TRANSPORT PHENOMENA IN MEMBRANES

A compilation of research papers submitted to
THE ALIGARH MUSLIM UNIVERSITY ALIGARH
for the award of the degree of

Doctor of Science

IN

CHEMISTRY

FASIH AHMAD SIDDIQI

DEPARTMENT OF CHEMISTRY
ALIGARH MUSLIM UNIVERSITY
ALIGARH INDIA
1983

To my inspirer Aligarh's

Prof. Rashid Ahmad Siddiqi

— great scholar and visionary

P R E F A C E

The last two decades have witnessed the extremely rapid growth in breadth and depth of the field of membrane science. The progress continues to be made at an almost breath taking pace which is amply depicted by the publication of innumerable volumes after volumes in this most important and fascinating field in which chemists, biochemists, biophysicists, biologists, pharmacologists, physiologists, immunologists, chemical engineers and molecular geneticists etc. are continuing to contribute both at the fundamental as well as at applied level.

In order to understand the extremely complex natural biomembrane systems, simpler and well defined model systems have been developed and studied in recent years. This has helped much in understanding the structure and dynamics of natural biomembranes. This thesis which is in the form of compilation of the recently published papers by the author (and coworkers) is an attempt in that direction and mainly deals with the studies of model systems. These are:

(i) Composite asymmetric polymeric membranes which can serve as model for nerve cells,

(ii) bilayer lipid membranes (BLM) which constitute one of the most realistic and useful models for biological

membranes and

(iii) the parchment membranes which behave like gastric mucosal membranes.

Transport of matter and of electric charge is irreversible in nature and a very large number of theoretical biologists are investigating transport phenomena in membranes from the basic theories of electrolyte conduction and are developing them by using thermodynamics of irreversible processes. Membranologists have now started thinking that equilibrium thermodynamics cannot very accurately describe the more complicated chemiosmotic schemes but the theory of irreversible thermodynamics as applied to biological systems may offer certain possibilities. Majority of biological phenomena at a molecular level develop at far from equilibrium and it is better to use the irreversible thermodynamic approach.

The various ionic processes in membrane systems have been listed in literature under five headings, namely, (i) ionic transport, "flux", (ii) membrane potential, (iii) electrical conductivity, (iv) ionic distribution equilibria and (v) spatial distribution of ions and potential within the membrane. In view of the above listing the various papers in this thesis have been grouped together in the form of following chapters. In Chapters 1 and 2 preparation

of composite membranes, measurement of impedances, asymmetric properties, water and ion permeabilities, electrolyte uptake etc. are described. Chapter 3 deals with the electrochemistry of bilayer lipid membranes (BLM). Electrical transients, steady-state mediated transport, channels (pores) and electronic processes in BLM are discussed. In Chapters 4 and 5 the theory of absolute reaction rate is applied to diffusion and various thermodynamic activation parameters are evaluated. Nernst-Planck formulae for electrical potentials and Ficks diffusion law have been used for diffusion rate measurements. Chapters 6 to 8 deal mainly with the studies of membrane potentials and bi-ionic potentials. Thermodynamically effective fixed charge density, membrane selectivity, permeability ratio etc. have been evaluated. Recently developed equations for membrane potentials and bi-ionic potentials based on irreversible thermodynamics have been applied for the evaluation of various membrane parameters.

The research work (mainly post-doctoral) described above was carried out by the author at the following advanced centres.

(1) University of Pennsylvania, School of Medicine, Department of Pharmacology (March 1969 - January 1972), U.S.A.

(2) Michigan State University, East Lansing, Department of Biophysics (March 1978 - October 1979), U.S.A.

The papers published from Aligarh Muslim University, India deal with the "studies of parchment membranes". Most of the work on this system was carried out at the author's membrane research laboratory in the department of Chemistry in collaboration with his students whose names appear in those papers, the most important being that of Dr. M. N. Beg who is now a colleague and an active member of the research group.

I am most grateful to my colleagues and coworkers in the department for their collaboration and pleasant association. In particular, I thank Prof. Wasiur Rahman, Chairman, Department of Chemistry and Dean Faculty of Science, Aligarh Muslim University for his encouragement and interest and who has been a constant source of inspiration throughout my stay at Aligarh. I would be failing in my duties if I do not thank Prof. M. S. Ahmad who has been helping me in achieving my academic pursuits for the last twenty years in the department.

I am also grateful to Prof. A. R. Kidwai, Prof. S. M. F. Rahman and (Late) Prof. M. O. Farooq who have helped me in the late fifties and sixties as Heads of the Department.

Prof. Wahid U. Malik supervised my Ph.D. work (1958-1961) and introduced me this fascinating field of membranes.

I owe much to him and no words are enough to thank him.

I am grateful to Prof. Tien of Michigan State University and Prof. Lakshminarayaniah of University of Pennsylvania with whom I have worked in U.S.A. These gentlemen who are the authorities in the field of membrane science have helped me a lot.

I am also appreciative of the support of the Chairman of the Department of Pharmacology, Prof. George B. Koelle, University of Pennsylvania and Chairman of the Department of Biophysics, Michigan State University, Prof. P. Johnson.

Thanks are due to various funding agencies, namely, (i) U.S. Public Health Service, (ii) U.S. National Institute of Health, (iii) Council of Scientific and Industrial Research (India), (iv) University Grants Commission (India), for providing the necessary funds for carrying out these investigations. I also thank the various reviewers for their critical evaluation of our papers and editors for publishing our papers in their esteemed journals. Amongst them are: Journal of Physical Chemistry, Biophysics J., J. of Membrane Science, J. of Polymer Science, J. Colloid and Interface Science, Lipid (all in U.S.A.); Z. Physik Chem., Kolloid-Z-Z. Polymer (Germany); J. De Chemie Physique (France), Electrochemica Acta (England); Electroanal Chem.

(Netherland); Acta Chim (Hungry); Bull. Chem. Society, Japan; Canadian Journal of Chemistry and Indian J. of Technology. I am also thankful to Prof. Milan Bier, Editor, "Membrane Processes in Industry and Medicine", (Plenum Press, New York, 1971) and to Prof. G. Milazzo, Editor, "Topics of Bioelectrochemistry and Bioenergetics" (John Wiley and Sons, New York, 1983) for including our articles in the form of two chapters dealing with membranes in these books.

Fasih Ahmad Siddiqi 9/11/83

Department of Chemistry
Aligarh Muslim University
Aligarh, India.

Fasih Ahmad Siddiqi
Reader

November, 1983.

Dr. Fasih Ahmad Siddiqi

LIST OF PUBLICATIONS:

1. Studies on the Sol-gel transformation of the ferro and ferricyanides of some metals. Part III. Gelation in chromic ferrocyanide. J. Phys. Chem., 66, 356 (1962) (U.S.A.).

2. Studies on the Sol-gel transformation of the ferro and ferricyanides of some metals. Part IV. Determination of pH and viscosity during gelation. J. Phys. Chem., 66, 357 (1962) (U.S.A.).

3. Studies in the membrane permeability of chromic ferro and ferricyanides. J. Colloid Sci., 18, 161-173 (1963) (U.S.A.).

4. Studies in the membrane permeability of cobalt and manganese ferrocyanide. Proc. Indian Acad. Sci., 56, 206-222 (1962).

5. Studies on Sol-gel transformation of chromic ferrocyanide. Kelloid-Z-Z. Polymer, 184, 41-47 (1962) (Germany).

6. Studies on the mixed gels of silica, alumina and ferric oxide. J. Prakt. Chem., 33, 152-160 (1965) (Germany).

7. Studies on the membrane permeability of cadmium ferro and ferricyanides. Bull. Chem. Soc. Japan, 40, 1746-1756 (1967).

8. Studies of membrane phenomena. Part I. Effect of temperature on diffusion of electrolytes through a parchment-supported silver iodide membrane. J. Electroanal. Chem., 23, 137-146 (1969) (England).

9. Studies of membrane phenomena. Part II. Determination of membrane potential and evaluation of membrane fixed charge density and permselectivity of parchment-supported silver iodide membrane. J. Electroanal. Chem., 23, 147-156 (1969) (England).

10. Studies with Inorganic precipitate membranes. Part I. Measurement of temperature dependence of electrolyte diffusion through membranes. Z. Physik Chem. (Frankfurt), 72, 298-306 (1970) (Germany).

11. Studies with Inorganic precipitate membranes. Part II. Evaluation of apparent fixed charge on membranes. Z. Physik Chem. (Frankfurt), 72, 307-314 (1970) (Germany).

12. Studies with Inorganic precipitate membranes. Part III. Consideration of energetics of electrolyte permeation through membranes. J. Polymer Sci., 9, 2853-2868 (1971) (U.S.A.).

13. Studies with Inorganic precipitate membrane. Part IV. Evaluation of apparent fixed charge on membranes. J. Polymer Sci., 9, 2869-2875 (1971) (U.S.A.).

14. Some asymmetry properties of composite membranes in "Membrane Process in Industry and Biomedicine", Edited by M. Bier (pp. 301-309), Plenum Publishing Corporation, New York (1971).

15. Studies with composite membranes. Part I. Preparation and Measurement of Impedances. Biophys. J., 11, 603-616 (1971) (U.S.A.)

16. Studies with composite membranes. Part II. Measurement of asymmetric properties. Biophys. J., 11, 617-628 (1971) (U.S.A.).

17. Studies with composite membranes. Part III. Measurement of water transport. Biophys. J., 12, 540-551 (1972) (U.S.A.)

18. Relationship between membrane potential and electrolyte uptake by ion-exchange membranes. J. Polymer Sci., 8, 2449-2455 (1970) (U.S.A.).

19. Ion and water movement in permselective membranes. Z. Physik Chem., 78, 150-163 (1972) (Germany).

20. Studies with Parchment-supported membranes. Application of Fick's Diffusion Law and Nernst-Planck Formulae for Electrical Potential, Consideration of Membrane Field strength and Energetics of Permeation of Biologically important cations. Bull. Chem. Soc. Japan, vol. 49 (2858-2863), No. 10, Oct. 1976.

21. Studies with parchment supported membranes. Determination of thermodynamically effective fixed charge density by various methods and evaluation of permselectivity. Bull. Chem. Soc. Japan, vol. 49 (2864-2868), No. 10, Oct. 1976.

22. Studies with model membranes. Evaluation of the thermodynamically effective fixed charge density and permselectivity of cobalt tungstate and mercuric chromate membranes. Electroanal. Chem., 80, 223-238, 1977 (England).

23. Studies with model membranes. X. Evaluation of the thermodynamically effective fixed charge density and permselectivity of mercuric and cupric iodide parchment-supported membranes. J. Polymer Sci., 15, 959-972, 1977 (U.S.A.).

24. Studies with model membranes. Evaluation of thermodynamic parameters from the transition state theory of rate processes for electrolyte diffusion through silver chloride parchment supported membrane. J. Polym. Sci., 15, 1935-1956 (1977) (U.S.A.).

25. Studies with Inorganic precipitate membrane. Part XI. Evaluation of the thermodynamically effective fixed charge density by various methods. Electro. Chimica Acta., 22, 631-637 (1977) (England).

26. Studies with Inorganic precipitate membrane. Part XII. Consideration of membrane field strength and energetics of permeation. Electro. Chimica Acta, 22, 639-646 (1977) (England).

27. Studies with model membranes. Part XVII. Evaluation of thermodynamic activation parameters and effective fixed charge density of parchment supported membranes. J. De Chemie Physique, 74, No. 9, 932-941 (1977) (France).

28. Studies with Inorganic precipitate membrane. Part XIX. Evaluation of effective fixed charge density. Canadian J. of Chemistry, 55, 1680-1686 (1977).

29. Studies with model membranes. Evaluation of thermodynamic parameters for diffusion and fixed charge density by methods based on thermodynamics of irreversible processes. J. Memb. Sci., 2, 245-265 (1977) (U.S.A.).

30. Studies with parchment supported membranes. Determination of thermodynamically effective fixed charge density and permselectivity. Acta Chimica, 93 (2), 123-133 (1977) (Hungry).

31. Studies with model membranes. Evaluation and comparison of thermodynamic effective fixed charge density by different methods. Kolloid-Z-Z. Polymer, 256, 552-562 (1978) (Germany).

32. Studies with Inorganic precipitate membranes. Membrane potential response, characterization and evaluation of effective fixed charge density. J. Electroanal. Chem., 89, 141-147 (1978) (England).

33. Studies with model membranes. Part XIX. Evaluation of permselectivity and thermodynamically effective fixed charge density of mercuric tungstate parchment supported membrane. Indian J. of Chemistry 16A, 7-11 (1978).

34. Studies with Inorganic precipitate membranes. XXV. Evaluation of membrane parameters and test of recently developed fixed charge theories of membrane potential. J. Memb. Sci., 2, 365-374 (1977) (U.S.A.).

35. Studies with model membranes. Part XXIV. Evaluation of membrane fixed charge density and biionic potential based on thermodynamics of irreversible processes. J. Memb. Sci., 4, 275-283 (1978) (U.S.A.).

36. Studies with model membranes. Test of the theories of membrane potential and biionic potentials based on non-equilibrium thermodynamics. J. Electroanal. Chem., 92 (2), 231-238 (1978) (England).

37. Studies with model membranes. Part XXIV. Evaluation of thermodynamic activation parameters, effective fixed charged density and test of the theory of bi-ionic potential based on the thermodynamics of irreversible processes. Canadian J. Chem., 56, 2205-2215 (1978).

38. Studies with model membranes. Part XXII. Evaluation of thermodynamic parameters and test of theories of membrane potential and bi-ionic potential based on non-equilibrium thermodynamics. J. Polymer Sci., 17, 539-550 (1978) (U.S.A.).

39. Studies with model membranes. XXV. Evaluation of fixed charge density and test of membrane potential and bi-ionic potential theories based on thermodynamics of irreversible Processes. J. De Chimie Physique (France), 76, 57-60 (1979).

40. Studies with Inorganic precipitate membranes. XXII. Evaluation of thermodynamically effective fixed charge density and test of the most recently developed theory of membrane potential based on the principles of non-equilibrium thermodynamics. Electrochimica Acta (England) 24, 85-88 (1979).

41. Studies with inorganic precipitate membranes. Part XXII. Evaluation of membrane selectivity from electrical potential and conductivity measurements. J. Electroanal. Chem. (England), 98(2), 231-240 (1979).

42. Studies with inorganic precipitate membranes. Evaluation of effective fixed charge density and selectivity of membrane from electrical potential measurements. Proc. Ind. Natl. Acad., 45A(6), 543-557 (1979).

43. Studies with Model Membranes. Evaluation of membrane parameters and test of the theory of bi-ionic potential based on the thermodynamics of irreversible processes. J. Membrane Science (U.S.A.), 4, 275-281 (1978).

44. Studies with Model Membranes. Evaluation of fixed charge density and test of membrane potential and bi-ionic potential theories based on thermodynamics of irreversible processes. J. de Chimie Physique (France), 76, 57-60 (1979).

45. Studies with Inorganic Precipitate Membranes. Membrane potential and bi-ionic potential. Bull. Chem. Soc. Japan, 52(9), 2696-2698 (1979).

46. Studies with parchment supported cobalt(II) phosphate membrane for potential use for a phosphate ion selective electrodes. Frezenius Z. Anal. Chem. (Germany), 298, 157-158 (1979).

47. Preparation of cupric palmitate membranes. Its characterization and evaluation of thermodynamically effective fixed charge density. Lipids (U.S.A.), 14(7), 682-686 (1979).

48. Micro-detection of L-cysteine, Methionine, Thiourea .... with potassium chromate in hydrochloric acid medium. The Analyst (England), 104, 977-979 (1979).

49. Evaluation of effective fixed charge density of stannic phosphate membrane from membrane potential measurements. Indian J. Tech., 17, 419-422 (1979).

50. Studies with polystyrene based zinc and ferric phosphate membranes. Evaluation of .... Indian J. Chem., 17A, 434-436 (1979).

51. Studies with Model Membranes. Evaluation of the thermodynamically effective fixed charge density and test of theories of membrane potential and bi-ionic potential based on thermodynamics of irreversible processes. J. Indian Chem. Soc., LXII, 199-202 (1980).

52. Studies with Inorganic Precipitate Membranes. Membrane potential, bi-ionic potential and evaluation of membrane parameters. Polish J. Chem., 54 (11-12), 2253 (1980).

53. Transport through inorganic precipitate membranes. Application of absolute reaction rate theory and theory of membrane potential. Indian J. Chem., 20A, 216-220 (1981).

54. Mechanism of ion transport through parchment supported lead orthovanadate membrane. Indian J. Tech., 19, 135-138 (1981).

55. Transport of Alkali chlorides in parchment supported cupric hydroxide membrane and application of absolute reaction rate theory. J. Electroanal. Chem., 122, 313-319 (1981) (England).

56. Antigen-antibody complement reaction studies on micro bilayer lipid membranes. Proceedings of VII International Biophysics and III Pan-American Biochemistry Congress (1981) (U.S.A.).

57. Electrochemistry of Bilayer Lipid Membrane (BLM) in "Topics in Bioenergetics and Biomembranes", vol. V. Edited by G. Milazzo, John Wiley & Sons, Inc. New York (1983).

58. Evaluation of membrane selectivity and bi-ionic potential of polystyrene-based ferric orthovanadate membrane. Indian J. Tech., 21, 78-82 (1983).

59. Metal ion transport through barium tungstate parchment supported membrane. J. Colloid & Interface Sci., (In press).

A number of papers are under communication to various international journals.

A book entitled "Coal" is under publication. Manuscript of the book entitled "Synthetic Membrane Models" is under preparation and would be soon submitted to John Wiley & Sons (New York).

C O N T E N T S

CHAPTER 1

STUDIES WITH COMPOSITE MEMBRANES

STUDIES WITH COMPOSITE MEMBRANES

I. Preparation and Measurement of Impedances

N. LAKSHMINARAYANAIAH *and* FASIH A. SIDDIQI

Reprinted from the Biophysical Journal, 1971, Vol. 11, No. 7, pp. 603–616 *Printed in U.S.A.*

STUDIES WITH COMPOSITE MEMBRANES

I. PREPARATION AND MEASUREMENT OF IMPEDANCES

N. LAKSHMINARAYANAIAH *and* FASIH A. SIDDIQI

From the Department of Pharmacology, School of Medicine, University of Pennsylvania, Philadelphia, Pennsylvania 19104.

ABSTRACT Simple and composite membranes have been prepared from 2% collodion solutions containing different amounts of polystyrenesulfonic acid (PSSA). Various membrane parameters such as water content, electrolyte uptake, exchange capacity, and permselectivity of these membranes have been determined. The resistance and capacitance of simple membranes have been measured as functions of both external electrolyte concentration and internal fixed charge density. The impedance characteristics of composite membranes also have been determined and discussed in terms of the resistance and capacitance characteristics of simple membranes from which the composite structures have been formed.

INTRODUCTION

Biological membranes show asymmetric behavior when the same drug or reagent is applied in different ways (Adelman and Senft, 1968; Lakshminarayanaiah, 1969 *a*). For example, it is observed in the case of the giant axon of the squid that tetrodotoxin blocks the initial inward sodium current through the nerve membrane when the toxin is applied externally (Narahashi et al., 1964; Nakamura et al., 1965). Internal application of the same drug at the same concentration has no effect on the sodium current, although at higher internal concentrations, it becomes effective (Narahashi et al., 1966). On the other hand, tetraethylammonium ion blocks the late outward potassium current through the nerve membrane when applied internally (Tasaki and Hagiwara, 1957; Armstrong and Binstock, 1965; Armstrong, 1966). Similarly, cesium ion is able to block the outward potassium current when applied internally (Chandler and Meves, 1965; Adelman and Senft, 1966), but is without effect on this current when applied externally (Pickard et al., 1964). These asymmetries in behavior indicate the existence of dissimilar membrane surfaces. This dissimilarity may arise from a number of factors, some of which are differences in fixed charge density, porosity, selectivity, etc., of the two membrane faces. Other biological membranes, for example, frog skin (Ussing,

1966), gastric mucosa (Rehm, 1966), toad bladder (DiBona et al., 1969), etc., are considered to possess composite structures. In order to understand the behavior of these complex biological systems, simple polymeric membranes for quite some time (Lakshminarayanaiah, 1965) and lipid bilayer membranes in recent years (Mueller et al., 1962 *a*, *b*) have been used as models by a number of investigators whose work has been reviewed by Lakshminarayanaiah (1969 *b*).

In a series of theoretical papers, Kedem and Katchalsky (1963 *a*, *b*, *c*) have discussed the behavior of complex membranes. Recently such complex membranes have been prepared (Liquori and Botre, 1964, 1967; Liquori et al., 1966; Hays, 1968; de Korosy, 1968) and used in a few studies as models (Botre et al., 1967; Hays, 1968) to understand the behavior of living membranes. We have been engaged in similar studies to develop complex artificial systems. Composite membranes of two types, layer type and sandwich type, have been prepared from 2% collodion solutions containing different amounts of polystyrenesulfonic acid (PSSA). The impedance characteristics of these, and also of the simple membranes from which the composite membranes have been formed, are described in this paper.

EXPERIMENTAL

Simple membranes of collodion containing various amounts of PSSA were prepared by following the steps given by Neihof (1954) for the dissolution method. Styrene polymer (The Borden Chemical Co., Philadelphia, Pa.) used for the preparation of PSSA had a molecular weight of 35,000. PSSA, after purification, had an acid value of 4.0 meq/g as opposed to 5.4 meq/g, the theoretical value which could be derived on the assumption that every benzene ring had one sulfonic acid group. Membranes were cast on clean and dry glass plates from a 2% solution of Parlodion (pyroxylin, purified nitrocellulose, Mallinckrodt Chemical Works, St. Louis, Mo.) in alcohol-ether (3:1 ratio) containing a definite amount of PSSA. A Gardner film-casting knife (Gardner Laboratory, Inc., Bethesda, Md.), preset to produce a membrane of definite thickness, was used to spread the membrane-forming solution which, on spreading, was allowed to dry for 1 hr at room temperature and for another ½ hr at 60–70°C in an oven. The simple membranes were designated A, B, C, D, E, F, G, and H, and contained 8.3, 4.2, 2.1, 1.0, 0.8, 0.2, 0.02, and 0.002 mg PSSA per ml of the membrane-forming solution, respectively. Some membranes were also cast from a solution of nitrocellulose (concentration ~2%) which was formed from the commercial collodion (USP, Fisher Scientific Company, Pittsburgh, Pa.). The final alcohol:ether ratio was 1:2.5.

The composite membranes, otherwise called asymmetric membranes, of two types described by Liquori and Botre (1964, 1967), were prepared by following their steps although the compositions of the membrane-forming solutions were different. Type one, called the layer-type membranes, designated AD, AF, AG, AH, and ADFGH, were formed by casting different layers of 2% Parlodion solutions containing varying amounts of PSSA (8.3–0.002 mg/ml), one on top of the other (layer of lowest PSSA content first), in the way described by Liquori and Botre (1964). For example, the composite membrane AD was formed by first forming the simple membrane D as described above. Then on top of it, membrane A was formed by spreading and drying the membrane-forming solution A, i.e., 2% Parlodion solution containing 8.3 mg PSSA per ml of membrane-forming solution. All these membranes

were formed from Parlodion solutions in which the alcohol:ether ratio was 3:1. Type two, called sandwich-type membranes, were formed as outlined by Liquori and Botre (1967) by trapping a layer of PSSA (4 mg/ml) between high charge density membrane (~2% collodion, USP, Fisher Scientific Company, containing 10 mg PSSA per ml) and low charge density membrane (~2% collodion, USP, Fisher Scientific Company, containing 1 mg PSSA per ml). In this case, the alcohol:ether proportion was 1:2.5.

The membranes, simple and composite, were converted into the sodium form by treating them with about 200 ml of a strong solution (2-3 N) of NaCl. They were usually left in this solution for future use. When they were required, they were taken out of this solution and washed thoroughly with deionized water and equilibrated for about 2 hr with gentle stirring in about 100 ml of the solution to be used in the experiment.

The water content, electrolyte uptake, and exchange capacity of the different membranes were estimated by following the procedures described in our earlier publications (Lakshminarayanaiah and Subrahmanyan, 1964; Lakshminarayanaiah and Brennen, 1966; Lakshminarayanaiah and Siddiqi, 1970). These membrane parameters, which were determined accurate to ±5% using at least three membranes, are given in Table I.

The electrochemical cells of the type

Hg_2Cl_2-Hg	Saturated KCl-agar	Electrolyte solution C_1	Membrane	Electrolyte solution C_2	Saturated KCl-agar	Hg_2Cl_2-Hg

were used for measuring electrical potentials arising across different types of membranes. The potentials were measured using a Keithley microvoltmeter (Keithley Instruments, Inc., Cleveland, Ohio) at room temperature (air-conditioned).

The concentration potentials arising across the simple membranes were measured by maintaining a tenfold difference in concentration (i.e., $(C_2/C_1) = 10$) in the range 0.001–1.0 N. At least four membranes were used in each concentration step. The mean and the standard error of the mean of these measurements were computed. The potentials measured

TABLE I

EQUILIBRIUM PROPERTIES OF SIMPLE AND COMPOSITE (LAYER-TYPE) MEMBRANES FORMED FROM 2% SOLUTION OF PARLODION IN ALCOHOL-ETHER (3:1 RATIO) CONTAINING DIFFERENT AMOUNTS OF POLYSTYRENESULFONIC ACID

Membrane	Amt of PSSA	Water content	Exchange capacity (Acid given into 2 N NaCl)	Chloride uptake in 0.1 N NaCl
	mg/ml	*g H_2O/100 g wet membrane in H-form*	*meq/g wet membrane*	*meq/g wet membrane*
A	8.3	39.0	0.57	7.0×10^{-3}
B	4.2	30.3	0.40	6.6×10^{-3}
C	2.1	12.2	0.35	4.6×10^{-3}
D	1.0	—	0.17	4.0×10^{-3}
E	0.8	10.7	0.08	4.0×10^{-3}
F	0.2	8.5	0.02	3.0×10^{-3}
G	0.02	7.0	0.01	—
H	0.002	7.0	0.01	3.0×10^{-3}
ADFGH	—	15.0	0.16	8.0×10^{-3}

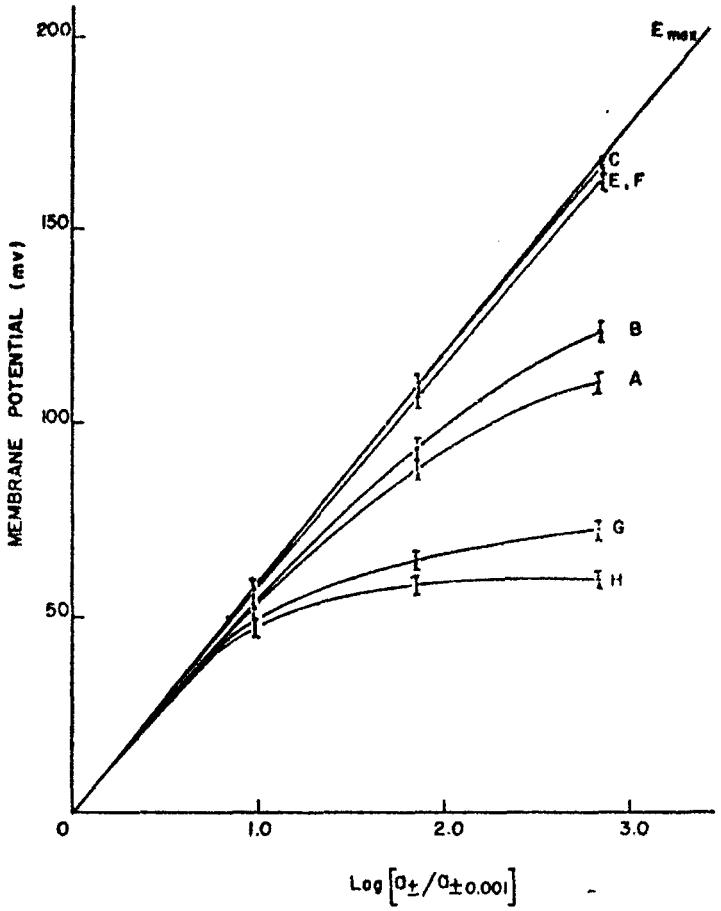

FIGURE 1 Electrical potentials (mv) arising across simple membranes plotted as a function of log $(a_{\pm}/a_{\pm 0.001})$. E_{max} represents the maximum theoretical Nernst potential. A, B, C, E, F, G, and H represent potentials arising across 2% Parlodion membranes (alcohol:ether ratio = 3:1) containing different amounts of PSSA (A = 8.3, B = 4.2, C = 2.1, E = 0.8, F = 0.2, G = 0.02, and H = 0.002 mg PSSA per ml of membrane-forming solution).

for the different concentration steps were added and the corresponding standard error for the added mean was calculated. The means with their standard errors (1 standard error) were plotted against log $(a_{\pm}/a_{\pm 0.001})$ where $a_{\pm}$ was the mean activity of the solution of higher concentration. This plot is shown in Fig. 1 along with the straight line E_{max} which represents the maximum theoretical value of the potential calculated according to the Nernst equation

$$E_{max} = \frac{RT}{F} \ln \frac{a_{\pm}}{a_{\pm 0.001}}. \qquad (1)$$

Electrical potentials were not observed across simple membranes when the same electrolyte of the same concentration (i.e., $C_1 = C_1$) was placed on its two sides. Under similar conditions, composite membranes, both layer and sandwich types, generated considerable potentials, and these are described in Part II (Lakshminarayanaiah and Siddiqi, 1971).

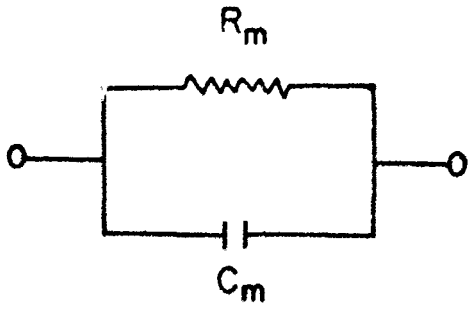

FIGURE 2 The equivalent electrical circuit for a simple membrane. R_m and C_m are membrane resistance and capacitance respectively.

The impedances of the membranes were measured on a General Radio Z-Y bridge (General Radio Co., Concord, Mass.) using the membrane cell described elsewhere (Lakshminarayanaiah and Subrahmanyan, 1968). The cell was kept in a water thermostat maintained at 25 ±0.01°C. In this method, purified mercury equilibrated with the solution in which the membrane had to be used was placed on either side of the membrane. Extensive use of this method has indicated that the following additional precautions should be taken to realize reproducible values:

(*a*) There should be no trapped air particularly at the corners of the cell near the membrane faces.

(*b*) Mercury is likely to be oxidized to form mercuric oxide which would form films on membrane faces and cause irreproducibility. This seems to be the major factor affecting the reproducibility of the results. Using only purified mercury has eliminated this problem in our studies and has given reproducible results.

The resistance R_s and the reactance X_s of the simple membranes, considered equivalent to the electrical circuit shown in Fig. 2, were measured on the General Radio Z-Y bridge. By the usual analysis (Lakshminarayanaiah and Shanes, 1965) the membrane resistance R_m and capacitance C_m were evaluated from the equations

$$R_m = R_s\left[1 + \left(\frac{X_s}{R_s}\right)^2\right], \tag{2}$$

$$\omega C_m R_m = \frac{X_s}{R_s}, \tag{3}$$

where $\omega = 2\pi f$ and f is the frequency (10^3 cycles/sec) used to measure R_s and X_s. R_m and C_m are expressed in ohms·cm² and μF/cm² respectively and are given in Table II as functions of both external electrolyte concentration and quantity of fixed charge present in the membrane. The impedance Z of a membrane is given by

$$Z = \sqrt{R_s^2 + X_s^2} \tag{4}$$

and the values derived for simple and layer-type composite membranes in equilibrium with 0.01 N NaCl solution are given in Table III. Similar values derived for the other simple and sandwich-type membranes are given in Table IV. All these impedance measurements had an error of ±10%.

TABLE II

MEMBRANE RESISTANCE R_m AND CAPACITANCE C_m OF SIMPLE MEMBRANES AS A FUNCTION OF EXTERNAL ELECTROLYTE CONCENTRATION*

Membrane‡	Amt PSSA	NaCl concentration (eq/liter) 10^{-4}		10^{-3}		10^{-2}		10^{-1}	
		R_m	C_m	R_m	C_m	R_m	C_m	R_m	C_m
	mg/ml	*ohms·cm²*	*μF/cm²*	*ohms·cm²*	*μF/cm²*	*ohms·cm²*	*μF/cm²*	*ohms·cm²*	*μF/cm²*
A	8.3	29.2	8.2	21.8	12.6	9.5	21.6	5.1	46.0
B	4.2	45.7	5.4	30.4	9.6	20.0	18.6	6.5	40.4
C	2.1	43.0	4.5	29.4	8.0	25.0	15.0	7.3	36.6
D	1.0	107.7	0.7	77.8	0.5	64.9	0.4	12.1	3.7
F	0.2	1.4×10^4	0.006	0.8×10^4	0.012	0.4×10^4	0.022	0.2×10^4	0.030
G	0.02	8.9×10^4	0.0018	6.6×10^4	0.0014	3.5×10^4	0.010	0.7×10^4	0.006
H	0.002	19.5×10^4	0.0006	11.0×10^4	0.0006	4.1×10^4	0.004	1.8×10^4	0.002

* Membrane thickness ~ 0.02 mm.
‡ 2% Parlodion; alcohol: ether (3:1).

TABLE III

IMPEDANCES OF SIMPLE AND COMPOSITE MEMBRANES IN EQUILIBRIUM WITH 0.01 N NaCl SOLUTION

Membrane*	Thickness	X_s	R_s	Z (equation 4)
	mm	*ohms*	*ohms*	*ohms*
Simple				
A	0.025	13‡	10‡	16.4
D	0.030	30‡	180‡	182
F	0.020	0.4×10^4	0.8×10^4	0.9×10^4
G	0.018	0.6×10^4	1.6×10^4	1.7×10^4
H	0.017	3.2×10^4	5.4×10^4	6.3×10^4
Composite layer type				
AD	0.040	10	10	14.2
AF	0.045	8.5	22.0	23.5
AG	0.040	13.5	30.0	32.9
AH	0.040	35.0	80.0	87.3
ADFGH	0.095	1.7×10^4	4.3×10^4	4.6×10^4

* 2% Parlodion; alcohol:ether (3:1).
‡ Values for R_m and C_m calculated from equations 2 and 3 for membranes A and D are 9.1 ohms·cm², 22.8 μF/cm² and 63.0 ohms·cm², 0.42 μF/cm². These values for a membrane thickness of 0.02 mm (i.e., ½ thickness of composite membrane AD) become 7.3 and 42.0 ohms·cm² for R_m of A and D, and 28.5 and 0.63 μF/cm² for C_m of A and D respectively.

TABLE IV

IMPEDANCES OF SIMPLE AND SANDWICH-TYPE MEMBRANES IN EQUILIBRIUM WITH 0.1 N NaCl SOLUTION

Membrane*	Amt of PSSA	Thickness	X_s	R_s	Z (equation 4)
	mg/ml	*mm*	*ohms*	*ohms*	*ohms*
High charge	10.0	0.200	9.0‡	21.0‡	22.8
Low charge	1.0	0.200	22.0‡	115.0‡	117.1
Sandwich	-	0.180	14.0	42.0	44.2

* 2% collodion; alcohol:ether (1:2.5).

‡ Values for R_m and C_m calculated from equations 2 and 3 for high and low charge density membranes are 8.5 ohms·cm², 8.0 μF/cm² and 40.6 ohms·cm², 0.8 μF/cm². Corrected for membrane area (0.34 cm²) and thickness (0.06 mm) these become 7.5 ohms (R_H) and 9.1 μF (C_H) for high charge density membrane and 36 ohms (R_L) and 0.91 μF (C_L) for low charge density membrane.

RESULTS AND DISCUSSION

The results of Table I show that the water content of the simple membranes with large quantities of PSSA in them is high. Consequently the quantity of PSSA present in the membrane determines both its porosity and the fixed charge density. How these two parameters interact to control the over-all permselectivity of the membrane is shown in Fig. 1. Although membranes A and B have high quantities of PSSA, they generate potentials which are lower than those generated by membranes C, E, and F containing low quantities of PSSA. Despite their high exchange capacities, membranes A and B because of their high water contents (i.e., high porosities) are not able to exclude coions such as chloride from the membrane phase (see last column of Table I). Thus these two factors, viz. the ability to prevent coion uptake brought about by the tightness of the membrane (i.e., less water present) and the presence of fixed negative charge (0.02 meq/g) on the membrane, are responsible for the high electrical potentials generated by membranes E and F. Membranes G and H have the tightness required for excluding coions as effectively as E and F. However, they do not have the capacity for generating the diffusion potentials because of the lack of fixed groups. These two factors are effectively combined in a suitable proportion in membrane C. It has an exchange capacity of 0.35 meq/g and 12.2% water and has the highest permselectivity in that the potentials are very close to the theoretically predicted E_{max} values given by equation 1.

In agreement with what has been described above, it is found that the resistance R_m of simple membranes which contain high PSSA is low, whereas the R_m of those which contain low PSSA is high (see Table II). This can be attributed to the presence of more charge carriers (counterions and coions) in the case of membranes

TABLE V
ELECTROLYTE CONTENT OF MEMBRANE E AS A FUNCTION OF EXTERNAL NaCl SOLUTION

Solution concentration	Na^+	Cl^-
eq/liter	*meq/g wet membrane*	*meq/g wet membrane*
0.0001	0.411	1.3×10^{-4}
0.001	0.411	1.5×10^{-3}
0.01	0.422	2.1×10^{-3}
0.1	0.442	4.0×10^{-2}
0.5	0.468	12.7×10^{-2}

of high PSSA content. On this basis, the increase in R_m with decrease in external electrolyte concentration observed in all cases given in Table II may be explained. As the external concentration is decreased, the electrolyte uptake of the membrane also is decreased. This can be seen in the electrolyte uptake data given in Table V for the membrane E. Similar behavior was noted in the case of composite membranes whose impedances also increased with decrease in the external electrolyte concentration (values not given).

The data obtained with simple membranes formed from collodion solutions (alcohol:ether ratio = 1:2.5) and given in Table IV show that the values for the membrane resistances for both high charge and low charge density membranes (thickness ~0.2 mm) are low compared to simple membranes (thickness ~0.02 mm) formed from Parlodion solutions (alcohol:ether ratio = 3:1). Obviously the increased proportion of ether in the membrane-forming solution made these membranes more porous. Membrane D (see Table II) corresponds to the low charge density membrane (see Table IV) in respect to its PSSA content. But the values for R_m of these two membranes are different. Increase of alcohol:ether proportion by about 7.5 times reduced the value of R_m of the low charge density membrane by nearly 0.06 times when proper correction for differences in the thickness of the two membranes was made.

The other interesting property of simple membranes is the change in the value of their capacitance when their PSSA and electrolyte contents are increased. Data given in Table II show that increase of both PSSA content and the concentration of the external electrolyte solution gave higher values for C_m. According to the parallel plate capacitor equation,

$$9 \times 10^{11} C_m = (\epsilon/4\pi d), \tag{5}$$

(where C_m is in farads per square centimeter, ϵ is the dielectric constant, and d is

the thickness in centimeters), this increase in the value of C_m can arise from a decrease in the thickness of the membrane or an increase in the dielectric constant of the membrane material or both. Increase of PSSA content of the membrane increased the membrane water content (see Table I) but for any given PSSA content, the membrane thickness remained practically constant when the concentration of the external electrolyte was changed. Since the species present in the membrane causing this change in C_m (i.e., PSSA, ions, and water) are all polar in nature, increase in C_m with increase in PSSA and electrolyte content of the membrane can be attributed to an increase in the value of ϵ. A similar effect of electrolyte concentration on C_m was noted also in our earlier studies with thin Parlodion membranes (Lakshminarayanaiah and Shanes, 1965).

Although values for R_m and C_m can be computed easily for simple membranes from bridge readings of R_r and X_r, such a calculation cannot be done for composite membranes primarily because they cannot be described by any definite equivalent circuit. Nevertheless, their impedances can be obtained from equation 4 These values given in Tables III and IV indicate some interesting points. The composite membrane AD formed from simple membranes A and D has a value for its impedance Z which is less than the value realized for either membrane A or D. In the case of other composite membranes (AF, AG, and AH) the Z values lie between the values obtained for the two simple membranes but are closer to the value of membrane A. In the case of the highly composite membrane ADFGH, the Z value is higher and closer to that of the membrane H.

It is very difficult to represent any of the composite membranes by equivalent circuits of the type shown in Fig. 2 for the simple membranes. However an ideal case, where the simple membranes (A, D, F, G, and H), retaining their identity, combine to form the composite membrane ADFGH, may be considered. This structure can be represented by the equivalent circuit shown in Fig. 3. Such an ideal system, in practice, is very difficult to construct. The interactions involved in its

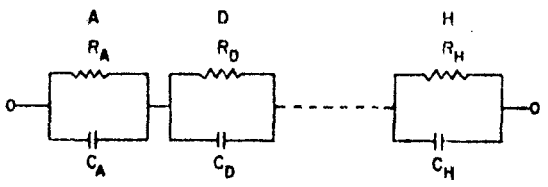

FIGURE 3

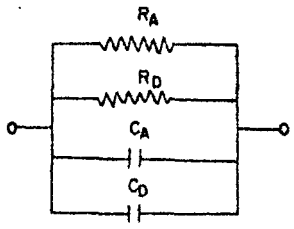

FIGURE 4

FIGURE 3 The equivalent electrical circuit for an ideal composite membrane built from simple membranes A, D, ···, H. R's and C's are simple membrane resistances and capacitances respectively.

FIGURE 4 A probable equivalent electrical circuit for the layer type composite membrane AD. R's and C's are simple membrane resistances and capacitances respectively.

formation are unknown and cannot be controlled. Many possibilities of composite membrane formation even from two simple membranes exist and some of these are examined below.

If we assume that the composite membrane AD conforms to the circuit given in Fig. 3, the impedance of the circuit for the two units A and D is given by

$$\frac{R_A}{1 + i\omega C_A R_A} + \frac{R_D}{1 + i\omega C_D R_D}, \tag{6}$$

where R_j and C_j are the resistance and capacitance of simple membrane j and $i = \sqrt{-1}$. Separating the real and imaginary parts of equation 6 yields

$$R_z = \frac{R_A}{1 + \omega^2 C_A^2 R_A^2} + \frac{R_D}{1 + \omega^2 C_D^2 R_D^2}, \tag{7}$$

$$X_z = \frac{\omega C_A R_A^2}{1 + \omega^2 C_A^2 R_A^2} + \frac{\omega C_D R_D^2}{1 + \omega^2 C_D^2 R_D^2}. \tag{8}$$

From equations 7 and 8, values for R_z and X_z can be computed, as the values of R_A, R_D, C_A, and C_D are known from independent measurements using simple membranes with 0.01 N NaCl solution (see Table VI). Substituting the values after correction for thickness (i.e., ½ thickness of membrane AD: R_A = 21.4 ohms, C_A = 9.7 μF, R_D = 123 ohms, and C_D = 0.214 μF) in the above equations, and solving them, give values of 128 and 32 (ohms) for R_z and X_z respectively. These do not agree with the observed values of 10.0 and 10.0 (see Table III). Similar disagreement was noted also in the case of the other membranes AF, AG, and AH. To compromise this discrepancy, one must add a series negative impedance to the membrane elements A and D. As no such negative impedance is known to exist in these artificial systems, the ideal circuit must be either rejected or modified. Rejection in favor of the other possibility, viz. formation of an entirely different membrane out of A and D possessing its own characteristics, gives some interesting results. Values of R_z and X_z for the membrane AD (i.e., 10.0 and 10.0 ohms) by the usual analysis using equations 2 and 3 give values of 6.8 ohms·cm² and 23.2

TABLE VI

VALUES OF R_m AND C_m FOR SIMPLE MEMBRANES (AREA = 0.34 cm²) IN EQUILIBRIUM WITH 0.01 N NaCl SOLUTION*

Membrane	A	D	F	G	H
Thickness, *mm*	0.025	0.030	0.020	0.018	0.017
R_j, *ohms*	26.7	185	1×10^4	1.8×10^4	7.3×10^4
C_j, *μF*	7.75	0.143	0.008	0.0033	0.0013

* Calculated according to equations 2 and 3 from the data given in Table III.

$\mu F/cm^2$ for R_m and C_m respectively. If the elements R_A, R_D, C_A, and C_D are coupled to form the circuit shown in Fig. 4, then the use of the values given above for R_A, R_D, C_A, and C_D yield the values 6.2 ohms·cm^2 and 29.1 $\mu F/cm^2$ for R_m and C_m. These values are close to those derived above from the simple circuit (Fig. 2); however, this agreement is considered fortuitous in view of the fact that such a scheme (Fig. 4) is found inapplicable to the other membranes AF, AG, and AH. Consequently, modifying the ideal scheme (Fig. 3) seems to be realistic. This modification is to assume that membrane A retains its characteristics and that the properties of membrane D in series with A are altered. Even this scheme fails because equations 7 and 8 lead to negative values for C_D. A better scheme is to assume that the membrane AD is composed oe three units, the two units A and D holding between them a third unit formed from A and D. This would conform in principle to the circuit shown in Fig. 3. As the middle unit is formed at the expense of A and D, the thicknesses of A and D will be affected. We assume (because equal volumes of A and D are used to form AD), for the sake of simplicity, that the thicknesses of A and D are reduced to the same extent, while their unit resistance (R_m) and capacitance (C_m) characteristics remain unaltered. Provided the thicknesses of the end units A and D are known, the unknown parameters of the middle unit can be quantitatively estimated. There is no straightforward way to derive these. The only way this can be done reasonably is to use the data of Table III with equations 7 and 8. These equations upon expansion to include the characteristics (R_k and C_k) of the middle unit, become

$$R_x = \frac{R'_A}{1 + \omega^2(R'_A)^2(C'_A)^2} + \frac{R_k}{1 + \omega^2 R_k^2 C_k^2} + \frac{R'_D}{1 + \omega^2(R'_D)^2(C'_D)^2}, \qquad (9)$$

$$X_x = \frac{\omega C'_A(R'_A)^2}{1 + \omega^2(R'_A)^2(C'_A)^2} + \frac{\omega C_k R_k^2}{1 + \omega^2 R_k^2 C_k^2} + \frac{\omega C'_D(R'_D)^2}{1 + \omega^2(R'_D)^2(C'_D)^2}, \qquad (10)$$

where R_x and X_x are the measured values for the composite membrane AD (see Table III) and R'_A, R'_D, C'_A, C'_D are the resistance and capacitance values for the simple membranes A and D corresponding to their reduced thicknesses (i.e., as they prevail in composite membrane AD). For any arbitrarily chosen thickness, for example 0.01, 0.001, 0.0001 mm, etc., values for R'_A, R'_D, C'_A, C'_D can be calculated from the values given in Table VI. Using these values in equations 9 and 10, sample calculations can be made to derive values for R_k and C_k. Such calculations gave negative values for the factor $[R_k/(1 + \omega^2 R_k^2 C_k^2)]$. However, when values of R'_A, R'_D, C'_A, C'_D corresponding to a membrane thickness of 0.0015 mm were used, a small positive value (0.3) was obtained for the same factor. Similar calculations using equation 10 gave a higher value (7.94) for the factor $[(\omega R_k^2 C_k)/(1 + \omega^2 R_k^2 C_k^2)]$. Solving these gave values of 210 ohms and 20 μF for R_k and C_k respectively. The results of similar calculations pertaining to the other composite membranes are collected in Table VII. The values of R_k (except membrane AD) de-

TABLE VII

CHARACTERISTICS OF THE MIDDLE UNIT PRESENT IN THE COMPOSITE MEMBRANE*

Composite membrane	AD	AF	AG	AH
Composite membrane thickness, *mm*	0.040	0.045	0.040	0.040
Assumed thickness of end units, *mm*	0.0015	0.00004	0.000034	0.000018
Middle unit thickness, *mm*	0.037	0.0449	0.0399	0.03996
Characteristics of simple membrane corresponding to the thickness assumed	(A) (D)	(A) (F)	(A) (G)	(A) (H)
R_l, *ohms*	1.6:9.3	0.043:20	0.036:34	0.019:72
C_l, μF	129:2.4	4850:4	5700:1.76	10780:1.67
$\frac{R_k}{1 + \omega^2 R_k^2 C_k^2}$	0.3	6.084	0.1864	34.3
$\frac{\omega R_k^2 C_k}{1 + \omega^2 R_k^2 C_k^2}$	7.94	0.4593	2.38	0.6
R_k, *ohms*	210	6.1	30.6	34.3
C_k, μF	20	1.97	65.7	0.08

* Computed from equations 9 and 10 using the known characteristics of simple membranes.

rived for the middle units, whose thicknesses are nearly the same as the thicknesses of the composite membranes themselves, appear reasonable. The exception noted (membrane AD) here confirms the fact, already mentioned above, that the various units are united according to Fig. 4 and not according to Fig. 3. The values of C_k also appear reasonable although the value for membrane AG is high. This is difficult to explain, but it could arise as a rare event where PSSA got localized without being uniformly dispersed during spreading. The other important point of this circuit analysis is the fact that the thicknesses of the end units are of microscopic dimensions (see Table VII). Whether these dimensions and the values derived for the characteristics of the middle units (i.e., R_k and C_k values) are real or not is difficult to prove. In any case, all the layer-type membranes including the highly complex membrane ADFGH can be described qualitatively by the series equivalent circuit of Fig. 3.

The situation with respect to the sandwich-type membrane is less complex than that with respect to the layer type. This is because during the formation of the sandwich type, the two simple membranes retain their individual characteristics to a large extent when they become part of the composite structure. The sandwich type therefore can be depicted with some degree of certainty by the circuit of Fig. 3. Using the same assumptions and approximations given above, values for R_k and C_k of the middle unit formed from high and low charge density membranes can be derived from the data given at the bottom of Table IV. When values of R_H, R_L, C_H, and C_L (H = high and L = low charge density membrane) corresponding to membrane thickness of 0.06 mm are used in equations 9 and 10, positive values of 1.2 and 4.2 are obtained for the factors $[R_k/(1 + \omega^2 R_k^2 C_k^2)]$ and $[(\omega R_k^2 C_k)/$

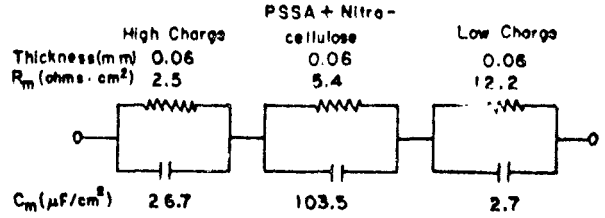

FIGURE 5 The equivalent electrical circuit for a sandwich-type composite membrane.

$(1 + \omega^2 R_k^2 C_k^2)]$. Solving these gives 15.8 ohms and 35.2 μF for R_k and C_k respectively. The value of R_k is intermediate between the values of R_H (7.5 ohms) and R_L (36 ohms), whereas the value of C_k is very high compared to the values of C_H (9.1 μF) and C_L (0.91 μF). This high value as discussed already is because of the presence of a high proportion of PSSA. Consequently the sandwich-type membrane can be represented quantitatively by the circuit of Fig. 5.

In essence then, when sandwich-type membranes are formed from simple membranes of high and low charge density, an extra unit is formed in the middle at the expense of the end units. These end units have their thicknesses reduced but retain their essential resistance and capacitance characteristics. In the case of the layer-type membranes also, a similar phenomenon happens, but the end units have their thicknesses reduced to microscopic dimensions. In either case the impedance is intermediate between the impedances of the high and low charge density simple membranes existing at the two ends of the composite structure; however, in this study, an exception is found in the case of the membrane AD.

This work has been supported by U. S. Public Health Service grant NB-08163.

Received for publication 12 May 1970 and in revised form 22 October 1970.

REFERENCES

ADELMAN, W. J., JR., and J. P. SENFT. 1966. *J. Gen. Physiol.* **50**:279.
ADELMAN, W. J., JR., and J. P. SENFT. 1968. *J. Gen. Physiol.* **51**(5, Pt. 2):102S.
ARMSTRONG, C. W. 1966. *J. Gen. Physiol.* **50**:491.
ARMSTRONG, C. W., and L. BINSTOCK. 1965. *J. Gen. Physiol.* **48**:859.
BOTRE, C., S. BORGHI, and M. MARCHETTI. 1967. *Biochim. Biophys. Acta.* **135**:162.
CHANDLER, W. K., and H. MEVES. 1965. *J. Physiol. (London).* **180**:788.
DE KOROSY, F. 1968. *J. Phys. Chem.* **72**:2591.
DIBONA, D. R., M. M. CIVAN, and A. LEAF. 1969. *J. Membrane Biol.* **1**:79.
HAYS, R. M. 1968. *J. Gen. Physiol.* **51**:385.
KEDEM, O., and A. KATCHALSKY. 1963 *a. Trans. Faraday Soc.* **59**:1918.
KEDEM, O., and A. KATCHALSKY. 1963 *b. Trans. Faraday Soc.* **59**:1931.
KEDEM, O., and A. KATCHALSKY. 1963 *c. Trans. Faraday Soc.* **59**:1941.
LAKSHMINARAYANAIAH, N. 1965. *Chem. Rev.* **65**:491.
LAKSHMINARAYANAIAH, N. 1969 *a.* Transport Phenomena in Membranes. Academic Press, Inc., New York. 363.

LAKSHMINARAYANAIAH, N. 1969 *b*. Transport Phenomena in Membranes. Academic Press, Inc., New York 10, 129, 224, 414.
LAKSHMINARAYANAIAH, N., and K. R. BRENNEN. 1966. *Electrochim. Acta.* **11**:949.
LAKSHMINARAYANAIAH, N., and A. M. SHANES. 1965. *J. Appl. Polym. Sci.* **9**:689.
LAKSHMINARAYANAIAH, N., and F. A. SIDDIQI. 1970. *J. Polym. Sci.* **8**(Pt. A-1):2949.
LAKSHMINARAYANAIAH, N., and F. A. SIDDIQI. 1971. *Biophys. J.* **11**:617.
LAKSHMINARAYANAIAH, N., and V. SUBRAHMANYAN. 1964. *J. Polym. Sci.* (Pt. A) **2**:4491.
LAKSHMINARAYANAIAH, N., and V. SUBRAHMANYAN. 1968. *J. Phys. Chem.* **72**:4314.
LIQUORI, A. M., and C. BOTRE. 1964. *Ric. Sci.* **34**(6):71.
LIQUORI, A. M., and C. BOTRE. 1967. *J. Phys. Chem.* **71**:3765.
LIQUORI, A. M., L. CONSTANTINO, and G. SEGRE. 1966. *Ric. Sci.* **36**:591.
MUELLER, P., D. O. RUDIN, H. TI TIEN, and W. C. WESCOTT. 1962 *a*. *Nature* (*London*). **194**:979.
MUELLER, P., D. O. RUDIN, H. TI TIEN, and W. C. WESCOTT. 1962 *b*. *Circulation*. **26**:1167.
NAKAMURA, Y., S. NAKAJIMA, and H. GRUNDFEST. 1965. *J. Gen. Physiol.* **48**:985.
NARAHASHI, T., N. C. ANDERSON, and J. W. MOORE. 1966. *Science* (*Washington*). **153**:765.
NARAHASHI, T., J. W. MOORE, and W. R. SCOTT. 1964. *J. Gen. Physiol.* **47**:965.
NEIHOF, R. 1954. *J. Phys. Chem.* **58**:916.
PICKARD, W. F., J. Y. LETTVIN, J. W. MOORE, M. TAKATA, J. POOLER, and T. BERNSTEIN. 1964. *Proc. Nat. Acad. Sci. U. S. A.* **52**:1177.
REHM, W. S. 1966. *Ann. N. Y. Acad. Sci.* **137**:591.
TASAKI, I., and S. HAGIWARA. 1957. *J. Gen. Physiol.* **40**:859.
USSING, H. H. 1966. *Ann. N. Y. Acad. Sci.* **137**:543.

STUDIES WITH COMPOSITE MEMBRANES

II. Measurement of Asymmetric Properties

N. LAKSHMINARAYANAIAH *and* YASIH A. SIDDIQI

Reprinted from the Biophysical Journal, 1971, Vol. 11, No. 7, pp. 617–628 *Printed in U.S.A.*

STUDIES WITH COMPOSITE MEMBRANES

II. MEASUREMENT OF ASYMMETRIC PROPERTIES

N. LAKSHMINARAYANAIAH *and* FASIH A. SIDDIQI

From the Department of Pharmacology, School of Medicine, University of Pennsylvania, Philadelphia, Pennsylvania 19104.

ABSTRACT Electrical potentials arising across composite membranes when they separate the same concentration of a (1:1) electrolyte or electrolytes have been measured. These potentials have been shown to arise from differences in the transport number of counterions contacting the two faces of the membrane which contained in its body a high concentration of electrolyte and polyelectrolyte. When the concentration of this trapped electrolyte or polyelectrolyte is low, the asymmetry potentials are small. Although measurements of current-voltage relations provided evidence for the existence of asymmetry between the two faces of the membrane, osmotic flow of water in either direction across the membrane and the salt flow in the two directions were symmetrical. These solvent and solute flux measurements lasted more than 30 hr. Short-term (about 4 hr) flux measurements, however, using tritiated water (THO), gave flows which were different in the two directions. Similarly, the salt flows measured using ^{22}Na isotope were different in the two directions. The usefulness of the present system as a model to use for studies concerned with carrier transport problems in biology has been pointed out.

INTRODUCTION

Composite membranes have been prepared from collodion and polystyrenesulfonic acid (PSSA) by Liquori and Botre (1964, 1967). These membranes have been used by Botre et al. (1967) to simulate bioelectrical potentials observed across the squid nerve membrane. Liquori (1968) has suggested that the difference in the selectivities of the two faces of the biological membrane may form the basis for sustaining the resting potential of the living cell. This simple physicochemical proposal has been inspired by the fact that a composite membrane containing a polyelectrolyte (sulfonated polystyrene) trapped between membrane layers of increasing charge density, generated an asymmetry potential when the same concentration of an electrolyte solution was placed on either side of it. De Korosy (1968) also observed similar asymmetry potentials across his own composite membranes, but he showed that the potentials were of a temporary nature. The results of our

studies pertaining to asymmetry potentials and other transport properties of composite membranes are presented in this part.

EXPERIMENTAL

The preparation of simple and composite membranes, layer as well as sandwich types, was according to the procedures given in Part I (Lakshminarayanaiah and Siddiqi, 1971 *b*). Some membranes conforming to the specifications of Liquori and Botre (1964, 1967) were also prepared.

Membrane pieces (~2.5 cm squares) were converted into the Na form by immersing them in about 200 ml of a strong solution (2–3 N) of NaCl. They were kept gently stirred for a few hours, and left there for future use. A few pieces when required were taken out, thoroughly washed with deionized water, and equilibrated for 2 hr with gentle stirring in about 100 ml of the NaCl solution to be used in the experiment. The solution was changed frequently during equilibration.

Asymmetry, biionic, and concentration potentials arising across simple and composite membranes were measured using an electrochemical cell of the type described in Part I (Lakshminarayanaiah and Siddiqi, 1971 *b*).

The membrane current (i) and voltage (V) relations were determined using an H-cell. The membrane bisected this cell into two halves, each of which contained the same electrolyte solution and two reversible Ag-AgCl electrodes. Two of these electrodes, one on each side of the membrane, were placed a few centimeters away from the membrane. The other two were placed close to the membrane faces. A constant current (determined from measured iR drop across a known resistor) from a constant current supply was passed through the membrane using the two distant electrodes. As a consequence, a change in membrane potential occurred, and this change was measured on a microvoltmeter connected to the two near electrodes. All these experiments were carried out at room temperature (air-conditioned).

Osmotic water flow in either direction was measured using the cell described in our earlier publication (Lakshminarayanaiah, 1967). 0.5 N NaCl solution on one side and deionized water on the other side of the membrane were used. The assembly was kept in a water thermostat at 25 ±0.01°C. The flow of water was followed on a cathetometer with time. At the end of the experiment which lasted at least 30 hr, the salt content of the water compartment was estimated on a Perkin-Elmer Atomic Absorption Spectrophotometer (Perkin-Elmer Corp., Instrument Div., Norwalk, Conn.).

RESULTS AND DISCUSSION

No asymmetry potential E_0, i.e. potential when the same electrolyte of the same concentration was placed on either side of the membrane, was observed across simple membranes of high or low charge density. Under similar conditions, composite membranes, both layer and sandwich types, gave potentials (high charge density side taken positive) shown in Fig. 1. Immediately on assembling the whole cell, the value for E_0 was noted (i.e., 2–3 min after mounting the membrane) and followed with time for 1–2 hr. The change in E_0 during this period was within ±8% of the initial value. Each point in Fig. 1 represents the mean of the initial values observed with at least four different membranes which were screened to keep the variability of the asymmetry potentials within ±10%. The values ob-

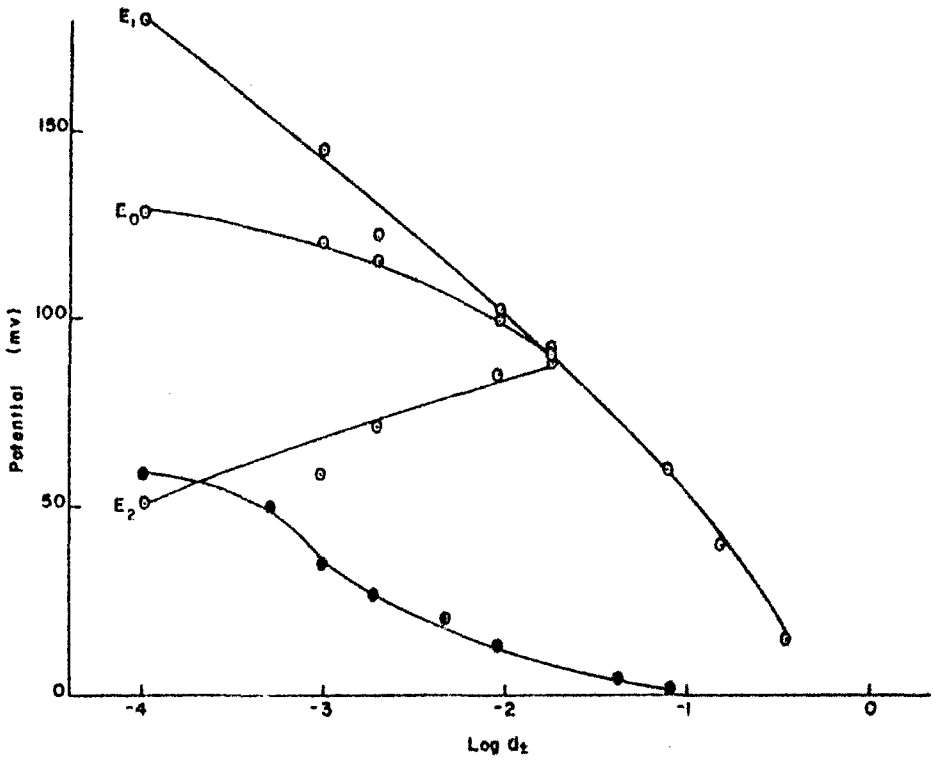

FIGURE 1 Electrical potentials arising across a composite membrane when it separates the same or different concentrations of NaCl, plotted against the activity of the external solution. ⊙ refers to layer-type composite membranes. E_0 refers to asymmetry potentials, i.e., potentials when the same concentration of NaCl is placed on both sides of the membrane. E_1 refers to concentration potentials with 0.02 N NaCl solution on one side of the membrane (low charge density side) and the concentration on the high charge density side is varied. E_2 refers again to concentration potentials when the concentration gradient is reversed. ● refers to asymmetry potentials arising across sandwich-type membrane.

served for E_0 across sandwich-type membranes are lower than those observed across layer types. The possible reason as to why this is so is discussed later.

The concentration potentials, i.e. potentials arising across the layer-type membranes when different concentrations of the same electrolyte solution are placed on one side keeping the concentration of the electrolyte on the other side constant, and vice versa, are also given in Fig. 1. The values of the potential are high when the electrolyte solution gradient is acting in the same direction as the asymmetry potential, whereas the values are low when the gradient is opposing the asymmetry potential. In either case, however, it is found (see Table I) that the observed value for any given concentration ratio does not agree with the value calculated (i.e., $E_0 \pm E_{max}$) by the algebraic addition of the theoretical concentration potential

TABLE I

ELECTRICAL POTENTIALS OBSERVED ACROSS A LAYER-TYPE MEMBRANE WHEN A CONCENTRATION POTENTIAL ACTS EITHER TO REINFORCE OR TO OPPOSE THE ASYMMETRY POTENTIAL

Electrolyte concn C_2 held constant	Electrolyte concn C_1 varied	Concn potential $E_{max} = \frac{RT}{F} \ln \frac{a_2}{a_1}$	Asymmetry potential E_0, C_1 on both sides	Concn potential (observed) with E_0		Concn potential (calculated)	
				Reinforcing	Opposing	$E_0 + E_{max}$	$E_0 - E_{max}$
eq/liter	*eq/liter*	*mv*	*mv*	*mv*	*mv*	*mv*	*mv*
0.02	0.0001	130.0	128	180	51.5	258	−2.0
0.02	0.001	72.6	120	145	59.0	193	47.4
0.02	0.002	55.4	115	122	71.5	170	59.6
0.02	0.01	16.5	102	100	85.0	119	85.5
0.02	0.02	0	90	87	91.0	90	90.0

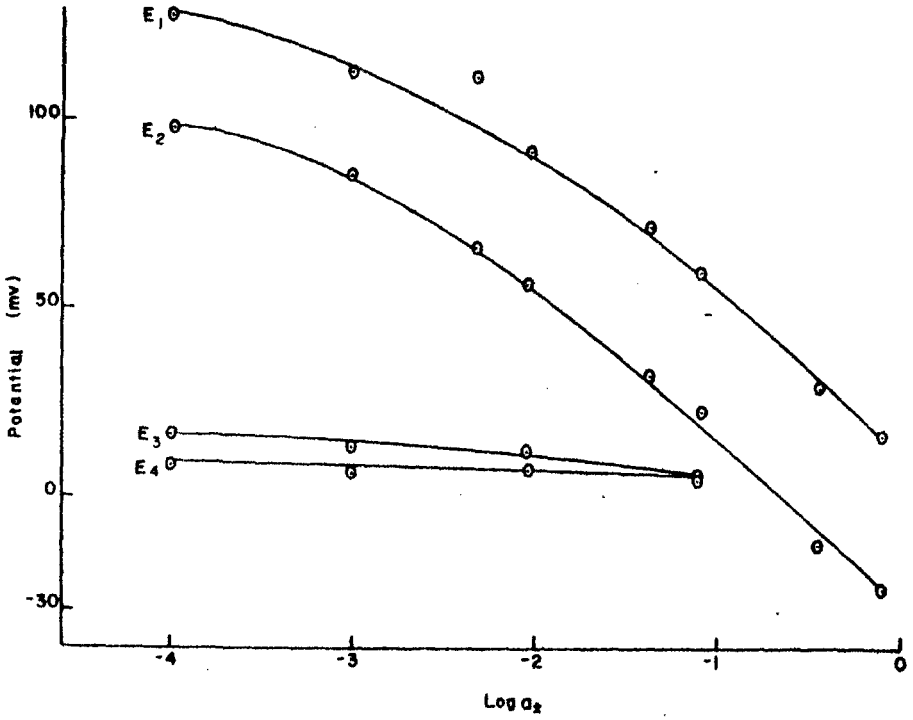

FIGURE 2 Biionic potentials observed across layer-type composite membranes when they separate the same concentration of NaCl and KCl solutions, plotted as a function of the activity of the external NaCl solution. E_1 refers to potentials when KCl solution is in contact with high charge density side and E_2 refers to potentials when KCl and NaCl are interchanged. E_3 and E_4 refer to biionic potentials observed across simple high charge and low charge density membranes.

E_{max}, viz. $E_{max} = (RT/F) \ln (a_2/a_1)$, where a_2 is the constant activity of the solution 2, and a_1 is the activity of the solution 1 which is varied, and the observed asymmetry potential E_0. An exception exists in the case $(C_2/C_1) = 2$ where the concentration gradient is opposing the asymmetry potential. In all the other cases, the discrepancy noted reflects the fact that the *composite membrane as a whole* generates low concentration potentials and thus has low permselectivity to the Na^+ ions.

The results of asymmetry po' ntials across composite membranes which were prepared according to the formula of Liquori and Botre (1964, 1967) followed the same pattern of behavior shown in Fig. 1; but the actual values, in the case of layer type, were lower, and in the case of sandwich type, a little higher, than those shown in Fig. 1.

The biionic potentials generated when layer-type membranes separa' 'd NaCl and KCl solutions of the same concentration are shown in Fig. 2. The E_1 curve shows the variation of biionic potential as a function of the activity of the outside NaCl solution when KCl solution is in contact with the high charge density side of the membrane. The potentials are reduced a little (i.e., E_2 curve) when the solutions are interchanged allowing NaCl to contact the high charge density surface. In the same figure appear also the biionic potentials (E_3 and E_4 curves) observed across simple high and low charge density membranes. These potentials are very low compared to those observed across layer-type membranes.

The basis for the existence of asymmetry potential across a composite membrane has been explored by Liquori and Botre (1964) from the standpoint of the concepts of the theory of membrane potential developed by Teorell (1935 *a*, *b*), and Meyer and Sievers (1936 *a*, *b*, *c*). They showed that the asymmetry potential arose as a result of the differences in the Donnan and diffusion potentials existing at the two asymmetric faces of the membrane. Later "a simple straightforward explanation" was given in terms of the model system shown in Fig. 3 (Liquori and Botre, 1967). The model system was composed of two simple membranes M_H and M_L which contained respectively high and low concentrations of fixed negative

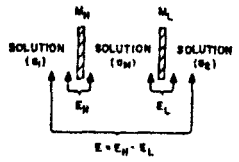

FIGURE 3 The model system for the composite membrane. M_H and M_L are simple membranes of high charge (PSSA = 2.5 mg/ml) and low charge (PSSA = 0.025 mg/ml) density separating three solutions of the same electrolyte of activity a_1, a_M, and a_2 contained in the three compartments. E_H is the concentration potential arising across the membrane M_H, and E_L is the concentration potential arising across the membrane M_L. E is the potential acting across the whole cell.

groups. The membranes were assembled in series to form a three-chambered cell. The middle chamber, which represented the interior of the composite membrane, contained a known concentration of the electrolyte (e.g., NaCl) solution. In the two outer compartments, NaCl solution of the same or different concentration was placed to measure asymmetry and/or concentration potentials across the whole membrane system.

In terms of the model system, the asymmetry potential is given by the algebraic sum of the membrane potentials which exist across the two simple membranes M_H and M_L. The membrane potential across M_H (i.e., E_{H_0}) is given by (Lakshminarayanaiah, 1969)

$$E_{H_0} = \frac{RT}{F}(2\bar{I}_{+(H)} - 1) \ln \frac{a_M}{a_1}. \quad (1)$$

Similarly the membrane potential E_{L_0} across M_L is given by

$$E_{L_0} = \frac{RT}{F}(2\bar{I}_{+(L)} - 1) \ln \frac{a_M}{a_2}, \quad (2)$$

where $\bar{I}_{+(H)}$ and $\bar{I}_{+(L)}$ are the transport numbers of counterions in membranes M_H and M_L respectively. a_1 and a_2 are the activities of the two solutions in the outer compartments. a_M is the activity of the solution used in the middle compartment. The net potential E across the composite membrane system (Fig. 3) is given by

$$E = E_{H_0} - E_{L_0} = \frac{RT}{F}\left[(2\bar{I}_{+(H)} - 1) \ln \frac{a_M}{a_1} - (2\bar{I}_{+(L)} - 1) \ln \frac{a_M}{a_2}\right]. \quad (3)$$

When $a_1 = a_2 = a$, the asymmetry potential E_0 is given by

$$E_0 = E_{H_0} - E_{L_0} = \frac{2RT}{F}[\bar{I}_{+(H)} - \bar{I}_{+(L)}] \ln \frac{a_M}{a}. \quad (4)$$

When $a_M = 0.35$ (i.e., $C_M = 0.5$ N NaCl solution), E_{H_0}, E_{L_0} and E_0 have been measured using a high charge density membrane (collodion containing 2.5 mg/ml of PSSA) and a low charge density membrane (collodion containing 0.025 mg/ml of PSSA) as a function of the activity of the external NaCl solution (see Fig. 4). Similarly values for E_0 when $a_M = 0.08$ (i.e., 0.1 N) and 0.009 (i.e., 0.01 N) have been determined also and are given in the same figure.

The data given in Fig. 4 show that the algebraic addition of the values of E_{H_0} and E_{L_0} agree with the values given for the curve E_0 (i.e., for 0.5 N NaCl). At other values of a_M similar agreement was obtained (values not given). So it is inferred that equations 1, 2, and 4 are valid for the model system. For the case when $a_1 \neq a_2$, equation 3 has been assumed to be valid. This is based on the fact that the values of E_1 or E_2 (see Fig. 4) measured across the whole membrane system were found to

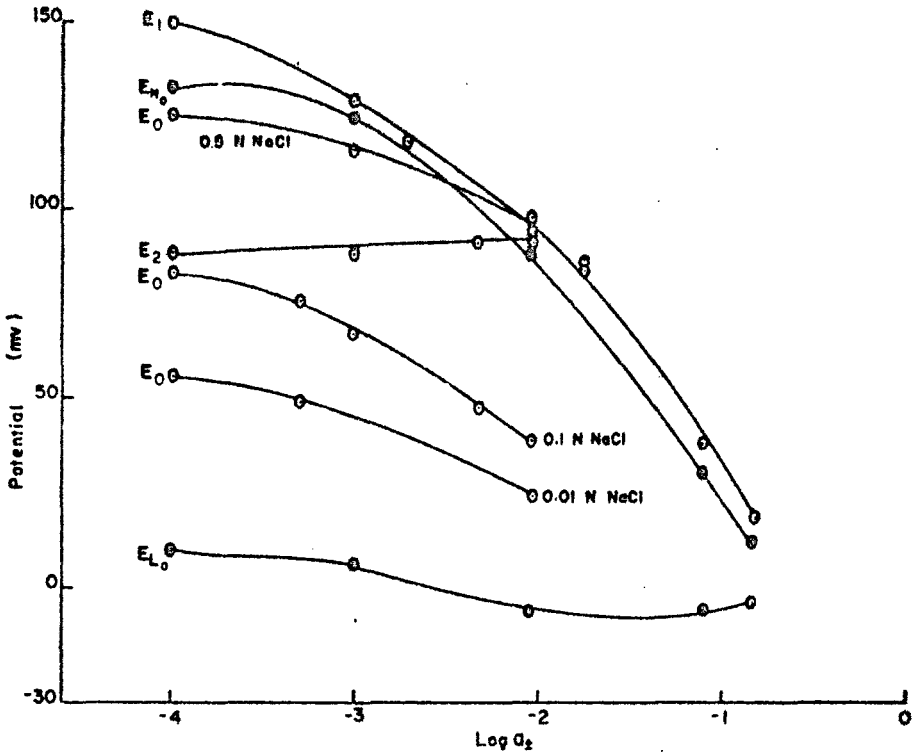

FIGURE 4 Electrical potentials arising across the model membrane system of Fig. 3, plotted as a function of the activity of the external NaCl solution. E_0's refer to the asymmetry potentials (i.e., $a_1 = a_2$) measured across the complete cell when the middle chamber contained 0.5, 0.1, and 0.01 N NaCl solution (values of a_M are 0.35, 0.079, and 0.009). E_{H_0} and E_{L_0} are the concentration potentials observed across simple membranes M_H and M_L when they separated 0.5 N NaCl solution on one side (middle chamber) and the other NaCl solution whose concentration is varied on the other side. Algebraic addition of E_{H_0} and E_{L_0} gave E_0 (0.5 N NaCl solution in the middle chamber). E_1 refers to the concentration potentials measured across the complete membrane cell when the middle compartment contained 0.5 N NaCl solution and compartment 2 contained 0.02 N NaCl solution and compartment 1 contained NaCl solution whose concentration is varied. E_2 refers to concentration potentials when the concentration gradient is reversed.

be equal to the values obtained by the algebraic addition of the potentials measured across the simple membranes M_H and M_L (these values not given). The measured values of E_1 in Fig. 4 correspond to the case when the concentration potential was acting in the same direction as the asymmetry potential. The measured values of E_2 pertain to the other case when the concentration potential opposed the asymmetry potential. The results of Fig. 4 simulate those observed across layer-type composite membranes (see Fig. 1). Equations 1–4 thus could be applied to explain the results of Fig. 1. To do this, one should know the values for a_M, $t_{+(H)}$, and $t_{+(L)}$ for the layer-type membrane. Values for $t_{+(H)}$ and $t_{+(L)}$ can be calculated from the

values of E_{H_0} and E_{L_0} (see Fig. 4) using equations 1 and 2. These results are given in Table II. Assuming that these values are appropriate for the two sides of the composite membrane, values for the asymmetry potential can be calculated from equation 4 substituting different values for a_M. Only for a value of 0.4 for a_M (i.e., concentration $\approx$0.6 N), results agreeing with the experimental values for the asymmetry potential in the region of low concentration are obtained (see Table III). At higher concentrations, the calculated values are lower than the observed values. This discrepancy could arise from (*a*) the actual values of $[\bar{t}_{+(H)} - \bar{t}_{+(L)}]$ being different from those used in the calculations, and (*b*) the value substituted for a_M in the calculations being too low. A simple calculation using equation 4 shows that the value for $[\bar{t}_{+(H)} - \bar{t}_{+(L)}]$ must be 0.77 for the solutions 0.5/0.1 N or 0.98 for the solutions 0.5/0.2 N to obtain agreement between calculated and observed

TABLE II

VALUES OF TRANSPORT NUMBER FOR HIGH AND LOW CHARGE DENSITY MEMBRANES M_H AND M_L CALCULATED FROM EQUATIONS 1 AND 2 WHEN 0.5 N NaCl SOLUTION IS KEPT IN THE MIDDLE COMPARTMENT

NaCl solution on two sides	$\bar{t}_{+(H)}$	$\bar{t}_{+(L)}$	$[\bar{t}_{+(H)} - \bar{t}_{+(L)}]$
eq/liter			
0.0001	0.82	0.52	0.30
0.001	0.91	0.52	0.39
0.002	0.92	0.50	0.42
0.01	0.97	0.46	0.51
0.02	0.96	0.46	0.50
0.10	0.85	0.45	0.40
0.20	0.77	0.36	0.41

TABLE III

ASYMMETRY POTENTIALS ACROSS LAYER-TYPE COMPOSITE MEMBRANES

NaCl solution on two sides	E_0 (observed)	E_0 (calculated)
eq/liter	*mv*	*mv*
0.0001	128	128
0.001	120	121
0.002	115	116
0.01	102	99.5
0.02	90.0	80.4
0.1	64.2	33.5
0.2	49.8	21.0

asymmetry potentials. These values for the term $|\bar{I}_{+(R)} - \bar{I}_{+(L)}|$ are too high to be true. Therefore, factor b may be responsible for the discrepancy. That this is so is apparent from the nature of the function log (a_M/a) of equation 4. In dilute solutions (e.g., $a = 0.002$ N) the value of log (a_M/a) changes little ($< 10\%$) for a given change in the value of a_M (say from 0.6 to 0.4 N) compared with a similar change ($> 30\%$) in the value of the function log (a_M/a) for the same change in a_M in strong solutions (e.g., $a = 0.2$ N).

The asymmetry potentials across sandwich-type membranes (see Fig. 1), unlike similar potentials observed by Liquori and Botre (see their Fig. 3, 1967), are low. We experienced considerable difficulty in preparing these membranes. Deposition of PSSA between M_R and M_L membranes always gave good sandwich membranes, which, when equilibrated with solutions, separated into the two membranes M_R and M_L. The results presented in Fig. 1 refer to those sandwich membranes which remained intact after repeated equilibrations with the electrolyte solutions. In Fig. 4 are given the values of E_0 realized with the three-chamber model system when 0.1 or 0.01 N NaCl solution was used in the middle chamber. Comparison of these different values of E_0 with those given in Fig. 1 for the sandwich type indicates a value of about 0.009 for a_M. It is apparent therefore that the magnitude of the asymmetry potential is controlled by the amount of electrolyte and polyelectrolyte trapped in the body of the composite membrane.

The results of biionic potentials (see Fig. 2) can be explained also in terms of equation 4. The transport numbers now correspond to the cations Na^+ and K^+ contacting the two membrane faces. As the membrane exhibits little discrimination between Na^+ and K^+ ions (see curves E_3 and E_4 of Fig. 2), the potential arising on that account is absent and all the observed potential therefore becomes attributable to the terms a_M and $|\bar{I}_{+(R)} - \bar{I}_{+(L)}|$.

The asymmetry potentials existing across layer-type membranes should exert some influence on the flow of charged species through them. To investigate this, current-voltage relations have been determined and these results are shown in Fig. 5. There is more current flowing through the membrane in one direction (positive current towards the high charge density side) than there is in the reverse direction. Because of the presence of more charges in the membrane when it is in contact with a stronger solution (i.e., 10^{-2} N compared with 10^{-4} N solution), more current is carried across the membrane. Similar experiments performed with simple membranes of high and low charge densities gave i-V relationships which were linear and nonrectifying. The values for the resistances derived from the slopes of the straight lines were 2.2×10^5, 6.8×10^5 ohms for high charge density membrane, and 9.6×10^7, 3.3×10^7 ohms for low charge density membrane when they were in contact with 10^{-4} and 10^{-2} N NaCl solutions respectively. The membrane area involved was 2.84 cm^2. The corresponding resistance values for the composite membrane were 2.6×10^6 ($-ve$ direction) and 4.8×10^5 ohms ($+ve$ direction) for 10^{-4} N solution and 2.0×10^5 and 3.5×10^4 ohms for 10^{-2} N solution. These

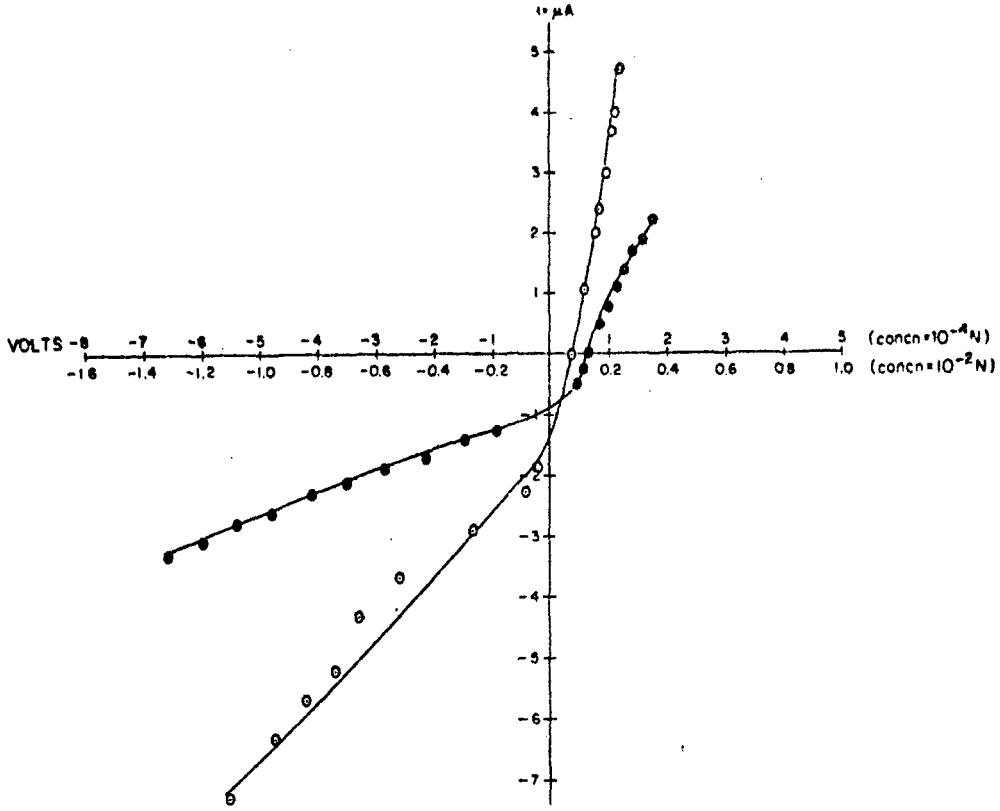

FIGURE 5 A plot of current i (μA) flowing through an area of 2.84 cm² layer-type membrane against voltage V (Volts) when there was 10^{-4} (●) and 10^{-2} N (⊙) NaCl solution on either side of the membrane.

values refer to the total resistance of the membrane and the solution films existing between the Ag-AgCl electrodes and the membrane faces. Since the solutions used in the measurements were dilute, the resistance of the solution alone was of the same order of magnitude as that due to membrane plus solution films. By this method reliable values for the resistance of the membrane only could not be derived.

Although the flow of current across the composite membrane is different in the two directions, the osmotic flow of water and the diffusional flow of salt, each of these measured in the two directions across the membrane, remained practically the same. The osmotic flow of water (0.5 N NaCl solution on high charge density side) was $(1.10 \pm 0.13) \times 10^{-8}$ ml/hr through 2.84 cm² membrane in one direction and $(0.96 \pm 0.12) \times 10^{-8}$ ml/hr in the reverse direction. The salt flow was 5.4×10^{-9} eq/cm²·hr in one direction and 5.7×10^{-9} eq/cm²·hr in the other direction. The average of these salt fluxes used in the unintegrated form of Fick's equation

(Stewart and Graydon, 1956), viz.,

$$\bar{D}_{app} = \frac{\Delta C V d}{A C_t t}, \qquad (5)$$

(where $\bar{D}_{app}$ = apparent diffusion coefficient of the electrolyte, ΔC = change in concentration on either side of the membrane in time t, V = volume of the solution on the low concentration side, d = membrane thickness, A = membrane area, and C_t = concentration on the high concentration side at the end of time t) gave a value of 1.6×10^{-11} ($cm^2 \cdot sec^{-1}$) for $\bar{D}_{app}$. Thus the diffusion of salt in these composite membranes is very low.

The results pertaining to water and salt flows are not in accord with the facts already considered about the behavior of the composite membranes, i.e., asymmetry potential and current rectification. The experiments carried out to measure significant flows of salt and water lasted more than 30 hr. Recent experiments reported elsewhere (Lakshminarayanaiah and Siddiqi, 1971 *a*) show that the asymmetry potentials when followed over this long period of time decay to low values. This is probably because of some structural change in the membrane. At this stage we do not know definitely what this structural change is. It may be that PSSA migrates from a region of high concentration to a region of low concentration. As a result, it is possible that the asymmetry of the membrane faces is reduced, if not completely destroyed. If this is true, salt flows in either direction will not be unequal. Similarly water flows in the two directions also may not be unequal. In order to obviate this difficulty involved in long-term experiments, we conducted some short-term experiments using suitable isotopes to measure both water and salt flows. THO with NaCl (10^{-2} N) on one side and only 10^{-3} N NaCl solution on the other side of the composite membrane, were used to follow the movement of THO for about 4 hr. The amount of THO that came to the "cold" side in this period of time was small. However, the average of a number of experiments gave the following results: flux of THO with THO on high charge density side = $(9.5 \pm 1.5) \times 10^{-3}$ ml/hr; flux of THO with THO on low charge density side = $(6.5 \pm 1.0) \times 10^{-3}$ ml/hr across 2.84 cm^2 membrane.

^{22}Na in 10^{-2} N NaCl solution was used to follow the salt flux. In this case also there was a small increase in the activity on the cold side. A number of experiments performed in 4-hr periods gave the following values: flux of salt with ^{22}Na on low charge density side = $(7.4 \pm 1.0) \times 10^{-9}$ eq/$cm^2 \cdot$hr; flux of salt with ^{22}Na on high charge density side = $(5.0 \pm 0.7) \times 10^{-9}$ eq/$cm^2 \cdot$hr. There is a definite trend towards rectification of water and salt flows, although the magnitude of the difference between the flows in the two directions is not as high as the initial membrane asymmetry demands.

The relevance of these studies to the behavior of the biological membrane may not be obvious. The composite membranes mimic none of the physical charac-

teristics of the living membrane, whereas in terms of function they show some resemblance, because of the asymmetry of the two faces, in generating asymmetry potentials when the same electrolyte concentration is placed on either side. This aspect has been well demonstrated by Botre et al. (1967) who were able to reproduce with the composite membrane the resting potentials observed across the squid axon membrane. Similar work performed with our membranes gave unsatisfactory results. The reasons for this are being investigated.

The present model seems to be an improvement over other models of the type, for example, ion exchange membranes, liquid ion exchangers, phospholipids deposited on Millipore filters, etc. (Lakshminarayanaiah, 1965). The distinct advantage of the present model is the fact that one can incorporate either into the body of the composite membrane or into the middle chamber of the three-compartment cell (Fig. 3) various enzymes or other carriers and investigate the properties of these carriers. The model could be improved by using membranes containing carboxylic, phosphate, or amino groups in place of M_H and M_L membranes, maintaining an asymmetry not only in regard to charge density but also in regard to the nature of the group. Although the biological membrane is known to contain phosphate, carboxylic, and amino groups, how they are distributed between the inner and outer surfaces of the membrane is unknown. An insight into this group distribution may be possible with the present model by measuring asymmetry potentials using membranes containing phosphate, carboxylic, and amino groups in different combinations. Studies of this type are in progress.

This work has been supported by U.S. Public Health Service grant NB-08163.

Received for publication 12 May 1970 and in revised form 22 October 1970.

REFERENCES

BOTRE, C., S. BORGHI, and M. MARCHETTI. 1967. *Biochim. Biophys. Acta.* 135:162.
DE KOROSY, F. 1968. *J. Phys. Chem.* 72:2591.
LAKSHMINARAYANAIAH, N. 1965. *Chem. Rev.* 65:554.
LAKSHMINARAYANAIAH, N. 1967. *J. Appl. Polym. Sci.* 11:1737.
LAKSHMINARAYANAIAH, N. 1969. Transport Phenomena in Membranes. Academic Press, Inc., New York. 199.
LAKSHMINARAYANAIAH, N., and F. A. SIDDIQI. 1971 *a. In* Membrane Processes in Industry and Biomedicine. M. Bier, editor. Plenum Publishing Corporation, New York. 301.
LAKSHMINARAYANAIAH, N., and F. A. SIDDIQI. 1971 *b. Biophys. J.* 11:603.
LIQUORI, A. M. 1968. *Farm. Ed. Sci.* 23:999.
LIQUORI, A. M., and C. BOTRE. 1964. *Ric. Sci.* 34(6):71.
LIQUORI, A. M., and C. BOTRE. 1967. *J. Phys. Chem.* 71:3765.
MEYER, K. H., and J. F. SIEVERS. 1936 *a. Helv. Chim. Acta.* 19:649.
MEYER, K. H., and J. F. SIEVERS, 1936 *b. Helv. Chim. Acta.* 19:665.
MEYER, K. H., and J. F. SIEVERS. 1936 *c. Helv. Chim. Acta.* 19:987.
STEWART, R. J., and W. F. GRAYDON. 1956. *J. Phys. Chem.* 60:750.
TEORELL, T. 1935 *a. Proc. Soc. Exp. Biol. Med.* 33:282.
TEORELL, T. 1935 *b. Proc. Nat. Acad. Sci. U. S. A.* 21:152.

STUDIES WITH COMPOSITE MEMBRANES

III. Measurement of Water Permeability

N. LAKSHMINARAYANAIAH *and* FASIH A. SIDDIQI

From the Department of Pharmacology, School of Medicine, University of Pennsylvania, Philadelphia, Pennsylvania 19104

BIOPHYSICAL JOURNAL VOLUME 12 1972

STUDIES WITH COMPOSITE MEMBRANES

III. Measurement of Water Permeability

N. LAKSHMINARAYANAIAH *and* FASIH A. SIDDIQI

From the Department of Pharmacology, School of Medicine, University of Pennsylvania, Philadelphia, Pennsylvania 19104

ABSTRACT The permeability of tritiated water (THO) across simple and layer-type composite membranes of collodion containing different amounts of polystyrenesulfonic acid has been measured and corrected for the effects of aqueous stationary layers present at the membrane-solution interfaces. It was found that the water permeabilities in the two opposite directions across the composite membranes were different, whereas they were the same across simple membranes. The theoretical permeability value for the composite membrane (formed by putting one simple membrane on top of another simple membrane of increasing charge density and gently pressing them together), calculated from the values due to simple membranes, was found to be always greater than the two measured values. It was shown that the aqueous layers trapped between membranes were not responsible for the low measured values. The factor causing this was ascribed to the mechanism which produced rectification of water flow in the composite membranes. Establishment of the THO concentration profile in the layered membranes showed that accumulation and depletion of THO in the membrane phase when the THO was flowing from the high charge density side to the low charge density side and vice versa, respectively, were responsible for the unequal flows observed across the composite membrane in the two directions.

INTRODUCTION

In part I in this series (Lakshminarayanaiah and Siddiqi, 1971 *a*), the preparation of simple and composite membranes of collodion containing polystyrenesulfonic acid and their impedances, and in part II (Lakshminarayanaiah and Siddiqi, 1971 *b*), some of the asymmetric properties of the layer-type composite membranes, have been described. Some preliminary values for the transport of salt and water across them given in part II showed that the magnitude of each of these flows in the opposite directions was different. A detailed report of the flow of THO in simple and in layer-type composite membranes is presented in this paper.

EXPERIMENTAL

The preparation of simple and layer-type composite membranes was carried out according to the procedures given in part I (Lakshminarayanaiah and Siddiqi, 1971 *a*). The composite

membranes used in this study were the same as those used in the earlier study described in Part II (Lakshminarayanaiah and Siddiqi, 1971 *b*). The concentrations of various membrane-forming solutions used in the preparation of both simple and composite membranes are given at the bottom of Table I.

Membrane pieces (~3 cm square) were converted into the Na form by immersing them in about 100 ml of 1 N NaCl solution in which they were left for future use. When they were required, a few pieces were taken out, gently stirred with deionized water with frequent changes of liquid for about 2 hr, equilibrated for 2–3 hr in about 100 ml of 0.001 N NaCl solution which also was changed often, and finally used in the experiments to be performed.

TABLE I

THO PERMEABILITY DATA FOR DIFFERENT SIMPLE MEMBRANE SYSTEMS

Membrane*	Single membrane permeability $P_s \times 10^6$ (equation 2)	Double membrane permeability $P_d \times 10^6$ (equation 2)	True membrane permeability $P_t \times 10^6$ (equation 5)	Stagnant layer thickness δ (equation 6)
	cm/sec	*cm/sec*	*cm/sec*	μ
M_1	352.00 ± 10.00‡	182.00 ±5.00‡	377.00	23
M_2	10.72 ± 0.30	5.41 ±0.16	10.92	210
M_3	5.48 ± 0.20	2.80 ±0.10	5.73	955
M_4	5.34 ± 0.20	2.75 ±0.10	5.66	1330
M_5	5.11 ± 0.20	2.60 ±0.10	5.30	828

* Membranes formed from 2% collodion solution (alcohol/ether ratio = 3/1) containing 2.91 (M_1), 0.41 (M_2), 0.10 (M_3), 0.04 (M_4), and 0.004 (M_5) mg of polystyrenesulfonic acid/ml of membrane-forming solution. Thickness of each single membrane = 0.002 cm.

‡ The mean and one standard error of the mean of 10–15 values derived from at least three membranes.

The cell used in the measurement of permeability of THO was of the type described elsewhere (Lakshminarayanaiah, 1967 *a*, *b*). The area of the membrane exposed to the "hot" (0.001 N NaCl solution containing THO on one side) and "cold" (0.001 N NaCl solution on the other side) solutions was 5.0 cm^2. The volume of each of the two chambers holding the membrane between two rubber gaskets was about 40 ml and contained exactly 35 ml of the hot or cold solution. Magnetic stirrers (size: length = 2.5 cm, diameter = 1.1 cm) were used in the two chambers and were kept rotating close to the membrane faces. The rate of rotation (200 rpm) was determined by using a Strobotac, Type 1531 (General Radio Co., Concord, Mass.). The flow of THO was followed by sampling aliquots (exactly 1 ml) of liquid on the cold side at regular intervals of time. The loss in the volume of liquid due to sampling was compensated by adding 1 ml of 0.001 N NaCl solution.

The aliquots taken for counting were transferred into polyethylene vials (capacity of each about 25 ml) to which 20 ml of Bray's solution (Bray, 1960) were added and mixed thoroughly. These were counted in a Packard Tri-Carb liquid scintillation counter (Packard Instrument Co., Inc., Downers Grove, Ill.). All these experiments were performed in an air-conditioned room at 22°C.

RESULTS

The measurement of the flow of THO across the membrane, simple or composite, is quite straightforward provided the stationary aqueous layers at the membrane-solution interfaces are eliminated. This is very difficult to carry out. One could use turbulent flow of solution to eliminate them. Such a technique, however, would require elaborate hardware (Klein et al., 1969). Other methods described in the literature (Lakshminarayanaiah, 1965, 1969 *a*) could be employed to overcome the boundary layer effects which generally lowered the value for the permeability of THO. In recent years a few more methods (Scattergood and Lightfoot, 1968; Hale and Govindan, 1969; Everitt and Haydon, 1969; Everitt et al., 1969; Andreoli and Troutman, 1971) have been described. In this study the method described by Everitt et al. (1969) has been used. This involved making two permeability measurements, one using a piece of the simple membrane and the other using two pieces of the same membrane contacting each other in series ("double" membrane). The apparent permeability P_t for the single and for the double membrane systems was calculated from the equation (Dainty and House, 1966)

$$P_t = \frac{2.303 V_1 V_2}{(V_1 + V_2) A \Delta t} \log \frac{C' V_1 + C'' V_2 - C''_{t_0}(V_1 + V_2)}{C' V_1 + C'' V_2 - C''_{t_0+\Delta t}(V_1 + V_2)}, \qquad (1)$$

where V_1 and V_2 are the volumes of compartments 1 (cold) and 2 (hot). C' and C'' are the initial concentrations (taken as counting rate per milliliter) at time $t = 0$ of radioactive isotope in compartments 1 and 2. C''_{t_0} and $C''_{t_0+\Delta t}$ are the concentrations in compartment 2 at $t = t_0$ and $t = t_0 + \Delta t$ respectively. Δt is thus the time in seconds between samplings. As $V_1 = V_2 = 35$ ml and $A = 5.0$ cm², equation 1 becomes

$$P_t = \frac{8.05}{\Delta t} \log \frac{C'' - 2C''_{t_0}}{C'' - 2C''_{t_0+\Delta t}}. \qquad (2)$$

A plot of log $([C'' - 2\,C''_{t_0}]/[C'' - 2\,C''_{t_0+\Delta t}])$ against time (Δt) gave a straight line (results not shown) whose slope multiplied by 8.05 gave the value for P_t; however in this work P_t was evaluated numerically.

Equation 1 is applicable to the steady state of flow of THO across the membrane. In all the experiments, the diffusion of THO was allowed to go on for about 5 hr. In this period, the radioactivity (counts per minute) accumulating on the cold side followed as a function of time was linear (results not given). The steady-state straight line, in the case of simple membranes, cut the time axis very close to zero and gave a value between 1 and 3 min for the holdup time, whereas in the case of composite membranes, the holdup time was between 10 and 18 min.

The apparent permeability P_t evaluated from equation 2 using a simple membrane has been related to the true membrane permeability P_t by the relation (Kedem and Katchalsky, 1963)

$$\frac{1}{P_s} = \frac{1}{P_t} + \frac{\delta_1 + \delta_2}{D}, \tag{3}$$

where δ_1 and δ_2 are the thicknesses of the stagnant boundary layers existing at the two membrane faces and D is the self-diffusion coefficient of THO whose value has been found to be 2.44×10^{-5} cm^2 sec^{-1} (Wang et al., 1953). Similarly for the double membrane, equation 3 becomes

$$\frac{1}{P_d} = \frac{2}{P_t} + \frac{\delta_1 + \delta_2}{D}, \tag{4}$$

where P_d is the apparent permeability of the double membrane. The value for P_t is given by solving equations 3 and 4. Thus

$$P_t = \frac{P_s \times P_d}{P_s - P_d}. \tag{5}$$

As the hydrodynamic conditions prevailing in the two chambers are almost similar, it is assumed that $\delta_1 = \delta_2 = \delta$. Consequently equations 3 and 4 give

$$\delta = \frac{2P_d - P_s}{P_s P_d} \times \frac{D}{2}. \tag{6}$$

The various measured values of P_s and P_d and the derived values of P_t and δ are given in Table I.

The permeability results pertaining to composite membranes are given in Table II. Two types of composite membrane systems were used in these studies. Type 1 was formed in the usual way (Lakshminarayanaiah and Siddiqi,-1971 *a*) by spreading and drying different membrane-forming solutions of collodion containing varying amounts of polystyrenesulfonic acid one on top of the other. These composite membranes have been designated as M_1M_5 and $M_1M_2M_3M_4M_5$. Type 2 was formed from simple membranes by putting one equilibrated (i.e., wet) membrane, for example M_1, on top of another simple wet membrane, for example M_5, and pressing them together so as to make good physical contact. These have been designated as M_1-M_5, M_1-M_3-M_5, and M_1-M_2-M_3-M_4-M_5. The values of apparent permeability P_s for the composite membrane systems were corrected for the presence of stagnant diffusion layers by using equation 3 and a value of 23 μ for δ_1 (layer in contact with high charge density membrane surface) and a value of 1037 μ (average of the three high values given in the last column of Table I) for δ_2 (layer in contact with low charge density membrane surface). These corrected values which correspond to P_t for the composite membranes are also given in Table II.

In the case of simple membranes M_1 through M_5, the permeability of the membrane was the same whether the flow of THO was in one direction or in the opposite direction. On the other hand, the results given in Table II for the various composite

TABLE II
THO PERMEABILITY DATA FOR THE LAYER-TYPE COMPOSITE MEMBRANE SYSTEMS

Membrane	Direction of THO flow	Apparent permeability $P_a \times 10^4$ (equation 2)	True permeability $P_t \times 10^4$ (equation 3)
		cm/sec	*cm/sec*
M_1M_4*	$M_1 \rightarrow M_4$	8.82 ±0.46	9.17
	$M_4 \rightarrow M_1$	7.49 ±0.38	7.75
M_1-M_4‡	$M_1 \rightarrow M_4$	4.33 ±0.21	4.41
	$M_4 \rightarrow M_1$	3.67 ±0.19	3.72
M_1-M_4-M_4	$M_1 \rightarrow M_4$	1.73 ±0.07	1.74
	$M_4 \rightarrow M_1$	1.55 ±0.06	1.56
$M_1M_2M_3M_4M_4$	$M_1 \rightarrow M_4$	1.53 ±0.05	1.54
	$M_4 \rightarrow M_1$	1.17 ±0.05	1.18
M_1-M_2 M_3-M_4 M_4	$M_1 \rightarrow M_4$	1.40 ±0.06	1.41
	$M_4 \rightarrow M_1$	1.14 ±0.06	1.15

* Membranes designated M_iM_j are formed by spreading and drying different membrane-forming solutions of collodion containing varying amounts of polystyrenesulfonic acid one on top of the other.
‡ Membranes designated M_i-M_j are formed from simple membranes M_i and M_j by putting them one on top of the other and pressing together to make good physical contact. Equilibrated wet membranes are used.

membranes show that the permeabilities in the two opposite directions across the membrane were different. When the THO solution was in contact with the high charge density surface of the composite membrane, the flow observed was higher than that observed in the opposite direction, i.e., when THO solution was contacting the low charge density surface of the membrane. Whether the difference in the values of the two permeabilities observed in the two directions was significant or not was established by carrying out a Student's t test on at least 12 sets of values. In the case of all composite membranes used in these studies (see Table II), the values of t were always greater than 4 and thus the difference in the two permeabilities in the opposite directions for a given composite membrane was significant.

DISCUSSION

The effect of the stationary boundary layers, as pointed out already, is to reduce the value of P_t, the true permeability of the species (THO) flowing through the membrane. The magnitude of the reduction in the value of P_t is determined as discussed elsewhere (Lakshminarayanaiah and Siddiqi, 1972) by (*a*) the size of the stirrers in relation to the area of the membrane, (*b*) the rate of stirring, (*c*) the distance at which the stirrers rotated from the membrane surfaces, and (*d*) the nature of the membrane. Factors *a–c* were adequately taken care of in this study by

using large stirrers rotating at 200 rpm as close to the membrane faces as possible. That the stirrers were fairly close to the membrane faces was indicated by the fact that a number of experiments had to be abandoned because of rupture of the membrane by rotating bars. The rotation of the bars at 200 rpm was also found satisfactory since speeds greater than 200 rpm never increased the THO permeability. With regard to factor (d), the results given in Tables I and II show that when the membrane resistance was low, i.e. simple membrane M_1, even thin stagnant layers (23 μ) have a significant effect on P_t. The P_t has increased in this case by about 7%. On the contrary, in the case of membranes M_2 through M_6 which have relatively high resistance compared with M_1 (see Lakshminarayanaiah and Siddiqi, 1971 *a*), the increase in the value of P_t is between 3 and 5% even though the boundary layer thickness is as high as 1000 μ. In the case of the relatively thick composite membrane $M_1M_2M_3M_4M_5$, the boundary layers have very little effect (< 1%) on the value of P_t. These facts are in accord with the information available in the literature (Helfferich, 1962 *a*; Lakshminarayanaiah, 1969 *b*).

In the earlier study (Lakshminarayanaiah and Siddiqi, 1971 *a*) it was shown from impedance measurements that the composite membrane M_1M_5 had the characteristics of three membranes, viz. M_1, M_5, and the third simple membrane formed from M_1 and M_5 and existing in between them. The permeability results also lead to the same conclusion as illustrated below.

If the composite membrane M_1M_5 retained the characteristics of M_1 and M_5, it should have according to equation 3, i.e.

$$\frac{1}{\bar{P}_{M_1M_5}} = \frac{1}{\bar{P}_{t(M_1)}} + \frac{1}{\bar{P}_{t(M_5)}},$$

a value of 5.23×10^{-6} cm/sec for its permeability to THO. This value is lower than either of the two observed values, i.e., 9.17 or 7.75×10^{-6} cm/sec (see Table II). Substituting the higher of the two values in the modified form of equation 3, viz.

$$\frac{10^6}{9.17} = \frac{d_1}{\bar{D}_1} + \frac{1}{P_{15}} + \frac{d_5}{\bar{D}_5}, \tag{7}$$

(where d_1 and d_5 are the thicknesses of membranes M_1 and M_5 as they prevail in the composite membrane M_1M_5, $\bar{D}_1$ and $\bar{D}_5$ are the diffusion coefficients of THO in membranes M_1 and M_5, and P_{15} is the permeability of the third unit to THO, the third unit being formed as stated already from M_1 and M_5), equation 7 becomes

$$P_{15} = \frac{1}{1.09 \times 10^5 - 9.55 \times 10^7 d}, \tag{8}$$

where the assumption $d_1 = d_5 = d$ and the following substitutions have been made: $\bar{D}_1 = P_{t(M_1)}d_1 = 7.54 \times 10^{-7}$, [$P_{t(M_1)} = 3.77 \times 10^{-4}$ cm/sec and $d_1 = 2 \times 10^{-3}$

cm; see Table I], $\bar{D}_5 = P_{i(M_5)}d_5 = 1.06 \times 10^{-5}$ cm² sec⁻¹ [$P_{i(M_5)} = 5.3 \times 10^{-4}$ and $d_5 = 2 \times 10^{-3}$ cm; see Table I].

From equation 8, values for P_{16} may be calculated by assigning different values for d. The results of such calculations are given in Table III. It is seen from these results that when $d = 0$, $P_{16} = 9.17 \times 10^{-6}$, i.e., one uniform membrane is formed; and when $d = 1.14 \times 10^{-3}$ cm, $P_{16} = \infty$. Also when $d = 1.113 \times 10^{-3}$ cm, $P_{16} = 3.77 \times 10^{-4}$, the same value as the high charge density membrane, and the thickness of this unit is 1.774×10^{-3} cm. That a uniform membrane is formed is not true as rectification of THO flow is observed; and that the end units have a thickness of 1.113×10^{-3} cm is also not true because this would give a composite membrane M_1M_5 (thickness $= 4 \times 10^{-3}$ cm) containing a high charge density membrane M_1 of thickness 2.887×10^{-3} cm, i.e. $1.774 \times 10^{-3} + 1.113 \times 10^{-3}$, and M_5 of thickness 1.113×10^{-3} cm. The thickness of M_1 can never be greater than 2×10^{-3} cm because the volume of membrane-forming solution and the area it occupies are fixed. Consequently it is established that the thickness of the end units must be less than 1.113×10^{-3} cm. What the values of P_{16} are when the end units have a thickness in the range $(1.1\text{–}0.1) \times 10^{-3}$ cm are given in Table III.

Unlike the composite membrane M_1M_5, the composite membrane M_1-M_5 formed by laying and pressing M_1 on top of M_5 has no intermediate unit in the sense in which it is supposed to exist in the membrane M_1M_5. Still there might be a thin liquid layer between the two membranes M_1 and M_5. The theoretical value for the permeability of this membrane system should still be 5.23×10^{-5} cm/sec as the contribution of the thin liquid layer to the over-all permeability of the whole membrane system would be very small. This theoretical value is higher than the

TABLE III

THICKNESS OF END UNITS OF M_1 AND M_5 AS THEY EXIST IN THE COMPOSITE MEMBRANE M_1M_5 AND THE PERMEABILITY P_{16} OF THE MIDDLE UNIT FORMED FROM M_1 AND M_5 CALCULATED ACCORDING TO EQUATION 8

Thickness of end units of composite membrane M_1M_5 $d \times 10^3$	Permeability of middle unit formed from M_1 and M_5 of the composite membrane M_1M_5 P_{16}
cm	*cm/sec*
1.14	∞
1.12	5.00×10^{-4}
1.113	3.77×10^{-4}
1.10	2.50×10^{-4}
1.00	7.40×10^{-5}
0.67	2.21×10^{-5}
0.10	1.01×10^{-5}
0.00	9.17×10^{-6}

two observed values (see Table II). This discrepancy might arise from (*a*) the presence of not so thin a liquid layer between M_1 and M_5 or (*b*) the same factor which caused the rectification of the THO flows. A simple calculation using equation 3, i.e.

$$\frac{10^6}{4.41} = \frac{10^6}{5.23} + \frac{10^6 d}{2.44},$$

(where 4.41×10^{-6} cm/sec is the observed permeability of THO across the composite membrane M_1-M_5 [see Table II], 5.23×10^{-6} cm/sec is the theoretical permeability value, 2.44×10^{-5} cm²/sec is the self-diffusion coefficient of THO, and d is the thickness of the trapped aqueous layer between membranes M_1 and M_5) gives a value of 0.88 cm for the thickness of the trapped aqueous layer. This value is too high (several orders higher than the thickness of the membranes put together) to be true. Similarly in the case of the other composite membrane systems, M_1-M_3-M_5 and M_1-M_2-M_3-M_4-M_5, the observed permeabilities (1.74 and 1.41×10^{-6} cm/sec respectively) are found to be lower than the calculated (theoretical) values (2.74 and 1.58×10^{-6} cm/sec). In these cases also, the thicknesses of the aqueous layers trapped between membranes are unbelievably high (5.1 and 1.7 cm). So the factor *a* mentioned above cannot be responsible for the discrepancy between the observed and the calculated values of THO permeability. It is very interesting to find that the observed permeability across the composite membrane $M_1M_2M_3M_4M_5$, i.e. 1.54×10^{-6} cm/sec, is close but still lower than the theoretical value of 1.58×10^{-6} cm/sec. Consequently it is believed that the factor *b* mentioned above is probably involved in generating low values for the THO permeability in composite membranes. So the important question raised by the above discussion is what is really causing the composite membranes to allow more THO to flow in one direction (i.e. $M_1 \rightarrow M_5$) than in the reverse direction, i.e., $M_5 \rightarrow M_1$.

The two faces of the composite membranes are asymmetrical in that one surface is more highly charged (M_1) than the other surface (M_5); besides, surface M_1 is more porous than surface M_5 (see Lakshminarayanaiah and Siddiqi, 1971 *a*). In general the flow of an uncharged species like THO through the composite membrane will not be influenced by the fixed charges present in the membrane (Helfferich, 1962 *b*). On the other hand, the porosity, i.e. the amount of water present in the membrane, will affect the flow of THO. This is very well reflected in the values of permeability given in the fourth column of Table I. M_1 which is more porous than M_5 is nearly 70 times more permeable to THO than is M_5. The permeability sequence of the individual units used in the composite membrane is as $M_1 > M_2 > M_3 \geq M_4 \geq M_5$.

It is generally recognized in the case of artificial membranes that the permeabilities of counterion, coion, and nonelectrolytes are all concentration dependent (Helfferich, 1962 *b*). We may include water also to show this behavior, although it is difficult to come up with a direct demonstration in the way the dependence of permeability

on concentration of a nonelectrolyte solute, noninteracting with the membrane matrix, can be demonstrated.

When a gradient of THO acts across a composite membrane it takes, as stated already, 10–18 min for the flow of THO to reach a steady state. During this period, i.e. holdup time, THO would move through the different units constituting the composite membrane at rates proportional to the corresponding permeabilities in those units. When the gradient is acting in the direction $M_1 \rightarrow M_5$, the rate at which THO moves through the M_1 unit is faster than the rate at which it is removed through the M_5 unit. Consequently one might expect, during the time the flow is reaching the steady state, accumulation of THO at some border line in the membrane phase. Similarly for the same reason, there will be depletion of THO at some border line in the membrane phase when the direction of the THO gradient is reversed, i.e., $M_5 \rightarrow M_1$. Following this, the steady state is reached when the rates of flow in the different units would be equal. When the flow has attained this state, the

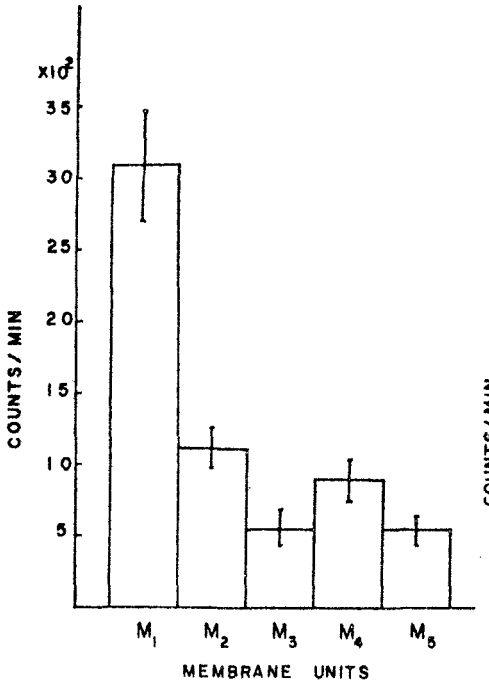

FIGURE 1

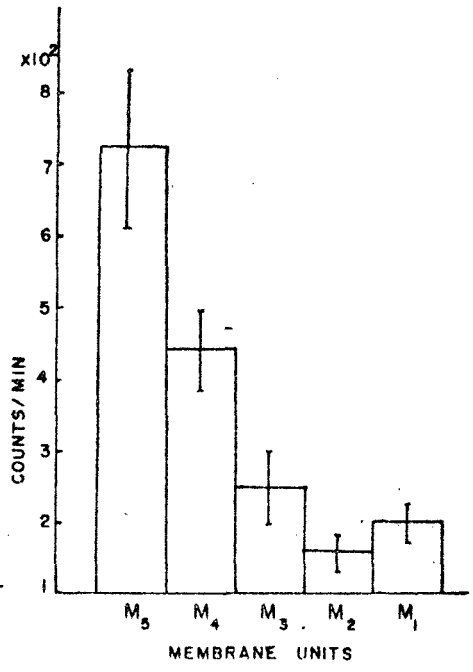

FIGURE 2

FIGURE 1 Concentration profile of THO in composite membrane (M_1-M_2-M_3-M_4-M_5) formed by putting one simple membrane on top of another and pressing them together when the THO gradient was acting in the direction $M_1 \rightarrow M_5$, where M_1 was the high charge density membrane and M_5 was the low charge density membrane.

FIGURE 2 Concentration profile of THO in composite membrane (M_5-M_4-M_3-M_2-M_1) formed by putting one simple membrane on top of another and pressing them together when the THO gradient was acting in the direction $M_5 \rightarrow M_1$, where M_5 was the low charge density membrane and M_1 was the high charge density membrane.

concentration profile in the membrane would have become stationary probably with a hump at some distance in the membrane when the gradient is in the direction $M_1 \rightarrow M_5$ and with a dip at some distance in the membrane when the gradient is acting in the reverse direction $M_5 \rightarrow M_1$. If this is true, the flow of THO in the direction $M_1 \rightarrow M_5$ would be greater than the flow in the reverse direction provided the over-all permeability is controlled by the nature of the concentration profile. This necessarily implies dependence of THO permeability on concentration, a fact already referred to above. In order to check these points, the concentration profile of THO in the composite membrane M_1-M_2-M_3-M_4-M_5 was determined. This was carried out as follows.

The membranes M_1 to M_5 were stacked in series to form a seven-member stack as M_1-M_1-M_2-M_3-M_4-M_5-M_5. Hot and cold solutions of 0.001 N NaCl were placed on the M_1 and M_5 sides respectively. The diffusion of THO was allowed to take place in the usual way for a period of about 3 hr, at the end of which the cell was emptied thoroughly. The membrane stack was removed from the cell carefully. The end membranes, the first M_1 and the last M_5, were discarded. The other five membranes M_1 through M_5 were carefully separated from one another and each was placed in a polyethylene vial into which 20 ml of Bray's solution were added, mixed, and counted in a liquid scintillation counter. This procedure was repeated by reversing the direction of THO flow, i.e., hot and cold solutions were placed on M_5 and M_1 sides respectively. The results realized are shown in Figs. 1 and 2.

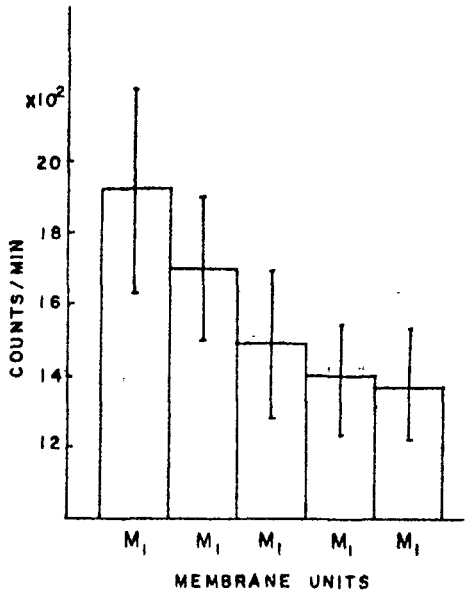

FIGURE 3 Concentration profile of THO in a uniform membrane formed from a stack of seven M_1 membranes. M_1 membrane contained 2.91 mg of polystyrenesulfonic acid/ml of membrane-forming collodion solution.

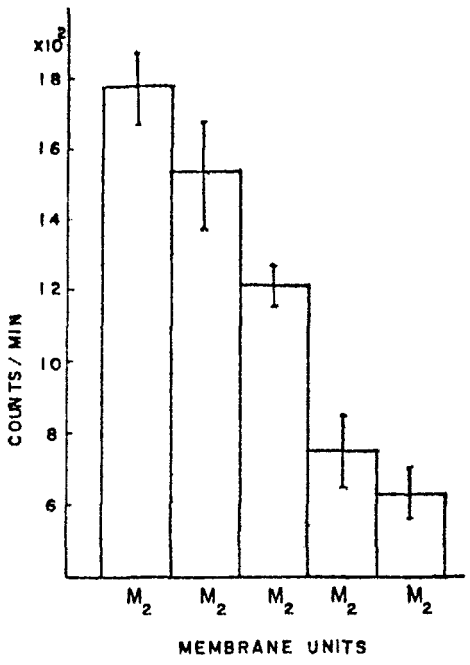

FIGURE 4

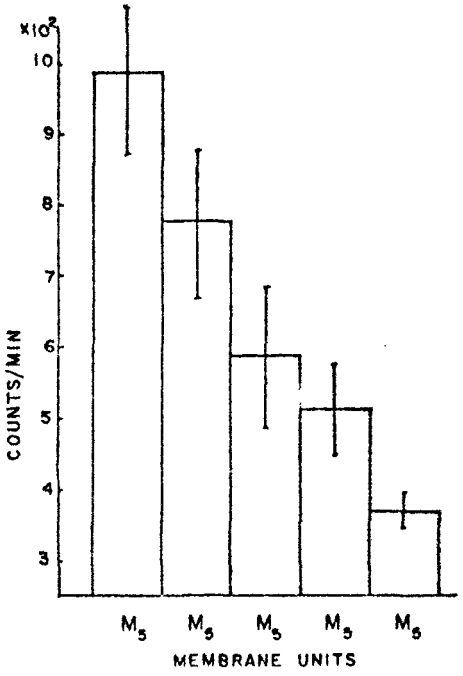

FIGURE 5

FIGURE 4 Concentration profile of THO in a uniform membrane formed from a stack of seven M_2 membranes. M_2 membrane contained 0.41 mg of polystyrenesulfonic acid/ml of membrane-forming collodion solution.

FIGURE 5 Concentration profile of THO in a uniform membrane formed from a stack of seven M_5 membranes. M_5 membrane contained 0.004 mg of polystyrenesulfonic acid/ml of membrane-forming collodion solution.

The normal concentration profile in a high, medium, or low charge density membrane system was also established using again a seven-membrane stack formed of seven high, medium, or low charge density membranes. These results are given in Figs. 3–5.

In the above experimental procedure, the amount of liquid trapped between membranes has been taken into account. Two other alternate treatments at the end of the experimental run were also followed to determine the amount of THO present in each membrane only of the stack. Treatment one consisted of giving each membrane after removal from the stack a quick dip in deionized water. Then it was transferred to the vial as usual. Treatment two consisted of gently pressing each membrane of the stack between filter papers and transferring it to the vial. These treatments removed the superficial liquid from the membranes. These procedures also gave profiles (results not given) similar to those shown in Figs. 1–5 although the counts were relatively low.

The results of Figs. 3–5 indicate that in a "uniform" membrane, whether it contained high, medium, or low density of fixed charges, there is a gradual decrease in

the concentration of THO in the membrane phase as THO moved down its gradient. On the other hand, the picture is different in the case of the composite membrane (see Figs. 1 and 2). When the THO gradient is in the direction $M_1 \rightarrow M_3$, the concentration of THO decreases up to the third unit (Fig. 1), then increases, and finally decreases. The maximum (i.e., accumulation) is located between M_3 and M_4 units of the composite membrane. When the gradient is reversed (i.e., $M_3 \rightarrow M_1$), the concentration of THO decreases, reaches a minimum, and then increases. The minimum (i.e., depletion of THO) is located between M_3 and M_1 units. Thus these conditions should lead to unequal flows of THO across the composite membrane in the opposite directions. The data given in Table II confirm this.

This work has been supported by U. S. Public Health Service grant NB-08163.

Received for publication 11 August 1971 and in revised form 24 September 1971.

REFERENCES

ANDREOLI, T. E., and S. L. TROUTMAN. 1971. *J. Gen. Physiol.* **57**:464.
BRAY, G. A. 1960. *Anal. Biochem.* **1**:279.
DAINTY, J., and C. R. HOUSE. 1966. *J. Physiol. (London).* **185**:172.
EVERITT, C. T., and D. A. HAYDON. 1969. *J. Theor. Biol.* **22**:9.
EVERITT, C. T., W. R. REDWOOD, and D. A. HAYDON. 1969. *J. Theor. Biol.* **22**:20.
HALE, D. K., and K. P. GOVINDAN. 1969. *J. Electrochem. Soc.* **116**:1373.
HELFFERICH, F. 1962 *a*. Ion Exchange. McGraw-Hill Book Company, New York. 348.
HELFFERICH, F. 1962 *b*. Ion Exchange. McGraw-Hill Book Company, New York. 350.
KEDEM, O., and A. KATCHALSKY. 1963. *Trans. Faraday Soc.* **59**:1941.
KLEIN, E., J. K. SMITH, and R. P. WENDT. 1969. *J. Polym. Sci. Part C.* **28**:209.
LAKSHMINARAYANAIAH, N. 1965. *Chem. Rev.* **65**:499.
LAKSHMINARAYANAIAH, N. 1967 *a*. *Biophys. J.* **7**:511.
LAKSHMINARAYANAIAH, N. 1967 *b*. *J. Appl. Polym. Sci.* **11**:1737.
LAKSHMINARAYANAIAH, N. 1969 *a*. Transport Phenomena in Membranes. Academic Press, Inc., New York. 132.
LAKSHMINARAYANAIAH, N. 1969 *b*. Transport Phenomena in Membranes. Academic Press, Inc., New York. 131.
LAKSHMINARAYANAIAH, N., and F. A. SIDDIQI. 1971 *a*. *Biophys. J.* **11**:603.
LAKSHMINARAYANAIAH, N., and F. A. SIDDIQI. 1971 *b*. *Biophys. J.* **11**:617.
LAKSHMINARAYANAIAH, N., and F. A. SIDDIQI. 1972. *Z. Phys. Chem. (Frankfurt am Main).* In press.
SCATTERGOOD, E. M., and E. N. LIGHTFOOT. 1968. *Trans. Faraday Soc.* **64**:1135.
WANG, J. H., C. V. ROBINSON, and I. S. EDELMAN. 1953. *J. Amer. Chem. Soc.* **75**:466.

MEMBRANE PROCESSES IN INDUSTRY AND BIOMEDICINE

EDITED BY MILAN BIER
Veterans Administration Hospital and
The University of Arizona, Tucson, Arizona

PLENUM PRESS • NEW YORK–LONDON • 1971

Reprinted from: MEMBRANE PROCESSES IN INDUSTRY AND BIOMEDICINE
Edited by Bier
(Plenum Press, 1971)

SOME ASYMMETRY PROPERTIES OF COMPOSITE MEMBRANES

N. Lakshminarayanaiah and Pasih A. Siddiqi

Department of Pharmacology, University of Pennsylvania School of Medicine, Philadelphia, Pa. 19104.

ABSTRACT

Composite membranes of two types, layer-type and sandwich-type, have been prepared from 2% collodion solutions containing different amounts of polystyrene sulfonic acid. The layer-type membranes were formed by evaporating first a collodion solution containing the least amount of the polyelectrolyte. On top of this collodion solutions containing increasing quantities of the polyelectrolyte were evaporated one after the other. Sandwich-type membranes were formed by trapping some polyelectrolyte between two simple membranes, one containing a small quantity and the other containing a large quantity of the polyelectrolyte.

Electrical potentials arising across these membranes when they separate the same concentration of (1:1) electrolyte have been measured as a function of concentration. Long term equilibration of these membranes with very dilute electrolyte solutions tend to lower the potentials observed in the first few hours of equilibration. These results are discussed in terms of a model system built from two simple membrane cells, one containing membrane of high charge density and the other containing membrane of low charge density, in such a way that one membrane cell opposed the emf of the other membrane cell.

INTRODUCTION

A group of Italian workers[1-3] have shown that composite membranes prepared from collodion-polystyrene sulfonic acid can mimic some of the properties of the squid nerve membrane. In fact one of them[4] has advanced a physico-chemical model for the nerve

membrane in terms of which the resting and action potentials have been explained. These studies intrigued us very much and we repeated their work. Short period (1-2 hr) equilibrations of the membrane with the electrolyte solutions, particularly the layer-type membranes, gave values for the asymmetry potential (i.e. emf generated when the same concentration of the electrolyte was placed on either side of the membrane) which agreed roughly in magnitude with the published values of the Italian workers[2]. In this paper, the results of long term equilibration and of other experiments are presented.

EXPERIMENTAL

The dissolution method reviewed by Neihof[6] was used to prepare simple membranes of collodion which contained various amounts of polystyrene sulfonic acid (PSSA). Styrene polymer (Borden Chemical Co., Philadelphia, Pa) was sulfonated and PSSA obtained following the procedure described by Neihof. Membranes were cast on clean and dry glass plates from a 2% solution of Parlodion (purified nitrocellulose, Mallinckrodt) in alcohol-ether mixture (3:1 by volume) containing different amounts of PSSA.

The composite membranes were prepared following the steps given by Liquori and Botre[1,2], although the compositions of solutions used to form membranes were different. The layer-type membranes were formed by casting different layers of 2% Parlodion solution containing various amounts of PSSA (8.3 to 0.02 mg/ml), one on top of the other, in the way described by Liquori and Botre[1]. The sandwich-type membranes were formed by trapping a layer of PSSA (4 mg/ml) between high charge density membrane (2% collodion, USP, Fisher, containing 10 mg/ml PSSA) and low charge density membrane (2% collodion, USP, Fisher, containing 1 mg/ml PSSA) in the way outlined by Liquori and Botre[2]. In this case alcohol to ether ratio was 1:2.5.

The membranes were converted into the Na form by treating them with 1.0 N solution of NaCl. They were washed with deionized water and equilibrated with the solution to be used in the experiment with frequent changes of the solution. The asymmetry potentials arising across composite membranes were measured on a Keithley microvoltmeter in an air conditioned room at 22°C using an all glass H-cell and saturated KCl-agar bridges.

RESULTS

Electrical potentials (high charge density side taken positive) arising across some of the composite membranes, both layer and sandwich types, when they were subject to short term equilibrations (1-2 hr) and separating the same electrolyte solution of NaCl are given in Figure 1. The membranes were screened to choose only the

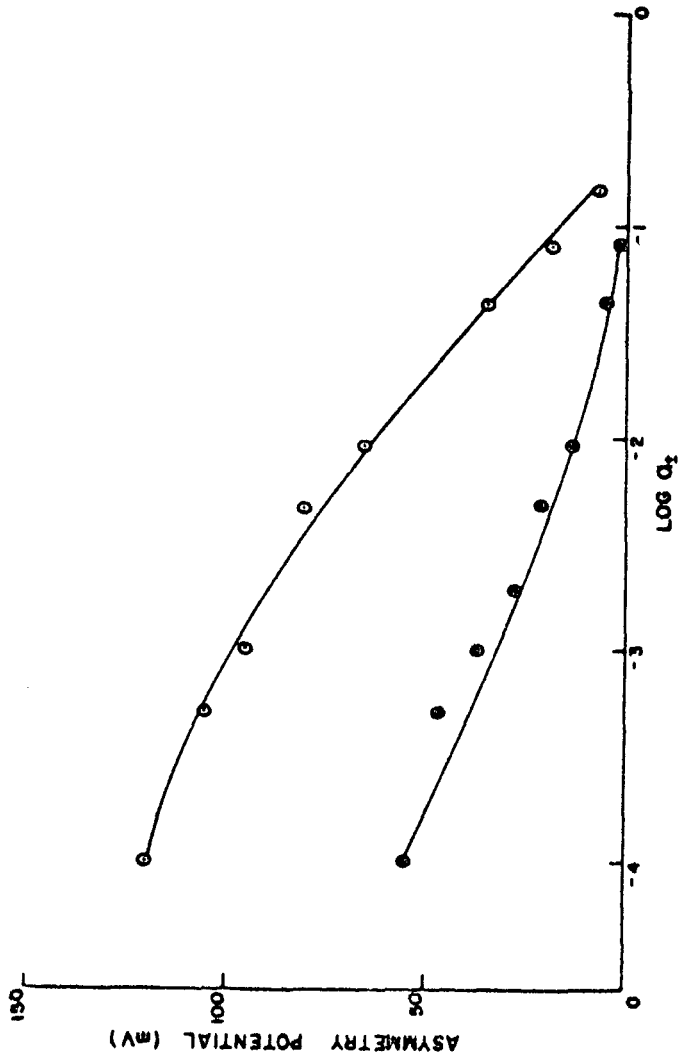

Fig. 1. Electrical potentials arising across a composite membrane when it separates the same concentration of NaCl plotted as a function of the activity of the external solution. (○) refer to asymmetry potentials across a layer-type membrane; (●) refer to asymmetry potentials across a sandwich-type membrane.

majority of those which gave good and steady emf values agreeing among themselves within ± 10%. There were however some membranes belonging to the same lot which gave emf values lower in magnitude to those given in Figure 1. The sandwich-type membranes with which we had the most difficulty in preparing them, gave asymmetry potentials which were lower than those given by layer-type membranes (see Figure 1) and those observed by Liquori and Botre[2] for similar membranes (see their Figure 3). Deposition of PSSA between the two simple membranes, one of low charge and the other of high charge density, always gave good sandwich-type membranes; but they separated into the individual units when kept in equilibrating solutions. The results given in Figure 1 were obtained from those sandwich-type membranes which remained intact after equilibration with the solutions. Inspite of repeated attempts, we were not successful in preparing sandwich-type membranes which gave emf values as high as those published by Liquori and Botre[2].

Four pieces cut out of a layer-type membrane formed on a glass plate gave 62, 61, 50 and 45 mV each for asymmetry potential after 2 hr equilibration with 0.01 N NaCl solution. This type of variability was noted in most cases and hence the need for screening these membranes. A piece of membrane that gave an asymmetry potential of 54 mV with 0.01 N NaCl solution in the first few hours of equilibration was used to follow the change in potential with time. These results are given in Figure 2. The potential decayed with time and similar decay was noted also at other concentrations. The decline was usually slow in the case of those membranes which gave low asymmetry potentials initially. Similar pattern was commonly observed with our sandwich-type membranes. Included in Figure 2 are the data realized using a genuine Liquori-Botre membrane (our sincere thanks to Prof. A. M. Liquori for supplying their sandwich-type membrane to one of us (F.A.S)) which contained a layer of PSSA trapped between two collodion films containing 0.5 and 0.005 equiv/Kg of PSSA. Even in this case, the asymmetry potentials decay with time. The magnitude of the emf observed at any given time and its rate of fall were determined by the way membranes were treated. For example, it was found that the potential was fairly high with 0.0001 N NaCl solution (about 120-130 mV) when the measurement was made immediately after washing the Na form of the membrane (i.e. in contact with 1.0 N solution) with deionized water. But it rapidly declined with time. On the other hand if the equilibration with 0.0001 N solution was carried out for 10-12 hr with frequent changes of solution, the value observed for the potential was low. Again the strength of the solution used in the measurement also affected the magnitude of the potential. Generally low values were observed with solutions whose concentration was greater than 0.01 N. The factors causing this behavior are discussed below.

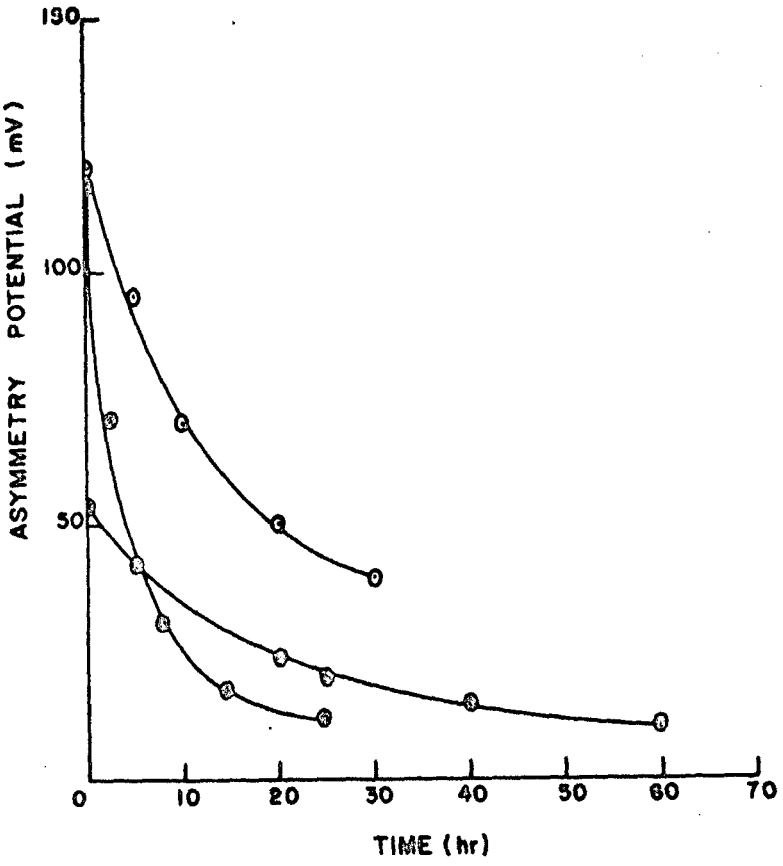

Fig. 2. The decline of asymmetry potential followed as a function of time. (⊖), (⊜) refer to a layer-type membrane in contact with 0.0001 and 0.01 N NaCl solution respectively. (⊜) refer to a genuine Liquori-Botre sandwich-type membrane in contact with 0.0001 N NaCl solution.

DISCUSSION

The asymmetry potential was considered by Liquori and Botre in their earlier paper[1] in terms of Donnan and diffusion potentials. Later[2] they proposed a model (see Figure 3) in which two membranes, one of high charge density M_H (i.e. highly selective to cations) and the other of low charge density M_L (i.e. low selectivity to

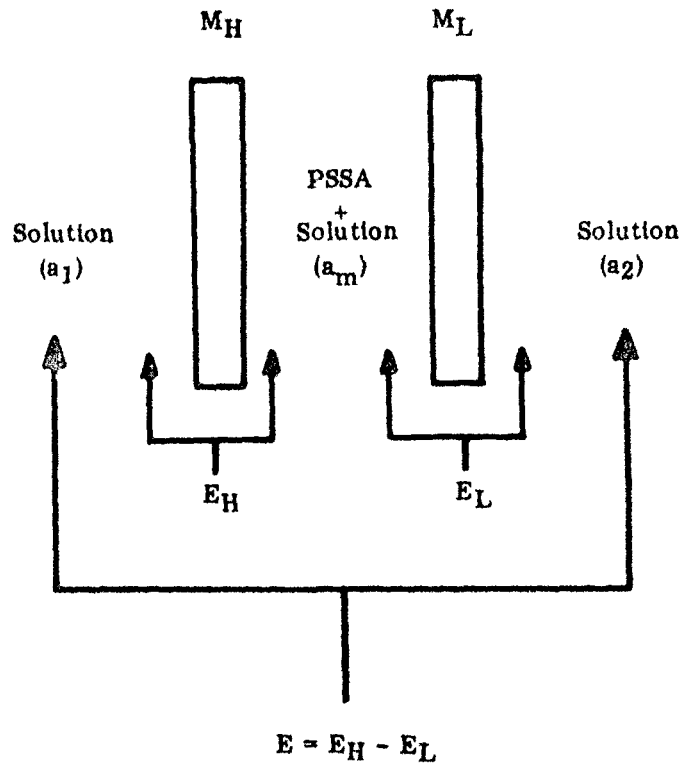

Fig. 3. The model for the composite membrane. M_H and M_L are simple membranes of high charge (PSSA = 2.5 mg/ml of membrane forming solution) and low charge (PSSA = 0.025 mg/ml) density respectively separating three solutions of the same electrolyte of activity a_1, a_m and a_2 contained in the three chambers. E_H is the concentration potential arising across membrane M_H and E_L is a similar potential arising across M_L. E is the potential across the complete electrochemical cell. E is the asymmetry potential developing across the whole cell when the activities a_1 and a_2 are equal.

cations), were considered to hold in between a high concentration of counterions associated with the polyelectrolyte (PSSA). In this arrangement, asymmetry potential arose as a result of the differences in the selectivities of the two membranes. Expressing selectivities in terms of counterion transport numbers, Lakshminarayana-

iah and Siddiqi[5] showed that the emf E across the composite cell (Figure 3) was given by

$$E = \frac{RT}{F}\left[(2\bar{t}_{+(H)} - 1)\ln\frac{a_m}{a_1} - (2\bar{t}_{+(L)} - 1)\ln\frac{a_m}{a_2}\right] \quad (1)$$

where $\bar{t}_{+(H)}$ and $\bar{t}_{+(L)}$ are the transport numbers of counterion in high charge and low charge density membranes respectively, a_m is the activity of counterions existing between the membranes, and a_1 and a_2 are the activities of the two solutions contacting high and low charge density membranes. When $a_1 = a_2 = a$, the asymmetry potential is given by

$$E = \frac{2RT}{F}\left[\bar{t}_{+(H)} - \bar{t}_{+(L)}\right]\ln\frac{a_m}{a} \quad (2)$$

Lakshminarayanaiah and Siddiqi[5] showed that the potential E arising across the model system (Figure 3) conformed to Eqs. (1) and (2) and as a result they came to the conclusion that the magnitude of E (Eq. (2)) arising across composite membranes was controlled more by a_m, the activity of cations associated with PSSA and free electrolyte, than by the factor $\left[\bar{t}_{+(H)} - \bar{t}_{+(L)}\right]$. The results of long term equilibration experiments and other results obtained with these membrane systems (see below) can be explained in terms of Eq. (2). Lack of good reproducibility of potentials observed with different pieces cut out of the same membrane can be attributed to the heteroporous structure of the membrane. In this type of structure, the different regions of the same membrane will trap different quantities of PSSA and electrolyte thereby giving different values for a_m. Similarly during long term equilibrations with dilute solutions, removal of trapped electrolyte will follow different pattern on the time scale depending on how big or small the membrane pores were. On the basis of this model, thorough washing and equilibration with dilute solutions of the composite membrane would give low values for the asymmetry potential. This is in agreement with our observations (see Figure 2). We always found short term equilibrations gave high potentials and long term equilibrations gave low values. Further use of membranes which were already used once before and therefore subject to washings and equilibrations always gave low values for the asymmetry potential. So long as the composite membrane retained a structure which stabilized the value for a_m, irrespective of the period of equilibration, steady and good potentials would be obtained. If the activity of trapped ions a_m is due to sorbed electrolyte which can be partially removed by washing and equilibration over a period of time, the potential would always decay with time as observed in the present studies. In view of this, it is not surprising to obtain with these membrane systems results which would not agree

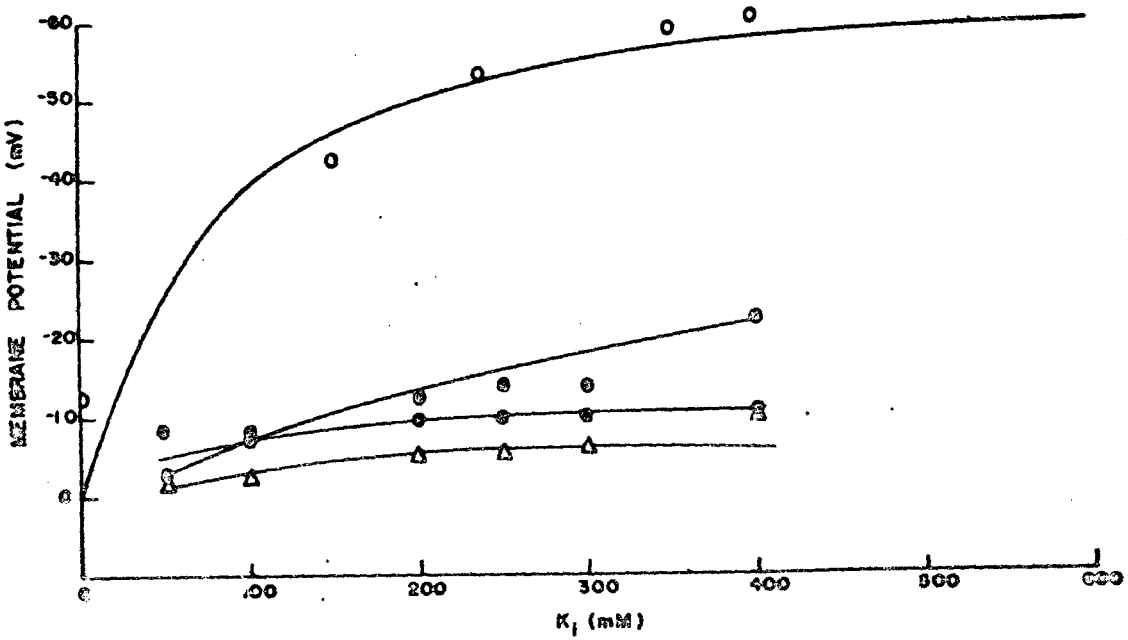

Fig. 4. Membrane potential across different membrane systems plotted as a function of K^+ concentration. The high charge density side indicated to be negative. The solid line represents the data of Baker et al[7] who used the "perfusion technique" to replace the natural axoplasm of the giant axon of the squid with different isotonic solutions containing varying amounts of K_i^+. (O) represent the data obtained by Botre et al[3] with a composite membrane when the "outside" solution was 0.45 M NaCl and 0.01 M KCl and the "inside" solution contained different amounts of K_i^+. The ionic strength of this solution was kept at 0.45 M by replacing K^+ with Na^+. (●), (○) and (▲) represent data of this study using a genuine Liquori-Botre sandwich-type membrane, a layer-type membrane and the model system of Figure 3 when the middle compartment contained 0.5 M NaCl solution respectively. The solutions used were the same as those used by Botre et al.

with those obtained by others. For example in Figure 4 are given the results obtained by Botre et al[3] with a composite membrane. These potentials give good agreement with the resting potentials measured by Baker et al[7] using the perfusion technique on a squid nerve membrane. In these experiments the natural axoplasm of the giant axon of the squid was replaced by isotonic solutions containing varying amounts of K_i^+. In the same figure are given also some of our results obtained with three membrane systems, viz. the genuine Liquori-Botre sandwich-type membrane, our layer-type membrane and the model system (Figure 3) with 0.5 M NaCl solution in the middle chamber. The solutions used on either side of the composite membranes are indicated in the legend to Figure 4. Although our results with the three systems are consistent, they do not agree with the published values of Botre et al[3].

REFERENCES

1. A. M. Liquori and C. Botre, Ric. Sci., 34, (6), 71 (1964).
2. A. M. Liquori and C. Botre, J. Phys. Chem., 71, 3765 (1967).
3. C. Botre, S. Borghi and M. Marchetti, Biochim. Biophys. Acta, 135, 162 (1967).
4. A. M. Liquori, Il Farmaco (Pravia) Ed. Sci., 23, 999 (1968).
5. N. Lakshminarayanaiah and F. A. Siddiqi, communicated elsewhere.
6. R. Neihof, J. Phys. Chem., 58, 916 (1954).
7. P. F. Baker, A. L. Hodgkin and T. I. Shaw, Nature, 190, 885 (1968).

ACKNOWLEDGMENTS

The work has been supported by Public Health Service grant NB-08163-02.

CHAPTER 2

ION AND WATER MOVEMENTS IN PERMSELECTIVE MEMBRANES AND RELATIONSHIP BETWEEN MEMBRANE POTENTIAL AND ELECTROLYTE UPTAKE

Sonderdruck: „Zeitschrift für Physikalische Chemie Neue Folge", 78 (1972) 150–163
Herausgegeben von G. Briegleb, Th. Förster, G. Schmid, G.-M. Schwab, E. Wicke

Ion and Water Movements in Permselective Membranes

By

N. Lakshminarayanaiah and Fasih A. Siddiqi

Department of Pharmacology, University of Pennsylvania, School of Medicine
Philadelphia, Pennsylvania 19104

(Received September 27, 1971)

AKADEMISCHE VERLAGSGESELLSCHAFT
FRANKFURT AM MAIN
1972

Abstract

The equilibrium properties such as water content and exchange capacity, and transport properties such as electrical conductance, ionic self diffusion coefficient and water transport have been measured for two cation exchange membranes of low water content in different cationic forms and for one anion exchange membrane of low water content in chloride form. The measured ionic conductance was found to be greater than the corresponding value derived from the ionic self diffusion coefficient. This discrepancy could not be attributed completely to electroosmosis. Part of it was found to arise from the migration of counterions along the polymer chains, a process similar to surface conduction.

Introduction

Maintenance of a chemical potential gradient of species i across a membrane, charged or uncharged, gives rise to unidirectional flow of i which is described by Fick's first law. An integrated form of Fick's equation[1] could be used to derive a value for the self diffusion coefficient $\bar{D}_i$ of the species by measuring its flux using a radioactive isotope of i. Under ideal conditions, $\bar{D}_i$ is related to the limiting equivalent conductance $\bar{\lambda}_i$ by the Nernst-Einstein relation[2], Viz.

$$\bar{D}_i = \frac{RT}{z_i F^2} \bar{\lambda}_i, \qquad (1)$$

where z_i is the valence of i, R, T and F are the gas constant, absolute temperature and the Faraday constant respectively. GOTTLIEB and

[1] N. LAKSHMINARAYANAIAH, J. physic. Chem. 74 (1970) 2385.

[2] R. A. ROBINSON and R. H. STOKES, Electrolyte Solutions, Butterworths, London 1959, p. 317.

SOLLNER[3], expressing eq. (1) for $z_i = 1$ in the form

$$J_i = \frac{RT}{\bar{\varrho} F^2} \tag{2}$$

(where J_i is the flux in equiv./sec and $\bar{\varrho}$ is the membrane resistance in ohms) found it applicable to a cation permeable membrane of oxidized collodion. But in the case of other membrances [collodion containing polystyrenesulfonic acid (PSSA), protamine or poly-2-vinyl-*N*-methyl pyridinium bromide (PVMP)], unsatisfactory agreement between J_{exp} and J_{cal} was found. J_{exp} was found to be greater than J_{cal} in the case of PVMP membranes and less than J_{cal} in the case of the other two types of membrances. The former type of discrepancy, i.e. $J_{exp} > J_{cal}$, is very unusual in that it is the first recorded example which remains unexplained although it could be attributed to ion association[4]. The latter finding, i.e. $J_{exp} < J_{cal}$, has been noted by a number of earlier investigators[5–8] who attributed the discrepancy to electroosmosis. MEARES and coworkers[8,9] have considered this problem quantitatively in detail. According to that theory, the portion of the equivalent conductance of the membrane due to electroconvection is given by[10]

$$k\, t_w \bar{V}_w \tag{3}$$

where k is the specific conductance, t_w is the transport number of water (moles/F) and $\bar{V}_w$ is the partial molar volume of water. All these quantities refer to the membrane phase.

Addition of eq. (3) to eq. (1) gives the theoretical equivalent conductance of the membrane. That is

$$\bar{\lambda}_{i\,(\mathrm{theo})} = z_i \frac{F^2}{RT} \bar{D}_i + k\, t_w \bar{V}_w . \tag{4}$$

---

[3] M. H. GOTTLIEB and K. SOLLNER, Biophys. J. 8 (1968) 515.

[4] J. O'M. BOCKRIS and A. K. N. REDDY, Modern Electrochemistry, Plenum Press, New York 1970, Vol. 1, p. 383.

[5] K. S. SPIEGLER and C. D. CORYELL, J. physic. Chem. 57 (1953) 687.

[6] A. DESPIC and G. J. HILLS, Discuss. Faraday Soc. 21 (1956) 150.

[7] N. LAKSHMINARYANAIAH, Ph. D. Thesis, University of London, London 1956.

[8] P. MEARES and H. H. USSING, Trans. Faraday Soc. 55 (1959) 244.

[9] W. J. MCHARDY, P. MEARES, A. H. SUTTON and J. F. THAIN, J. Colloid and Interface Sci. 29 (1969) 116.

[10] N. LAKSHMINARAYANAIAH, in: Electrochemistry, Vol. 2, Specialist Periodical Reports, The Chemical Society, London (to be published).

The directly measured $\bar{\lambda}_{i(obs)}$ for the membrane is given by

$$\bar{\lambda}_{i(obs)} = \frac{k\bar{t}_i}{z_i \bar{C}_i}, \tag{5}$$

where $\bar{C}_i$ is in moles per cubic centimeter of ions i in the membrane. Eq. (4) is valid for an ideal membrane system in which there is complete interaction only between mobile ions and water. In reality, due to interactions of mobile components with the membrane matrix and its fixed groups, values of $\bar{\lambda}_i$ predicted by eq. (4) will deviate from the observed values. The extent of these interactions has been evaluated by McHARDY et al.[9] by introducing an empirical constant into eq. (4), viz.

$$\bar{\lambda}_{i(obs)} = z_i \frac{F^2}{RT} \bar{D}_i + \bar{\alpha}_i k \bar{t}_w \bar{V}_w . \tag{6}$$

The values for $\bar{\alpha}_i$ have been computed for a cation exchange membrane (ZeoKarb 315) of high water content ($\sim 67\%$) by carrying out measurements of self diffusion coefficient, water transport number and electrical conductance of the membrane as functions of external electrolyte concentration. Similar studies but using two cation and one anion exchange membranes of low water contents ($< 20\%$) in equilibrium with an electrolyte environment (0.01 N) in which the transport number of the counterion $\bar{t}_i$ is unity, are presented in this paper.

Experimental

The membranes used were the commercially available AMF C-103, AMF C-104 and AMF A-100 (American Machine and Foundry Company) which were of the strong acid and strong base types containing sulfonic acid and quaternary ammonium groups. The membranes were treated and equilibrated with the different 0.01 N electrolyte solutions in the way described previously[1,11]. Their equilibrium properties, viz. thickness, water content and exchange capacity, were determined in the usual way[1,12].

Measurements of electrical conductance[13], water transport number[14] and self diffusion coefficient[1,15] were made following our methods

[11] N. LAKSHMINARAYANAIAH, J. Macromol. Sci.-Phys. B 5 (1971) 159.

[12] N. LAKSHMINARAYANAIAH and V. SUBRAHMANYAN, J. Polymer Sci., Part A 2 (1964) 4491.

[13] V. SUBRAHMANYAN and N. LAKSHMINARAYANAIAH, J. physic. Chem. 72 (1968) 4314.

[14] N. LAKSHMINARAYANAIAH and V. SUBRAHMANYAN, J. physic. Chem. 72 (1968) 1253.

[15] N. LAKSHMINARAYANAIAH, Biophys. J. 7 (1967) 511.

referred to. The isotopes used in the measurements of self diffusion coefficients were ^{22}Na, ^{86}Rb, ^{137}Cs, ^{45}Ca and ^{36}Cl.

Table 1. *Different parameters of the membrane in equilibrium with various 0.01 N electrolyte solutions*

Membrane system	Thickness d, cm	Water content g/100 g wet membrane	ml H_2O/equiv. of counterion	Exchange capacity $\bar{C}_i$ (equiv./cm³) · 10³
		AMF A-100		
Cl	0.0221	16.5	159	1.08
		AMF C-103		
Na^+	0.0142	16.8	190	0.94
Rb^+	0.0142	12.6	154	0.89
Cs^+	0.0142	12.3	175	0.77
Ca^{2+}	0.0135	12.0	139	0.95
		AMF C-104		
Na^+	0.0150	12.9	141	0.98
Rb^+	0.0150	11.5	144	0.88
Cs^+	0.0150	11.6	158	0.81
Ca^{2+}	0.0142	10.4	125	0.95

Table 2. *Transport parameters for membranes in contact with 0.01 N solutions*

Membrane system	Sp. conductance $\bar{k} \cdot 10^3$ ohm^{-1} cm^{-1}	Eq. conductance $\bar{\lambda}_i$ ohm^{-1} cm^2 equiv^{-1}	Water transport l_w mole F^{-1}
		AMF A-100	
Cl^-	2.11	1.95	3.8
		AMF C-103	
Na^+	1.70	1.81	7.5
Rb^+	1.97	2.21	4.9
Cs^+	1.67	2.17	5.0
Ca^{2+}	0.47	0.49	7.4
		AMF C-104	
Na^+	1.39	1.42	6.5
Rb^+	1.73	1.97	4.1
Cs^+	1.23	1.52	4.5
Ca^{2+}	0.36	0.38	7.3

Results

The equilibrium parameters determined for the various membranes are given in Table 1. The overall errors of these parameters were estimated to be $\pm$ 4%.

The specific conductance (k) and the equivalent conductance ($\bar{\lambda}_t$) evaluated for the various membranes in different ionic forms are collected in Table 2. Although the resistance of the membrane could be measured to better than $\pm$ 1%, estimation of membrane area and thickness were accurate to $\pm$ 3%.

Water transport

Application of a d.c. field to the system, electrolyte solution⇌membrane⇌electrolyte solution, allows cations to move to the cathode and anions to the anode through the membrane. The electrolyte environment is such that there are few coions present in the membrane phase and consequently all the current is carried through the membrane by counterions whose transport is accompanied by movement of water. Necessarily therefore, there is flow of water into the anode chamber in the case of anion exchange membranes (AMF A-100) and into the cathode chamber in the case of cation exchange membranes (AMF C-103 and C-104).

Measurement of this water flow, i.e. l_w, accurate to $\pm$ 2%, was carried out using the volume method at different current densities in the range 0.32 -16.0 mA/cm^2. Unlike membranes of high water content whose values of l_w were strongly dependent on the density of current employed during electrolysis[14,16] the membranes used in this study had low water contents and showed no such dependence of l_w on current density although AMF C-103 in *Na*-form showed a slight increase in l_w at 0.32 mA/cm^2. The value given in Table 2 for the *Na*-form of this membrane was the limiting value realized in the current density range 2—16 mA/cm^2. All of the values of l_w have been corrected appropriately for the electrode reactions.

Self diffusion coefficient

The measurement of self diffusion coefficient is quite straight forward provided the irksome stationary aqueous layers at the membrane-solution interfaces have been eliminated. This could be done by using turbulent flow technique which however requires elaborate

[16] N. LAKSHMINARAYANAIAH, Desalination 3 (1967) 97.

hardware[17,18]. There are also other methods which have been reviewed by LAKSHMINARAYANAIAH[19]. Recently some more methods have been described[20–24]. In this study, the method described by EVERITT et al.[23] has been used. This consists in making two permeability measurements, one using a piece of the membrane and the other using two pieces of the same membrance contacting each other in series, in an H-cell of the type described elsewhere[16,25]. The apparent permeabilities P_t for the single and for the double (series) membrane systems were evaluated from the equation[26]

$$P_t = \frac{2.303\, V_1 V_2}{(V_1 + V_2) A \Delta t} \log \frac{C' V_1 + C'' V_2 - C''_{t_0}(V_1 + V_2)}{C' V_1 + C'' V_2 - C''_{t_0+\Delta t}(V_1 + V_2)}, \qquad (7)$$

where V_1 and V_2 are the volumes of compartments 1 ("cold" side) and 2 ("hot" side). C' and C'' are the initial concentration (taken as counting rate per milliliter) of radioactive isotope in compartments 1 and 2, i e. at time $t = 0$. C''_{t_0} and $C''_{t_0+\Delta t}$ are the concentrations in compartment 2 at time $t = t_0$ and $t = t_0 + \Delta t$ respectively. Δt therefore is the time elapsing between samplings in seconds.

For the single membrane the apparent permeability P_a is given by[27]

$$\frac{1}{P_a} = \frac{1}{P_t} + \frac{\delta_1 + \delta_2}{D}, \qquad (8)$$

where P_t is the corrected value for the presence of the boundary layers of thickness δ_1 and δ_2 at the two membrane faces and D is the self diffusion coefficient of the species concerned in the aqueous

[17] E. KLEIN, J. K. SMITH and R. P WENDT, J. Polymer Sci., Part C 28 (1969) 209.

[18] E. KLEIN, P. D. MAY, J. K. SMITH and N. LEGER, Biopolymers 10 (1971) 647

[19] N. LAKSHMINARAYANAIAH, Transport Phenomena in Membranes, Academic Press, New York 1969, p. 132; Chem. Rev. 65 (1965) 499.

[20] E. M. SCATTERGOOD and E. N. LIGHTFOOT, Trans. Faraday Soc. 64 (1968) 1135.

[21] D. K. HALE and K. P. GOVINDAN, J. electrochem. Soc. 116 (1969) 1373.

[22] C. T. EVERITT and D. A. HAYDON, J. Theoret. Biol. 22 (1969) 9.

[23] C. T. EVERITT, W. R. REDWOOD and D. A. HAYDON, J. Theoret. Biol. 22 (1969) 20.

[24] T. E. ANDREOLI and S. L. TROUTMAN, J. gen. Physiol. 57 (1971) 464.

[25] N LAKSHMINARAYANAIAH, J. appl. Polymer Sci. 11 (1967) 1737.

[26] J. DAINTY and C. R. HOUSE, J. Physiol. [London] 185 (1966) 172.

[27] O. KEDEM and A. KATCHALSKY, Trans. Faraday Soc. 59 (1963) 1941.

boundary layers. Similarly for the two membranes in series, eq. (8) becomes

$$\frac{1}{\bar{P}_b} = \frac{2}{\bar{P}_t} + \frac{\delta_1 + \delta_2}{\bar{D}} \tag{9}$$

where P_b is the apparent permeability of the "double membrane". The value for P_t may be obtained from eqs. (8) and (9). Thus

$$P_t = \frac{P_a P_b}{P_a - P_b} \tag{10}$$

In view of the symmetry of the membrane system and of identical hydrodynamic conditions, i.e. stirring, employed, one can assume that $\delta_1 = \delta_2 = \delta$. Thus eqs. (8) and (9) give

$$\delta = \frac{2P_b - P_a}{P_a P_b} \cdot \frac{D}{2} \tag{11}$$

AMF C 104 membrane in *Na* form was used to determine P_a and P_b under a variety of experimental conditions. Two different *H*-cells were used. One was a small cell each compartment of which had a capacity of about 30 ml and contained initially 26 ml of the hot or cold 0.01 N *NaCl* solution. These solutions were kept well stirred using rotating teflon coated magnetic bars. The area of the membrane exposed to the solutions was 5.0 cm². The second cell was a large one the capacity of each half cell of which was about 300 ml and contained 250 ml of hot or cold 0.01 N *NaCl* solution. These solutions were kept very well stirred. Besides, the solutions at the two membrane solution interfaces were also kept well stirred by using teflon coated magnetic bars of different sizes. The area of the membrane exposed to the solutions in this cell was 2.86 cm². The results realized in these two cells when different stirring conditions were employed are given in Table 3. The values of P_a and P_b had an error of $\pm$ 3%.

The results given in Table 3 indicate a number of interesting features concerning the thickness of the boundary layers. The stirrers in the small cell were rotating at a distance of about 3 cm from the membrane faces whereas in the bigger cell they were rotating at a distance of about 12 cm. The values of P_t realized (Table 3, rows 1 and 2) are about the same. On the other hand, the thicknesses of the boundary layers are different (45 and 26 μ). These results in themselves are consistent. But they become fictitious in relation to the other values of P_a, P_b and P_t and the thickness of the stagnant layer when both the bulk solutions and the interfacial regions of the membrane are stirred (see Table 3, row 3). Stirring the interfacial

regions with small stirrers gave higher values for P_a, P_b and P_t. The value of P_t is nearly twice the value realized when only bulk solutions are stirred and the thickness of the boundary layer is larger than either of the thicknesses obtained when only bulk solutions in the two cells are stirred. Although the value of P_t is as it should be,

Table 3. *Permeability data for AMF C-104 membrane in Na and Ca forms*

Cell	Stirring conditions	Dimensions of stirring bars length · dia cm · cm	P_a Eq.(7) cm/sec · 10^4	P_b Eq.(7) cm/sec · 10^4	P_t Eq.(10) cm/sec · 10^4	δ Eq.(11) μ
		Membrane in *Na*-form				
Small H-cell Each half-cell contained 26 ml. Membrane area = 5 cm²	Only bulk solutions stirred 300 rpm*	1.6 · 1.0	3.46	1.96	4.52	45
Large H-cell Each half-cell contained 250 ml. Membrane area = 2.86 cm²	Only bulk solutions stirred 400 rpm*	2.5 · 1.1	3.95	2.14	4.67	26
Large cell	Bulk solution 400 rpm and interfacial stirring 300 rpm	2.5 · 1.1 1.0 · 0.3	4.73	3.18	8.82	72
Large cell	Bulk solution 400 rpm and interfacial stirring 300 rpm	2.5 · 1.1 1.6 · 1.0	7.92	4.86	12.60	31
		Membrane in *Ca*-form				
Large cell	Bulk solution 400 rpm and interfacial stirring 300 rpm	2.5 · 1.1 1.6 · 1.0	1.03	0.54	1.13	35

* The rpm's were determined with the help of a Strobotac, Type 1531 (General Radio Company, Concord, Mass.).

the value of δ (72 μ) points to the conclusion that when bulk solutions only are stirred the solutions at the membrane interfaces are quite stagnant and form, as it were, part of the membrane faces. When the size of the stirrers rotating at the membrane-solution interfaces is increased the values of P_a, P_b and P_t increased further (see Table 3, row 4) and the value of δ decreased to 31 μ. This means that the small stirrers used at the interfacial regions of the membrane were not providing adequate stirring. Use of higher stirring rates or even larger stirrers which could be rotated conveniently at the interfaces did not further reduce the thickness of the boundary layer and gave values for P_a, P_b and P_t which agreed with those given in Table 3 and row 4. So it is believed that the P_t value of $12.6 \cdot 10^{-4}$ cm/sec has been properly corrected for the presence of boundary layers. This is further confirmed by an indirect estimate of the upper limit of this value which is $19.4 \cdot 10^{-4}$ cm/sec (see discussion).

Ca-form of AMF C-104 membrane was also used in this "double membrane" technique to derive values for P_a, P_b, P_t and δ which are given in the last row of Table 3. The value of δ is close to the value realized with the *Na*-form of the membrane, AMF C-104.

Table 4. *Permeability and self diffusion coefficient data for membranes in contact with 0.01 N solution*

Membrane system	P_a Eq. (7) cm/sec · 10^4	D_i Eq. (1) cm²/sec · 10^5	P_i Eq. (8) cm/sec · 10^4	$\bar{P}_i$ Eq. (12) cm/sec · 10^6	Self diffusion coefficient $\bar{D}_i$ Eq. (13) cm²/sec · 10^7
			AMF A-100		
Cl^-	8.72	2.03	12.15	11.24	2.48
			AMF C-103		
Na^+	6.05	1.33	8.62	9.18	1.30
Rb^+	7.60	2.07	10.00	11.24	1.60
Cs^+	10.31	2.06	15.39	19.95	2.83
Ca^{2+}	0.90	0.79	0.97	1.02	0.14
			AMF C-104		
Na^+	7.92	1.33	12.60	12.87	1.93
Rb^+	10.98	2.07	16.90	19.20	2.88
Cs^+	11.00	2.06	17.00	21.00	3.15
Ca^{2+}	1.03	0.79	1.13	1.19	0.17

In the case of this membrane and other membranes in other ionic forms, only values of P_a shown in Table 4 were determined. Using 33 μ as the value for δ and the corresponding value of D calculated from eq. (1), i.e.

$$D_i = \frac{2.66 \times 10^{-7}}{z_i} \lambda_i \qquad \text{(at 25 °C)} \tag{1}$$

(where λ_i is the limiting equivalent conductance of the ion concerned[28]) in eq. (8), the values for P_i were calculated for the *Cl*-form of AMF A 100, *Na*, *Rb*, *Cs* and *Ca*-forms of AMF C-103 and *Rb* and *Cs*-forms of AMF C-104 membranes. All these values and those of D_i calculated according to the above equation are given in Table 4.

Although the values of P_i have been corrected for the boundary layers, they require a further correction in order to refer them to the membrane phase. This arises from the fact that the membranes, being charged, accumulate the mobile species according to the Donnan relation[28,29]

$$P_i C_i = \bar{P}_i \bar{C}_i, \tag{12}$$

where C_i is the external concentration of counterion (0.01 N), $\bar{C}_i$ is the concentration in the membrane and $\bar{P}_i$ is the true permeability of the membrane to the species concerned. The relationship of $\bar{P}_i$ to the diffusion coefficient $\bar{D}_i$ of the species is given by

$$\bar{P}_i = \frac{\bar{D}_i}{d}, \tag{13}$$

where d is the thickness of the membrane. The values of $\bar{D}_i$ calculated in this manner are given in the last column of Table 4.

Discussion

As the membranes used in this study have been used in earlier investigations[1,11] it is interesting to note that the values of the different parameters agree to a reasonable extent, the striking exception however being the values of the counterion diffusion coefficients which are all higher than the values reported in the earlier publications[1,11]. Despite the fact that good stirring was employed in those studies, it was not doing the job it was meant to do, as brought out in the present investigations. The discrepancy is evidently due to the

[28] R. Schlögl and F. Helfferich, Z. Elektrochem., Ber. Bunsenges. physik. Chem. 56 (1952) 644.

[29] R. Caramazza, W. Dorst, A. J. C. Hoeve and A. J. Staverman, Trans. Faraday Soc. 59 (1963) 2415.

existence of boundary layers which are not completely removed by the stirring of both bulk and interfacial solutions. That the present values of $\bar{D}_i$ are probably the true values can be inferred from an indirect check using the equations developed by SCATTERGOOD and LIGHTFOOT[20]. These equations are

$$l_w = (\bar{x}_w/\bar{D}_{1w})/[(\bar{x}_1/\bar{D}_{1w}) + (\bar{x}_m/\bar{D}_{wm})] \quad (14)$$

$$L_p = (\bar{x}_w \bar{C} \bar{V}_w^2)/[\{(\bar{x}_1 \bar{D}_{1w}) + (\bar{x}_m/\bar{D}_{wm})\} RTd] \quad (15)$$

$$k = (\bar{C}_1 F^2/RT)/[(\bar{x}_w/\bar{D}_{1w}) + (\bar{x}_m/\bar{D}_{1m}) - (l_w \bar{x}_1/\bar{D}_{1w})] \quad (16)$$

$$(1/\bar{D}_1) = [(\bar{x}_1 + \bar{x}_{1^*1})/\bar{D}_{1^*1}] + [\bar{x}_w/\bar{D}_{1w}] + [x_m/\bar{D}_{1m}], \quad (17)$$

where $\bar{x}_i$'s are mole fractions, D_{ij}'s are Stefan-Maxwell diffusivity coefficients, C is the total concentration of various species in the membrane, * indicates the radioactive isotope of the counterion 1, w and m represent water and membrane matrix respectively. Taking the case of AMF C-104 membrane in Na-form, the present $\bar{D}_1$ value is $1.93 \cdot 10^{-7}$ cm^2/sec in contrast to the value of $7.33 \cdot 10^{-8}$ reported earlier[1]. The counterion diffusion coefficient is related to the other Stefan-Maxwell diffusivity coefficients by eq. (17). As the equilibrium properties and the values of l_w and those of k of this study are close to the corresponding values determined in earlier studies[1,11], it is reasonable to assume that the values of L_p, the hydraulic permeability of the membrane, are also similar. Consequently the values of $\bar{D}_{1w}$, $\bar{D}_{1m}$ and $\bar{D}_{wm}$ evaluated earlier[1,11] usings eqs. (14—16) would remain practically unaffected; whereas the values of $\bar{D}_{1^*1}$ would be affected due to the fact that the values of $\bar{D}_1$ used in the calculations are not the true values. As the last two terms of eq. (17) are known, an upper limit to the value of $\bar{D}_1$ can be estimated from that equation. This value should be equal to $2.97 \cdot 10^{-7}$ cm^2/sec, i.e. $(1/\bar{D}_1) = (\bar{x}_w/\bar{D}_{1w}) + (\bar{x}_m/\bar{D}_{1m}) = 3.37 \cdot 10^6$ (see ref. [1] for the values of $\bar{x}_i$'s and $\bar{D}_{ij}$'s), as all other values greater than this would lead to absurd values (the values will be negative) for the term $(\bar{x}_1 + \bar{x}_{1^*1}/)\bar{D}_{1^*1}$. Consequently it is believed that the measured value of $1.93 \cdot 10^{-7}$ for $\bar{D}_1$ which appears to be reasonable compared to the theoretically possible maximum value of $2.97 \cdot 10^{-7}$ cm^2/sec is the true value. Accordingly the other values of $\bar{D}_1$ given in the last column of Table 4 are considered reasonable and close to the true values. Under the circumstances, the values for $\bar{D}_{1^*1}$ derived from $\bar{D}_1$ values given in the earlier publications[1,11] (all values of $\bar{D}_1$ are lower than the corresponding values given in

Table 5. *Corrected values of $\bar{D}_{1^*1}$ for different membrane systems*

	AMF A-100	AMF C-103			AMF C-104		
	Cl^-	Na^+	Rb^+	Cs^+	Na^+	Rb^+	Cs^+
$\bar{D}_{1^*1} \cdot 10^5$ (cm²/sec)	2.43	1.47	2.26	7.08	5.88	8.90	22.8

Table 4) are in error and therefore they are withdrawn. The corrected values of $\bar{D}_{1^*1}$ are given in Table 5.

The results of equivalent conductances given in Table 2 and of self diffusion coefficients given in Table 4 for the cation exchange membranes in different ionic forms present some interesting structural aspects concerning the two membranes, AMF C-103 and C-104. The ionic conductances of each membrane in different cation forms follow the sequence $Ca^{2+} < Na^+ < Rb^+ > Cs^+$. *Ca*-form of the membrane has the lowest conductance although the sequence of the limiting conductances of different ions in aqueous solutions is as $Na^+ < Ca^{2+} < Rb^+ > Cs^+$. This may be attributed to the greater association of Ca^{2+} ion, because of the presence of two charges on the ion, with two fixed negative charges on the membrane. The self diffusion coefficients corresponding to each membrane follow the sequence $Ca^{2+} < Na^+ < Rb^+ < Cs^+$. This sequence is the same as the sequence followed by the ionic conductances except for the Cs^+ ion whose conductance and self diffusion coefficient are respectively less and greater than those of Rb^+ ion. This may be due to the bigger size of the unhydrated Cs^+ ion which can sit at the entrance of a membrane pore and block it. This would lead to low conductance and high diffusion in relation to those of the Rb^+ ion.

An intrigueing aspect of the results of ionic conductances and self diffusion coefficients of the two membranes is the fact that the conductances of AMF C-103 membrane in different ionic forms are greater and the self diffusion coefficients are smaller than the corresponding values of the conductances and self diffusion coefficients of AMF C-104 membrane. This anomaly is very difficult to reconsile with the accepted notion that ionic conductance and self diffusion are governed by the same molecular mechanism, the basis on which eq. (1) is founded. In view of this, an explanation for the above anomaly is sought elsewhere. It is established from water flow measurements[30]

[30] N. Lakshminarayanaiah and M. S. White, J. Polymer Sci., Part A 7 (1969) 2235.

that the dimensions of the pore radii of AMF C-103 and C-104 membranes are 8.6 and 6.4 Å respectively and that there are more pores per unit membrane area in AMF C-104 membrane than there are in C-103 membrane. It is our belief (derived from working with these membranes over the years) that these membranes are inhomogeneous (see also Ref.[20]). Consequently, the chances are that there would be more uncharged and probably dead end pores in AMF C-104 membrane than there would be in AMF C-103 membrane. In such a situation the electrical conductance of C-104 membrane would be less than that of C-103 membrane; whereas its self diffusion coefficient would be greater due to isotope occupancy of the dead end pores.

The values of the self diffusion coefficients have been converted to equivalent conductances using eq. (1) and these values are given in Table 6. All these values are lower than the corresponding values of $\bar{\lambda}_i$ measured directly. This, as pointed out by earlier investigators[5–8], is due to electroosmosis whose contribution to conductance could be calculated from eq. (3). These values also are given in Table 6. The theoretical equivalent conductance calculated according to eq. (4) (see Table 6, column 4) in every case is less than the directly measured equivalent conductance. In order to allow close agreement between

Table 6. *Calculated and observed equivalent conductances of membranes in different ionic forms*

Membrane system	$\bar{\lambda}_i$ Eq. (1)	Electroosmotic contribution Eq. (3)	$\bar{\lambda}_{i\,(cal)}$ Eq. (4)	$\bar{\lambda}_{i\,(obs)}$ Eq. (5)	$\bar{\alpha}_i$ Eq. (6)
		AMF A-100			
Cl^-	0.93	0.144	1.07	1.95	7.08
		AMF C-103			
Na^+	0.49	0.230	0.72	1.81	5.73
Rb^+	0.60	0.174	0.77	2.21	9.25
Cs^+	1.06	0.150	1.21	2.17	7.39
Ca^{2+}	0.11	0.063	0.17	0.49	6.02
		AMF C-104			
Na^+	0.73	0.163	0.89	1.42	4.23
Rb^+	1.08	0.128	1.21	1.97	6.95
Cs^+	1.18	0.100	1.28	1.52	3.40
Ca^{2+}	0.13	0.047	0.18	0.38	5.31

the calculated and observed λ_i values, a drag factor $\bar{\chi}_i$ has been introduced by McHARDY et al.[9] [see eq. (6)] who found the values of $\bar{\chi}_i$ to be less than unity for counterions when the high water content membrane (ZeoKarb 315) was in the homoionic state. Similar calculations carried out for the different counterions used with various membranes of this study gave values for $\bar{\chi}_i$ (see Table 6, last column) which are all greater than unity and lie in the range 3–9. Low values for $\bar{\chi}_i$ and less than unity were attributed to, (a) counterion retardation due to its interaction with the polymer matrix, fixed charges and coions which opposed the forward drag of the electroosmotic flow, and (b) movement of water in the immediate neighbourhood of the counterions being slower than the average rate of electroosmotic flow. The reverse of factor (b), i.e. faster movement of water in the neighbourhood of counterions lined along the polymer chains will account for the high values realized for $\bar{\chi}_i$. But it is very difficult to visualize how this could arise. Even considering that all water associated with an equivalent of counterion in the membrane phase (see Table 1, column 4) is mobile, the calculated values of $\bar{\lambda}_i$ would still be less than the measured values. Our earlier studies[1,11] have shown that the interactions of counterions with the fixed charges of the membrane matrix are stronger than their interactions with water (see Table 4 of Ref. [1] and Table 3 of Ref. [11]). Consequently the mobile counterions will be aligned along the polymer chains to which the negative or positive groups are attached. Application of an electric field to measure counterion conductance in the membrane would lead to ion migration, some of which might occur along the surface of the polymer chains. This part of ion migration is similar to surface conduction which has been decribed in a few systems[31]. In view of the compact structure of the charged membrane, i.e. low water content, and the electrolyte environment in which the membrane is held, i.e. complete absence of coions in the liquid of the membrane pores, it becomes reasonable to assign a major portion of the measured conductance to ion migration occurring along the surface of the pores in the membrane. So it seems probable that surface conduction is involved in generating high values for $\bar{\alpha}_i$.

The work was supported in part by U. S. Public Health Service grant NB-08163.

[31] J. T. DAVIES and E. K. RIDEAL, Interfacial Phenomena, Academic Press, New York 1961, p. 108.

JOURNAL OF POLYMER SCIENCE: PART A-1 VOL. 8, 2949–2955 (1970)

Relationship Between Membrane Potential and Electrolyte Uptake by Ion-Exchange Membranes

N. LAKSHMINARAYANAIAH and FASIH A. SIDDIQI,*
Department of Pharmacology, University of Pennsylvania School of Medicine, Philadelphia, Pennsylvania 19104

Synopsis

Electrical potentials arising across three cation-selective membranes of low water content when they separate solutions of different concentration of the same NaCl electrolyte have been measured at 25°C. Also, electrolyte uptake by these membranes when they are in equilibrium with different soutions of NaCl has been estimated. These data together with the apparent membrane transport number derived from membrane potential have been used to check a simple relation given by Lakshminarayanaiah.

INTRODUCTION

The electrical potentials arising across membranes separating different salt solutions are usually measured by using cells of the type:

Reference electrode	Solution 1	‖ Membrane ‖	Solution 2	Reference electrode

The reference electrode may be a reversible electrode of the type Ag–AgCl in chloride solutions or calomel connected to the solutions through KCl–agar bridges. In the former case, the total potential is equal to the sum of electrode potential and membrane potential. In the latter case, the cell potential directly gives the membrane potential. These measurements are not unambiguous as they involve all the extra nonthermodynamic assumptions about single-ion activity coefficients, diffusion potentials at KCl bridges, etc. These measurements are taken as routine to characterize the selectivity of membranes.[1]

The membrane potential measured at different concentrations, C_1 and C_2 ($C_2 > C_1$), of the same electrolyte is related to the transport number of the cation in the case of cation-exchange membrane by the relation:

$$\bar{t}_{+(app)} = (E/2E_{max}) + 0.5 \qquad (1)$$

* On study leave from the Department of Chemistry, Aligarh Muslim University Aligarh, India.

where E is the membrane potential measured by using calomel electrodes and KCl–agar salt bridges, E_{max} is the theoretically possible maximum value of the membrane potential given by the equation:

$$E_{max} = \left(\frac{RT}{F}\right) \ln (a_1/a_2) \tag{2}$$

where a_1 and a_2 are the activities of the two solutions of concentrations C_1 and C_2 and R, T, and F have their usual significance. The cation transport number given by eq. (1) is not a true value as it does not take into account the transfer of water and so is called the apparent transport number $\bar{l}_{+(app)}$. This has been related to the true transport number ($\bar{l}_+$) by two treatments which are reviewed elsewhere by Lakshminarayanaiah.[2] Treatment one gives the relation,[2-4]

$$\bar{l}_+ = \bar{l}_{+(app)} + 0.018 m_\pm \bar{l}_w \tag{3}$$

where $\bar{l}_w$ is the transport number of water and $m_\pm$ is the mean molality of the solution used in the measurements. Treatment two, originally given by Oda and Yawataya[5] is expressed by Arnold and Swift[6] in the form

$$\bar{l}_+ = \left(\frac{\bar{l}_w}{\bar{W}_e}\right)(1 + S) + \bar{l}_{+(app)} [1 - (\bar{l}_w/\bar{W}_e)] \tag{4}$$

where $\bar{W}_e$ is the number of moles of water per equivalent of fixed ion-exchange site in the membrane and S is the equivalent of coions per equivalent of fixed site sorbed by the membrane.

Lakshminarayanaiah,[2] working with crosslinked phenol sulfonate membranes of high water content (>50%) showed that eqs. (3) and (4) generated identical values for $\bar{l}_+$ and consequently the two equations were considered equivalent, leading to a simple relationship between electrolyte uptake and $\bar{l}_{+(app)}$, viz.,

$$m_\pm = \bar{X}_m [S + \bar{l}_{-(app)}] \tag{5}$$

where $\bar{X}_m$ is the number of equivalents of fixed groups associated with 1000 g of membrane interstitial water and $\bar{l}_{+(app)} + \bar{l}_{-(app)} = 1$. In this paper, electrolyte uptake, membrane potential and other relevant measurements are presented to check the validity of eq. (5) in the case of three cation-exchange membranes of low water content (<22%).

EXPERIMENTAL

Membranes

Three cation-exchange membranes of different water content and exchange capacity were used in this study. Polyethylene–styrene graft copolymer type AMF C-104 membrane containing sulfonic acid groups was supplied by the American Machine and Foundry Company. The other two membranes were prepared from Parlodion [purified pyroxylin (nitrocellulose), Mallinckrodt] and sulfonated polystyrene (SPS) following

the method reviewed by Neihof.[7] A 2% solution of Parlodion (P) in alcohol–ether (3:1) containing 0.25 g of SPS was used to prepare a P-SPS membrane of high charge density. Again, 2% P solution containing 0.025 g of SPS was used to prepare a P-SPS membrane of low charge density. About 10 ml of the P-SPS solution was spread on a clean, dry glass plate by using a Boston-Bradley doctor blade (Gardner Laboratory, Bethesda, Md). The solution was allowed to dry in air for about 3 hr and then dried in an oven at 80°C for another hour, after which the membrane was removed from the glass plate under water. The doctor blade was adjusted to give a membrane, about 0.02 mm thick, after drying. The AMF membrane was about 0.12 mm thick. All the membranes were conditioned in deionized water and converted to the Na form by equilibrating them with 1N NaCl solution. These membranes were washed thoroughly with deionized water and equilibrated with the required NaCl solution with frequent solution changes.

Water Content

Pieces of membrane equilibrated with the appropriate NaCl solution were blotted with filter paper, placed in a weighing bottle and weighed. They were then dried to constant weight in a vacuum desiccator at 70°C. The accuracy of this measurement was ±5%.

Exchange Capacity and Coion Uptake

A known weight of surface dried membrane already equilibrated in the required NaCl solution was treated with exactly 10 ml of 0.1*N* HNO_3 solution and kept stirred for about 24 hr. The liquid was decanted carefully and the membrane was washed a number of times with deionized water. The decanted liquid with the washings was analyzed for its acid content in the usual way. The chloride was estimated by using Aminco-Cotlove automatic chloride titrator (American Instrument Company, Silver Spring, Md.). The overall accuracy of these estimations was determined by the homogeneity of the membranes used, and we therefore estimate the accuracy of these measurements to be ±5%.

Membrane Potential

These measurements were made following the procedures described elsewhere.[8] Calomel and KCl–agar bridges were used in the measurements. Here again, for any given membrane, although the potentials could be measured accurate to ±0.5 mV on the 30-mV scale of a 151 Keithley microvoltmeter, the overall accuracy (about 5%) was determined by the different membranes used in the measurements.

RESULTS AND DISCUSSION

The different equilibrium parameters determined for the membranes as a function of external electrolyte concentration are given in Table I

and the membrane potentials are given in Table II. The $l_{+(app)}$ values calculated from eq. (1) are related to the molality of the external solution by the interpolation procedure described by Oda and Yawataya[8] and illustrated by Lakshminarayanaiah.[2] The values of $l_{+(app)}$ so derived and re-

TABLE I
Parameters for the Membrane in Equilibrium with NaCl Solution at 25°C

Parameter	Electrolyte solution, N	AMF C-104	High-charge P-SPS	Low-charge P-SPS
Water content, g/100 g wet membrane	0.001	13.0	21.0	8.5
	0.01	13.0	20.8	8.0
	0.1	12.5	20.5	7.5
	0.5	12.0	19.0	7.0
Exchange capacity, meq/g wet membrane	0.001	0.560	0.410	0.037
	0.01	0.500	0.420	0.038
	0.1	0.504	0.437	0.039
	0.5	0.558	0.445	0.040
Chloride (coion) uptake, meq/g wet membrane	0.001	0.4×10^{-3}	1.5×10^{-3}	1.5×10^{-3}
	0.01	1.1×10^{-3}	2.1×10^{-3}	2.3×10^{-3}
	0.1	1.6×10^{-3}	4.6×10^{-3}	6.4×10^{-3}
	0.5	9.1×10^{-3}	12.8×10^{-3}	6.8×10^{-3}

TABLE II
Emf's across Membrane Cell at 25°C

Hg, Hg_2Cl_2 | Saturated KCl-agar | NaCl (m_1) || Membrane || NaCl (m_2) | Saturated KCl-agar | Hg_2Cl_2, Hg

				Emf, mV		
m_1	m_2	a_1	a_2	AMF C-104	High-charge P-SPS	Low-Charge P-SPS
0.001004	0.002004	0.00098	0.00193	17.4	16.8	12.5
0.002004	0.005005	0.00193	0.00473	22.3	21.8	14.8
0.005005	0.1005	0.00473	0.00932	16.7	16.2	11.8
0.01005	0.02005	0.00932	0.0180	16.0	15.5	11.5
0.02005	0.05006	0.0180	0.0428	21.0	19.6	12.5
0.05006	0.1006	0.0428	0.0783	14.5	12.5	9.8
0.1006	0.2026	0.0783	0.148	14.0	11.3	8.5
0.2026	0.5066	0.148	0.344	18.2	13.0	10.5
0.5066	1.024	0.344	0.666	12.8	8.0	7.3

lated to the concentration of the external solution are given in Figure 1 for the three membranes. The values of $m_{\pm}$, $\bar{X}_m$, and S derived from the results of Table I are given in Table III. From these values $l_{-(app)}$ is calculated using eq. (5). These calculated values of $l_{+(app)}$ along with

TABLE III
Parameters for the Membrane in Contract with NaCl Solution

Membrane	External solution molality $m_{\pm}$	$\bar{X}_m$, eq/1000 g water	m_{Cl^-}, eq/1000 g water $\times 10^{-3}$	S, eq (Cl-) per eq. of $\bar{X}_m \times 10^{-3}$	$l_{-(app)}$ [eq. (5)] $\times 10^{-3}$	$l_{+(app)}$ Calcd	$l_{+(app)}$ Found
AMF C-104	0.001004	4.31	3.1	0.7	−0.5	1.001	0.999
	0.01005	3.84	8.2	2.1	+0.5	1.000	0.976
	0.1006	4.02	12.8	3.2	+1.8	0.998	0 954
	0.5066	4.65	75.8	16.3	+92.7	0.907	0.905
High-charge P-SPS	0.001004	1 95	7.2	3.6	−3.0	1.003	0.985
	0.01005	2.02	10.1	5.2	−0.03	1.000	0.962
	0.1006	2.13	22.4	10.5	+36.7	0.963	0.884
	0.5066	2.39	67.4	28.2	+184	0.816	0.776
Low-charge P-SPS	0.001004	0.44	17.6	40.6	−38.0	1.038	0.963
	0.01005	0.48	28.5	60.1	−39.0	1.039	0.840
	0.1006	0.52	84.7	163	+30.0	0.970	0.796
	0.5066	0.57	97.0	170	+715	0.285	0 733

those values derived from membrane potential measurements are also given in Table III.

Comparison of the results given in the last two columns of Table III indicate that the calculated values of $\bar{l}_{+(app)}$ [eq. (5)] are close (within 5%) to the corresponding observed values in the case of AMF C-104 membrane; whereas in the case of the other P-SPS membrane of high charge density, the agreement lies between 2 and 10%. In the case of the P-SPS membrane of low charge density, the agreement is poor, although in the very dilute region the divergence is about 7%. This study restricted to one

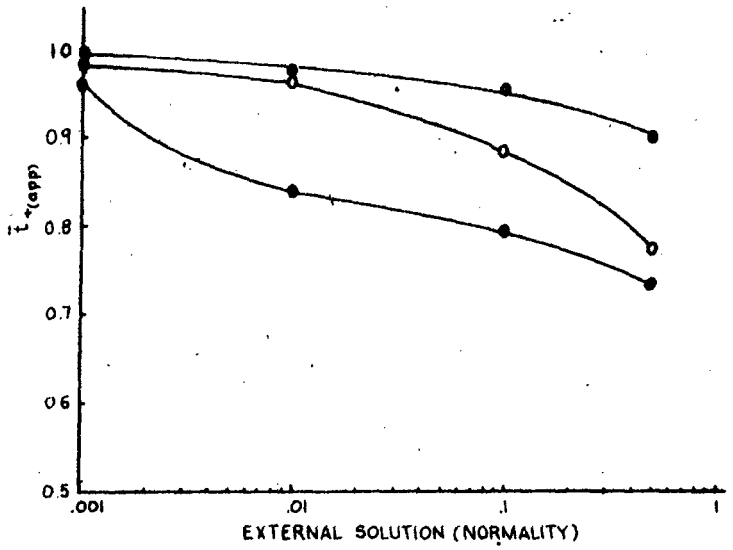

Fig. 1. Apparent transport number [$\bar{l}_{+(app)}$] derived from membrane potential data related to the external solution concentration: (⊕) AMF C-104 membrane; (○) P-SPS membrane of high charge density; (●) P-SPS membrane of low charge density.

electrolyte and three membranes of low water content (<22%) leads to the conclusion that eq. (5) could be used, in the case of high charge density membrane, to predict values for $\bar{l}_{+(app)}$ (within 10%) from the electrolyte content of the membrane phase. It seems to be inapplicable to membranes of low charge and low water content. Whether it can predict values for membranes of low charge and high water content requires further investigation.

The work was supported by Public Health Service Grant NB-08163-01.

References

1. N. Lakshminarayanaiah, *Transport Phenomena in Membranes*, Academic Press, New York, 1969, p. 196.
2. N. Lakshminarayanaiah, *J. Phys. Chem.*, **73**, 07 (1969).
3. D. K. Hale and D. J. McCauley, *Trans. Faraday Soc.*, **57**, 135 (1961).

4. V. Subrahmanyan and N. Lakshminarayanaiah, *J. Sci. Ind. Res.* (India), **21B**, 229 (1962).
5. Y. Oda and T. Yawataya, *Bull. Chem. Soc. Japan*, **29**, 673 (1956).
6. R. Arnold and D. A. Swift, *Austral. J. Chem.*, **20**, 2575 (1967).
7. R. Neihof, *J. Phys. Chem.*, **58**, 916 (1954).
8. N. Lakshminarayaniah and V. Subrahmanyan, *J. Polym. Sci. A*, **2**, 4491 (1964).

Received February 17, 1970

CHAPTER 3

ELECTROCHEMISTRY OF BILAYER LIPID MEMBRANES (BLM)

Topics of Bioelectrochemistry and Bioenergetics Volume 5
Edited by G. Milazzo

BIOELECTROCHEMISTRY
and
BIOENERGETICS

Electrochemistry of Bilayer Lipid Membranes

F. A. SIDDIQI and H. TI TIEN
Biophysics Department, Michigan State University, East Lansing, Michigan 48824 (USA)

John Wiley & Sons, Inc.
New York London Sydney Toronto

Topics of Bioelectrochemistry and Bioenergetics Volume 5
Edited by G. Milazzo

BIOELECTROCHEMISTRY *and* BIOENERGETICS

Electrochemistry of Bilayer Lipid Membranes

F. A. SIDDIQI and H. TI TIEN
Biophysics Department, Michigan State University, East Lansing, Michigan 48824 (USA)

John Wiley & Sons, Inc.
New York London Sydney Toronto

Topics of Bioelectrochemistry and Bioenergetics Volume 5
Edited by G. Milazzo

Electrochemistry of Bilayer Lipid Membranes

F. A. SIDDIQI and H. TI TIEN

Biophysics Department, Michigan State University, East Lansing, Michigan 48824 (USA)

Contents

1. Introduction

The basic structure of all biological membranes appears to be unique and possesses a common design with lipids in the form of a bilayer, with proteins *floating* about or spanning across the bilayer, and with other constituents such as

pigments, if present, organized in some array in the bilayer. The strongest experimental evidence in support of such a supposition is provided by the electron microscopy of biological membranes and organells (ZINGSHEIM[1], WEISSMANN and CLAIBORNE[2], BAUMEISTER and HAHN[3]).

Since biological membranes are ultrathin structures, and composed mainly of two classes of compounds, lipid and proteins, it is obvious that the chemical composition and thickness of any adequate model should be similar to those of biological membranes. A good experimental model should therefore possess a lipid bilayer structure, onto which proteins, pigments and the like can interact. Biological membranes generally exist as liquid structures bound on either side by an aqueous phase; thus there are two coexisting liquid|liquid interfaces (or a biface) associated with each membraneous structure. Furthermore, many biological membranes have been shown to function in a vectorial or directional manner, *e.g.*, glucose accumulation in red blood cells by carrier-facilitated or active transport. These characteristics impose corresponding requirements on any model membrane system. It has been evident for some time that if the lipid bilayer were indeed the major structural component of biological membranes, knowledge concerning the properties and the formation of such a structure *in vitro* would be of considerable significance, both experimentally and theoretically. It was readily apparent that a detailed physicochemical description of biological membranes would be best approached by studies of simpler well-defined models.

The search for a more realistic model has led to the discovery of a method for forming bilayer lipid membranes (BLM) in aqueous media in 1960.[4] The details have been described in the monographs on BLM by JAIN[5], TIEN[6], and in numerous reviews BANGHAM[7], ANTONOV *et al.*[8], PAPAHADJOPOULOS[9], MARKIN and CHIZMADZHEV[10], OHKI[11], DE LEVIE[12], ANDERSEN[13], SHAMOO and TIVOL[14].

Bilayer lipid membranes (BLM) can now be formed in aqueous media from a variety of materials. These materials include brain lipids, proteolipids, purified phospholipids, oxidized cholesterol, synthetic surfactants, chloroplast extracts, carotenoid pigments, and synthetic amphiphiles[6,15,16]. The intrinsic properties of unmodified BLM (*e.g.*, formed from either egg lecithin, or oxidized cholesterol) in 0.1 *M* NaCl are similar to those expected from an ultrathin layer of liquid hydrocarbon. Upon the introduction of additives to the BLM system, the intrinsic or passive properties of the BLM can be drastically modified. Categorically, the BLM modifiers may be divided into five groups:

(*a*) those that alter the passive electrical properties,
(*b*) those that change the mechanical properties,
(*c*) those that confer ion selectivity,
(*d*) those that induce electrical excitability, and
(*e*) those that generate photoelectric effects.

The modified BLM systems at present constitute realistic experimental models for a variety of biological membranes[6]. Biologically relevant phenomena such as

excitability, ion selectivity, antibody-antigen reaction, active ion transport, and photoelectric effects have been demonstrated. The light-induced phenomena in photoactive BLM provide strong evidence for the existence of electronic charge carriers in the membrane immersed in aqueous solution.

Unmodified BLM's have been found to represent a high energy barrier for ions. The energy barrier arises mainly as a result of the electrostatic energies of the charged species in the membrane and the aqueous phase having unequal dielectric constants. From BORN's electrostatic equation, one can evaluate the value of the energy barrier, E, which is given by

$$E = \frac{Q^2}{8\pi r}\left(\frac{1}{\epsilon_m} - \frac{1}{\epsilon_w}\right)$$

where Q and r are the charge and radius of the ion, and ϵ_m and ϵ_w are the dielectric constants of the membrane and the aqueous phase, respectively. Substituting reasonable values into the BORN equation, E is in the order of 1 eV ($\sim 40\,kT$). The BORN equation indicates that the energy barrier is inversely proportional to the size of the charged species and higher barrier for polyvalent ions. Electrically, the BLM is equivalent to a parallel arrangement of a resistor (R_m) and capacitor (C_m). Typical values for R_m and C_m are, respectively, 10^8–$10^{10}\,\Omega\,cm^2$ and 0.3–1 $\mu F\,cm^{-2}$.

The high BLM resistance may be lowered by many orders of magnitude in the presence of a host of compounds, the well known ones are considered in detail in this review. These interesting compounds interact with the hydrophobic interior of BLM in one of the two ways:

(*i*) increasing the ion concentration in the membrane by means of complex formation (*i.e.*, ion carrier), and

(*ii*) interrupting the lipid bilayer by means of pore (channel) formation through the membrane.

Extensive experimental work with BLM has, in the past decade, firmly established these mechanisms as the molecular basis of ion transport across membranes.

Recent studies on BLM, not covered in this paper or found in the previous reviews are listed here for the interested reader. WHITE[17] discussed the physical chemistry of BLM relating to biological membrane organization. The interfacial tension of BLM was given a statistical mechanical analysis by SUEZAKI[18] and was experimentally measured by KOZA *et al.*[19] and SNYDER *et al.*[20]. Other physical properties have been reported by WALDBILLIG and SZABO[21], LIN[22], NAGLE and SCOTT[23]. Permeability and diffusion characteristics have been investigated by TVERDISLOV *et al.*[24], JONES and NICKSON[25], KAISER *et al*[26], ROSENBERG and FINKELSTEIN[27], and WALTER and GUTKNECHT[28]. BLM containing chlorophylls or bacteriorhodopsin have been reported in several papers (DANCSHAZY *et al.*[29], FRAGATA[30], HERMANN and RAYFIELD[31], HONG[32]). In addition, SCIBONA *et al.*[33] reported non-isothermal potentials of BLM and GRUPE *et al.*[34] studied the effect of quaternary

tri-alkyl-ammonium halides on BLM. In another interesting paper ROHR and ROONEY[35] have described the influence of ultrasound on BLM. Finally, a number of original papers on or related to BLM have recently appeared (KUNITAKE and YAMADA[36], HO *et al.*[37], GROTE *et al.*[38], BERESTROVSKY *et al.*[39], SHAMOO[40], SZUNDI[41], KAFKA *et al.*[42], KOSSI and LEBLANC[43], THOMPSON *et al.*[44], KORYTA[45], EBIHARA *et al.*[46], FETTIPLACE and HAYDON[47], GRUEN and HAYDON[48], REPKE *et al.*[49], YOSHIDA *et al.*[50], DELY *et al.*[51], REIG *et al.*[52], KHARITONENKOV *et al.*[53]).

2. Membrane interfaces

2.1. *Electrical double layer theory and BLM*

The essence of all membrane models is to allow the polar groups of the phospholipid bilayer and those of membrane protein to project into the aqueous phases surrounding them (membrane|solution interfaces). At physiological pH the polar groups are considered to be mostly negatively charged and some water molecules are associated with them. To maintain electroneutrality, cations (counterions) which are probably hydrated must be adjacent to the negative groups and form an electrical double layer which is characteristic of all phase boundaries. The extrapolation of the concepts of membrane|solution interface which have been evolved over the years by electrochemists for the double layer existing at the metal electrode-solution interface is illustrated in Fig. 1. In the compact part of the double layer there will be a few co-ions (ions of the same charge as that of the membrane) and the concentration of counterions will be high compared to the concentration in bulk solution. As one enters the diffuse part of the double layer, counter- and co-ions coexist.

Two broad aspects of the electrical phenomena at interfaces deserve attention. The first refers to the consequences of having electrical charges at the interface in an electrolyte solution and the second concerns the nature of the electrical potentials that occur at phase boundaries. GOUY-CHAPMAN treated this problem and derived a relationship between the potential across the double layer, surface charge, and concentration of ions in solution (see PAYNE[54] for a recent discussion). This theory has been applied in recent years to membranes (TIEN and DIANA[55]; TIEN[6]; McLAUGHLIN *et al.*[56]) to explain shifts in conductance-voltage relations following changes in the concentration of ions and in so doing has been used to derive values for the density of charges present on the membrane (GILBERT and EHRENSTEIN[57], MOZHAYERA and NAUMOV[58], MULLER and FINKELSTEIN[59], LAKSHMINARAYANAIAH[60]). A brief account of the relations and their applications are given below.

If U is the potential at a distance x from the membrane interface the local concentration n_i of ion i of valence z_i will be

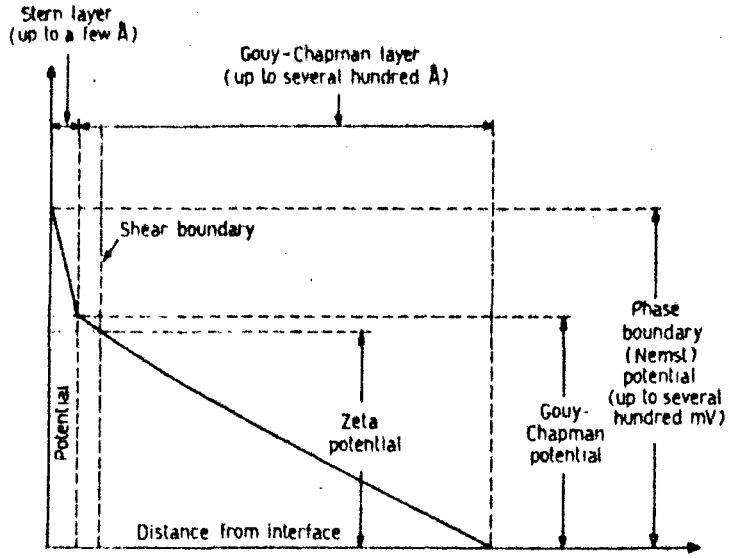

Fig. 1. A graphic representation of an electrical double layer. The fixed charges and counterions are not shown. The phase boundary potential is also known as the total interfacial potential.

$$n_i = n_i^0 \exp\left(\frac{-z_i e U}{kT}\right) \tag{1}$$

where n_i^0 refers to the bulk average stoichiometric concentration; e, the electronic charge; k, BOLTZMANN's constant; and T, the absolute temperature. The net charge density $\rho(x)$ at point x is given by

$$\rho(x) = \sum_i z_i e n_i^0 \exp\left(\frac{-z_i e U}{RT}\right) \tag{2}$$

if ion distribution is governed by only electrostatic interactions. In equation (2) n^+ and n^- are the numbers of cations and anions per unit volume. POISSON's equation relates U in one dimension to ρ by the equation

$$\frac{d}{dx}\left(\frac{dU}{dx}\right) = -\frac{4\pi\rho(x)}{\epsilon} \tag{3}$$

where ϵ is the dielectric constant.

Equation (3) takes into account any variation ϵ in the double layer as a function of x. Substitution of equation (2) in equation (3) gives

$$\frac{d}{dx}\left(\frac{dU}{dx}\right) = -\frac{4\pi e}{\epsilon}\sum n_i^0 z_i \exp\left(\frac{-x_i e U}{kT}\right) \tag{4}$$

using $\epsilon = \bar{\epsilon}$, a mean value of ϵ in the double layer (the value of ϵ is not very sensitive to variation of x except in the close vicinity of the membrane interface) and the identity

$$2\frac{d^2U}{dx^2} = \frac{d}{dU}\left(\frac{dU}{dx}\right)^2 \tag{5}$$

equation (4) gives on integration

$$\frac{dU}{dx} = \frac{8\pi kT}{\bar{\epsilon}}\sum_i n_i^0\left[\exp\left(\frac{-z_i e U}{kT}\right) - 1\right]^{1/2} \tag{6}$$

for the boundary conditions

$$U(x) = U_0 \text{ at } x = 0; \qquad \frac{dU}{dx} = 0 \text{ at } x = \infty.$$

The surface charge density σ on the membrane is related to $\rho(x)$ by

$$\sigma = -\int_0^\infty \rho(x)\,dx. \tag{7}$$

If a is the distance of closest approach of the ions to the membrane, then integration of equation (3) and substitution into equation (7) gives the relation

$$\sigma = \frac{\epsilon a}{4\pi}\left(\frac{dU}{dx}\right)_{x=a} \tag{8}$$

for the electric field at a, where ϵ_a is the dielectric constant in the region $x \leq a$. Equating ϵ_a to $\bar{\epsilon}$, although this assumption is unsatisfactory at the membrane surface, and substituting equation (8) in equation (6) gives, on rearrangement

$$\sigma = \frac{kT\bar{\epsilon}}{2\pi}\sum_i n_i^0\left[\exp\left(\frac{-z_i e U}{kT}\right) - 1\right]^{1/2}. \tag{9}$$

In most work, $\bar{\epsilon}$ is generally equated to the dielectric constant of bulk water, although this is considered very unsatisfactory. Expressing n_i as $c_i N_A/1000$ (where N_A is the Avogadro number and c_i the bulk solution concentration, moles per liter), σ as the surface charge density in electronic charges per square angström, and $U = U_0$ at $x = a$, equation (9) at 22 °C becomes

$$\sigma = \frac{1}{272}U_0\left\{\sum_i e_i\left[\exp\left(\frac{-z_i e U_0}{kT}\right) - 1\right]\right\}^{1/2}. \tag{10}$$

This equation becomes

$$\sigma = \frac{\sqrt{c}}{136}\sinh\frac{z\mathcal{F}U_0}{2RT} \tag{11a}$$

for ions of valence z, and

$$\sigma = \frac{1}{272}\left[c_+\left(\exp\left\{\frac{\mathcal{F}U_0}{RT}\right\} + \exp\left\{-\frac{\mathcal{F}U_0}{RT}\right\} - 2\right) + c^{2+}\left(2\exp\left\{\frac{\mathcal{F}U_0}{RT}\right\} + \exp\left\{-\frac{2\mathcal{F}U_0}{RT}\right\} - 3\right)\right]^{1/2} \quad (11b)$$

for solutions containing (1:1) and (2:1) electrolytes.

In the foregoing considerations, the binding of divalent ions to negative sites on the membrane was ignored. GILBERT and EHRENSTEIN[57] and McLAUGHLIN *et al.*[61], have taken into account by considering the relation

$$[C^{2+}] + [S^{2-}] = [CS]; K_a = \frac{[CS]}{[C][S]} \quad (12)$$

where $[C^{2+}]$ is the concentration of divalent cation at the membrane containing sites of concentration $[S^{2-}]$ and K_a is the association constant (liters per mole). The relation between the maximum charge density on the membrane (σ_{max}) in the absence of divalent ions to that (σ) in the presence of the ion is given by

$$\sigma = \frac{\sigma_{max}}{1 + K_a[C^{2+}]_{bulk}\exp\left[-2\mathcal{F}U_0/(RT)\right]}. \quad (13)$$

Equations (12) and (13) have been used to evaluate both σ_{max} and K_a. In the above treatment, it has been generally stressed that the values derived for σ refer to the region of the membrane at which ionic channels exist. Whether the charge density near the channel region (assumption of membrane inhomogeneity, *i.e.*, discrete distribution of charge) indicates also the charge density of the whole membrane (assumption of homogeneity, *i.e.*, uniform charge distribution) requires some other independent evidence, although the two models (discrete and uniform) for the distribution of charges on the membrane have been theoretically considered by BROWN[62]. He has shown that the uniform-charge and *open-portal* (mouth of the channel uncharged) models describe the behavior of the biological membranes better than the *charged-portal* model. Further it has been shown that the spacing between charges according to the discrete model, is about two thirds the spacing predicted by the uniform model, although both models predict equal affinities of either monovalent or divalent cations to the membrane sites. The resolution of these minor but important (from the point of view of channel structure) differences rests on an independent method of estimation of charge density based on the uniform-charge model. Such a procedure has been described by LAKSHMINARAYANAIAH[60] as well as by SIDDIQI[63] *et al.*, who applied the theories of membrane potential developed earlier (KOBATAKE *et al.*[64], BUCK[65]) for the determination of thermodynamically effective fixed charge density of model membrane systems.

One of the notable applications of the double layer theory to membrane

electrochemistry is in the estimation of pH at membrane interface (SACHS[66]) which is usually different from the pH of the bulk solution. The bulk and membrane interface pH is related by equation (1) by letting $n_i = [H]_i$, the hydrogen ion concentration at a negatively charged membrane, $n_i^0 = [H]_b$, the hydrogen ion concentration in the bulk phase and remembering $pH = -\log [H]$, one obtains

$$[pH]_i = [pH]_b + \frac{eU_0}{2.3kT}. \tag{14}$$

Equation (14) shows that only when $U_0 = 0$, there is no difference between interface and bulk pH. Therefore, for a negatively charged membrane the pH at the interface is lower than $[pH]_b$. The *correct* value may be obtained if U_0 is known. In general, U_0 could be estimated in terms of the zeta potential (ξ), the electrical potential at the plane of shear. For example, PAPAHADJOPOULOS and WATKINS[67] have found a reasonable agreement between the values calculated from equation (14) and the electrophoresis measurements on spherical bilayer lipid membranes (liposomes). Recently, VAZ *et al.*[68], using a fluorescent pH indicator (dimyristoyldansylcephalin) estimated the pH adjacent to the BLM interface and have found that the hydrogen ion concentration is electrostatically enhanced, the enhancement being dependent on the interface charge density and bulk phase salt concentration. Their results suggest that the dansyl chromophore is located at the charged membrane interface.

BRENNER *et al.*[69] find that image forces have a small effect on the capacitance of a single conducting planar electrode. For example, at a bulk salt concentration of 0.1 *M* the surface charge density required to maintain a 25 mV surface potential is 8 % higher when imaging is included in the calculation than when imaging is neglected. The repulsive pressure between two electrodes at such a salt concentration and surface potentials is decreased by 4 % when imaging at one of the electrodes is taken into account. The decrease in force is roughly independent of the separation between the electrodes. This independence suggests that only the effective coefficient of the pressure is altered by the inclusion of imaging; the distance dependence of the interaction is not affected. The effects of imaging are usually more pronounced at high bulk salt concentration; at a given salt-concentration the largest effects occur at small separations between the plates.

2.2. *Transmembrane potentials of BLM*

OHKI[11,70] proposed another type of theory of transmembrane potential for asymmetric membrane. This membrane potential arises from the difference between two diffuse surface potentials on two sides of membrane which are produced by the fixed charges at the membrane surface and the surrounding electrolyte solution. The following membrane system may exhibit this membrane potential, that is, a membrane can be considered to be impermeable to ions

compared to the diffusion of ions in the aqueous phase. The membrane has a hydrophobic interior and hydrophilic surface facing electrolyte solution phases. If one surface of the membrane is different from the other membrane surface with respect to their surface charges, two different diffuse double layer potentials would be produced on two different sides of the membrane. Assuming that there is no potential gradient in the membrane, a potential on one side of the membrane away from the membrane surface would be different from that on the other side of the membrane. A phospholipid bilayer system which has asymmetrical distribution with the surface charges might correspond to one which demonstrates such a membrane potential. OHKI[70] observed the membrane potential with asymmetrical phospholipid membranes consisting of acidic phospholipids in which one surface of the membrane is charged differently from the other surface. The two surface charge densities are designated by σ and σ'. Using linearized POISSON's equation, OHKI[70] obtained the following relation between membrane potential U_m and surface charge densities σ and σ'.

$$U_m = \frac{4\pi d}{\epsilon_1}\left(\frac{\sigma - \sigma'}{2 + (\epsilon_0 \kappa d/\epsilon_1)}\right) \tag{15}$$

where κ is the DEBYE-HÜCKEL constant, ϵ_0 and ϵ_1 are the dielectric constant of the medium and that of the membrane respectively, and d is the thickness of the membrane. If $(\epsilon_0 \kappa d/\epsilon_1) \ll 2$ (in BLM prepared in 0.1 M NaCl this condition holds), equation (15) is approximately reduced to

$$U_m = \frac{4\pi}{\epsilon_0 \kappa}(\sigma - \sigma'). \tag{16}$$

Equation (16) gives the membrane potential U_m which results from the charge asymmetry of the membrane. The following relation exists among δ, q, q', and the surface charge densities (σ, σ').

$$\frac{e\delta}{A} = \frac{e(q - q')}{A} = \sigma - \sigma'. \tag{17}$$

Where A is the unit area (as a convenience $A = 50\ \text{Å}^2$, e is the electronic charge, q the coefficients of fixed charge per unit area A. Therefore, δ is defined by the difference between two coefficients of fixed charges of the membrane surfaces.

3. Ionic adsorption and conductance of BLM

3.1. *Simple square-barrier constant field approximation*

It has become obvious that many membrane-permeable ions are strongly adsorbed at the membrane|water interfaces. Ionic adsorption changes the surface

charge density, and hence the aqueous diffuse double layers adjacent to the membrane. Such ionic adsorption may also modify the so-called dipole potential, an effect which can be observed in pure form with neutral molecules. DE LEVIE[12] has recently considered specifically ionic effects, which appear to play a significant role in the adsorption onto phospholipid membranes of, *e.g.*, substituted phenols (SMEJTEK *et al.*[71]), and local anesthetics (McLAUGHLIN[72]). DE LEVIE[12] has used simple square-barrier constant field approximation to describe ion permeation through the BLM.

The permeability of ions through BLM is effected by ionic adsorption. The surface excess of adsorbed ions Γ is given by

$$\Gamma = c_w \exp\left(-\frac{\Delta G_{ads}}{RT} - \frac{n\mathcal{F}U_o}{RT}\right). \tag{18}$$

In equation (18) Γ denotes the surface excess of adsorbed ions, c_w the corresponding aqueous concentration just outside the aqueous space charge layer, U_o the potential difference between the bulk aqueous solution and the adsorption site, and ΔG_{ads} the GIBBS energy of adsorption of the ion onto the membrane. There is every reason to believe that membrane-soluble ions can be adsorbed partially or completely at the lipid side of the water|membrane interface, because there they can interact hydrophobically while experiencing only a fraction of the full BORN repulsion of the middle of the membrane (KETTERER *et al.*[73]). It is therefore even more pertinent with membranes than it is with metals to consider the possible presence of a charge-free interfacial region between the aqueous diffuse double layer and the plane of adsorbed surface charge density, quite analogous to Stern's compact double layer.

The importance of the compact double layer potential has recently been emphasized in connection with the adsorption of tetraphenylborate. DE LEVIE[12] obtained various expressions for the dependence of conductance on concentration. The slope of the curve of direct current *versus* direct voltage, the so-called *d.c.* conductance, is usually determined for BLM interposed between the two aqueous solutions of identical composition. In such experiments, the membrane composition is usually also symmetrical (*i.e.*, the same on both sides), and the ionic strength of the aqueous solutions is typically kept constant with inert electrolyte when the concentration of the adsorbing species is varied.

The effect of concentration on conductance has recently been studied by DE LEVIE[12]. He has derived various expressions to show that as the concentration c_w of the absorbing ion in the aqueous phase is increased, at constant ionic strength, the dependence of the conductance on c_w changes from a strict proportionality to a cube root relationship. A conductance proportional to the cube root of its aqueous concentration has been reported at high concentration of pentachlorophenol, where the permeant species is the pentachloro-phenolate anion (SMEJTEK *et al.*[71]). WANG and BRUNER[74] working with dipicrylaminate anion have also

reported two regions of direct and cube root proportionality confirming the findings of DE LEVIE[12].

The model presented by DE LEVIE[12] is a simple electrostatic one, and does not take into account the discrete nature of the charges involved. McLAUGHLIN[72] and ANDERSEN *et al.*[75] have shown that absorbed neutral molecules can have a dramatic effect on ion permeabilities by modifying dipole potential barriers near the membrane interfaces. The absorbed ions having permanent dipole moment or highly polarizable can also exert similar effect.

3.2. *Dielectric saturation of the aqueous layers adjacent to charged BLM*

BLM has recently been studied by WANG and BRUNER[74] when it is exposed to the intense electric field. High field dielectric measurements provide evidence that bulk water does indeed play normal saturation. The experimental evidence for dielectric saturation of water in more intense electric fields is provided by the measurements of differential or integral capacitance of mercury aqueous electrolyte interface. ROBINSON and LEVINE[76] presented a theoretical treatment of the integral capacitance of charged aqueous interfaces and studied the static dielectric permittivity of aqueous electrolyte solution to show the evidence of saturation. In this connection WANG and BRUNER[74] employed BLM formed from dioleyl lecithin — the zwitterionic head groups of which carry no net charge for such studies of dielectric saturation. When dipicrylamine is introduced into the surrounding aqueous solution, such BLM acquire a net negative charge due to adsorption of dipicrylamine anion (DPA^-). KETTERER *et al.*[73] have studied the current relaxations accompanying the application of a voltage step to this system. They have shown that the transport of DPA^- across BLM takes place in three distinct steps, namely interfacial adsorption, translocation across the membrane and desorption. They have also observed that the initial currents are of much greater magnitude than steady-state currents. This clearly indicates that the membrane translocation step is much faster than the interfacial reactions. Experiments performed at high voltage steps show that all absorbed DPA^- ions can be transferred to one membrane|solution interface completely eradicating the initially equal distribution of absorbed charges between two interfaces. A graphical integration of the observed current time transient provides a direct and model independent measure of the density of charge present on the membrane solution interface prior to application of voltage step. The relationship between the density of adsorbed membrane surface charge and concentration of adsorbate has been found to be linear so long as the surface charge density is sufficiently low as not to perturb the aqueous phase concentration of adsorbate near the interfaces. As the surface charge density increases, however, a point will be reached at which impinging hydrophobic anions will experience electrostatic repulsion by those already adsorbed, leading to a sublinear increase of surface charge density with further increase of absorbate concentration in the aqueous phase.

3.3. *GOUY-CHAPMAN theory of self-limited adsorption*

According to the classical GOUY-CHAPMAN theory the relationship between electrostatic potential U_s, at a plane carrying a surface charge density, σ_s adjoining a symmetric electrolyte solution is given by

$$\frac{\sigma_s}{2\sigma_0} = \sinh\left(\frac{ezU_s}{2kT}\right) \tag{19}$$

where $\sigma_0 = \dfrac{1}{2\epsilon\epsilon_0 RTc_0}$. This term σ_0 is a characteristic charge density which involves the relative permittivity or static dielectric constant of solvent. The permittivity of free space is given by ϵ_0 and c_0 is the concentration of indifferent electrolyte. In equation (19) is measured relative to $U = 0$ in the bulk solution, e is the magnitude of electronic charge and $z = z^+ = -z^-$ is the valency of ion, the other terms have their usual meaning. The magnitude of surface charge density due to the absorbed DPA^- is related to its concentration in the bulk phase by

$$|\sigma_s| = \beta c_w[DPA^-]\exp\left(-\frac{e|U_s|}{kT}\right) \tag{20}$$

where β is the partition coefficient.

At low surface potential when $|U_s| \ll kT$ equation (9) is reduced to

$$|\sigma_s| = \beta c_w[DPA^-] \tag{21}$$

and under the condition of $\dfrac{e|U_s|}{kT} \gg 1$ the expression for $|\sigma_s|$ is given by

$$|\sigma_s| = \sigma_0\left[\frac{\beta c_w[DPA^-]}{\sigma_0}\right]^{z/(z+2)} \tag{22}$$

By the use of equations (21) and (22) WANG and BRUNER[74] showed that a log–log plot of $|\sigma_s|$ *vs.* $c_w[DPA^-]$ which covers a sufficient range give a linear segment of unit slope at low concentration of DPA^- followed by a smooth transition to another linear segment of lower slope $[z/(z+2)]$ at higher concentration of DPA^-. At low concentration there seems to be agreement between theory and experimental result but with increasing salt concentration this agreement is lost, the observed surface charge density at onset of self-limited adsorption increases much less rapidly than predicted by the theory. The magnitude of membrane surface potential increases more rapidly with surface charge density. Increase in the density of adsorbed surface charges results in an increase in the field strength which becomes sufficiently intense to cause dielectric saturation of water in diffuse charge layers. Such saturation, causing a decrease of effective dielectric constant of aqueous boundary layers accounts for a more rapid than expected increase of $|U_s|$ with $|\sigma_s|$.

WANG and BRUNER[74] assumed simplified characterization of dielectric saturation depicted in Fig. 2. The macroscopic polarization, P, of water is assumed to increase initially with E, the macroscopic average electric field in the dielectric with a slope characterized by the static dielectric constant ϵ. This constant ϵ takes into account of polarization from all sources. This total polarization increases with field until a transition field, σ_t is reached at which polarization due to orientation of permanent dipoles reaches a limiting value P_o. This contribution remains constant at all higher fields. Further increase of P with E is attributed solely to atomic and electronic polarization. At the boundary of the membrane WANG and BRUNER[74] have shown that there will be a particular value of surface charge density, $|\sigma_t|$, for which the electric field at the boundary will be E_t, and the corresponding membrane surface potential will be $|U_t|$. The relation betwen $|U_s|$ and $|\sigma_s|$ for all values of $|\sigma_s| < |\sigma_t|$ will be given by equations (19) and (20) and as illustrated by the solid line portion of curve *I* of Fig. 3. When $|\sigma| > |\sigma_t|$ then one will have $E > E_t$ over some fraction of the boundary layer which is designated as the high field fraction. If the dielectric constant of the entire layer could be characterized by ϵ' then the relation between $|\sigma_s|$ and $|U_s|$ would be as illustrated by dashed line curve *II* of Fig. 3. Actually curve *II* is used to relate the surface charge

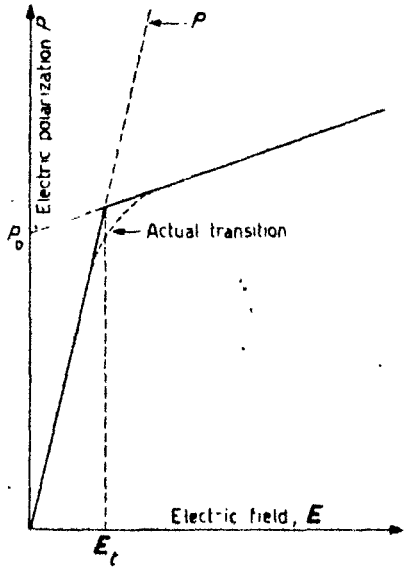

Fig. 2. The dependence of electric polarization, P, of water upon the macroscopic average electric field, E, according to the transition field model. An abrupt change of slope at the transition field, E_t, is assumed by the model. The actual transition from low to high field polarization is illustrated qualitatively by the dashed line curve smoothly connecting the linear segments. The extrapolated polarization, P_o, represents the maximum dipolar contribution to the total polarization (WANG and BRUNER[69]).

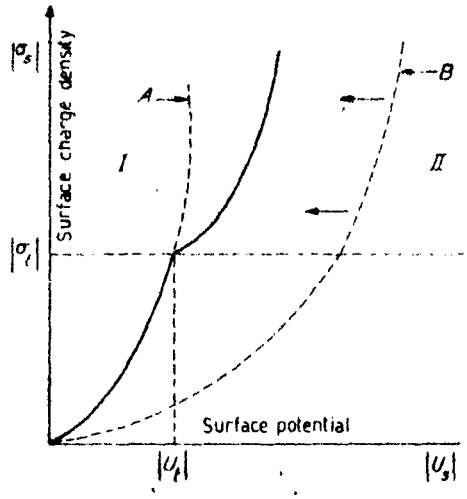

Fig. 3. The relation between $|U|$ and $|\sigma|$. The solid line curve illustrates the dependence of membrane surface density upon surface potential, as assumed by the transition field model (WANG and BRUNER[69]).

difference $|\sigma_s| - |\sigma_t|$, to the potential differences across the high field fraction of the boundary layer. When the field in the boundary layer decays to E_t the corresponding potential must be $|U_t|$. The transition field of WANG and BRUNER[72] leads to the remarkable conclusion that the power law dependence of $|\sigma_s|$ upon c_n [DPA] in the range of self limited adsorption remains identical to that of the unmodified GOUY-CHAPMAN theory at all concentrations of indifferent electrolyte.

3A. *Voltage-dependent conductance induced in BLM by monazomycin*

MULLER and FINKELSTEIN[59] have studied very thoroughly the steady-state conductance-voltage (g-U) characteristics of BLM in the presence of micromolar amounts of monazomycin, and the dependence of this characteristic on concentrations of monazomycin, salt, and divalent cations. Monazomycin is an antibiotic of proposed empirical formula $C_{62}H_{119}O_{20}N$ produced by *Streptomyces*. It contains many hydroxyl groups, one sugar residue, and one amino group which gives it a single positive charge over the pH range of 5.6 to 6.8. Two types of BLM have been studied:

(1) the membranes made with a lipid bearing no net charge, *i.e.*, from phosphatidylethanolamine (PE), and

(2) the membranes from phosphatidylglycerol (PG) which is a negatively charged lipid.

For the case of PE membranes the dependence of conductance (g) on potential (U) can be written in the form

$$g \propto \exp\left(\frac{neU}{kT}\right) \tag{23}$$

where e is the charge on the electron, k is the BOLTZMANN constant, T is the absolute temp and n is a constant. Equation (23) has been derived simply by assuming that the number of open (conducting) and closed (non-conducting) channels is governed by the BOLTZMANN distribution. The average value of n with PE membranes is about 4.4. Since $kT/e = 25.6\,\text{mV}$ at 25 °C, this means that the conductance changes e-fold about every 6 mV. Such a steep exponential dependence of conductance on voltage is also observed for sodium and potassium conductance of nerve (HODGKIN[77]).

The dependence of steady-state conductance on voltage, monazomycin concentration, and salt concentration can be expressed by

$$g \propto [\text{K}^+][\text{monazomycin}]^s \exp\left(\frac{neU}{kT}\right) \tag{24}$$

with $s \simeq 5$ and $n \simeq 4.4$. Divalent cations have no effect on the conductance of PE-treated membranes. The conductance-voltage (g-U) characteristic of monazomycin-treated phosphatidylglycerol (PG) membrane is similar to that of PE membranes. The log of steady-state conductance is proportional to the membrane potential and like PE membranes can be expressed by equation (23). Also in agreement with data on PE membranes, conductance varies as the 5th power of monazomycin concentration, and the membranes display good selectivity for univalent cations. In three respects, however, the behaviour of PG membranes is quite different from that of PE membranes:

(*a*) the monazomycin concentration necessary to achieve a given conductance at a given voltage is much less (about 0.02-fold),

(*b*) symmetrical increases of uni-univalent salt concentration produce dramatic *decreases* in conductance at a given voltage, instead of the linear increases seen with PE membranes,

(*c*) divalent cations profoundly shift the g-U characteristic, whereas they are virtually without effect on PE membranes.

MULLER and FINKELSTEIN[59] have applied diffuse double layer theory to PG membranes and have demonstrated that the differences of behavior between PE and PG membranes are the simple consequences of the negative surface charge on PG membranes. It is assumed that the phosphate group of the PG molecules produces a negative surface charge density on the membrane. At equilibrium there will exist a surface potential U_0 at the membrane solution interface (one interface on each side of the membrane). The only quantity of interest is the value of U_0. In order to calculate this, BOLTZMANN distribution and POISSON's equation

are combined to obtain the POISSON–BOLTZMANN equation which is then solved under appropriate boundary conditions. The area of the membrane is assumed to be infinite, so that all quantities vary on the coordinate x normal to the membrane surface $x = 0$ at the membrane surface. In order to make things simpler, only ions of significant concentration are one univalent cation, one univalent anion, and one divalent cation, *i.e.*, K^+, Cl^-, and Ca^{2+}.

From the above considerations one can have some idea about the effect of surface potential on the g-U characteristic of charged PG BLM. These BLM have approximately 1 charge per 60 Å^2. The sensitivity of PG membranes to monazomycin can be seen in the following way. The concentration of any univalent cation, i^+, at the membrane-solution interfaces is given by the BOLTZMANN distribution:

$$[i]_0 = [i^+]_\infty \exp\left(-\frac{eU_0}{kT}\right). \tag{25}$$

In particular this is true for potassium and monazomycin (which, because of its amino group, is a univalent cation in the pH range 5.6–6.8). For PE BLM, the interfacial concentrations of these ions are the same as in bulk solution, since $U_0 \simeq 0$ (because $\sigma = 0$). For PG BLM, however, their interfacial concentrations are much higher. In 0.01 M KCl, with $U_0 \simeq -180$ mV, the interfacial concentrations of K^+ and monazomycin$^+$ are about 10^3 times higher than in the bulk solution (see equation 25). Thus, even if PG and PE BLM have the same intrinsic sensitivity to monazomycin, PG will seem much more sensitive. The increase of monazomycin concentration has by far the greater effect on conductance. Conductance varies linearly with (surface) concentration of K^+. Thus a 10^3-fold concentration increase raises membrane conductance proportionally. On the other hand, since conductance is proportional to the 5th power of monazomycin concentration, a 10^3-fold increase in its concentration raises membrane conductance by a factor 10^{15}. One can also appreciate why increases of KCl concentration drastically reduce the conductance of PG BLM. If $Ca^{2+} = 0$, a ten-fold increase in KCl concentration decreases by about 60 mV. This reduces the interfacial concentration of monazomycin by 10-fold and hence decreases conductance by a factor of 10^5.

The divalent cations reduces U_0 which lowers the interfacial concentrations of both K^+ and monazomycin$^+$. The reduced interfacial concentration is the major reason for the lowering of conductance. The amount of divalent cations that need to be present is only 0.01th of KCl concentration to obtain shift in g-U curve. MULLER and FINKELSTEIN[59] concluded that the difference between PG and PE BLM results from the alteration of the negative surface potential of PG BLM. The membrane responds only to interfacial concentration of monazomycin. The asymmetric addition of divalent cation to the *trans* side (the solution in which monazomycin is not present) of PG membranes shifts the g-U characteristic to the

right along the voltage axis because of intramembrane potential difference. There is no change with the asymmetric addition of divalent cations to the *cis* side because of compensation of the two effects like

(*i*) internal field in the membrane which is now of the sign to drive monazomycin into the membrane and

(*ii*) the reduced monazomycin at the interface which makes it less available to be driven in by this field.

The diffuse double layer theory seems to explain the data obtained by MULLER and FINKELSTEIN[59] very nicely. The agreement between the divalent cation effects obtained by McLAUGHLIN *et al.*[56] using the K^+ carrier nonactin and the results of MULLER and FINKELSTEIN using monazomycin is quite close. The value of surface charge of cholesterol-free PG BLM determined by McLAUGHLIN is 1 charge per 38 Å^2 in good agreement with the result of MULLER and FINKELSTEIN which is 1 charge per 60 Å^2. These results lend strong support to the underlying theory, since the nonactin and monazomycin systems are so different. Nonactin forms a 1:1 complex with K^+ and acts as a simple carrier of that ion; the conductance is linear with the nonactin concentration and not voltage-dependent. Monazomycin, on the other hand, certainly does not function as a simple carrier, and the conductance is proportional to a large power of the antibiotic concentration and is strongly voltage-dependent.

3.5. *Inactivation of monazomycin-induced conductance*

HEYER *et al.*[78] described the phenomena of inactivation of the monazomycin-induced conductance. These mechanisms of achieving inactivation are interesting because of the information they give about the structure of monazomycin channels, and because of their possible relevance to inactivation in excitable cells.

The steady-state conductance (g_{ss}) of a monazomycin treated BLM is given by

$$g_{ss} = L[K^+]_o[mon^+]_o^n \exp\left(\frac{neU_m}{kT}\right) \tag{26}$$

where the concentrations of permeant ion (*i.e.* K^+) and of monazomycin (mon^+) at the membrane surfaces are subscribed as "o", and L is a constant of proportionality, S and n are empirically determined constants. The other terms have their usual meaning ($kT/e = 25.6$ mV at 300 °K). The potential U_m is the sum of the potential difference (U) across the membrane as ordinarily measured with electrodes placed in the bathing solutions, and of the difference in the two surface potentials (U_{oc} and U_{oi}) associated with any fixed surface charge that the membrane might have. These are shown in Fig. 4 and the relation is given by the following expression

$$\begin{aligned} U_m &= (U_c - U_i) + (U_{oc} - U_{oi}) \\ &= U + (U_{oc} - U_{oi}). \end{aligned} \tag{27}$$

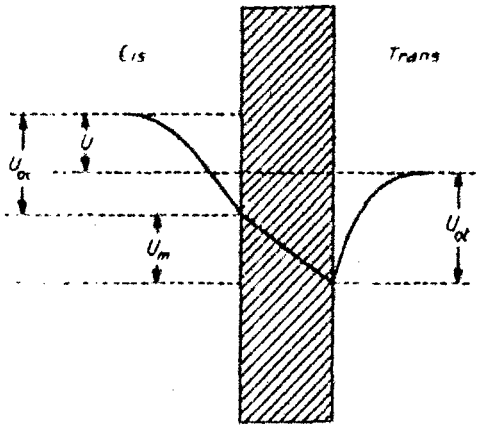

Fig. 4 Schematic representation of surface potential ($U_{\alpha c}$ and $U_{\alpha t}$), the potential difference across the membrane proper (U_m) and the measured (or applied) potential difference across the BLM (U). The potential drops in solution (due to the diffuse double layers) occurs over tens of angstroms (HEYER *et al.*[78])

The subscripts c and t refer to the two sides of the membrane (*cis* and *trans*), side c being the solution into which monazomycin is introduced. It was found that the conductance increases when side c is made more positive; such a change in U_m is in the direction to *drive* more of the positively charged monazomycin into the BLM, with the consequence that more ion-conducting channels form. U, the potential difference between sides c and t, is the quantity actually controlled by *voltage clamping*. With only monazomycin added to the *cis* compartment, conductance (current) rises in s-shaped manner to a steady-state value in response to a step change of potential from zero to some positive value. The steady-state conductance, g_{ss}, is a steep exponential function of the voltage of the form described earlier by equation (23).

$$g_{ss} \propto \exp\left(\frac{neU}{kT}\right) \tag{28}$$

where n is approximately equal to 5. Thus, g_{ss} increase e-fold for a 4–6 mV increase in potential. A semi-logarithmic plot of g_{ss} *versus* U yields a straight line, and is shown in Fig. 5*A*. When quaternary ammonium ions (QA), are also added to the *cis* compartment, a step change of potential from zero to some positive value causes the conductance to increase to a peak and then to decline to a much lower steady-state value; in other words, the monazomycin induced conductance inactivates. A semi-logarithmic plot of g_{ss} *versus* U now yields a curve that is concave downwards, although at smaller value of g_{ss}, it approaches a straight line (as shown in Fig. 5*B*) with the same slope as that obtained with monazomycin alone. The magnitude of inactivation, as measured by the ratio of the peak-conductance

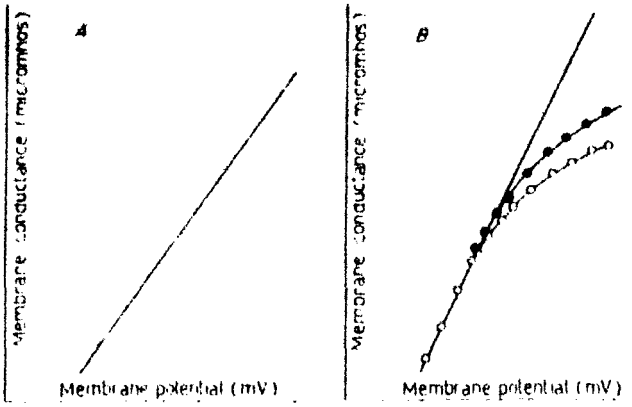

Fig. 5. (*A*) Steady-state g-U characteristic with monazomycin in *cis* compartment (*B*) Steady-state g-U characteristics on a single BLM with both monazomycin and different amounts of quaternary ammonium ions (C_{+}) in the *cis* compartment (HEYER *et al.*[78]).

to the steady-state conductance is greater when the slope of log g_{ss} *versus* U curve is smaller; where the log g_{ss} *versus* U curve is linear, the kinetic response is indistinguishable from that of monazomycin alone. Increasing amounts of QA results in greater bending (at a given conductance) in the log g_{ss} *versus* U curve from the limiting straight line (Fig. 5*B*).

The mechanism of QA-induced inactivation is explained by HEYER *et al.*[78] in the following manner. Due to the negative charge of PG BLM on each face there exists a negative surface potential U at each interface as shown in Fig. 6.4. Reversible binding of QA occurs at the *trans* surface which results in the reduction of *trans* surface charge density σ_t because QA is positive. In this way U_t becomes less negative thereby reducing U_m also. The consequence of this is that a negative potential difference which is not measurable by the recording electrode exists across the membrane proper and adds algebraically to any macroscopically applied positive potential shown in Fig. 6*B*.

The potential difference across the membrane proper (U_m) is seen by monazomycin. It is observed that log g_{ss} *versus* U curve is shifted to the right along the voltage axis by an amount equal to the decrease of *trans* surface potential. This shift in surface potential (U_m) depends on the quaternary ammonium (QA) concentration in the *trans* compartment. QA when added to the *cis* compartment, binds to the *cis* surface. The subsequent change in (U_m) has little effect on log g_{ss} *versus* U curve for the same reason that Ca^{2+} or Mg^{2+} added to the *cis* compartment has little effect. Namely, the effects of reducing mon^{+} and increasing U_m, the two consequences of the change in U_m cancel each other. QA has additional property of crossing the membrane to the *trans* compartment and binds the *trans* surface, making U_m more positive, consequently U_m is reduced, and the

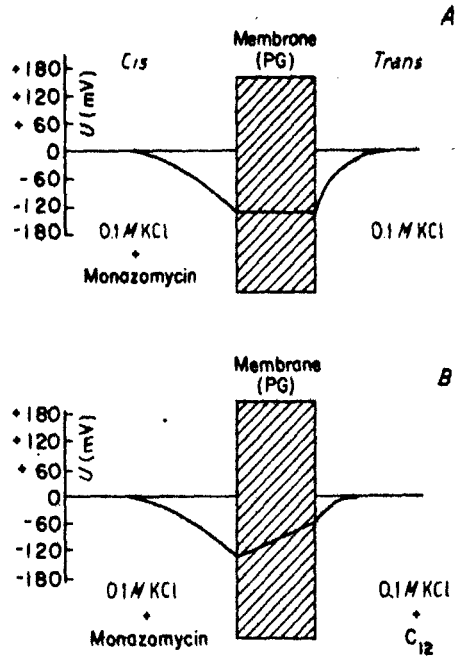

Fig. 6. (*A*) Diagram of the potential profiles (in the absence of an applied voltage) of a PG BLM separating symmetrical salt solutions. (*B*) Same as (*A*) except that C_{12} is present in the *trans* compartment. Because C_{12} binds to the surface, it reduces the *trans* negative surface charge density and hence makes the *trans* surface potential more positive. Consequently, there is a negative potential difference across the membrane proper that is seen by monazomycin but is not measured by the recording electrodes. This potential difference adds algebraically to any applied potential, U (HEYER *et al.*[78]).

monazomycin-induced conductance decreases. Thus inactivation occurs because the reduction of the potential difference across the membrane proper lowers the membrane conductance from the value it would achieve in the absence of QA.

The mechanism of QA permeation given by HEYER *et al.*[78] through monazomycin treated membrane is

(*i*) QA either passes through the lumen of the channel, or

(*ii*) crosses the modified region of the bilayer immediately adjacent to the channel.

The second of these possibilities is less likely. Formally large partition coefficient for QA between channel and surrounding aqueous solution explain various experimental observation. This must mean that there is a hydrophobic region associated with the channel to which QA binds. The hydrophobic region to which the aliphatic chain of the ions binds includes the bilayer itself; the polar amino end of the ion is in the lumen of the aqueous channel. The tail of the ion lies between the

monomeric subunits (*i.e.*, the individual monazomycin molecules) that form the channel. QA ions that pass through the channel in this way may have entered directly from solution or by first binding to the lipid and then slipping in between the monazomycin monomers.

The molecular basis for monazomycin is also given by HEYER *et al.*[78]. They postulate that monazomycin molecule is long enough to span the BLM, with its positively charged amino groups at one end and an uncharged but very polar region (perhaps the sugar moiety) at the other. They also imagine that one face of the long part of the molecule contains most of the hydroxyl groups, the polar faces from about five molecules form the hydrophilic lining of the pore. It is proposed that monazomycin monomers (or small aggregates such as dimers) can achieve a metastable, high energy state (called the spanned state) with the positively charged end of the molecule at the *trans* lipid|water interface and the polar end remains at the *cis* interface. Once in the spanned state, monazomycin can diffuse in the plane of the BLM and either form pores by mass aggregation or return to its original state on the *cis* surface. Once formed, the channel breaks up in such a way that some, or all, of its components wind up in the *trans* solution. The cause of the rise of voltage-dependent conductance is that the membrane potential lowers the free energy difference between the aqueous and spanned state. The potential is supposed to increase the concentration of monazomycin in the spanned state. This mechanism of channel formation is essentially the same as postulates by BOHEIM[79] for alamethicin. The scheme presented by HEYER *et al.*[78] constitutes a new permeability process in which individual molecules are impermeant but capable of forming permeant aggregates.

MOORE and NEHER[80] have used fluctuation and relaxation analysis to characterize a voltage-dependent BLM system. They have used monazomycin and to some extent alamethicin to produce multistate ion conducting channels which are voltage-dependent and show a steep relationship between the mean conductance and the membrane potential. These channels are probably formed by an aggregation reaction which is preceded by a voltage-dependent reorientation of the individual molecule. The equivalence of fluctuation analysis and small step relaxation experiments have been shown for gramicidin channels, which are presumed to have only one conducting state. The fluctuations of multistate processes arise from changes in the number of channel conductance itself (EISENBERG *et al.*[81]). MOORE and NEHER suggested that the estimated unit conductance is predominantly a function of multiplicity of state and that the mean unit conductance of a monazomycin channel may be smaller than the estimated value. The kinetic data obtained by MOORE and NEHER and consistent with a model similar to that proposed by others for both monazomycin and alamethicin (BOHEIM[79]; EISENBERG *et al.*[81]; MULLER and FINKELSTEIN[59]). Single channel conductance of BLM in the presence of monazomycin has also been studied by BAMBERG and JENKO[82]. They have reported that they could not find different conductance levels of the channel as was found in the case of

alamethicin (see Section 6.2) but they have not excluded the possibility of existence of different states of pore with their experiment. BAMBERG and JENKO have concluded that the monazomycin channels under experimental conditions (performed by them) do not interact with each other. At $T = 25\,^{\circ}C$ a mean life of 30 ms was found by them. The current-voltage behavior of the single channels is completely linear. It was impossible for them to find in the case of single channel experiments any voltage-dependence, in contrast to the dramatic voltage dependence of the macroscopic membrane conductance. Further, from the temperature dependence of the single channel conductance, a value has been calculated for the activation energy E for the ion transfer through the pore. For $T = 11\,^{\circ}C$ BAMBERG and JENKO obtained a value of 6.6 ps and for $25\,^{\circ}C$ a value of 16 ps. The activation energy was about 10 kcal/mole. This value is slightly higher than the value which was found for the gramicidin A channel (7.13 kcal/mole) by BAMBERG and LAUGER[83]. The discrepancy is in agreement with the hypothesis, that a pore with a smaller single channel conductance has a higher activation energy than a pore with a higher conductance. It seems reasonable that in a pore with a lower conductance the ions have to pass through a higher energy barrier than in a large pore.

4. Electrical transients in BLM

It is now recognized that hydrophobic ions absorb strongly into a region of a bilayer lipid membrane (BLM) near the membrane solution interface. Numerous studies have been made of the electrical properties of a BLM exposed to the lipid soluble ions tetraphenylborate ($TPhB^{-1}$) (LIBERMAN and TOPALY[84]; LEBLANC[85]; KETTERER *et al.*[73]; GRIGOREV *et al.*[86]; ANDERSEN and FUCHS[87]; HAYDON and HLADKY[88]; GAVACH and SANDEAUX[89]; BENZ *et al.*[90]; GAVACH *et al.*[91]; ANDERSEN *et al.*[75]; FELDBERG and DELAGO[92]) and dipicrylamine (KETTERER *et al.*[73]; DE LEVIE and VUKADIN[93]). The behavior of these two compounds is well understood, at least at low concentrations.

KETTERER *et al.*[73] showed that both conductance and the number of absorbed hydrophobic ions increase linearly with the aqueous concentration. The ion moves between two energy wells with a single time constant when a voltage is applied across the BLM and the voltage required is independent of concentration. ANDERSEN and FUCHS[87] established that the major contribution to the barrier properties of these membranes is the large electrostatic charging energy (primarily the BORN energy due to the difference in dielectric constants) necessary to move an ion out of an aqueous phase into the hydrocarbon phase in the BLM interior (FINKELSTEIN and CASS[94]). The membrane permeable ions are large organic ions or small inorganic with ion carriers, *e.g.* K^+-nonactin, K^+-valinomycin, *etc.* The electrostatic energy requirement is not constant through the BLM and the aqueous phases. The charging energy is only one component of the

total potential energy of an ion or ion–ion carrier complex within the BLM. Other components are hydrophobic interactions between the ion and the aqueous phases (TANFORD[95]), electrostatic potential differences (both surface and dipole potentials) between the membrane interior and the bulk aqueous phases and short range (packing) interactions between the ion and molecules in the BLM. The sum of these four components constitutes the potential energy barrier to ion transport through the BLM. The potential energy of an ion within the membrane may also be affected by an applied potential difference. This is, however, not a part of the potential energy barrier. Ion transport through the membrane, and its dependence on the applied potential, is determined by the shape of the potential energy barrier through BLM. All the four terms in the potential energy barrier are of importance in determining the magnitude of the membrane permeability (conductance). The potential dependence of ion transport through the middle of the membrane will be determined by the electrostatic charging energy term because it is the only term which changes significantly through the entire BLM. Any of the four terms, as well as other terms (ion–ion carrier association and dissociation kinetics) may be of importance for the current-carrying species across the membrane|solution interfaces.

The shape of the potential energy barrier for a current-carrying species is used to calculate the current-voltage characteristics of the membrane in the presence of this species (LAUGER and NEUMCKE[96]). A number of workers CIANI *et al.*[97]; HLADKY[98]; LAPRADE *et al.*[99]; STARK *et al.*[100]) studied the kinetics of ion–ion carrier association and dissociation reactions through the BLM. There are divergent reports about the *correct* shape of the potential energy barrier to ion transport in the centre of BLM.

ANDERSEN and FUCHS[87] have emphasized on the role of *effective potential* influencing ion movement within the BLM and not on the applied potential. They have proposed the use of the current carriers that do not cross the membrane|solution interfaces to any significant extent, once the membrane is loaded. The organic anion, *e.g.*, tetraphenylborate absorbs strongly into the membrane|solution boundary regions. These ions provide information about the shape of the potential energy barrier in the middle of the membrane, independent of assumptions about what happens at the membrane solution interfaces. This system, therefore, serves as a simple model for the transport of ion–ion carrier complexes through these membranes. In addition, it may serve as a model for some properties of the *gating currents* observed in excitable membranes (ARMSTRONG and BEZANILLA[101]; KEYNES and ROJAS[102]).

4.1. *Kinetics of tetraphenylborate ($TPhB^-$) transport through BLM at low concentration*

Simple EYRING type barrier model has been used by KETTERER *et al.*[73], to describe the kinetics of tetraphenylborate ($TPhB^-$) through BLM. Their

description gave quite a good picture of the events occurring but somewhat lacked quantitativeness. ANDERSEN and FUCHS[87] studied it very thoroughly particularly the shape of potential energy barrier in the middle of the BLM. Their approach of describing the potential energy barrier to ion-transport through the centre of BLM is similar to that of image force barrier of LAUGER and NEUMCKE[96].

The BLM is treated as a thin slab of hydrocarbon having a thickness of 50–70 Å and polar group 13 Å with dielectric constant, ϵ_m, between two aqueous phases with dielectric constant $\epsilon_{H_2O} = 80$ (Fig. 7)[6]. Only one charged species (current carrier) which is $TPhB^-$ is present within the membrane. The salient features of the treatment given by ANDERSEN and FUCHS[87] are as follows. The potential energy barrier to ion transport through BLM is represented by $E_{(x)}$. In the bulk phase this is supposed to be zero. Near the solution membrane interface at a distance equal to the ion radius r, the value of $E_{(x)}$ begins to change as shown in Fig. 8*A*. The potential energy $E_{(x)}$ has a deep narrow minimum near the two interfaces. In the case of large hydrophobic ions and ion–ion carrier complex one always gets such type of minima. Due to electrostatic charging energy, the two minima are separated by a broad barrier in the centre of BLM. The absorbed $TPhB^-$ ions in the BLM are concentrated in two very narrow strips near the solution membrane interface as shown in Fig. 8*B*. The applied potential difference across the BLM lowers the potential energy of ion in one minima as compared to the other (the positive). The $TPhB^-$ within the BLM tends to accumulate into the *positive*

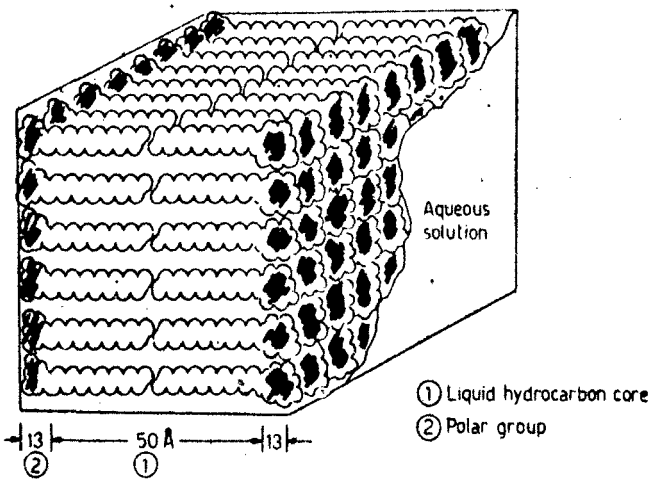

Fig. 7. Three-dimensional model of black lecithin membrane. The thickness of the liquid hydrocarbon core is about 50 Å. The polar portion of the membrane is estimated to have a thickness varying from about 5 Å for compact head groups to about 13 Å for a fully extended configuration at each end. The diameter of the area occupied per head group is about 8 Å.

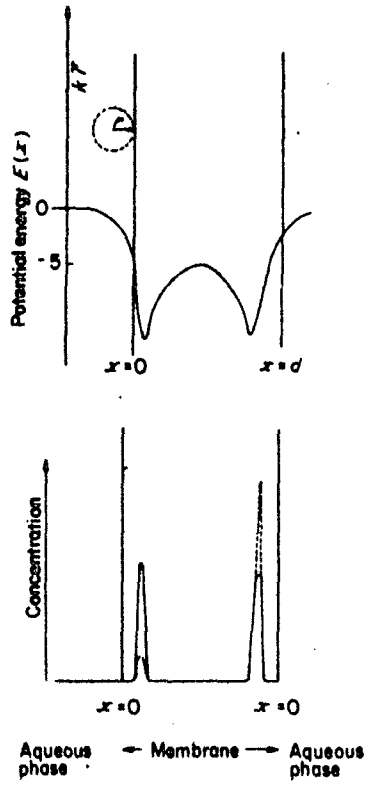

Fig. 8. (*A*) Schematic representation of the potential energy barrier to ion transport across a bimolecular lipid membrane. (*B*) Schematic representation of concentration profile for $TPhB^-$ within the bilayer. The full line is drawn for the potential difference of 0 mV, the stippled line is drawn for a potential difference of about 75 mV (ANDERSEN and FUCHS[87]).

minima and thus gives rise to a current through the membrane. The charge movement through the BLM is obtained in the following manner. At a time $t = 0$, a potential difference, U is applied suddenly across the membrane. The $TPhB^-$ ions will move through the membrane and the ion concentration within the membrane will shift from the equilibrium profile to some new profile which will be a function of voltage (U) and time (t). The integrated charge movement through the BLM is found to be equal to the net entry of ions into the membrane plus the net change in the number of absorbed ions. Theoretically it has been calculated that 3×10^{-16} mol of $TPhB^-$ can move through bacterial phosphatidyl ethanolamine (PE) BLM in 10 milliseconds (ms) while experimentally it has been observed that 4×10^{-15} mol of $TPhB^-$ can move in the same interval of time. From this result ANDERSEN and FUCHS[87] concluded that so many $TPhB^-$ ions absorb into the

membrane|solution boundary region (in a potential energy minima) that it is possible to disregard any ion transport through the membrane so that the number of ions absorbed into the membrane is constant. Thus,

(*i*) the current through the interior of BLM will be carried by $TPhB^-$,

(*ii*) the current through the BLM can not be maintained at the initially *high* level but will relax towards a very low value which is determined by the transport of $TPhB^-$ across the interfaces, and

(*iii*) one boundary region will become depleted of $TPhB^-$ while the other will accumulate $TPhB^-$ ions.

When no current is flowing across the BLM one can calculate the relative concentration of $TPhB^-$ in the two boundary regions using BOLTZMANN distribution. The number of ions ΔN transported through the centre of BLM is given by

$$\Delta N(U) = N_{abs} \tanh \frac{\beta q U}{2k\bar{T}} \tag{29}$$

where N_{abs} is the total number of ions absorbed into one boundary region of the membrane, q is the charge, and β is the fraction of the applied potential that is actually effective in moving ions through the membrane. From equation (29) it can be seen that the number of ions moved through the membrane during a current transient reaches an upper limit, N_{abs}, with increasing potential.

Ion transport through BLM may be described by the NERNST–PLANCK electrodiffusion equations provided one includes a term to describe variations in the potential energy barrier through the membrane. The current-transients can be expressed in terms of the mobility of the current carrying species ($TPhB^-$) within the membrane and $U(X)$ the electrostatic potential due to an externally applied potential. Even though concentration profiles and ion flux change with time, one can regard the transport process to be pseudo-stationary if the charging time constant τ_c (the time constant for changes of concentration profiles in the center of the BLM at $t = 0$) is much smaller than the time constant τ, of the observed current transient. The current through the membrane $I(U,t)$ is defined as $I(U,t) = qJ(U,t)$. The membrane conductance $g_m(U,t)$ is usually defined as

$$g_m(U,t) = \frac{I(Ut)}{U - U'(t)} \tag{30}$$

where $U'(t)$ denotes electromotive force which is a function of time. The electromotive force defined above is a measure of polarization within the membrane. $U'(t)$ may be regarded as a diffusion potential between the two potential energy minima within the membrane, thus emphasizing the difference between ion transport within the membrane compared with current flow across the membrane when $B < 1$. It is consequently advantageous to define a barrier

conductance $g_b(U, t)$, as

$$g_b(U, t) = \frac{I(U, t)}{\beta U - U(t)} \tag{31}$$

where βU is the actual electrical potential difference influencing ion movement within the membrane.

Charge movement across BLM in the presence of TPhB$^-$ has been given by ANDERSEN and FUCHS[57] in the following manner. The current $I(t)$ is shown in Fig. 9 as a function of time after a stimulus. After an initial very fast current transient, which charges the membrane capacitance, the current through the membrane declines with a time constant, τ, of about 1.4 ms (*on* response). At the end of the stimulus the membrane capacitance discharges and one observes a current relaxation, of opposite polarity to the first, with a time constant of about 2.0 ms (*off* response). The initial current $I(0)$ is obtained by plotting $I(t)$ *versus* time and extrapolating the *slow* transient back to $t = 0$. As can be seen in Fig. 10 the *slow* current relaxations are exponential for more than three time constants, indicating that only a few percent of the ions have moved across the two membrane solution interfaces during current transients.

The number of coulombs moved through the BLM during a single current transient given by $\int_0^\infty I(t)\,dt$ may be approximated by

$$\int_0^\infty I(0)\exp\left(-\frac{t}{\tau}\right)dt = I(0)\tau. \tag{32}$$

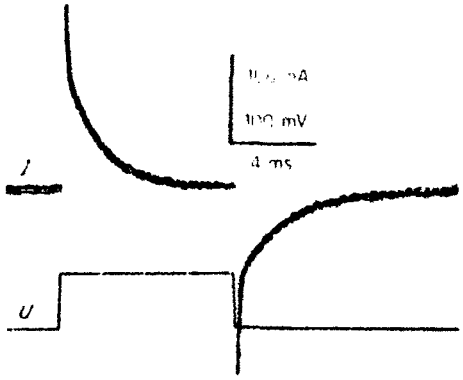

Fig. 9. An oscillogram of TPhB$^-$ current transient in a BPE-decane membrane. The top trace shows current, the lower trace potential as a function of time. Stimulus 60 mV, duration 8 ms. The aqueous phases contained 0.1 *M* NaCl and 7×10^{-8} *M* tetraphenyl borate, membrane area 1.2 mm^2. $T = 25$ °C (ANDERSEN and FUCHS[57]).

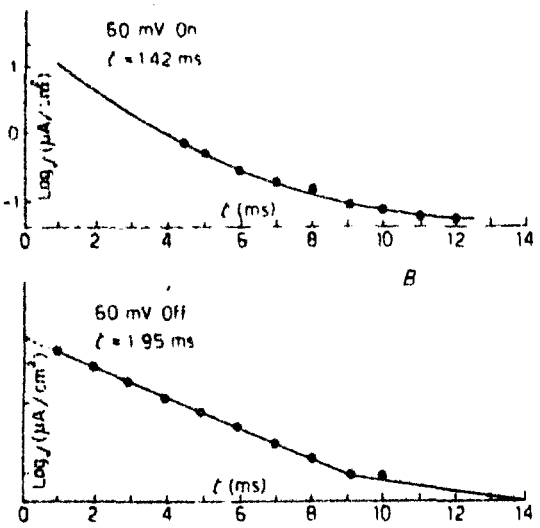

Fig. 10 (*A*) Plot of log current *versus* time for an *on* response. (*B*) Plot of log current *versus* time for an *off* response (ANDERSEN and FUCHS[87]).

In Fig. 11 the plots of the charge moved *versus* applied potential are shown. It is apparent that the charge moved through the membrane reaches an upper limit with increasing potential. This upper limit which is interpreted to be qN_{abs} corresponds to the complete depletion of $TPhB^-$ ions in one boundary region in Fig. 8*B*. Fig. 11 also demonstrates that the charge moved through the BLM during the on-response is exactly matched by charge moving back during the off-response.

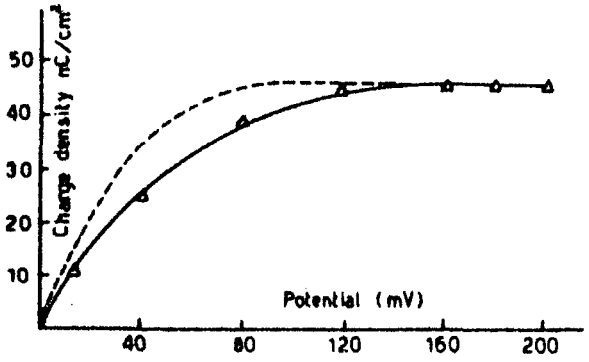

Fig. 11. Plot of the charge moved through the membrane, as a function of the applied potential. The solid line is the predicted behavior if the effective potential is 75 % of the applied potential. The stippled line is the predicted behavior if the effective potential is equal to the applied potential (ANDERSEN and FUCHS[87]).

The decline in current with time should, according to the model, be due to a charge accumulation in one boundary phase (the positive) and a corresponding depletion in the other. The time constant for the charge accumulation should be identical to that for the current transient itself. The charge accumulated at time t, $Q(t)$ is described by $Q(t)[1 - \exp(-t/\tau)]$ where τ is the time constant of the on-response and $Q(\infty) = I(0)\tau$. In Fig. 12 the plot of $\log [Q(\infty) - Q(t)]$ is shown. This is a straight line with $\tau = 1.30$ ms, for the on-response is 1.35 ms. ANDERSEN and FUCHS[87] concluded that the observed current relaxations are mainly due to charge redistribution with the BLM and only secondarily to membrane conductance changes. From Fig. 11 it can be seen that the agreement is excellent for 0.75, but poor for $\beta = 1.0$. β is obtained by calculating

$$\frac{\Delta N(U)}{\tanh [\beta q U/(2kT)]} = N_{ads} \tag{33}$$

for all U, both on and off-responses. For bacterial phosphatidylethanolamine membranes $\beta = 0.77 \pm 0.04$ while $\beta = 0.92 \pm 0.04$ for dioleoylphosphatidylethanolamine membranes.

Study of the BLM conductance and absorption of ions as a function of concentration show interesting behavior. In Fig. 13 the total number of ions, actually coulombs absorbed into one boundary region of a BLM is plotted as a

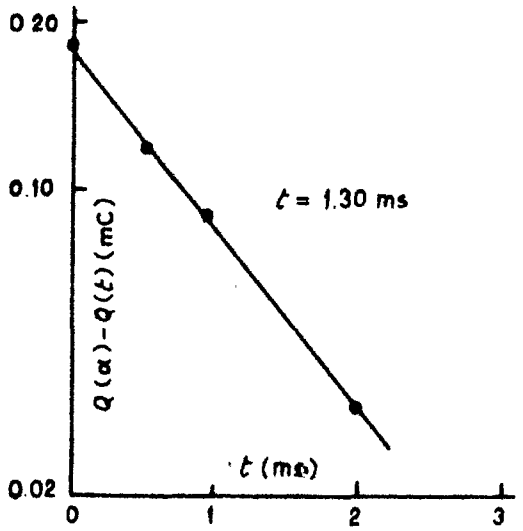

Fig. 12. Membrane polarization as a function of time. $\log (Q(\infty) - Q(t)$ is plotted *versus* time. $Q(\infty)$ denotes the amount of charge absorbed into one boundary phase of the membrane. $Q(t)$ denotes the amount of charge transferred through the membrane at time t after applying the potential. The aqueous phase contained 0.1 *M* NaCl plus 7×10^{-8} *M* tetraphenylborate 25 °C (ANDERSEN and FUCHS[87]).

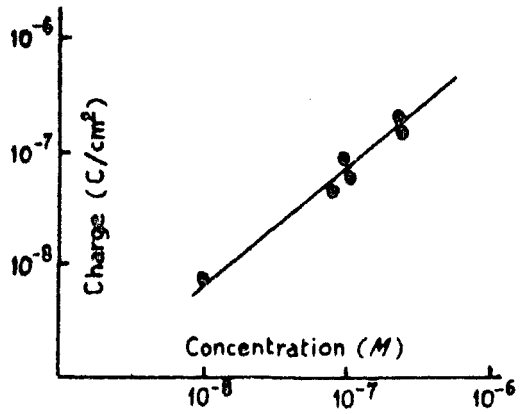

Fig. 13. Absorption of tetraphenylborate ions into the BLM boundary layer. 0.1 *M* NaCl plus various concentrations of tetraphenylborate at 25 ± 1.0 °C (ANDERSEN and FUCHS[87]).

function of the concentration of $TPhB^-$. The number of ions absorbed is a linear function of $TPhB^-$ concentration up to $3 \times 10^{-7} M$ $TPhB^-$. At higher concentrations of $TPhB^-$ ion movement across the membrane solution interface becomes significant compared with the ion movement through the center of the membrane. The time course of the current transient is no longer a single exponential and diffusion polarization plays a significant role in determining the time course of the current.

The above description of ANDERSEN and FUCHS[87] for the transport of lipid soluble ion through BLM can also serve as a model for carrier-mediated ion transport through these membranes. BENZ *et al.*[103]; KETTERER *et al.*[73]; LAPRADE *et al.*[99]; LAUGER and NEUMCKE[96]; STARK *et al.*[100] used potential dependence of membrane conductance or relaxation time constant for the analysis of transport mechanism. The general behavior of the $TPhB^-$-BLM system described by ANDERSEN and FUCHS[87] is phenomenologically somewhat similar to the *gating currents* in the squid giant axon (ARMSTRONG and BEZANILA[101]; KEYNES and ROJAS[102]) with respect to the time course of currents and their potential dependence. They believe that the *gating currents* can be analyzed by a model very similar to the one described by them.

4.2. *Kinetics of tetraphenylborate ($TPhB^-$) transport through BLM at high concentration*

The behavior of lipid soluble ion namely tetraphenylborate has recently been studied again by ANDERSEN *et al.*[75] and GAVACH *et al.*[91] at higher concentration. Serious anomalies are observed when the $TPhB^-$ solution is not

dilute. Neither the conductance nor the number of lipid soluble ions absorbed into the wells, for example, continues to increase linearly with the aqueous concentration. Attempts to explain these deviations from the simple model in terms of a buildup of space charge within the membrane, a limited number of binding sites, or a limited aqueous solubility of the ion are discussed critically by ANDERSEN *et al.*[75]. They demonstrated that as the concentration of lipid-soluble ions increases, the time-course of the current can no longer be described by a single exponential relaxation and that increasingly large potentials must be applied to the membrane to move a given fraction of charge between the two wells. They have further proposed that these and other anomalies are all due to the absorption of charge and the concomitant production of electrostatic *boundary potentials* within the membrane, a phenomenon first discussed by MARKIN *et al.*[104] and LIBERMAN and MARGULIS[105]. The salient features of the theory of electrostatic interactions among hydrophobic ions in BLM developed by ANDERSEN *et al.*[75] are described here.

A BLM is located between the symmetrical aqueous phases which contain equal concentrations of the hydrophobic anion tetraphenylborate ($TPhB^-$). An aqueous diffuse double layer potential due to the adsorption of $TPhB^-$ into the membrane is present at the surface of membrane. The chemical (mainly hydrophobic) and electrostatic (mainly pre-existing dipole potential and induced ion-dipole or image charge potentials) potential energies combine to establish deep potential energy well for $TPhB^-$ ion near the membrane solution interfaces as depicted in Fig. 14*a*. Partitioning of $TPhB^-$ takes place into the wells, while their counter ions Na^+ remain behind forming a diffuse double layer in each aqueous phase as shown in Fig. 14*b*. This charge separation (Fig. 14*c* heavy line) changes the electrostatic potential difference between the bulk aqueous phases and the planes of absorbed charge. The adsorption of $TPhB^-$ produces a change in the electrostatic potential between the bulk aqueous phase and the membrane solution interface as shown in Fig. 14*c* light line. If the absorbed anions are located within the low dielectric constant interior of the membrane an additional change in potential will be produced within the membrane. The absorbed charges are smeared uniformly over the planes located at $x = \delta$ and $x = d - \delta$. The counter ions may be considered to be located in two planes at $x = -1/\kappa$ and $x = d + (1/\kappa)$ where $(1/\kappa)$ is the DEBYE length as shown in Fig. 14*d*. Here four planes of charge and three dielectric regions are defined in the following way: an outer region between $-(1/\kappa)$ and δ with an effective dielectric constant ϵ_r, *outer*, an inner region between δ and $d - \delta$ with an effective dielectric constant ϵ_r, *inner* (probably close to 2) and an outer region between $d - \delta$ and $d + (1/\kappa)$ with an effective dielectric constant ϵ_r, *outer*. The specific capacitances of the outer and inner regions are given by C_0 and C_i respectively. The absorbed $TPhB^-$ ions produce changes in the electrical potentials across these regions. These changes in electrostatic potential are defined as the outer potentials U_0' and U_0'' and the inner potential, U_i (Fig. 14*d*).

When no potential is applied across a membrane in equilibrium with the

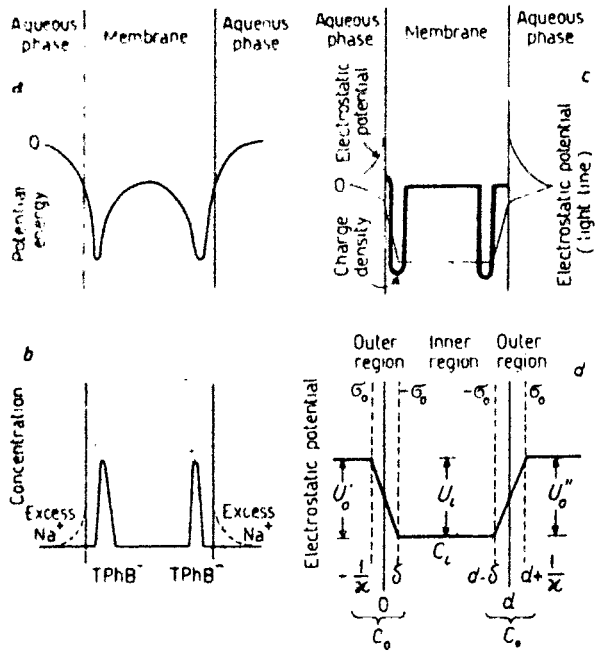

Fig. 14. Schematic representation of the three-capacitor model. (*a*) The potential energy profile experienced by a single TPhB ion as it crosses a BLM. For simplicity it is assumed that no interfacial barrier exists. (*b*) The concentration profiles for TPhB and Na^+, measured with respect to their concentrations in the bulk aqueouses phases. (*c*) The charge distribution (heavy lines) and electrostatic potential profile (light lines) in the membrane and aqueous diffuse double layers. (*d*) The three-capacitor model for the electrostatic potential. The loci of the adsorbed $TPhB^-$ ions $(\delta, d-\delta)$ and aqueous counterions $\left(-\frac{1}{\kappa}, d+\frac{1}{\kappa}\right)$ define four planes and three regions of the membrane. These regions can be regarded as three capacitors (ANDERSEN *et al.*[75]).

symmetrical aqueous phases, the outer potential on the left side of the membrane is (setting the potential of the left bulk aqueous phase equal to zero):

$$U_0' = -\frac{\sigma'}{C_0} = -\frac{\sigma^0}{C_0} \tag{34}$$

and the outer potential on the right side of the membrane is:

$$U_0'' = \frac{\sigma''}{C_0} = \frac{\sigma^0}{C_0} \tag{35}$$

where σ' and σ'' are the magnitudes of the absorbed charge density in the left and right-hand wells, respectively, and σ^0 is the magnitude of the adsorbed charge

density in either well at equilibrium. In all the derivations, the absorbed species is an anion.

It has also been assumed that there is no ion transport across the outer regions once adsorption equilibrium is attained. For the adsorption of the total charge in the membrane, $(\sigma' + \sigma'')$, the presence of an external applied potential is not necessary and the resulting intramembrane charge densities are defined by:

$$\sigma' + \sigma'' = 2\sigma^0 \tag{36}$$

with $|\sigma'| = |\sigma''| = |\sigma^0|$.

Furthermore, while $|\sigma'|$ and $|\sigma''|$ may be modified by an external potential their sum $2|\sigma^0|$ remains independent from the applied potential. The application of a potential, U'_m, (Fig. 15) or equivalently the injection of charge or passage of current through non-polarizable electrodes in the aqueous phases introduces additional charge density σ_c, into the plane at $x = d + (1/\kappa)$ (*i.e.*, the aqueous double layer on the right side of the membrane) while it removes the same quantity of charge from the plane at $x = -(1/\kappa)$ where κ is the reciprocal DEBYE length.

The situation immediately after the application of a potential is shown schematically in Fig. 15*a*. The situation after some charge has moved within the

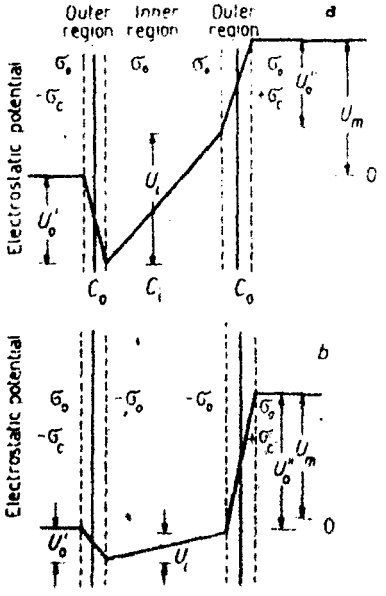

Fig. 15. (*a*) Schematic representation of the potential profiles after a potential difference, U'_m, has been applied across the BLM but before any charge translocation has occurred. (*b*) Schematic representation of the potential profile across a BLM after some charge translocation has occurred. The field in the membrane interior is now less than in (a) (ANDERSEN *et al.*[15]).

membrane is shown in Fig. 15*b*. Using GAUSS theorem, the potential change across each of the three regions is given by U_0', U_i and U_0''.

The total membrane potential, U_m, is the sum of these potential changes

$$U_m = U_0' + U_i + U_0''$$

$$= \sigma_c\left(\frac{2}{C_0} + \frac{1}{C_i}\right) + \frac{\sigma' - \sigma^0}{C_i} \tag{37}$$

where C_0 is the inner capacitor and C_i is the outer capacitor. The specific membrane capacitance C_m is found to be simply series combination of two outer capacitors and the inner capacitor. ANDERSEN *et al.*[75] have defined a term b as given by

$$b = \frac{C_m}{C_i}. \tag{38}$$

It is to be noted that b is the fraction of the total membrane potential which falls across the inner membrane region either before any charge translocation has taken place ($\sigma' = \sigma'' = \sigma^0$) or in the limit of zero adsorbed charge ($\sigma^0 \to 0$). It is clear that

$$0 \leq b < 1. \tag{39}$$

A value of $b = 0$ means that there is a single potential energy well in the middle of the membrane. When the ions are adsorbed to the membrane solution interface, the value of b approximately approaches unity.

5. Steady-state carrier mediated transport through BLM

FELDBERG and KISSEL[106] applied a charge pulse technique to the studies of steady-state carrier mediated transport through BLM. They have followed more closely the electrochemical approach used by a number of workers interested in electrode kinetics (KUDIRKA *et al.*[107]). The charge pulse technique is one of the best methods for measuring both steady-state and relaxation phenomena. The BLM has two elements; one is capacitive and the other resistive. The capacitive element is supposed to be in parallel with the resistive element. The principal of the experimental procedure described by FELDBERG and KISSEL for this technique is as follows. In an infinitely small interval of time, a precisely known charge is injected which gives an ideal charge pulse. Because of this charge pulse, a voltage is instantaneously developed across the capacitive element which decays through the resistive element. The manner in which the voltage decays is the manifestation of the events taking place in the BLM. For example, the rate processes associated with the membrane conductance can be thoroughly investigated with the knowledge obtained with the voltage decay. The voltage decay time constant may be large or small. If the rate processes are rapid relative to

voltage decay time constant they are assumed to be at a steady rate.

The equations used for the steady-state carrier mediated transport are based on HLADKY's presentation[108] and of LAUGER and STARK's model[109]. The symmetrical cases, where the composition of the salt solutions on each side of the membrane are identical, are considered. The symbol, Γ, denotes the concentration of species on or near each membrane surface in moles/cm^2. The carrier and carrier-ion complex are concentrated in a planar region located just inside the polar head group on each side of the BLM. It is also assumed that all carrier molecules (complexed or uncomplexed) are membrane bound in the time scale of the experiment and that a given carrier concentration in the bulk lipid *n*-decane mixture establishes a given concentration of free carrier in the BLM.

Several interesting data have been obtained by steady state measurements of actin-mediated ammonium ion transport applying the above theory. First is the constancy of the rate parameter k_u for all the four actins (nonactin, monactin, dinactin, and trinactin). This suggests that the membrane energy barrier for the four different ammonium actin complexes is essentially the same (this supports the conclusion of EISENMAN *et al.*[110], that the overall size and shape of the actin antibiotics are independent of the degree of methylation). Second is the observation that k_s is much greater than k_u. LAPRADE, *et al.*[99] made a similar observation in studies of actin-mediated transport in dioleate (GDO) BLM and rationalized it by pointing out that the carrier complex must overcome the dielectric energy barrier as discussed by LAUGER and NEUMCKE[111]. LAPRADE *et al.* also noted that the values of the instantaneous current (for high concentration of NH_4^+ with trinactin in BLM) predicted from steady-state data were much higher than the values directly measured using voltage-clamp techniques.

GINSBURG and STARK[112] while studying the facilitated transport of di- and tri-nitrophenolate ions across BLM by valinomycin and nonactin have suggested a model, which, based on the generation of mobile defect structure by the incorporation of large molecules, allows one to explain facilitated transport without the assumption of stable chemical bonds between a carrier and its transported substrate. The surprising result of an enhanced permeability of various nitrophenolate anions in the presence of macrocyclic compounds has encouraged GINSBURG and STARK to put forward a molecular interpretation. All the three substances used by them, namely valinomycin (10^{-7} *M*), nonactin (10^{-6} *M*) and enniatin B (10^{-5} *M*), are known as carriers for cations such as potassium. Therefore, one might imagine that they also act as carriers for certain anions. This would require the existence of stable carrier-anion complexes. The structure of these complexes must, however, be completely different from the structure of the cation complexes, since the size of a picrate anion is far too large to allow its incorporation into the interior of macrocyclic carrier (as in the case of cation). GINSBURG and STARK have raised the question whether specific carrier-anion complexes must be postulated in order to explain facilitated

transport. They have considered the non-facilitated transport of nitrophenolate-anions. The first step in the movement of these anions across a BLM is their adsorption to an interface (ANDERSEN and FUCHS[97]). The height of the energy barrier which limits the diffusion across the membrane is determined by several factors. Firstly, a specific interaction of the ion with the interface will enlarge the depth of the energy minima. Secondly, the image forces acting on an ion near the interface of two media with different dielectric constants give rise to a broad barrier in the middle of the membrane (NEUMCKE and LAUGER[113]). Finally, the intermolecular interaction of adjacent hydrocarbon chains of the lipid molecules hinders the penetration of *foreign molecules*. This interaction is fundamental for the maintenance of a liquid crystalline order inside the membrane[6]. The diffusion of any solute is limited by the amount of free volume available in the frame of this structural order. Such free volume is present through the existence of defect structures. The diffusion of solutes across the hydrocarbon-like interior of biological and model membranes has been described in a way analogous to diffusion process in polymers. Special defect structures found to be present in paraffins, in polyethylenes and other polymers (PECHOLD[114]), have also been suggested for lipid membranes and have been considered as *intrinsic carriers* for small solutes such as water molecules. Large molecules, however, do not fit into these intrinsic defect structures with a diameter of one to several Å in the lateral direction. The presence of valinomycin or nonactin (diameter 12–16 Å) must considerably disturb the order of their lipid environment, *i.e.* introduce additional disorder. Since the flexibility of hydrocarbon chains in a BLM is limited, the distortion in the proximity of those molecules will inevitably create additional free volume. This may be occupied by other, smaller *foreign molecules*. In the light of these considerations the following possibility shown in Fig. 16 of facilitated diffusion has been envisaged by GINSBURG and STARK[112].

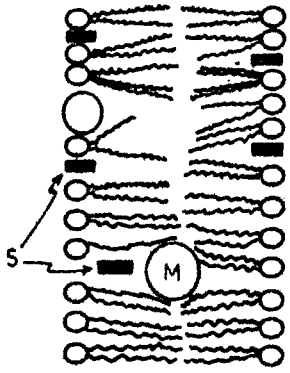

Fig. 16. Schematic representation of the transport of a species S facilitated by a mobile mediator M. The small molecule S can exist inside the free space generated by the large molecule M within the liquid crystalline lattice of lipid molecules. It moves concomitantly with M across the membrane (GINSBURG and STARK[112]).

A large *mediator* M allows the incorporation of a small solute S, otherwise largely confined to the interface, into the interior of the membrane by the generation of free volume in the environment of M. If M itself is mobile inside the membrane, it will transport *free volume* from one interface to the other and simultaneously solute S inside this volume. Though no direct chemical interaction between M and S is assumed (as in the case of a carrier mechanism), a charged solute S will be able to transfer the driving force, exerted by an electric field, to the coupled movement of S and M.

The energy profile of macrocyclic compounds valinomycin and nonactin has been found to be similar to that of hydrophobic ions by different methods (HALL *et al.*[115]). They are preferentially confined to the membrane/water interface, but have a relatively high probability per unit time of crossing the barrier of the membrane interior. A kinetic analysis performed on the basis of voltage-jump current relaxation experiments yielded values for the translocation rate constant of the neutral species of about 10^3 10^5 s^{-1}, depending on the type of carrier and the kind of lipid (LAPRADE *et al.*[99]). A similar analysis of the hydrophobic ions dipicrylamine and tetraphenylborate gave values of 380 and 9 s^{-1}, respectively, for dioleoyl lecithin BLM (KETTERER *et al.*[73]). The high translocation rate constant of valinomycin and nonactin, in combination with their size indicate that they might serve as mediators for the transport of picrate anions. With 10^{-7} *M* valinomycin in the aqueous phases, about 10^{12} molecules are absorbed to 1 cm^2 of the BLM composed of about 2×10^{14} dioleoyl lecithin molecules/cm^2 (BENZ *et al.*[103]). The application of GOUY-CHAPMAN theory of charged interfaces allows the calculation of the number of charges, which are responsible for a given electrical surface potential. The absorption density of about 3×10^{13} picrate anions/cm^2 at 10^{-3} *M* picrate in the aqueous phase has been obtained. Though this number is only an approximation it might indicate that a relatively dense packing of picrate in the aqueous phase has been obtained. They could considerably favor the occupation of free defect structures in the proximity of valinomycin molecules. The conductance depends roughly on the third power of the *actual* picrate concentration. This seems to imply, in the light of present argument, that the probability of occupation of empty defect structures generated by valinomycin is drastically enhanced with increased packing density of picrate at the BLM surface. In other words, picrate anions prefer the adsorption sites at the interface at low packing density.

5.1. *Valinomycin*

The effect of ionophores such as valinomycin or gramicidin A on the cation permeability of natural as well as reconstituted BLM has been extensively studied. Valinomycin behaves as a translational carrier for potassium or rubidium ions. Gramicidin behaves differently. It forms polar pores which allow the passage of monovalent cations from one side of the membrane to the other[6]. Steady state as

well as non-steady state electrical methods have been applied to elucidate the mechanism by which these substances act. Valinomycin promotes cation permeation through BLM by forming 1:1 complex with the cation, which are mobile inside the membrane. A complex kinetic analysis has been used for the determination of concentration and mobility. Non linearity of stationary current-voltage curves and current relaxation data have been used for the evaluation of various parameters. The time course of current following a voltage jump depends in a characteristic way on the molecular events of a specific transport model. Simple carrier model which treats the BLM as a single step energy barrier has been applied by STARK *et al.*[100]; BENZ *et al.*[103]; GAMBALE *et al.*[116]. All the rate constants which according to this model are required to describe carrier mediated ion transport have been evaluated. Related charge pulse methods[103,106,117] have confirmed this type of analysis. These treatments provide information about the number of ions which are transported by a single carrier molecule per second.

The kinetic analysis of the carrier model has been given by LAUGER and STARK[109]. The effect of ion carriers like valinomycin on the conductance of BLM has been described on the basis of a simple model. Positively charged 1:1 complexes MS^+ formed between a carrier molecule S from the membrane and an ion M^+ from water represent the mobile charge carriers inside the BLM. Their formation at the membrane|water interface as well as their translocation across the diffusion barrier of the membrane interior are described by rate constants. This model has been found to predict sufficiently well the concentration dependence of the zero current conductance and of the non-linearity of steady state current-voltage characteristics. Dansylysine-valinomycin, a fluorescent analogue of the ionophore valinomycin was incorporated in BLM by POHL *et al.*[118]. Its concentration inside the membrane was determined from electrical relaxation experiments, which were analyzed on the basis of the proposed carrier model. A conductance increment per carrier molecule of about 3×10^{-17} s^{-1} was obtained for dansylysine-valinomycin in the membrane.

5.2. *Nigericin*

The group of ionophore antibiotics including nigericin, monensin, dianemycin and X-206 has been attracting considerable interest lately. These compounds are polyethers, polyalcohols and monocarboxylic acids with molecular weights in the range from 700 to 1000. They are capable of extracting alkali cations from aqueous solutions into organic solutions and affecting exchange transport of potassium and hydrogen ions in various biological systems. Nigericin is the most extensively studied representative of this group. At low concentrations (about 10^{-7} *M*) nigericin inhibits mitochondrial respiration and higher concentrations (10^{-6}-10^{-5} *M*) it uncouples oxidative phosphorylation[119]. Nigericin affects transmembrane exchange of potassium for protons in mitochondria at concentrations as low as 10^{-7} *M* (PRESSMAN *et al.*[120]). Nigericin can complex

with potassium, in which the carboxyl group is deprotonated and the antibiotic forms a collar about the cations. The complex remains stable as a result of the interaction between the cation and the dipole parts of the antibiotic and as a result of the hydrogen bond between the opposite ends of the molecule with the deprotonated carboxyl group on one side and the hydroxyl group on the other. The complex so formed is a zwitterion. Thus, nigericin can transport alkali ions in an electrically neutral form of zwitterions and protons in an electrically neutral non-dissociated form. MARKIN *et al.*[121] have studied the electrical properties of the BLM in the presence of nigericin and have analyzed the possible mechanisms for the electric charge transport. They have developed an ion transport model and have assumed that in the membrane the species move by the EYRING hopping mechanism; that is in the membrane the species are located in the potential wells near the surface hopping between them with rate constants. The potential applied to the BLM is assumed to change the hopping rates of the charge particles. They have assumed that nigericin in the BLM works as an ion carrier. It means that nigericin molecules repeatedly shuttle inside the membrane before they cross its boundaries, so that the net nigericin flux across BLM is negligible in comparison with the net ion fluxes. The total flux of all forms of nigericin across membrane in the steady state is zero, which has been explained in terms of the induced ion transport across BLM. This theory in its present form is based on models of carriers, relay race, and collective transport advanced by MARKIN and CHIZMADZHEV[122]. But neither the carrier model nor the relay race model explains the transmembrane potential of variable polarity. This effect has been predicted theoretically only in the collective transport model though under entirely different conditions Thus, MARKIN *et al.*[121] were compelled to consider the collective transport model or more exactly, a special case of it —the model of dimers. They have reported that the potassium and hydrogen dimers of nigericin can transport charges across BLM. Their theory predicts a characteristic shape of the curve with the maximum. Analyzing the electrical properties of BLM they have concluded that nigericin inside the membrane commutes between its interfaces carrying ions from one solution to another. This kind of motion is called small loop. Their experimental data also suggest that dimers are considerably more effective in transporting charges than the nigericin anion and that permeability for potassium compounds is considerably higher than the permeability of hydrated compounds.

5.3. *Phloretin*

This compound is the classical reversible inhibitor of the hexose transport system in the human red blood cell membrane; it also slows the movement of glycerol and urea and powerfully inhibits chloride movement[123]. In addition, phloretin affects non electrolyte and ion transport across several other biological membranes (*e.g.*, KOTYK *et al.*[124], OWEN *et al.*[125]). The physico-chemical mechanism responsible for the effect of phloretin on a variety of BLMs and

transport systems has been given by ANDERSEN *et al.*[75]. They reported that phloretin and certain other dipolar organic molecules increase carrier-mediated and lipophilic cation conductances and decrease carrier-mediated and lipophilic anion conductances of BLM. Phloretin produces trivial changes in the conductance of BLM separating NaCl or KCl solutions. In the case of modified BLMs phloretin increases cation conductance and decreases anion conductances. The BLMs have to be first treated with ion carriers, or lipophilic ions. This has been found for K^+-*nonactin*, K^+-*valinomycin*, $TPhAs^+$, $TPhB^-$, $CCCP^-$, *etc.* Moreover, these conductance changes are very large. For example, 1.5×10^{-4} *M* phloretin increases K^+-nonactin conductance 10^5-fold and decreases CCCP conductance 10^3-fold on BLMs. These conductance changes clearly reflect changes in permeability to the original conducting species, since ion selectivity is not altered.

Phloretin's action can be interpreted as follows. There exists a positive potential difference of several hundred millivolts between the hydrocarbon interior of a membrane and the adjacent aqueous phases, shown in Fig. 17. This potential difference arises from oriented dipoles (of either the lipids themselves or water) near the lipid-water interface. Phloretin adsorbs at this interface and, probably by the orientation of its own large dipole moment, introduces a dipole potential of opposite polarity to the pre-existing one. Thus, the positive potential in the BLM interior is reduced. Consequently, the BLM becomes more permeable to cations, because of their increased partition coefficient into the membrane interior, and less permeable to anions, because of their decreased partition coefficient.

Para- and *meta*-nitrophenols have qualitatively similar effects to those of phloretin; *i.e.*, they increase cation conductances and decrease anion

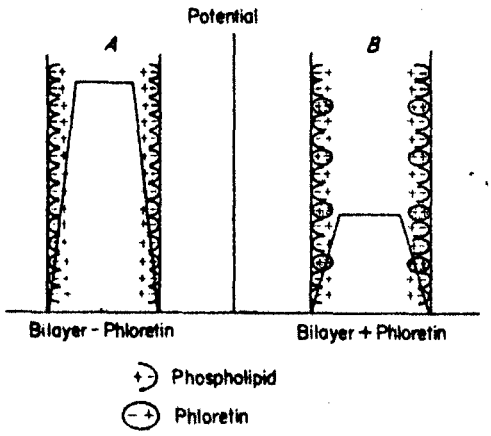

Fig. 17. Schematic representation of the electrical dipole potential profile within a BLM in the absence (*A*) and presence (*B*) of phloretin (ANDERSEN *et al.*[75]).

conductances. The fact that un-ionized phloretin and *m*- and *p*-nitrophenols greatly enhance cation conductances and greatly depress anion conductances is due to the reduction of positive dipole potentials in BLM. This reciprocal action on positive and negative species implies that these molecules act mainly by reducing the electrostatic potential of the membrane interior with respect to the aqueous phases. As this is not achieved from changes in BLM surface charge, it must result from changes in the dipole potential at the membrane interface, since surface charges and surface dipoles can only affect the interior potential of thin membranes, *i.e.*, thickness less than the DEBYE length within the BLM. In thick membranes they are screened by compensating ions in the diffuse double layers.

6. Channels (pores) in BLM

The basic mechanism involved in nerve signal has been described phenomenologically and mathematically by HODGKIN[77] and KATZ[126] (for a recent monograph see SCOTT[127]). Their *ionic theory* of membrane excitability has received general acceptance, although the turning *on* and *off* pathways for the movement of specific ions (Na^+ and K^+) across nerve cell membrane and the physical understanding of the ion *gating* process is still not very clear. The electrical potential across plasma membrane may be a consequence of:

(*a*) the ion asymmetries between cytoplasm and surrounding medium, and
(*b*) the relative permeability of the membrane to these ions. In excitable cells the action potential results because the membrane permeabilities (or conductances) to several of these ions (in the squid giant axon these are Na^+ and K^+) are strongly voltage dependent. According to the ionic theory, metabolism serves only to establish and maintain ionic asymmetries; given the asymmetries, the action potential arises from the voltage-dependent conductance changes in the membrane independent of metabolism.

In the past two decades, numerous investigators have confirmed the essentials of the HODGKIN–HUXLEY–KATZ theory for a wide variety of excitable cells (SCOTT[127]). Although the particular ion conductances that are under voltage control vary with the type of cell, in all systems studied the basis of electrical excitability is the strong dependence of ion or several ion conductances on membrane potential. This being the case, the central question concerning the mechanism of excitability becomes: what are the physico-chemical events that occur in the membrane in response to changes in membrane potential? That is, how does an electric field alter the permeability of the membrane to a given ion? There is indirect evidence that the permeability increase results from the opening of numerous small pores of two kinds in the membrane, each with a conductance of about 0.1 nmho. The estimate of pore conductance rests largely on the fact that certain subthreshold potentials occur more often than the others, with a spacing between most likely potentials of about 0.15 mV.

The changes of this kind have been detected in BLM. Several substances provide models which may be examples of rather general mechanisms by which voltage gating can be accomplished. A proteinaceous material of bacterial origin discovered by MUELLER *et al*.[4,128] (TIFN[6]) called *excitability inducing material* (EIM) interacts with BLM to produce a voltage-dependent conductance system that mimics in many respects the properties of biological excitable systems. MUELLER and RUDIN[129,130] subsequently discovered that two antibiotics alamethicin and monazomycin also induce dramatic voltage-dependent conductance changes in BLM. Since the thickness of BLM is comparable to the dimensions of (macro) molecules, special conduction mechanism becomes possible, in which molecules or molecular aggregates form ion-conducting channels across the BLM.

6.1. *Excitability inducing material (EIM)*

The conductance of BLM can be increased several orders of magnitude by modifying membranes with *excitability inducing material*[6]. The conductance induced by this material exhibits negative resistance regions, and, under certain conditions, action potentials similar to those found in some excitable cells have been produced (MUELLER *et al*.[4], MUELLER and RUDIN[129]). BEAN *et al*.[131] have presented convincing evidence that the conductance properties of membranes so modified are a result of the formation of discrete, proteinaceous, trans-membrane channels which have two or more well-defined conductance states. LATORRE *et al*.[132] and EHRENSTEIN *et al*.[133] have investigated the properties of these channels in oxidized cholesterol BLMs (ROBINSON and STRICKHOLM[134]). For a single voltage polarity, only two distinct channel conductance states were generally observed in these membranes, and the ratio of the high to low conductance was approximately 5:1. BEAN[131] observed that in other membrane preparations the channel had three or more conductance states at a given polarity. One of the low conductance states corresponded approximately to the low conductance states observed in oxidized cholesterol BLMs, and a nearly zero conductance state was also frequently observed.

In BLMs containing many channels of EIM, the conductance change following a step change in potential (voltage-clamp) has been observed by BEAN *et al*.[131] to follow an exponential rise or decay involving one or two decay constants. EHRENSTEIN *et al*.[133] found that for oxidized cholesterol BLMs the conductance change following a step change from zero to some higher voltage was an exponential decay with a single decay constant. They also determined the voltage dependence of the decay constants for one voltage polarity and found a good correlation between the decay constants in membranes containing many channels and the average time that single channels existed in either the high or low conductance states. The transition rates for the opening and closing of the channels

were found to depend exponentially on the voltage across the BLM.

Recently HOFFMAN *et al.*[135] have reported observations of voltage-clamped oxidized cholesterol BLMs with EIM which have several rather than two conductance states at a given voltage polarity. They have presented evidence of the multistate conductance behavior of the membranes containing either a single channel or several hundred channels. They have also considered the kinetics for the conductance transition following a step change to voltage. The decay constants for the transitions to a quasi-steady-state and the relative conductance of this state were determined for a range of negative and positive clamping voltages and they have compared the experimental results with models. They have also speculated on the types of models for the channels which are consistent with the experimental data.

The multi-state behavior of EIM-modified BLMs was conclusively demonstrated by HOFFMAN *et al.*[135] in single-channel experiments. Many levels were observed for both positive and negative polarizations, although the actual conductances of various states varied slightly among different channels. Although a given conductance state could occur at either positive or negative voltages, each state was much more frequent at one polarity or the other. The conductance states most frequently observed at negative clamping voltages was approximately 0.3, 0.1, 0.03 and 0 $n\Omega^{-1}$, and at positive voltages approximately 0.25, 0.05, 0.03 and 0 $n\Omega^{-1}$. A zero conductance state means that the channel conductance was not distinguishable within experimental error from the conductance of the unmodified BLM. Fig. 18*a* shows that for small negative voltages a channel is nearly always in a state with conductance 0.3 $n\Omega^{-1}$. Fig. 18*b* shows several conductance levels at positive polarization. The sudden absence of fluctuation in the zero conductance state is a common phenomenon in these BLMs but this probably does not indicate removal of the channel because a return to a higher conductance state is frequently observed upon changing to a lower voltage or voltages of opposite polarity. However, the duration of polarization at large voltages seems to affect the ability of a channel in the zero conductance state to return to a higher conductance state. Channels have been observed which, when forced into the zero conductance state by large positive voltages lasting several minutes, could not be brought to a higher conductance state even after prolonged polarization at negative voltage up to the membrane's breakdown voltage. This would seem to explain the irreversible decrease in conductance observed in BLMs containing many channels. Multiple conductance states as well as a zero conductance state are also observed at negative voltages, as shown in Fig. 19. HOFFMAN *et al.*[135] have demonstrated that for a given voltage polarity, the channels are multi-state rather than two-state systems and that the irreversible transition to low conductance states in many-channel membranes is probably due to channels going to near-zero conductance states, from which a return to higher conductance states is improbable. The existence of several conductance states in a single channel gives rise to several decay constants in the decay of the conductance for many channel membranes following a step

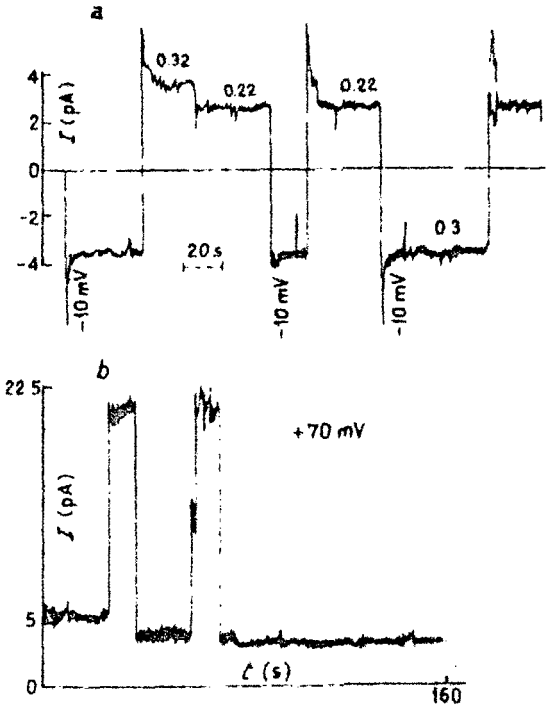

Fig. 18. Single channel conductance states. In (*a*) and (*b*) the channel conductance (0.32, 0.22 and 0.3 $n\Omega^{-1}$) at selected levels is given in units of $n\Omega^{-1}$: both (*a*) and (*b*) are records (as pA) of a single membrane formed from reoxidized cholesterol (HOFFMAN *et al.*[135]).

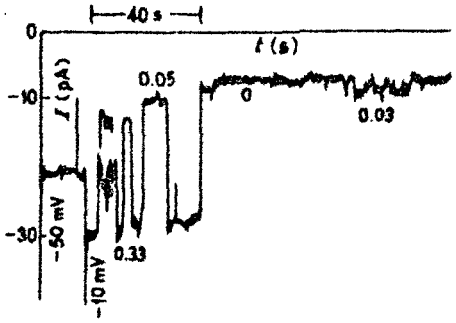

Fig. 19. Single channel conductance states. This is a record of the current of a single channel at −70 mV. Several conductance states (0.33, 0.05 and 0.03 $n\Omega^{-1}$) are apparent although the channel is in the zero conductance state most of the time. The membrane is formed from reoxidized cholesterol in decane (HOFFMAN *et al.*[135]).

change in voltage. Since some of the time constants are very large, a quasi-steady-state can be reached, and the decay to this quasi-steady-state is reasonably well described by a single decay constant. The voltage dependence of the decay constant and quasi-steady-state relative conductance (in terms of models in which the energy levels of and barriers between the conductance states of the channels) depend linearly on the voltage across the BLM. This voltage dependence could represent either a dipole interaction with the electric field or a charge-gaining energy by moving through the electric field.

6.2. *Alamethicin*

This compound exhibits a strongly voltage dependent conductance in BLM formed from 2.5 % sphingomyelin in tocopherol, chloroform, methanol (5:3:1) (MUELLER and RUDIN[129]). In BLM of this composition, addition of alamethicin to one side produces an increase in electrical conductance when voltages of either polarity are applied. The conductance increase occurs at a somewhat lower voltage when the side to which the alamethicin is added is positive. GORDON and HAYDON[136] published the first evidence that alamethicin produces discrete steps in conductance. They also state that the discrete steps come in *groups* but they did not provide quantitative evidence for this. GORDON and HAYDON have also stated that the conductance of a discrete level is independent of BLM thickness, is approximately proportional to electrolyte concentration, and is nearly independent of voltage but shows a slight bend toward the current axis in the voltage-current curves at higher voltages. CHERRY *et al.*[137] found that alamethicin in BLM also induced a conductance increase independent of voltage and that the type of ion influences the rate at which the current increases with voltage. EISENBERG *et al.*[138] showed how macroscopic phenomena, voltage-current curves, and negative resistance in the presence of salt gradient, for example, are related to microscopic events, which presumably involve interactions of only a relatively few molecules. On the macroscopic level EISENBERG *et al.* presented observations of voltage-current curves, time responses of current to a voltage step and time averaged fluctuations at high conductance levels. On a microscopic level they have also measured, in the same system used for macroscopic observations, discrete conductance levels of the kind reported by GORDON and HAYDON[136]. They have, in addition, made quantitative measurements on the relative likelihood of given discrete levels and have shown that the strongly voltage dependent conductance must depend on the voltage dependence of the probability of formation of a single entity, which they called as a *pore*. Each pore can then exist in several conductance states, corresponding to the discrete levels. The conductance of an individual pore fluctuates between five levels ranging from roughly 0.1 to 1.0 nmho in 0.1 *M* KCl. The pores are formed preferentially in the lowest conductance state (zeroth level) and also they disappear preferentially from that state. Thus, a pore, once formed, has a high probability of fluctuating through all its

levels before disappearing. There is an e-fold increase in the number of pores at equilibrium for a rise in potential of 4.94 mV. These results also explain the observation of MAURO *et al.*[139].

The kinetic of formation and disappearance is interpreted in terms of a three-state scheme: pre-pore, activated state, and pore. Each of these three states has its own energy level. The energy of the pre-pore is the lowest and that of the activated state is highest. The rate of formation will be determined, in part, by the difference in energy between the pre-pore and the activated state. The number of pre-pore at a given voltage will be determined by the alamethicin concentration and the salt concentration. The rate of disappearance will be determined, in part, by the difference in energy between the pore and the activated state. The equilibrium between pore and pre-pore will be determined by the difference in energy between the two states. If it is assumed that the energy of the pore is not affected by the potential, one can calculate that the energy level of the pore is lowered by kT when the potential is raised by 3.94 mV.

The equilibrium concentration of pores increases with the 9th power (9.2 ± 1.1) of the alamethicin concentration and with the 4th power (4.2 ± 0.35) of salt concentration. The number of pores can be written

$$n = n_i [\text{salt}]^4 [\text{alameth}]^9 \exp\left(\frac{U - U_i}{3.94}\right) \tag{40}$$

where n_i is the number of pores at $U = U_i$ (U_i is the characteristic voltage at a fixed conductance g_i) and is independent of voltage. U_i is a constant depending on the type of salt and membrane area.

Gordon and Haydon[136] also showed from the studies of the fluctuations that can be detected in very small membrane currents, that alamethicin forms transient pores of some 0.6 nm in diameter and that, for small inorganic ions, these are poorly selective. They have demonstrated that the sensitivity of the BLM conductance to the applied potential arises only to a slight extent from the current-voltage relations for the individual pores, and that the main effect stems from the influence of the potential on the frequency of opening of the pores. From the properties of BLM containing alamethicin in a wide variety of electrolytes, and from other evidence, it is concluded that alamethicin reacts to the electric field more probably because it has a large dipole moment than because it binds ions. They have proposed that the conducting complex is capable of functioning in either of two orientations, and that it is these two possibilities that give rise to certain differences in the single channel characteristics for the two directions of the field.

6.3. *Gramicidin A*

This is a linear polypeptide antibiotic which makes biological membranes and BLM permeable to alkali cations and protons[6]. Thus, much current interest exists in gramicidin A as a model transmembrane channel. HLDAKY and HAYDON[98]

showed that BLM containing a very small amount of gramicidin A exhibit discrete changes in conductance that are due to the formation and breakdown of individual gramicidin channels. A number of experiments have suggested that the gramicidin A transmembrane channel is a dimer. According to a proposal by URRY *et al.*[140] the structure of such a gramicidin channel consists of a helix which is formed by head to head association of two gramicidin A molecules in the BLM. This hypothesis is supported by the finding that the chemically dimerized malonyl-bis-desformyl gramicidin increases the membrane conductance and creates single channels in the BLM, the diameter of the hydrophobic interior is 4 Å. An alternate structure of the gramicidin channel, in which two gramicidin molecules consists of a double helix has also been proposed[141]. The dimerization process in the membrane has been investigated with electrical relaxation experiments (BAMBERG and LAUGER[83]) and the results have been confirmed by a number of investigators (ZINGSHEIM and NEHER[142], KOLB *et al.*[143]) who analyzed the electrical noise induced by the opening and closing of the gramicidin channels in a multichannel membrane system. Recently it was shown by BAMBERG and BENZ[144] that an electrical field can directly influence dimerization process of gramicidin in the BLM. BAMBERG and JANKO[82] more recently studied the BLM prepared by dioleoyl phosphatidylcholine and measured bi-ionic potentials with malonyl-bis-desformyl gramicidin (Gramicidin A was dimerized with carbon-suboxide). This substance increases the BLM conductance in a manner similar to that of the monomer gramicidin. In order to prove that the molecule forms cation-selective channels as the monomer does, and not unspecific pores, the dilution potential and bi-ionic potential were measured in the presence of univalent electrolytes. In the case of dilution potentials they obtained the theoretical value of cation induced potential (58 mV with 1.0 *M*|0.1 *M* NaCl). The ion specificity with respect to cations was measured by determination of bi-ionic potential. In such experiments the GOLDMAN equation was applied (bi-ionic potential = 44 mV with 1.0 *M* CsCl|1.0 *M* NaCl). An evaluation of bi-ionic potential data disclosed a permeability ratio $P_{Cs}/P_{Na} = 5.7$. This value is in close agreement which was found by HAYDON and HLADKY[88] for the monomer gramicidin.

The kinetics of dimerization of two monomer gramicidin molecules have been studied by BAMBERG and LAUGER[83] by voltage-clamp experiments. A voltage jump disturbs the equilibrium between monomers and conducting dimers in the BLM. The equilibrium in the BLM,

$$G + G \underset{k_D}{\overset{k_r}{\rightleftharpoons}} G_2 \tag{41}$$

is shifted toward the side of the conducting dimers at higher voltages. According to the dimer model of the channel the membrane current is proportional to the dimer concentration in the BLM. After a voltage clamp the current should relax to a higher stationary level. It has been successfully demonstrated (BAMBERG and

BENZ[144]) for several lipid-membrane systems that the current density $j(t)$ is governed by a single exponential for a wide range of gramicidin A induced conductances.

$$j(t) = j_\infty + (j_0 - j_\infty)\exp\left(-\frac{t}{\tau}\right) \tag{42}$$

where j_0 is the initial and j_∞ the steady-state current density. The relaxation time τ is given by

$$\frac{1}{\tau} = k_D + \sqrt{\frac{k_r k_D g_\infty}{N_A \Lambda}} \tag{43}$$

where k_D is the dissociation rate constant, k_r the association rate constant for the dimerization process, N_A AVOGADRO's constant and g_∞ the steady-state conductance of the membrane, which is reached after a long period of time (t). Λ is the single channel conductance of gramicidin A. The model for the dimerization of gramicidin A in a BLM requires that the relaxation amplitude becomes smaller with increasing membrane conductance. At higher levels of conductance, *i.e.* at high concentrations of gramicidin, the molecule should be present mainly in the dimerized form, so that the relaxation amplitude becomes smaller with increasing conductance.

The properties of malonyl-bis-desformyl-gramicidin (MbdG) channels have been studied by BAMBERG and JANKO[82] for different lipid systems. Fig. 20*a* shows a typical experiment, whereas in Fig. 20*b* the result is compared with the current fluctuation arising from appearing and disappearing gramicidin A channels. The conditions for both experiments were identical. To understand the mechanism, it is more interesting to study the kinetic behavior of MbdG channels on the single channel basis than the single channel conductance. The single channel lifetime is dramatically increased compared with the monomer gramicidin A. This result is expected on the basis of the dimer hypothesis. According to URRY's model[140], a chemically dimerized molecule should produce channels with a very long lifetime, since the MbdG cannot switch off, due to dissociation. The inactivation of such a channel can only occur by its diffusion into a part of the membrane, where, for geometrical reasons, the channels cannot exist in the conducting form.

Another remarkable phenomenon is shown in Fig. 20, the rapid switching on and off of probably the same channel. This fluctuation could arise from the same channel and presumably is not due to the association and dissociation of two dimer molecules to form a tetramer, producing new channels. This could be possible, according to a proposal by VEATCH and STRYER[141]. These authors propose an alternate channel model to the hypothesis by URRY. They postulate that two monomer gramicidin molecules can form a parallel and an antiparallel helix, respectively. The conductance and fluorescence energy transfer studies of channels

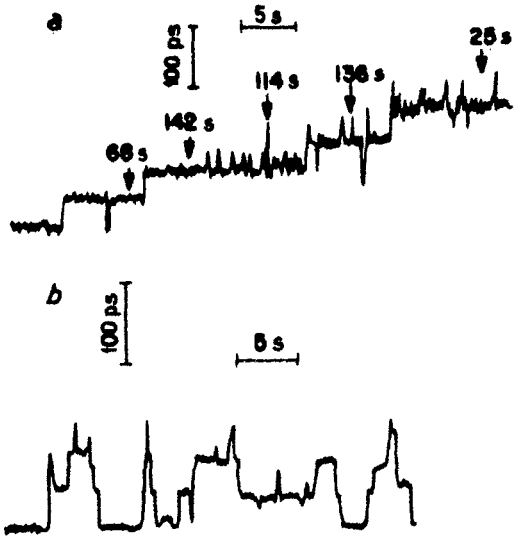

Fig. 20. (*a*) Single channel response of malonyl-bis-desformylgramicidin. Lipid, diphytanoyl phosphatidyl-choline/cholesterol. *U*-100 mV (*b*) Single channel response of gramicidin A, under identical conditions as in (*a*) (BAMBERG and JANKO[82]). The figures on the graph refer to the lifetime of the channel.

containing two kinds of gramicidin have been carried out. These studies of hybrid channels were designed to determine the number of molecules in a channel. The single-channel conductance of gramicidin C in BLM is 0.68 that of gramicidin A. BLMs containing both gramicidin C and gramicidin A exhibit three kinds of channels: a pure gramicidin A, a pure gramicidin C channel, and a hybrid channel with an intermediate conductance (0.82 that of gramicidin A). The dependence of the frequencies of these three kinds of channels on the mole fractions of gramicidin A and gramicidin C in the membrane-forming solution fits a dimer model. The fluorescence studies, like single-channel conductance measurements, showed that there are two molecules of gramicidin in a channel. Finally, SZABO and URRY[145] have found that N-acetyl gramicidin greatly increased the rate of dissociation of conductance channels in BLM and concluded that their results further supported the head-to-head dimer structure for the ion-conducting gramicidin A channel.

6.4. *Hemocyanin*

Hemocyanins are oxygen-transporting blood proteins and contain 0.18 to 0.24 % copper, probably univalent. Electron-micrographs and ultra-centrifugal analysis indicate that the hemocyanin molecule in dilute salt solution at neutral pH is roughly cylindrical in shape with a diameter of about 30 nm. Reversible

association occurs, if divalent cations are added to the media or if pH is readjusted to 5–7 (VAN BRUGGEN *et al.*[146]; KONINGS *et al.*[147]). It has been reported that keyhole limpet hemocyanin markedly increased the ionic conductance in oxidized cholesterol and brain BLM (PANT and CONRAN[148]). LATORRE *et al.*[149] have recently found evidence that hemocyanin forms discrete channels in BLM. The channel conductance is constant for negative potentials, but at high positive potentials the conductance fluctuates between several levels. The electrical responses of individual hemocyanin channels in oxidized cholesterol BLM demonstrate that the voltage-dependent conductance of many-channel BLM arises from two different mechanisms. These are the voltage-dependent redistribution of channels among several discrete single-channel conductance states and the continuously voltage-dependent conductance of the single-channel states themselves. The relaxation time for the discrete conductance changes is of the order of seconds and the relaxation time of the continuous conductance changes is of the order of 10^{-4} seconds. As salt concentration in the bathing medium is increased, the single channel conductance first increases linearly and then saturates. The characteristics of the saturation curves suggest that the continuous conductance changes occur at the edges of the channel and that the mean time an ion spends in the channel is 4 nanoseconds.

LATORRE *et al.*[149] attempted to provide some insight into the continuous changes of the hemocyanin channel by consideration of the saturation properties. They used a model for saturation based on the assumption that no more than one ion can be in a given pore at a given time. In this model, the mean time that an ion spends in the channel is an important parameter. If this time is long enough and ions enter the channel fast enough, the channel will be occupied for a substantial fraction of time. Since an occupied channel cannot accept an additional ion, it becomes more difficult to increase the current through the channel, thus causing saturation. This model can be described quantitatively as follows:

Let g = channel conductance; K = constant of proportionality; c = salt activity; f = probability that channel is occupied; t = mean time an ion spends in channel; and R = rate of ions entering channel. The channel conductance is proportional to the salt concentration and to the probability that the channel is available. The probability that the channel is available is simple $(1 - f)$. Therefore

$$g = Kc(1 - f). \tag{44}$$

f is equal to the product of the mean time an ion spends in the channel and the rate of ions entering the channel. Thus,

$$f = tR. \tag{45}$$

R is proportional to channel conductance. For g in units of mhos and applied potential 100 mV in magnitude

$$R = 0.625 \times 10^{18} g. \tag{46}$$

The constant in equation (46) is obtained by dividing the current corresponding to 100 mV and 1 mhos by the charge of an electron. Combining equations (44–46) one obtains equation (47)

$$g = \frac{Kc}{1 + 0.625 \cdot 10^{18} Kc} \tag{47}$$

which is a saturation equation. For low concentration, conductance is proportional to activity, and for high concentration, it is independent of activity. The parameter K, which is a measure of conductance at low concentration, is about 3.5 times larger at -100 mV than at $+100$ mV. This variation of K can be interpreted as a variation of probability of an ion getting into the channel. The value of t which is determined by the maximum conductance, is approximately the same for the low potentials. At -100 mV, $t = 3.2$ ns. Thus, the average time an ion spends in the channel does not vary for all the continuous changes of the channel within the uppermost discrete levels but the probability of an ion getting into the channel does vary. This can be described by a barrier model where the ionic potential profile within the channel does not change, but the ionic barriers at the inner and outer surfaces of the channel do change. The model implies that the continuous changes in channel conductance correspond to conformational changes at the edges of the hemocyanin channel. Another property that can provide information about channel structure is ion selectivity. The hemocyanin channel is highly selective to cations relative to anions, but that there is not a large selectivity difference between monovalent cations. Hemocyanin differs from both excitability inducing material and alamethicin in that discrete states of individual hemocyanin channels have voltage-dependent conductance and in that for at least one discrete single-channel state, the current through the hemocyanin channel saturates with increasing salt concentration. More recently, ANTOLINI and MENESTRINA[150], and McINTOSH *et al.*[151] reported that currents through the hemocyanin channel show saturation at increasing concentrations of KCl, which in some aspects are similar to those obtained with alamethicin and Excitability-Inducing Material (HOFFMAN *et al.*[135]).

6.5. *Miscellaneous studies*

SCHEIN *et al.*[152] have incorporated into BLM a voltage-dependent anion-selective channel (VDAC) obtained from *Paramecium Aurelia*. VDAC-containing BLM have the following properties:

(1) The steady-state conductance of a many-channel membrane is maximal when the transmembrane potential is zero and decreases as a steep function of both positive and negative voltage.

(2) The fraction of time that an individual channel stays open is strongly voltage dependent in a manner that parallels the voltage dependence of a many-channel membrane.

(3) The conductance of the open channel is about 500 pmho in 0.1 to 1.0 M salt solutions and is ohmic.
(4) The channel is about 7 times more permeable to Cl^- than to K^+ and is impermeable to Ca^{2+}.

Analysis of the voltage dependence is as follows.

Assume that the channel can exist (for positive voltages) in either an open (o) or a closed (c) state, and that the relative number in each state is given by the BOLTZMANN distribution

$$\frac{N_o}{N_c} = \frac{N_o}{N_t - N_o} = \exp\left(-\frac{E(U)}{kT}\right) \tag{48}$$

where N_o and N_t are the number of channels in the open and closed states, respectively, $N_t (= N_o + N_c)$ is the total number of channels, and $E(U)$ is the voltage-dependent energy difference between the two states. Suppose that it requires the movement of charges associated with the channel to switch the channel from the open to the closed state. If ne is the equivalent number of charges which move through the entire transmembrane potential U_m, then

$$E(U) = ne(U_m - U_o) \tag{49}$$

and equation (48) becomes:

$$\frac{N_o}{N_t - N_o} = \exp\left[-\frac{ne(U_m - U_o)}{kT}\right]. \tag{50}$$

Calling $g_{s,V}$, the conductance of a single channel in the open state, then the total conductance ($g_{t,V}$) is given by

$$g_{t,V} = N_o g_{s,V} \tag{51}$$

$$g_{t,max} = N_t g_{s,V} \tag{52}$$

and equation (50) becomes

$$\frac{g_{t,V}}{g_{t,max} - g_{t,V}} = \exp\left[-\frac{ne(U_m - U_o)}{kT}\right]. \tag{53}$$

This is the simple two-state model for the channel. $g_{t,max}$ is the maximum value of $g_{t,V}$ (it occurs around $U_m = 0$), U_o is the switching voltage (at $U_m = U_o$ there is an equal number of channels in the open and closed), e is the electronic charge, k is the Boltzmann constant, T is temperature in degree Kelvin. Fig. 21 is a plot of $\ln \frac{g_{t,V}}{g_{t,max} - g_{t,V}}$ versus U and gives a straight line as predicted by equation (53). From the slope and intercept one obtains $n = 4.5$ and $U_o = \pm 20$ mV (values of n range from 4 to 8; values of U_o range from ± 15 to 20 mV). A value of $n = 4.5$ means that at

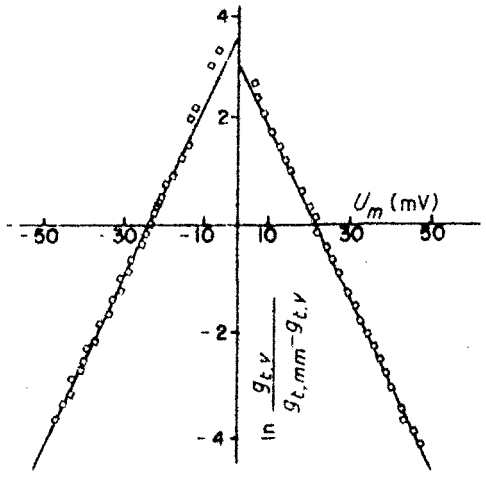

Fig 21. Plots of $\ln [g_{t,V}/(g_{t,max} - g_{t,V})]$ *versus* U. $g_{t,V}$ the conductance at any point minus the ohmic conductance. U is the potential (mV). $g_{t,max}$ is the maximal conductance minus the ohmic conductance (SHEIN *et al.*[152]). The two branches corresponds to positive and negative values of U, respectively.

voltages where $g_{t,V} \ll g_{t,max}$, $g_{t,V}$ changes e-fold for every 5.5 mV shift in membrane potential.

Another paper from SCHEIN *et al.*[152] reported that colicins, bactericidal proteins of molecular weights 5×10^4 to 10^5 produced by *E. coli*, can form voltage-dependent and ion-permeable channels in phospholipid BLM. Their observations are of interest and may be related to the known effects of the functional group of colicins (K, El and Ia) on the bacterial cell. The colicins exert their bactericidal effects by a conformational change of the cytoplasmic membrane thereby promoting a net efflux of ions from the cell.

BENZ *et al.*[153] reported formation of large, ion-permeable channels in BLM by porin, one of the major proteins of the outer membrane of *E. coli*. This protein has been observed to increase BLM conductance by many orders of magnitude in concentrations of the order of 10 mg/cm^3. At lower concentrations, the BLM resistance decreases in a stepwise fashion, the single conductance change being about $2 \times 10^{-9} \Omega^{-1}$. SCHINDLER and ROSENBUSCH[154] have observed similar discrete conductance steps in BLM.

In recent years, one of the most interesting studies with BLMs, initiated by DEL CASTILLO *et al.*[155], is concerned with antigen-antibody-complement interactions (KINSKY and NICOLOTT[156]; WOBSCHALL and McKEON[157]; MICHAELS *et al.*[158]; MOUNTZ and TIEN[159]). In particular MICHAELS *et al* have shown that complement components, when incorporated into BLM, increase transmembrane ion flow. They believe that the conductance

increase is due to formation of channels of insertion of complement peptides. Further, MICHAELS *et al.* found that, on the basis of their conductivity data, interaction of the terminal components in the fluid lipid bilayer phase leads to the formation of complexes that are inactive with respect to BLM. Similar to the liposome experiments (KINSKY and NICOLOTT[156]), the BLM experiments (MICHAELS *et al.*[158]) suggest that the lipid moiety of cells is the target of attack by complement. Optimistically, they have concluded that, for certain types of experiments, the BLMs offer distinct advantages over liposomes. The mode of assembly of the channel can be studied more effectively with BLM than with liposomes.

KAKA *et al.*[42] have reported that dopamine-B-hydroxylase (DBH), an enzyme that catalyzes the conversion of dopamine (DA) to norepinephrine in adrenal medullary chromaffin granules, increases the electrical conductance of BLM. From their data, KAKFA *et al.* suggest that DBH forms ion-conducting channels and that the enzyme requires DA, its substrate, and Ca^{2+} for activity. Other proteins such as cytochrome oxidase, proteolipid apoprotein (TING-BEALL *et al.*[160]), asialoglycoprotein (BLUMENTHAL *et al.*[161]), plasma lipoproteins (MARTSENJSKY *et al.*[162], REPKE *et al.*[49]) and calcium binding glycoprotein (ANTONOV *et al.*[8]) greatly enhance the conductance of the BLM. An ion-transport system in a BLM has been reconstituted using Na^+ K^+ ATPase (SHAMOO and TRIVOL[14]). SHAMOO and TRIVOL reviewed this work and provided excellent criteria for the reconstitution of ion transport systems.

Stepwise increase in BLM conductance by liposomes prepared from the electric organ of *Torpedo californica* has also been reported[163]. Liposomes are lipid microvesicles or in single layer form are BLMs in spherical configuration and have been extensively studied along with the BLM system (for reviews see TIEN[6]; SHAMOO and TIVOL[14]; FENDLER[164]). To make these systems even more versatile, fusion of BLMs with loposomes has been carried out (ANTONOV *et al.*[8]; COHEN *et al.*[165]). This novel approach facilitates the introduction of ionophores, dyes, proteins, bacteriorhodopsin or other compounds of interest from liposomes into the BLM (LOPEZ and TIEN[166]). Interactions between liposomes and the BLM in most cases are increased in the presence of Ca^{2+}. One of the ubiquitous biological phenomenon, exocytosis, is being studied using the combined liposome-BLM system (COHEN *et al.*[165]). SUEZAKI[167], on theoretical grounds, has attempted to clarify the thermodynamic relationship between the stability of BLMs and liposomes.

Finally, exploitation of the BLM system for clinical and analytical purposes goes back to the experiments of DEL CASTILLO *et al.*[155] in 1966 (MOUNTZ and TIEN[159]). Recently, THOMPSON *et al.*[44] reported the use of the BLM as an electrochemical sensor and reported the limits of detection for amphotericin B and valinomycin which are, respectively, 10^{-9} *M* and 10^{-11} *M*. The nature of membrane responses at selective interactions of BLMs are discussed in terms of analytical parameters. In the study of the complex processes of drug absorption,

INUI *et al.*[168] have used the BLM system as a model for the intestinal lipid membrane. Although these methods are useful as laboratory tools, one severe drawback is the lack of long-term stability of the BLM. Perhaps the use of Nucleopore filters[195] as a BLM support might prolong the life expectancy of conventional BLM.

7. Electronic processes in BLM

Central to membrane bioenergetics is the redox reaction across the membrane. This entails the generation, separation and transport of charges (electrons and holes) leading eventually to redox reactions on opposite sides of the membrane. The energy stored in separated charges and redox compounds may be used to drive vital processes such as oxidative and photophosphorylation. In this section we are concerned with redox reactions (electronic processes) associated with BLM only (for reviews of the earlier literature see TIEN[6,169,170], MAUZERALL[171]). For electronic processes in other membrane systems, a number of papers are of interest (TABUSHI and FUNAKURA[172], SPARNAAY[173], DIGBY[174], PETHIG[175]).

7.1. *Electrostenolysis in BLM*

The BLM system consists of a BLM separating two aqueous solutions, in which the BLM is considered electrically as equivalent to a pico-ohm resistor in parallel with a large capacitor. The two solutions serve as electrical contact to the membrane, which are in turn contacted by reference electrodes connected to an external monitoring device. At each of the solution|BLM interfaces, a junction potential may be generated as a result of charge separation (ions and/or electrons and holes) in the interfacial region. Although each of these junction potentials is not directly measurable, the potential difference ($\phi_i - \phi_o$) of the BLM system can be readily determined, providing the monitoring device has an internal resistance 2-3 orders greater than the BLM resistance. Referring to Fig. 22, the transport process of charges across the BLM can be either ionic or electronic. In the latter case corresponding redox reactions occur, since the lifetimes of electrons and holes are ephemeral in the bathing solution.

First of all, is there any experimental evidence to support the idea of electron conduction in a membrane immersed in an aqueous environment? and, if so, what is the source of electrons in the membrane? The answers to these questions have been provided by the classical phenomenon of electrostenolysis[6]. The phenomenon can be described as follows. When a direct current is passed through a membrane (or barrier) of high electrical resistance separating two aqueous solutions, coupled electrochemical reactions occur on opposite sides of the membrane. Oxidation takes place on the side facing the negative electrode. Implicit in these reactions is a transverse movement of electrons across the membrane.

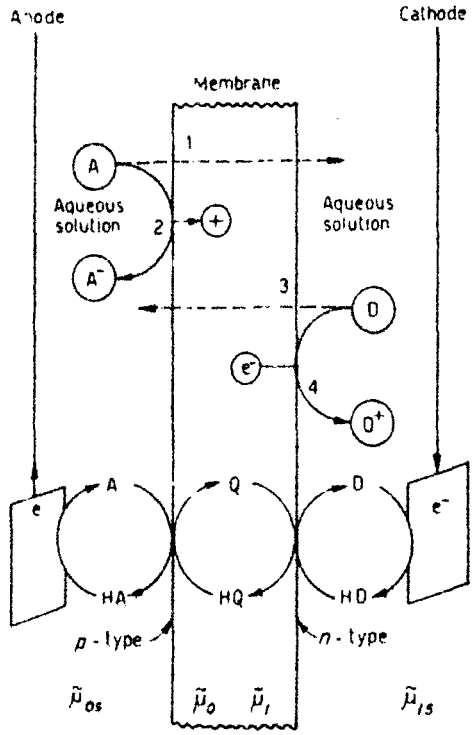

Fig. 22. Electronic processes in BLM. A = electron acceptor, D = electron donor. Also shown are redox reactions involving H^+ where a quinonoid compound (Q = oxidized form; HQ = reduced form) acts as a H-carrier in the membrane. The membrane|solution interface is considered to be analogous to a SCHOTTKY like barrier. $\tilde{\mu}$'s are electrochemical potentials. 1, 3 = ion transport: 2, 4 = electronic processes.

A dramatic demonstration of electrostenolysis in BLM has been seen in the following experiment[176]. If an oxidized cholesterol BLM is interposed between a solution of cupric nitrate and sodium sulphide, a shining mirror is observed to cover the entire BLM area in 3–10 minutes. The brightness of the mirror has been found to depend on several variables such as the concentration of $Cu(NO_3)_2$, the BLM resistance, the pH of the bathing solution, the duration and magnitude of the applied voltage. For example, using the cell arrangement: *aqueous solution* (0.05 cm^3 saturated Na_2S to 10 cm^3 of 0.1 *M* Na-acetate, pH = 4)|*Oxidized cholesterol BLM*|*aqueous solution* (0.02 *M* $Cu(NO_3)_2$ in 0.1 *M* Na acetate pH = 4), the mirror formation was observed within 100 seconds. If a pair of calomel electrodes were used to monitor the potential difference across the BLM, a voltage of 0 to about 50 mV was detected when mirror became visible. This voltage rose to about 200 mV when the entire BLM surface was covered by the mirror. The brightest mirror observed was at a voltage around 350 mV. If the BLM resistance was lowered by the addition of tetraphenylborate (2×10^{-4} *M*) to the bathing

solution, the mirror began to form within 30 seconds after adding $Cu(NO_3)_2$ to one side of the BLM. Concurrently, the membrane voltage rose quickly to about 150 mV and eventually levelled off at about 300–350 mV.

Pertinent to the above experiment is the confirmation of the classical concept that a suitably constituted interface can behave as a bipolar redox electrode, in which a liquid|liquid interface between distilled water and a solution of saturated KI has been used[176]. This has been accomplished by carefully layering a column of distilled water on top of the saturated KI solution. To aid visualization of the products at the interface as a result of electrostenolysis, phenophthalein and potato starch were added, respectively, to the distilled water and saturated KI solution. After applying a voltage of 100–250 V *via* a pair of platinum electrodes for 10–15 minutes, a faint brownish coloration appeared at the interface and became more intense with time resulting eventually in a highly visible dark-violet layer characteristic of the iodine starch complex. (The observed current flow was 4–10 mA.) In another experiment using similar conditions except that potato starch was omitted in the saturated KI solution, the interface acquired a pinkish color similar to that of the dye in an alkaline solution. These phenomena were not observed when saturated KI was replaced by a solution of saturated KCl. A straight forward interpretation of the results is that the interface between distilled water and saturated KI solution functions as a bipolar electrode. On one side of the interface iodide ions are oxidized to molecular iodine and on the other side hydrogen ions are discharged in accordance with the classical concept of electrostenolysis. Similar reactions were demonstrated in BLM, in that the time dependence of BLM conductance (current) in the presence of 0.1 *M* KCl and 0.1 *M* KI at 60 mV was measured. In the case of KCl solution, the BLM current displayed practically no time-dependency. As has been shown previously (LAUGER *et al.*[177], FINKELSTEIN and CASS[94]), the conductance of BLM in solutions containing iodide depends on the presence of trace amounts of iodine, being 2–3 orders of magnitude higher than the solution containing iodide only. Thus, the results obtained can be explained in terms of electrostenolysis in which the BLM served as a bipolar electrode just as in the case of the water|saturated KI solution interface. Upon passing a *d.c.* current, I^- is oxidized to iodine. The resulting product prefers a low dielectric medium (*i.e.*, the BLM) to aqueous solution by a factor of 50 times. The enhanced conductance of BLM, under these circumstances, has been attributed to the tendency of iodide and iodine to form polyiodides[94] which have a considerable solubility in the lipid phase and facilitate ion transport across the BLM.

7.2. *Redox potentials in BLM*

From thermodynamics the overall free energy change associated with an electrical cell reaction is given by

$$\Delta G = -nF\Delta U \tag{54}$$

where ΔU is the electric potential of the cell. Consider the BLM system as an electrical cell shown in Fig. 23, each solution|membrane interface is assumed to behave as a redox electrode. From equation (54) the individual free energy terms are denoted by μ. Thus, as indicated in the left side of the BLM (Fig. 23) $\mu_A + \mu_e = \mu_{A^-}$. Similarly, in the right side

$$D - e \rightarrow D^+ \tag{55}$$

and

$$\mu_D - \mu_e = \mu_{D^+}. \tag{56}$$

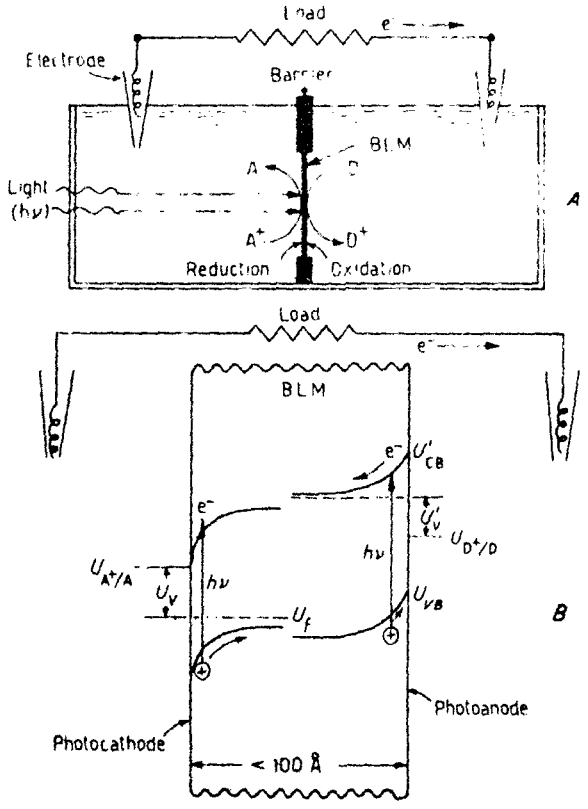

Fig. 23. Electron transfer scheme. (*A*) The BLM acts as bipolar electrode, on one side of which reduction takes place ($A^+ \rightarrow A$) and on the other side oxidation occurs ($D \rightarrow D^+$). (*B*) The BLM|electrolyte interface is likened to that of a SCHOTTKY barrier (semiconductor|metal interface). Excitation of electrons can take place in the band bending interfacial region whose depth depends on charge density and band bending (TIEN[170]).

In writing these equations the electrons involved are considered as one of the reactions. Since $\mu_i = \mu^0 + RT \ln a_i \simeq \mu^0 + RT \ln [i]$, where μ^0 is a constant, R and T have the usual significance, a is the activity and $[i]$ the concentration of the ionic species when the activity coefficient is taken to be unity. The free energy of the electron, μ_e, is given by

$$\mu_e = -\mathcal{F} U_{out} = \mu_{A^-} - \mu_A \simeq \mu^0_{A^-} - \mu^0_A + RT \frac{[A^-]}{[A]} \tag{57}$$

for the outer (left) solution|membrane interface, where U_{out} = the electrode potential. For the inner (right) solution|membrane interface, we have

$$\mu_e = -\mathcal{F} U_{in} = \mu_D - \mu_{D^+} \simeq \mu^0_D - \mu^0_{D^+} + RT \frac{[D]}{[D^+]} \tag{58}$$

At steady state, the free energy difference of the electron across the BLM is equal to

$$-\frac{\Delta \mu_e}{\mathcal{F}} = \Delta U_m = (U^0_{A/A^-} - U^0_{D^+/D}) + \frac{RT}{\mathcal{F}} \ln \frac{[A][D]}{[A^-][D^+]} \tag{59}$$

when $[A^-] = [A]$ and $[D^+] = [D]$, we have

$$\Delta U_m = U^0_{A/A^-} - U^0_{D^+/D} = U^0_{redox}.$$

Experimental confirmation of equation (59) has been sought in the BLM system. Thus far, only very limited success has been achieved (TIEN and SHIEH, unpublished data, 1975). The difficulty lies perhaps in finding suitable compounds for incorporation in the lipid bilayer phase, which can serve as pathways for electron tunnelling and conduction.

Finally, in connection with redox reactions in biomembrane systems, mention must be made of MITCHELL's work, whose chemiosmotic hypothesis of phosphorylation is currently receiving a great deal of attention. The 1978 Nobel Prize in Chemistry was awarded to MITCHELL on his chemiosmotic theory[178]. The essential features of MITCHELL's hypothesis are based on a redox membrane of high electrical resistance impermeable to ions.

7.3. *Modified BLM as semiconductors*

Electronic processes in biological membranes have been repeatedly suggested (TIEN[6]; ELEY *et al.*[179]) to be important, especially in connection with coupled redox reactions in mitochondria, energy transfer and conversion in chloroplasts, and sensory transduction in visual systems. Electronic processes (including electron conduction) in photoactive BLMs have been reported (TIEN[180]; KARVALY and PANT[181]; SCHADT[182]; HONG[183]; ALEXANDROWICZ and BERNS[184]; HUEBNER[185]; LUTZ *et al.*[186]; FELDBERG *et al.*[187]; TIEN[170]). In photoelectric BLMs, the membrane is considered to be *liquid*

crystalline possessing semiconductor characteristics[6]. Viewed in this manner, the language of solid-state physics can be used to the BLM system without much change. For example, the free energy of an electron in the BLM may be described in terms of the FERMI energy level, E_f. Similarly, a FERMI level has been defined for electrolyte solutions (GERISCHER[188]). Fig. 23 illustrates a BLM separating two aqueous solutions with redox couples, $A|A^-$ and $D^+|D$. In terms of electrochemical potential, $\tilde{\mu}$, one can write, at equilibrium

$$\tilde{\mu}_e = \tilde{\mu}_A - \tilde{\mu}_A \tag{60}$$

for the reaction

$$A + e^- \rightleftharpoons A^- \tag{61}$$

where $\tilde{\mu}_e$ = the electrochemical potential of electrons in the BLM. This term is identical to the FERMI energy level of electrons, E_f. The FERMI level of the redox couple ($A|A^-$) is related to the standard electrode potential $U^0_{A|A^-}$, which is based on the hydrogen scale, by

$$E_{F(redox)} = E^0_{F(H)} - e^- U^0_{A|A^-} \tag{62}$$

where $E^0_{F(H)}$ has been estimated to be about -4.5 eV. In Fig. 23 at the reference electrodes reversible electrochemical reactions occur which provide electronic carriers for the external circuit. If one assumes that the left BLM|solution interface behaves as a "*p*-type" semiconductor and the right BLM|solution interface as a "*n*-type", the FERMI level within the BLM can be related to the changes in the composition of the bathing solutions. Therefore, an equal change in $\tilde{\mu}$'s must occur. Thus, for the left interface

$$\Delta\tilde{\mu}_A = \Delta\tilde{\mu}_{oS} = \Delta\tilde{\mu}_o \tag{63}$$

and for the right interface

$$\Delta\tilde{\mu}_R = \Delta\tilde{\mu}_i = \Delta\tilde{\mu}_{iS}. \tag{64}$$

For a *p*-type BLM, the electron carrier concentration is given by

$$n = N_{A^-} - N_A. \tag{65}$$

The change in $\tilde{\mu}$ is then equal to

$$\Delta\tilde{\mu}_o = RT\ln\frac{n_f}{n_i} \tag{66}$$

where n_f and n_i denote the final and initial electron concentrations (TIEN[6]). Introducing equation (65) into equation (66) we have

$$\Delta\tilde{\mu}_o = RT\ln\frac{(N_{A^-f} - N_{Af})}{(N_{A^-i} - N_{Ai})}. \tag{67}$$

If $N_{A,i} \gg N_{A,f}$ and $N_{A,i} \simeq N_{A,0}$

$$\Delta\tilde{\mu}_e = RT\ln\frac{n_f}{n_i} \simeq RT\ln\frac{N_{A,f}}{N_{A,i}} \tag{68}$$

The bulk phase, $\tilde{\mu}_{e,s}$, will have an activity of the donor species, a

$$\Delta\tilde{\mu}_{e,s} = RT\ln\frac{a_{A,f}}{a_{A,i}} \tag{69}$$

From equations (65), (68), and (69), we have

$$\frac{n_f}{n_i} = \frac{N_{A,f}}{N_{A,i}} = \frac{a_{A,f}}{a_{A,i}} \tag{70}$$

In a similar manner, we can obtain an expression for a *n*-type BLM, which is

$$\frac{n_f}{n_i} = \frac{N_{D,f}}{N_{D,i}} = \frac{a_{D,f}}{a_{D,i}} \tag{71}$$

It should be noted that, combining equations (70) and (71), the overall expression for the membrane potential in terms of acceptor and donor concentrations is identical to that of equation (59).

One final comment should be made concerning Fig. 22 in which a quinone type carrier is depicted. Quinonoid compounds such as ubiquinone, vitamin K, and plastoquinone have been implicated in mitochondrial and photosynthetic membrane systems[178]. Of evident interest BLMs containing such compounds should be carried out in testing hypotheses of electron transfer and redox mechanisms.

The pigmented BLMs have been used to mimic the thylakoid membrane of the chloroplast and the visual receptor of the eye[6,32]. Lately, photoactive BLMs have found their place in the field of photochemical conversion and storage of solar energy (BOLTON and HALL[189], GERISCHER[190], LICHTIN[191]). For instance, with suitable electron acceptors and donors in the bathing solution separated by a pigmented BLM, light-induced redox reactions can occur at opposite interfaces. It might be possible to couple BLMs of this type in such a way as to effect photolysis of water into hydrogen and oxygen[195].

Of more immediate interest to membrane biology and biophysics are experiments using fluorescent probes in BLMs reported by LOEW *et al.*[192], DRAGSTEN and WEBB[193] reported that BLM-containing Merocyanine 540 responds to a potential step in two distinct time constants; one in less than 6 μs and the other 0.1 s. Both response amplitudes are proportional to applied voltages. The relationship between optical properties and the applied field, known as electrochromism, has been observed by LOEW *et al.*[194]. They have presented evidence for a charge-shift electrochromic mechanism and suggested that it

might be possible to develop a universal set of probes for monitoring membrane potentials. Since the fluorescence response to a potential step of a BLM is much less than 6 μs, the apparatus developed by HUEBNER[185] for pigmented BLM studies should be of interest

8. Concluding remarks and perspective

Since its inception in 1960, the bilayer lipid membrane (BLM) has served as one of the most useful models for biological membranes[6]. As evidenced in this review, many investigators have been able to modify its intrinsic characteristics by adding molecular constituents which endow it with dynamical properties resembling, for example, the nerve membrane. Considering the fragility of the BLM and its associated experimental difficulties, it is truly astonishing that so much data have been gathered on BLM. In this review we have summarized mainly one aspect of BLM research, namely, the electrochemistry. In this area alone, many more experiments could have been carried out, had there been a more stable BLM to work with. In concluding, we would like to call attention that such a system is now available. Previously, the BLM has been by necessity formed singly and in such a way that leaves it very fragile and having a lifetime only a few hours at best. The new BLM system is constructed by filling the smooth circular pores of known diameter and density in a commercially available polycarbonate membrane. Under an ideal situation this new BLM system can be visualized as tens of thousands of micro BLM simultaneously generated in the polycarbonate support[195]. The membranes formed in this manner exhibit far superior stability and manipulability as well as having longer lifetimes and larger areas than can be achieved with conventional BLM. Since the new BLM system has the desirable quality of long-term stability, it would be interesting not only to repeat some of the difficult and uncertain experiments reviewed here but to carry out new experiments such as antigen-antibody-complement interactions and transport studies hitherto plagued by BLM instability problems. The BLM system has furnished and will continue to furnish much important information directly pertinent to the problems posed by membrane biology and biophysics in areas such as active transport, phosphorylation, photosynthesis, vision, immunology, nerve conduction, and energy transduction. The BLM system should also be useful in understanding membrane genesis in nature and in other membrane-mediated life processes.

Acknowledgements

Preparation of this review was assisted by a NIH grant (GM-14971) from the National Institutes of Health.

References

1 H P ZINGSHEIM, *Biochim. Biophys. Acta*, MRI: 339 (1972)
2 G WEISSMANN and R CLAIBORNE, in *Cell Membrane: Structure, Function and Pathology*, Hospital Practice Publ. Co., New York (1975)
3 W BAUMEISTER and M. HAHN, *Prog. Surf. Membr. Sci.*, **11**, 227 (1976)
4 P MUELLER, D O RUDIN, H T TIEN, and W C WESCOTT, *Nature (London)*, **195**, 979 (1962)
5 M K JAIN, *The Biomolecular Lipid Membrane*, Von Nostrand Reinhold, New York (1972)
6 H T TIEN, *Bilayer Lipid Membranes (BLM): Theory and Practice*, Dekker, Inc., New York, 672 (1974)
7 A D BANGHAM, *Prog. Biophys. Mol. Biol.*, **18**, 29 (1968)
8 V F ANTONOV, Y G ROVIN, and L T TRIFMOV, *A Bibliography of Bilayer Lipid Membranes: 1962 1975*, All Union Institute for Scientific Information, Moscow, 229 (1979)
9 D PAPAHADJOPOULOS, In *Biological Horizons in Surface Science*, L M Prince and D F Sears (Editors), Academic Press, New York (1973)
10 V S MARKIN and YU A CHIZMADZHEV, *Induced Ion Transport in Bilayer Lipid Membranes*, Moscow Publishing House, Moscow (1974)
11 S OHKI, *Prog. Surf. Membr. Sci.*, **10**, 117 (1976)
12 R DELEVIE, *J. Electroanal Chem. Interfacial Electrochem.*, **69**, 265 (1976)
13 O S ANDERSEN, In *Membrane Transport in Biology*, C C TOSTESON (Editor), Springer Verlag, Berlin, Heidelberg (1978) Chapter II
14 A E SHAMOO and W F TIVOL, *Curr. Top. Membr. Transp.*, **14**, 57 (1980)
15 T KUNITAKE and Y OKAHATA, *J. Am. Chem. Soc.*, **102**, 549 (1980)
16 H H HUB, B HUPFER, H KOCH and H RINGSDORF, *Angew. Chem.*, **19**, 938 (1980)
17 S H WHITE, *Science*, **207**, 1075 (1980)
18 Y SUEZAKI, *J. Theor. Biol.*, **71**, 279 (1978)
19 W P KOZA, G E KLINZING and S H CHIANG, *J. Colloid. Interface Sci.*, **66**, 455 (1978)
20 T S SNYDER, S H CHIANG, G E KLINGZING and A P TIRIO, *J. Colloid. Interface Sci.*, **61**, 31 (1978)
21 R C WALDBILLIG and G SZABO, *Biochim. Biophys. Acta*, **557**, 295 (1979)
22 G S B LIN, *Bull. Math. Biol.*, **42**, 601 (1980)
23 J F NAGLE and H L SCOTT, *Phys. Today*, **31**, 38 (1978)
24 V A TVERDISLOV, S FL KARADAGI, O V MARTSENYUK and E N GERASIMOVA, *Biofizika*, **25**, 841 (1980)
25 M N JONES and H K NICKSON, *Biochim. Biophys. Acta*, **509**, 260 (1978)
26 G KAISER, P LAMBOTTE, P FALMAGNE, C CAPIAU, J ZANEN and J M RUYSSCHA, *Arch. Int. Physiol. Biochim.*, **89**, 22 (1981)
27 P A ROSENBERG and A FINKELSTEIN, *J. Gen. Physiol.*, **72**, 341 (1978)
28 A WALTER and J GUTKNECHT, *Biochim. Biophys. Acta.*, **641**, 183 (1981)
29 Z DANCSHAZY, P ORMOS, L A DRACHEV and V P SKULACHEV, *Biophys. J.*, **24**, 423 (1978)
30 M FRAGATA, *J. Colloid. Interface Sci.*, **66**, 470 (1978)
31 T M HERMAN and G W RAYFIELD, *Biophys. J.* **21**, 111 (1978)
32 F T HONG, *Adv. Chem. Ser.*, **188**, 211 (1980)
33 G SCIBONA, B SCUPPA, C FABIANI and C CIAVOLA, *Biochim. Biophys. Acta*, **506**, 30 (1978)
34 R GRUPE, E PREUBER and H GORING, *Stud. Biophys.*, **69**, 81 (1978)

35. K. R. ROHR and J. A. ROONEY, *Biophys. J.*, **23**, 33 (1978)
36. T. KUNITAKE and S. YAMADA, *Polym. Bull.*, **1**, 35 (1978)
37. T. L. HO and L. D. HAMILTON, *M. Kagaku To Seibutsu (Chem. Biol.)*, **23**, 65 (1978)
38. J. R. GROTE, R. M. SYREN and S. W. FOX, *BioSystems*, **10**, 287 (1978)
39. G. N. BERESTOVSKY, M. Z. GYULKHANDANYAN, V. G. IVKOV and V. D. RAZHIN, *J. Membr. Biol.*, **43**, 227 (1978)
40. A. F. SHAMOO, *J. Membr. Biol.*, **43**, 227 (1978)
41. I. SZUNDI, *Chem. Phys. Lipids*, **22**, 153 (2978)
42. M. S. KAFKA, R. BLUMENTHAL, G. A. WALKER and H. B. POLLARD, *Membr. Biochem.*, **1**, 279 (1978)
43. G. N. KOSSI and R. M. LEBLANC, *J. Colloid. Interface Sci.*, **80**, 426 (1981)
44. M. THOMPSON, P. J. WORSFOLD, J. M. HOLUK and E. A. STUBLEY, *Anal. Chim. Acta*, **104**, 195; **117**, 121 (1979)
45. J. KORYTA, *Electrochim. Acta*, **24**, 293 (1979)
46. L. EBIHARA, J. E. HALL, R. C. MacDONALD and T. J. McINTOSH, *Biophys. J.*, **28**, 185 (1979)
47. R. FETTIPLACE and D. A. HAYDON, *J. Physiol. Rev.*, **60**, 510 (1980)
48. D. W. R. GRUEN and D. A. HAYDON, *Biophys. J.*, **30**, 129 (1980); *Pure Appl. Chem.*, **53**, 1229 (1980)
49. H. REPKE, A. BEREZI and H. MATTHIES, *Acta Biol. Med.*, **39**, 657 (1980)
50. M. YOSHIDA, A. F. CLARK and P. D. SWANSON, *J. Membr. Sci.*, **7**, 101 (1980)
51. M. DELY, P. PRAGER and A. PUPPI, *Stud. Biophys.*, **85**, 115 (1981)
52. F. REIG, J. M. G. ANTON, G. VALENCIA and J. J. DOMINQUE, *Fette Seifen. Anstrichm.*, **83**, 367 (1981)
53. I. G. KHARITONENKOV, S. ELKARADA, D. J. BUCHER, J. A. ZAKAMIRD and V. A. TVERDISLOV, *Biochim. Biophys. Res. Commun.*, **102**, 308 (1981)
54. R. PAYNE, *J. Electroanal. Chem. Interfacial Electrochem.*, **41**, 277 (1973)
55. H. T. TIEN and L. DIANA, *J. Colloid Interface Sci.*, **24**, 287 (1967)
56. S. McLAUGHLIN, G. SZABO, G. EISENMAN and S. M. CIANI, *Proc. Natl. Acad. Sci. (U.S.A.)*, **67**, 1268 (1970)
57. D. L. GILBERT and G. EHRENSTEIN, *Biophys. J.*, **9**, 447 (1969)
58. G. N. MOZHAYEVA and A. P. NAUMOV, *Biofizika*, **17**, 412, 618, 801 (1972)
59. R. V. MULLER and A. FINKELSTEIN, *J. Gen. Physiol.*, **60**, 285 (1972)
60. N. LAKSHMINARAYANAIAH, *J. Membr. Biol.*, **29**, 243 (1976)
61. S. McLAUGHLIN and M. EISENBERG, *Annu. Rev. Biophys. Bioeng.*, **4**, 335 (1975)
62. R. H. BROWN, Jr., *Prog. Biophys. Mol. Biol.*, **28**, 343 (1974)
63. F. A. SIDDIQI, M. N. BEG, I. R. KHAN, A. HAQ, S. K. SAKSENA and B. ISLAM, *Can. J. Chem.*, **56**, 2205 (1978)
64. Y. KOBATAKE and N. KAMO, *Prog. Polym. Sci. Jpn.*, **5**, 257 (1973)
65. R. P. BUCK, *CRC Crit. Rev. Anal. Chem.*, 323 (1975)
66. G. SACHS, *Gastroenterology*, **75**, 750 (1978)
67. D. PAPAHADJOPOULOS and J. C. WATKINS, *Biochim. Biophys. Acta*, **135**, 639 (1967)
68. W. L. C. VAZ, A. MICKSCH and F. JAHING, *Eur. J. Biochem.*, **83**, 299 (1978)
69. S. L. BRENNER, V. A. PARSEGIAN and D. GINGELL, *J. Phys. Chem.*, **82**, 1727 (1978)
70. S. OHKI, *J. Colloid and Interface Sci.*, **27**, 318 (1971)
71. P. SMEJTEK, K. HSU and W. H. PERMAN, *Biophys. J.*, **16**, 319 (1976)
72. S. McLAUGHLIN, in *Molecular Mechanism of Anesthesia*, B. R. FINK (Editor), Progress in Anesthesiology, Raven Press, Inc., New York (1975) Vol. 1, p. 193
73. B. KETTERER, B. NEUMCKE and P. LAUGER, *J. Membr. Biol.*, **5**, 225 (1971)

74. C. C. WANG and L. J. BRUNER, *J. Membr. Biol.*, **38**, 311 (1978)
75. O. S. ANDERSEN, S. FELDBERG, H. NAKADOMARI, S. LEV and A. McLAUGHLIN, *Biophys. J.*, **21**, 35 (1978)
76. R. ROBINSON and S. LEVINE, *J. Electroanal. Chem. Interfacial Electrochem.*, **47**, 395 (1973)
77. A. L. HODGKIN, *The Conduction of Nervous Impulse*, Thomas, Springfield, Ill. (1964)
78. E. J. HEYER, R. U. MULLER and A. FINKELSTEIN, *J. Gen. Physiol.*, **67**, 703, 731 (1976)
79. G. BOHEIM, *J. Membr. Biol.*, **19**, 277 (1974)
80. L. E. MOORE and E. NEHER, *J. Membr. Biol.*, **27**, 347 (1976)
81. M. EISENBERG, J. F. HALL and C. A. MEAD, *J. Membr. Biol.*, **14**, 143 (1973)
82. E. BAMBERG and K. JANKO, *Biochim. Biophys. Acta*, **465**, 486 (1977)
83. E. BAMBERG and P. LAUGER, *Biochim. Biophys. Acta*, **367**, 127 (1974)
84. E. A. LIBERMAN and V. P. TOPALY, *Biofizika*, **14**, 452 (1969)
85. O. H. LEBLANC, Jr., *Biochim. Biophys. Acta*, **193**, 300 (1969)
86. P. A. GRIGOREV, L. N. YERMISHKIN and V. S. MARKIN, *Biofizika*, **17**, 788 (1972)
87. O. S. ANDERSEN and M. FUCHS, *Biophys. J.*, **15**, 795 (1975)
88. D. A. HAYDON and S. B. HLADKY, *Q. Rev. Biophys.*, **5**, 187 (1972)
89. C. GAVACH and R. SANDEAUX, *Biochim. Biophys. Acta*, **413**, 33 (1975)
90. R. BENZ, K. JANKO and P. LAUGER, *Biochim. Biophys. Acta*, **551**, 238 (1979)
91. C. GAVACH, P. SETA, R. SANDEAUX and D. CROS, in *Electrical Phenomena at the Biological Membrane Level*, E. ROUX (Editor), Elsevier, Amsterdam (1977) p. 419
92. S. W. FELDBERG and A. B. DELGADO, *Biophys. J.*, **21**, 71 (1978)
93. R. DE LEVIE and D. VUKADIN, *J. Electroanal. Chem. Interfacial Electrochem.*, **62**, 95 (1975)
94. A. FINKELSTEIN and A. CASS, *J. Gen. Physiol.*, **52**, 145 (1968)
95. C. TANFORD, *The Hydrophobic Effect*, John Wiley and Sons, New York (1973)
96. P. LAUGER and B. NEUMCKE, *Lipid Bilayers*, G. EISENMANN (Editor), Marcel Dekker, Inc., New York, Chap. 1
97. S. M. CIANI, G. EISENMAN, R. LAPRADE and G. SZABO, in *Membranes*, G. EISENMAN (Editor), Marcel Dekker, New York (1973) Vol. 2, Chap. 2
98. S. B. HLADKY and D. A. HAYDON, *Biochim. Biophys. Acta*, **274**, 294 (1972)
99. R. LAPRADE, S. M. CIANI, G. EISENMAN and G. SZABO, in *Membranes*, G. EISENMAN (Editor), Marcel Dekker, Inc., New York (1974) Vol. 3, Chap. 2
100. G. STARK, B. KETTERER, R. BENZ and P. LAUGER, *Biophys. J.*, **11**, 981 (1971)
101. C. M. ARMSTRONG and F. BENZANILLA, *J. Gen. Physiol.*, **63**, 533 (1974)
102. R. D. KEYNES and E. ROJAS, *J. Physiol. (London)*, **255**, 157 (1976)
103. R. BENZ, G. STARK, K. JANKO and P. LAUGER, *J. Membr. Biol.*, **14**, 339–364 (1973)
104. V. S. MARKIN, P. A. GRIGOREV and L. N. YERMISHKIN, *Biofizika*, **16**, 1011 (1971)
105. Y. A. LIBERMAN and D. M. MARGULIS, *Biofizika*, **19**, 450 (1974)
106. S. W. FELDBERG and G. KISSEL, *J. Membr. Biol.*, **20**, 269 (1975)
107. J. M. KUDIRKA, P. H. DAUM and C. G. ENKE, *Anal. Chem.*, **44**, 309, 614 (1972)
108. S. B. HLADKY, *Biochim. Biophys. Acta*, **352**, 71 (1974)
109. P. LAUGER and G. STARK, *Biochim. Biophys. Acta*, **211**, 458 (1970)
110. G. EISENMAN, G. SZABO, S. CIANI, S. McLAUGHLIN and S. KRASNE, in *Prog. Surf. Membr. Sci.*, **6**, 254 (1973)

111 P. LAUGER and B. NEUMCKE, Marcel Dekker, Inc., New York, Chap. 1 (1973)
112 H. GINSBURG and G. STARK, *Biochim. Biophys. Acta*, **455**, 685 (1976)
113 B. NEUMCKE and P. LAUGER, *Biophys. J.*, **9**, 1160 (1969)
114 W. PECHOLD, *Kolloid Z.Z. Polym.*, **288**, 1 (1968)
115 J. E. HALL, C. A. MEAD and G. SZABO, *J. Membr. Biol.*, **11**, 75 (1973)
116 F. GAMBALE, A. GLIOZZI, I. M. PEPE, M. ROBELLO and R. ROLANDI, *Gazz. Chim. Ital.*, **109**, 441 (1979)
117 R. BENZ and P. LAUGER, *J. Membr. Biol.*, **27**, 171 (1976)
118. W. G. POHL and J. TEISSIE, *Z. Naturforsch. Teil.*, C **30**, 147 (1975)
119 O. S. ESTRADA, S. H. GRAVEN and H. A. LARDY, *J. Biol. Chem.*, **242**, 2925 (1968)
120 B. C. PRESSMAN, E. J. HARRIS, W. S. JAGGER and J. H. JOHNSON, *Proc. Natl. Acad. Sci. U.S.A.*, **58**, 1949 (1967)
121. V. S. MARKIN, V. S. SOKOLOV, L. I. BOGUSLAWSKY and L. S. JAZUZHINSKY, *J. Membr. Biol.*, **25**, 23 (1975)
122. U. A. CHIZMADZEV, I. G. ABIDOR, V. F. PASTUSCHENKO and V. B. ARAKELYAN, *Bioelectrochem. Bioenerg.*, **6**, 37 (1979)
123 R. B. GUNN, J. O. WIETH and D. C. TOSTESON, *J. Gen. Physiol.*, **65**, 731 (1975)
124. A. KOTYK, J. KOLINSKÁ, J. VERES and J. SZAMMER, *Biochem. Z.*, **342**, 129–138 (1965)
125. J. D. OWEN, D. M. STEGGALL and E. M. EYRING, *J. Membr. Biol.*, **19**, 79 (1974)
126. B. KATZ, *Nerve Muscle and Synapse*, McGraw-Hill, New York (1966)
127. A. C. SCOTT, *Neurophysics*, Wiley and Sons, Inc., New York (1977)
128. P. MUELLER, D. O. RUDIN, H. T. TIEN and W. C. WESCOTT, *J. Phys. Chem.*, **67**, 534 (1963)
129. P. MUELLER and D. O. RUDIN, *J. Theor. Biol.*, **18**, 222 (1968)
130. P. MUELLER and D. O. RUDIN, in *Current Topics in Bioenergetics* (1969)
131 R. C. BEAN, W. C. SHEPHERT and J. T. EICHNER, in *The Role of Biogenic Amines and Physiological Membranes in Modern Drug Therapy*, J. H. BIEL and L. G. ABOOD (Editors), p. 124, Marcel Dekker, Inc., New York (1971)
132. R. LATORRE, G. EHRENSTEIN and H. LECAR, *J. Gen. Physiol.*, **70**, 72 (1972)
133. G. EHRENSTEIN, R. BLUMENTHAL, R. LATORRE and H. LECAR, *J. Gen. Physiol.*, **63**, 707 (1974)
134. R. L. ROBINSON and A. STRICKHOLM, *Biochim. Biophys. Acta*, **509**, 9 (1978)
135. R. A. HOFFMAN, D. D. LONG, R. A. ARNDT and L. D. ROPER, *Biochim. Biophys. Acta*, **455**, 780 (1976)
136. L. G. M. GORDON and D. A. HAYDON, *Biochim. Biophys. Acta*, **255**, 1014 (1972)
137. R. J. CHERRY, D. CHAMPAN, E. G. FINER, H. HAUSER, M. C. PHILLIPS, G. G. SCHIPLEY and A. I. McMULLEN, *Nature (London)*, **224**, 692 (1969)
138. M. EISENBERG, J. F. HALL and C. A. MEAD, *J. Membr. Biol.*, **14**, 143 (1973)
139. A. MAURO, R. P. NANAVATI and E. HEYER, *Proc. Natl. Acad. Sci. U.S.A.*, **69**, 3742 (1972)
140. D. W. URRY, M. C. GOODALL, J. D. GLICKSON and D. F. MAYERS, *Proc. Natl. Acad. Sci. U.S.A.*, **68**, 1, 907 (1971)
141. W. R. VEATCH and L. STRYER, *Mol. Biol.*, **113**, 89 (1977)
142. H. D. ZINGSHEIM and E. NEHER, *Biophys. Chem.*, **2**, 197 (1974)
143. H. A. KOLB, P. LAUGER and E. BAMBERG, *J. Membr. Biol.*, **20**, 133 (1975)
144. E. BAMBERG and R. BENZ, *Biochim. Biophys. Acta*, **426**, 570 (1976)
145. G. SZABO and D. W. URRY, *Science*, **203**, 55–57 (1978)
146. E. F. J. VAN BRUGGEN, V. SCHUITEN, E. H. WIEBENGA and GRUBER, *J. Mol. Biol.*, **7**, 249 (1963)
147. W. N. KONINGS, R. J. SIEZEN and M. BRUBER, *Biochim. Biophys. Acta*, **194**, 376 (1969)

148. H. C. PLANT and P. CONRAN, *J. Membr. Biol.*, **8**, 357 (1972)
149. R. LATORRE, O. ALVAREZ, G. EHRENSTEIN, M. ESPINOZA and J. REYES, *J. Membr. Biol.*, **25**, 163 (1975)
150. R. ANTOLINI and G. MENESTRINA, *FEBS Lett.*, **100**, 377 (1979)
151. T. J. McINTOSH, S. A. SIMON and R. C. MacDONALD, *Biochim. Biophys. Acta*, **597**, 445 (1980)
152. S. J. SHEIN, B. L. KAGAN and A. FINKELSTEIN, *Nature (London)*, **276**, 154 (1978)
153. R. BENZ, J. ISHII and T. NAKAE, *J. Membr. Biol.*, **56**, 19 (1980)
154. H. SCHINDLER and J. P. ROSENBUSH, *Proc. Natl. Acad. Sci. U.S.A.*, **75**, 3751 (1978)
155. J. DEL CASTILLO, A. RODRIQUEZ, C. A. ROMERO and SANCHEZ, *Science*, **153**, 185 (1966)
156. S. C. KINSKY and R. A. NICOLOTTI, *Annu. Rev. Biochem.*, **46**, 49 (1977)
157. D. WOBSCHALL, C. McKEON, *Biochim. Biophys. Acta*, **413**, 317 (1975)
158. D. W. MICHAELS, A. S. ABAMOWITZ, C. H. HAMMER and M. M. MAYER, *Proc. Natl. Acad. Sci. U.S.A.*, **73**, 3852 (1976)
159. J. MOUNTZ and H. T. TIEN, *J. Bioenerg. Biomembr.*, **69**, 1 (1979)
160. H. P. TING-BEALL, M. B. LEES and J. D. ROBERTSON, *J. Membr. Biol.*, **51**, 33 (1979)
161. R. BLUMENTHAL, R. D. KLAUSNER and J. M. WIENSTEI, *Nature (London)*, **288**, 333 (1980)
162. O. V. MARTSENJSKY, N. V. PEROVA, E. N. GERASIMOX, V. A. TVERDISLOV and S. ELKARADA, *Vopr. Med. Khim.*, **26**, 484 (1980)
163. R. CORONADO and C. MILLER, *Nature (London)*, **280**, 807 (1979)
164. J. H. FENDLER, *J. Phys. Chem.*, **84**, 1485 (1980)
165. F. S. COHEN, J. ZIMMERBE, A. FINKELSTEIN, *J. Gen. Physiol.*, **75**, 251 (1980)
166. J. LOPEZ and H. T. TIEN, *Biochim. Biophys. Acta*, **597**, 433 (1980)
167. Y. SUEZAKI, *J. Colloid Interface Sci.*, **73**, 529 (1980)
168. K. I. INUI, K. TABARA, R. HORI, A. KANEDA, S. MURANISH and H. SEZAKI, *J. Pharm. Pharmacol.*, **29**, 22 (1977)
169. H. T. TIEN (Editor), *Photochem. Photobiol.*, **24** (1976)
170. H. T. TIEN, in *Photosynthesis in Relation to Model Systems*, J. BARBER (Editor), Elsevier North-Holland Pub., New York, Chapter 4 (1979)
171. D. MAUZERALL, in *Light-induced Charge Separation in Biology and Chemistry*, H. GERISCHER (Editor), Verlag-Chimie, Berlin, pp. 241-254 (1979)
172. I. TABUSHI and M. FUAKURA, *J. Am. Chem. Soc.*, **98**, 4684 (1976)
173. M. J. SPARNAAY, in *Electrical Phenomena at the Biological Membrane Level*, Elsevier, Amsterdam, pp. 43-58 (1977)
174. P. S. B. DIGBY, *Symp. Expt. Biol.*, **26**, 445 (1970)
175. R. PETHIG, *Dielectric and Electronic Properties of Biological Materials*, Wiley, New York, Chapters 7 and 8 (1972)
176. H. T. TIEN, B. KARVALY and P. K. SHEIH, *J. Colloid Interface Science*, **72**, 185 (1977)
177. P. LAUGER, W. LESSLAUER, E. MARTI and E. RICHTER, *Biochim. Biophys. Acta*, **135**, 20 (1976)
178. P. MITCHELL, *Chemiosmotic Coupling and Energy Transduction*, Blynn, Res. Ltd., Bodmin, Cornwall, England; *FEBS Lett.*, **56**, 1 (1975)
179. D. D. ELEY, N. C. LOCKHART and C. N. RICHARDS, *J. Bioenerg. Biomembr.*, **9**, 289 (1977)
180. H. T. TIEN, *Nature (London)*, **219**, 272 (1968)
181. B. KARVALY and H. C. PANT, *Stud. Biophys.*, **33**, 51 (1972)

182. N. SCHADT, *Biochim. Biophys. Acta*, **323**, 351 (1973)
183. F. HONG, *Photochem. Photobiol.*, **24**, 155 (1976)
184. G. ALEXANDROWICZ and D. S. BERNS, *Photobiochem. Photobiophys.*, **1**, 353 (1980)
185. J. S. HUEBNER, *Biochim. Biophys. Acta*, **406**, 178 (1978); *Photochem. Photobiol.*, **30**, 233 (1979)
186. H. U. LUTZ, H. W. TRISSL and R. BENZ, *Biochim. Biophys. Acta*, **345**, 257 (1974)
187. S. W. FELDBERG, G. H. ARMEN, J. A. BELL, C. K. CHANG and C. B. WANG, *Biophys. J.*, **34**, 149 (1980)
188. H. GERISCHER, in *Physical Chemistry, IX*, H. EYRING (Editor), Academic Press, New York (1970)
189. J. R. BOLTON and D. O. HALL, *Annu. Rev. Energy*, **4**, 353 (1979)
190. H. GERISCHER, *Top. Appl. Phys.*, **31**, 115 (1979)
191. N. N. LICHTIN, *Chem. Technol.*, **10**, 254 (1980)
192. L. M. LOEW, S. SCULLY, L. SIMPSON and A. S. WAGGONER, *Nature (London)*, **281**, 497 (1979)
193. P. R. DRAGSTEN and W. W. WEBB, *Biochemistry*, **17**, 5228 (1978)
194. L. M. LOEW and L. L. SIMPSON, *Biophys. J.*, **34**, 353 (1980)
195. J. MOUNTZ and H. T. TIEN, *Photochem. Photobiol.*, **28**, 395 (1978)

CHAPTER 4

STUDIES IN THE MEMBRANE PERMEABILITY OF PARCHMENT SUPPORTED INORGANIC MEMBRANES

Reprinted from JOURNAL OF COLLOID SCIENCE, Volume 18, No. 2, February 1963

JOURNAL OF COLLOID SCIENCE **18**, 161-173 (1963)

STUDIES IN THE MEMBRANE PERMEABILITY OF CHROMIC FERRO AND FERRICYANIDES

Wahid U. Malik and Fasih A. Siddiqi

Chemical Laboratories, Muslim University, Aligarh, India

Received May 29, 1962

The complexity of the membrane phenomenon is well known. A number of controlling factors have been listed from time to time. According to Teorell (1) the problem can be approached from five different angles, viz., (*1*) ionic transport, (*2*) membrane potential, (*3*) electrical conductivity, (*4*) ionic distribution equilibria, and (*5*) the spatial distribution of ions and potentials within the membrane. In the transport of charged or uncharged particles across the membrane, Wiebenga (2) and Staverman (3) considered the membrane as a surface of discontinuity setting up different resistances to the passages of various molecular or ionic species, while Teorell (4) and Mackie and Meares (5) had thought in terms of its quasi-homogeneous nature. Davison and Danielli (6) and also Zwolinsky, Eyring, and Reese (7) had postulated the existence of an inhomogeneous intermediate phase lending a potential barrier on the two sides of the membrane.

Experimental evidence in partial support of what has been described above, is forthcoming on the basis of extensive investigations carried out with the help of classical copper ferrocyanide (8) membranes. Very little, however, appears to have been done with other membranes. Recently work (9) in this direction was undertaken in these laboratories as a side problem to our main investigations on the sol-gel transformation in inorganic gel-forming mixtures (10). The present communication deals with studies on the permeability of electrolytes through the less familiar metal ferrocyanogen compounds, namely, chromic ferro- and ferricyanides. Earlier work on these compounds (11) has shown that their gels form a uniform homogeneous film on a parchment support.

EXPERIMENTAL

Chromic ferrocyanide membranes were prepared by keeping a parchment thimble (Whatman B.T.L.) containing chromic chloride (0.5 *M*) immersed at 80°C. in a potassium ferrocyanide solution (0.5 *M*) for about 2 hours. The solutions were then interchanged and kept for the same time.

The same procedure was employed for chromic ferricyanide with the only difference that the reaction bath was maintained at 90°C. A uniform deposit of the gels on the thimbles was realized in both cases.

Permeability Determination

The diffusion experiments were carried out by the constant-flow method employing apparatus described by Austin, Hartung, and Willis (12) using the constant-flow principle. The membrane was obtained in the form of a circular disc (50 mm. in diameter) after spreading out the gel deposited thimble. The membrane was washed several times with doubly distilled water to remove all the adsorbed ions before carrying out the diffusion experiments with a particular electrolyte. The hydrostatic pressures on each side of the membrane was always kept equal by maintaining the flow of electrolyte and conductivity water across the membrane. The analysis of the effluent coming out of the lower half cell was made conductometrically by a W.T.W. type L.B.R. bridge. By knowing the rate of flow and concentration of effluent coming out of the lower half of the cell (from concentration conductance curves) the permeability in millimoles per hour was determined at 10, 15, 20, 25, and 30°C.

The results are summarized in Table I.

Permeability of Various Electrolytes through Pretreated Membranes

The effect of pretreated membranes on the permeability of various electrolytes was studied by soaking the membranes in solutions containing

TABLE I

Permeability in Millimoles per Hour over the Range 10°–30°C.

Electrolyte (0.2 *M*)	Chromic ferrocyanide membrane					Chromic ferricyanide membrane				
	10°	15°	20°	25°	30°	10°	15°	20°	25°	30°
KCl	0.1245	0.1521	0.1883	0.2362	0.2781	0.1523	0.1817	0.2253	0.2521	0.2896
KNO_3	0.0952	0.1123	0.1312	0.1526	0.1752	0.1233	0.1513	0.1725	0.1962	0.2381
K_2SO_4	0.0412	0.0482	0.0561	0.0653	0.0741	0.0552	0.0663	0.0794	0.0922	0.1073
NaCl	0.0861	0.1023	0.1192	0.1462	0.1694	0.1125	0.1326	0.1632	0.1916	0.2152
$NaNO_3$	0.0721	0.0851	0.1012	0.1283	0.1401	0.0982	0.1124	0.1262	0.1523	0.1822
Na_2SO_4	0.0381	0.0452	0.0541	0.0632	0.0721	0.0512	0.0625	0.0734	0.0852	0.0962
KBr	—	—	—	0.2162	—	—	—	—	0.2312	—
KCNS	—	—	—	0.1212	—	—	—	—	0.1423	—
CH_3COOK	—	—	—	0.0985	—	—	—	—	0.0312	—
NaBr	—	—	—	0.1204	—	—	—	—	0.1332	—
CH_3COONa	—	—	—	0.0786	—	—	—	—	0.0912	—
K_3FeCy_6	—	—	—	—	—	—	—	—	0.0210	—
K_4FeCy_6	—	—	—	0.0121	—	—	—	—	—	—

their constituent metal ions (0.2 *M*) for 8 hours and measurements were carried out at 25°C. The results are summarized in Table II.

Membrane Potential

The potential developed by setting up the concentration cell of the type described by Michaelis (13)

Saturated calomel electrode	Electrolyte C_1	Electrolyte C_2	Saturated calomel electrode

Membrane

$C_1 = 10C_2$

was taken as a measure of the membrane potential. The measurements were carried out with the help of a Tinsley low-range potentiometer type 3387B under the following conditions:

1. Keeping the solutions (0.1, 0.01 *M*) stationary on both sides of the membrane;

2. Allowing the solutions to circulate across the membrane thereby realizing conditions approximating those for the constant-flow method. In case (*1*) it took some time to realize steady conditions across the membrane. What happened was that the potential increased initially, attaining a maximum value after some time (15 to 20 minutes), and then started decreasing slowly. The maximum potential attained in each case was taken as a measure of the membrane potential. Once the membrane had been treated like this with a particular electrolyte, it served well for the potential

TABLE II

Permeabilities in Millimoles per Hour at 25°C. for Pretreated Membranes

Electrolyte (0.2 *M*)	Chromic ferrocyanide membrane		Chromic ferricyanide membrane	
	K_4FeCy_6 treated membrane	$CrCl_3$ treated membrane	K_3FeCy_6 treated membrane	$CrCl_3$ treated membrane
KCl	0.1574	0.2382	0.1782	0.2528
KBr	0.1411	0.2178	0.1648	0.2406
KNO_3	0.1018	0.1605	0.1496	0.2076
KCNS	0.0912	0.1232	0.1086	0.1502
K_2SO_4	0.0338	0.0513	0.0512	0.1006
CH_3COOK	0.0663	0.0891	0.0785	0.1103
NaCl	0.0985	0.1472	0.1365	0.2065
NaBr	0.0812	0.1213	0.0962	0.1412
$NaNO_3$	0.0852	0.1272	0.1134	0.1503
Na_2SO_4	0.0325	0.0594	0.0513	0.0843
CH_3COONa	0.0528	0.0698	0.0705	0.0922

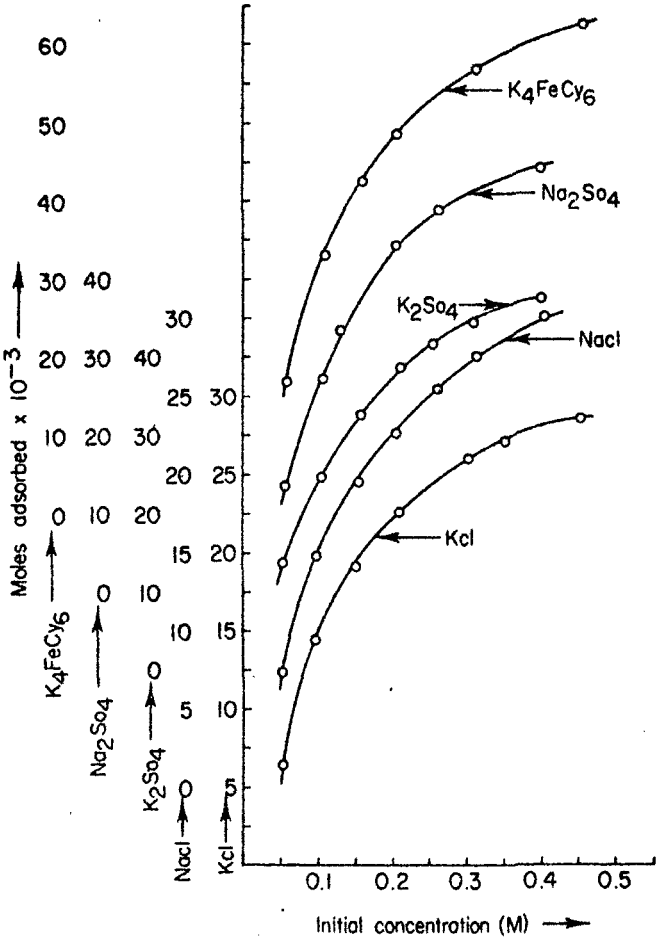

FIG. 1

measurement, since introduction of the electrolyte after this stage gave potential values almost the same as those previously noted for the maximum potential. The flow method, however, proved to be more useful and comparable values were obtained in less than 5 minutes. Only this method was, therefore, adopted with pretreated membranes. The results are summarized in Tables III and IV.

Adsorption

In order to obtain further experimental support for our results on permeability and membrane potential, the adsorption of various electrolytes on chromic ferro- and ferricyanide gels was investigated. The method employed was as follows. The gels were first prepared by mixing 0.5 *M* solu-

TABLE III

Potentials in Millivolts for Chromic Ferrocyanide Membranes

Electrolyte (0.1, 0.01 *M*).....	KCl	NaCl	KBr	NaBr	KNO_3	$NaNO_3$	KCNS	CH_3COOK	CH_3COONa	K_2SO_4	Na_2O_4	K_4FeCy_6
Stationary method	24.0	25.5	27.0	28.5	29.0	31.0	32.5	34.5	36.0	37.5	39.0	44.5
Flow method	22.0	23.5	24.5	25.5	27.0	29.0	30.0	32.5	34.0	35.0	37.5	42.0
After treatment with K_4FeCy_6	27.5	28.0	28.5	29.5	32.5	37.0	35.5	37.0	39.5	45.5	46.5	—
After treatment with $CrCl_3$	23.5	24.5	25.0	26.0	27.5	30.0	31.0	33.0	36.0	36.0	38.0	—

TABLE IV

Potentials in Millivolts for Chromic Ferricyanide Membranes

Electrolyte (0.1, 0.01 *M*).....	KCl	NaCl	KBr	NaBr	KNO_3	$NaNO_3$	KCNS	CH_3COOK	CH_3COONa	K_2SO_4	Na_2SO_4	K_3FeCy_6
Stationary method	16.5	18.0	19.0	21.5	23.5	25.5	28.0	30.0	32.0	32.5	34.5	43.5
Flow method	15.0	16.5	17.5	18.5	21.5	23.0	26.5	27.0	30.0	30.5	32.5	42.0
After treatment with K_3FeCy_6	19.5	21.5	21.0	23.5	24.5	26.5	29.5	31.5	33.5	38.0	39.5	—
After treatment with $CrCl_3$	16.0	17.0	18.0	19.5	22.5	23.5	27.0	27.5	31.0	31.0	33.0	—

tions of chromic chloride and potassium ferrocyanide at 80°C. and allowing to stand for one hour. The gel obtained was washed several times with water and dried at 110°C. in an air oven for about 2 hours. Then 1.0 g. of the finely powdered gel was placed in a Pyrex conical flask and varying amounts of electrolytes (KCl, NaCl, K_2SO_4, Na_2SO_4, K_3FeCy_6, and K_4FeCy_6) added. The total volume was made up to 100 ml. After allowing the flasks to stand for 24 hours in a water thermostat maintained at 25°C. the volume of the supernatant liquid was estimated, either volumetrically or gravimetrically. Experiments with chromic ferricyanide gel were carried out under exactly identical conditions. Here the gel was obtained by heating the mixture of the reactants at 90°C. for about 2 hours. The results are depicted in Figs. 1 and 2.

Discussion

The two main factors which may be considered to determine the permeability of ions through membranes are: (*1*) charges on the membrane pores, due to either adsorption or ionization, which act as barriers to the diffusing

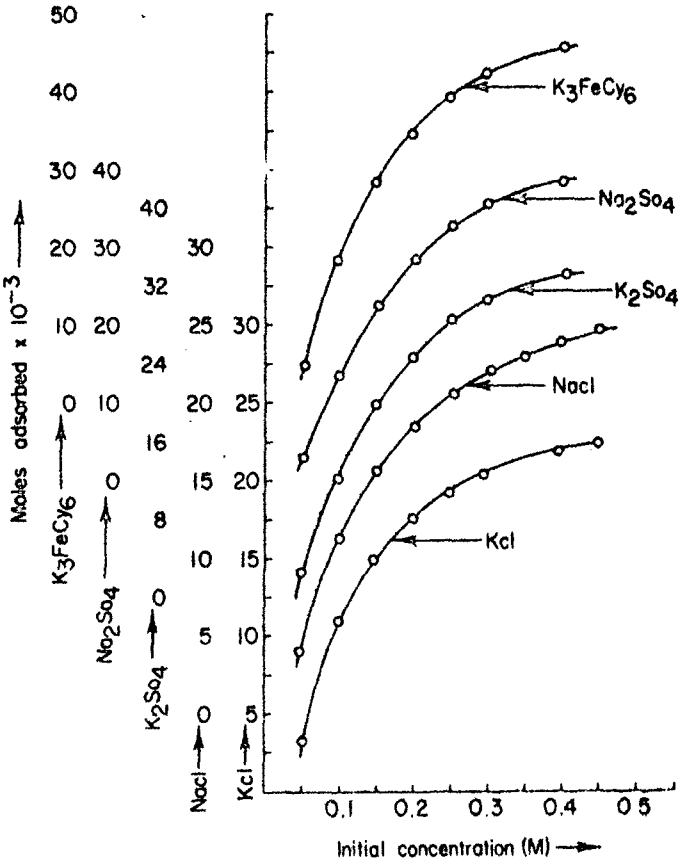

FIG. 2

ions, as postulated by Meyer and Sievers (14) and Teorell (4): (*a*) sieve action whereby screening of ions according to their size takes place, larger ions diffusing out more slowly than the smaller ones and vice versa, according to Collander (15), Willis (16), and Sollner (17). Our permeability results with chromic ferro- and ferricyanide membranes show that the first factor plays a more dominant role in the diffusion process, and sieve action may be of only secondary importance here. The contention is borne out in more than one way on the basis of the following facts.

On considering the relative permeability of the anions (both for potassium and sodium salts) it will be seen that the following order exists for both the membranes:

$$Cl^- > Br^- > NO_3^- > CNS^- > CH_3COO^-$$

$$> SO_4^- > FeCy_5^{--} > FeCy_6^{---}$$

Although the order may apparently lead to the conclusion that the ion size is the controlling factor, a closer analysis of the results would reveal that such is not the case. On the other hand, free diffusion of ions is restricted owing to the interposition of the membrane with the result that nowhere the order of free diffusion.

$$FeCy_6^{---} > SO_4^{--} > Br^- > Cl^- > NO_3^- > CNS^-$$

is realized.

Further confirmation is forthcoming on the basis of adsorption studies where it is found that the order of adsorbability is $FeCy_6^{---} > FeCy_6^{--} > SO_4^{--} > Cl^-$, which is just the reverse of the order of the permeability given above. Besides, the difference in permeability values for the untreated and pretreated membranes lends support to the role of adsorption here. Thus with potassium ferro- or ferricyanide treated membranes the rate of diffusion is retarded to such a great extent that the diffusion rate of SO_4^{--} becomes nearly half that of the original and the permeability ratio Cl^-/SO_4^{--} increases on passing from the untreated to the pretreated membrane. To explain this behavior it may well be assumed that the stronger adsorption of $FeCy_6^{4-}$ or $FeCy_6^{3-}$ by the membrane surface results in a restricted movement of the anions and that the retardation would naturally be more marked with bivalent sulfate than the univalent chloride. Moreover, the nature of the membrane material is significant. The adsorption results show that chromic ferrocyanide is a better adsorbant than the ferricyanide and the ferrocyanide membrane would have lower permeability values than the ferricyanide membrane as observed.

The potential measurement besides giving a relationship between membrane potential and permeability (the larger the membrane potential the lesser the permeability) provides a method of determining the anion mobility, through the equation (18):

$$E = \frac{\frac{u}{Z_c} - \frac{v}{Z_a}}{u + v} \frac{RT}{F} \ln \frac{f_1 C_1}{f_2 C_2},$$

where E is the membrane potential, C_1 and C_2 are the concentrations of the electrolyte solutions in grams-equivalent per liter, f_1 and f_2 are the corresponding activity coefficients, Z_c and Z_a are the valencies of the cation and anion, respectively. Assuming that u remains unchanged in the case of a negative membrane, we can calculate v from the above equation. The apparent mobilities of anions, for the treated and untreated membranes, were as follows in Tables V and VI.

From the above observations it is clear that the surface charge controls the movement of ions across the membrane. These results confirm the views of Meyer and Sievers (14) and also of Teorell (4), who postulated

TABLE V

Anion Mobilities for a Chromic Ferrocyanide Membrane

Electrolyte	Anion	True mobility	Apparent mobility (stationary method)	Apparent mobility (flow method)	Apparent mobility (K_4FeCy_6 treated membrane)
KCl	Cl^-	76.4	50.92	51.24	47.67
NaCl	Cl^-	76.4	34.97	36.02	35.52
KNO_3	NO_3^-	71.5	46.13	47.75	43.39
$NaNO_3$	NO_3^-	71.5	30.81	31.86	27.83
K_2SO_4	$\frac{1}{2}SO_4^-$	80.0	36.44	37.94	29.99
Na_2SO_4	$\frac{1}{2}SO_4^-$	80.0	23.66	24.47	20.01
K_4FeCy_6	$\frac{1}{4}FeCy_6^{---}$	111.0	18.72	20.98	—

TABLE VI

Anion Mobilities for a Chromic Ferricyanide Membrane

Electrolyte	Anion	True mobility	Apparent mobility (stationary method)	Apparent mobility (flow method)	Apparent mobility (treated membrane)
KCl	Cl^-	76.4	57.38	58.78	54.72
NaCl	Cl^-	76.4	38.27	39.24	34.17
KNO_3	NO_3^-	71.5	50.66	51.29	49.78
$NaNO_3$	NO_3^-	71.5	34.92	35.22	33.23
K_2SO_4	$\frac{1}{2}SO_4^-$	80.0	39.72	40.61	35.35
Na_2SO_4	$\frac{1}{2}SO_4^-$	80.0	26.04	27.70	23.46
K_3FeCy_6	$\frac{1}{3}FeCy_6^{---}$	100.9	22.65	23.10	—

a number of fixed charges due to either adsorption or ionization resulting in the setting up of a Donnan equilibrium. The change in the mobilities of ions calculated are due to the combined effects of the mobilities of the ions and their tendency to enter the membrane from the bulk of the solution as modified by surface and electrical forces. The pretreatment of the membrane with $FeCy_6^{4-}$ or $FeCy_6^{3-}$ ions with resulting decrease of permeability and increase of potential (consequent decrease in mobility) is strong evidence that the consequent increase in membrane selectivity is due to the surface charges present. These charges originated from other ions and were increased by further adsorption. The low values of permeability of CH_3COO^- and CNS^- ions are also due to the fact that they have very low free mobilities. The case of $FeCy_6^{---}$ or $FeCy_6^{----}$ may also be interpreted by considering the pore size, although the effect of adsorption is more important. The effect of valency also plays an important role for multivalent ions like $FeCy_6^{---}$ or $FeCy_6^{----}$, for which the greater electrical re-

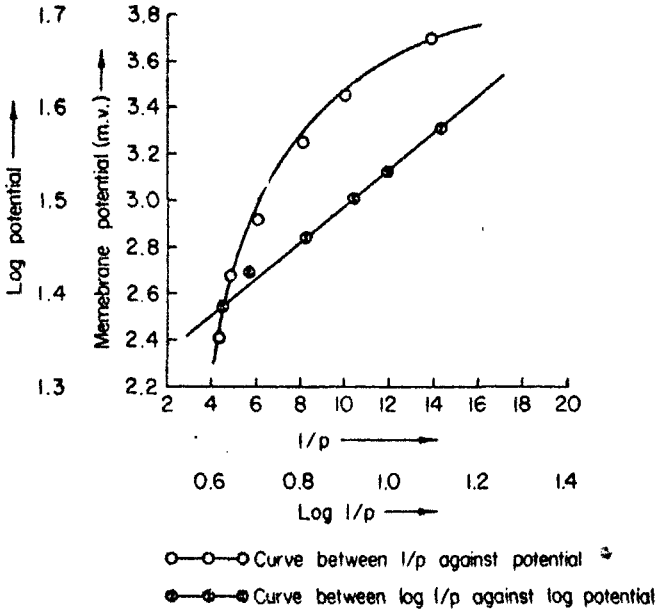
Log potential
Membrane potential (m.v.)
1.7
1.6
1.5
1.4
1.3
3.8
3.6
3.4
3.2
3.0
2.8
2.6
2.4
2.2
2 4 6 8 10 12 14 16 18 20
1/p
0.6 0.8 1.0 1.2 1.4
Log 1/p
Curve between 1/p against potential
Curve between log 1/p against log potential

FIG. 3

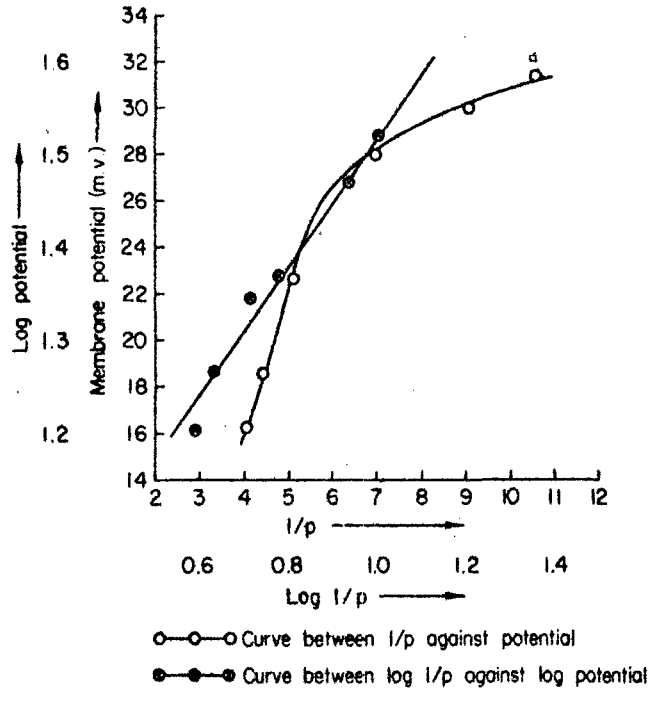
Log potential
Membrane potential (m v.)
1.6
1.5
1.4
1.3
1.2
34
32
30
28
26
24
22
20
18
16
14
2 3 4 5 6 7 8 9 10 11 12
1/p
0.6 0.8 1.0 1.2 1.4
Log 1/p
Curve between 1/p against potential
Curve between log 1/p against log potential

FIG. 4

pulsion is also responsible for the decrease in permeability in comparison to univalent Cl^- ions.

A close relationship between permeability and membrane potential is also revealed by plots (Figs. 3 and 4) of the reciprocal of permeability $1/p$, against membrane potential, (for K^+ salts), and from this follows an empirical relationship of the form $Y = ax^-$, where a and n are constants and x and y represent permeability and potential, respectively. The values of the constants are $a = 13.65$ and $n = 2.50$ for chromic ferrocyanide and $a = 7.49$ and $n = 1.60$ for chromic ferricyanide. This relationship is similar to the Freundlich adsorption isotherm and brings out to some extent the interconnection between adsorption, on the one hand, and permeability and membrane potential, on the other.

The results for permeability show a strong dependence on temperature. From the temperature coefficient as determined by plotting log $(p \times 10^2)$ against $1/T \times 10^3$ (Figs. 5, 6), p being permeability and T the absolute temperature, the energy of activation of the diffusion process (i.e., E) was

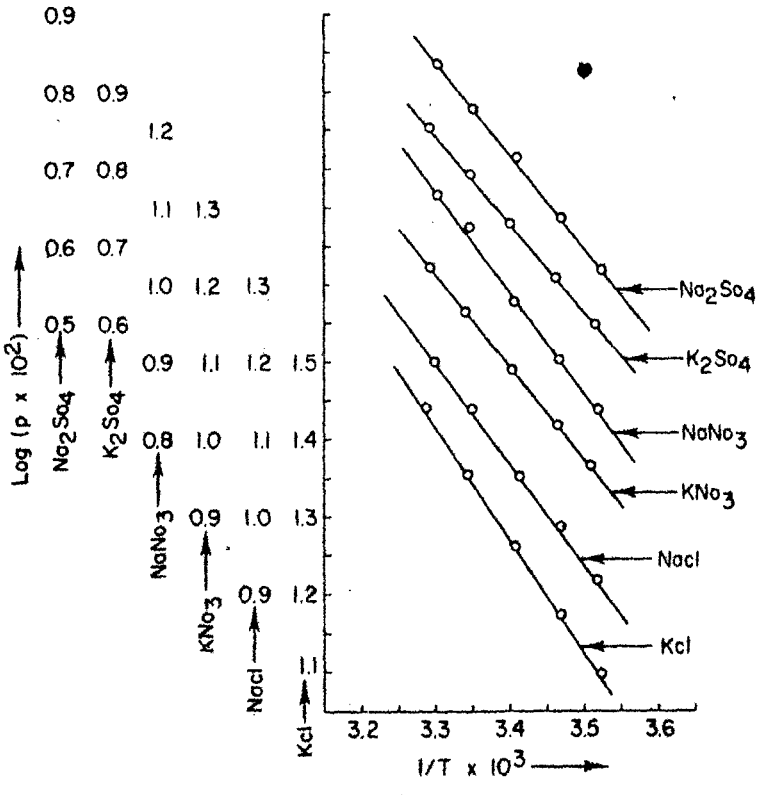

FIG. 5

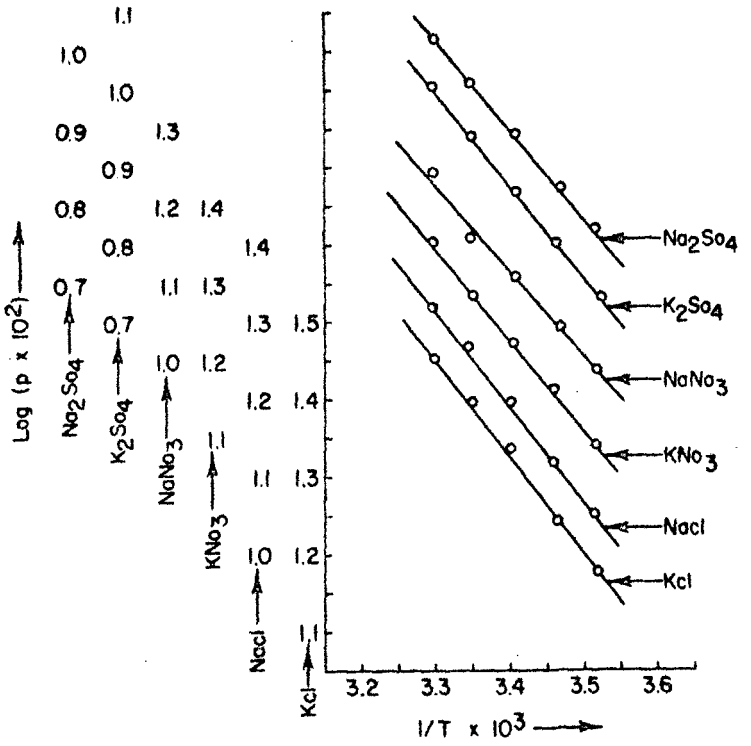

FIG. 6

calculated from the slope which is equal to $E/2.303\ R$. The values of E are in calories per mole.

Membrane	KCl	KNO_3	K_2SO_4	NaCl	$NaNO_3$	Na_2SO_4
Chromic ferrocyanide	6446	5296	5181	5805	5757	5425
Chromic ferricyanide	5757	5328	5327	5711	5183	5489

The value of the activation energy for the free diffusion of KCl reported in the literature is 4400 calories per mole, and is smaller than those calculated above. Evidently there is more of a barrier with the membrane present than with free diffusion. These results confirm the values by Tolliday, Woods, and Hartung (19) of 5100 calories per mole for KCl, and 5900 calories per mole for K_2SO_4 (0.2 M).

So far attention has been focused only on the changes occurring at the surface of the membrane. The condition existing inside the membrane during the flow of electrolyte is also worth discussion. The order of permeability of the different anions for these membranes: $Cl^- > Br^- > NO_3^- >$

$CNS^- > CH_3COO^- > SO_4^{--} > FeCy_6^{---} > FeCy_6^{----}$ is more or less the reverse of what is known as the Hofmeister series. From this interesting observation it may be concluded that the permeability order can be taken as an index of the peptizing action of the ions.

It therefore appears that those ions which can easily peptize the membrane material diffuse more easily than others. Such behavior in the case of metal ferro- and ferricyanides is not surprising since they exhibit properties typical of lyophilic colloidal systems (11).

Summary

The permeability of various electrolytes (with a common cation) through parchment-supported chromic ferro- and ferricyanide membranes was investigated, employing the constant flow method. The permeability order was found to be $Cl^- > Br > NO_3^- > CNS^- > CH_3COO^- > SO_4^{--} > FeCy_6^{---} > FeCy_6^{----}$ in both cases. A considerable decrease in these values was observed when potassium ferro- and ferricyanide treated membranes were used. Adsorption and membrane potential studies revealed an order that was just the reverse of that for permeability. The energy of activation for the diffusion process for various electrolytes was found to lie between 5000 and 6500 calories per mole, values which are higher than those determined for the free diffusion of electrolytes.

The role of Hofmeister series has been considered in relation to the peptizing of the membrane material during the diffusion process and such peptizing appears to be one of the factors controlling the permeability phenomenon.

Acknowledgment

Thanks are due to Prof. A. R. Kidwai for providing facilities and to C.S.I.R. (India) for the award of a fellowship to one of us (F. A. S.).

References

1. Teorell, T., *Discussions Faraday Soc.* No. **21**, 9-25 (1956).
2. Wierenga, *Rec. trav. chim.* **65**, 973 (1946).
3. Staverman, A. J., *Trans. Faraday Soc.* **48**, 176 (1952).
4. Teorell, T., *Proc. Soc. Exptl. Biol. Med.* **33**, 282 (1935).
5. Mackie and Meares, *Proc. Roy. Soc. (London)* **A232**, 498 (1955).
6. Davison and Danielli, "The Permeability of Natural Membrane," Chapter 21, and Appendix A. Cambridge, 1943.
7. Zwolinsky, Eyring, and Reese, *J. Phys. Chem.* **53**, 1426 (1949).
8. Weiser, H. B., *J. Phys. Chem.* **34**, 335 (1930).
9. Hasan, A., Malik, W. U., and Bhattacharya, A. K., *J. Ind. Chem. Soc.* **32**, 501 (1955); Malik, W. U., and Ali, S. A., *Kolloid-Z* **175**, 139 (1961).
10. Malik, W. U., and Bhattacharya, A. K., *J. Phys. Chem.* **59**, 488 (1955); Malik, W. U., and Bhattacharya, A. K., *J. Phys. Chem.* **60**, 490 (1955); Malik, W. U., and Ali, S. A., *Kolloid Z.* **170**, 45 (1960).

11. MALIK, W. U., AND SIDDIQI, F. A., *J. Phys. Chem.* **66**, 356 (1962); *J. Phys. Chem.* **66**, 357 (1962); *Kolloid-Z.* **184**, 1, 41–47 (1962).
12. AUSTIN, A. T., HARTUNG, E. J., AND WILLIS, G. M., *Trans. Faraday Soc.* **40**, 520 (1944).
13. MICHAELIS, *Kolloid-Z.* **62**, 1 (1933); MICHAELIS AND FUJITA, *Biochem. Z.* **142**, 398 (1923); *Z. physik. Chem.* **110**, 266 (1924).
14. MEYER AND SIEVERS, *Helv. Chim. Acta* **19**, 649 (1936); *Trans. Faraday Soc.* **33**, 1073 (1937).
15. COLLANDER, *Kolloid-Beih.* **19**, 72 (1924); *ibid.* **20**, 273 (1925).
16. WILLIS, G. M., *Trans. Faraday Soc.* **38**, 172 (1942).
17. SOLLNER, K., *J. Phys. Chem.* **49**, 265 (1945); SOLLNER, K., AND GREGOR, H. P., *J. Am. Chem. Soc.* **67**, 346 (1945).
18. WILLIS, G. M., *Trans. Faraday Soc.* **38**, 171 (1942).
19. TOLLIDAY, J. D., WOODS, E. F., AND HARTUNG, E. J., *Trans. Faraday Soc.* **45**, 148 (1949).

Sonderdruck: „Zeitschrift für Physikalische Chemie Neue Folge", 72 (1970) 298–306
Herausgegeben von G. Briegleb, Th. Förster, G. Schmid, G.-M. Schwab, E. Wicke

Studies with Inorganic Precipitate Membranes

I. Measurement of Temperature Dependence of Electrolyte Diffusion through Membranes

By

FASIH A. SIDDIQI, N. LAKSHMINARAYANAIAH and SANTOSH K. SAXENA

Department of Pharmacology, University of Pennsylvania, School of Medicine
Philadelphia, Pennsylvania, 19104

and

Department of Chemistry, Aligarh Muslim University, Aligarh, India

With 3 figures

(Received September 10, 1970)

AKADEMISCHE VERLAGSGESELLSCHAFT
FRANKFURT AM MAIN
1970

Abstract

The permeability of various electrolytes through parchment-supported silver chloride, silver phosphate and silver tungstate membranes has been measured at 10, 15, 20, 25 and 30°C. At any given temperature, the order of permeability increased as $Li^+ < Na^+ < K^+$ for univalent cations and as $Ba^{2+} < Sr^{2+} < Mg^{2+} < Ca^{2+}$ for divalent cations; whilst Al^{3+} had the lowest permeability. The data have been considered from the standpoint of the theory of rate processes and the values for the entropy of activation ($\Delta S'$) have been derived assuming an equilibrium distance of 3 Å in the membrane. The values of $\Delta S'$ were low and in the majority of cases were negative. This was interpreted to mean that the electrolyte permeation took place with a minimum of disturbance of the membrane structure, i.e. little disorder.

Introduction

The nonelectrolyte permeability data in respect of plant and animal cells available in the literature have been examined by ZWOLINSKI et al.[1] by applying the theory of rate processes[2]. Similarly SHULER et al.[3] considered the kinetics of membrane permeation for

[1] B. J. ZWOLINSKI, H. EYRING and C. E. REESE, J. physic. Chem. **53** (1949) 1426.

[2] S. GLASSTONE, K. J. LAIDLER and H. EYRING, The Theory of Rate Processes, McGraw-Hill Book Co., New York 1941.

[3] K. E. SHULER, C. A. DAMES and K. J. LAIDLER, J. chem. Physics **17** (1949) 860.

nonelectrolytes through collodion membranes. There are any number of studies of gas permeation through polymer membranes described in the literature. With the availability of thin lipid membranes[4], TIEN and TING[5] measured their permeability to water and considered the permeation process from the concepts of the theory of absolute reaction rates. In recent years, a number of workers[6-8] have investigated the electrolyte permeability characteristics of parchment-supported inorganic precipitate membranes. In this paper, the electrolyte permeability of three inorganic membranes at different temperatures using a number of electrolytes is considered from the standpoint of the theory of rate processes.

Experimental

The membranes of silver chloride, silver phosphate and silver tungstate were prepared by the method of interaction suggested by WEISER[9]. The membranes were prepared by impregnating the parchment paper with the gel. First the parchment paper was soaked in distilled water for 2 hours and then tied carefully to the flat mouth of a beaker in which 0.2 M $AgNO_3$ solution was taken. This was suspended for about 72 hours in a 0.2 M solution of a suitable salt, potassium chloride, sodium phosphate or sodium tungstate. The two solutions were interchanged and kept for another 72 hours. The membranes were washed with deionized water for the removal of the free electrolyte. Microscopic examination of these membranes showed a uniform deposition of the precipitate on the surface. The membranes were always kept in deionized water in the dark.

The diffusion experiments were carried out following the method of AUSTIN et al.[10] based on the constant flow principle. The membrane in the form of a circular disc (functional area = 19.6 cm^2) was washed several times with deionized water to remove adsorbed electrolyte

[4] N. LAKSHMINARAYANAIAH, Transport Phenomena in Membranes, Academic Press, New York 1969, pp. 436–456.

[5] H. T. TIEN and H. P. TING, J. Colloid and Interface Sci. 27 (1968) 702.

[6] W. U. MALIK and F. A. SIDDIQI, Proc. Indian Acad. Sci. A 56 (1962) 206; J. Colloid Sci. 18 (1963) 161

[7] W. U. MALIK, H. ARIF and F. A. SIDDIQI, Bull. chem. Soc., Japan 40 (1967) 1746.

[8] F. A. SIDDIQI and S. PRATAP, J. electroanalyt. Chem. 23 (1969) 137.

[9] H. B. WEISER, J. physic. Chem. 34 (1930) 335, 1826.

[10] A. T. AUSTIN, E. J. HARTUNG and G. M. WILLIS, Trans. Faraday Soc. 40 (1944) 520.

and fixed in the leak-proof all glass cell which finally rested on a magnetic stirrer plate. The upper and lower parts of the transport cell were connected, past manometers, to reservoirs of 0.2 M electrolyte solution and of deionized water, respectively. On leaving the cell, the water passed past two stout platinized platinum electrodes which were used to follow the conductance change of the effluent. The rate of flow was 180 ml/hour. Similarly the electrolyte flow was maintained usually at 300 ml/hour. The hydrostatic pressure on each side of the membrane was kept equal always by adjusting the rates of flow of solution and water.

From calibration curves relating conductance to electrolyte concentration previously established for the conductivity cell referred to above (cell constant $= 9.85 \cdot 10^{-3}$ cm^{-1}), the concentration of the effluent was determined. This combined with the rate of flow of the effluent enabled permeability P in millimoles per hour to be calculated at any given temperature. The whole cell assembly was kept immersed in a water thermostat maintained to an accuracy of $\pm 0.1^{\circ}$. The experiments were carried out at 10, 15, 20, 25 and 30 °C.

Results and discussion

In Figs. 1—3 are given the plots of log P against $(1/T)$, where T is the absolute temperature at which the experiment was conducted, for the three membranes and different (1:1), (2:1) and (3:1) electrolytes which were all chlorides.

The two important factors which control electrolyte permeability through a membrane are charge on the membrane and its porosity. Parchment paper, except for the presence of some stray and end carboxyl groups, contains very few fixed groups. Deposition of inorganic precipitates gives rise to a net negative or positive charge on the membrane. Due to this, the membrane in contact with electrolytes will have the type of ionic distribution associated with the electrical double layer. Flow of electrolyte by diffusion, because of the presence of net charge, negative or positive, on the membrane, gives rise to the membrane potential whose magnitude depends on how effectively the coion (chloride ion in the case of negatively charged membrane) is excluded from the membrane phase. This potential, whose value will be different from the liquid junction potential ordinarily observed under similar conditions in the absence of the membrane, regulates the flow of electrolyte by increasing the speed of the slow moving ion and also by decreasing the speed of

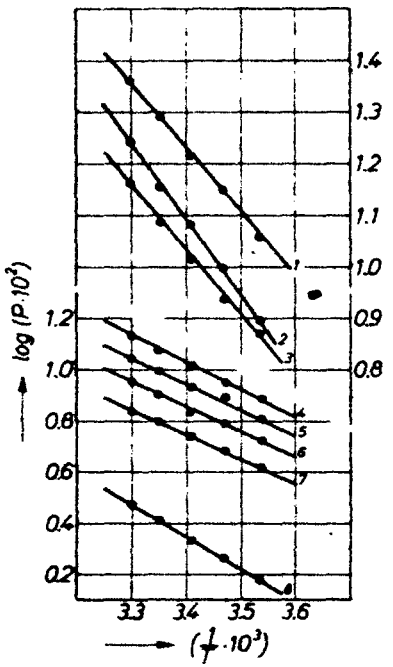

Fig. 1

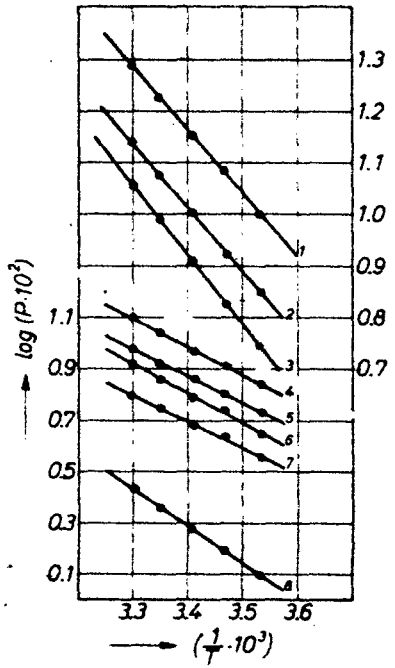

Fig. 2

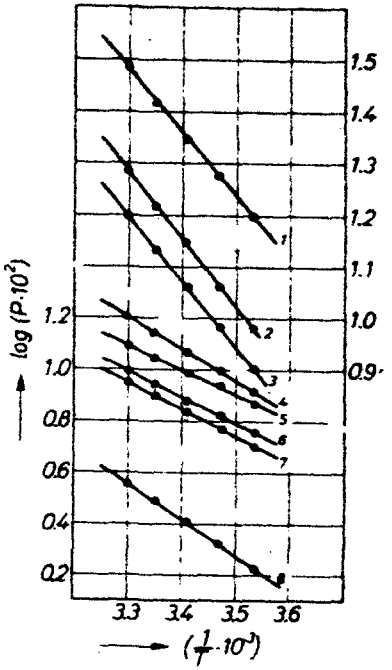

Fig. 3

Fig. 1. The variation in permeability P (mM/hour) of a silver chloride membrane with temperature in presence of different electrolytes. *1* = KCl; *2* = $NaCl$; *3* = $LiCl$; *4* = $CaCl_2$; *5* = $MgCl_2$; *6* = $SrCl_2$; *7* = $BaCl_2$ and *8* = $AlCl_3$

Fig. 2. The variation in permeability P (mM/hour) of a silver phosphate membrane with temperature in presence of different electrolytes. *1* = KCl; *2* = $NaCl$; *3* = $LiCl$; *4* = $CaCl_2$; *5* = $MgCl_2$; *6* = $SrCl_2$; *7* = $BaCl_2$ and *8* = $AlCl_3$

Fig. 3. The variation in permeability P (mM/hour) of a silver tungstate membrane with temperature in presence of different electrolytes. *1* = KCl; *2* = $NaCl$; *3* = $LiCl$; *4* = $CaCl_2$; *5* = $MgCl_2$; *6* = $SrCl_2$; *7* = $BaCl_2$ and *8* = $AlCl_3$

the fast moving ion. This regulated rate of flow (i.e. permeability) measured for different electrolytes through various membranes at a given temperature decrease in the order $K^+ > Na^+ > Li^+$ for monovalent cations and $Ca^{2+} > Mg^{2+} > Sr^{2+} > Ba^{2+} > Al^{3+}$ for *di* and *tri* valent cations. In the case of different electrolyte types, the permeability sequence of (2:1) type overlap with that of (1:1) type, although (3:1) type has the lowest permeability.

The effect of temperature is to increase the electrolyte permeability through the membrane (see Figs. 1—3). At higher temperatures, considerably higher fraction f of the total number of a given kind would possess excess energy ΔE according to Boltzmann distribution $f = e^{-\Delta E/RT}$. Under these conditions, those ionic species which have lost sufficient water of hydration to be smaller than the size of the membrane pore would enter the membrane. This is subject to the condition that the membrane has undergone no irreversible change in its structure. That no such change in structure of the membrane is brought about is evident from the linear plots of log P *vs* $(1/T)$ given in Figs. 1—3. The slope of these lines which is equal to $(E_a/2.303\,R)$, gave the activation energy E_a required for the diffusion process. The values so derived are given in Table 1.

The theory of absolute reaction rates[2] has been applied to diffusion processes in membranes by several investigators[1-3,5,11,12]. Following ZWOLINSKI et al.[1], one may write

$$P' = \frac{\lambda^2 kT}{d\hbar}\, e^{-\Delta F'/RT}, \qquad (1)$$

where P' is permeability in cm/sec*, k is the Boltzmann constant, d is the membrane thickness, $\hbar$ is the Planck constant and λ is the

* P' (cm/sec) is related to P (mM/hour) by the relation.

$$P' = \frac{P \cdot 10^{-6}}{3.6\, A\, \Delta C}$$

where A is membrane area (cm²) and ΔC is the difference in the electrolyte concentration existing across the membrane (mole/cm³). Substitution of the respective values for A and ΔC gives

$$P' = 7.1 \cdot 10^{-6}\, P.$$

The slopes of linear plots of log P *vs* $(1/T)$ and of log P' *vs* $(1/T)$ will remain equal.

[11] R. M. BARRER and G. SKIRROW, J. Polymer Sci. **3** (1948) 549.

[12] W. D. STEIN, The Movement of Molecules across Cell Membranes, Academic Press, New York 1967, pp. 70—89.

Table 1. *Experimental activation energy E_a and other thermodynamic parameters calculated from the transition state theory of rate processes for electrolyte diffusion through membranes*

Temperature 25 °C

Electrolyte	KCl	$NaCl$	$LiCl$	$CaCl_2$	$MgCl_2$	$SrCl_2$	$BaCl_2$	$AlCl_3$
Membrane: Silver chloride								
E_a (kcal)	6.44	6.22	5.99	5.30	4.95	4.84	4.72	6.22
$\Delta H'$ (kcal)	5.85	5.63	5.40	4.71	4.36	4.24	4.13	5.23
$\Delta F'$ (kcal)	5.64	5.90	6.00	5.98	6.12	6.23	6.37	6.90
$\Delta S'$ (E.U.)	0.70	−0.92	−2.02	−4.27	−5.90	−6.69	−7.52	−4.28
Membrane: Silver phosphate								
E_a (kcal)	6.45	6.22	6.10	5.76	5.30	5.18	5.07	6.68
$\Delta H'$ (kcal)	5.86	5.63	5.51	5.17	4.71	4.59	4.48	6.09
$\Delta F'$ (kcal)	5.80	6.02	6.13	6.05	6.19	6.30	6.44	6.98
$\Delta S'$ (E.U.)	0.18	−1.30	−2.06	−2.95	−4.97	−5.74	−6.60	−2.98
Membrane: Silver tungstate								
E_a (kcal)	6.22	5.99	5.76	5.54	5.18	5.07	4.84	6.45
$\Delta H'$ (kcal)	5.63	5.40	5.17	4.95	4.59	4.48	4.25	5.86
$\Delta F'$ (kcal)	5.66	5.93	6.06	6.09	6.22	6.36	6.37	6.99
$\Delta S'$ (E.U.)	−0.13	−1.79	−2.99	−3.83	−5.46	−6.33	−7.13	−3.82

Table 2. *Thermodynamic quantity $\Delta S'$ for permeation of various substances through different membrane systems*

Diffusing Species	Membrane	Entropy factor λ $(e^{\Delta S'/R})^{1/2}$ (Å)	$\Delta S'$ (E.U.)	Ref.
H_2	Butadiene acrylonitrile	182	16.0	13,14a
N_2	Butadiene acrylonitrile	130	14.7	13,14a
N_2	Butadiene-methylmethacrylate	150	15.3	13,14a
N_2	Butadiene polystyrene	24	7.8	13,14a
H_2	Neoprene	74	12.4	13,14a
N_2	Neoprene	215	16.7	13,14a
H_2	Chloroprene	150	15.3	13,14a
H_2	Silicone rubber (sheet)	1.3	− 3.4	15
N_2	Silicone rubber (sheet)	0.85	− 5.0	15
O_2	Silicone rubber (sheet)	0.61	− 6.3	15
H_2	Glass	$4 \cdot 10^{-2}$	− 17.1	2
Sucrose	Collodion	$1.1 \cdot 10^{-2}$	− 22.2	2
Lactose	Collodion	$4.3 \cdot 10^{-2}$	− 16.8	2
Mannitol	Collodion	$8.1 \cdot 10^{-2}$	− 23.4	2
Raffinose	Collodion	$2.4 \cdot 10^{-2}$	− 19.1	2
H_2O (sucrose solution)	Collodion	$1.2 \cdot 10^{-2}$	− 21.8	2
H_2O	Polyethylene	$3.9 \cdot 10^{3}$	28.4	16
H_2O	Polypropylene	$25 \cdot 10^{3}$	35.8	16
H_2O	Lipid bilayer (oxidized cholesterol)	$5.5 \cdot 10^{-2}$	− 15.8	5
H_2O (Endosmosis)	Arbacia eggs (unfertilized)	$14.4 \cdot 10^{3}$	31.6	1b
Proprionamide	Arbacia eggs (unfertilized)	$26.9 \cdot 10^{3}$	34	1b
Butyramide	Arbacia eggs (unfertilized)	$12.1 \cdot 10^{4}$	40	1b
Nonelectrolyte (glycerol, glycols, thiourea)	Oxerythrocyte	7.7	3.7	17

[a] Calculations correspond to $\lambda^2 = 10^{-15}$ cm; [b] Calculations correspond to $\lambda = 5$ Å and all other results correspond to $\lambda = 3$ Å.

average distance between equilibrium positions in the process of diffusion. $\Delta F'$ is the free energy of activation for permeability and is releated by the Gibbs-Helmholtz equation

$$\Delta F' = \Delta H' - T\Delta S' \tag{2}$$

to enthalpy $\Delta H'$ and entropy $\Delta S'$ of activation for permeability. $\Delta H'$ is related to Arrhenius energy of activation by the equation

$$E_a = \Delta H' + RT. \tag{3}$$

As the values of d (measured by micrometer calipers) and of the universal constants are known, values for $\Delta H'$, $\Delta F'$ and $\Delta S'$ can be calculated provided the value of λ is known. Different investigators[1-3,5,11] have used values ranging from 1—5 Å for λ. In this work, a value of 3 Å has been used in the calculations and the values so derived for the different quantities are given in Table 1. For purposes of comparision, in Table 2 are given the values of $\Delta S'$ determined by various investigators for a variety of systems.

The values of $\Delta S'$ (see Table 2) are either positive or negative for membranes. According to EYRING and coworkers[1,2] the values of $\Delta S'$ indicate the mechanism of flow; large positive $\Delta S'$ is interpreted to reflect breakage of bonds, while low values indicate that permeation has taken place without breaking bonds. The negative $\Delta S'$ values are considered to indicate either the formation of covalent bond between the permeating species and the membrane material or that the permeation through the membrane may not be the rate limiting step.

On the contrary, BARRER and coworkers[11,14,15] have developed the concept of "zone activation" and applied it to the permeation of gases through polymer membranes. According to this zone hypothesis, a high $\Delta S'$, which has been correlated with high energy of activation for diffusion, means either the existence of a large zone of activation or the reversible loosening of more chain segments of the membrane. A low $\Delta S'$ then means either a small zone of activation or no loosening of the membrane structure on permeation. In view of these differences in the interpretation of $\Delta S'$, SHULER et al.[3], who found negative $\Delta S'$ values for sugar permeation through collodion membranes, have taken

[13] Ref. [1], p. 544.

[14] R. M. BARRER, Trans. Faraday Soc. 38 (1942) 322.

[15] R. M. BARRER and H. T. CHIO, J. Polymer Sci. *Pt. C*, 10 (1965) 111.

[16] H. YASUDA and V. STANNETT, J. Polymer Sci. 57 (1962) 907.

[17] Ref. [12], p. 89.

the view that "it would probably be correct to interpret the small negative values of $\Delta S'$ mechanically as interstitial permeation of the membrane (minimum of chain loosening) with partial immobilization in the membrane (small zone of disorder)". On the other hand, TIEN and TING[5], who found negative $\Delta S'$ values for the permeation of water through very thin (50 Å thickness) bilayer membrane, stressed the possibility that the membrane may not be the rate determining step. Based on additional experimental data, they came to the conclusion that the solution-membrane interface was the rate limiting step for the permeation of water.

The data of the present study (see Table 1) show that electrolyte permeation gives rise to very small negative values for $\Delta S'$ (except two cases with KCl) whose magnitude however depends on the value chosen for λ, the distance between equilibrium positions during permeation. The values of $\Delta S'$ for all the three membranes used, indicated similar behaviour for all the electrolytes. Since the membranes used in this study are fairly thick (~ 0.03 cm) compared to bilayers, it is believed that the membrane and not the solution-membrane interface, controlled the rate determining step in the process of electrolyte diffusion. The small negative values of $\Delta S'$ therefore according to SHULER et al.[3] reflected the fact that the permeation process occurred with partial immobilization in the membrane, the partial immobility for various electrolytes increasing in the order

$$KCl < NaCl < LiCl \approx AlCl_3 < CaCl_2 < MgCl_2 < SrCl_2 < BaCl_2.$$

Acknowledgements

The writing of this work has been supported in part by Public Health Service Grant NB-08163-02.

Thanks are due to Dr. S. M. F. RAHMAN, Head, Chemistry Department, for providing laboratory facilities and to CSIR (India) for the award of a fellowship to S.K.S.

JOURNAL OF POLYMER SCIENCE: PART A-1 VOL. 9, 2853-2867 (1971)

Studies with Inorganic Precipitate Membranes. III.* Consideration of Energetics of Electrolyte Permeation through Membranes

FASIH A. SIDDIQI, N. LAKSHMINARAYANAIAH, and MOHAMMAD N. BEG, *Department of Pharmacology, University of Pennsylvania School of Medicine, Philadelphia, Pennsylvania 19014, and Department of Chemistry, Aligarh Muslim University, Aligarh, India*

Synopsis

The permeability of various electrolytes through parchment-supported ferrocyanide membranes of manganese, cobalt, silver, and cadmium has been measured at 10, 15, 20, 25, and 30°C. The order of permeability at a given temperature was $Cl^- > NO_3^- > CNS^- > CH_3COO^- > SO_4^{2-}$ for both monovalent and divalent cations. For any given anion, the cations followed the sequence $NH_4^+ > Li^+ > Ba^{2+} > Ca^{2+} > Mg^{2+} > Al^{3+}$. This sequence has been correlated with the size of the hydrated ion. Further, the data have been considered from the standpoint of the theory of rate processes and the values for the entropy of activation ($\Delta S'$) have been derived assuming an equilibrium distance of 3 Å in the membrane. The values of $\Delta S'$ were all negative and decreased with increasing valence of the ions. This was interpreted to mean electrolyte permeation with partial immobilization in the membrane.

INTRODUCTION

Zwolinski et al.[1] in 1949 examined the nonelectrolyte premeability data available in the literature for various plant and animal cells by applying the theory of absolute reaction rates.[2] Similarly Shuler et al.[3] considered the kinetics of membrane permeation for nonelectrolytes through collodion membranes. With the availability of thin lipid membranes,[4] Tien and Ting[5] measured their permeability to water and considered the permeation process from the standpoint of the theory of rate processes. In recent years, a number of investigators[6-8] have investigated the electrolyte permeability characteristics of parchment-supported inorganic precipitate membranes. In this paper, the electrolyte permeability of four inorganic membranes at different temperatures in a number of electrolytes is considered on the basis of the concepts of the theory of absolute reaction rates.

* The permeability and the charge density characteristics of parchment-supported membranes of silver chloride, silver phosphate, and silver tungstate are described in Parts I and II, see *Z. physik. Chem.* (Frankfurt), 72, 298, 307 (1970).

EXPERIMENTAL

Preparation of Parchment-Supported Inorganic Membranes

Manganese, cobalt, silver, and cadmium ferrocyanide membranes were prepared following the procedures described elsewhere.[8] To precipitate these substances in the interstices of the parchment paper, 0.2*M* solution of potassium ferrocyanide was kept inside the glass tube, to one end of which was tied the parchment paper. This was suspended for 72 hr in a 0.2*M* solution of a suitable salt of magnanese (chloride), cobalt (chloride), silver (nitrate), or cadmium (chloride). The two solutions were interchanged later and kept for another 72 hr. The membranes were washed with deionized water for removal of free electrolyte.

Measurement of Membrane Potential

The apparatus used was similar to the one used by Siddiqi and Pratap.[8] The membrane was held between two half cells (capacity ca. 125 ml), each of which contained 125 ml of the electrolyte solution. Initially the concentrations C_1 and C_2 were 0.001 and 0.1*M*, respectively. In each half cell there were two firmly fixed platinized platinum electrodes to follow concentration changes on a conductivity bridge and an anion reversible Ag–AgCl electrode to measure the electrical potentials arising across the membrane. The whole cell was immersed in a water thermostat maintained at 25 ± 0.1°C. The various salt solutions (chlorides of Li^+, Na^+, K^+, NH_4^+, Ba^{2+}, Ca^{2+}, Mg^{2+}, and Al^{3+}) were prepared from B.D.H. AR-grade chemicals by use of deionized water. The solutions in both the chambers were kept well stirred by magnetic stirrers.

Exactly known weights or volumes of two test solutions were introduced (say at zero time), and the platinized platinum electrodes were connected to the conductance bridges to follow conductance change with time. No appreciable change in conductance was noted within the 5-hr period on the C_2 side (0.1*M*), and so we have assumed this concentration to be practically constant and followed only the conductance change on the C_1 side. The exact concentration of this solution was determined from a calibration curve where conductance was plotted against concentration. The Ag–AgCl electrodes were connected to a Pye precision vernier potentiometer to monitor the potential across the membrane with time.

Measurement of Electrolyte Permeability

The diffusion experiments were performed by the method of Austin et al.[9] based on the constant flow principle. The membrane in the form of a circular disk (functional area = 19.6 cm^2) was washed thoroughly to remove adsorbed electrolyte and fixed in the leak-proof all-glass cell which finally rested on a magnetic stirrer plate. The upper and lower portions of the cell were connected, past manometers, to reservoirs of 0.2*M* electrolyte solution and of doubly distilled water, respectively. On leaving the cell, the water passed two platinized platinum electrodes which were used to

follow the conductance change of the effluent. The rate of this flow was 180 ml/hr. Similarly the electrolyte flow was maintained usually at 300 ml/hr. The hydrostatic pressure on each side of the membrane was kept equal by adjusting the rates of flow of solution and water.

From calibration curves relating conductance to electrolyte concentration previously established for the conductivity cell, the concentration of the effluent was determined. This, combined with the rate of flow of the effluent, enabled permeability P in millimoles per hour to be calculated at any given temperature. The whole cell assembly was kept immersed in a water thermostat maintained constant to an accuracy of ±0.1°C. The experiments were carried out at 10, 15, 20, 25, and 30°C.

RESULTS AND DISCUSSION

The potential difference between Ag–AgCl electrodes placed on either side of the membrane is the algebraic sum of the electrode potential difference E_e (i.e., concentration potential) and the membrane potential E_m. E_e is obtained by calculation from the measured concentrations of the solutions C_1 and C_2 on the two sides of the membrane from the equation

$$E_e = (RT/Z_-F) \ln (C_2\gamma_2/C_1\gamma_1) \quad (1)$$

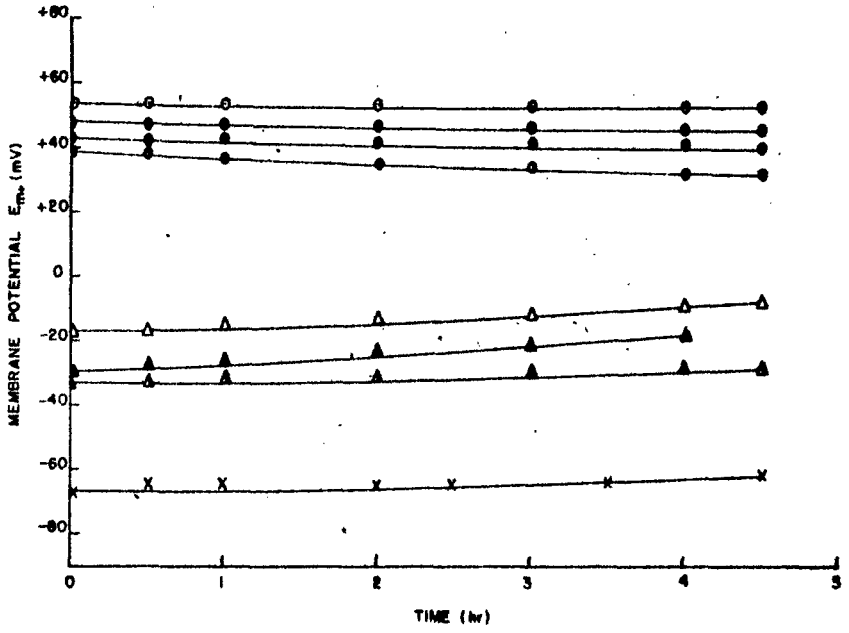

Fig. 1. Variation of membrane potential E_m with time occurring across a parchment-supported manganese ferrocyanide membrane when it separated 0.1 and 0.001 M solutions of the same electrolyte. The electrolytes used were; chlorides of (⊙) Li^+; (●) Na^+; (⊕) K^+; (◑) NH_4^+; (▲) Ca^{2+}; (Δ) Ba^{2+}; (▲) Mg^{2+}; and (×) Al^{3+}.

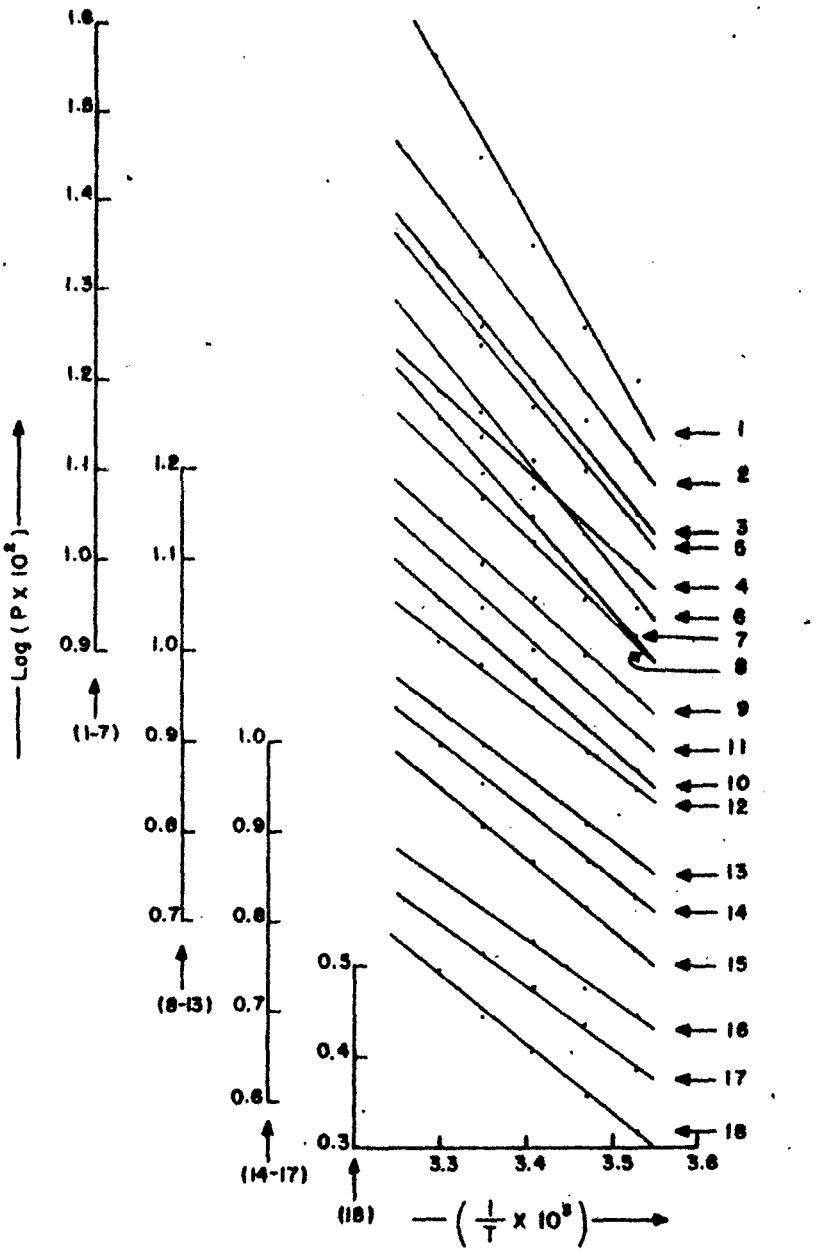

Fig. 2. Variation in permeability P (mmole/hr) of a manganese ferrocyanide membrane with temperature in presence of different electrolytes: (*1*) NH_4Cl; (*2*) NH_4NO_3; (3) NH_4CNS; (4) $(NH_4)_2SO_4$; (*5*) LiCl; (*6*) $LiNO_3$; (*7*) Li_2SO_4; (*8*) $BaCl_2$; (*9*) $Ba(NO_3)_2$; (*10*) $Ba(CH_3COO)_2$, (*11*) $CaCl_2$; (*12*) $Ca(NO_3)_2$; (*13*) $Ca(CH_3COO)_2$, (*14*) $MgCl_2$; (*15*) $Mg(NO_3)_2$; (*16*) $Mg(CH_3COO)_2$; (*17*) $MgSO_4$; (*18*) $AlCl_3$.

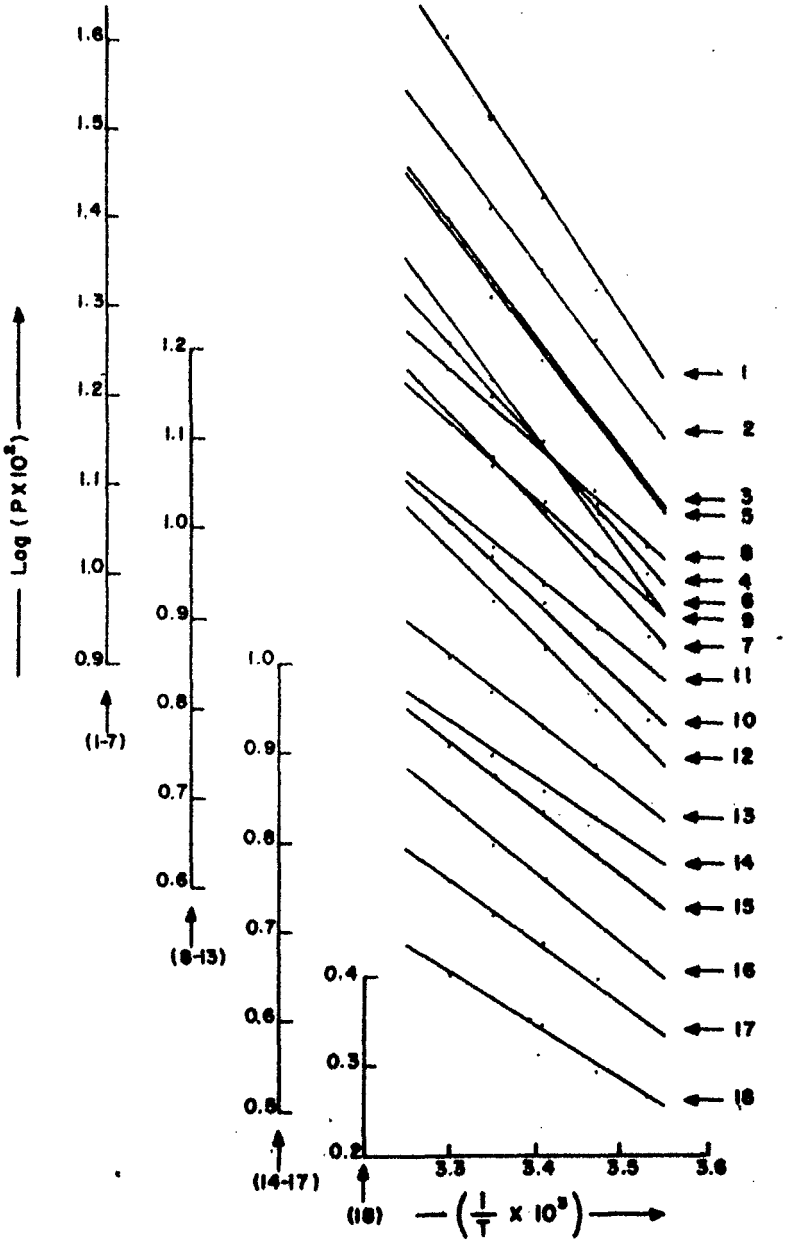

Fig. 3. Variation in permeability P(mmole/hr) of a cobalt ferrocyanide membran with temperature in presence of different electrolytes: (*1*) NH_4Cl; (*2*) NH_4NO_3; (*3* NH_4CNS; (*4*) $(NH_4)_2SO_4$; (*5*) LiCl; (*6*) $LiNO_3$; (*7*) Li_2SO_4; (*8*) $BaCl_2$; (*9*) $Ba(NO_3)_2$; (*10*) $Ba(CH_3COO)_2$; (*11*) $CaCl_2$; (*12*) $Ca(NO_3)_2$; (*13*) $Ca(CH_3COO)_2$; (*14*) $MgCl_2$; (*15*) $Mg(NO_3)_2$; (*16*) $Mg(CH_3COO)_2$; (*17*) $MgSO_4$; (*18*) $AlCl_3$.

where the γ are the activity coefficients of the electrolyte solutions. Since Z_- is always unity, E_s at 25°C is given by

$$E_s = 59.16 \log (C_2\gamma_2/C_1\gamma_1)$$

As E_s and $(E_s + E_m)$ measured directly are known, E_m can be obtained by subtraction.

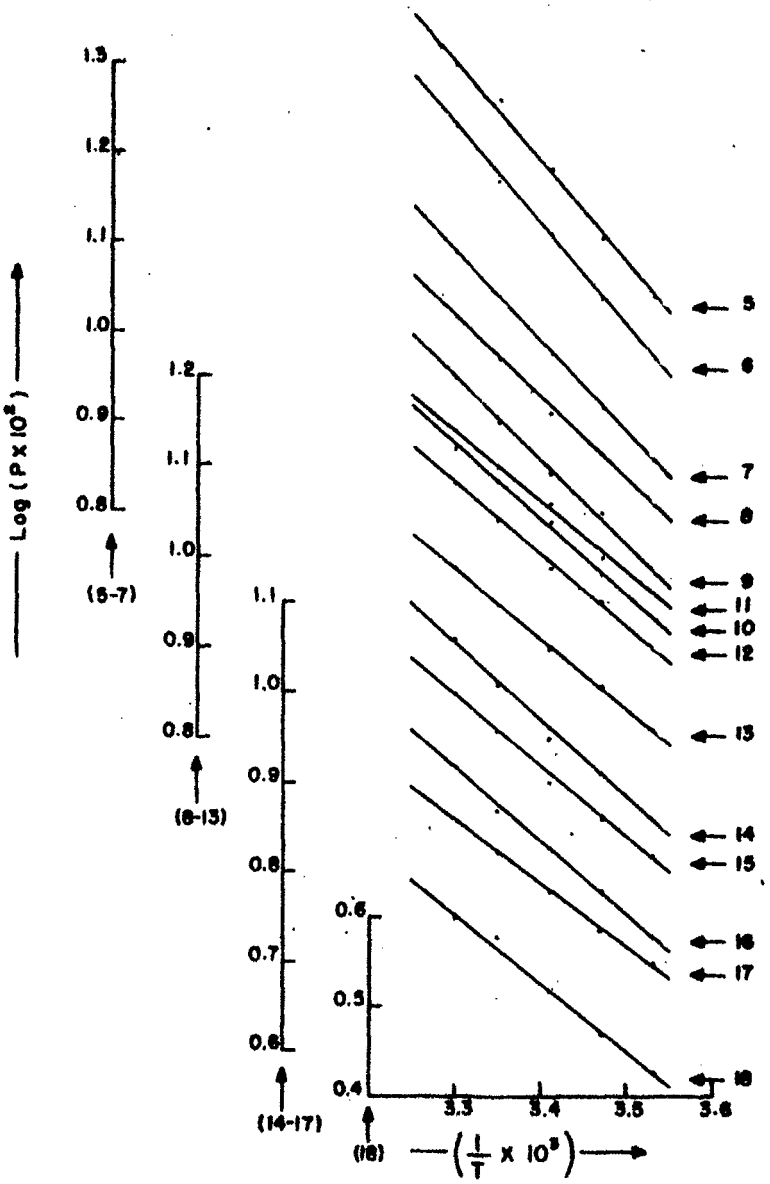

Fig. 4. Variation in permeability P (mmole/hr) of a silver-ferrocyanide membrane with temperature in presence of different electrolytes: (*6*) LiCl; (*6*) $LiNO_3$; (*7*) Li_2SO_4; (*8*) $BaCl_2$; (*9*) $Ba(NO_3)_2$; (*10*) $Ba(CH_3COO)_2$; (*11*) $CaCl_2$; (*12*) $Ca(NO_3)_2$; (*13*) $Ca(CH_3COO)_2$; (*14*) $MgCl_2$; (*15*) $Mg(NO_3)_2$; (*16*) $Mg(CH_3COO)_2$; (*17*) $MgSO_4$; (*18*) $AlCl_3$.

The changes in E_m noted with time are shown in Figure 1 for various electrolytes diffusing through a manganese ferrocyanide membrane. Little change in the values of E_m with time is noted. Similar values for E_m (not

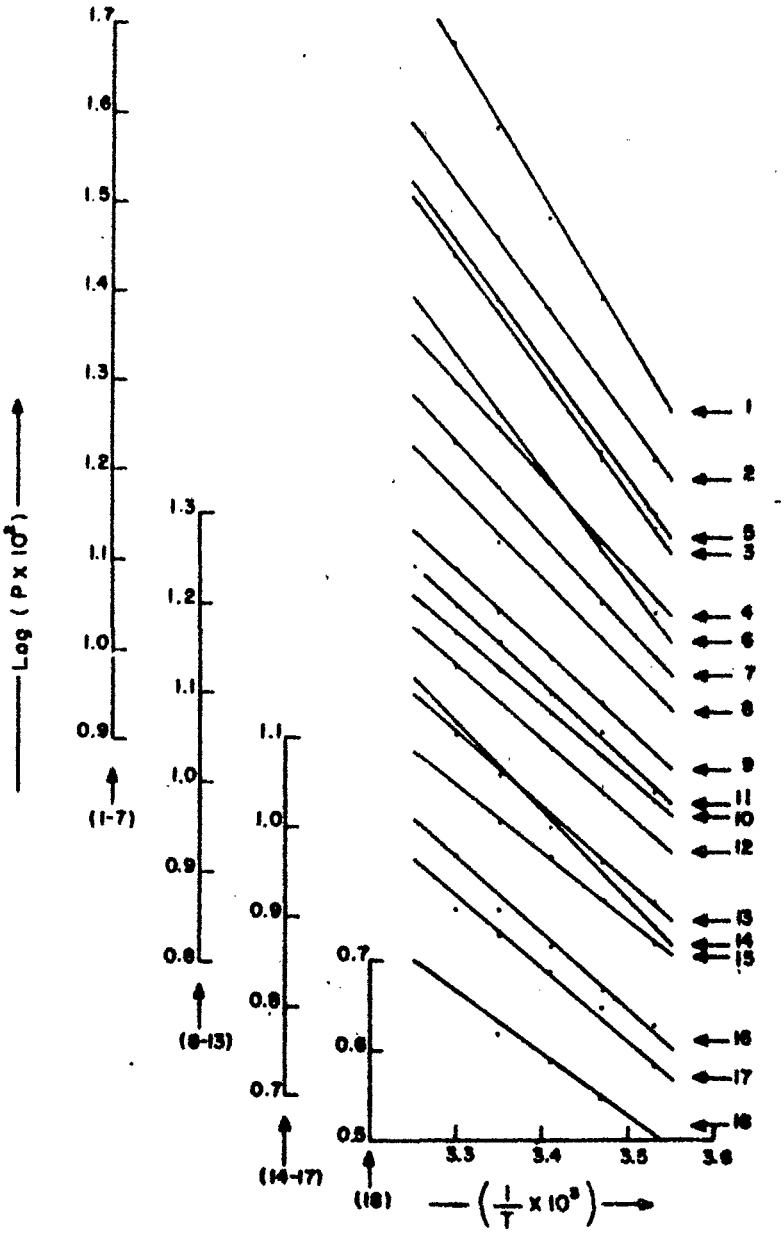

Fig. 5. Variation in permeability P(mmole/hr) of a cadium ferrocyanide membrane with temperature in presence of different electrolytes: (*1*) NH_4Cl; (*2*) NH_4NO_3; (*3*) NH_4CNS; (*4*) $(NH_4)_2SO_4$; (*5*) LiCl; (*6*) $LiNO_3$; (*7*) Li_2SO_4; (*7*) $BaCl_2$; (*8*) $Ba(NO_3)_2$; (*10*) $Ba(CH_3COO)_2$; (*11*) $CaCl_2$; (*12*) $Ca(NO_3)_2$; (13) $Ca(CH_3COO)_2$; (*14*) $MgCl_2$; (*15*) $Mg(NO_3)_2$; (*16*) $Mg(CH_3COO)_2$; (*17*) $MgSO_4$; (*18*) $AlCl_3$.

given) were observed with the other three membranes also. An interesting point with these values of E_m is the fact that in the case of (1:1) electrolytes, the values are all positive (i.e., dilute solution side C_1 taken positive). This means that the membrane is cation-selective. In the case of 2:1 and 3:1 electrolytes, E_m changes sign and therefore becomes anion-selective. This change in the selectivity character of the membrane is due to adsorption of multivalent ions leading to a state where a net positive charge is left on the membrane surface making it anion-selective. Adsorption of Al^{3+} makes the membrane more anion-selective than it is with the adsorption of other divalent cations. Such behavior is not peculiar to these systems. Rosenberg et al.[10] found in the case of thorium counterion, negative electroosmotic transport of water. The ion was so strongly adsorbed on a cation exchange membrane that it conferred anion selectivity to the membrane, and thus water was transferred in the opposite direction (i.e., to the anode chamber instead of to the cathode chamber). Similarly Schulz[11] found, in the case of sodium diphosphate, adsorption of the diphosphate anion on the surface of the anion exchange membrane, Permplex A-100. This reversed the charge on the membrane and also the direction of water flow. This surface-charge reversal occurred in every one of the membranes and electrolytes (2:1 and 3:1) used in this study.

In Figures 2–5 are given the plots of log P against $(1/T)$, where T is the absolute temperature at which the experiments were conducted, for the four membranes and different 1:1, 2:1, and 3:1 electrolytes.

The two important factors which control electrolyte permeability through a membrane are charge on the membrane and its porosity. Parchment paper, except for the presence of some stray and end carboxyl groups, contains very few fixed groups. Deposition of inorganic precipitates gives rise to a net negative charge on the membrane surface in the case of 1:1 electrolyte leading to the type of ionic distribution associated with the electrical double layer. However, as discussed above, use of 2:1 or 3:1 electrolytes leaves a net positive charge on the membrane and again results in the formation of the electrical double layer. Flow of electrolyte by diffusion, because of the presence of a net charge ($-ve$ or $+ve$) on the membrane, gives rise to the membrane potential, as opposed to the liquid junction potential ordinarily observed under similar conditions in the absence of the membrane, which regulates the flow of electrolyte by increasing the speed of the slow moving ion and also by decreasing the speed of the fast moving ion. This regulated rate of flow (i.e., permeability) measured for different electrolytes through the various membranes at any given temperature decreases in the order $Cl^- > NO_3^- > CNS^- > CH_3COO^- > SO_4^{2-}$ for both monovalent and divalent cations. For any given anion, the cations follow the sequence

$$NH_4^+ > Li^+ > Ba^{2+} > Ca^{2+} > Mg^{2+} > Al^{3+}$$

Electrolyte types follow the sequence 1:1 > 2:1 > 3:1.

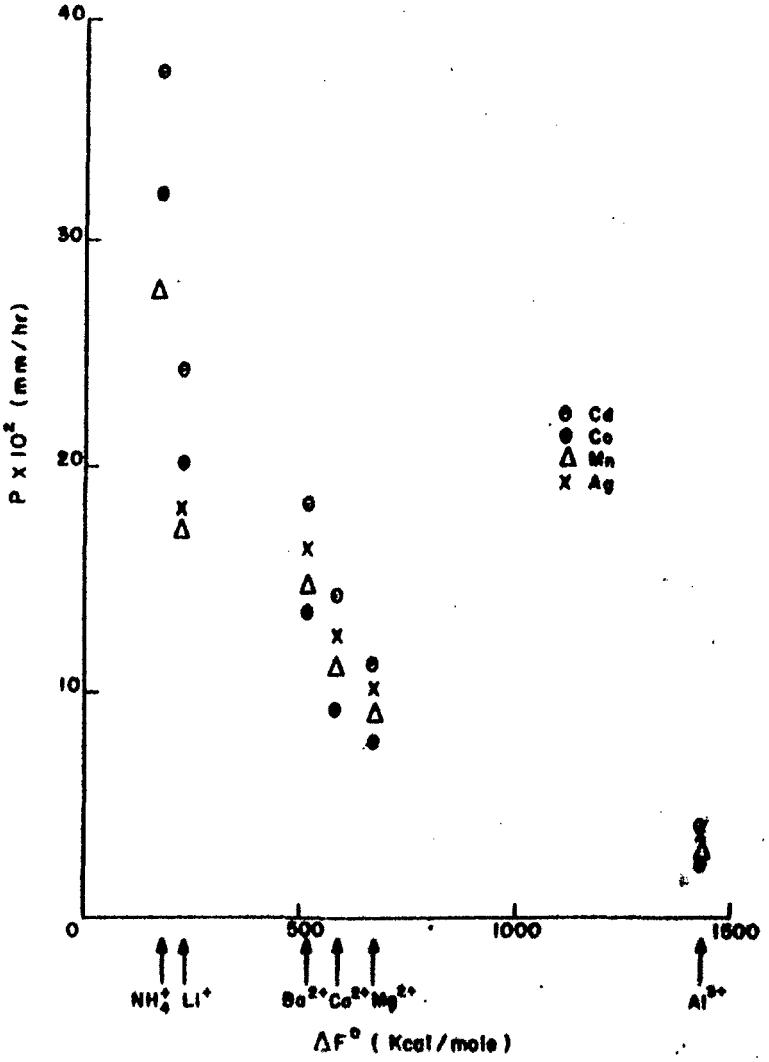

Fig. 6. Permeability P(mmole/hr) at 25°C of various electrolytes (chlorides) through different membranes plotted against the free energy ($\Delta F°$) of hydration of cations: (Δ) manganese ferrocyanide; (●) cobalt ferrocyanide; (×) silver ferrocyanide; (⊙) cadium ferrocyanide.

Membrane porosity in relation to the size of the species (hydrated) flowing through the membrane seems to determine the above sequence. Although the sizes of the hydrated electrolytes are not known with certainty, there are a few tabulations[12,13] of the number of moles of water associated with some electrolytes. However, in Figure 6, a plot of permeability of different electrolytes (chlorides) against free energy of hydration of cations[14] is given for the four membranes. It is seen that permeability decreases with increasing hydration energy, that is, greater size due to increase in hydration. This points to the fact that the electrolyte is diffusing along pores or

TABLE I

Experimental Activation Energy E_a and Other Thermodynamic Parameters Calculated from the Transition State Theory of Rate Processes for Electrolyte Diffusion through Membranes (Temperature = 25°C)

Electrolyte	Manganese ferrocyanide				Cobalt ferrocyanide			
	E_a, kcal	$\Delta H'$, kcal	$\Delta F'$, kcal	$\Delta S'$, e.u.	E_a, kcal	$\Delta H'$, kcal	$\Delta F'$, kcal	$\Delta S'$, e.u.
NH_4Cl	7.37	6.78	8.55	−6.0	7.55	6.96	8.58	−5.8
NH_4NO_3	6.07	5.48	8.72	−10.9	6.07	5.48	8.72	−10.8
NH_4CNS	5.53	4.94	8.83	−13.1	5.97	5.38	8.85	−11.6
$(NH_4)_2SO_4$	4.97	4.38	9.00	−15.5	5.07	4.48	9.01	−15.2
$LiCl$	5.50	4.91	8.85	−13.2	5.90	5.31	8.85	−11.9
$LiNO_3$	5.48	4.89	8.95	−13.6	5.80	5.21	8.99	−12.7
$LiSO_4$	4.79	4.20	9.05	−16.3	4.61	4.02	9.10	−17.1
$BaCl_2$	4.24	3.65	8.95	−17.8	3.96	3.37	9.08	−19.2
$Ba(NO_3)_2$	3.96	3.37	9.05	−19.1	3.96	3.37	9.18	−19.5
$Ba(CH_3COO)_2$	3.85	3.26	9.15	−19.8	3.95	3.36	9.32	−20.1
$CaCl_2$	3.76	3.17	9.11	−19.9	3.59	3.00	9.30	−21.1
$Ca(NO_3)_2$	3.59	3.00	9.20	−20.8	4.22	3.63	9.40	−19.4
$Ca(CH_3COO)_2$	3.40	2.81	9.31	−21.8	3.22	2.63	9.52	−23.1
$MgCl_2$	3.41	2.82	9.24	−21.5	2.95	2.36	9.41	−23.7
$Mg(NO_3)_2$	3.45	2.86	9.30	−21.6	3.33	2.74	9.44	−22.5
$Mg(CH_3COO)_2$	3.32	2.73	9.43	−22.5	3.21	2.62	9.55	−23.2
$MgSO_4$	3.22	2.63	9.50	−23.0	3.13	2.54	9.65	−23.9
$AlCl_3$	3.68	3.09	9.93	−22.9	2.86	2.67	10.10	−26.3

TABLE II

Experimental Activation Energy E_a and Other Thermodynamic Parameters Calculated from the Transition State Theory of Rate Processes for Electrolyte Diffusion through Membranes (Temperature = 25°C)

Electrolyte	Silver ferrocyanide				Cadmium ferrocyanide			
	E_a, kcal	$\Delta H'$, kcal	$\Delta F'$, kcal	$\Delta S'$, e.u.	E_a, kcal	$\Delta H'$, kcal	$\Delta F'$, kcal	$\Delta S'$, e.u.
NH_4Cl	—	—	—	—	7.65	7.06	8.56	−5.1
NH_4NO_3	—	—	—	—	6.36	5.77	8.70	−9.9
NH_4CNS	—	—	—	—	6.26	5.67	8.81	−10.5
$(NH_4)_2SO_4$	—	—	—	—	5.16	4.57	8.98	−14.8
$LiCl$	5.53	4.94	8.80	−13.0	6.36	5.77	8.79	−10.1
$LiNO_3$	5.49	4.90	8.93	−13.5	5.99	5.40	8.97	−12.0
Li_2SO_4	4.61	4.02	9.10	−17.1	4.79	4.20	9.07	−15.3
$BaCl_2$	4.24	3.65	8.85	−17.5	4.61	4.02	8.95	−16.5
$Ba(NO_3)_2$	4.15	3.56	8.95	−18.1	4.24	3.65	9.07	−18.2
$Ba(CH_3COO)_2$	3.95	3.36	9.03	−19.0	4.15	3.56	9.15	−18.8
$CaCl_2$	3.68	3.09	9.00	−19.8	4.24	3.65	9.11	−18.3
$Ca(NO_3)_2$	3.58	2.99	9.10	−20.5	3.68	3.09	9.20	−20.5
$Ca(CH_3COO)_2$	3.57	2.98	9.23	−21.0	3.58	2.99	9.31	−21.2
$MgCl_2$	3.96	3.37	9.13	−19.4	4.61	4.02	9.25	−17.6
$Mg(NO_3)_2$	3.59	3.00	9.21	−20.9	3.68	3.09	9.31	−20.9
$Mg(CH_3COO)_2$	3.59	3.00	9.34	−21.3	3.50	2.91	9.45	−21.9
$MgSO_4$	3.32	2.73	9.38	−22.3	3.49	2.90	9.50	−22.1
$AlCl_3$	3.41	2.82	9.72	−23.1	3.32	2.73	9.86	−23.9

channels of dimensions adequate to allow the substance to penetrate the membrane. The state of hydration of the penetrating electrolyte may be considered to exist in a dynamic condition so that at higher temperatures considerably higher fraction f of the total number of a given kind would possess excess energy ΔE according to the Boltzmann distribution $f = e^{-\Delta E/RT}$ (R is the gas constant). Under these circumstances, those ionic species which have lost sufficient water of hydration to be smaller than the size of the pore would enter the membrane. This way the permeability would increase with increase in temperature, subject however to the proviso that the membrane has undergone no irreversible change in its structure. That no such structural change is involved is evident from the linear

TABLE III
Thermodynamic Parameters $\Delta S'$ for Permeation of Various Substances through Different Systems[a]

Diffusing species	Diffusion system: Medium	Entropy factor $\lambda[e^{\Delta S'/R}]^{1/2}$, Å	$\Delta S'$, e.u.	Reference
Water	Water	11.0	9.5	
Phenol	Methyl alcohol	1.4	1.3	
Phenol	Benzene	1.4	1.3	2a[b]
$C_2H_2Br_4$	$C_2H_2Cl_4$	1.0	0	
Bromine	CS_2	0.4	−3.6	
Mannitol	Water	2.8	4.1	16b[b]
H_2	Butadiene acrylonitrile membrane	182	16.0	
N_2	Butadiene acrylonitrile membrane	130	14.7	
N_2	Butadiene methyl methacrylate membrane	150	15.3	
Ar	Butadiene methyl methacrylate membrane	93	13.4	
N_2	Butadiene polystyrene membrane	24	7.8	2b,17[c]
Ar	Butadiene polystyrene membrane	33	9.3	
H_2	Neoprene membrane	74	12.4	
N_2	Neoprene membrane	215	16.7	
Ar	Neoprene membrane	185	16.2	
H_2	Chloroprene membrane	130	15.3	
H_2	Silicone rubber membrane (sheet)	1.3	−3.4	
N_2	Silicone rubber membrane (sheet)	0.85	−5.0	
O_2	Silicone rubber membrane (sheet)	0.61	−6.3	18
He	Silicone rubber membrane (sheet)	0.87	−4.0	
Ar	Silicone rubber membrane (sheet)	0.83	−5.1	

TABLE III (*continued*)

Diffusion system		Entropy factor $\lambda[e^{\Delta S'/R}]^{1/2}$,		
Diffusing species	Medium	Å	$\Delta S'$, e.u.	Reference
H_2	Glass membrane	4×10^{-2}	−17.1	3
He	Glass membrane	4×10^{-2}	−17.1	
Sucrose	Collodion membrane	1.1×10^{-2}	−22.2	
Lactose	Collodion membrane	4.3×10^{-2}	−16.8	
Mannitol	Collodion membrane	8.1×10^{-2}	−23.4	
Raffinose	Collodion membrane	2.4×10^{-2}	−19.1	
H_2O (sucrose) solution	Collodion membrane	1.2×10^{-2}	−21.8	
H_2O	*n*-Hexadecane liquid	2.8	−0.2	19
H_2O	Hexamethyltetracosane liquid	4.8	1.9	
H_2O	Polyethylene membrane	3.9×10^{3}	28.4	20
H_2O	Polypropylene membrane	25×10^{3}	35.8	
H_2O	Lipid bilayer membrane (oxidized cholesterol)	5.5×10^{-1}	−15.8	5
H_2O (Endosmosis)	Arbacia eggs (unfertilized)	14.4×10^{3}	3.16	1[d]
Propionamide	Arbacia eggs (unfertilized)	26.9×10^{3}	34	
Butyramide	Arbacia eggs (unfertilized)	12.1×10^{4}	40	
Nonelectrolyte (glycerol, glycols, thiourea)	Oxerythrocyte membrane	7.7	3.7	16b

[a] All results correspond to $\lambda = 3$ Å unless otherwise noted.
[b] Calculations correspond to $\lambda = 1$ Å.
[c] Calculations correspond to $\lambda^2 = 10^{-16}$ cm^2.
[d] Calculations correspond to $\lambda = 5$ Å.

plots of log P versus $(1/T)$ given in Figures 2–5. The slope of these lines which is equal to $(E_a/2.303R)$ gave the activation energy E_a required for the diffusion process. The values so derived are given in Tables I and II.

The theory of absolute reaction rates[2] has been applied to diffusion processes in membranes by several investigators.[1–3,15,16a] Following Zwolinski et al.,[1] we may write

$$P' = (\lambda^2 kT/dh)\, e^{-\Delta F'/RT} \tag{2}$$

where P' is the permeability,* k is the Boltzmann constant, d is membrane

* P', (cm/sec) is related to P (mmole/hr) by the relation

$$P' = P \times 10^{-6}/3.6A\Delta C$$

where A is membrane area (19.6 cm^2) and ΔC is the difference in the electrolyte concentration existing across the membrane (0.2 mole/l.). Introducing these values gives $P' = 7.1 \times 10^{-4} P$. The slopes of linear plots of log P vs $(1/T)$ and of log P' vs $(1/T)$ will be equal.

thickness, h is Planck constant, and λ is the average distance between equilibrium positions in the process of diffusion. $\Delta F'$ is the free energy of activation for permeability and is related by Gibbs-Helmholtz equation:

$$\Delta F' = \Delta H' - T'\Delta S' \tag{3}$$

to enthalpy $\Delta H'$ and entropy $\Delta S'$ of activation for permeability. $\Delta H'$ is related to Arrhenius energy of activation E_a by the equation

$$E_a = \Delta H' + RT \tag{4}$$

As the values of d (manganese ferrocyanide membrane = 0.03556 cm; cobalt ferrocyanide = 0.03048 cm; silver ferrocyanide = 0.03810 cm; cadmium ferrocyanide = 0.02794 cm) and of the universal constants are known, values of $\Delta H'$, $\Delta S'$, and $\Delta F'$ can be calculated provided the value for λ is known. Different investigators[1-3,5,15] have used values ranging from 1 to 5 Å for λ. In this work, a value of 3 Å has been used in the calculations, and the values so derived for the different thermodynamic parameters are given in Tables I and II. For purposes of comparison, in Table III, are given the values of $\Delta S'$ determined by various investigators for a variety of systems.

The values of $\Delta S'$ (see Table III) are either positive or negative for membranes. There are a few values which are close to zero and correspond to liquid systems. According to Eyring and co-workers,[1,2] the values of $\Delta S'$ indicate the mechanism of flow; large positive $\Delta S'$ is interpreted to reflect breakage of bonds, while low values indicate that permeation has taken place without breaking bonds. The negative $\Delta S'$ values are considered to indicate either formation of covalent bond between the permeating species and the membrane material or that the permeation through the membrane may not be the rate determining step.

On the contrary, Barrer[15,17,18] has developed the concept of "zone activation" and applied it to the permeation of gases through polymer membranes. According to this zone hypothesis, a high $\Delta S'$, which has been correlated with high energy of activation for diffusion, means either the existence of a large zone of activation or the reversible loosening of more chain segments of the membrane. A low $\Delta S'$, then means either a small zone of activation or no loosening of the membrane structure on permeation. In view of these differences in the interpretation of $\Delta S'$, Shuler et al.,[3] who found negative $\Delta S'$ values for sugar permeation through collodion membranes, have stated that "it would probably be correct to interpret the small negative values of $\Delta S'$ mechanically as interstitial permeation of the membrane (minimum chain loosening) with partial immobilization in the membrane (small zone of disorder)." On the other hand, Tien and Ting,[5] who found negative $\Delta S'$ values for the permeation of water through very thin (50 Å thickness) bilayer membrane, stressed the possibility that the membrane may not be the rate-determining step. Based on additional experimental data, they came to the conclusion that the solution–membrane interface was the rate-limiting step for permeation.

The data of the present study (see Tables I and II) indicate that electrolyte permeation gives rise to negative values for $\Delta S'$, whose magnitude however depends on the value chosen for λ, the distance between equilibrium positions in the process of diffusion. The values of $\Delta S'$ for all the four membranes used in this study show similar behavior for the different electrolytes. It is in general found that as the valence of the individual ion is increased, the decrease in the value of $\Delta S'$ is increased. Since the membranes used in this study are fairly thick compared to bilayers, it is believed that the membrane and not the solution-membrane interface controlled the electrolyte permeation process. The negative values of $\Delta S'$ therefore, as suggested by Shuler et al.,[3] indicated electrolyte permeation with partial immobilization in the membrane, the partial immobility increasing in a relative manner with increase in the valence of the ions constituting the electrolyte.

The writing of this work has been supported in part by Public Health Service grant NB-08163-02. Thanks are due to Dr. S. M. F. Rahman, Head of the Chemistry Department, for providing laboratory facilities.

References

1. B. J. Zwolinski, H. Eyring, and C. E. Reese, *J. Phys. Chem.*, **53**, 1426 (1949).
2. S. Glasstone, K. J. Laidler, and H. Eyring, *The Theory of Rate Processes*, McGraw-Hill, New York, 1941, (a) p. 525; (b) p. 544.
3. K. E. Shuler, C. A. Dames, and K. J. Laidler, *J. Chem. Phys.*, **17**, 860 (1949).
4. N. Lakshminarayanaiah, *Transport Phenomena in Membranes*, Academic Press, New York, 1969, pp. 436–456.
5. H. T. Tien and H. P. Ting, *J. Colloid Interface Sci.*, **27**, 702 (1968).
6. W. U. Malik and F. A. Siddiqi, *Proc. Indian Acad. Sci.*, **A56**, 206 (1962); *J. Colloid Sci.*, **18**, 161 (1963).
7. W. U. Malik, H. Arif, and F. A. Siddiqi, *Bull. Chem. Soc. Japan*, **40**, 1746 (1967).
8. F. A. Siddiqi and S. Pratap, *J. Electroanal. Chem.*, **23**, 137 (1969).
9. A. T. Austin, E. J. Hartung, and G. M. Willis, *Trans. Faraday Soc.*, **40**, 520 (1944).
10. N. W. Rosenberg, J. H. B. George, and W. D. Potter, *J. Electrochem. Soc.*, **104**, 11 (1957).
11. G. Schulz, *Z. Anorg. Allgem. Chem.*, **301**, 97 (1959).
12. H. S. Harned and B. B. Owen, *The Physical Chemistry of Electrolyte Solutions*, 3rd ed., Reinhold, New York, 1958, p. 525.
13. R. A. Robinson and R. H. Stokes, *Electrolyte Solutions*, 2nd ed., Butterworths, London, 1959, p. 62.
14. Y. Marcus and A. S. Kertes, *Ion Exchange and Solvent Extraction of Metal Complexes*, Interscience, New York, 1969, p. 13.
15. R. M. Barrer and G. Skirrow, *J. Polym. Sci.*, **3**, 549 (1948).
16. W. D. Stein, *The Movement of Molecules across Cell Membranes*, Academic Press, New York, 1967, (a) pp. 70–89; (b) p. 89.
17. R. M. Barrer, *Trans. Faraday Soc.*, **38**, 322 (1942).
18. R. M. Barrer and H. T. Chio, in *Transport Phenomena in Polymeric Films* (*J. Polym. Sci. C*, **10**), C. A. Kumins, Ed., Interscience, New York, 1965, p. 111.
19. P. Schatzberg, in *Transport Phenomena in Polymeric Films* (*J. Polym. Sci. C*, **10**), A. Kumins, Ed., Interscience, New York, 1965, p. 87.
20. H. Yasuda and V. Stannett, *J. Polym. Sci.*, **57**, 907 (1962).

Received January 12, 1971

CHAPTER 5

APPLICATION OF FICKS DIFFUSION LAW AND NERNST-PLANCK FORMULAE FOR ELECTRICAL POTENTIALS

ELECTROANALYTICAL CHEMISTRY AND INTERFACIAL ELECTROCHEMISTRY 137
Elsevier Sequoia S.A., Lausanne Printed in The Netherlands

STUDIES OF MEMBRANE PHENOMENA

I. EFFECT OF TEMPERATURE ON DIFFUSION OF ELECTROLYTES THROUGH A PARCHMENT SUPPORTED SILVER IODIDE MEMBRANE

FASIH A. SIDDIQI AND SURENDRA PRATAP
Department of Chemistry, Aligarh Muslim University, Aligarh (India)

(Received February 6th, 1969)

INTRODUCTION

The findings of Teorell[1] that gastric mucosal membrane, in some formal aspects at least, behaved exactly like parchment membrane led us to investigate a very large number of parchment-supported membranes as models for biological membranes. In previous communications[2-5] the membrane potential (E) was related to the permeability (P) parameter by a Freundlich adsorption-type equation $E = aP^{1/n}$, and the constants a and n characterizing the membranes were evaluated. It soon was realized that the electrolytic resistance of the membrane R_m plays an important role in the diffusion process. This communication deals with the determinations of the membrane resistance R_m, the membrane concentration potential, E_m, and diffusion rate D_r, at various temperatures. The evaluation of the energy and enthalpy of activation of diffusion of biologically important electrolytes and their relationship with various thermodynamic quantities of aqueous ions is also considered. These investigations emphasize the importance of hydration and the energetics of the associated processes in membrane phenomena. The fixed charge theory of Teorell[6], and Meyer and Sievers[7] as well as the views of Sollner[8], Gregor[9], Schmid[10] and Eisenman[11] have been applied to elucidate the electrochemical nature of the membranes investigated.

EQUATION USED FOR DIFFUSION RATE MEASUREMENT

The equations used in these investigations to calculate diffusion rates were modifications of those which apply to the migration of ions under the influence of a potential gradient. The equation:

$$\frac{dQ_+}{dt} = \frac{1}{Z_+ R_m F}\left[\frac{Z_-}{Z_+ + Z_-}\frac{E_m}{E_{c+}} + \frac{Z_+}{Z_+ + Z_-}\right][E_{c+} - E_m] \qquad (1)$$

where

Q_+ = mmoles of cations
Z_+, Z_- = valency of cation and anion respectively
E_m = membrane concentration potential
E_{c+} = potential difference (mV) equivalent to a given difference in cation concentration

E_c = potential difference (mV) equivalent to a given difference in anion concentration
F = Faraday (96,500 C)
R_m = electrolytic resistance of membrane (Ω)
t = diffusion time (s),

which was deduced by Kittleberger[12], was employed for the determination of the diffusion rate. For uni-univalent electrolytes, $Z_+ = Z_-$, eqn. (1) then becomes

$$D_t = \frac{dQ}{dt} = \frac{dQ_+}{dt} = \frac{1}{FR_m}\left[\frac{1}{2}\frac{E_m}{E_{c'}} + \frac{1}{2}\right][E_{c'} - E_m] \quad (2)$$

where D_t is the diffusion rate and Q is mmoles of salt.

EXPERIMENTAL

Preparation of parchment-supported silver iodide membrane

The membrane was prepared by impregnating parchment paper with silver iodide. The paper was first soaked with distilled water and then tied carefully to a glass tube (cylinder). A 0.2 *M* solution of potassium iodide was put inside the paper container which was then suspended for 72 h in a 0.2 *M* $AgNO_3$ solution contained in a beaker. The parchment paper was then taken out and washed repeatedly with distilled water to remove the adsorbed electrolytes. The solutions of potassium iodide and silver nitrate were then interchanged. The paper was then immersed in them for another 72 h. This process was repeated a number of times until a very fine deposit of silver iodide was obtained on the paper. The membrane, yellow in colour, was observed under a microscope; there was a fine deposition over the whole surface.

Apparatus and procedure

The assembly used for the diffusion rate measurement is shown in Fig. 1. It consisted of two half-cells (125-ml capacity) having flanges to fit each other. The vertical female joints, T and T', attached to each half-cell provided introduction for the electrolyte and the conductivity cell electrodes. The test membrane in the form of a disc slightly larger than the cell was installed between the flanges of the half-cells. One Ag/AgCl J-shaped electrode and one Ag/AgCl disc electrode passed through two narrow holes in each half-cell very close to the membrane as shown in Fig. 1. A narrow tube was slipped over the ends of the J-shaped and the disc electrodes and waxed firmly. Some mercury was also placed in each of the tubes to provide connection to the copper wire leads.

The conductivity cell electrodes dipping in the salt solutions in the two half-cells were used to determine the salt concentration of the test solutions. Various salt solutions (KCl, NaCl and LiCl) were prepared from B.D.H. AR-grade chemicals. Initially, they were usually 0.2 *M* and 0.002 *M* in the two half-cells. No appreciable change was observed within 5–6 h in 0.2 *M* electrolyte concentration and we have therefore assumed this concentration to be practically unchanged.

The potential difference between the Ag/AgCl J-shaped electrodes in test solutions on opposite sides of the membrane is the algebraic sum of concentration potential E_c and membrane potential E_m. E_c was obtained by calculation from the measured concentrations of the two test solutions and $(E_m + E_c)$ was obtained

directly. The membrane concentration potential E_m was then obtained by subtraction. Under the conditions of the experiment, the dilute side was always positive and E_m was taken with its proper sign.

The electrolytic resistance of the membrane R_m was determined by applying an external e.m.f. to the Ag|AgCl disc electrodes in the solutions on opposite sides of the membrane and measuring the change in the potential difference of the Ag|AgCl J-shaped electrodes. To determine the current in the circuit, the IR drop across a known resistance R (1000 Ω) in series with the cell was also measured. This measuring current was kept as low as possible in order to minimise the transfer of ions during the 2 or 3 min required for each resistance measurement.

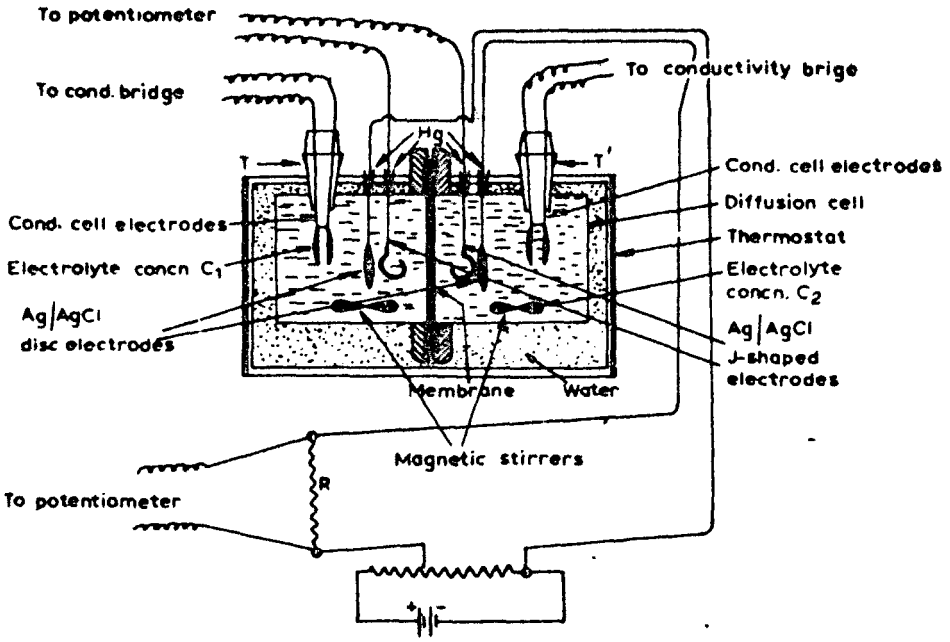

Fig. 1. Apparatus for diffusion rate measurement and electric circuit for measurement of the membrane resistance R_m.

The experimental procedure involved setting up a cell with a membrane and silver–silver chloride electrodes (both J-shaped as well as disc-shaped). Known volumes of the two test solutions (approx. 125 ml of each) were introduced and the conductivity cell electrodes fixed in place. The assembly had magnetic stirrers in each half-cell and was placed in a thermostat maintained at the required temperature. The measurements needed were the determination of (*a*) the salt concentration of the two test solutions, (*b*) the membrane concentration potential and (*c*) the membrane resistance in order to compute the diffusion rate.

Two sets of calibration curves were needed in this experiment, one to obtain the concentration from the measured conductivity and the other to obtain the concentration potential E_c. In the first case, the curves were plots of conductance *vs.* concentration. The curves from which concentration potentials were obtained were plots of e.m.f. *vs.* log fc from the equation:

$$\text{e.m.f.} = \frac{2.303\,RT}{F} \log fc \qquad (3)$$

(for uni-univalent electrolytes)

For all electrolytes, $E_{c\cdot}$ was equal to the difference between the e.m.f. values of the dilute and concentrated test solutions.

With R_m in ohms and $E_{c\cdot}$ and E_m in millivolts, eqn. (2) gives the rate of diffusion of an electrolyte through the membrane in mmol s^{-1}.

The potential and conductance measurements were made by means of a Pye precision vernier potentiometer (No. 7568) and Cambridge conductivity bridge (No. L-350140), respectively.

RESULTS AND DISCUSSION

The equation for the diffusion rate for a uni-univalent electrolyte is given by eqn. (2) which clearly shows that D_t depends mainly upon two main factors, membrane resistance R_m and membrane potential E_m. The changes in the diffusion rate over a range of nearly 6 h for the chlorides of alkali metal ions are shown in Fig. 2. The variations in the membrane resistance and membrane potential over the same time range are shown in Figs. 3 and 4 respectively. As the diffusion rate depends markedly

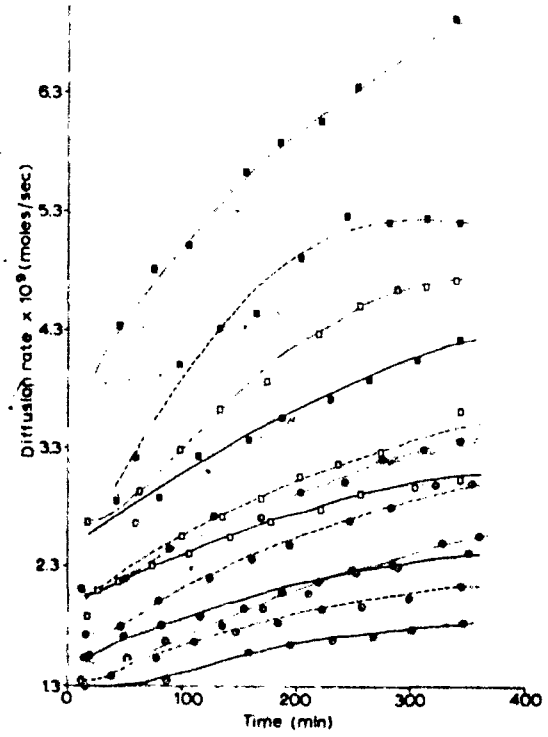

Fig. 2. Rates of diffusion (D_t) of various electrolytes through silver iodide membrane at different temps. LiCl (straight lines) (⊙) 10°, (●) 18°, (□) 25°, (■) 35°C. NaCl: the same with a dashed line. KCl: the same with a dotted line.

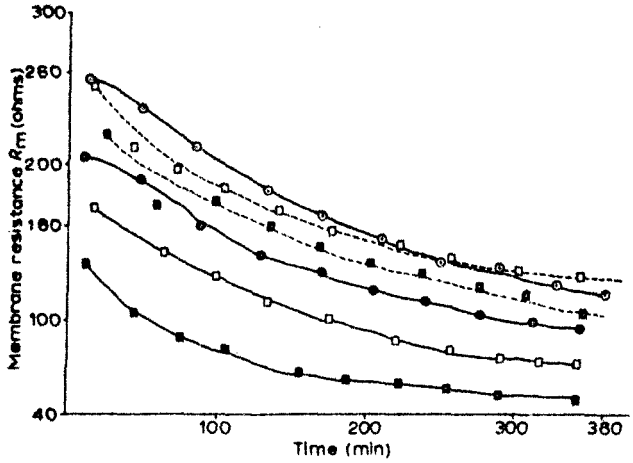

Fig. 3. Plots of membrane resistance *vs.* time for KCl at different temperatures, and for NaCl and LiCl at 25°C (dashed lines). KCl: (○), 10°; (●), 18°; (□), 25°; (■), 35°C. NaCl: (▨); LiCl: (□).

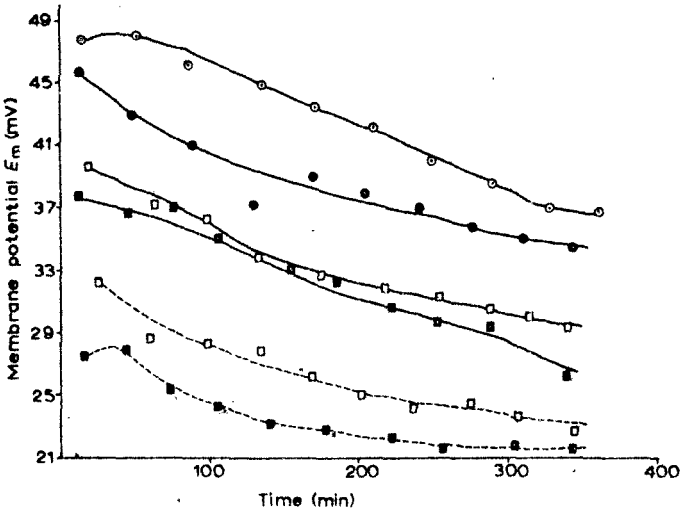

Fig. 4. Plots of membrane potential *vs.* time for KCl at different temperatures and for NaCl and LiCl at 25°C (dashed lines). Designations as in Fig. 3 for KCl. Dotted lines: NaCl: (□); LiCl: (■).

on temperature, it was thought worthwhile to study the effect of temperature on membrane resistance and membrane potential. The behaviour of membrane resistance and membrane potential for KCl at various temperatures is shown in Figs. 3 and 4 respectively. The effect of temperature on membrane resistance and membrane potential was found to be similar for NaCl and LiCl; representative curves for NaCl and LiCl at 25°C are also shown in the same Figures.

In order to obtain the energy of activation of diffusion of the three electrolytes (*viz.* KCl, NaCl and LiCl), plots of log D_r *vs.* $1/T$ (T is the absolute temperature) were drawn for the three electrolytes and from the slope, the energy of activation E_A, was evaluated. As is clear from Figs. 2, 3 and 4, the changes in D_r, R_m and E_m are appreciably lower after 300 min, so these values at 340 min were chosen for each

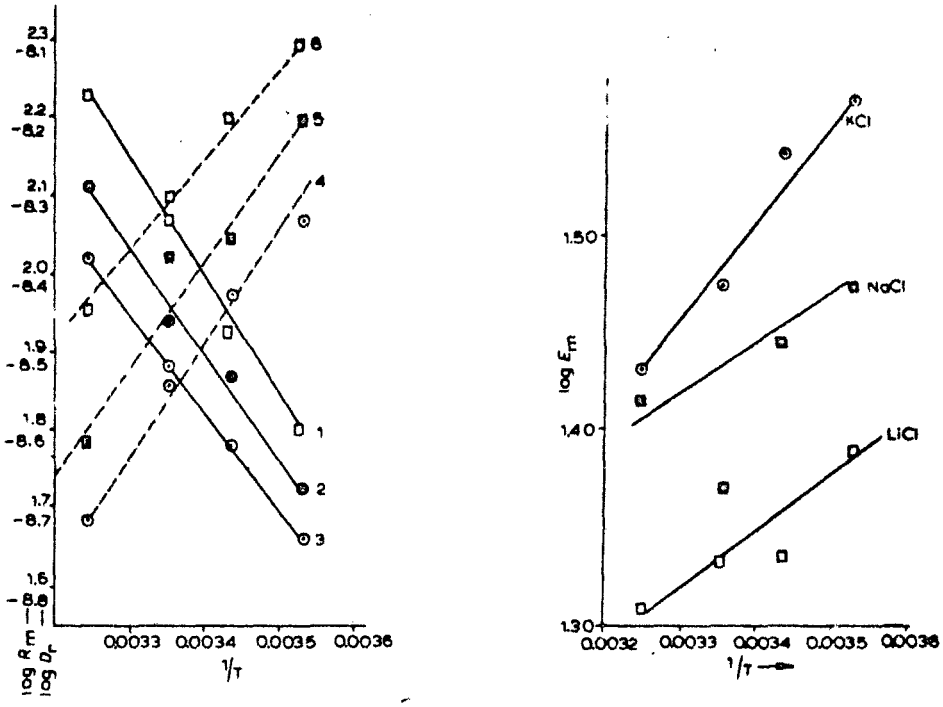

Fig. 5. Plots of log D_r (full line) and log R_m (dashed line) *vs.* $1/T$ (both at 340 min) for different electrolytes. (□) (1), KCl; (●) (2), NaCl; (⊙) (3), LiCl. (⊙) (4), KCl; (■) (5), NaC (□) (6), LiCl.

Fig. 6. Plots of log E_m *vs.* $1/T$ for different electrolytes.

TABLE 1

VALUES OF MEMBRANE RESISTANCE R_m, MEMBRANE POTENTIAL E_m, AND DIFFUSION RATE D_r (AT THE 340TH MINUTE) FOR VARIOUS ELECTROLYTES AT DIFFERENT TEMPERATURES USING PARCHMENT-SUPPORTED SILVER IODIDE MEMBRANE

($C_1/C_2 = 0.2\ M/0.002\ M$)

Electrolyte	*Temp./°C*	R_m/Ω	E_m/mV	$10^9\ D_r/mol\ s^{-1}$
KCl	10	118.0	37.0	2.50
	18	94.5	34.8	3.37
	25	72.0	29.7	4.70
	35	48.0	27.0	6.83
NaCl	10	158.5	29.7	2.12
	18	111.5	27.9	2.94
	25	106.0	23.5	3.45
	35	61.0	26.0	5.20
LiCl	10	198.5	24.5	1.82
	18	160.0	21.6	2.39
	25	126.0	21.4	3.07
	35	90.0	20.3	4.18

electrolyte to make a comparative study. In order to draw the plots of log D_r, log R_m and log E_m *vs.* $1/T$, the values of D_r, R_m and E_m chosen for each electrolyte at each temperature were those at the 340th minute. The plots of log D_r and log R_m *vs.* $1/T$ for different electrolytes are shown in Fig. 5; those of log E_m *vs.* $1/T$ are shown in Fig. 6. The values of D_r, R_m and E_m for different electrolytes at different temperatures (at the 340th minute) are summarized in Table 1.

The energies of activation of diffusion for the three electrolytes are in the order: KCl, 6974; NaCl, 6132; LiCl, 5675 cal mol^{-1}.

The enthalpies of activation ΔH^* (at 25°C) for the three electrolytes are as follows: KCl, 6382; NaCl, 5540; LiCl, 5083 cal mol^{-1}.

A critical evaluation of the experimental results on the diffusion rates has to take into consideration the following factors which are responsible for slowing down the diffusion through the membrane compared to the diffusion in free solution.

1. A part of the cross section of the membrane is occupied by the frame-work (cellular material and silver iodide precipitate).

2. Diffusion of the electrolyte takes place through a tortuous and hence longer path.

3. The frame-work impedes the diffusion of large hydrated ions.

4. Interaction of the fixed ionic groups of the frame-work retards the diffusion.

Moreover, pore geometry also plays a role in explaining the retardation in diffusion rate. In the system investigated, all homogenous membrane elements are taken to be charged, rigid capillary structures or gels which may be adequately described by the classical fixed charge theory of Teorell. The charged membrane is to be viewed as a set of parallel capillaries having a diameter large with respect to the thickness of the electrical double layer at the walls.

The interpretation of the results of the diffusion rate studies can be discussed in terms of ionic sizes, solvation, mobilities, adsorption properties and other thermodynamic properties. The theory put forward by Gregor[9] in relation to the ionic selectivity depends largely on the use of hydrated ionic volumes. As our discussion is largely dependent upon ionic hydration, it seems necessary to mention some concept of ionic hydration as applied to membrane phenomena. Levine and Bell[13] have considered the region of water surrounding an ion as a coordinated hydration shell, and call it an ion complex. Its formation and breaking would be accompanied by substantial free energy and entropy changes. Stern and Amis[14] considered that ions may possess solvation sheaths of water molecules "bound" to give distinct molecular species. Stokes and Robinson[15] have given the number of bound molecules (N_h) in their hydration shell by the interaction of ions and the surrounded water. This number N_h is not the same as the conventional number of water molecules in the first layer around the ion, it is rather a number introduced to allow for the average effect of all ion–solvent interaction. The following are the values of N_h and a_0 (mean distance of approach in Å units) for the three cations[18]

	N_h	a_0 (Å)
KCl	1.9	3.63
NaCl	3.5	3.97
LiCl	7.1	4.32

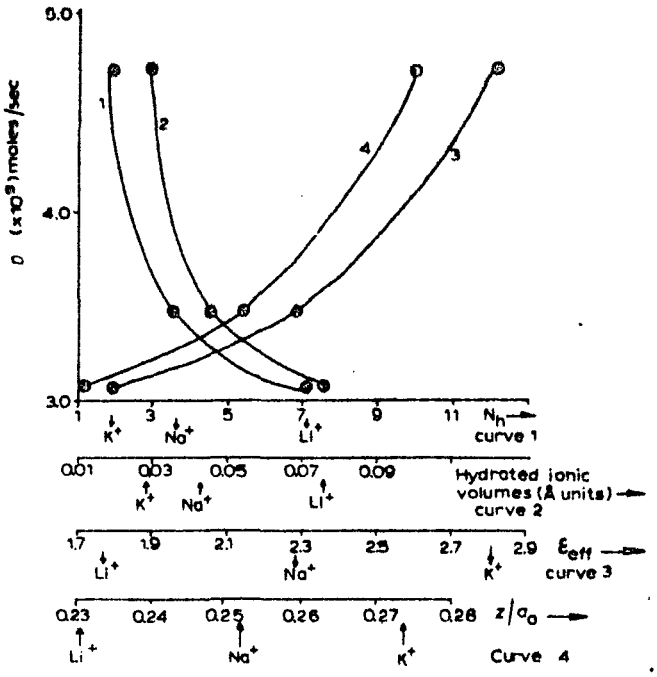

Fig. 7. Plots of: (1), N_h; (2), hydrated ionic volumes; (3), E_{eff}; (4), Z/a_0 *vs.* D_r, where the D_r values are those at 340 min and 25°C.

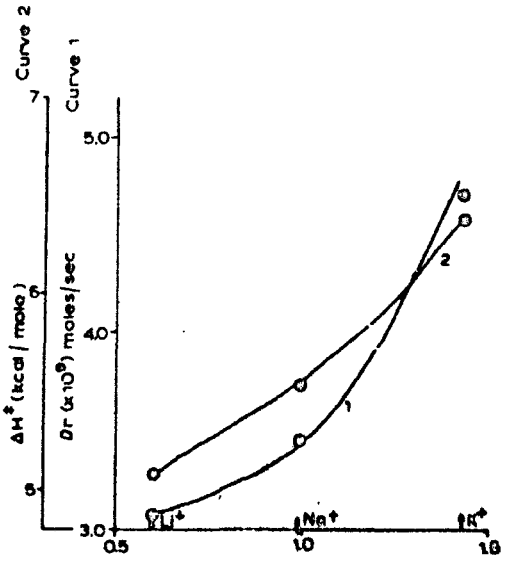

Fig. 8. Plots of: (1), D_r; (2) ΔH^* *vs.* heats of hydration. D_r-values are those at the 340th min and 25°C; ΔH^*-values are those at 25°C.

According to Gregor's theory of ion selectivity[9], of two exchangeable cations the one with the smaller hydrated radius will be preferred by the exchanger. Depending on the size and electrical charge pattern of a pore, it may either admit or repel a solute particle. This is the basis of ion selectivity and applies equally to the material in a thin sheet (a membrane) or in bulk (an ion exchanger). It has been proposed by Mullins[16] that the hydration of the materials of the pores themselves may provide a favourable water environment for particular ions or molecules, so that they slip into the pore away from their previous water molecules. According to the Mullins argument this could result in selection of a particular size with discrimination against both smaller and larger hydrated ions. However it is more general to regard the state of hydration as being in a dynamic condition so that a fraction f of the number of a given kind of particles in the solution has a reduced hydration corresponding to excess energy ΔE mole, according to the Boltzmann distribution $f = \exp(-\Delta E/RT)$. Thus, it can be said that those ions that have lost sufficient water of hydration to become smaller than the pore, can enter the material.

To obtain a quantitative relation between the ease of penetration and the ion size (hydrated) it will be necessary to know the electrostatic force that acts between the ions and the material of the membrane, since this force provides energy equal to ΔE to displace water of hydration. Eisenman[11] has pointed out that the order of the ease of penetration of univalent cations will depend upon the energy for the ion-fixed charge interaction. The values of the activation energies as determined for a silver iodide membrane for the three electrolytes are found to lie between 5.6 and 7.0 kcal mole^{-1}. It is quite probable that the pores of the membrane may have such a size that they allow some of the hydrated sheaths along with the ions to pass through. However in Fig. 7, plots of the hydration numbers and the hydrated ionic volumes *vs.* D_r show that Li^+ having the highest value has the lowest D_r value. The plots of D_r and enthalpy of activation ΔH^* *vs.* heats of hydration (Fig. 8) of the individual ions show that Li^+ having the lowest value of heat of hydration has the lowest values of D_r and ΔH^*.

Noyes[17] while dealing with the thermodynamics of ion hydration as a measure of the effective dielectric properties of water, has regarded the thermodynamic changes during hydration as a measure of the effective dielectric properties of solvent and shows that $\varepsilon_{effective}$ is primarily a function of the size (crystallographic radii) of such a cation and is virtually independent of charge on it. As, during the diffusion process, adsorbability and polarizability play an important part which will certainly influence and thereby diminish the effective hydration (the higher adsorbability of Li^+, Na^+, K^+ are linked closely with their stepwise stronger polarizabilities and, hence, effective hydration is diminished to a larger extent[8]) it would be quite logical to relate the effective dielectric constant with D_r. The plots of ε_{eff} *vs.* D_r are shown in Fig. 7, the highest values of ε_{eff} of K^+ giving the largest value of D_r.

ACKNOWLEDGEMENT

The authors are grateful to Dr. S. M. F. Rahman, Head of the Chemistry Department, for providing facilities for carrying out these investigations.

SUMMARY

The diffusion of LiCl, NaCl and KCl through parchment-supported silver

iodide membrane has been studied at various temperatures. The diffusion rate is in the order: KCl > NaCl > LiCl. The membrane resistance R_m and the membrane potential E_m are found to decrease with increase in temperature. The membrane resistance is in the order: $R_m(LiCl) > R_m(NaCl) > R_m(KCl)$ whereas the membrane potential is in the order: $E_m(KCl) > E_m(NaCl) > E_m(LiCl)$. The results have been discussed in the light of TMS theory and the views of Sollner, Gregor and Eisenman. The diffusion rate and the enthalpy of activation of diffusion have been related to the number of hydration, heats of hydration and other ionic quantities.

REFERENCES

1 T. TEORELL, *Discussions Faraday Soc.*, 21 (1956) 9.
2 W. U. MALIK AND S. A. ALI, *Kolloid-Z*, 175 (1961) 139.
3 W. U. MALIK AND F. A. SIDDIQI, *Proc. Indian Acad. Sci.*, A 56 (1962) 206.
4 W. U. MALIK AND F. A. SIDDIQI, *J. Colloid Sci.*, 18 (1963) 161.
5 W. U. MALIK, H. ARIF AND F. A. SIDDIQI, *Bull. Chem. Soc. Japan*, 40 (1967) 1741.
6 T. TEORELL, *Proc. Soc. Exp. Biol. Med.* 33 (1935) 282; *Z. Elektrochem.*, 55 (1951) 460; *Proc. Nat. Acad. Sci., U.S.*, 21 (1935) 152; *J. Gen. Physiol.*, 21 (1937) 107
7 K. H. MEYER AND J. F. SIEVERS, *Helv. Chim. Acta*, 19 (1936) 649, 665, 987.
8 K. SOLLNER, *J. Phys. Chem.*, 49 (1945) 47, 171; *J. Electrochem. Soc.*, 97 (1950) 139 C; *Ann. N.Y. Acad. Sci.*, 57 (1953) 177.
9 H. P. GREGOR, *J. Am. Chem. Soc.*, 70 (1948) 1293; 73 (1950) 642.
10 G. SCHMID, *Z. Elektrochem.*, 54 (1950) 424, *ibid.*, 55 (1951) 229; *ibid.*, 56 (1952) 181; G. Schmid and H. Schwartz, *Z. Elektrochem.*, 55 (1951) 295, *ibid.*, 55 (1951) 684; *ibid.*, 56 (1952) 35.
11 G. EISENMAN, *Biophys. J., Suppl.*, 2 (1962) 259; G. EISENMAN, in A. KLEINZELLER AND A. KOTYK (Eds.), *Membrane Transport and Metabolism*, Academic Press, New York, 1961, pp. 163-179.
12 W. W. KITTLEBERGER, *J. Phys. Chem.*, 55 (1949) 392.
13 S. LEVINE AND G. M. BELL, *Discussions Faraday Soc.*, 42 (1966) 9.
14 K. H. STERN AND E. S. AMIS, *Chem. Rev.*, 59 (1959) 1.
15 R. H. STOKES AND R. A. ROBINSON, *J. Am. Chem. Soc.*, 70 (1948) 1870.
16 R. J. HARRIS (Ed.), *Transport and Accumulation in Biological Systems*, Butterworths Scientific Publ. (London), 1960 edition.
17 R. M. NOYES, *J. Am. Chem. Soc.*, 84 (1962) 513.
18 H. S. HARNED AND B. B. OWEN, *Physical Chemistry of Electrolyte Solutions*, Reinhard Publishing Corp., New York, N.Y., 3rd ed., 1955, p. 548.

REPRINTED FROM

BULLETIN

OF THE

CHEMICAL SOCIETY OF JAPAN

VOL. 49, NO. 10, OCTOBER, 1976

THE CHEMICAL SOCIETY OF JAPAN

Studies with Parchment Supported Membranes. VII. Application of Fick's Diffusion Law and Nernst-Planck Formulae for Electrical Potential—Consideration of Membrane Field Strength and Energetics of Permeation of Cations

Fasih A. Siddiqi, M. Nasim Beg, Abdul Haque, and Surendra P. Singh
Division of Physical Chemistry, Department of Chemistry, Aligarh Muslim University, Aligarh, India

(Received December 8, 1975)

Electrolytic transport processes occurring across parchment supported membranes have been described by Nernst-Planck flux equation taking into account the membrane resistance R_m, membrane potential E_m *etc.* E_m values for various electrolytes display very interesting phenomena. In the case of 1:1 electrolyte the E_m values are all positive, while in the case of (2:1) and (3:1) electrolytes surface charge reversal takes place. The diffusion rate sequence and selectivity of the membrane for different uni-, bi-, and tri-valent cations was found to be primarily dependent on the difference in the hydration energies of counter ions in the external solution. On the basis of Eisenman-Sherry theory the diffusion rate sequence of alkali metal cations point towards the weak field strength of the fixed charge groups. Various thermodynamic parameters, ΔH^*, ΔF^*, and ΔS^* were evaluated by applying the theory of absolute reaction rates to the diffusion process through parchment supported membranes. The values of ΔS^* were found to be negative, indicating that diffusion takes place with partial immobilization in the membrane phase. The relative partial immobility was found to increase with increase in the valence of the ions constituting the electrolyte. A formal relation between $\Delta H_{hydration}$, $\Delta F_{hydration}$, and $\Delta S_{hydration}$ of cations with the corresponding values of ΔH^*, ΔF^*, and ΔS^* for diffusion, was also found to exist for these membranes.

Transport processes occuring across membranes are of great interest for biologists, who use them as simple models for physiological membranes in order to understand the behavior of complex cell membranes in terms of established physico-chemical principles. It was demonstrated by Teorell[1] that the gastric mucosal membrane, in some formal aspects at least, behaved exactly like parchment membrane. His findings, that electrolytic transport processes in stomach could be handled by something similar to Fick's diffusion law and that Nernst-Planck formulae for electrical potential were applicable, has encouraged us to proceed further with the studies of (a) the parchment supported membranes[2-9] and (b) the asymmetric polymeric membranes[10-14] which mimic some of the properties of nerve cells[15,16] as models for biological system.

This paper deals with the studies of diffusion rate of biologically important electrolytes through parchment supported membranes. The results are discussed in the light of Eisenman-Sherry field strength model[17-20] and the theory of absolute reaction rates.[21-23]

Experimental

The parchment supported membranes of (i) silver (ii) cadmium hexacyanoferrate(II) and (iii) barium phosphate were prepared by the method of interaction described by Siddiqi *et al.*[4,9] In order to precipitate these substances in the interstices of the parchment paper, 0.2 M solution of potassium hexacyanoferrate(II) was kept inside a glass tube to one end of which was tied the parchment paper. This was suspended for 72 h in a 0.2 M solution of silver nitrate or cadmium chloride (for hexacyanoferrate(II) membranes). The two solutions were interchanged later and kept for another 72 h. A similar procedure was adopted for the preparation of barium phosphate membrane by taking 0.5 M solutions of barium chloride and potassium di-hydrogen orthophosphate. The membranes thus prepared were washed with deionized water for removal of free electrolytes.

The apparatus and procedures to measure membrane potential E_m, membrane resistance R_m, and electrolyte concentrations were described by siddiqi *et al.*[2] The membrane was held between two half cells, each containing 125 ml of the electrolyte solution. Initially the concentrations C_1 and C_2 were 0.001 and 0.1 M, respectively. Each of the half cell was fitted with two platinized platinum electrodes firmly fixed to follow concentration changes and two anion reversible Ag–AgCl electrodes-one a disc type to pass a small d. c. current and the other a J-shaped wire electrode placed 1.7 cm apart from the membrane surface to measure membrane potential (Pye precision potentiometer No. 7568) and changes in membrane potential following current flow. The solutions in both the half cells were kept well stirred by magnetic stirrers. The whole cell assembly was immersed in a water thermostat maintained at 10, 15, 20, 25, and 30 °C (±0.1 °C).

Conductance changes on the dilute solution side was followed by means of the conductivity bridge (Cambridge Instrument Co. England No L-350140). The exact concentration of the solution at any given time was estimated from a calibration curve. The membrane resistance was determined by applying an external emf to the disc-type Ag–AgCl electrodes and measuring the change in potential across the membrane using J-type wire electrodes. The current passed through the membrane system was determined by measuring IR drop across a precision kilo-ohm resistor. The current was kept very low in order to minimize the ion transfer during the period (2—3 min) required for each resistance measurement. The direction of current flow was reversed in each successive measurement. The resistance measurements gave a value for the system electrolyte solution (R_e')-Membrane (R_m)-electrolyte solution (R_e''). In order to measure R_m directly, the wire electrodes should be placed strictly on the membrane surfaces. When this was done, resistance values were not reproducible This procedure was therefore abondoned in favor of the former and corrections for the electrolyte resistances R_e' and R_e'' were applied to derive a value for R_m. Since the geometry of the system (area=24.6 cm² and the distance at which wire electrode was placed from the membrane face = 1.7 cm) and the specific conductance of the electrolyte solutions were known accurately (better than 0.5%), the sum $(R_e'+R_e'')$ can be computed easily. Thus R_m, the membrane resistance only, can be derived as the difference between the measured total resistance and the sum of the

calculated electrolyte resistances ($R_e' + R_e''$). Although the membrane potential could be measured to a better accuracy than $\pm 1\%$, the estimation of membrane resistance was accurate to $\pm 3\%$.

Results and Discussion

The transport phenomena are often described by some extended form of the Nernst-Planck flux equation.[24] Evaluation of flows requires integration of these flux equations under suitable boundary conditions governing the behavior of the membrane system. Some time ago, Kittelberger[25] from the simple laws of electrolysis, developed the equation

$$\frac{dQ_+}{dt} = \frac{1}{Z_+ FR_m}\left[\frac{RT}{Z_+F}\ln\frac{a_2}{a_1} - E_m\right] \times\left[\left(\frac{Z_+Z_-}{Z_+ + Z_-}\right)\left(\frac{E_m}{\frac{RT}{F}\ln\frac{a_2}{a_1}}\right) + \frac{Z_+}{Z_+ + Z_-}\right] \quad (1)$$

where Q_+ is the milli-equivalents of cations diffusing in time t s, Z_+, Z_- are the valencies of cation and anion, respectively, R_m is the resistance in ohm of the membrane, E_m is the membrane potential in millivolts, a_1 and a_2 are the activities of the two electrolyte solutions on either side of the membrane, R, T, and F have their usual meanings to describe the rate of flow of a charged species or electrolyte through a membrane.

$$\frac{Z_+Z_-}{Z_+ + Z_-}\frac{E_m}{\frac{RT}{F}\ln\frac{a_2}{a_1}} + \frac{Z_+}{Z_+ + Z_-} \quad (2)$$

is the cation transport number expressed in terms of observed membrane potential E_m. The term

$$\frac{RT}{Z_+F}\ln\frac{a_2}{a_1} - E_m \quad (3)$$

is the effective potential acting on the ion.

The emf measured across the membrane using the J-type Ag-AgCl electrodes is made up of two components, the electrode potential difference E_e due to the Ag-AgCl electrodes existing in the two chloride solutions of different activity a_1 and a_2, and the membrane potential E_m arising across the membrane due to flow of electrolyte through it. E_e is given by the equation

$$E_e = \frac{RT}{Z-F}\ln\frac{C_2\nu_2}{C_1\nu_1} \quad (4)$$

where ν's are the activity coefficients of the electrolyte solutions. Since $(E_e + E_m)$ is measured directly, E_m can be evaluated by substraction.

Changes in E_m and R_m with time are shown in Figs. 1 and 2 for various electrolytes diffusing through a cadmium hexacyanoferrate(II) membrane. At any given time, the membrane resistance R_m increases in the order; KCl, NaCl, LiCl, for electrolytes (1:1), $CaCl_2$, $MgCl_2$, $BaCl_2$ for electrolytes (2:1), and electrolyte (3:1) $AlCl_3$ produces the highest value for R_m.

E_m values for the various electrolytes display a very interesting phenomenon. In the case of (1:1) electrolytes, the values are all positive (dilute solution side C_1 taken as positive) indicating thereby that the membrane is cation selective. In the case of (2:1) and (3:1) electrolytes, E_m changes sign. This indicates that the

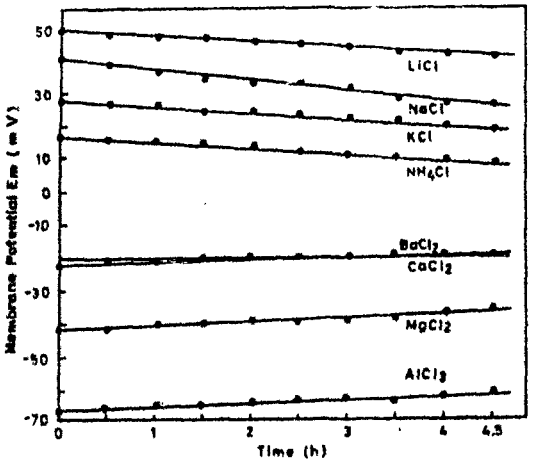

Fig. 1. Plots of membrane potential E_m against time for various electrolytes with cadmium hexacyanoferrate(II).

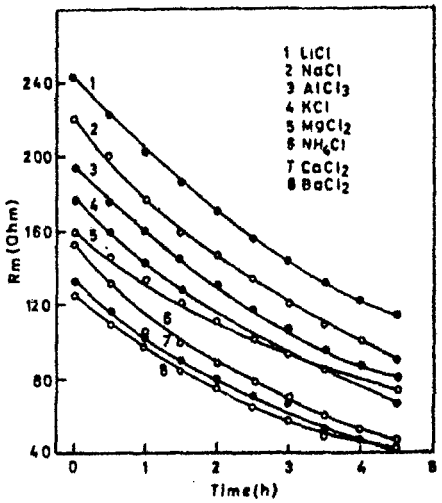

Fig. 2. Plots of R_m against time for various electrolytes with cadmium hexacyanoferrate(II).

membrane has become anion selective. The change in the selectivity character of the membrane is evidently due to adsorption of multivalent ions leading to a state where a net positive charge is left on the membrane surface taking it anion selective. Adsorption of Al^{3+} makes the membrane more anion selective than it is with the adsorption of other divalent cations. Such behavior seems to be observed with a number of other systems.[26-28]

The surface charge reversal occurred in every one of the membranes and electrolytes (2:1) and (3:1) and can be seen in the results given in Table 1 (a, b). E_m and R_m values are recorded.

With the help of Eq. 1, the rate at which various electrolytes diffuse through the membranes can be calculated. For electrolyte (1:1), ($Z_+ = Z_- = 1$), Eq. 1 becomes

$$\frac{dQ_+}{dt} = \frac{dQ_-}{dt} = \frac{dQ}{dt} = \frac{1}{2FR_m}\left[59.16\log\frac{C_2\nu_2}{C_1\nu_1} - E_m\right] \times\left[\frac{E_m}{59.16\log\frac{C_2\nu_2}{C_1\nu_1}} + 1\right] \quad (5)$$

For electrolyte (2:1), ($Z_+ = 2$ and $Z_- = 1$), it becomes

Table 1(a). Values of membrane potential E_m, membrane resistance R_m, and diffusion rate D_r at the end of 1/2 and 4 h periods at 25 °C[a]

Membrane	Silver Hexacyanoferrate(II)						Cadmium hexacyanoferrate(II)					
Thickness	0.0381 cm						0.0279 cm					
Electrolyte	E_m (mV)		R_m (ohm)		D_r (μ mol/h)		E_m (mV)		R_m (ohm)		D_r (μ mol/h)	
	1/2 h	4 h	1/2 h	4 h	1/2 h	4 h	1/2 h	4 h	1/2 h	4 h	1/2 h	4 h
LiCl	77.5	61.4	260	143	3.7	6.3	47.5	43.0	223	123	7.0	9.2
NaCl	70.0	52.0	231	127	5.1	9.0	39.0	28.0	200	100	8.2	15.3
KCl	63.7	44.1	214	114	6.3	12.6	26.5	20.0	160	70	11.5	17.5
NH_4Cl	—	—	—	—	—	—	16.6	10.6	133	53	16.0	26.3
$BaCl_2$	−1.5	−20.9	117	55.5	5.0	8.5	−21.5	−17.3	118	50	6.3	11.5
$CaCl_2$	−11.6	−31.0	134	73.5	4.8	6.6	−21.6	−19.6	117	49	6.0	9.2
$MgCl_2$	−35.0	−40.4	181	108	4.0	5.0	−41.9	−35.0	147	79	5.0	6.3
$AlCl_3$	−67.4	−75.0	226	140	0.8	0.5	−65.6	−61.5	177	87	1.5	2.8

a) Area of membrane=24.6 cm².

Table 1(b). Values of membrane potential E_m, membrane resistance R_m, and diffusion rate D_r at the end of 1/2 and 3 h periods at 25 °C[a]

Membrane	Barium phosphate					
Thickness	0.03612 cm					
Electrolyte	E_m (mV)		R_m (ohm)		D_r (μ mol/h)	
	1/2 h	3 h	1/2 h	3 h	1/2 h	3 h
KCl	12.72	7.10	155.0	55.0	10.483	22.70
NaCl	4.53	−0.73	180.2	84.0	7.894	15.624
LiCl	3.12	0.60	221.1	136.0	7.107	9.493

a) Area of membrane=24.6 cm².

$$\frac{dQ_+}{dt} = \frac{1}{2}\frac{dQ_-}{dt} = \frac{dQ}{dt} = \frac{1}{3FR_m}\left[29.58 \log \frac{C_2\nu_2}{C_1\nu_1} - E_m\right] \times \left[\frac{-E_m}{59.16 \log \frac{C_2\nu_2}{C_1\nu_1}} + 1\right] \quad (6)$$

For electrolyte (3: 1), ($Z_+=3$ and $Z_-=1$), it becomes

$$\frac{dQ_+}{dt} = \frac{1}{3}\frac{dQ_-}{dt} = \frac{dQ}{dt} = \frac{1}{4FR_m}\left[19.72 \log \frac{C_2\nu_2}{C_1\nu_1} - E_m\right] \times \left[\frac{-E_m}{59.16 \log \frac{C_2\nu_2}{C_1\nu_1}} + 1\right] \quad (7)$$

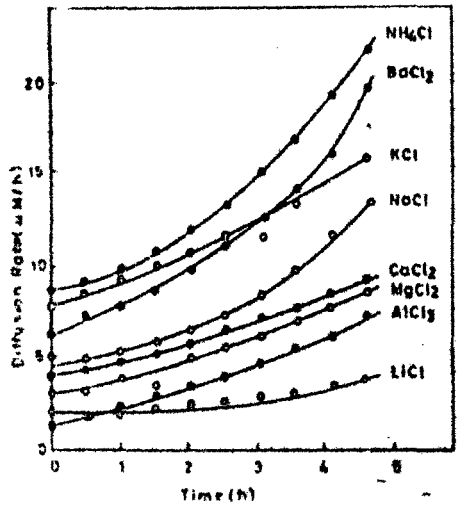

Fig. 3. Plots of diffusion rate *vs.* time through ...m hexacyanoferrate(II).

The electrolyte fluxes dQ/dt *i.e.* D_r calculated from Eqs. 5—7 for various electrolytes at 25 °C are given in Table 1 for all the three membranes. The reproducibility of the results were within ±3% at a certain temperature. The changes in R_m, E_m, and D_r with time for cadmium hexacyanoferrate(II) membrane are shown in Figs. 1—3, while comparative values for various cations are given in Fig. 3a.

The diffusion rate derived from the electrometrically or conductometrically determined changes in the salt concentration of the test solution C_1 is called "observed diffusion rate," while the values computed from the measured concentration potential and electrolytic resistance of the membrane *i.e.* from Eqs. 5—7 is designated the "computed" diffusion rate. The "computed" and "observed" diffusion rates of KCl, NaCl, LiCl for barium phosphate membrane are shown in Fig. 4a. For

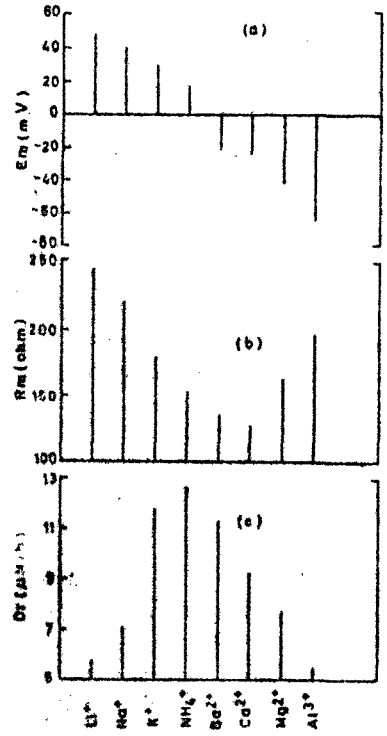

Fig. 3a. Plots of E_m, R_m, and D_r against the various electrolytes for cadmium hexacyanoferrate(II).

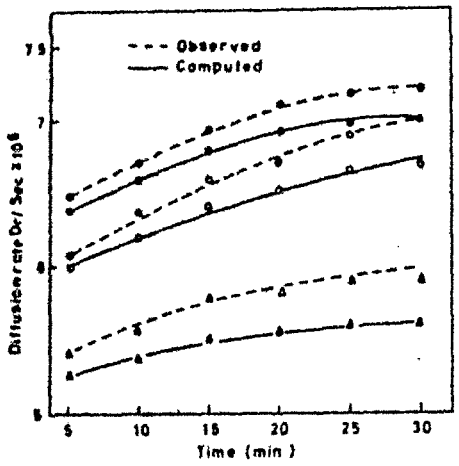

Fig. 4a. Plots of observed and computed diffusion rate against time for ●: KCl, ○: NaCl, and △: LiCl with barium phosphate membrane.

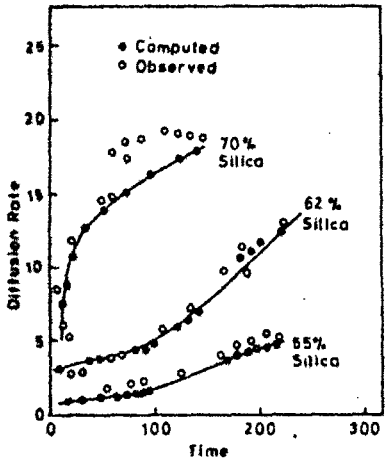

Fig. 4b. Plots of observed and computed diffusion rate against time for hydrochloric acid through polyvinyl butyral membrane.

the sake of comparison the rates of diffusion of hydrochloric acid through poly (vinyl butyral) membranes obtained by Kittelberger[28] are also given in Fig. 4b. Agreement is fair in both cases.

The diffusion of the electrolyte through the membrane is slower than in free solution. The order does not remain the same due to various reasons; (a) only a part of the frame work is available for free diffusion, (b) the diffusion paths in the membrane phase are more tortuous and therefore longer (*i.e.* the tortuousity factor), (c) the large hydrated ions in the narrow mesh region of the membrane might be impeded in their mobility by the frame work and (d) the interaction of the diffusing species with the fixed groups on the membrane matrix. Parchment paper, except for the presence of some stray and end carboxyl groups, contains very few fixed groups. Deposition of inorganic precipitate gives rise to a net negative charge on the membrane surface in the case of electrolyte (1: 1) leading to the type of ionic distribution associated with the electrical double layer. However, use of electrolyte (2: 1) or (3: 1) leaves a net positive charge on the membrane and results in the formation of the electrical double layer. The system is considered as having charged capillary structures or gels which can be judged in the light of classical fixed charge theory of Teorell,[29] Meyer and Sievers,[30] Sollner,[31] Gregor,[32] and Schmid.[33,34] Flow of electrolyte by diffusion because of the presence of a net charge ($-ve$ or $+ve$) on the membrane gives rise to the membrane potential as opposed to the liquid junction potential ordinarily observed under similar conditions in the absence of the membrane, which regulates the flow of electrolyte by increasing the speed of slow moving ion and by decreasing the speed of the faster moving ion. The regulated rate of flow (*i.e.* diffusion) measured for different electrolytes through the investigated membranes follow the sequence: $NH_4^+ > K^+ > Na^+ > Li^+$ and $Ba^{2+} > Ca^{2+} > Mg^{2+} > Al^{3+}$.

Depending on the size and electrical charge pattern of a pore, it may either admit or repel a solute particle. This is the basis of ion selectivity. Mullins[35] proposed that the hydration of the materials of the pores themselves may provide a favorable water environment for particular ions or molecules, so that they slip into the pores away from their previous water molecules. This could result in selection of a particular size with discrimination against both smaller and larger hydrated ions. In order to obtain a quantitative relation between the ease of penetration and the ion size, it is necessary to know the electrostatic force which acts between the ions and the material of the membranes, since this force provides energy to displace water of hydration. Eisenman *et al.*[17-19] pointed out that the order of the ease of penetration of cations depends on the energy available from the ion-fixed charge interaction. From a simplified model, in which field strength was taken as a controlling variable, the Coulomb energies of interaction of alkali cations with the charged sites were compared with the free energy of hydration of cations. A simplified theory of selectivity for four alkaline earths (Mg^{2+}, Ca^{2+}, Sr^{2+}, and Ba^{2+}) in a cation exchange membrane has been worked out by Sherry.[20] Specificity is determined by the difference between the free energy of hydration of

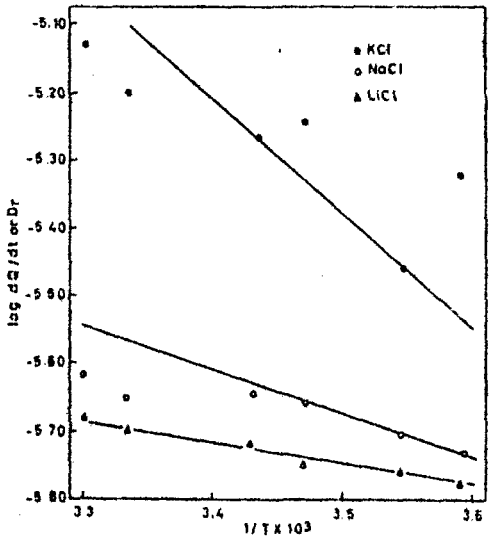

Fig. 5. Plots of log D_r *vs.* $1/T$ for different electrolytes with barium phosphate membrane.

Table 2(a). Experimental activation energy E_a and other thermodynamic parameters calculated from transition state theory of rate processes for various electrolytes diffusion, through membrane (Temperature=25 °C)

Membrane	Silver hexacyanoferrate(II)				Cadmium hexacyanoferrate(II)			
Electrolyte	E_a kcal mol^{-1}	ΔH^* kcal mol^{-1}	ΔF^* kcal mol^{-1}	ΔS^* e.u.	E_a kcal mol^{-1}	ΔH^* kcal mol^{-1}	ΔF^* kcal mol^{-1}	ΔS^* e.u.
LiCl	5.53	4.94	8.80	−13.0	6.36	5.77	8.79	−10.1
NaCl	5.97	5.38	8.85	−11.6	7.15	6.37	8.68	− 7.9
KCl	6.26	5.67	8.81	−10.5	7.50	6.95	8.58	− 5.8
NH_4Cl	—	—	—	—	7.65	7.06	8.56	− 5.1
$BaCl_2$	4.24	3.65	8.85	−17.5	4.61	4.02	8.95	−16.5
$CaCl_2$	3.68	3.09	9.90	−19.8	4.24	3.65	9.11	−18.3
$MgCl_2$	3.96	3.37	9.13	−19.4	4.61	4.02	9.25	−17.6
$AlCl_3$	3.41	2.82	9.72	−23.1	3.32	2.73	9.86	−23.9

Table 2(b). Experimental activation energy E_a and other thermodynamic parameters calculated from transition state theory of rate processes for various electrolytes diffusion, through membrane (Temperature=25 °C)

Membrane	Barium phosphate			
Electrolyte	E_a kcal mol^{-1}	ΔH^* kcal mol^{-1}	ΔF^* kcal mol^{-1}	ΔS^* e.u.
KCl	5.45	4.84	7.83	−10
NaCl	4.21	3.61	8.08	−15
LiCl	3.09	2.50	9.06	−22

alkaline earth cations and their Coulomb energies of interaction with the negatively charged sites. On the basis of Eisenman-Sherry theory,[17-20] the diffusion rate sequence obtained with the investigated membranes point towards the weak field strength of charged groups.

The theory of absolute reaction rates[21-25] has been applied to diffusion processes in membranes by several investigators.[23-29] According to Laidler *et al.*[22-25] the integral diffusion coefficient D is given by the expression

$$D = Ae^{-E_a/RT} \tag{8}$$

where E_a is the observed activation energy for diffusion and A is the frequency factor. Thus, if log D is plotted against $1/T$, the slope gives (Fig. 5) the value of energy of activation for the diffusion process. These values of E_a were determined for a number of electrolytes and with all the three membranes, and are given in Tables 2 (a, b).

According to Zwolinski *et al.*,[21] we have

$$D = \lambda^2\left(\frac{KT}{h}\right)\exp(\Delta S^*/R)\exp\left(\frac{-\Delta H^*}{RT}\right) \tag{9}$$

where λ is the distance between successive equilibrium positions of diffusing species, ΔS^* the entropy of activation, ΔH^* the enthalpy of activation, k, h, R, and T having their usual meanings.

The Eyring enthalpy of activation ΔH^* is calculated from the activation energy E_a (previously determined) by means of the relation

$$\Delta H^* = E_a - RT \tag{10}$$

Assuming λ to be equal to 3 Å for different electrolytes (values 1—5 Å for λ have been used by different investigators) and substituting the value of diffusion coefficient D, the value of ΔS^* has been calculated. The free energy of activation ΔF^* is then calculated by the Gibbs-Helmholtz equation

$$\Delta F^* = \Delta H^* - T\Delta S^* \tag{11}$$

The values so derived for the different thermodynamic parameters are given in Tables 2 (a, b).

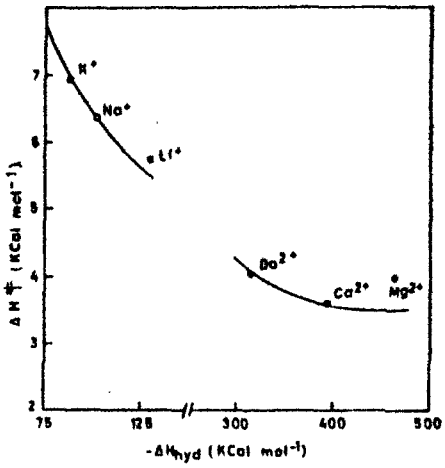

Fig. 6a. Plots of ΔH^* for the diffusion of various electrolytes (at 25 °C) against $-\Delta H_{hyd}$ for the respective cations through cadmium hexacyanoferrate(II).

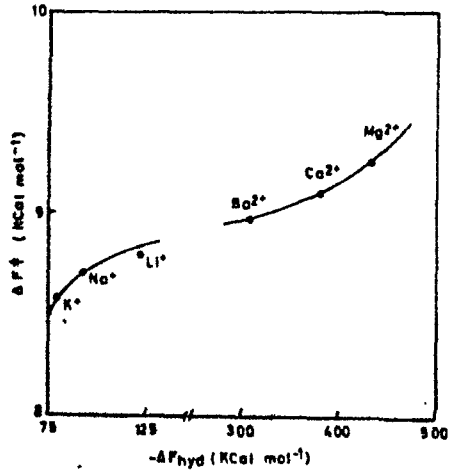

Fig. 6b. Plots of ΔF^* for the diffusion of various electrolytes (at 25 °C) against $-\Delta F_{hyd}$ for the respective cations through cadmium hexacyanoferrate(II).

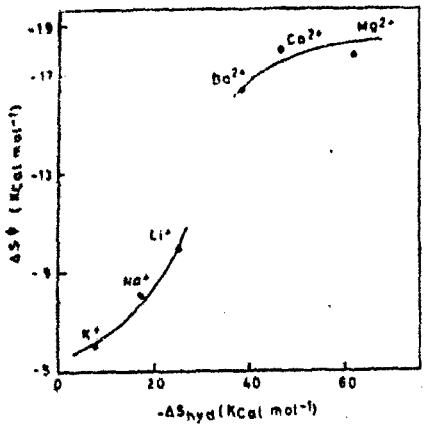

Fig. 6c. Plots of ΔS^* for the diffusion of various electrolytes (at 25 °C) against $-\Delta S_{hyd}$ for the respective cations through cadmium hexacyanoferrate(II).

The results indicate that electrolyte permeation gives rise to negative values of ΔS^*. The values of ΔS^* for all the three membranes show a similar behavior for different electrolytes. With increase in valence of the individual ion, the decrease in the values of ΔS^* is enhanced. It is believed that the membrane and not the solution-membrane interface controls the electrolyte diffusion process. The negative values of ΔS^* as suggested by Schular *et al.*[23] indicate electrolyte diffusion with partial immobilization in the membrane, the relative partial immobility increasing with increase in the valence of ions constituting the electrolyte. In Fig. 6 (a, b, c) the individual ionic contribution to the properties of aqueous ions given by Noyes[40] namely $\Delta H_{hydration}$, $\Delta F_{hydration}$, and $\Delta S_{hydration}$, of Li^+, Na^+, K^+, as well as those of Ba^{2+}, Ca^{2+}, and Mg^{2+} are plotted against the corresponding ΔH^*, ΔF^*, and ΔS^* values for diffusion through the membrane. It is found that at least some formal relationship exists between these thermodynamic parameters.

The authors are grateful to Prof. Wasiur Rahman, Head of Department of Chemistry, for providing research facilities and to C.S.I.R. (India) for financial assistance to A. H. and S. P. S.

References

1) T. Teorell in "Membrane Phenomena," *Discuss. Faraday Soc.*, **21**, 9 (1956).
2) F. A. Siddiqi and S. Pratap, *J. Electroanal. Chem.*, **23**, 137, 147 (1969).
3) F. A. Siddiqi, N. Lakshminarayanaiah, and S. K. Saksena, *Z. Phys. Chem., (Frankfurt)*, **72**, 298, 307 (1970).
4) F. A. Siddiqi, N. Lakshminarayanaiah, and M. N. Beg, *J. Polym. Sci.*, **9**, 2868 (1971).
5) F. A. Siddiqi, M. N. Beg, and S. P. Singh, *J. Polym. Sci.*, in press.
6) F. A. Siddiqi, M. N. Beg, and P. Prakash, *J. Electroanal. Chem.*, in press.
7) W. U. Malik and F. A. Siddiqi, *Proc. Indian Acad. Sci.*, **A56**, 206 (1962).
8) W. U. Malik and F. A. Siddiqi, *J. Colloid Sci.*, **18**, 161 (1963).
9) W. U. Malik, H. Arif, and F. A. Siddiqi, *Bull. Chem. Soc., Jpn.*, **40**, 1741 (1967).
10) N. Lakshminarayanaiah and F. A. Siddiqi, *Biophys. J.*, **11**, 603, 617 (1971).
11) N. Lakshminarayanaiah and F. A. Siddiqi, *Biophys. J.*, **12**, 540 (1972).
12) N. Lakshminarayanaiah and F. A. Siddiqi in "Membrane Processes in Industry and Biomedicine," ed. by M. Bier, Plenum Publishing Corporation, New York (1971).
13) N. Lakshminarayanaiah and F. A. Siddiqi, *J. Polym. Sci.*, **8**, 2949 (1970).
14) N. Lakshminarayanaiah and F. A. Siddiqi, *Z. Phys. Chem., (Frankfurt)*, **78**, 150 (1972).
15) A. M. Liquori and C. Botre, *Ric. Sci.*, **34**, 6 (1964).
16) A. M. Liquori and C. Botre, *J. Phys. Chem.*, **71**, 3765, (1967).
17) G. Eisenman in "Membrane Transport and Metabolism," ed. by A. Kleinzeller and A. Kobyk, Academic Press, New York (1961).
18) G. Eisenman, "The Glass Electrode," Interscience Publishers, Inc., New York (1965).
19) G. Eisenman, *Biophys. J.*, **2**, 259 (1962).
20) H. Sherry in "Ion Exchange," Vol. 2, ed. by J. A. Marinsky, Dekker, New York (1968).
21) B. J. Zwolinski, H. Eyring, and C. E. Reese, *J. Phys. Chem.*, **53**, 1426 (1949).
22) S. Glasston, K. J. Laidler, and H. Eyring, "The Theory of Rate Processes," McGraw-Hill, New York (1941).
23) E. K. Shuller, C. A. Dames, and K. J. Laidler, *J. Chem. Phys.*, **17**, 860 (1949).
24) R. Schlögl, "Estofftransport durch Membranen," Steinkopff, Darmstadt (1964); *Ber. Bunsenges Phys. Chem.*, **70**, 400 (1966).
25) W. W. Kittelberger, *J. Phys. Colloid Chem.*, **53**, 392 (1949).
26) N. W. Rosenberg, J. H. B. George, and W. D. Potter, *J. Electrochem. Soc.*, **104**, 111 (1957).
27) N. Lakshminarayanaiah, *J. Electrochem. Soc.*, **116**, 338 (1969).
28) G. Schulz, *Z. Anorg. Allgem. Chem.*, **301**, 97 (1959).
29) T. Teorell, *Proc. Soc. Exptl. Biol.*, **33**, 282 (1935); *Proc. Natl. Acad. Sci., (U.S.A.)*, **21**, 152 (1935); *Progr. Biophys. Chem.*, **3**, 305 (1953).
30) K. H. Meyer and J. F. Sievers, *Helv. Chim. Acta*, **19**, 649, 665, 987 (1936).
31) K. Sollner, *J. Phys. Chem.*, **49**, 47 171 (1945); *J. Electrochem. Soc.*, **97**, 139C (1950); *Ann. N. Y. Acad. Sci.*, **57**, 177 (1953).
32) H. P. Gregor, *J. Am. Chem. Soc.*, **70**, 1293 (1948); *ibid.*, **73**, 642 (1950).
33) G. Schmid, *Z. Elektrochem.*, **54**, 424 (1950); *ibid.*, **55**, 229 (1951); *ibid.*, **56**, 181 (1952).
34) G. Schmid and H. Schwarz, *Z. Elektrochem.*, **55**, 295 (1951); *ibid.*, **55**, 684 (1951); *ibid.*, **56**, 35 (1952).
35) L. J. Mullins in "Transport and Accumulation in Biological Systems," ed. by E. J. Harris, Butterworths Scientific Publication, London (1960).
36) H. T. Tien and H. P. Ting, *J. Colloid Interface Sci.*, **27** 702 (1968).
37) R. M. Barrer, *Trans. Faraday Soc.*, **38**, 322 (1942).
38) R. M. Barrer and G. Skirrow, *J. Polymer Sci.*, **3**, 549 (1948).
39) R. M. Barrer and H. T. Chio, in "Transport Phenomena in Polymeric Films," ed. by C. A. Kumins, Interscience, New York (1965).
40) R. M. Noyes, *J. Am. Chem. Soc.*, **84**, 513 (1962).

JOURNAL OF POLYMER SCIENCE: Polymer Chemistry Edition VOL. 15, 1935–1956 (1977)

Studies with Model Membranes. IX. Evaluation of Thermodynamic Parameters from the Transition State Theory of Rate Processes for Electrolyte Diffusion through Silver Chloride Parchment-Supported Membranes

FASIH A. SIDDIQI, SANTOSH K. SAKSENA, and IBADUR RAHMAN KHAN, *Division of Physical Chemistry, Department of Chemistry, Aligarh Muslim University, Aligarh, U.P. India*

Synopsis

Diffusion rate of biologically important electrolytes through parchment-supported silver chloride membrane have been determined by the use of Nernst-Planck equation at various temperatures taking into account membrane resistance R_m, membrane potential E_m, etc. The diffusion rates were found to be primarily dependent upon the difference in the hydration energies of the counterion in the external solution. On the basis of Eisenman-Sherry theory the diffusion rate sequence of alkali metal cations point towards the weak field strengths of the fixed charge groups. The various thermodynamic parameters, namely, $\Delta H^{\ddagger}$, $\Delta F^{\ddagger}$, and $\Delta S^{\ddagger}$ were evaluated. The values of $\Delta S^{\ddagger}$ found to be negative, indicating that the diffusion is taking place with partial immobilization in the membrane phase. A formal relation between $\Delta H_{\text{hydration}}$, $\Delta F_{\text{hydration}}$, and $\Delta S_{\text{hydration}}$ of cations with the corresponding values of $\Delta H^{\ddagger}$, $\Delta F^{\ddagger}$, and $\Delta S^{\ddagger}$ for diffusion was also found to exist for the investigated system.

In order to understand the behavior of complex cell membranes, we have been engaged for quite some time in developing a complex artificial system of membranes, namely, parchment-supported membranes,[1-9] which in some formal aspect at least behave like gastric mucosal membranes,[10] and asymmetric composite polymeric membranes,[11-16] which mimic some of the properties of nerve cells.[17,18]

Theories of membrane behavior, particularly those of complex ones, have been discussed by Kedem and Katchalsky[19] in a series of theoretical papers. The various theories according to Schlogl[20] may be roughly divided into three groups, depending on the nature of the flux equation used in the treatment. Older theories or their modern refinements based on the Nernst-Planck flux equation, fall into one group. A second group comprises the theories which use the principle of irreversible thermodynamics. The third group is made up of those theories which utilize the concepts of the theory of rate processes. These have been reviewed in a number of monographs, particularly that of Lakshminarayanaih.[21]

This series of communications deals with studies of diffusion rates of biologically important electrolytes through silver chloride parchment-supported

membrane; Kittelberger's equation,[22] found suitable for both the "paint type" and parchment-supported membranes,[1,2] is used. The results are discussed in the light of the views put forward by Sollner,[23-25] Gregor,[26,27] Schmid,[29] and Hellferich.[30] The field-strength model of Eisenman[31-33] and Sherry[34] and the theory of absolute reaction rates have also been applied in explaining various aspects, particularly those of hydrated ionic size and the energetics of hydration of the permeating species.

EXPERIMENTAL

The silver chloride parchment-supported membrane was prepared by the method of interaction suggested by Weiser.[35] First, parchment paper was soaked in distilled water for 2 hr and then tied carefully to the flat mouth of a beaker containing 0.2*M* $AgNO_3$ solution. This was suspended for about 72 hr in a 0.2*M* solution of potassium chloride. The two solutions were interchanged and kept for another 72 hr. The silver chloride membrane thus prepared was washed with deionized water for removal of free electrolyte. The apparatus and procedures used to measure membrane potential, resistance, and electrolyte concentrations are those described by Siddiqi et al.[1,2] The capacity of each of the two half cells holding the membrane was about 130 ml. A known volume of each of the two test solutions (approximately 125 ml of each) was introduced and conductivity cell electrodes fixed in place. An assembly with magnetic stirrers in each half cell was placed in a thermostat maintained at 25 ± 0.1°C. The actual experimental procedure was to set up the cell with membrane and silver–silver chloride electrode (both J-shaped as well as disk electrodes). The solutions in both the half cells were kept well stirred by using magnetic stirrers. Various salt solutions (chlorides of Li^+, Na^+, K^+, Ca^{2+}, Ba^{2+}, Mg^{+2}, and Al^{3+}) were prepared from BDH analytical-grade chemicals with deionized water. They were normally 0.1*M* and 0.001*M* in the two half cells initially. No appreciable change in 0.1*M* electrolyte concentration was observed (within an interval of 4–5 hr), and we thus assumed this concentration to be practically unchanged.

When once the cell was set up; the experimental procedure was to follow the conductance change on either side of the membrane with time. On the high-concentration side (0.1*M*), it was found that in the time period (about 5 hr) the experiment ran, there was no significant change in conductance of the solution. It was therefore assumed that the concentration of this side remained constant and only the conductance change on the dilute solution side was followed with time on the conductivity bridge. The exact concentration of the solution at any given time was estimated from a calibration curve where conductance was recorded against concentration. J-type wire electrodes connected to a Pye precision vernier potentiometer monitored the membrane potential with time. The membrane resistance was determined by applying an external emf to disk-type Ag–AgCl electrodes and measuring the change in potential across the membrane using the J-type wire electrodes. The current passed through the membrane system was determined by measuring the IR drop across a precision Kilo-ohm resistor. The current was kept very low to minimize ion transfer during the period (about 2–3 min) required for each resistance measurement. The direction of current flows was reversed in each successive measurement.

The diffusion cell used in these studies was such that J-type wire electrodes

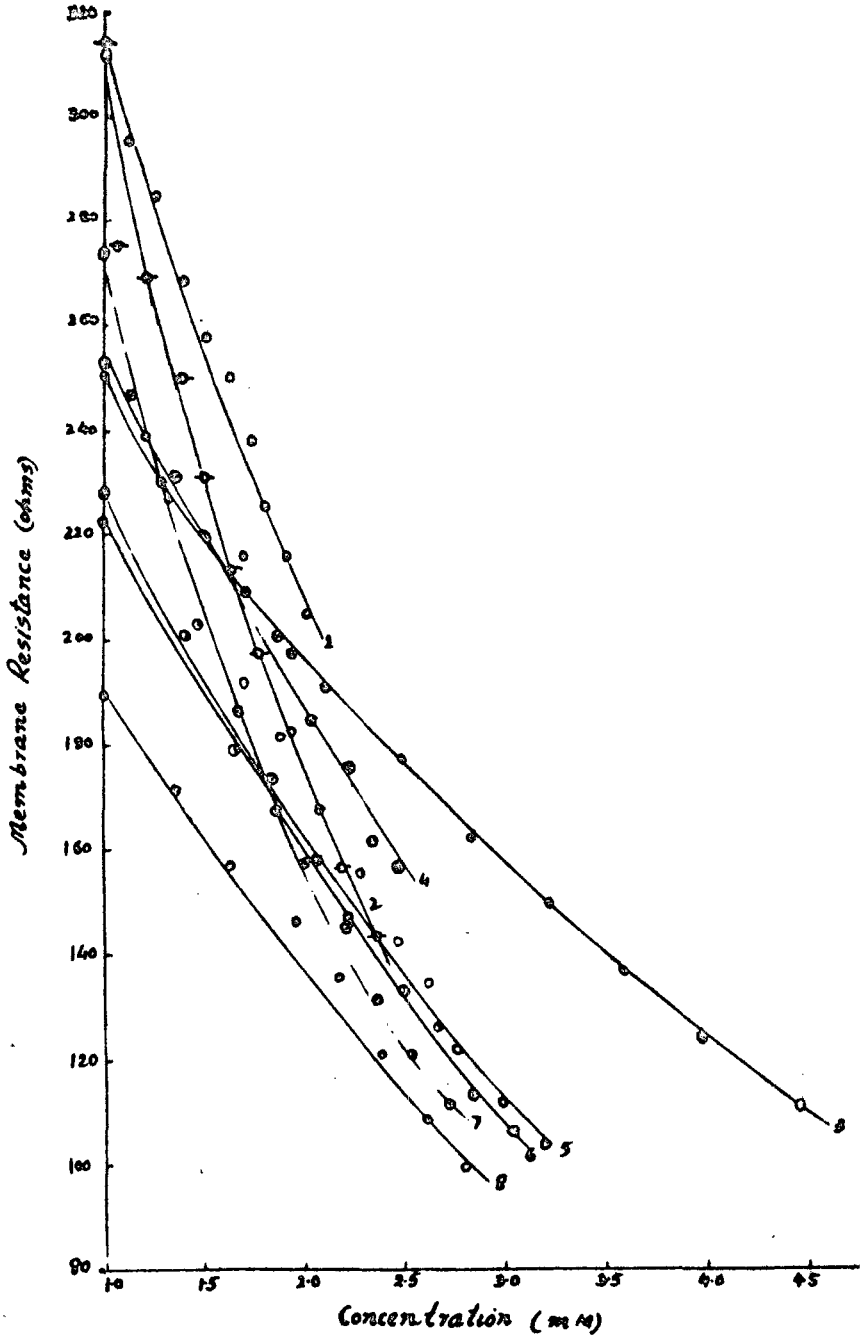

Fig. 1. Plots of membrane resistance R_m against concentrations for various electrolytes across a silver chloride membrane: (*1*), $AlCl_3$; (2) LiCl; (*3*) KCl; (*4*) $BaCl_2$; (5) $MgCl_2$; (6) $SrCl_2$; (7) NaCl; (*8*) $CaCl_2$.

fixed vertically parallel to the membrane faces were each 1.7 cm away from the membrane faces. Consequently, the resistance measurements gave a value for the system electrolyte solution (R_e')-membrane (R_m)-electrolyte solution (R_e'').

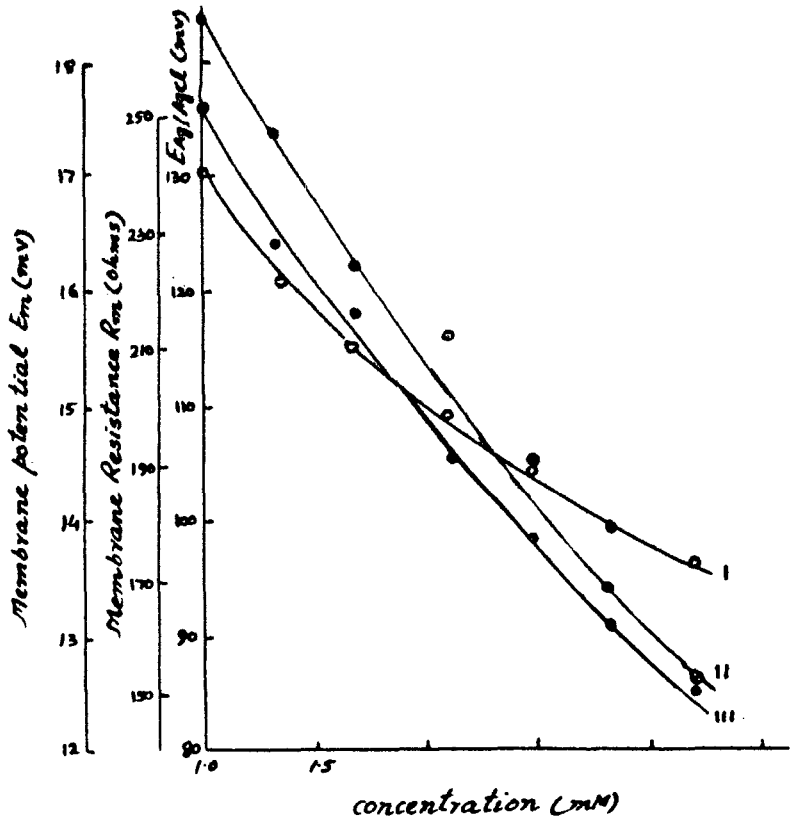

Fig. 2. Values of (*I*) $E_{Ag/AgCl}$; (*II*) E_m, and (*III*) R_m plotted against concentration for KCl across a silver chloride membrane; 1:1 electrolyte.

To measure R_m directly, the wire electrodes had to be placed strictly on the membrane faces. When this was done, resistance values were not reproducible. This procedure was therefore abandoned in favor of the former, and correction for the electrolyte resistances R_e' and R_e'' was applied to derive a value for R_m. Since the geometry of the system (area = 24.6 cm^2, distance of each wire electrode from the membrane face = 1.8 cm) and the specific conductance of the electrolyte solutions were known accurately (better than ± 0.5%), the sum $(R_e' + R_e'')$ can be computed easily. Thus R_m, the membrane resistance only, can be derived as the differences between the measured total resistance and the sum of the calculated electrolyte resistance $(R_e' + R_e'')$.

RESULTS AND DISCUSSION

When an ionic gradient is maintained using two solutions of different concentration of the same electrolyte on either side of the membrane, diffusion of the electrolyte from the region of high concentration takes place. There will be flow of water in the opposite direction. Besides, an electric field due to differences in the mobilities of cations and anions is established across the membrane. If the membrane contains a large number of groups, say negatively charged, the potential generated (dilute solution side positive) will be many times larger than

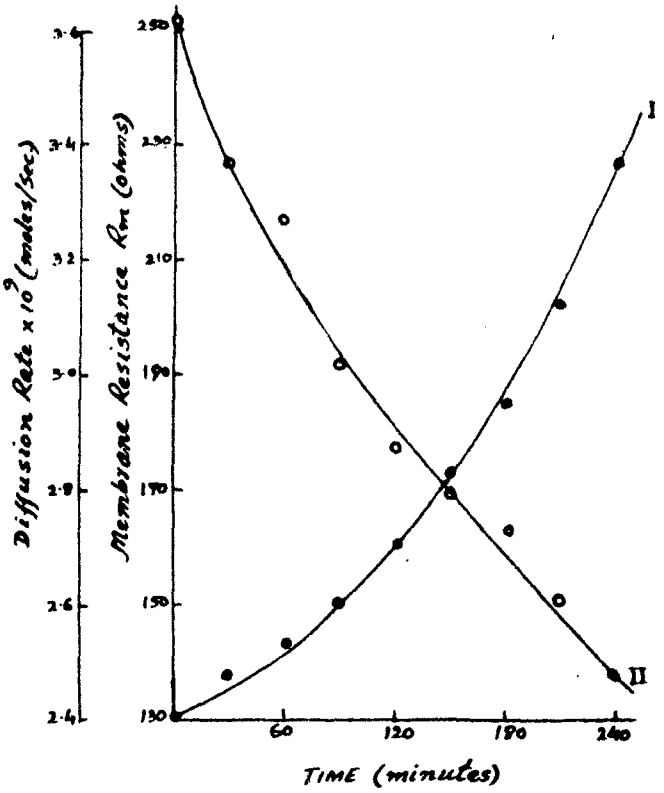

Fig. 3. Plots of (*I*) diffusion rate and (*II*) membrane resistance against time for KCl across a silver chloride membrane; 1:1 electrolyte.

the liquid junction potentials which are normally observed when the same two solutions are brought together with or without an "uncharged" membrane in between. These transport phenomena are often described by some extended form of Nernst-Planck flux equations.[36] Evaluation of flows requires integration of these flux equations under suitable boundary conditions governing the behavior of the membrane system. Sometime ago, Kittelberger[22] from the simple laws of electrolysis, developed eq. (1):

$$\frac{dQ_+}{dt} = \left(\frac{1}{Z_+FR_m}\right)\left[\frac{RT}{Z_+F}\ln\frac{a_2}{a_1} - E_m\right] \times \left[\frac{Z_+Z_-}{Z_+ + Z_-}\frac{E_m}{(RT/F)\ln(a_2/a_1)}\right] + \left[\frac{Z_+}{Z_+ + Z_-}\right] \quad (1)$$

where Q_+^* is the milliequivalents of the cation diffusing in time t (sec); Z_+, Z_- are the valences of the cation and anion respectively, R_m is the resistance (in ohms) of the membrane, E_m is the membrane potential (in millivolts), a_1 and a_2 are the activities of the two electrolyte solutions on either side of the membrane; R, T, and F have their usual significance. Equation (1) describes the rate of flow of a charged species or electrolyte through a membrane. The term

$$\left(\frac{Z_+Z_-}{Z_+ + Z_-}\right)\left[\frac{E_m}{(RT/F)\ln(a_2/a_1)}\right] + \left(\frac{Z_+}{Z_+ + Z_-}\right)$$

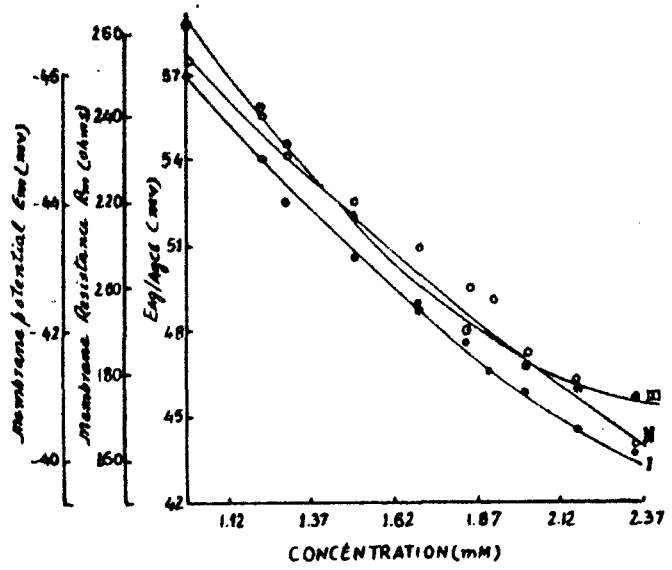

Fig. 4. Values of (*I*) $E_{Ag/AgCl}$; (*II*) E_m, and (*III*) R_m plotted against concentration for $BaCl_2$ across a silver chloride membrane; 2:1 electrolyte.

is the cation transport number expressed in terms of observed membrane potential E_m when electrolyte solutions of activity a_1 and a_2 exist on either side of the membrane. The term

$$[(RT/Z_+F) \ln (a_2/a_1) - E_m]$$

is the effective potential acting on the ion.

The emf measured across the membrane using the J-type Ag–AgCl electrode is made up of two components. The first is the electrode potential difference E_e due to the Ag–AgCl electrodes existing in two chloride solutions of different activity a_1 and a_2, and the second is due to the membrane potential E_m arising across the membrane due to flow of electrolyte through it. E_e is given by eq. (2):

$$E_e = (RT/Z_-F) \ln (C_2\nu_2/C_1\nu_1) \quad (2)$$

where the ν are the activity coefficients of the electrolyte solutions. Since Z_- is always unity and $C_1\nu_1$ (a_1) and $C_2\nu_2$ (a_2) are known, E_e can be computed. As ($E_e + E_m$) is measured directly, E_m can be evaluated by subtraction.

The changes in membrane resistance R_m against concentration for various electrolytes diffusing through silver chloride membranes are shown in Figure 1, while the changes in membrane potential E_m and membrane resistance R_m with concentration and diffusion rate and membrane resistance with time are shown in Figures 2–7 for 1:1, 2:1, and 3:1 electrolytes. At any given time, the membrane resistance R_m increases in the order KCl < NaCl < LiCl for 1:1 electrolytes, and $CaCl_2$ < $MgCl_2$ < $SrCl_2$ < $BaCl_2$ for 2:1 electrolytes; 3:1 electrolyte produces the highest value for R_m.

E_m values for the various electrolytes display a very interesting phenomenon. In case of 1:1 electrolytes, the values are all positive (dilute solution side C_1 taken

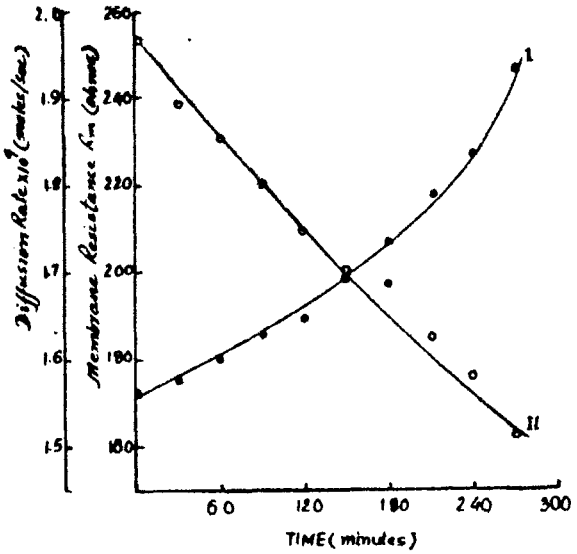

Fig. 5. Plots of (*I*) diffusion rate and (*II*) membrane resistance against time for $BaCl_2$ across a silver chloride membrane; 2:1 electrolyte.

as positive), indicating thereby that the membrane is cation-selective. In case of 2:1 and 3:1 electrolytes, E_m changes sign, as shown in Figure 8. This means that the membrane has become anion-selective. This change in the selectivity character of the membrane is evidently due to adsorption of multivalent ions leading to a state where a net positive charge is left on the membrane surface making it anion-selective. Adsorption of Al^{3+} makes the membrane more anion-selective than it is with the adsorption of either divalent cations. Such behavior seems to be a common phenomenon observed with a number of other systems. For example, Rosenberg et al.[37] found in the case of thorium counterions, negative electroosmotic transport of water. The ion was so strongly adsorbed on a cation-exchange membrane that it conferred anion selectivity to the membrane and thus water was transferred in the opposite direction, i.e., to the anode chamber instead of the normal flow which moves into the cathode chamber in the case of monovalent cations and cation-exchange membrane.[38] Similarly, Schulz[39] found, in the case of sodium diphosphate, adsorption of the diphosphate anion on the surface of the anion exchange membrane, Permplex A-100. This reversed the charge on the membrane and also the direction of electroosmotic flow of water.

This surface charge reversal occurred in every one of the membranes and electrolytes 2:1 and 3:1 used in this study and can be seen in the results given in Table I, in which E_m and R_m values, as obtained at the end of 2- and 4-hr periods, are recorded.

With the help of eq. (1), the rate at which various electrolytes diffuse through the membranes can be calculated. For 1:1 electrolyte, ($Z_+ = Z_- = 1$), eq. (1) becomes:

$$dQ_+/dt = dQ_-/dt = dQ/dt$$

$$= \left(\frac{1}{2FR_m}\right)\left[59.16 \log \frac{C_2\nu_2}{C_1\nu_1} - E_m\right]\left[\frac{E_m}{59.16 \log (C_2\nu_2/C_1\nu_1)} + 1\right] \quad (3)$$

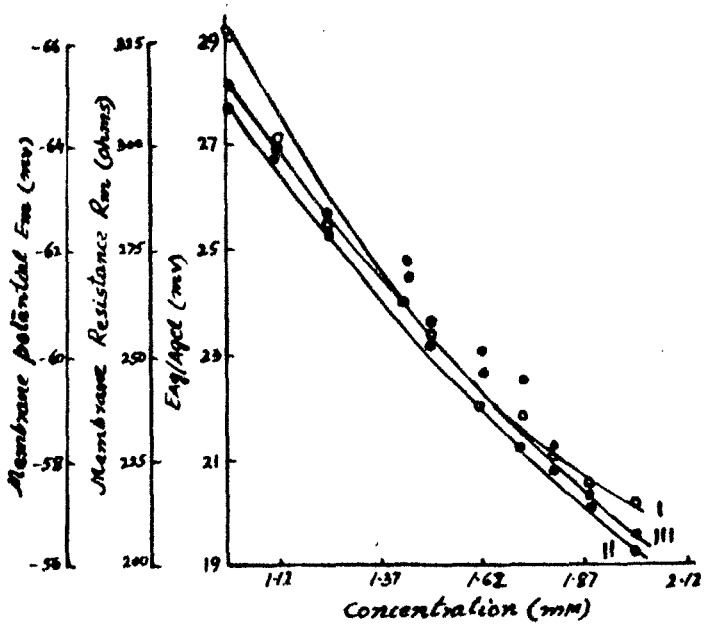

Fig. 6. Values of (*I*) $E_{Ag/AgCl}$, (*II*) E_m, and (*III*) R_m plotted against concentration for $AlCl_3$ across a silver chloride membrane; 3:1 electrolyte.

For 2:1 electrolyte, ($Z_+ = 2$ and $Z_- = 1$), it becomes:

$$dQ_+/dt = dQ_-/2dt = dQ/dt$$

$$= \frac{1}{3FR_m}\left[29.58 \log \frac{C_2\nu_2}{C_1\nu_1} - E_m\right]\left[\frac{E_m}{59.16 \log (C_2\nu_2/C_1\nu_1)} + 1\right] \quad (4)$$

For 3:1 electrolyte, ($Z_+ = 3$ and $Z_- = 1$), it becomes:

$$dQ_+/dt = dQ_-/3dt = dQ/dt$$

$$= \frac{1}{4FR_m}\left[19.72 \log \frac{C_2\nu_2}{C_1\nu_1} - E_m\right]\left[\frac{E_m}{59.16 \log (C_2\nu_2/C_1\nu_1)} + 1\right] \quad (5)$$

The electrolyte fluxes dQ/dt, i.e., D_r calculated from eqs. (3)–(5) for various electrolyte at 25°C are given in Table I. The changes in R_m, E_m and D_r with time and with cations are shown in Figure 8.

The diffusion rate derived from the electrometrically or conductometrically determined changes in the salt concentration of the test solution C_1 is called the observed diffusion rate, while the values computed from the measured concentration potential and electrolytic resistance of the membrane, i.e., from eqs. (3)–(5), is designated the computed diffusion rate. In Figures 9 and 10 are shown the computed and observed diffusion rates of KCl, NaCl, LiCl for silver chloride membrane. For comparison the rates of diffusion of hydrochloric acid through poly(vinyl butyral) membranes obtained by Kittelberger[22] are also shown. It is found that in both the cases the agreement is quite satisfactory.

Equation (1) seems to be a quite simple and elementary way to describe accurately the rather complex processes going on in the membrane; other techniques described by Newman[40] and by Smyrl and Newman[41] which begin with

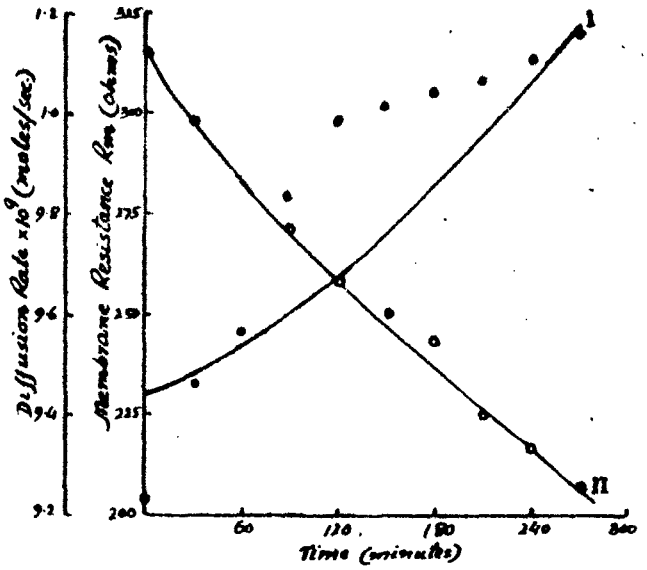

Fig. 7. Plots of (*I*) diffusion rate and (*II*) membrane resistance against time for $AlCl_3$ across a silver chloride membrane; 3:1 electrolyte.

the Stefan-Maxwell transport equations are available, they are not widely applicable to our system. The Nernst-Planck equation on which eq. (1) is based can be applied to parchment membrane as they have been applied to electrolytic transport processes in stomach.[10]

The diffusion experiments at the same time provided a method for calculation of the diffusion coefficients D_c of the electrolyte. Ciric and Graydon[42] have suggested eq. (6)

$$D_c = (VL/2A)\,[\ln (\Delta C_0/\Delta C_f)/\Delta t] \qquad (6)$$

where L is membrane thickness (cm), A is the membrane area (cm^2), V is the volume of the half cell (15 ml), and ΔC_0 is the difference in concentration of the diffusing species between half cell at zero time and ΔC_f = differences in con-

TABLE 1

Experimental Activation Energies and the Eyring Activation Parameters Derived from Transition State Theory of Rate Processes for Diffusion of Various Electrolytes through Parchment-Supported Silver Chloride Membrane

Electrolyte	$D_r \times 10^9$, mole/sec	$\bar{D}_c \times 10^7$, cm^2/sec	E_a, kcal/mole
KCl	2.70	4.050	6.442
NaCl	2.34	2.624	6.217
LiCl	1.93	2.221	5.987
$BaCl_2$	1.65	1.157	4.722
$CaCl_2$	1.94	2.268	5.300
$SrCl_2$	1.64	1.454	4.836
$MgCl_2$	1.93	1.784	4.952
$AlCl_3$	0.99	0.477	6.218

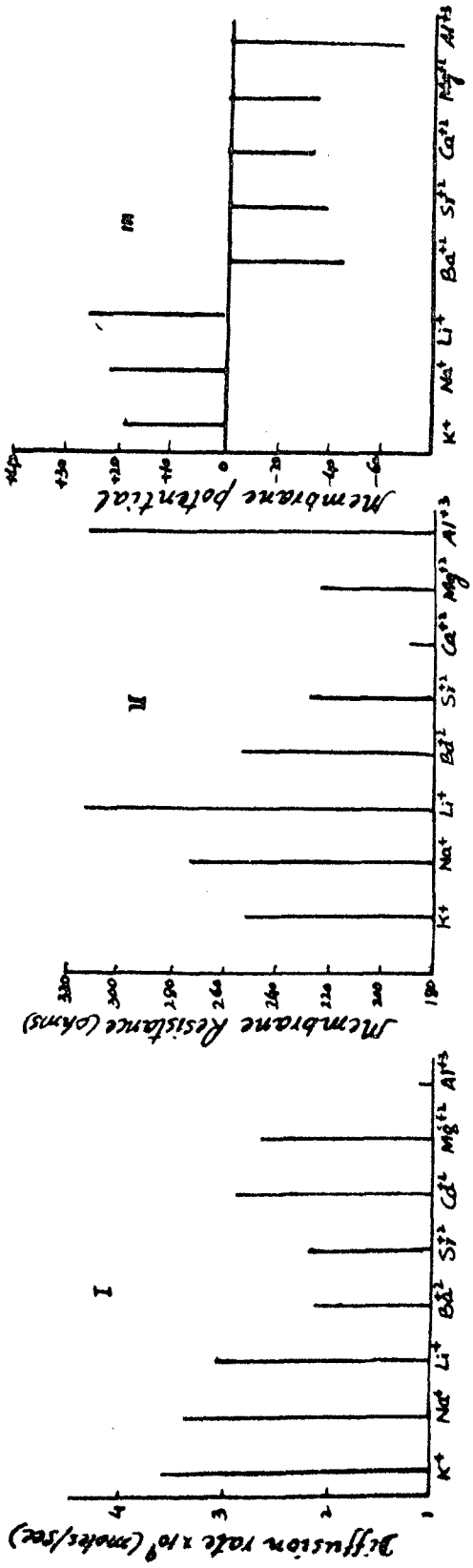

Fig. 8. Plots of (*I*) diffusion rate, (*II*) membrane resistance, and (*III*) membrane potential plotted for various cations across silver chloride membrane.

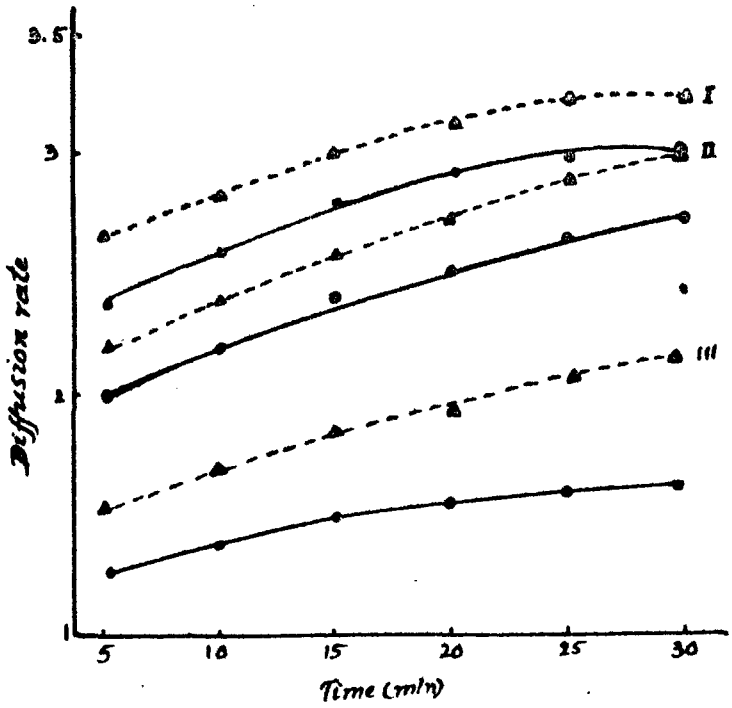

Fig. 9. Plots of (- -▲- -) observed and (--●- -) computed diffusion rate against time for (*I*) KCl, (*II*) NaCl, and (*III*) LiCl with silver chloride membrane.

centration of the diffusing species between half cells at time t, t being the time in minutes.

Plots of ln $(\Delta C_0/\Delta C_f)$ against t gave straight lines and are shown in Figure 11, from which the value of diffusion coefficients are calculated and given in Table II.

The diffusion of the electrolyte through the membrane is slower than in the free solution. Moreover, the order does not remain the same due to various reasons: (a) only a part of the framework is available for free diffusion; (b) the diffusion paths in the membrane phase are more tortuous and therefore longer (i.e., the tortuosity factor); (c) the large hydrated ions in the narrow mesh region of the membrane may be impeded in their mobility by the frame work; and (d) interactions of the diffusing species with fixed groups occur on the membrane matrix. Parchment paper, except for the presence of some stray and carboxylic end groups, contains very few groups. Deposition of the inorganic precipitates gives rise to a net negative charge on the membrane surface in the case of 1:1 electrolyte leading to the type of ionic distribution associated with the electrical double layer. However, as discussed earlier, use of 2:1 or 3:1 electrolyte leaves a net positive charge on the membrane and again results in the formation of the electrical double layer. The system investigated is considered as having charged rigid capillary structures or gels which can be judged in the light of classical fixed charge theory of Teorell,[43] Meyer and Sievers,[44] Sollner[23-25] Gregor,[26,27] and Schmid.[28,29] Flow of electrolyte by diffusion because of the presence of a net charge ($-V_e$ or $+V_e$) on the membrane gives rise to the membrane potential as opposed to the liquid junction potential ordinarily observed under similar conditions in the absence of the membrane, which regulates the flow of electrolyte

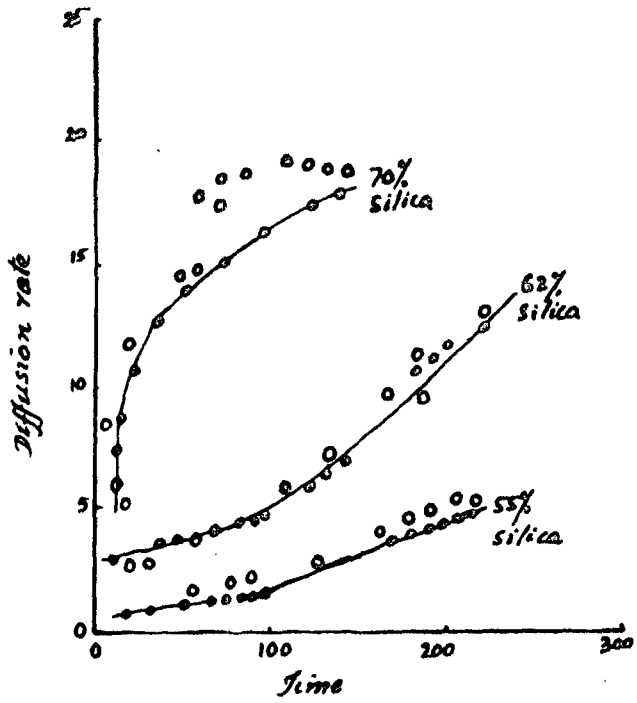

Fig. 10. Plots of (○) observed and (●) computed diffusion rate against time for hydrochloric acid through poly(vinyl butyral) membrane

by increasing the speed of the slow moving ion and also by decreasing the speed of the faster moving ion. This regulated rate of flow (i.e., diffusion) measured for different electrolytes through the membrane follows the sequence $K^+ > Na^+ > Li^+$ and $Ba^{2+} > Ca^{2+} > Mg^{2+} > Al^{3+}$.

Depending on the size and electrical charge pattern of a pore, it may either admit or repel a solute particle. This is the basis of ion selectivity and applies equally to material in a thin sheet (a membrane) or in bulk (an ion exchanger). It has been proposed by Mullins[45] that the hydration of the materials of the pores themselves may provide a favorable water environment for particular ions or molecules, so that they slip into the pores away from their previous water molecules. According to Mullins's argument, this could result in selection of a particular size with discrimination against both smaller and larger hydrated ions. However, it is more general to regard the state of hydration as being in a dynamic condition so that a fraction of the number of a given kind particles in the solution has a reduced hydration corresponding to excess energy ΔE per mole according to Boltzmann distribution $f = \exp\{-\Delta E/RT\}$. To obtain a quantitative relation between the ease of penetration and the ion size it will be necessary to know the electrostatic force which acts between the ions and the materials of the membrane since this force provides energy equal to ΔE to displace water of hydration. Eisenman et al.[31-33] have pointed out that the rank order of ease of penetration of univalent cations will depend on the energy available from the ion-fixed charge interaction.

In the theory of Eisenman, hydration, however, is connected in terms of its energetics rather than in terms of hydrated ionic radius or volume. Electrostatic interactions are regarded as the primary cause of diffusion. Eisenman's

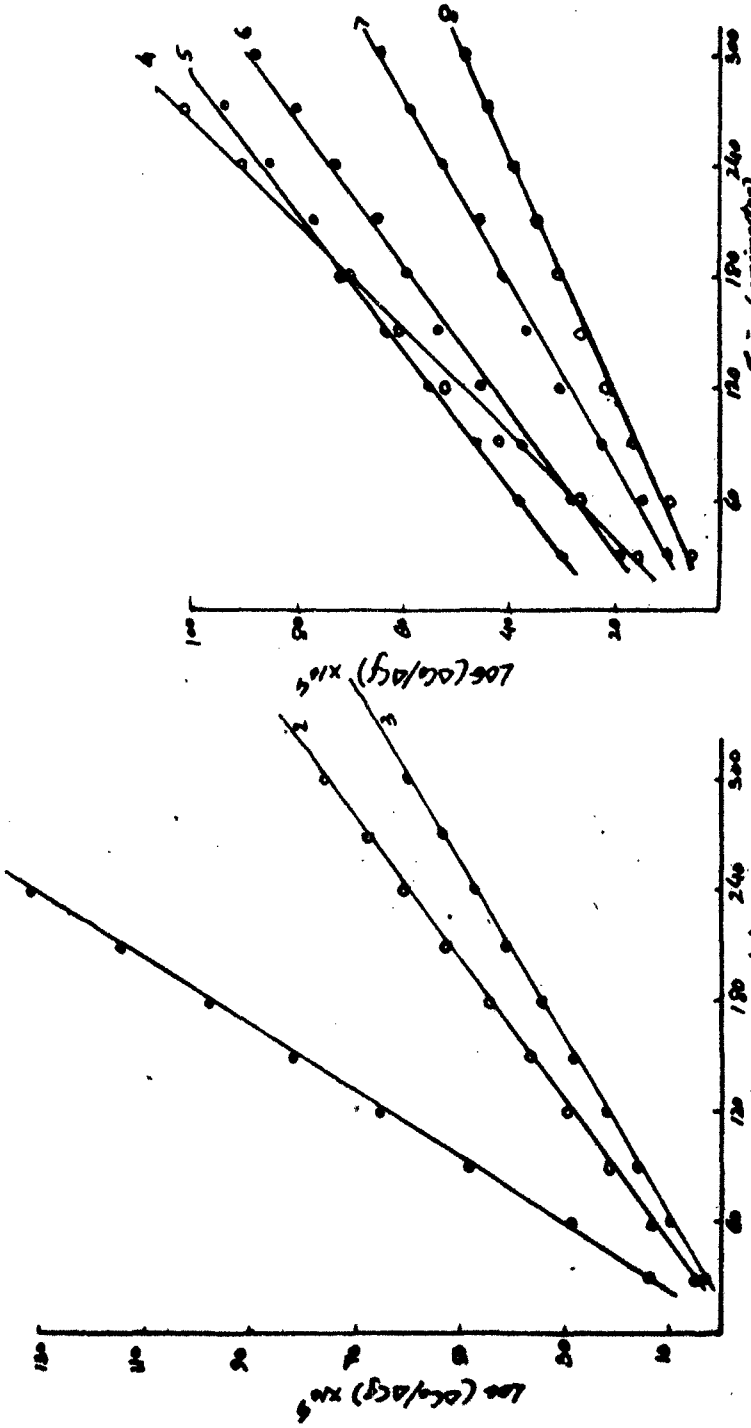

Fig. 11. Plots of $\log (\Delta C_0/\Delta C_f) \times 10^4$ against time for various electrolytes: (1) KCl; (2) NaCl; (3) LiCl; (4) $CaCl_2$ (5) $MgCl_2$ (6) $SrCl_2$, (7) $BaCl_2$, and (8) $AlCl_3$. ΔC_0 = initial concentration difference of the diffusing species across the silver chloride membrane at zero time. ΔC_f = final concentration difference of the diffusing species across the silver chloride membrane at time t.

theory[31-33] takes into account: (1) the electrostatic interactions between the fixed groupings and the ion and (2) the free energies required to remove from (or arrange around) the fixed grouping and the counterion as many water molecules as are necessary to permit the contact (or close approach) of the fixed grouping and the counterion. Such free energies would be closely related if not actually proportional to the standard free energies of the fixed group and the counterion. Rosseinsky,[46] while discussing the electrode potentials and hydration energies has given comparative values of various thermodynamic parameters which have been reproduced in Figures 12–18. These include (Fig. 14) the partial molal volume V, the conductance λ°, (3) $S^\circ_{Con} - \frac{3}{2} R \ln M$, $-\Delta F_{ai}$ free energy change of (aqueous) ionization, and ΔF_h standard free energy change of hydration. From Figure 14 it is quite evident that Mg^{++} has the smallest value while Ba^{++} has the highest one. It would be quite worthwhile to relate the properties like ionic free energy, heat capacity, and free energy of hydration, to the diffusion rate D_r. The plots of D_r against all these thermodynamic extensive properties are shown in Figures 15–18.

Although the sizes of the hydrated electrolytes are not known with certainty, there are few tabulations[47-49] of the number of moles of water associated with some electrolytes. A plot of diffusion rates of different electrolytes against free energy of hydration of cations[50] is given in Figure 14 for the silver chloride membrane. It is seen that diffusion rate decreases with increasing hydration energy, that is greater size due to increase of hydration. Chu et al.[51] ascribe anion exchange selectivity primarily due to differences in hydration energies of counterions in the external solution. According to these authors the hydration shells are largely broken down in the exchanger phase. Since this requires energy, it is the ions with the lowest hydration energy which are preferentially taken up by the exchangers. Eisenman[31-33] observed that cation selectivity was controlled by the field strengths of the negative fixed charge sites in the glass. For negative sites with very high field strengths, the ion–site interaction was much stronger than the ion–water interaction, so that the relative affinities were in the opposite sequence (the order of the hydrated radii) for sites with very weak field strengths, since the ion–site interaction was then much weaker than the ion–water interaction. From a simplified model, in which field strength was taken as the controlling variable, the Coulomb energies of interactions of alkali cation with the sites were compared with the free energy of hydration of cations.

TABLE II

Values of Diffusion Coefficients D_c for Various Electrolytes through Parchment-Supported Silver Chloride Membrane

No.	Electrolytes	$D_c \times 10^7$, cm^2/sec
1	KCl	1.7400
2	NaCl	0.780
3	LiCl	0.648
4	$BaCl_2$	0.625
5	$CaCl_2$	1.093
6	$SrCl_2$	0.796
7	$MgCl_2$	0.858
8	$AlCl_3$	0.518

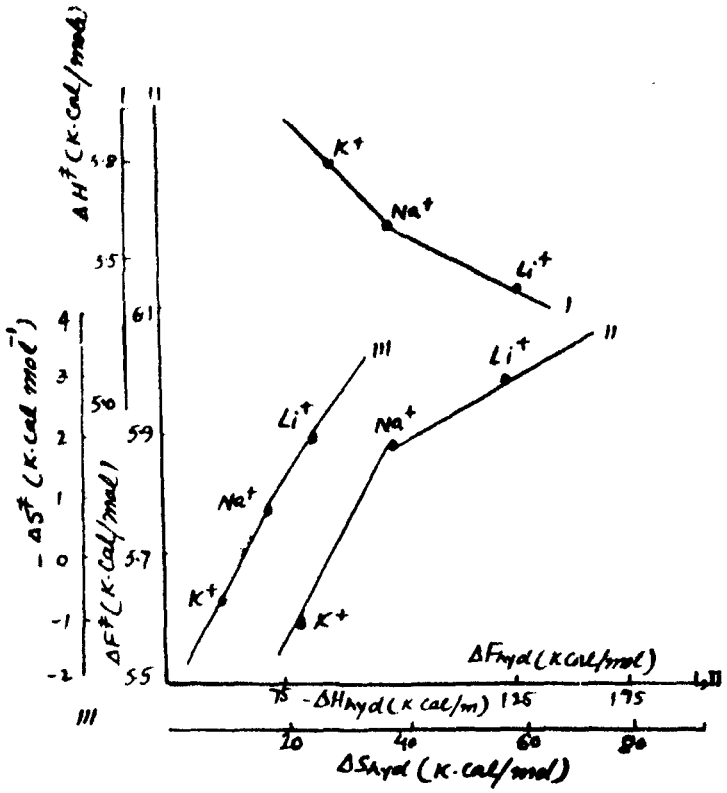

Fig. 12. Plots of (*I*) $\Delta H^{\ddagger}$ (kcal/mole) vs. ΔH_{hyd} (kcal/mole), (*II*) $\Delta F^{\ddagger}$ vs. ΔF_{hyd}, and (*III*) $\Delta S^{\ddagger}$ vs. ΔS_{hyd} for a silver chloride membrane.

Eisenman correctly predicted the various cation sequences intermediate between those of hydrated and nonhydrated radii, actually observed in artificial membranes including glass electrodes.

A simplified theory of selectivity for the four alkaline earths (Mg^{2+}, Ca^{2+}, Sr^{2+}, and Ba^{2+}) in a cation-exchange membrane with univalent negatively charge sites has been worked out by Sherry[34] along the lines of Eisenman's treatment for alkali cations. Specificity is considered to depend upon the values of two parameters: the field strength of the anionic sites and the distance between adjacent sites. Specificity is determined, as in Eisenman's model, by the difference between free energy of hydration of alkaline earth cations and their Coulomb energies of interaction with the negatively charged sites, very weak sites yielding no specificities in the order of the hydrated radii of the cations at any site spacing, and very strong sites yielding the sequence of the nonhydrated radii until large site spacings are reached. Sherry's model predicts that out of 24 sequences obtainable by permutations of the four alkaline earths, only seven should actually be observed as selectivity sequence, the two extreme ones being $Ba^{2+} > Ca^{2+} > Mg^{2+}$ for low field-strength group and $Mg^{2+} > Ca^{2+} > Ba^{2+}$ for high field strength. On the basis of Eisenman-Sherry theory, the diffusion rate sequence obtained in our case point towards the weak field strength of the charge groups of the membrane investigated. These findings are in complete agreement with our results of membrane charge-density measurements which were found to be low.

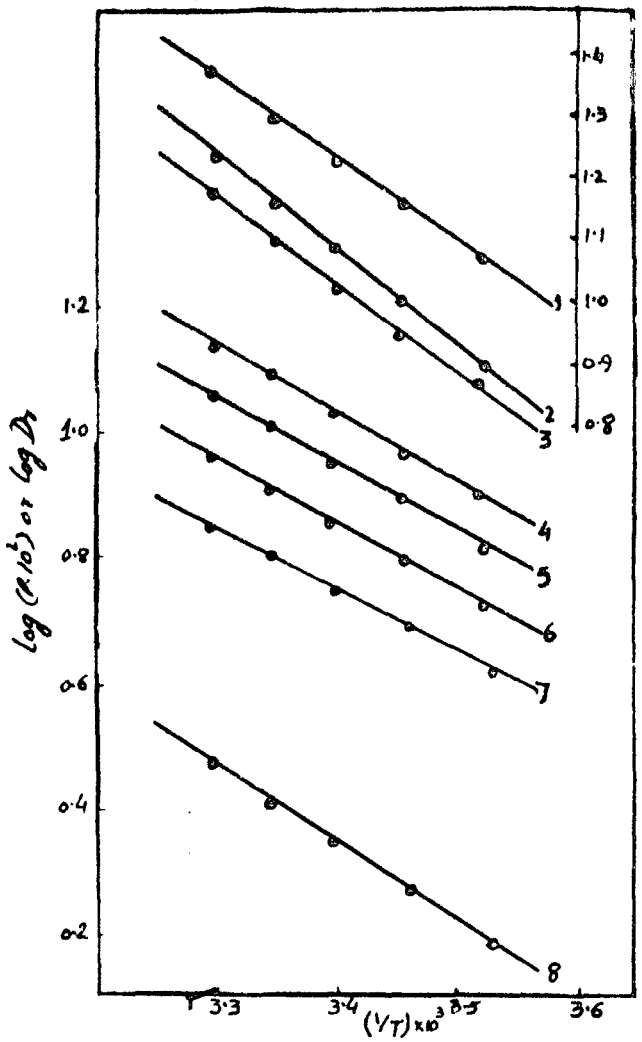

Fig. 13. Variation in permeability P (mm/hr) or D_t of a silver chloride membrane with temperature in presence of (1) KCl, (2) NaCl (3) LiCl, (4) $CaCl_2$, (5) $MgCl_2$, (6) $SrCl_2$, (7) $BaCl_2$ and (8) $AlCl_3$ electrolytes.

The theory of absolute reaction rates has been applied to diffusion processes in membranes by several investigators.[52-54] According to Laidler et al.[53,54] the integral diffusion coefficient $\bar{D}_c$ is given by eq. (7):

$$\bar{D}_c = Ae^{-E_a/RT} \tag{7}$$

where E_a is the observed activation energy for diffusion and A is the frequency factor. Thus, if $\bar{D}_c$ is plotted against $1/T$, the slope gives the value of energy of activation for the diffusion process. For a number of electrolytes and with silver chloride membrane the values of E_a were determined and are given in Table I. Also according to Zwolinski et al.[52-54]

$$\bar{D}_c = \lambda^2 (KT/h) \exp\{\Delta S^{\ddagger}/RT\} \exp\{-\Delta H^{\ddagger}/RT\} \tag{8}$$

where λ is the distance between successive equilibrium positions of diffusing species, $\Delta S^{\ddagger}$ is the entropy of activation, $\Delta H^{\ddagger}$ the enthalpy of activation, K is the

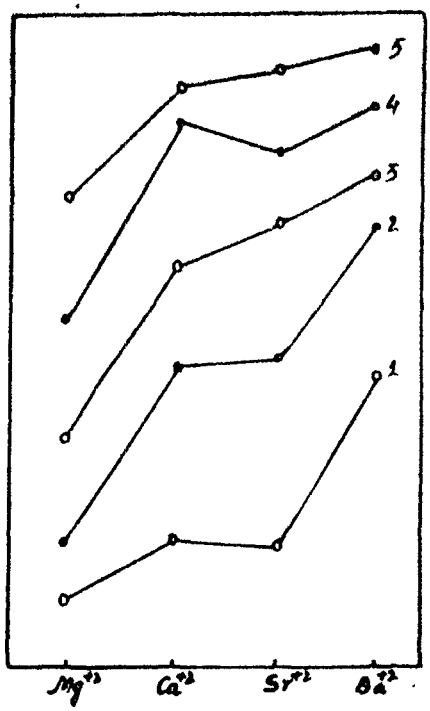

Fig. 14. Plots of (*1*) partial molal volume of ions in solution V, (*2*) λ°, (*3*) $S^\circ_{con} - \frac{1}{2} R \ln M$, (*4*) $-\Delta F_{ai}$ (aqueous) ionization, and (*5*) ΔF_h standard free energy change of hydration across a silver chloride membrane.

Boltzmann constant, h is the Planck constant, R the gas constant, and T the absolute temperature.

The Eyring enthalpy of activation $\Delta H^\ddagger$ is calculated from the activation energy E_a (previously determined) by using relation (8):

$$\Delta H^\ddagger = E_a - RT \tag{8}$$

λ being assumed to be equal to 3 Å for different electrolytes. (Different investigators[52-55] have used values ranging from 1 to 5 Å for λ.) On substituting the value of diffusion coefficient $\bar{D}_c$, the value of $\Delta S^\ddagger$ has been calculated. The free energy of activation $\Delta F^\ddagger$ is then calculated from the Gibbs-Helmoltz equation:

$$\Delta F^\ddagger = \Delta H^\ddagger - T\Delta S^\ddagger$$

The values so derived for the different thermodynamic parameters are given in Table II. For purposes of comparison, the values of $\Delta S^\ddagger$ determined by various investigators for a variety of systems are given in Table III.

The values of $\Delta S^\ddagger$ are either positive or negative for membranes. These are a few values which are close to zero and correspond to liquid system. According to Eyring et al.,[52,53] the values of $\Delta S^\ddagger$ indicate the mechanism of flow: large positive $\Delta S^\ddagger$ is interpreted to reflect breakage of bonds while low values indicate that diffusion has taken place without breaking bonds. Negative $\Delta S^\ddagger$ values are considered to indicate either that a covalent bond is formed between the permeating species and the membrane material or that permeation through the membrane may not be the rate-determining step.

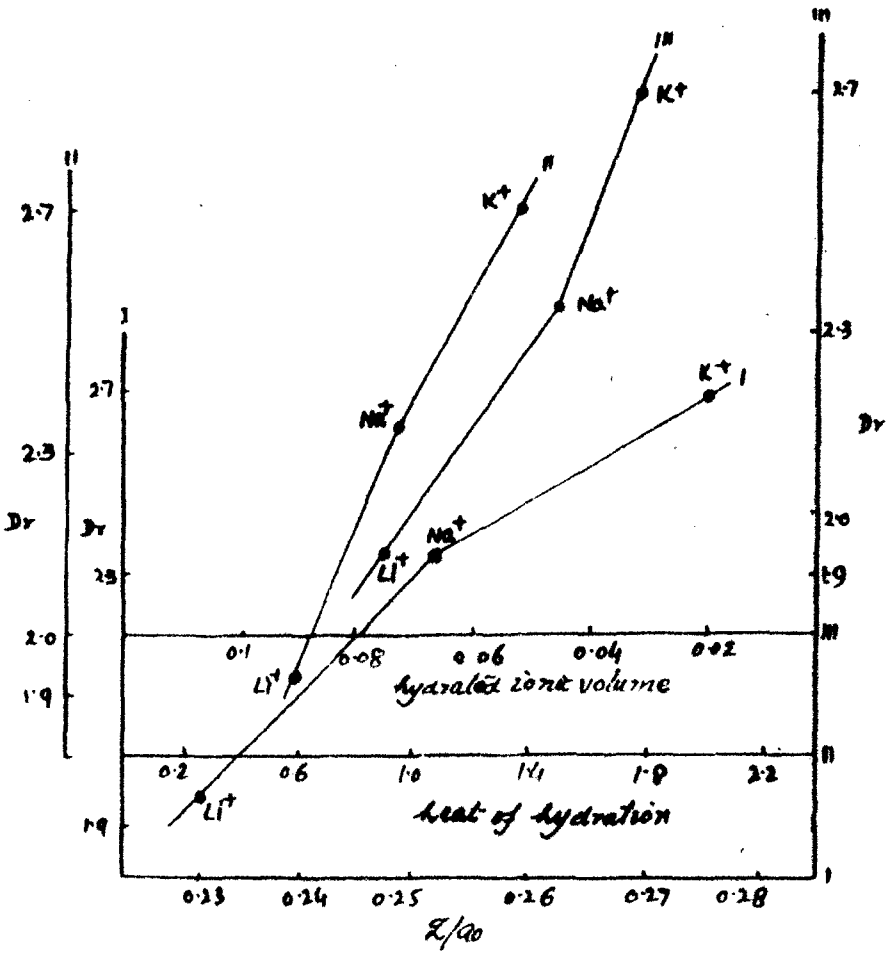

Fig. 15. Plots of D_r against (*I*) Z/A_0 (*II*) heat of hydration, and (*III*) hydrated ionic volume across a silver chloride membrane.

On the contrary, Barrer[56-58] has developed the concept of "zone activation" and applied it to the permeation of ases through polymer membranes. According to this zone hypothesis, a high $\Delta S^{\ddagger}$, which has been correlated with high energy of activation for diffusion, means either the existance of a large zone of activation or the reversible loosening of the more chain segments of the membrane. A low $\Delta S^{\ddagger}$, then means either a small zone of activation or no loosening of membrane structure on permeation. In view of these differences in the interpretation of $\Delta S^{\ddagger}$, Schuler et al.,[54] who found negative $\Delta S^{\ddagger}$ for sugar permeation through collodion membranes, have stated that "It would probably be correct to interpret the small negative values of $\Delta S^{\ddagger}$ mechanically as interstitial permeation of the membrane (minimum chain loosening) with partial immobilization in the membrane (small zone of disorder)." On the other hand, Tien and Ting[55] who found negative $\Delta S^{\ddagger}$ values for the permeation of water through very thin (50 Å thickness) bilayer membranes, stressed the possibility that the membrane may not be the rate-determining step. Based on additional experimental data, they came to the conclusion that the solution membrane interface was the rate-limiting step for permeation.

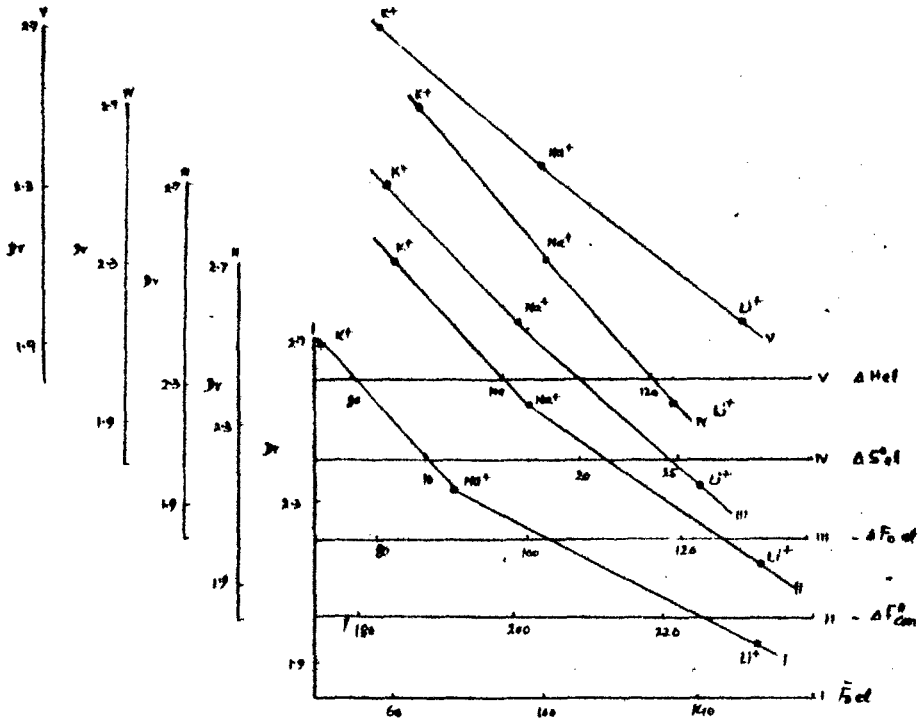

Fig. 16. Plots of D_r against (*I*) F_0 el, (*II*) $-\Delta F°_{con}$, (*III*) $-\Delta F_0$ el (*IV*), $\Delta S°_{el}$, and (*V*) $\Delta H°_{el}$ across a silver chloride membrane.

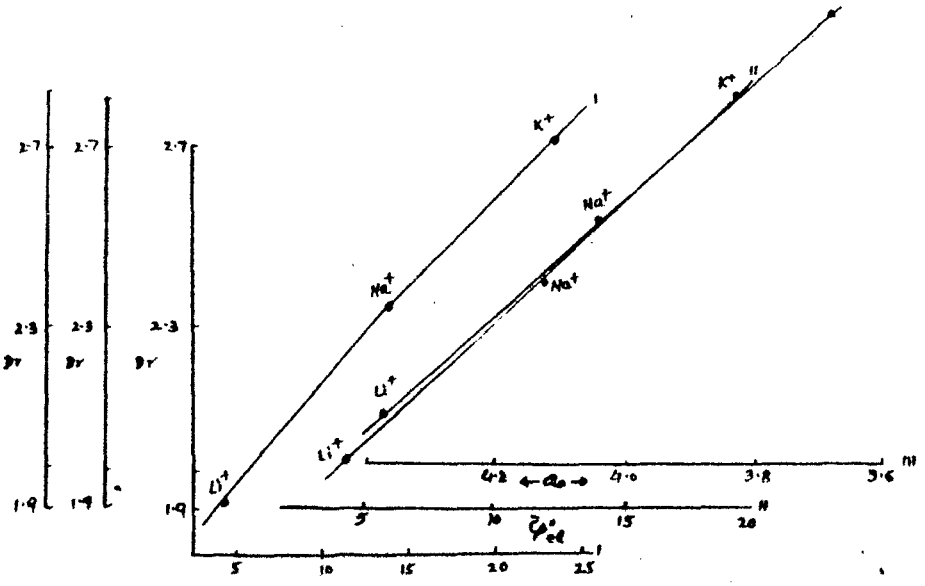

Fig. 17. Plots of D_r against (*I*) entropy, (*II*) $\bar{C}_{el}$, and (*III*) A_0 across the silver chloride membrane.

The data of the present study (Table III) indicate that electrolyte permeation gives rise to negative values of $\Delta S^{\ddagger}$, the magnitude of which depends on the value chosen for the distance λ between equilibrium positions during diffusion. Since the membranes used in this study are fairly thick as compared to bilayers, it is

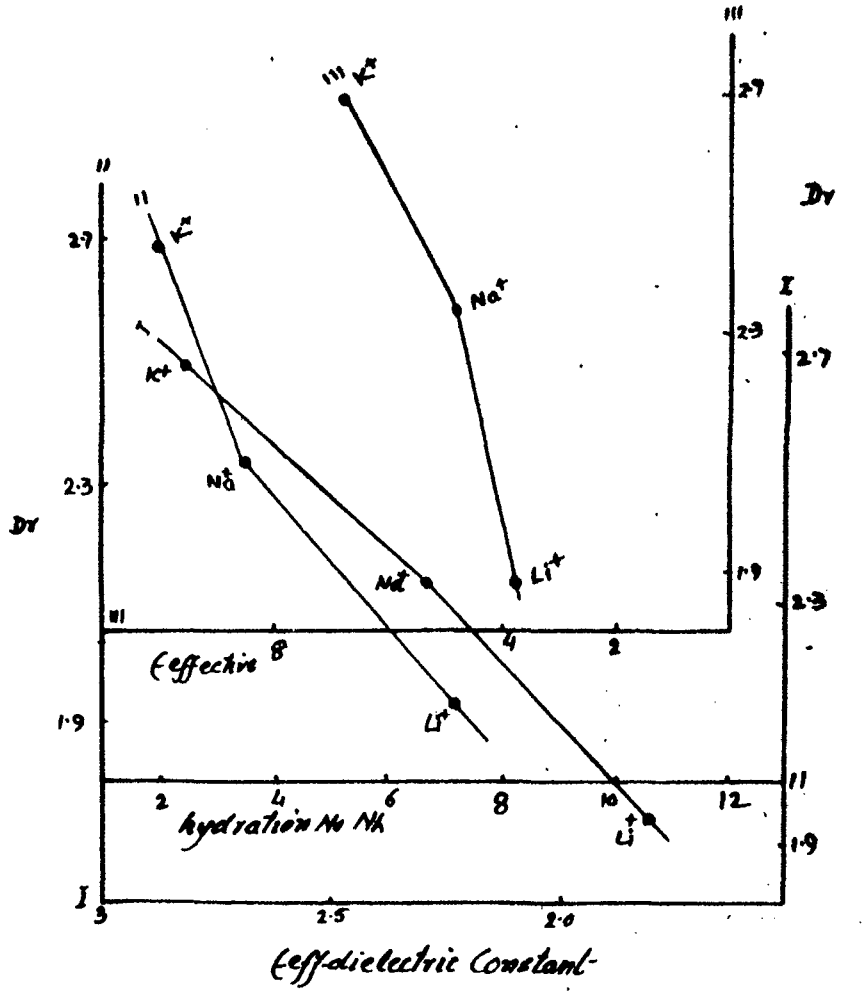

Fig. 18. Plots of D_r against (*I*) effective dielectric constant ϵ_{eff}, (*II*) hydration number N_h, and (*III*) ε effective, across a silver chloride membrane.

believed that the membrane and not the solution–membrane interface controls the electrolyte diffusion process. The negative values of $\Delta S^{\ddagger}$, therefore, as suggested by Schuler et al.,[54] indicate electrolyte diffusion with partial immo-

TABLE III

Thermodynamic Parameters Calculated from the Transition State Theory of Rate Processes for Electrolyte Diffusion through Parchment-Supported Silver Chloride Membrane

Electrolytes	$\Delta H^{\ddagger}$, kcal/mole	$\Delta S^{\ddagger}$, cal/deg mole	$\Delta F^{\ddagger}$, kcal/mole	$\lambda(\exp \Delta S^{\ddagger}/RT)^{1/2}$, Å
KCl	5.850	0.6971	5.642	3.575
NaCl	5.625	−0.9192	5.899	2.380
LiCl	5.395	−2.020	5.997	1.804
$BaCl_2$	4.130	−7.520	6.370	0.447
$CaCl_2$	4.708	−4.270	5.980	1.018
$SrCl_2$	4.244	−6.690	6.230	0.552
$MgCl_2$	4.360	−5.90	6.120	0.674
$AlCl_3$	5.626	−4.280	6.900	1.016

bilization in the membrane, the partial immobility increasing in a relative manner with increase in the valence of ions constituting the electrolyte. In Figure 12 the individual ionic contribution to the properties of aqueous ions given by Noyes,[50] namely, $\Delta H_{\text{hydration}}$, $\Delta F_{\text{hydration}}$, and $\Delta S_{\text{hydration}}$ of Li^+, Na^+, and K^+ are plotted against corresponding $\Delta H^{\ddagger}$, $\Delta F^{\ddagger}$, and $\Delta S^{\ddagger}$ values for diffusion through the membrane. It is found that at least some formal relationship exists between these thermodynamic parameters.

The authors are grateful to Prof. Wasi ur Rahman, Head of the Department of Chemistry, for providing research facilities, and to C.S.I.R. (India) for the award of fellowships to two of them (S.K.S. and I.R.K.).

References

1. F. A. Siddiqi and S. Pratap, *J. Electroanal. Chem.*, **23**, 137 (1969).
2. F. A. Siddiqi and S. Pratap, *J. Electroanal. Chem.*, **23**, 147 (1969).
3. F. A. Siddiqi, N. Lakshminarayanaiah, and S. K. Saksena, *Z. Physik. Chem.* (Frankfurt), **72**, 298 (1970).
4. F. A. Siddiqi, N. Lakshminarayanaiah, and S. K. Saksena, *Z. Physik. Chem.* (Frankfurt), **72**, 307 (1970).
5. F. A. Siddiqi, N. Lakshminarayanaiah, and M. N. Beg, *J. Polym. Sci. A-1*, **9**, 2853 (1971).
6. F. A. Siddiqi, N. Lakshminarayanaiah, and M. N. Beg, *J. Polym. Sci. A-1*, **9**, 2868 (1971).
7. W. U. Malik and F. A. Siddiqi, *Proc. Indian Acad. Sci.*, **A56**, 206 (1962).
8. W. U. Malik and F. A. Siddiqi, *J. Colloid Sci.*, **18**, 161 (1963).
9. W. U. Malik and F. A. Siddiqi, *Bull. Chem. Soc. Japan*, **40**, 1741 (1967).
10. T. Teorell, *Discuss. Faraday Soc.*, **21**, 9 (1956).
11. N. Lakshminarayanaiah and F. A. Siddiqi, *Biophys. J.*, **11**, 603 (1971).
12. N. Lakshminarayanaiah and F. A. Siddiqi, *Biophys. J.*, **11**, 617 (1971).
13. N. Lakshminarayanaiah and F. A. Siddiqi, *Biophys. J.*, **12**, 540 (1972).
14. N. Lakshminarayanaiah and F. A. Siddiqi, in *Membrane Processes in Industry and Biomedicine*, M. Bier, Ed., Plenum Press, New York, 1971, p. 301.
15. N. Lakshminarayanaiah and F. A. Siddiqi, *J. Polym. Sci.*, **8**, 2949 (1970).
16. N. Lakshminarayanaiah and F. A. Siddiqi, *Z. Physik. Chem.* (Frankfurt), **78**, 150 (1972).
17. A. M. Liquori and C. Botre, *Ric. Sci.*, **34**, 6 (1964).
18. A. M. Liquori and C. Botre, *J. Phys. Chem.*, **71**, 3765 (1967).
19. O. Kedem and A. Katchalsky, *Trans. Faraday Soc.*, **59**, 1918, 1931, 1941, (1963).
20. R. Schlögl, *Discussions Faraday Soc.*, **21**, 46 (1956).
21. N. Lakshminarayanaiah, *Chem. Rev.*, **53**, 392 (1949); *Transport Phenomena in Membranes*, Academic Press, New York, (1969).
22. W. W. Kittelberger, *J. Phys. Chem.*, **53**, 392 (1949).
23. K. Sollner, *J. Phys. Chem.*, **49**, 47, 171 (1945).
24. K. Sollner, *J. Electrochem. Soc.*, **97**, 139C (1950).
25. K. Sollner, *Ann. New York Acad. Sci.*, **57**, 177 (1953).
26. H. P. Gregor, *J. Amer. Chem. Soc.*, **70**, 1293 (1948).
27. H. P. Gregor, *J. Amer. Chem. Soc.*, **73**, 642 (1950).
28. G. Schmid, *Z. Elektrochem.*, **54**, 424 (1950); *ibid.*, **55**, 229 (1951); *ibid.*, **56**, 181 (1952).
29. G. Schmid and H. Schwarz, *Z. Elektrochem.*, **55**, 295 (1951); *ibid.*, **56**, 35 (1952).
30. F. Helfferich, *Ion Exchange*, McGraw-Hill, New York, 1962.
31. G. Eisenman, in *The Glass Electrode*, Interscience, New York, 1965.
32. G. Eisenman, *Biophys. J.*, **2**, 259 (1962).
33. G. Eisenman, in *Membrane Transport and Metabolism*, A. Kleinzellers and A. Kotyk, Eds., Academic Press, New York, 1961.
34. H. Sherry in *Ion Exchange* Vol. 2, J. A. Marinsky, Ed., Dekker, New York, 1968.
35. H. B. Weiser, *J. Phys. Chem.*, **34**, 335, 1826 (1930).
36. R. Schlögl, *Stofftransport durch Membrane*, Steinkopff, Darmstadt (1964); *Ber. Bunsenges. Phys. Chem.*, **70**, 400 (1966).

37. N. W. Rosenberg, J. H. B. George, and W. D. Potter, *J. Electrochem. Soc.*, **104**, 111 (1957).
38. N. Lakshminarayanaiah, *J. Electrochem. Soc.*, **116**, 338 (1969).
39. G. Schulz, *Z. Anorg. Allgem. Chem.*, **301**, 97 (1959).
40. J. Newman, *Adv. Electrochem. Eng.*, **5**, 87 (1967).
41. W. H. Smyrl and J. Newman, *J. Phys. Chem.*, **72**, 4660 (1968).
42. J. Ciric and W. F. Graydon *J. Phys. Chem.*, **66**, 1549 (1962).
43. T. Teorell, *Proc. Soc. Exptl. Biol.*, **33**, 282 (1935); *Proc. Natl. Acad. Sci. (US)*, **21**, 152 (1935); *Progr. Biophys. Biophys. Chem.*, **3**, 305 (1953).
44. K. H. Meyer and J. F. Sievers, *Helv. Chim. Acta*, **19**, 649, 665, 987 (1936).
45. L. J. Mullins, in *Transport and Accumulation in Biological Systems*, E. J. Harris, Ed., Butterworths, London, 1960.
46. D. R. Rosseinsky, *Chem. Rev.*, **65**, 466 (1965).
47. H. S. Harned and B. B. Owen, *The Physical Chemistry of Electrolyte Solutions* (3rd ed.), Reinhold, New York, 1958.
48. R. A. Robinson and R. H. Stokes, *Electrolyte Solutions* (2nd ed.), Butterworths, London, 1959, p. 62.
49. J. O. Bockris and P. P. S. Sabija, *J. Phys. Chem.*, **76**, 2298 (1972).
50. R. M. Noyes, *J. Amer. Chem. Soc.*, **84**, 513 (1962).
51. B. Chu, D. C. Shitnej, and R. M. Diamond, *J. Inorg. Nucl. Chem.*, **24**, 1405 (1962).
52. B. J. Zwolinsky, H. Eyring, and C. E. Reese, *J. Phys. Chem.*, **53**, 1426 (1949).
53. S. Glasstone, K. J. Laidler, and H. Eyring, *The Theory of Rate Processes*, McGraw-Hill, New York, 1941, p. 525.
54. K. E. Shuler, C. A. Dames, and K. J. Laidler, *J. Chem. Phys.*, **17**, 860 (1949).
55. H. T. Tien and H. P. Ting *J. Colloid Interface Sci.*, **27**, 702 (1968).
56. R. M. Barrer, *Trans. Faraday Soc.*, **38**, 322 (1942).
57. R. M. Barrer and G. Skirrow, *J. Polym. Sci.*, **3**, 549 (1968).
58. R. M. Barrer and H. T. Chio, in *Transport Phenomena in Polymeric Films* (*J. Polym. Sci. C*, **10**), C. A. Kumins, Ed., Interscience, New York, 1965, p. 111.

Received June 17, 1976

J. Electroanal. Chem., 122 (1981) 313–319
Elsevier Sequoia S.A., Lausanne – Printed in The Netherlands

TRANSPORT OF ALKALI CHLORIDES IN PARCHMENT SUPPORTED CUPRIC HYDROXIDE MEMBRANE AND APPLICATION OF ABSOLUTE REACTION RATE THEORY

MOHAMMAD N BEG, FASIH A. SIDDIQI, K. AHMAD and I. ALTAF

Physical Chemistry Division, Department of Chemistry, Aligarh Muslim University, Aligarh 202001 (India)

(Received 26th September 1980)

ABSTRACT

The preparation of a parchment supported cupric hydroxide membrane is described. Membrane conductance in contact with various alkali–metal chlorides at different concentrations and temperatures have been measured in order to investigate the mechanism of transport of simple salts through the membrane. Various thermodynamic parameters E_a, $\Delta H^{\neq}$, $\Delta G^{\neq}$ and $\Delta S^{\neq}$ and also the interionic distance, d, were evaluated by the application of absolute reaction rate theory. The activation energies for electrolytic conduction follow the sequence of crystallographic radii of alkali–metal cations, which shows that activation energy depends on the size of the penetrant species. The activation energy decreases with increase in the bathing electrolyte concentrations. It has been concluded that the membrane is weakly charged and ionic species retain their hydration shell at least partially while diffusing through the membrane pores. The values of $\Delta S^{\neq}$ were found to be negative, suggesting that the partial immobilization of ions takes place, most probably, due to the interstitial permeation and ionic interaction with the fixed charge groups of the membrane skeleton.

INTRODUCTION

Diffusion of salts in polymers is closely related to the transport phenomena in various systems, namely, ion exchange, desalination, dyeing and biological systems. Many studies and various theories on diffusion of simple salts in membranes have been reported and are reviewed comprehensively by Helfferich [1,2] Lakshminarayanaiah [3], Buck [4] and others in an expanding literature.

The theory of absolute reaction rates has been applied to the diffusion process in membranes by several investigators. Zwolinski et al. [5] examined the permeability data available in the literature for various plant and animal cells by applying the theory of rate processes. Similarly Shuller, Dames and Laidler [6] considered the kinetics of membrane permeation of non-electrolytes through collodion membranes. Tien and Ting [7] studied water permeation through thin lipid membranes and considered the permeation process from the standpoint of the theory of rate process. Clough et al. [8], Li and Gainer [9], and Navari et al. [10] have applied absolute reaction rate theory to the diffusion of solute in polymer solutions. They attached importance to the influence of the polymer on the activation energy for diffusion. Recently, Tsimboukis and

Petropoulos [11] determined the diffusion coefficient of alkali metal ions through cellulose acetate membranes and discussed the results in terms of the pore structure model, and Iijima et al. [12] used activation analysis for the investigation of the mechanism of the diffusion of ions of simple salts through polyamide membranes.

In a series of communications we have [13—17], on the basis of the Eisenman [18—20] and Sherry [21] model of membranes selectivity, and from membrane potential measurements and utilizing various recently developed theories based on the principles of irreversible thermodynamics, demonstrated that the inorganic precipitate membranes, both parchment supported and polystyrene based, possess a small density of fixed charge. In this paper we describe a series of membrane conductance measurements in contact with alkali—metal chlorides at different concentrations and temperatures in order to investigate the transport mechanism of simple salts in inorganic precipitate membranes by the application of absolute reaction rate theory.

EXPERIMENTAL

Cupric hydroxide membranes were prepared by the method of interaction suggested by Beg and co-workers [13—17]. Parchment paper (supplied by Baird and Tatlock Ltd., London) was first soaked in distilled water and then tied to the flat bottom of a glass tube. A 0.1 *M* solution of potassium hydroxide was taken inside it. It was then suspended in a solution of 0.1 *M* $CuCl_2$ for about 72 h. The two solutions were later interchanged and kept for another 72 h. The membrane thus obtained was washed with deionized water for the removal of free electrolytes. It was then cut into a circular disc form and sealed between two half-cells of an electrochemical cell (using adhesive) of the type shown in Fig. 1 of ref. 17. The half-cells were first filled with electrolyte solutions to equilibrate the membrane. The solutions were then replaced by purified mercury without removing the adhering surface liquid [22]. Platinum electrodes dipping in mercury were used to establish electrical contact. The membrane conductance was monitored on a direct reading conductivity meter 303 (Systronics) at a frequency of 10^3 Hz. All measurements were carried out using a water thermostat maintained at temperatures of 25, 30, 35, 40, 45 and 50°C (±0.1°C). The electrolyte solutions were prepared from analytical grade reagents and deionized water.

Extensive use of the method has indicated that, to obtain reproducible results, there should be no trapped air particularly at the membrane—mercury interfaces and the mercury used should be purified as it easily becomes oxidized.

RESULTS AND DISCUSSION

The specific conductance of parchment supported $Cu(OH)_2$ membranes in contact with various 1 : 1 electrolyte solutions at a temperature range of 25—50°C (±0.1°C) have been measured and the results are shown in Fig. 1.

The specific conductance of the membrane increases almost linearly with the square root of the concentration of the bathing electrolyte solutions and

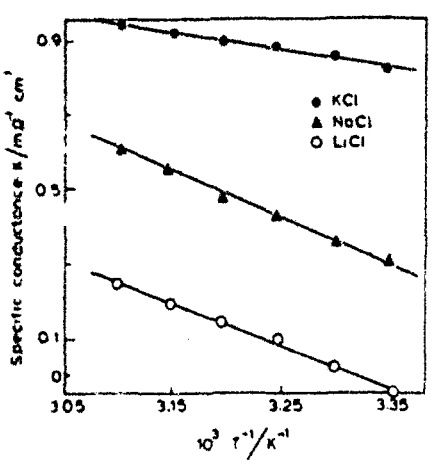

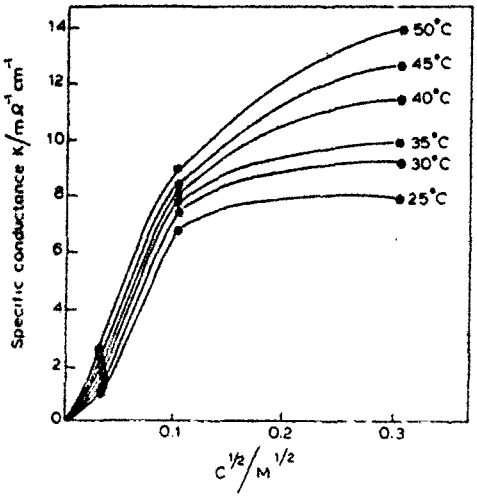

Fig. 1 Arrhenius plot of specific conductance.

Fig. 2. Plots of specific conductance ($m\Omega^{-1}$ cm^{-1}) against square root of concentrations for KCl at different temperatures through cupric hydroxide membranes.

attains a maximum limiting value. This behaviour was seen with all the electrolytes used and at every temperature.

The flow of ion and water is generally larger in the more open structure of the membrane and decreases as the membrane shrinks in more concentrated solution, due, in part at least to increased obstruction of the polymer matrix as diffusional pathways become more tortuous and that fractional pore volume decreases. On the other hand, the electrical conductivity should increase with the increased salt uptake. These two opposing effects operate simultaneously and at higher concentration, as shown in Fig. 2; the effect of salt uptake by the membrane overcomes the effect of increased tortuosity and thus membrane conductance becomes almost constant. This is in accordance with the findings of Paterson in the case of C60N and C60E membranes with NaCl used as invading electrolyte, as well as those of Iijima et al. [12] for nylon membranes with various alkali chlorides. The sequence of membranes conductance for the alkali–metal ions under the same condition (0.01 *M*, 25°C) was

$$K^+ > Na^+ > Li^+$$

which is parallel to mobility of alkali metal ions in aqueous solution. This sequence refers to the fact that the membrane is weakly charged [18–21] and the ionic species retain their hydration shells, at least partially [13]. This is in full agreement with our results of charge density determinations (charge $\approx 10^{-3}$ m*M*). The selectivity of alkali metal ions in ion-exchange resin has been discussed in detail by Reichenberg [23].

Membrane porosity in relation to the size of the species (hydrated) flowing through the membrane seems to determine the above sequence. Although the sizes of the hydrated electrolytes are not known with certainty, there are a few

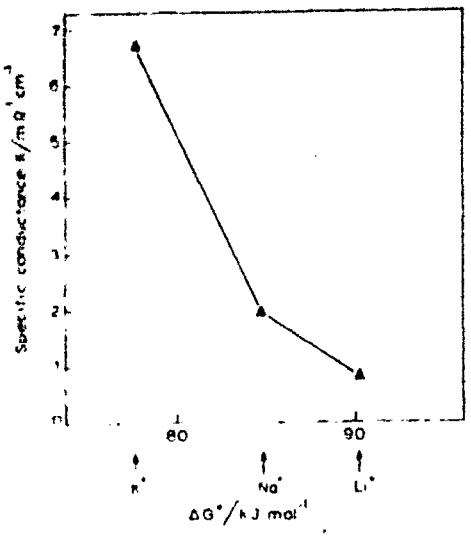

Fig 3 Specific conductance ($m\Omega^{-1}$ cm^{-1}) of various 1 : 1 electrolytes at 25°C through cupric hydroxide membranes plotted against the free energy of hydration (ΔG^0) of cations.

tabulations [24,25] of the number of moles of water associated with some electrolytes. However, in Fig. 3 a plot of specific conductance of different electrolytes (chlorides) against the free energy of hydration of cation [26] is given for the membrane. It is seen that specific conductance decreases with increasing hydration energy, i.e., greater size due to increase in hydration. This points to the fact that the electrolyte is diffusing along pores or channels of dimensions adequate to allow the entrance to penetrate the membrane. The state of hydration of the penetrating electrolyte may be considered to exist in a dynamic condition, so that at higher temperatures a considerably higher fraction of the total number of a given kind would possess excess energy ΔE per mole according to the Boltzmann distribution $f = e^{-\Delta E/RT}$ (R is the gas constant). Under theses circumstances, those ionic species which have lost sufficient water of hydration to become smaller than the size of the pore would enter the membrane. In this way the specific conductance would increase with increase in temperature, subject, however, to the proviso that the membrane has undergone no irreversible change in its structure. That no such structural change is involved is evident from the linear plots of log π vs. $1/T$ shown in Fig. 1. The slope of these gives the energy of activation as required by the Arrhenius equation.

Table 1 shows that the activation energy decreases with the increase in concentration of the bathing electrolyte solution, and that for different electrolytes at a particular concentration it follows that:

$$E_{a_{K^+}} > E_{a_{Na^+}} > E_{a_{Li^+}}$$

The activation energies for electrolytic conduction follow the sequence of crystallographic radii of the alkali metal cations. When the penetrant moves in a polymer substance containing a relatively small amount of water, its motion

TABLE 1

Values of thermodynamic parameters, energy of activation E_a, free energy of activation $\Delta G^{\neq}$ and entropy of activation $\Delta S^{\neq}$, for parchment supported cupric hydroxide membrane in contact with different concentrations of various 1 : 1 electrolyte solutions

Electrolyte concentration c/mol l^{-1}	Parameters		
	E_a/kJ mol^{-1}	$\Delta G^{\neq}$/kJ mol^{-1}	$\Delta S^{\neq}$/J K^{-1} mol^{-1}
KCl			
0 1	18.4	73.4	241
0 01	25.0	71.1	163
0.001	25.4	75.5	176
0.0001	25.4	78.0	185
NaCl			
0.01	24 3	74.2	177
LiCl			
0 1	18.3	72.1	190
0 01	22.0	75.7	190
0 001	24.5	78.5	189

may be governed by the segmental mobility of the polymer, and its diffusivity may depend on the probability that the segment will make a hole large enough to accommodate a penetrant species [27]. In such a system the activation energy will depend on the size of the penetrant species, i.e., the activation energy will increase with the penetrant size. If this is the case in our system, the dependence of the activation energy on the kind of alkali metal ion may be interpreted in terms of the crystallographic radius of the ion, which is consistent with the result obtained in the diffusivity measurement in the same system [12].

The theory of absolute reaction rates has been applied to diffusion processes in the membrane by several investigators [5—7,28,29]. Following Eyring [5,30] we have:

$$\pi = (RT/Nh)\, e^{-\Delta H^{\neq}/RT}\, e^{\Delta S^{\neq}/R} \qquad (1)$$

where π is the membrane conductance, h the Planck constant, R the gas constant, N the Avogadro constant and T the absolute temperature. Here, $\Delta G^{\neq}$ is the free energy of activation for the diffusion of ions and is related by the Gibbs--Helmholtz equation:

$$\Delta G^{\neq} = \Delta H^{\neq} - T\Delta S^{\neq} \qquad (2)$$

$\Delta H^{\neq}$ is related to the Arrhenius energy of activation E_a by

$$E_a = \Delta H^{\neq} + RT \qquad (3)$$

A plot of log $\pi Nh/RT$ vs. $1/T$ from experimental data gives a straight line, the slope and the intercept of which gives the value for $\Delta H^{\neq}$ and $\Delta S^{\neq}$ as demanded by eqn. (1). This justifies the applicability of eqn. (1) to the system under investigation. The derived values of $\Delta H^{\neq}$ and $\Delta S^{\neq}$ were then used to obtain the value of $\Delta G^{\neq}$ and E_a, using eqns. (2) and (3). The values of various

thermodynamic activation parameters E_a, ΔH^*, ΔG^* and ΔS^* derived in this way for the diffusion of various electrolytes in the membrane are given in Table 1. The results indicate that the electrolyte permeation is associated with negative values of ΔS^*. According to Eyring and co-workers [5,30], the values of ΔS^* indicate the mechanism of flow, the large positive ΔS^* being interpreted to reflect breakage of bonds, while low values indicate that permeation has taken place without breaking bonds. The negative ΔS^* values are considered to indicate either formation of covalent bonds between the permeating species and the membrane material, or that the permeation through the membrane may not be the rate-determining step.

Conversely, Barrer [28,31,32] has developed the concept of "zone activation" and applied it to the permeation of gases through polymer membranes. According to this zone hypothesis, a high ΔS^*, which has been correlated with high energy of activation for diffusion, means either the existence of a large zone of activation or the reversible loosening of more chain segments of the membrane. A low ΔS^*, then, means either a small zone of activation or no loosening of the membrane structure on the permeation. In view of these differences in the interpretation of ΔS^*, Shuller et al. [6], who found negative values of ΔS^* for sugar permeation through the collodion membrane, have stated that "it would probably be correct to interpret the small negative values of ΔS^* mechanically as interstitial permeation of the membrane (minimum chain loosening) with partial immobilization in the membrane (small zone of disorder)". On the other hand, Tien and Ting [7], who found negative ΔS^* values for the permeation of water through very thin (5 nm thickness) bilayer membrane, stressed the possibility that the membrane may not be the rate-determining step, but the solution–membrane interface was the rate-limiting step for permeation. Negative ΔS^* values may be ascribed to the partial immobilization of ions and its interaction with the membrane fixed-charge groups.

On the other hand we have [33]:

$$\pi = \pi_0 e^{-E_a/RT} \quad (4)$$

and

$$\pi_0 = 2.72\,(kTd^2/h)\,e^{\Delta S^*/R} \quad (5)$$

where k is the Boltzmann constant and d is the interionic jump distance, i.e. the distance between equilibrium positions of diffusing species in the membrane. Equation (4) predicts that a plot of log π vs. $1/T$ gives a straight line and E_a may be obtained. Substituting the value of parameter ΔS^* and E_a in eqns. (4) and (5) we obtain the value of interionic distance ≈0.15 nm. This value of d is not unusual in these systems. Various investigators [5–7,13,25,34,35] have used values of d ranging from 0.1 to 0.5 nm.

The results of all these investigations are that the membrane conductance can be determined at different temperatures with reasonable accuracy. The membrane is weakly charged and ionic species retain their hydration shell at least partially while diffusing through the membrane pores. Negative ΔS^* values suggest that the partial immobilization of ions takes place most probably due to interstitial permeation and ionic interaction with the fixed-charge groups of the membrane skeleton. The interionic jump distance for the system was 0.15 nm.

ACKNOWLEDGEMENTS

The authors are grateful to Prof. Wasiur Rahman, Head of the Department of Chemistry, for providing research facilities, and to U.G.C. (India) for the award of fellowship to one of us (K.A.)

REFERENCES

1 F. Helfferich, Ion Exchange, McGraw-Hill, New York, 1962.
2 F. Helfferich in J.A. Marinski (Ed.), Ion Exchange: A Series of Advances, Marcel Dekker, New York, 1966, Ch. 2.
3 N. Lakshminarayanaiah, Chem. Rev., 53 (1949) 392; Transport Phenomena in Membranes, Academic Press, New York, 1969.
4 R.P. Buck, CRC Crit. Rev. Anal. Chem., (1976) 323.
5 B.J. Zwolinski, H. Eyring and C.E. Reese, J. Phys. Chem., 53 (1949) 1426.
6 K.E. Shuller, C.A. Dames and K.J. Laidler, J. Chem. Phys., 17 (1949) 860.
7 H.T. Tien and H.P. Ting, J. Colloid Interface Sci., 27 (1968) 702.
8 S.B. Clough, A.E. Read, A.B. Metzner and V.C. Behn, A.I.Ch. J., 8 (1962) 346.
9 S.U. Li and J.L. Gainer, Ind. Eng. Chem. Fund., 7 (1968) 433.
10 R.M. Navari, J.L. Gainer and K.R. Hall, A.I.Ch.J., 17 (1971) 1028.
11 D. Tsimboukis and J.H. Petropoulos, 17th Discussion Meeting on Dyeing Chemistry, Sen-I-Gakkai (The Society of Fibre Science and Technology, Japan), 1975, preprint.
12 T. Iijima, T. Obara, M. Ieshiki, T. Seki and K. Adochi, J. Colloid Interface Sci., 63 (1978) 421.
13 F.A. Siddiqi, N. Lakshminarayaniah and M.N. Beg, J. Polym. Sci., 9 (1971) 2853.
14 F.A. Siddiqi, M.N. Beg and S.P. Singh, J. Polym. Sci., 15 (1977) 959.
15 M.N. Beg, F.A. Siddiqi and R. Shyam, Can. J. Chem., 55 (1977) 1680.
16 M.N. Beg, F.A. Siddiqi, R. Shyam and M. Arshad, J. Membrane Sci., 2 (1977) 365.
17 M.N. Beg, F.A. Siddiqi, R. Shyam and I. Altaf, J. Electroanal. Chem., 98 (1979) 231.
18 G. Eisenman, The Glass Electrode, Interscience, New York, 1965, p. 215.
19 G. Eisenman, Biophys. J. Suppl., 2 (1962) 259.
20 G. Eisenman in A. Kleinzellers and A. Kotyk (Eds.), Membrane Transport and Metabolism, Academic Press, New York, 1961, p. 163.
21 H. Sherry in J.A. Marinsky (Ed.), Ion Exchange, Vol. 2, Marcel Dekker, New York, 1969, p. 89.
22 V. Subramanyan and N. Lakshminarayanaiah, J. Phys. Chem., 72 (1968) 4314.
23 D. Reichenberg in J.A. Marinsky (Ed.), Ion Exchange: A Series of Advances, Marcel Dekker, New York, 1966, Ch. 7.
24 H.S. Harned and B.B. Owen, The Physical Chemistry of Electrolyte Solutions, Reinhold, New York, 3rd edn., 1958, p. 525.
25 R.A. Robinson and R.H. Stokes, Electrolyte Solutions, Butterworths, London, 2nd edn., 1959, p. 62.
26 Y. Marcus and A.S. Kertes, Ion Exchange and Solvent Extraction of Metal Complexes, Interscience, New York, 1969, p. 13.
27 C.A. Kumins and T.K. Kwei in J. Crank and G.S. Park (Eds.), Diffusion in Polymers, Academic Press, London, 1968, Ch. 4.
28 R.M. Barrer and G. Skirrow, J. Polym. Sci., 3 (1948) 549.
29 W.D. Stein, The Movement of Molecules Across Cell Membranes, Academic Press, New York, 1967, pp. 70–89.
30 S. Glasstone, K.J. Laidler and H. Eyring, The Theory of Rate Processes, McGraw-Hill, New York, 1941, pp. 525–544.
31 R.M. Barrer, Trans. Faraday Soc., 35 (1942) 322.
32 R.M. Barrer and H.T. Chio in C.A. Kumins (Ed.), Transport Phenomena in Polymeric Films (J. Polym. Sci. C, 10), Interscience, New York, 1965, p. 111.
33 R.M. Barrer, R.F. Bartholomew and L.V.C. Rees, J. Phys. Chem. Solids, 21 (1961) 12.
34 F.A. Siddiqi, S.K. Saksena and I.R. Khan, J. Polym. Sci., 15 (1977) 1935, 1956.
35 A. Dyer and J.M. Fawcett, J. Inorg. Nucl. Chem., 28 (1966) 615.

CHAPTER 6

EVALUATION OF APPARENT FIXED CHARGE DENSITY ON MEMBRANES

JOURNAL OF POLYMER SCIENCE: PART A-1 VOL. 9, 2869-2875 (1971)

Studies with Inorganic Precipitate Membranes. IV.* Evaluation of Apparent Fixed Charge on Membranes

FASIH A. SIDDIQI, N. LAKSHMINARAYANAIAH, and MOHAMMAD N. BEG, *Department of Pharmacology, University of Pennsylvania School of Medicine, Philadelphia, Pennsylvania 19104 and Department of Chemistry, Aligarh Muslim University, Aligarh, India*

Synopsis

Membrane potentials arising across four parchment-supported ferrocyanide membranes of manganese, cobalt, silver, and cadmium when they separate 1:1 electrolyte solutions of concentration C_1 and C_2 such that $C_1 = 10C_2$, have been measured. The data have been used according to the procedure prescribed by one of the theories of membrane potential due to Teorell and Meyers and Sievers to derive values for the quantity of charge present on the membranes. An alternative procedure employed by Altug and Hair has been considered and found to overestimate the value for the charge on the membranes.

Introduction

From the results discussed in Part III,[1] it is evident that parchment-supported inorganic precipitate membranes have the ability to generate potentials when they are used to separate electrolyte solutions of different concentration. This property is attributed to the presence of a net charge (negative in the case of 1:1 electrolytes and positive in the case of 2:1 or 3:1 electrolytes) on the membrane probably due to adsorption of anions or cations. The quantity of charge required to generate potentials, particularly when dilute solutions are used, is very small.[2a] This, of course, is dependent on the porosity of the membrane. If the membrane pores are too wide, any amount of charge on the membrane does little to generate good potentials. But if the membrane pores are narrow, a little charge on it can give ideal potentials according to the Nernst equation

$$E_{max} = (RT/F) \ln (a_1/a_2) \quad (1)$$

where a_1 and a_2 are the activities of the two solutions on either side of the membrane in an electrochemical cell of the type

$Hg-Hg_2Cl_2$	saturated KCl–agar	solution a_1	Membrane	solution a_2	saturated KCl–agar	Hg_2Cl_2-Hg

* The permeability and the charge density characteristics of parchment-supported membranes of silver chloride, silver phosphate, and silver tungstate are described in Parts I and II, see *Z. Physik. Chem.* (Frankfurt), 72, 298,307 (1970).

E_m is the membrane potential and R, T, and F have their usual significance. In this paper the quantity of charge present on ferrocyanide membranes of manganese, cobalt, silver, and cadmium, when they are in contact with 1:1 electrolytes, is evaluated.

Experimental

The membranes were prepared as outlined in Part III.[1] The potential developed across the cell was measured by using a Pye precision vernier potentiometer (No. 7568). The concentration of solutions used in the above cell was always $C_1 = 10C_2$, where $C\gamma = a$ (γ is the activity coefficient).

Results and Discussion

The values of membrane potential measured across four ferrocyanide membranes with the use of various 1:1 electrolytes are given in Table I.

The fixed groups present in well characterized ion-exchange membranes can be easily estimated by titration. This procedure was used by Sollner et al.[3,4] to estimate the end groups and stray carboxyl groups present in the collodion material. Because of the difficulty in obtaining adequate amount of the material, Lakshminarayanaiah[5] in his studies with thin membranes of Parlodion, used two methods—the isotopic and the potentiometric—to evaluate the apparent fixed charge on the membrane material. In the present studies, the titration method proved inconvenient and very inaccurate, while the isotopic method was discarded in view of the strong ionic adsorption phenomenon exhibited by these systems. Consequently the potentiometric method was used. This method is based on the fixed charge theory of membrane potential proposed simultaneously by Teorell[6] and by Meyers and Sievers[7], the important features of which have been reviewed by Lakshminarayanaiah.[8,2b]

The membrane potential E_m in millivolts according to the theory, applicable to a highly idealized system is given by the equation (at 25°C)

$$E_m = 59.2\left[\log \frac{C_1(\sqrt{4C_2^2 + \bar{X}^2} + \bar{X})}{C_2(\sqrt{4C_1^2 + \bar{X}^2} + \bar{X})} + \bar{U} \log \frac{\sqrt{4C_1^2 + \bar{X}^2} + \overline{XU}}{\sqrt{4C_2^2 + \bar{X}^2} + \overline{XU}}\right] \quad (2)$$

where $\bar{U} = (\bar{u} - \bar{v})/(\bar{u} + \bar{v})$, $\bar{u}$ and $\bar{v}$ are the mobilities of cation and anion, respectively, in the membrane phase (overbars refer the parameter to the membrane phase). $\bar{X}$ is the charge on the membrane expressed in equivalents/liter of imbibed solution. In order to evaluate this parameter for the simple case of 1:1 electrolyte and membrane carrying a net negative charge of unity ($\bar{X} = 1$), theoretical concentration potentials E_m existing across the membrane were calculated as a function of C_2, the ratio (C_1/C_2) being kept at a constant value of 10 for different mobility ratio $(\bar{u}/\bar{v})$ and plotted as shown in Figure 1. The observed membrane potential values given in Table I for different membranes and KNO_3 electrolyte were plotted

TABLE I

Membrane potential observed in a membrane cell at 25°C

$Hg\text{-}Hg_2Cl_2$ | saturated KCl-Agar | (1:1) electrolyte solution (C_1) | Membrane | (1:1) electrolyte solution (C_2) | saturated KCl-Agar | Hg_2Cl_2-Hg (E_m in millivolts)								
	Solution concn, mole/l.		E_m for 1:1 electrolytes, mV					
Membrane	C_1	C_2	KNO_3	$NaNO_3$	NH_4NO_3	KCl	NaCl	NH_4Cl
Manganese ferrocyanide	0.002	0.0002	32.5	38.5	39.0	37.0	40.0	41.5
	0.01	0.001	26.5	31.5	34.5	32.0	35.5	37.5
	0.02	0.002	20.5	26.5	29.0	18.0	22.5	28.5
	0.05	0.005	14.0	19.5	22.0	14.5	19.0	24.5
	0.10	0.01	11.5	17.5	18.5	12.0	12.5	21.5
	0.20	0.02	9.5	14.0	16.5	2.6	9.8	14.5
Cobalt ferrocyanide	0.002	0.0002	46.5	53.2		45.2	57.0	
	0.005	0.0005	45.0	47.2		43.5	42.0	
	0.01	0.001	43.1	41.5		41.5	39.5	
	0.02	0.002	36.5	32.5		35.5	30.0	
	0.05	0.005	26.0	29.0		24.2	25 0	
	0.10	0.01	25.5	27.0		22.0	23.5	
Silver ferrocyanide	0.002	0.0002	36.0	35.2				
	0.005	0.0005	34.3	34.2				
	0.01	0.001	32.8	31.5				
	0.02	0.002	30.9	27.4				
	0.05	0.005	27.3	24.4				
	0.10	0.01	22.1	24.6				
Cadmium ferrocyanide	0.002	0.0002	34.1	39.7		27.6		
	0.005	0.0005	32.8	39.4		26.3		
	0.01	0.001	32.0	35.4		25.3		
	0.02	0.002	31.9	31.9		24.5		
	0.05	0.005	30.5	31.2		22.3		
	0.10	0.01	30.3	30.0		20.4		

in the same graph as a function of $\log(1/C_2)$. The experimental curve for any given membrane was shifted horizontally and ran parallel to one of the theoretical curves. The extent of this shift gave $\log \bar{X}$ and the parallel theoretical curve gave the value for $(\bar{u}/\bar{v})$. In Table II are given the values of $\bar{X}$ and $(\bar{u}/\bar{v})$ derived in this way for the different membranes and elec-

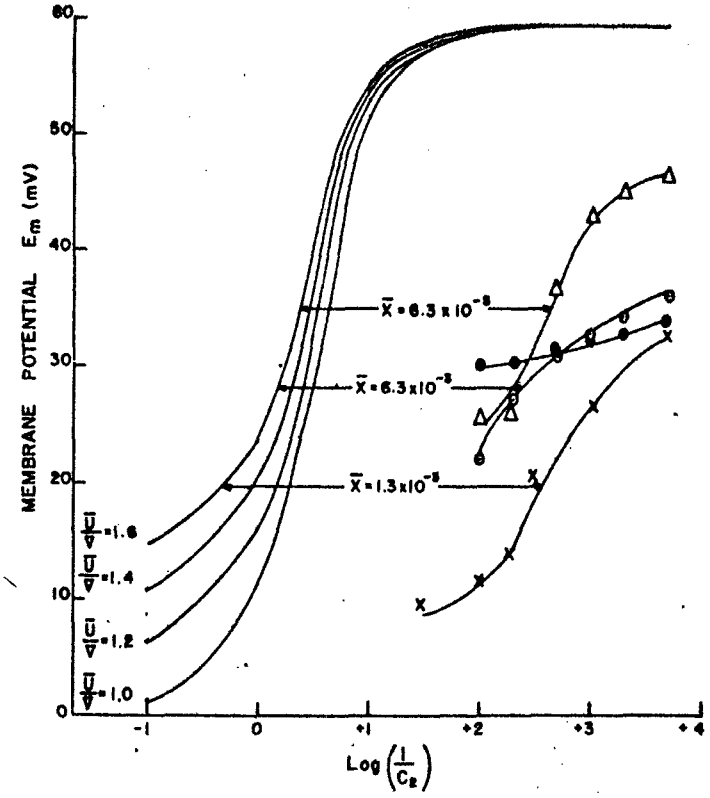

Fig. 1. Evaluation of membrane charge density $\bar{X}$ and the mobility ratio $\bar{u}/\bar{v}$ in the membrane phase. Smooth curves on the left are the theoretical concentration potentials for a cation selective membrane ($\bar{X}$ = 1), 1:1 electrolyte and constant solution concentration ratio (C_1/C_2) = 10 as a function of log ($1/C_2$). The different curves are for different mobility ratios ($\bar{u}/\bar{v}$). The experimental values of E_m for the four ferrocyanide membranes: (×) manganese, (Δ) cobalt, (⊙) silver, and (●) cadmium and KNO_3 electrolyte solution are plotted in the same graph against log ($1/C_2$). Shift of the experimental curve coinciding with one of the theoretical curves gave log $\bar{X}$, and the coinciding curve gave the mobility ratio.

trolytes. In a modification of this type of plotting, Altug and Hair[9] evaluated $\bar{X}$ for glass membranes, choosing the solution values for $\bar{u}$ and $\bar{v}$ and calculating the total membrane potential for different values for $\bar{X}$. The membrane potentials were plotted against log ($1/C_2$) giving now a family of theoretical curves for different values of $\bar{X}$ and constant value of $(\bar{u}/\bar{v})$. The theoretical curve with which the experimental curve overlapped gave

TABLE II

Values Derived for the Membrane Parameters $\bar{X}$ and $(\bar{u}/\bar{v})$

Membrane	Parameter	KNO_3	$NaNO_3$	NH_4NO_3	KCl	NaCl	NH_4Cl
Manganese ferrocyanide	$(\bar{X}) \times 10^3$, eq/l.	1.3	1.6	1.7	3.7	3.2	4.6
	$(\bar{u}/\bar{v})$	1.6	1.8	1.8	1.4	1.4	1.6
Cobalt ferrocyanide	$(\bar{X}) \times 10^3$, eq/l.	6.3	2.9		4.6	2.2	
	$(\bar{u}/\bar{v})$	1.6	1.8		1.6	1.8	
Silver ferrocyanide	$(\bar{X}) \times 10^3$ eq/l.	6.3	1.0				
	$(\bar{u}/\bar{v})$	1.6	>2.0				
Cadmium ferrocyanide	$(\bar{X}) \times 10^3$, eq/l.	2.1	3.2		0.3		
	$(\bar{u}/\bar{v})$	>2.0	>2.0		>2.0		

TABLE III

Apparent Transport Number of Counterion (l_+) and the Mobility Ratio ($\bar{u}/\bar{v}$) in the Membrane Phase Derived from Transport Number Values

KNO_3 concentration		Manganese ferrocyanide		Cobalt ferrocyanide		Silver ferrocyanide		Cadmium ferrocyanide	
C_1	C_2	l_+	$\bar{u}/\bar{v}$	l_+	$\bar{u}/\bar{v}$	l_+	$\bar{u}/\bar{v}$	l_+	$\bar{u}/\bar{v}$
0.002	0.0002	0.78	3.5	0.89	8.1	0.81	4.3	0.79	3.8
0.005	0.0005			0.88	7.3	0.79	3.8	0.78	3.5
0.01	0.001	0.73	2.7	0.87	6.7	0.78	3.5	0.77	3.4
0.02	0.002	0.66	1.9	0.82	4.6	0.76	3.3	0.77	3.4
0.05	0.005	0.63	1.7	0.75	3.0	0.73	2.7	0.76	3.3
0.10	0.01	0.61	1.6	0.70	2.3	0.69	2.2	0.76	3.3
0.20	0.02	0.59	1.4						

the value for $\bar{X}$. A similar procedure was used by Siddiqi and Pratap[10] (also see Beg and Saxena[11]) to determine the value for $\bar{X}$ for a parchment-supported silver iodide membrane. The value derived by them was 0.01 eq/l. The results of the present study given in Table II for the four parchment-supported membranes are all lower, and the values for the mobility ratio are all higher than unity, the value used by Siddiqi and Pratap for KCl solution. Since the mobility ratios in solutions of KNO_3, $NaNO_3$, NH_4NO_3, KCl, NaCl, and NH_4Cl are 1.03, 0.70, 1.03, 0.97, 0.66, and 0.95, respectively—all lower than the values given in Table II—use of this alternate procedure resorted to by Altug and Hair[9] would give values for $\bar{X}$ different from those given in Table II. A typical calculation made for KNO_3 solution and silver ferrocyanide membrane gave a value of about 2×10^{-2} eq/l. ($\bar{u}/\bar{v} = 1.03$) as opposed to a value of 6.3×10^{-3} eq/l. and ($\bar{u}/\bar{v} = 1.6$). Consequently, it is believed that the approach of Altug and Hair overestimated the value of $\bar{X}$. Further it is not realistic to use the solution mobility ratio in these calculations in view of the fact that the membrane potential data of Table I lead to values for mobility ratios for the membrane phase (KNO_3 solution) given in Table III. These values, which are all higher than 1.03 and decrease with increase in the concentration of the external solution, were derived from eqs. (3)–(5).

For 1:1 electrolyte, the counterion transport number l_+ is given by[20]

$$l_+ = (E_m/2E_{max}) + 0.5 \tag{3}$$

$$(\bar{u}/\bar{v}) = (l_+/l_-) \tag{4}$$

$$l_+ + l_- = 1 \tag{5}$$

l_- is the coion transport number and E_{max} is given by eq. (1).

The trend noted in the data given in Table III was also observed in the case of other electrolytes and membranes. The important point emerging from this data is that the mobility ratio goes through a change, considerable in some cases, in the membrane phase. Usually in the case of cation selective membrane (value of $\bar{X}$ high) $(\bar{u}/\bar{v}) \rightarrow \infty$ in dilute solutions and only when the membrane is in equilibrium with concentrated solutions $(\bar{u}/\bar{v}) \rightarrow (u/v)_{solution}$. In view of this, the approach of Teorell and Meyer and Sievers is unreliable to use to evaluate $\bar{X}$ for ion-exchange membranes which have a high concentration of fixed groups. This point has been well illustrated by Lakshminarayanaiah[8] for phenolsulfonate membrane. It is not that unreliable for a membrane which has a low concentration of $\bar{X}$, as found in this study, due to the fact that the change in the values of the factor $(\bar{u}/\bar{v})$ is not as drastic as it is with membranes of high charge density.

The writing of this work has been supported in part by Public Health Service Grant NB-08163-02. Thanks are due to Dr. S. M. F. Rahman for providing laboratory facilities.

References

1. F. A. Siddiqi, N. Lakshminarayanaiah, and M. N. Beg, *J. Polym. Sci. A-1*, **9**, 2853 (1971).
2. N. Lakshminarayanaiah, *Transport Phenoemna in Membranes*, Academic Press, New York, 1969, (a) p. 196; (b) p. 203; (c) p. 199.
3. K. Sollner, C. W. Carr, and I. Abrams, *J. Gen. Physiol.*, **25**, 411 (1942).
4. K. Sollner and J. Anderman, *J. Gen. Physiol.*, **27**, 433 (1944).
5. N. Lakshminarayanaiah, *J. Appl. Polym. Sci.*, **10**, 1687 (1966).
6. T. Teorell, *Proc. Soc. Exptl. Biol. Med.*, **33**, 182 (1935); *Proc. Nat. Acad. Sci. U. S.*, **21**, 152 (1935).
7. K. H. Meyers and J. F. Sievers, *Helv. Chim. Acta*, **19**, 649, 665, 987 (1936).
8. N. Lakshminarayanaiah, *Chem. Rev.*, **65**, 491 (1965).
9. I. Altug and M. L. Hair, *J. Phys. Chem.*, **72**, 599 (1968).
10. F. A. Siddiqi and S. Pratap, *J. Electroanal. Chem.*, **23**, 147 (1969).
11. M. A. Beg and S. K. Saxena, *Kolloid Z-Z Polym.*, **243**, 67 (1971).

Received January 12, 1971

Sonderdruck: „Zeitschrift für Physikalische Chemie Neue Folge", 72 (1970) 307–315
Herausgegeben von G. Briegleb, Th. Förster, G. Schmid, G.-M. Schwab, E. Wicke
Akademische Verlagsgesellschaft, Frankfurt am Main

Studies with Inorganic Precipitate Membranes

II. Potentiometric Evaluation of Apparent Fixed Charge on Membranes

By

FASIH A. SIDDIQI, N. LAKSHMINARAYANAIAH and SANTOSH K. SAXENA

Department of Pharmacology, University of Pennsylvania, School of Medicine
Philadelphia, Pennsylvania, 19104

and

Department of Chemistry, Aligarh Muslim University, Aligarh, India

With 2 figures

(Received September 10, 1970)

Abstract

Membrane potentials arising across three parchment-supported membranes of silver chloride, silver phosphate and silver tungstate when they separate (1:1) electrolyte solutions of concentration C_1 and C_2 such that $C_1 = 10\,C_2$, have been measured. The data have been used according to the procedure prescribed by one of the theories of membrane potential due to TEORELL, MEYER and SIEVERS to derive values for the quantity of charge present on the membranes. An alternative procedure to do this and employed by ALTUG and HAIR has been considered and found to overestimate in a majority of cases the value for the charge on the membranes.

Introduction

The parchment-supported inorganic precipitate membranes can generate emfs which are greater than normal liquid junction potentials when they are used to separate electrolyte solutions of different concentration. This property can be attributed to the existence of a net charge [negative in the case of (1:1) electrolyte and positive in the case of (2:1) or (3:1) electrolytes] on the membrane probably due to adsorption of anions or cations. The quantity of charge required to generate good potentials, particularly when dilute solutions are used, is very small[1]. This is dependent on the porosity of the mem-

[1] N. LAKSHMINARAYANAIAH, Transport Phenomena in Membranes, Academic Press, New York 1969, p. 196.

brane. If the membrane pores are too big, any amount of charge on the membrane gives very low potentials. But on the other hand, if the membranes are tight, a little charge can give ideal potentials according to the Nernst equation

$$E_{max} = \frac{RT}{F} \ln \frac{a_1}{a_2}, \qquad (1)$$

where a_1 and a_2 are the activities of the two solutions on either side of the membrane in an electrochemical cell of the type, $Hg—Hg_2Cl_2$

saturated $KCl-Agar$	solution a_1	membrane	solution a_2	saturated $KCl—Agar$	$Hg_2Cl_2—Hg.$

E_{max} is the theoretical membrane potential, R, T and F have their usual significance. The quantity of charge present on silver chloride, silver phosphate and silver tungstate membranes when they separate solutions of (1:1) electrolyte is evaluated in this part.

Experimental

The membranes were prepared as outlined in part I[2]. The emf developed across the above cell, when the concentration ratio C_1/C_2 ($a_1 = C_1\gamma_1$ and $a_2 = C_2\gamma_2$ where γ is the activity coefficient) was kept constant at 10, was measured using a Pye precision vernier potentiometer (No. 7568).

Results and discussion

The values of membrane potential measured across the three membranes of silver chloride, silver phosphate and silver tungstate employing various (1:1) electrolytes are given in Table 1.

The fixed groups present in well characterized ion exchange membranes can be easily estimated by titration. This procedure was used by SOLLNER et al.[3,4], to estimate the stray and end carboxyl groups present in the collodion material. Because of the difficulty in obtaining adequate quantity of the material, LAKSHMINARAYANAIAH[5], in his studies with thin membranes of Parlodion, used the other two methods, viz. isotopic and potentiometric, to evaluate the apparent

---

[2] F. A. SIDDIQI, N. LAKSHMINARAYANAIAH and S. K. SAXENA, Z. physik. Chem. Neue Folge 72 (1970) 298.

[3] K. SOLLNER, C. W. CARR and I. ABRAMS, J. gen. Physiol. 25 (1942) 411.

[4] K. SOLLNER and J. ANDERMAN, J. gen. Physiol. 27 (1944) 433.

[5] N. LAKSHMINARAYANAIAH, J. appl. Polymer Sci. 10 (1966) 1687.

Table 1. *Membrane potential observed in a membrane cell,* $Hg-Hg_2Cl_2$ | *saturated KCl–Agar* | *(1:1) electrolyte solution* (C_1) | *membrane* | *(1:1) electrolyte solution* (C_2) | *saturated KCl–Agar* | Hg_2Cl_2-Hg *at 25°C*

E_m is in millivolts.

Solution conc. (mole/l)		(1:1) electrolyte					
C_1	C_2	$LiCl$	$NaCl$	KCl	NH_4Cl	KNO_3	KCH_3COO
				Silver chloride membrane			
0.01	0.001	51.0	50.7	45.3	48.8	52.0	53.2
0.02	0.002	48.5	47.6	42.3	46.7	46.0	49.7
0.05	0.005	39.0	35.0	33.5	37.4	38.2	41.4
0.10	0.01	34.6	28.6	24.6	28.5	30.7	34.0
0.20	0.02	24.5	23.0	21.3	19.2	25.4	26.8
				Silver phosphate membrane			
0.01	0.001	47.3	46.0	44.3	46.7	48.3	55.0
0.02	0.002	45.3	42.0	36.6	43.5	46.4	53.4
0.05	0.005	41.6	39.2	30.0	34.6	35.5	49.2
0.10	0.01	34.3	33.4	27.3	25.2	31.0	41.3
0.20	0.02	26.1	24.8	22.6	20.7	27.1	34.0
				Silver tungstate membrane			
0.01	0.001	48.6	46.6	41.7	48.9	46.6	48.5
0.02	0.002	46.1	41.6	37.7	45.2	43.2	45.4
0.05	0.005	41.4	32.5	28.7	34.6	34.6	36.8
0.10	0.01	36.6	29.5	22.5	25.6	22.7	28.2
0.20	0.02	25.2	24.5	19.7	21.0	15.4	21.7

charge on the membrane material. In the present studies, both the titration and the isotopic methods were discarded because of (1) the nature of the material involved and (2) the strong ionic adsorption phenomenon exhibited by these systems. Consequently, the potentiometric method was used. This method is based on the fixed charge theory of membrane potential proposed simultaneously by TEORELL[6] and by MEYER and SIEVERS[7], the important features of which have been recently reviewed by LAKSHMINARAYANAIAH[8].

[6] T. TEORELL, Proc. Soc. exp. Biol. Med. **33** (1935) 192; Proc. nat. Acad. Sci. USA **21** (1935) 152.

[7] K. H. MEYER and J. F. SIEVERS, Helv. chim. Acta **19** (1936) 649, 665, 987.

[8] N. LAKSHMINARAYANAIAH, Chem. Rev. **65** (1965) 491; Ref. (1), p. 203.

According to the theory, the membrane potential E_m is composed of two Donnan potentials at the two solution-membrane interfaces and a diffusion potential arising from the unequal concentrations of the mobile ions at the two membrane faces. The total potential therefore at 25 °C is given by (in millivolts)

$$E_m = 59.16 \left[\log \frac{C_1 (\sqrt{4 C_2^2 + X^2} + X)}{C_2 (\sqrt{4 C_1^2 + X^2} + X)} + \bar{U} \log \frac{\sqrt{4 C_1^2 + X^2} + X \bar{U}}{\sqrt{4 C_2^2 + X^2} + X \bar{U}} \right], \tag{2}$$

where $\bar{U} = (\bar{u} - \bar{v})/(\bar{u} + \bar{v})$, $\bar{u}$ and $\bar{v}$ are the mobilities of cation and anion respectively in the membrane phase (overbars refer the para-

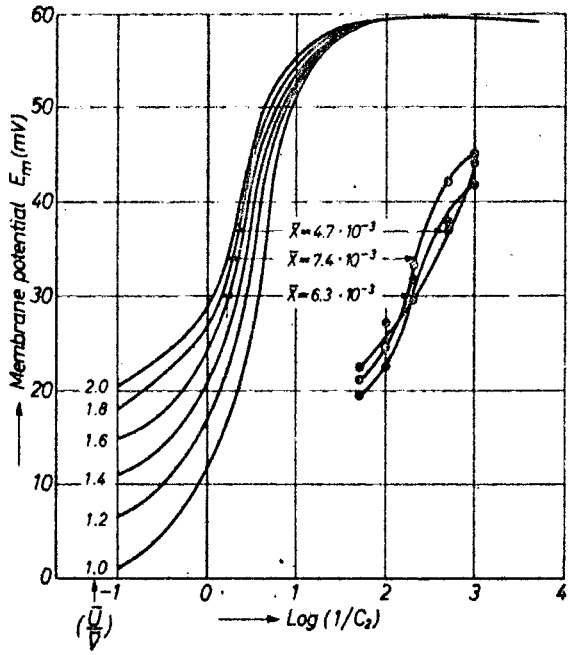

Fig. 1. Evaluation of membrane charge density ($\bar{X}$) and the mobility ratio ($\bar{u}/\bar{v}$) in the membrane phase. Smooth curves on the left are the theoretical concentration potentials for a cation selective membrane ($\bar{X} = 1$), 1:1 electrolyte and constant solution concentration ratio (C_1/C_2) = 10 as a function of log ($1/C_2$). The different curves are for different mobility ratios ($\bar{u}/\bar{v}$). The experimental values of E_m for the three membranes of silver chloride (⊙), silver phosphate (⊗) and silver tungstate (●) and KCl electrolyte solution are plotted in the same graph against log ($1/C_2$). Shift of the experimental curve coinciding with one of the theoretical curves gave log $\bar{X}$ and the coinciding curve gave the mobility ratio.

meters to the membrane phase). $\bar{X}$ is the effective charge on the membrane expressed in equivalents/liter of imbibed solution. In order to evaluate this for the simple case of (1:1) electrolyte and membrane carrying a net negative charge of unity (i.e. $\bar{X} = 1$) theoretical values for E_m were calculated as a function of C_2, the ratio of C_1/C_2 being kept at a value of 10 for the different values of the mobility ratio $\bar{u}/\bar{v}$ and plotted as shown in Fig. 1. The observed values of membrane potential given in Table 1 for different membranes and *KCl* electrolyte were plotted in the same graph as a function of log $(1/C_2)$. The experimental curve for any given membrane was shifted horizontally and ran parallel to one of the theoretical curves. The shift gave the value of log $\bar{X}$ and the parallel theoretical curve gave the value for $\bar{u}/\bar{v}$. In Table 2 are given the values of $\bar{X}$ and $\bar{u}/\bar{v}$ so derived for the different membranes and the electrolytes. In a modification of this type of plotting, ALTUG and HAIR[9] evaluated $\bar{X}$ on glass membranes choosing the aqueous electrolyte solution values for $\bar{u}$ and $\bar{v}$ and calculating the values for E_m assigning different values for $\bar{X}$. The membrane potential values of E_m so calculated were plotted against log $(1/C_2)$ giving now a family of theoretical curves for different values of $\bar{X}$ and constant value of $\bar{u}/\bar{v}$. The theoretical curve with which the experimental curve overlapped gave the value for $\bar{X}$. Similar procedure was used by SIDDIQI and PRATAP[10] to deter-

Table 2. *Values derived for the membrane parameters $\bar{X}$ (equiv/liter) and $(\bar{u}/\bar{v})$*

Parameter	*LiCl*	*NaCl*	*KCl*	NH_4Cl	KNO_3	KCH_3COO
			Silver chloride membrane			
$(\bar{X}) \cdot 10^2$	1.7	1.2	0.7	1.5	1.4	2.1
$(\bar{u}/\bar{v})$	1.8	1.8	2.0	1.6	2.0	1.8
			Silver phosphate membrane			
$(\bar{X}) \cdot 10^2$	2.2	1.5	0.5	1.2	1.0	3.2
$(\bar{u}/\bar{v})$	1.8	2.0	2.0	1.6	>2.0	1.4
			Silver tungstate membrane			
$(\bar{X}) \cdot 10^2$	2.2	1.0	0.6	1.5	1.1	1.3
$(\bar{u}/\bar{v})$	2.0	2.0	1.8	1.6	1.6	1.8

[9] I. ALTUG and M. L. HAIR, J. physic. Chem. 72 (1968) 599.
[10] F. A. SIDDIQI and S. PRATAP, J. electroanalyt. Chem. 23 (1969) 147.

mine a value for $\bar{X}$ for a parchment-supported silver iodide membrane. Since the mobility ratios in solutions of *LiCl*, *NaCl*, *KCl*, NH_4Cl, KNO_3 and KCH_3COO are as 0.56, 0.66, 0.97, 0.95, 1.03 and 1.8 respectively, all lower than the values given in Table 2 (except the case of KCH_3COO), use of this alternate method of plotting the data resorted to by ALTUG and HAIR[9] may be expected to give values for $\bar{X}$ different from those given in Table 2. In Fig. 2 are given the plots of E_m values, both theoretical and experimental, according to ALTUG

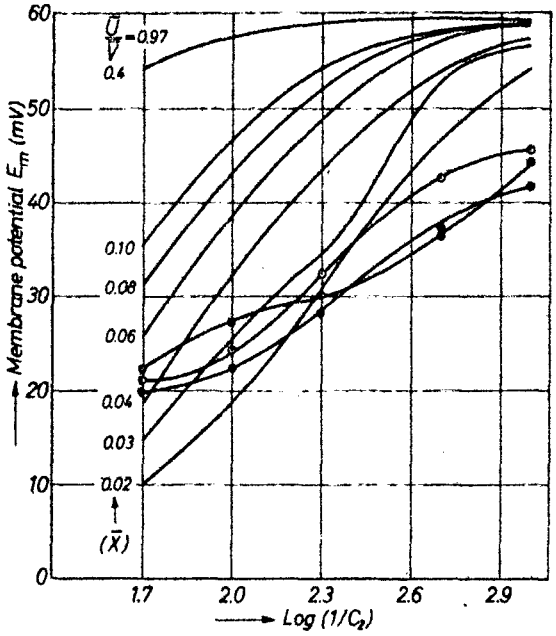

Fig. 2. Evaluation of membrane fixed charge density ($\bar{X}$) assuming the solution mobility ratio of 0.97 for *KCl* solution to be applicable to the membrane phase. The theoretical curves (solid lines) are the plots of membrane potential E_m calculated for different assigned values of $\bar{X}$ as a function of log ($1/C_2$). The experimental values of E_m for the three membranes of silver chloride (○), silver phosphate (⊗) and silver tungstate (●) and *KCl* electrolyte solution are plotted in the same graph against log ($1/C_2$). The theoretical curve best fitting the experimental curve gave the value for $\bar{X}$

and HAIR for the three membranes and *KCl* electrolyte. The values of $\bar{X}$ which roughly fit the theoretical curves are 0.03 equiv./liter for silver chloride membrane and 0.02 for silver phosphate and tungstate membranes. In the case of other electrolytes also, roughly the same

values for $\bar{X}$ were obtained for the three membranes. The value of 0.03 derived for the silver chloride membrane is higher than the values given in Table 2. Similarly the value of 0.02 derived for the silver phosphate and tungstate membranes is higher except in the case of the electrolytes *LiCl* and KCH_3COO. In a similar type of study using parchment-supported ferrocyanide membranes of manganese, cobalt, silver and cadmium, SIDDIQI et al.[11], came to the conclusion that the method of plotting used by ALTUG and HAIR overestimated the value for $\bar{X}$. In this study also similar trend is noted in a majority of cases, the exceptions being *LiCl*-silver phosphate and tungstate membrane systems and KCH_3COO-silver phosphate membrane system (see Table 2). Further it is not very realistic to use the solution mobility values for the ratio $\bar{u}/\bar{v}$ in the calculations in view of the fact that the membrane potential data of Table 1 lead to values for the mobility ratio in the membrane phase given in Table 3 (note however the exceptional case of KCH_3COO where the mobility ratio for the solution phase is the same as the ratio derived for the membrane phase in the case of silver chloride and tungstate membranes). These values which are all higher than unity were derived from the following equations. For (1:1) electrolyte, the transport number of the counterion $\bar{t}_+$ is given by[12]

$$\bar{t}_+ = (E_m/2\,E_{max}) + 0.5 \tag{3}$$

$$(\bar{u}/\bar{v}) = (\bar{t}_+/\bar{t}_-) \quad \text{and} \quad \bar{t}_+ + \bar{t}_- = 1 \tag{4}$$

($\bar{t}_-$ is the transport number of the coion). E_{max} is given by Eq. (1). The important point of the data of Table 3 is the fact that the mobility ratio goes through a considerable change in the membrane phase, always decreasing with increase in the external electrolyte concentration. In the case of ion exchange membranes (cation selective) which have a high value for $\bar{X}$, normally in dilute solutions, the ratio $(\bar{u}/\bar{v})$ tends to infinity and only when the membrane is in equilibrium with concentrated solutions, does $(\bar{u}/\bar{v}) \rightarrow (u/v)_{solution}$. In view of this, the approach of TEORELL, MEYER and SIEVERS is unreliable to use to evaluate $\bar{X}$ for ion exchange membranes. LAKSHMINARAYANAIAH[5] illustrated this point in the case of phenolsulfonate membrane which

[11] F. A. SIDDIQI, N. LAKSHMINARAYANAIAH and M. N. BEG, communicated elsewhere.

[12] N. LAKSHMINARAYANAIAH, Ref. [1], p. 199.

had a base exchange titration capacity of 0.933 mole/liter. The overall value for $\bar{X}$ and the value for the mobility ratio derived by the theory were 0.15 and 1.7 respectively. The upper end of the experimental curve gave a value of 0.9 for $\bar{X}$ and a high value for $\bar{u}/\bar{v}$, while the lower end gave a value of 0.4 for $\bar{X}$ and a value of less than unity

Table 3. *Apparent transport number of counterion $\bar{t}_+$ and the mobility ratio ($\bar{u}/\bar{v}$) in the membrane phase*

Concentration (mole/l)		(1:1) electrolyte											
		KCl		*LiCl*		*NaCl*		NH_4Cl		KNO_3		KCH_3COO	
C_1	C_2	$\bar{t}_+$	$\bar{u}/\bar{v}$	$\bar{t}_+$	$\bar{u}/\bar{v}$	$\bar{t}_+$	$\bar{u}/\bar{v}$	$\bar{t}_+$	$\bar{u}/\bar{v}$	$\bar{t}_+$	$\bar{u}/\bar{v}$	$\bar{t}_+$	$\bar{u}/\bar{v}$
Silver chloride membrane													
0.01	0.001	0.90	9.0	0.95	19.0	0.94	15.7	0.99	99.0	0.95	19.0	0.95	19.0
0.02	0.002	0.87	6.7	0.93	13.3	0.92	11.5	0.92	11.5	0.91	10.1	0.92	11.5
0.05	0.005	0.80	4.0	0.85	5.7	0.81	4.3	0.84	5.3	0.85	5.7	0.85	5.7
0.10	0.01	0.72	2.6	0.81	4.3	0.75	3.0	0.76	3.2	0.78	3.5	0.79	3.8
0.20	0.02	0.70	2.3	0.72	2.6	0.71	2.4	0.68	2.1	0.73	2.7	0.73	2.7
Silver phosphate membrane													
0.01	0.001	0.89	8.1	0.91	10.1	0.90	10.0	0.91	10.1	0.92	11.5	0.97	32.3
0.02	0.002	0.82	4.5	0.90	10.0	0.87	6.7	0.89	8.1	0.90	10.0	0.95	19.0
0.05	0.005	0.77	3.3	0.87	6.7	0.85	5.7	0.81	4.3	0.85	5.7	0.92	11.5
0.10	0.01	0.75	3.0	0.81	4.3	0.80	4.0	0.73	2.7	0.79	3.8	0.85	5.7
0.20	0.02	0.71	2.4	0.74	2.8	0.73	2.7	0.69	2.2	0.75	3.0	0.80	4.0
Silver tungstate membrane													
0.01	0.001	0.86	6.1	0.93	13.3	0.91	10.1	0.93	13.3	0.91	10.1	0.91	10.1
0.02	0.002	0.83	4.9	0.91	10.1	0.87	6.7	0.90	10.0	0.88	7.3	0.89	8.1
0.05	0.005	0.76	3.2	0.87	6.7	0.79	3.8	0.81	4.3	0.81	4.3	0.81	4.3
0.10	0.01	0.71	2.4	0.83	4.9	0.77	3.3	0.74	3.8	0.71	2.4	0.74	3.8
0.20	0.02	0.68	2.1	0.73	2.7	0.73	2.7	0.69	2.2	0.64	1.8	0.68	2.1

for $\bar{u}/\bar{v}$. These considerations, although not sanctioned by the theory emphasize the fact that both $\bar{X}$ and $\bar{u}/\bar{v}$ are dependent on the concentration of the external electrolyte solution. This dependence well established for ion exchange membranes[13] which have a high value

[13] G. J. HILLS, P. W. M. JACOBS and N. LAKSHMINARAYANAIAH, Proc. Roy. Soc. [London], Ser. A 262 (1961) 257.

for $\bar{X}$ tends to be low for membranes of the type used in the present study. Consequently, the use of the theory of TEORELL, MEYER and SIEVERS to derive a value of $\bar{X}$ is not that unreliable in these cases due to the fact that the change in the values of the factor $\bar{u}/\bar{v}$ is not as drastic (see Table 3) as it is with an ion exchange membrane.

Acknowledgments

The writing of this work has been supported in part by Public Health Service Grant NB-08163-02.

Thanks are due to Dr. S. M. F. RAHMAN, Head of the Department of Chemistry for providing laboratory facilities and to CSIR (India) for the award of a fellowship to S.K.S.

J. Electroanal. Chem., 89 (1978) 141–147

STUDIES WITH INORGANIC PRECIPITATIVE MEMBRANES

XI. MEMBRANE POTENTIAL RESPONSE, CHARACTERIZATION AND EVALUATION OF EFFECTIVE FIXED CHARGE DENSITY

MOHAMMAD N. BEG, FASIH A. SIDDIQI, R. SHYAM and I. ALTAF

Physical Chemistry Division, Department of Chemistry, Aligarh Muslim University, Aligarh-202001 (India)

(Received 9th July 1976; in revised form 20th July 1977)

ABSTRACT

Membrane potentials arising across parchment supported nickel and cobalt phosphate membranes when they separate 1 : 1 electrolyte solutions of concentration c_1 and c_2 such that $c_1 = 10\ c_2$, have been measured. The membranes in contact with dilute solutions have been found to carry a negative charge whereas the charge reversal was observed when the membrane was separating concentrated solutions. The membrane potential data have been used according to the procedure prescribed by Teorell-Meyer-Sievers theory (the TMS theory) to derive the value of effective fixed charge density of membranes. The electrical double layer at the membrane—solution interface has been suggested to control the over all rate of diffusion.

INTRODUCTION

Biological membranes, for example, frog skin [1], gastric mucosa [2], toad bladder [3] are considered to possess complex structures. Mueller [4] generated the first bimolecular lipid layer membrane which has been used as model by a number of investigators [5]. Recently other complex membranes have been prepared by Liquori et al. [6,7], Hays [8], De Korosy [9], Lakshminarayanaiah and Siddiqi [10], Siddiqi and Beg et al. [11–15], etc. and utilized as a useful representation of living systems.

One of the most consistent properties of biological system is the presence of a voltage across the cellular surfaces. The mechanism whereby this potential arises is still in dispute. Some consider it to be a diffusion potential while others suggest the voltage to be an adsorption potential [16]. Teorell [17] considered the presence of charge on the membrane skeleton responsible for the development of potential across it. His further findings, that electrolyte transport processes in stomach could be handled by something similar to Fick's diffusion law and that Nernst-Planck formula for electrical potential were applicable, has encouraged us to proceed further with the study of parchment supported membranes which in some formal aspect at least behave like the gastric mucosal membrane.

This paper describes the preparation of parchment supported cobalt and nickel phosphate membranes to be utilized as biological model. Electrical potential of

the membranes interposed between two aqueous solutions of a 1 : 1 electrolyte have been measured for the investigation of the actual mechanism of ion permeation as well as to evaluate the effective fixed charge density which is an important parameter governing the membrane phenomena [11–15, 17, 18, 26].

EXPERIMENTAL

Cobalt and nickel phosphate membranes were prepared by the method of interaction suggested by Siddiqi and Beg [11–15]. To precipitate these substances in the interstices of the parchment paper, 0.2 *M* solution of sodium triorthophosphate was kept inside the glass tube, to one end of which was tied the parchment paper previously soaked in water. This was suspended for 72 h in a 0.2 *M* solution of cobalt chloride. The two solutions were interchanged later and kept for another 72 h. The membrane was washed with deionized water for the removal of free electrolyte. Similar procedure was adopted for the preparation of nickel phosphate membrane by taking 0.2 *M* solution of nickel chloride in place of cobalt chloride. Both the membranes were found to be more shining and transparent than any other parchment supported membranes reported earlier [11–15]. The electrochemical cell of the type

$Hg-Hg_2Cl_2$	Saturated KCl–agar	Solution c_1	Membrane	Solution c_2	Saturated KCl–agar	Hg_2Cl_2–Hg

were used for measuring electrical potentials arising across the different types of membranes by maintaining a tenfold difference in concentration (i.e., $c_1/c_2 = 10$) in the range 1×10^{-4} *M* to 0.1 *M* and using a Pye precision vernier potentiometer (No. 7568). The whole cell assembly was immersed in a water thermostat maintained at 25 ± 0.1°C. The various salt solutions (chloride of Li^+, Na^+ and K^+) were prepared from analytical grade reagents (B.D.H.) by use of deionized water. The parchment paper was supplied by Baird and Tatlock (London) Ltd.

RESULTS AND DISCUSSION

Parchment supported inorganic precipitate membranes have the ability to generate potentials when they are used to separate electrolyte solutions of different concentration [11–15]. This property is attributed to the presence of a net charge on the membrane probably due to adsorption of anions or cations. The quantity of charge required to generate potentials, particularly when dilute solutions are used, is small. This, of course, is dependent on the porosity of the membrane. If the membrane pores are too wide, any amount of charge on the membrane does little to generate good potentials. But if the membrane pores are narrow, a little charge on it can give ideal potentials according to the Nernst equation

$$E_{max} = (RT/F) \ln(a_1/a_2) \qquad (1)$$

where a_1 and a_2 are the activities of the two solutions on either side of the membrane in an electrochemical cell of the type mentioned in the experimental part

TABLE 1

Values of the membrane potential E_m/mV across cobalt and nickel phosphate membranes*

Electrolyte concentration	Membrane					
	cobalt phosphate			nickel phosphate		
	KCl	NaCl	LiCl	KCl	NaCl	LiCl
0.1/0.01	−34.30	−38.65	−35.00	−42.40	−42.30	−40.50
0.05/0.005	−31.36	−36.80	−32.60	−40.25	−40.28	−38.00
0.01/0.001	−28.50	−21.70	−16.40	−32.00	−24.50	−21.50
0.005/0.0005	−10.50	−14.50	−10.40	−15.00	−13.00	−6.90
0.001/0.0001	+1.50	−5.00	+5.00	+1.50	+9.00	+4.50
0.0005/0.00005	+9.00	+10.00	+15.50	+10.25	+10.25	+8.00
0.0001/0.00001	+10.00	+15.00	+20.00	+12.50	+12.50	+15.25

* Dilute solution side taken as *+ve*.

of this paper; E_{max} is the membrane potential and R, T and F have their usual significance.

The values of the membrane potential E_m measured across both nickel and cobalt phosphate membranes with the use of the chloride of potassium, sodium and lithium are given in Table 1. An interesting point with the values of E_m is the fact that these are +ve when the membrane is separating dilute solutions of the electrolytes (dilute solution side c_2 taken as *+ve*). This means that the membrane is cation selective, and when the membrane is used to separate concentrated solutions the values of E_m are *−ve*, i.e., the membrane becomes anion selective. Such reversal in selectivity character is not peculiar to these systems [11,12].

The two important factors which control electrolyte permeability through a membrane are charge on the membrane and its porosity. Parchment paper, except for the presence of some stray and end carboxylic group, contains very few fixed groups. Deposition of inorganic precipitate gives rise to a net negative charge on the membrane surface in the case of dilute solutions of a 1 : 1 electrolyte leading to the type of ionic distribution associated with the electrical double layer. The stepwise change in membrane potential or the selectivity character of the membrane-electrolyte system may readily be explained in terms of the structural changes produced in the electrical double layer at the interfaces. Parchment supported nickel and cobalt phosphate membranes are considered negatively charged in contact with water. It is probable that in these cases the negative charge is due to the firm attachment of hydroxyl ions from the water and PO_4^{3-} ions from the solution constituting the membrane. An equivalent number of protons and/or cations, some closely held in the fixed part of the double layer and the remainder in the diffuse portion, will be left in the solution. By the addition of uni-univalent electrolytes, there will be a tendency for the cations to accumulate on the solution side of the fixed double layer, by increasing the positive charge density, the interfacial potential difference changes thereby changing the overall membrane potential. If the electrolyte concentration is made

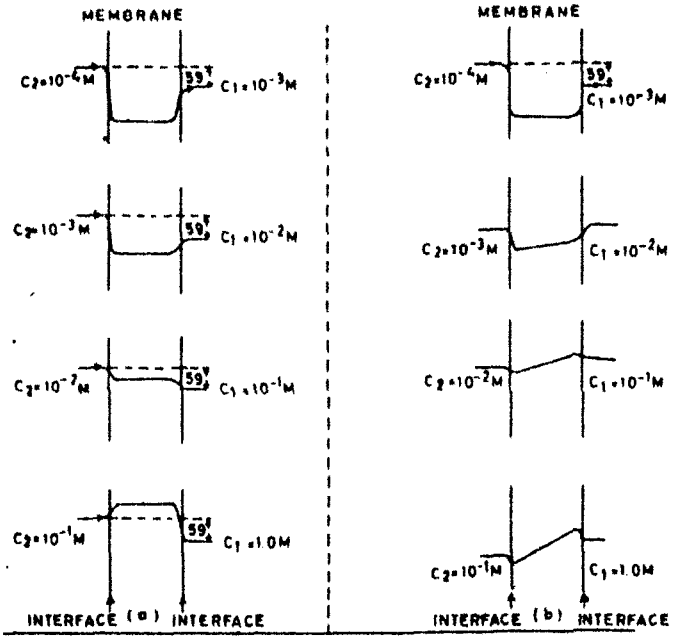

Fig. 1a, b. Hypothetical potential profiles existing across the membranes.

large, the sign of the electrical potential may eventually be reversed leading to a state where the membrane becomes anion selective. Figure 1 depicts a family of hypothetical potential profiles existing across the membranes.

The fixed groups present in well characterized ion-exchange membranes can be easily estimated by titration. This procedure was used by Sollner et al. [19] to estimate the end groups and stray carboxylic groups present in the collodion material. Lakshminarayanaiah [10] in his studies with thin membranes of parlodion, used two methods — the isotopic and the potentiometric to evaluate the apparent fixed charge on the membrane material. In the present studies, the titration method proved inconvenient and very inaccurate, while the isotopic method was discarded in view of the strong ionic adsorption phenomena exhibited by these systems. Consequently the potentiometric method was used. This method is based on the fixed charge theory of membrane potential proposed simultaneously by Teorell [17] and Meyer and Sievers [18]. According to this theory membrane potential is considered to be composed of two Donnan potentials at the two solution—membrane interfaces and a diffusion potential arising from unequal concentration of the two membrane faces. These authors derived following equation for membrane potential in millivolts (at 25°C) applicable to a highly idealized system, viz:.

$$E_m = 59.2\left[\log\frac{c_1}{c_2}\frac{\sqrt{4c_2^2+\bar{x}^2}+\bar{x}}{\sqrt{4c_1^2+\bar{x}^2}+\bar{x}} + \bar{U}\log\frac{\sqrt{4c_1^2+\bar{x}^2}+\bar{X}\bar{U}}{\sqrt{4c_2^2+\bar{x}^2}+\bar{X}\bar{U}}\right] \quad (2)$$

where $\bar{U} = (\bar{u}-\bar{v})/(\bar{u}+\bar{v})$, $\bar{u}$ and $\bar{v}$ are the mobilities of cation and anion respectively in the membrane phase; $\bar{x}$ is the charge on the membrane expressed in

equivalents/litre of imbibed solution. Equation (2) has been frequently used for the evaluation of the fixed charge density $\bar{x}$ of a membrane [20]. In order to evaluate this parameter for the simple case of 1 : 1 electrolyte and membrane carrying a net negative charge of unity ($\bar{x} = 1$), theoretical concentration potentials E_m existing across the membrane are calculated as function of c_2, the ratio c_1/c_2 being kept at constant value for different mobility ratios ($\bar{u}/\bar{v}$). The observed membrane potential values are then plotted in the same graph as a function of $\log(1/c_2)$. The experimental curve is shifted horizontally until it coincides with one of the theoretical curves. The extent of this shift gives $\log \bar{x}$ and the coinciding theoretical curve, the value of ($\bar{u}/\bar{v}$). Similar procedure was tried here to evaluate fixed charge density $\bar{x}$ of cobalt and nickel phosphate membranes. But in both the membranes the observed membrane potential curves on shifting horizontally did not overlap with any of the theoretical curves particularly in the dilute ranges. As a result eqn. (2) was used in another way, in the way Teorell did, to evaluate $\bar{x}$. A family of curves similar to those in Fig. 2 were constructed assigning $x = 1$ and successively decreasing values to $\bar{x}(\bar{x} < 1)$ keeping $\bar{u}/\bar{v} = 0.2$. The curves thus obtained have same shape and limits but are transposed along the $\log c_2$ axis. The value of $\bar{x}$ is then given by the curve with which the experimental curve coincided. The values thus derived are given in Table 2. In addition to the value of $\bar{x}$, the plotting in this form correctly predicts diffusion potential at the limit $\bar{x} = 0$. The diffusion potential values derived in this way were found to have approximately the same magnitude and sign as the potential developed across the membranes when these are used to separate highly concentrated solu-

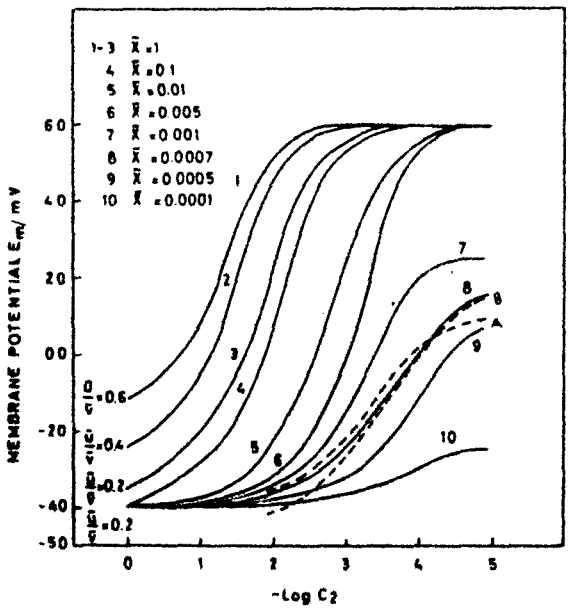

Fig. 2. Smooth curves are the theoretical concentration potentials for $\bar{x} = 1$ and different mobility ratios $\bar{u}/\bar{v}$ (1—3), and $\bar{x} < 1$ (4—10) for $\bar{u}/\bar{v} = 0.2$. Broken lines are the experimental values of E_m for (A) cobalt and (B) nickel phosphate membranes using KCl electrolyte solution.

TABLE 2

Values of the effective fixed charge density of cobalt and nickel phosphate membranes

Electrolyte	Membrane			
	cobalt phosphate		nickel phosphate	
	$\bar{x}$ /eq. l^{-1}	diff. potential/mV	$\bar{x}$ /eq. l^{-1}	diff. potential/mV
KCl	0.65×10^{-3}	−34.30	0.75×10^{-3}	−42.40
NaCl	1.88×10^{-3}	−38.65	1.41×10^{-3}	−42.30
LiCl	2.98×10^{-3}	−35.00	2.45×10^{-3}	−40.50

tions of an electrolyte (Table 2). In view of this limiting diffusion potential value, the variation in membrane potential with the change in external electrolyte concentrations may be ascribed to be due to the structural changes produced in the electrical double layer at the membrane-solution interfaces. Thus the system under investigation may be more conveniently described as consisting of two mini cells — one with constant emf corresponding to the limiting diffusion potential and the other with variable emf representing the interfacial potential difference (0—60 mV approximately). Since the total membrane potential changes sign as the concentration of the electrolytes across the membrane are changed, it may be concluded that these mini cells are combined together in series but operating in opposite direction.

The parchment supported cobalt and nickel phosphate membranes in contact with various 1 : 1 electrolytes are thus considered as the homogeneous membrane elements with charged rigid capillary structures or gels having a diameter large as compared to the thickness of the electrical double layer at the walls in accordance with the classical fixed charge theory of Teorell [17], Meyer and Sievers [18], Sollner [19], Sollner and Gregor [21], Schmidt [22] and Kobatake and co-workers [23—26] etc. Flow of electrolyte by diffusion, because of the presence of a net charge on the membrane gives rise to membrane potential, as opposed to the liquid junction potential observed under similar conditions in the absence of the membrane, which regulates the flow of electrolyte by increasing the speed of the slow moving ion and also by decreasing the speed of the fast moving ion. The electrical double layer at the membrane-solution interface seems to be the rate-determining step as suggested by Tien and Ting [27] for bilayer membranes.

ACKNOWLEDGEMENT

The authors are grateful to prof. W. Rahman, Head, Department of Chemistry, for providing necessary laboratory facilities.

REFERENCES

1 H.H. Uasing, Ann. N.Y. Acad. Sci., 137 (1966) 543.
2 W.S. Rehm, Ann. N.Y. Acad. Sci., 137 (1966) 591.

3 D.R. Dibona, M.M. Civan and A. Leaf., J. Membrane Biol., 1 (1969) 79.
4 P. Muller, D.O. Rudin, H.T. Tien and W.C. Wescott, Circulation, 26 (1962) 1167; Nature 194 (1962) 979; J. Phys. Chem., 67 (1963) 534.
5 N. Lakshminarayanaiah, Chem. Rev., 65 (1965) 491.
6 A.M. Liquori and C. Botre, Ric. Sci., 34 (8) (1964) 71; J. Phys. Chem., 71 (1967) 3765.
7 A.M. Liquori, L. Constantino and G. Segre, Ric. Sci., 36 (1966) 591.
8 R.H. Hays, J. Gen. Physiol., 51 (1968) 385.
9 F. de Korosy, J. Phys. Chem., 72 (1968) 2591.
10 N. Lakshminarayanaiah and F.A. Siddioi, Biophys. J., 11 (1971) 600, 617; ibid., 12 (1972) 540.
11 F.A. Siddiqi, N. Lakshminarayanaiah and M.N. Beg, J. Polym. Sci., A-1, 9 (1971) 2853; J. Polym. Sci., A-1, 9 (1971) 2869.
12 F.A. Siddiqi, M.N. Beg, S.P. Singh and A. Hao, Bull. Chem. Soc., Japan. 49 (1976) 2858, 2864; Electrochimica Acta., 22 (1977) 631, 638.
13 F.A. Siddiqi, M.N. Beg and S.P. Singh, J. Polymer Sci., 15 (1977) 959.
14 F.A. Siddiqi, M.N. Beg and P. Prakash, J. Electroanal. Chem., 80 (1977) 228.
15 M.N. Beg, F.A. Siddiqi and R. Shyam, Can. J. Chem., 55 (1977) 1680.
16 M. Goldsmith, D. Har and R. Damadian, J. Phys. Chem., 79 (1975) 842.
17 T. Teorell, Proc. Soc. Expti. Biol. Med., 33 (1935) 182; Proc. Nat. Acad. Sci. U.S., 21 (1935) 152.
18 K.H. Meyer and J.F. Sievers, Helv. Chim. Acta., 19 (1936) 649, 665, 987.
19 K. Sollner, J. Phys. Chem., 47 (1945) 171.
20 N. Lakshminarayanaiah, Transport Phenomena in Membranes, Academic Press, New York, (1969) 202–203.
21 K. Sollner and H.P. Gregor, J. Colloid Sci., 7 (1952) 37.
22 G. Schmid, Z. Elektrochem, 54 (1950) 424; ibid., 55 (1951) 229; ibid., 56 (1952) 181.
23 M. Yuasa, Y. Kobatake and H. Fujita, J. Phys. Chem., 72 (1968) 2871.
24 T. Ueda, H. Kamo, N. Ishida and Y. Kobatake, J. Phys. Chem., 76 (1972) 2447.
25 Noaki, Kamo, Masako and Y. Kobatake, J. Phys. Chem., 77 (1973) 92.
26 Y. Kobatake and Kamo, Prog. Poly. Sci., Japan., 5 (1975) 257.
27 H.T. Tien and H.P. Ting, J. Colloid Interface Sci., 27 (1968) 702.

ELECTROANALYTICAL CHEMISTRY AND INTERFACIAL ELECTROCHEMISTRY 147
Elsevier Sequoia S.A., Lausanne Printed in The Netherlands

STUDIES OF MEMBRANE PHENOMENA

II. DETERMINATION OF MEMBRANE POTENTIALS AND EVALUATION OF THE MEMBRANE FIXED CHARGE DENSITY AND PERMSELECTIVITY OF PARCHMENT-SUPPORTED SILVER IODIDE MEMBRANE

FASIH A. SIDDIQI AND SURENDRA PRATAP
Department of Chemistry, Aligarh Muslim University, Aligarh (India)

(Received February 6th, 1969)

INTRODUCTION

For the characterisation of the selectivity of ionic membranes, the electrical potentials arising across the ionic membrane have been measured by constructing a cell of the type

$$\text{Ref.electrode} \mid \underset{1}{\text{Solution}} \mid \text{Membrane} \mid \underset{2}{\text{Solution}} \mid \text{Ref.electrode}$$

the reference electrodes being the saturated calomels connected to the solutions by means of a KCl–agar bridge. The cell potential in this method gives directly the membrane potential. The calculation of the membrane potential and the theoretical approaches for it have been classified into three main groups: (*a*) the idealised theory of Teorell, Meyer and Sievers (TMS) and its refinements[1]; (*b*) the pseudo-thermodynamic approach and the treatment based on thermodynamics of irreversible processes[2] and (*c*) the kinetic approach[3].

In part I of these investigations, the electrochemical behaviour of the membrane was treated on the basis of TMS theory. In this communication the evaluation of Donnan potentials, diffusion potentials, membrane fixed charge density and permselectivity has been carried out on the basis of the TMS model of an ionic membrane.

EXPERIMENTAL

Preparation of the silver iodide membrane

The membrane was prepared as described in Part I[19].

Measurement of the membrane potential

The potential developed by setting up the concentration cell of the type described by Michaelis[4]

$$\text{SCE} \mid \underset{a_1}{\text{Solution}} \mid \text{Membrane} \mid \underset{a_2}{\text{Solution}} \mid \text{SCE}$$

$a_1 = 10a_2$

was taken as a measure of the membrane potential. The measurements were carried out using a Pye precision vernier potentiometer (No. 7568).

RESULTS AND DISCUSSION

The results of the membrane potential measurements may be discussed in terms of the theories put forward by Michaelis[4], Meyer and Sievers[5] and also by Teorell[6]. Michaelis held the view that the selective permeability and potential of the collodion membranes were due to preferential adsorption modifying the differential diffusion rates. Willis[7] extended this theory to cupric ferrocyanide, and Malik and Siddiqi[8] applied it to a large number of parchment-supported metal ferro- and ferricyanide membranes thus confirming the earlier view of Sollner[9] that the behaviour of collodion membrane is due to the surface charges fixed on the membrane matrix.

For the evaluation of membrane fixed charge density ($\omega\bar{x}$) by the potentiometric method, Teorell[6] and Meyer[10] have given a method which has been developed and reviewed by Lakshminarayaniah[11]. Recently, Altug and Hair[12] have given an ingenious and indirect method, which has also been developed on the lines of Teorell's model, for the evaluation of $\omega\bar{x}$.

The essential feature of the original fixed charged theory of Teorell[6] was the assumption that the overall membrane potential was composed of three potential jumps: two Donnan potentials at each solution–membrane interface (denoted by π_1 and π_2), and one residing inside the membrane, the internal potential or driving potential being denoted by $\phi_2-\phi_1$. The overall total membrane potential E_{calc} is thus given by:

$$E_{calc} = (\pi_1+\pi_2)+(\phi_2-\phi_1) \tag{1}$$

π_1 and π_2 have been calculated according to the equation:

$$\pi_1 = \frac{-RT}{F}\ln r_1 \tag{2(a)}$$

and

$$\pi_2 = \frac{RT}{F}\ln r_2 \text{ (for uni-univalent electrolytes)} \tag{2(b)}$$

where r_1 and r_2, the Donnan distribution ratios, are determined with the help of the equation

$$r = \left\{1+\left(\frac{\omega\bar{x}}{2a}\right)^2\right\}^{\frac{1}{2}} - \left(\frac{\omega\bar{x}}{2a}\right) \tag{3}$$

where a is the external solution concentration. The diffusion potential $\phi_2-\phi_1$ for uni-univalent electrolyte is given by:

$$\phi_2-\phi_1 = \frac{u-v}{u+v}\frac{RT}{F}\ln\left(\frac{a_1(r_1u+v/r_1)}{a_2(r_2u+v/r_2)}\right) \tag{4}$$

u and v being the cation and anion mobilities in the membrane. However, in the present calculations, these are assumed to be the same as in solution. Owing to the practical difficulty of measuring ionic activity in the membrane phase, concentrations have

been used in place of activities, as suggested by Altug and Hair[12].

In order to determine the fixed charge density of a parchment-supported silver iodide membrane, various values (*e.g.* -0.4 *N*, -0.1 *N*, etc.) were given to $\omega\bar{x}$ and for each value the total membrane potential was calculated for different concentrations of KCl using the above equations. The curves of total membrane potential *vs.* concentration were plotted for various $\omega\bar{x}$-values. At the same time, a curve was plotted between the experimentally determined membrane potential values for KCl and the concentrations of KCl (the concentration range being the same in the two cases). The fixed charge density $\omega\bar{x}$ is then the same as that of the theoretical curve which overlaps the experimental curve.

The values of the Donnan potential $(\pi_1 + \pi_2)$, the diffusion potential $(\phi_2 - \phi_1)$, and the total membrane potential E_{calc} for various concentrations of KCl (for various values of $\omega\bar{x}$) are given in Table 1A. The values of the observed membrane potential E_{obs} across the silver iodide membrane for various concentrations of KCl are given in Table 1B, (Fig. 1).

TABLE 1A

CALCULATED VALUES OF DONNAN POTENTIAL $(\pi_1 + \pi_2)$, DIFFUSION POTENTIAL $(\phi_2 - \phi_1)$ AND TOTAL MEMBRANE POTENTIAL E_{calc} ACROSS THE SILVER IODIDE MEMBRANE IN KCl OF VARIOUS CONCENTRATIONS, ASCRIBING VARIOUS VALUES TO $\omega\bar{x}$ (THE MEMBRANE FIXED CHARGE DENSITY) (AT 20°C)

$\omega\bar{x}/N$	Concns. $a_1/a_2/M$	$(\pi_1 + \pi_2)/mV$	$(\phi_2 - \phi_1)/mV$	E_{calc}/mV
−0.4	1/0.1	31.4	−0.74	30.66
	0.1/0.01	56.58	−0.05	56.53
	0.05/0.005	57.73	−0.01	57.72
	0.01/0.001	58.2	0.00	58.2
	0.001/0.0001	58.2	0.00	58.2
−0.1	1/0.1	10.89	−1.07	9.82
	0.1/0.01	46.21	−0.38	45.83
	0.05/0.005	53.3	−0.17	53.13
	0.01/0.001	57.85	0.00	57.85
	0.001/0.0001	58.2	0.00	58.2
−0.06	1/0.1	6.72	−1.1	5.62
	0.1/0.01	38.5	−0.58	37.92
	0.05/0.005	48.51	−0.32	48.19
	0.01/0.001	55.9	−0.12	55.78
	0.001/0.0001	58.2	0.00	58.2
−0.02	1/0.1	2.27	−1.12	1.15
	0.1/0.01	19.7	−0.96	18.74
	0.05/0.005	31.2	−0.75	30.45
	0.01/0.001	53.2	−0.17	53.03
	0.001/0.0001	58.2	0.00	58.2
−0.01	1/0.1	1.12	−1.28	−0.16
	0.1/0.01	10.89	−1.07	9.82
	0.05/0.005	19.68	−0.95	18.73
	0.01/0.001	46.25	−0.38	45.87
	0.001/0.0001	57.85	0.00	57.85

TABLE 1B

OBSERVED VALUES OF MEMBRANE POTENTIAL E_{obs} ACROSS THE SILVER IODIDE MEMBRANE IN KCl AT VARIOUS CONCENTRATIONS (AT 20 °C)

Concn. a_1, a_2	1 M 0.1 M	0.1 M 0.01 M	0.05 M 0.005 M	0.01 M 0.001 M	0.001 M 0.0001 M
Observed membrane potential E_{obs} (mV)	0.4	13.9	23.0	41.0	51.67

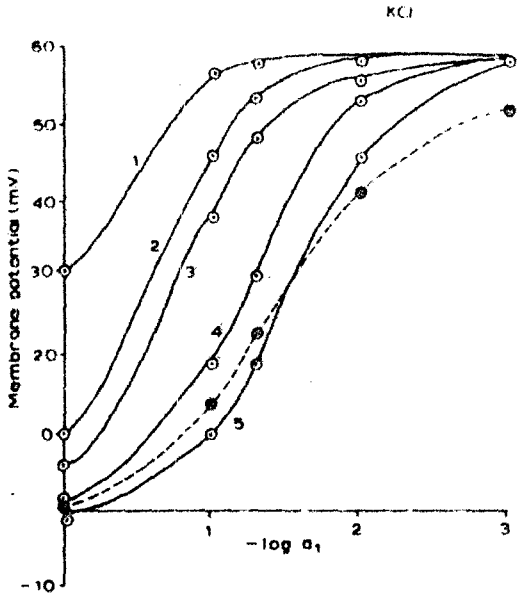

Fig. 1. Membrane potentials across silver iodide membrane in KCl of varying concns. (○) Calcd. values assuming $\omega\bar{x}$ equal to: (1) 0.4, (2) 0.1, (3) 0.06, (4) − 0.02, (5) − 0.01 N (●) Observed values (with dashed line).

The fixed charge density of the silver iodide membrane was thus found to be − 0.01 N. Assuming the same value for fixed charge density, the values of Donnan potentials, diffusion potentials and total membrane potentials were calculated for NaCl, LiCl and NH_4Cl at various concentrations. The calculated and observed values are given in Table 2 and shown in Figs. 2, 3 and 4.

A very good agreement between the observed and calculated values of membrane potential is observed in the case of KCl and NH_4Cl, thus showing that the behaviour of the silver iodide membrane is closely allied to Teorell's model. The agreement is only fair for NaCl but in the case of LiCl the deviation is quite marked. It should be noted that in our calculations we have assumed that the ionic mobilities in the membrane are the same as those in the free solution. The diffusion data in the literature show that the ion mobilities go through a considerable change in a charged phase, and hence apparent anionic mobilities (assuming cationic mobilities to be constant) were calculated as suggested by Willis[7].

The electrochemical nature of the membrane and its influence on the mobilities

TABLE 2

CALCULATED VALUES OF DONNAN POTENTIAL $(\pi_1+\pi_2)$, DIFFUSION POTENTIAL $(\phi_2-\phi_1)$ AND TOTAL MEMBRANE POTENTIAL E_{calc} (ASSUMING $\omega\bar{x}=-0.01$ N), AND THE OBSERVED VALUES OF MEMBRANE POTENTIAL E_{obs} ACROSS THE SILVER IODIDE MEMBRANE IN NaCl, LiCl AND NH_4Cl OF VARIOUS CONCENTRATIONS (AT 20°C)

Electrolyte	*Concns.* $a_1/a_2/M$	$(\pi_1+\pi_2)/mV$	$(\phi_2-\phi_1)/mV$	E_{calc}/mV	E_{obs}/mV
NaCl	1/0.1	1.12	−12.12	−11.0	−0.9
	0.1/0.01	10.89	−11.96	−1.07	8.20
	0.05/0.005	19.68	−10.99	8.69	20.11
	0.01/0.001	46.25	−4.8	41.45	40.75
	0.001/0.0001	57.85	−0.1	57.73	48.7
LiCl	1/0.1	1.12	−19.1	−17.98	0.5
	0.1/0.01	10.89	−19.22	−8.33	13.1
	0.05/0.005	19.68	−18.08	1.6	18.34
	0.01/0.001	46.25	−8.38	37.87	40.57
	0.001/0.0001	57.85	−0.22	57.63	47.75
NH_4Cl	1/0.1	1.12	−1.16	−0.04	−0.13
	0.1/0.01	10.89	−1.1	9.79	15.45
	0.05/0.005	19.68	−0.99	18.69	21.6
	0.01/0.001	46.25	−0.39	45.86	43.4
	0.001/0.0001	57.85	0.00	57.85	45.0

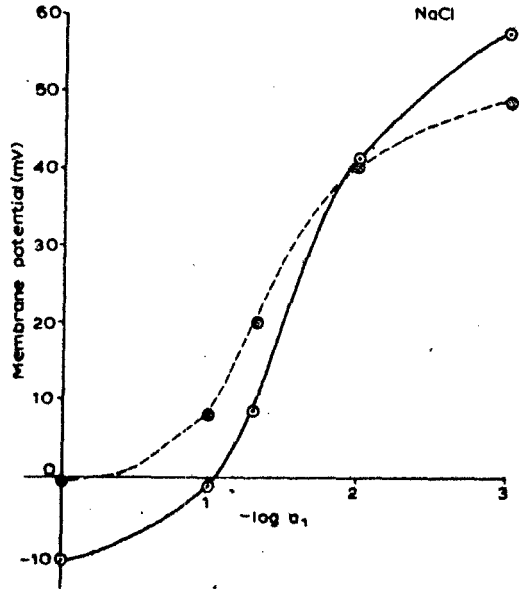

Fig. 2. Membrane potentials across silver iodide membrane in NaCl of varying concns. (⊙) Calcd. values assuming $\omega\bar{x}=-0.01$ N; (●) observed values.

of anions were also studied by calculating the mobility from the equation:

$$E_m=\frac{\frac{u}{z_+}-\frac{v}{z_-}}{u+v}\times\frac{RT}{nF}\ln\frac{f_1c_1}{f_2c_2}\qquad(E_m\text{ is the membrane potential})\qquad(5)$$

where the various terms have their usual meanings. This procedure has been used by Willis[7] in the case of a cupric ferrocyanide membrane, and Malik and Siddiqi[8] in the case of a large number of metal ferrocyanide and ferricyanide membranes. The apparent anionic mobilities were calculated over the concentration range 1 – 0.0001

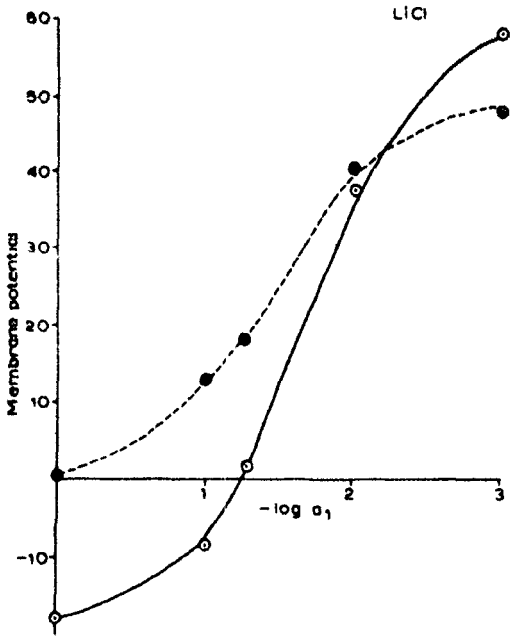

Fig. 3. Membrane potentials across silver iodide membrane in LiCl of varying concns. (⊙) Calcd. values assuming $\omega\bar{x} = 0.01$ N; (●) observed values.

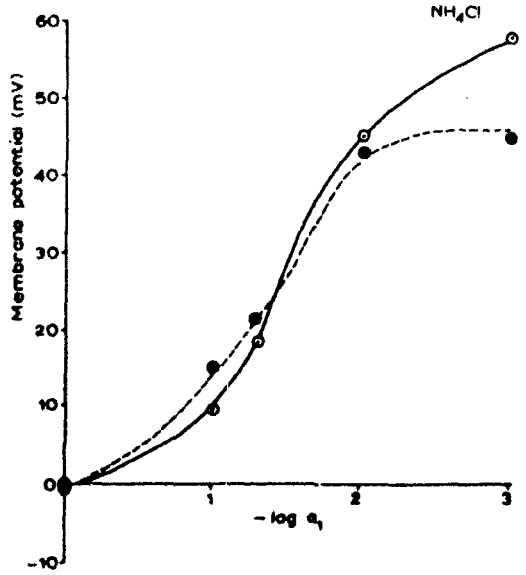

Fig. 4. Membrane potentials across silver iodide membrane in NH_4Cl of varying concns. (⊙) Calcd. values assuming $\omega\bar{x} = 0.01$ N; (●) observed values.

M, keeping $a_1/a_2 = 10$. The values of the mobility u for NH_4^+, K^+, Na^+, and Li^+ were taken to be those in free solution. The plots of log $1/a_1$ (where a_1 is the higher concentration) *vs.* apparent anion mobility for all the four electrolytes are shown in Fig. 6. The values of the transport numbers of cations t_+ were calculated from the equation:

$$t_+ = \frac{z_+ z_-}{z_+ + z_-}\left(\frac{E_m F}{RT \ln \frac{f_1 c_1}{f_2 c_2}}\right) + \frac{z_+}{z_+ + z_-} \tag{6}$$

for different electrolytes at various concentrations. The transport numbers of chloride

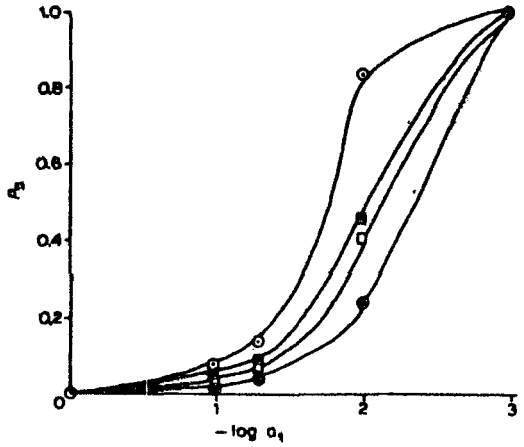

Fig. 5. Plots of P_a *vs.* log $1/a_1$ for various electrolytes. (⊙) NH_4Cl, (●) KCl, (□) NaCl, (■) LiCl.

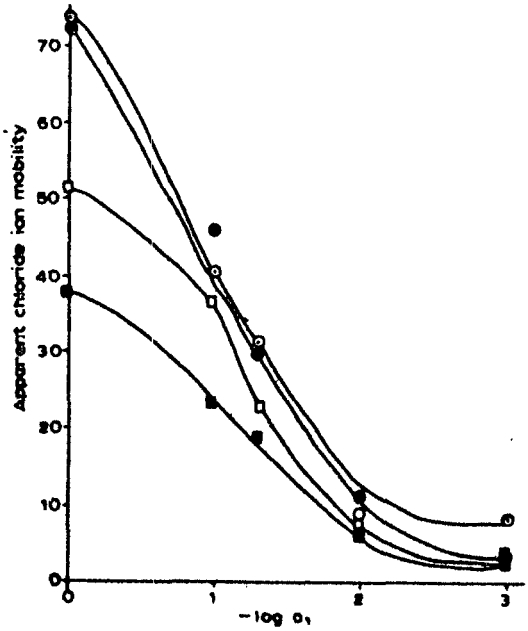

Fig. 6. Plots of apparent an ion mobility *vs.* log $1/a_1$ for various electrolytes. Designations as Fig. 5.

ion in an anionic membrane such as permionic ARX-44 were investigated by Clark *et al.*[13] They plotted t against $\bar{n}$ where $\bar{n}$ is the geometric mean of the concentrations of two solutions across the membrane. A similar procedure was adopted in the case of the membrane under investigation and log $\bar{n}$ was plotted against t_+ for different cations, the plots are shown in Fig. 7. From the Figure it is quite clear that the values of the transport numbers of cations continue to decrease with increase in concentration Jacobs[14] while using membranes of polymethacrylic acid in KOH solution over a wide concentration range found similar behaviour, *i.e.* t_+ decreased with increasing concentration of the electrolyte.

The permselectivity P_s[15] of the membrane is given by

$$P_s = \frac{t_+ - t_+}{1 - t_+} \tag{7}$$

where t_+ is the transport number in the membrane phase under highly idealized conditions of the TMS model 1 and is given by:

$$t_+ = \frac{E_m}{2E_{max}} + 0.5 \tag{8}$$

According to Spiegler *et al.*[16], the permselective materials are defined as the media which transfer certain types of ion in preference to others. Tolliday *et al.*[17] have reported that cupric ferrocyanide membrane behaves similarly in some respects to the electronegative membrane of Sollner. The values of P_s calculated from the above equations are plotted *vs* log 1 a_1 (see Fig. 5). The permselectivity P_s increases abruptly in the region log $1/a_1$ → 1.5 2.5. The values of t_+, t_+, P_s and apparent anion mobility for various concentrations of different electrolytes are summarized in Table 3.

The chief results of all these investigations show that the membrane potential can be determined with reasonable accuracy, and that in the case of a dilute solution it is somewhat closer to the maximum value (highest value of t_+ and therefore greatest

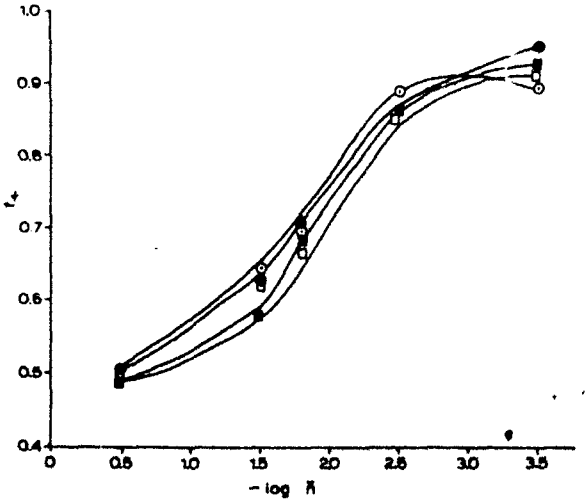

Fig. 7. Plots of t_+ *vs.* log $1/\bar{n}$ for various electrolytes. Designations as Fig. 5.

TABLE 3

VALUES OF t_-, t_+, P_s AND APPARENT ANION MOBILITY FOR VARIOUS ELECTROLYTES AT DIFFERENT CONCENTRATIONS FOR SILVER IODIDE MEMBRANE (AT 20°C)

Electrolyte	*Concns.* $a_1/a_2/M$	t_-	t_+	P_s	*Apparent anion mobility*/* $cm^2\Omega^{-1}equiv.^{-1}$
NH_4Cl	1/0.1	0.498	0.498	0.0	73.7
	0.1/0.01	0.643	0.671	0.0784	40.7
	0.05/0.005	0.698	0 74	0.139	31.6
	0.01/0.001	0.887	0.982	0.84	9.3
	0.001/0.0001	0.893	1	1	8.8
KCl	1/0.1	0.5038	0.504	0.0004	72.3
	0.1/0.01	0.628	0.634	0.0161	43.6
	0.05/0.005	0.709	0.722	0.0446	30.2
	0.01/0.001	0.863	0.896	0.241	11.7
	0.001/0.0001	0.9507	1	1	3.8
NaCl	1/0.1	0.491	0.491	0.00	51.6
	0.1/0.01	0.575	0.584	0.02	37.0
	0.05/0.005	0.682	0.706	0.074	23.3
	0.01/0.001	0.86	0.918	0.411	8.1
	0.001/0.0001	0.9248	1	1	4.1
LiCl	1/0.1	0.504	0.505	0.002	38.1
	0.1/0.01	0.620	0.637	0.0447	23.6
	0.05/0.005	0.667	0.692	0.075	19.4
	0.01/0.001	0.859	0.924	0.461	6.4
	0.001/0.0001	0.917	1	1	3.5

* Relative to free solution mobility of K^+ being taken as 73.5.

value of P_s). With more concentrated solutions this is not so, the membrane potential is progressively smaller than the maximum value. This is readily explained in terms of a decrease in membrane selectivity with increasing concentration of co-ions and diffusion of electrolyte through the membrane. All ion exchange membranes lose permselectivity with increase in concentrations of the solutions they separate. The parchment-supported silver iodide membrane shows high selectivity in the dilute range. In some ways this membrane is similar to an anion exchange membrane. This view is further confirmed by the observation of Heymann and Rabinov[18] that, like purified cellulose, parchment also contains exchangeable cations (and therefore acid groups) as part of its structure which may account for its negative charge. The exchangeable cations of this structure will be free to move in the pores and give an apparent increase in the cation mobility and therefore a decrease in the anion mobility (Fig. 6). Within the pores there will be a diffuse ionic atmosphere from the charged wall. The thickness of this atmosphere depends upon electrolyte concentration; in very dilute solutions of the electrolyte which are in contact with the membrane, the thickness becomes so great that only cations are present in the pores and the membrane is cation-permeable only (high value of P_s). As the concentration increases, the thickness of the ionic atmosphere decreases and anions will also be present; at high enough concentrations the ionic atmosphere will be negligible in comparision to the pore radius and the effect of the membrane vanishes.

Spiegler *et al.*[16] working with ion-exchange resin systems have explained the loss in permselectivity as due to increasing penetration of anions and cations into cation and anion exchange resins, respectively, and to the water transport. If the solutions are concentrated, the membrane acts as an inert material and the potential difference between the two solutions approaches the liquid junction potential value.

ACKNOWLEDGEMENT

The authors are grateful to Dr S. M. F. Rahman, Head of the Chemistry Department, for providing facilities for carrying out these investigations.

SUMMARY

Membrane potentials across parchment-supported silver iodide membrane in NH_4Cl, KCl, NaCl and LiCl solutions of various concentrations have been determined to evaluate fixed charge density ($\omega\bar{x}$) and permselectivity of the membrane; $\omega\bar{x}$ of silver iodide membrane has been found to be -0.01 *N*. The effect of concentration on transport numbers, apparent anion mobility and permselectivity has been studied. The results have been discussed in the light of the TMS theory.

REFERENCES

1 K. H. Meyer and J. F. Sievers, *Helv. Chim. Acta*, 19 (1936) 649, 665, 987. T. Teorell, *Proc. Soc. Expt. Biol. Med.*, 33 (1935) 282; *Proc., Nat. Acad. Sci. U.S.*, 21 (1935) 152; *Z. Elektrochem.*, 55 (1951) 460; *Discussions Faraday Soc.*, 21 (1956) 22.
2 G. Scatchard, *J. Am. Chem. Soc.*, 75 (1953) 2883; *Discussions Faraday Soc.*, 21 (1956) 30; G. J. Hills, P. W. M. Jacobs and N. Lakshminarayaniah, *Proc. Roy. Soc., (London)*, A 262 (1961) 257; Y. Kobatake, *J. Chem. Phys.*, 28 (1958) 146; A. J. Staverman, *Trans. Faraday Soc.*, 48 (1952) 176.
3 M. Nagasawa and I. Kagawa, *Discussions Faraday Soc.*, 21 (1956) 52; M. Nagasawa and Y. Kobatake, *J. Phys. Chem.*, 56 (1952) 1017.
4 L. Michaelis, *Kolloid-Z*, 62 (1933) 1; Michaelis and Fujita, *Biochem. Z.*, 142 (1923) 398; *Z. Physik. Chem.*, 110 (1924) 266.
5 K. H. Meyer and J. F. Sievers, *Helv. Chim. Acta*, 19 (1936) 649.
6 T. Teorell, *Proc. Soc. Expt. Biol. Med.*, 33 (1935) 282; *Z. Elektrochem.*, 55 (1951) 460; *Proc. Natl. Acad. Sci. U.S.*, 21 (1935) 152; *J. Gen. Physiol.*, 21 (1937) 107.
7 G. M. Willis, *Trans. Faraday Soc.*, 38 (1942) 172.
8 W. U. Malik and F. A. Siddiqi, *Proc. Indian Acad. Sci.*, A 56 (1962) 206; *J. Colloid. Sci.*, 18 (1963) 161; *Bull. Chem. Soc. Japan*, 40 (1967) 8, 1741.
9 K. Sollner, *J. Phys. Chem.*, 49 (1945) 47; *J. Electrochem. Soc.*, 97 (1950) 139 C; *Ann. N.Y. Acad. Sci.*, 57 (1953) 177.
10 K. H. Meyer, *Trans. Faraday Soc.*, 33 (1937) 1073.
11 N. Lakshminarayaniah, *J. Appl. Polymer Sci.*, 10 (1966) 1687.
12 I. Altug and M. L. Hair, *J. Phys. Chem.*, 72 (1968) 599.
13 J. T. Clark, J. A. Marinsky, W. Juda, N. W. Rosenberg and S. Alexander, *J. Phys. Chem.*, 56 (1952) 100.
14 P. W. M. Jacobs, *Discussions Faraday Soc.*, 21 (1956) 198.
15 A. G. Winger, G. W. Bodamen and R. Kunin, *J. Electrochem. Soc.*, 100 (1953) 178.
16 K. S. Spiegler, R. L. Yoest and M. R. J. Wyllie, *Discussions Faraday Soc.*, 21 (1956) 174.
17 J. D. Tolliday, E. F. Woodo and E. J. Hartung, *Trans. Faraday Soc.*, 45 (1949) 148.
18 E. Heymann and G. Rabinov, *J. Phys. Chem.*, 47 (1943) 655.
19 F. A. Siddiqi and S. Pratap, *J. Electroanal. Chem.*, 23 (1969) 137.

CHAPTER 7

APPLICATION OF IRREVERSIBLE THERMODYNAMICS METHOD FOR CHARGE DENSITY EVALUATION

JOURNAL OF POLYMER SCIENCE: Polymer Chemistry Edition VOL. 15, 959-972 (1977)

Studies with Model Membranes. X. Evaluation of the Thermodynamically Effective Fixed Charge Density and Permselectivity of Mercuric and Cupric Iodide Parchment-Supported Membranes

FASIH A. SIDDIQI, MOHAMMAD N. BEG, and SURENDRA P. SINGH,
Physical Chemistry Division, Department of Chemistry, Aligarh Muslim University, Aligarh (U.P.), India

Synopsis

Thermodynamically effective fixed charge densities of mercuric and cupric iodide parchment supported membranes were estimated by methods of Teorell, Meyer, and Sievers; Altug and Hair; and the most recent one of Kobatake and co-workers based on the thermodynamics of irreversible processes. The two limiting forms of Kobatake's equation for dilute and concentrated ranges gave identical values of charge densities. It is interesting to note that these two values of limiting cases are closer to the Teorell-Meyer-Sievers and Altug-Hair values. The theoretical predictions for membrane potential by the Kobatake equation were borne out quite satisfactorily by experimental results obtained with both the membranes.

INTRODUCTION

In order to understand the mechanism of transport through biological membranes, we have been carrying out extensive investigations on (a) parchment-supported membranes[1-11] which, in some formal aspects at least, according to Teorell,[12] behaved exactly like gastric mucosal membrane; and (b) asymmetric polymeric membranes[13-16] which mimic some of the properties of nerve cells.[17,18] Teorell's finding, that electrolyte transport processes in the stomach could be handled by something similar to Fick's diffusion law and that Nernst-Planck formulae for electrical potentials were applicable, has encouraged us to proceed further with the study of parchment membranes. This paper deals with the evaluation of the thermodynamically effective fixed charge density of mercuric and cupric iodide parchment-supported membranes by using well-accepted theories of Teorell, Meyer, and Siever;[19,20] Altug and Hair;[21] and the most recent one of Kobatake et al.[22-27] based on the thermodynamics of irreversible processes.

EXPERIMENTAL

Preparation of Membranes

The membranes of mercuric and cupric iodide were prepared by the method of interaction suggested by Weiser.[28] First, parchment paper was soaked in

distilled water for 2 hr and then tied carefully to the flat mouth of a beaker containing 0.2*M* mercuric chloride. This was suspended for about 72 hr in a 0.2*M* solution of potassium iodide. The two solutions were interchanged later and kept for another 72 hr. The mercuric iodide membrane thus prepared was washed with deionized water for the removal of free electrolyte. A similar procedure was adopted for the preparation of cupric iodide membrane by taking 0.2*M* solutions of cupric chloride and potassium iodide.

Measurement of Membrane Potential

The potential developed by setting up a concentration cell of the type described by Michaelis,[29] Sollner and Gregor,[30] and Marshall and Ayers:[31]

$$\text{S.C.E.} \mid \underset{C_1}{\text{Solution}} \mid \text{Membrane} \mid \underset{C_2}{\text{Solution}} \mid \text{S.C.E.}$$

$$C_2 = 10C_1$$

was taken as a measure of membrane potential. The measurements were carried out at 25°C by using a Pye precision vernier potentiometer (No. 7568).

THEORY

The earliest effort towards developing a membrane model was made by Michaelis,[32] who considered that the charge on the membrane was due to the adsorption of one kind of ion. Later, Teorell, Meyer, and Sievers (TMS)[19,20] developed a theory of membrane with charges fixed in the lattice. In the TMS theory there is an equilibrium process at each solution–membrane interface which has a formal analogy with the Donnan equilibrium. In addition, there is an internal salt-diffusion potential which was first represented by the Henderson equation and later by the more nearly correct Planck expression.[33] Further assumptions of TMS theory are (a) all single ion activity coefficients to be unity; (b) the cation and anion mobilities and fixed charge concentration are constant throughout the membrane phase and are independent of the salt concentration; and (c) the transference of water may be neglected. The implications of these assumptions have been discussed by Hills, Jacobs, and Lakshminarayanaiah.[34]

The membrane potential E_m in millivolts according to TMS theory, applicable to highly idealized system at 25°C is given by

$$E_m = 59.2 \log \left[\frac{C_1(\sqrt{4C_2^2 + \bar{X}^2} + \bar{X})}{C_2(\sqrt{4C_1^2 + \bar{X}^2} + \bar{X})} \right] + \bar{U} \log \frac{\sqrt{4C_1^2 + \bar{X}^2} + \bar{X}\bar{U}}{\sqrt{4C_2^2 + \bar{X}^2} + \bar{X}\bar{U}} \quad (1)$$

where

$$\bar{U} = (\bar{u} - \bar{v})/(\bar{u} + \bar{v}) \quad (2)$$

$\bar{u}$ and $\bar{v}$ are the mobilities of the cation and the anion, respectively, in the membrane phase (overbar refer to the parameters to the membrane phase), C_1 and C_2 are the concentrations of the electrolyte solutions on either side of the membrane, and $\bar{X}$ is the charge density expressed in equivalents/liter of imbibed solution in the membrane phase.

Altug and Hair[21] have given an ingenious and indirect method which has been

developed on the lines of Teorell's model for the evaluation of membrane charge density $\omega\bar{X}$, where $\bar{X}$ represents the number of ionized sites per unit volume and $\omega = \pm 1$, depending on the nature of the charged sites. According to Teorell's model, the behavior of a charged membrane in an electrolyte solution can be characterized in terms of ionic mobilities, concentrations, and the fixed charge in the membrane.

According to the fixed-charge theory of Teorell, the overall membrane potential is composed of three potential jumps: two Donnan potentials at each solution–membrane interface (denoted by π_1 and π_2) and one residing inside the membrane, the internal potential or driving potential being denoted by $\phi_2 - \phi_1$. The overall total membrane potential E_{cal} is thus given by

$$E_{cal} = (\pi_1 + \pi_2) + (\phi_2 - \phi_1) \tag{3}$$

where

$$\pi_1 = -(RT/F) \ln r_1 \tag{4}$$

and

$$\pi_2 = (RT/F) \ln r_2 \tag{5}$$

Here r_1 and r_2, the Donnan distribution ratios, are determined with the help of eq. (6):

$$r = [1 + (\omega\bar{x}/2a)^2]^{1/2} - (\omega\bar{x}/2a) \tag{6}$$

where a is the external solution activity. The diffusion potential $(\phi_2 - \phi_1)$ for 1:1 valent electrolyte is given by

$$\phi_2 - \phi_1 = \left(\frac{u - v}{u + v}\right) \frac{RT}{F} \ln \left[\frac{a_1(r_1u + v/r_1)}{a_2(r_2u + v/r_2)}\right] \tag{7}$$

where u and v are the cationic and anionic mobilities in the membrane. However, in the present calculations, these are assumed to be the same as in bulk solution. Subscripts 1 and 2 refer to the solution on each side of the membrane. The use of concentration, rather than activities is an assumption based on the practical difficulty of measuring ion activites in a membrane phase as suggested by Altug and Hair.[21] On substituting these values in eq. (3), the final expression is given by eq. (8):

$$E_{cal} = \left(\frac{u - v}{u + v}\right) \frac{RT}{F} \ln \left[\frac{a_1(r_1u + v/r_1)}{a_2(r_2u + v/r_2)}\right] + \frac{RT}{F} \ln \frac{r_2}{r_1} \tag{8}$$

Kobatake et al. (22) derived eq. (9) for the electric current density I_c, relative to the frame of reference fixed to the membrane, using the basic flow equations provided by the thermodynamics of irreversible processes:

$$I_c = -F(l_+C_+ + l_-C_-)(d\phi/dx) - RT[l_+C_+(d \ln a_+/dx) - l_-C_-(d \ln a_-/dx)] + F(C_+ - C_-)U_m \tag{9}$$

Here l_+ and l_- are molar mobilities of $+ve$ and $-ve$ ions defined in terms of the mass fixed frame of reference, U_m is the velocity of the local center of mass, ϕ is the electric potential, C_+ and C_- are concentrations of $+ve$ and $-ve$ ions in moles per cubic centimeter of solution, a_+ and a_- are activities of positive and negative ions in moles per cubic centimeter of solution, R is the molar gas con-

stant, T is the absolute temperature of the system, and F is the Faraday constant.

For the evaluation of U_m, the viscous force acting on 1 cm^3 of solution in the membrane is represented by $-(1/K)U_m$, where K is a constant which is considered to depend on the viscosity of the solution and the structural details of the polymer network of which the membrane is composed. The same volume of solution undergoes an electric force which is represented by

$$-F(C_+ - C_-)(d\phi/dx) \tag{10}$$

In the steady state, the sum of these two forces is zero, so that

$$U_m = -KF(C_+ - C_-)(d\phi/dx) \tag{11}$$

Kobatake et al. have considered a membrane which is ionized negatively with a charge density θ (in mole/cm^3); then the requirement that the electric neutrality must be realized in any element of the membrane gives the relation

$$C_+ - C_- = \theta \tag{12}$$

Since in the system considered here no electric field is applied externally across the membrane, no net charge is transported from one side of the membrane to the other. This means that I_c must be zero at a cross section of the membrane. On substituting eqs. (11) and (12) into eq. (9), putting I_c equal to zero, and solving for $d\phi/dx$, the expression (13) is obtained:

$$\frac{d\phi}{dx} = \frac{-(RT/F)[l_+(C_- + \theta)(d \ln a_+/dx) - l_-C_-(d \ln a_-/dx)]}{(l_+ + l_-)C_- + l_+\theta + KF\theta^2} \tag{13}$$

To proceed further, the activities a_+ and a_- must be known as function of C_-.

Assumptions for a_+ and a_-

Kobatake et al. have assumed the following relations:

$$a_+ = C_-$$
$$a_- = C_- \tag{14}$$

and

$$\nu_+ = C_-/(C_- + \theta)$$
$$\nu_- = 1 \tag{15}$$

Here ν_+ and ν_- are the activity coefficients of $+ve$ and $-ve$ ions in the membrane.

Equation for Membrane Potential

With eqs. (14), (15) assumed for a_+ and a_-, eq. (13) becomes

$$\frac{d\phi}{dx} = -\left(\frac{RT}{F}\right)\frac{(l_+ - l_-)C_- + l_+\theta}{[(l_+ + l_-)C_- + l_+\theta + KF\theta^2]C_-}\left(\frac{dC}{dx}\right) \tag{16}$$

When the bulk solution on both sides of the membrane is vigorously stirred, no potential gradient is set up, so that the desired membrane potential $\Delta\phi$ is obtained by integrating $d\phi/dx$ over the thickness of the membrane. The final expression for the membrane potential is given by eq. (17):

$$\Delta\phi = -\left(\frac{RT}{F}\right)\left[\frac{1}{\beta}\ln\frac{C_2}{C_1} - \left(1+\frac{1}{\beta}-2\alpha\right)\times\ln\left(\frac{C_2+\alpha\beta\theta}{C_1+\alpha\beta\theta}\right)\right] \tag{17}$$

where

$$\alpha = l_+/(l_+ + l_-) \tag{18}$$

$$\beta = 1 + (KF\theta/l_+) \tag{19}$$

and the parameters have been assumed to be independent of salt concentration.

Kobatake et al.[22] have derived two useful limiting forms of eq. (17). When C_2 becomes sufficiently small with ν fixed, eq. (17) may be expanded to give eq. (20):

$$|\Delta\phi_r| = \frac{1}{\beta}\ln\nu - \frac{\nu-1}{\alpha\beta\nu}\left(1+\frac{1}{\beta}-2\alpha\right)\frac{C_2}{\theta}+\ldots \tag{20}$$

where

$$\Delta\phi_r = F\Delta\phi/RT \tag{21}$$

It has also been shown by Kobatake et al. that at a fixed ν, the inverse of an apparent transference number t_{app} for the co-ion species in a negatively charged membrane is proportional to the inverse of the concentration C_2 in the region of high salt concentration. Here t_{app} is defined by the relation [eq. (22)]:

$$|\Delta\phi_r| = (1-2t_{\text{app}})\ln\nu \tag{22}$$

Substituting for $\Delta\phi$ from eq. (17) and expanding the resulting expression for $1/t_{\text{app}}$ in powers of $1/C_2$ gives eq. (23):

$$\frac{1}{t_{\text{app}}} = \frac{1}{(1-\alpha)} + \frac{(1+\beta-2\alpha\beta)(\nu-1)\alpha}{2(1-\alpha)^2\ln\nu}\left(\frac{\theta}{C_2}\right)+\ldots \tag{23}$$

Kobtake et al. developed another theory for the evaluation of charge density of membranes.[27] In this theory both the activity coefficients and mobilities of small ions in charged membranes can be expressed by the expressions [eqs. (24) and (25)]:

$$\nu_+ = \nu_+^\circ(C_- + \phi X)/(C_- + X)$$

$$\nu_- = \nu_-^\circ \tag{24}$$

$$u_+ = u_+^\circ(C_- + \phi X)/(C_- + X)$$

$$u_- = u_-^\circ \tag{25}$$

Here ν_i, u_i, ν_i°, and u_i° ($i = +, -$) stand for the activity coefficient and mobility of ions species i in the membrane and in the bulk solution, respectively. C_- and X are the concentration of anion adsorbed in the membrane (in mole/liter of water in the membrane), and the stoichiometric concentration of charges fixed in the membrane. According to the convention suggested by Guggenheim,[35]

ν_+^* can be equated with ν_-^* for 1:1 electrolyte, and they are replaced by the mean activity coefficient $\nu_\pm^*$ of the electrolyte component. In eq. (24), ϕ represents the fraction of counterions in the unbound form, i.e., excluding those tightly bound to the polymer skeleton constituting the membrane. ϕX is referred to as the thermodynamically effective fixed charge density of the membrane.

Consider a system in which a negatively charged membrane is immersed in an electrolyte solution of concentration C. Under this condition, the Donnan equilibrium for small ions holds between the membrane phase and the solution. Then we have

$$(\nu_\pm^*)^2 C^2 = \nu_+ C_+ \nu_- C_- \tag{26}$$

The mass fixed transference number of anion in the membrane, τ_-, is defined by

$$\tau_- = u_- C_- / (u_+ C_+ u_- C_-) \tag{27}$$

Introducing eqs. (24), (25), and (26) into eq. (27) together with the electrical neutrality condition, i.e., $C_+ = C_- + X$ we obtain

$$\tau_- = 1 - \alpha \frac{(4\xi^2 + 1)^{1/2} + 1}{(4\xi^2 + 1)^{1/2} + (2\alpha - 1)} \tag{28}$$

where

$$\xi = C/\phi X \tag{29a}$$

and

$$\alpha = u_+^*/(u_+^* + u_-^*) \tag{29b}$$

On the other hand, the apparent transference number of anion in the membrane, t_{app} is defined from the observed membrane potential $\Delta\phi$ by the Nernst equation:

$$\Delta\phi = -(RT/F)(1 - 2t_{app}) \ln (C_2/C_1) \tag{30}$$

Here C_1 and C_2 are the concentration of the external solution on the two sides of the membrane, and R, T, and F have their usual thermodynamic meaning. It has been found by Kobatake et al.[26] that the difference between τ_- and t_{app} was less than 2% in the wide range of salt concentration, when the averaged concentration $(C_1 + C_2)/2$ was replaced by C. Therefore, if we replace τ_- by t_{app}, and C by $(C_1 + C_2)/2$, eq. (28) is applicable even when the concentration on the two sides of the membrane are different. Rearrangement of eq. (28) leads to:

$$\frac{1}{(4\xi^2 + 1)^{1/2}} = \frac{1 - t_{app} - \alpha}{\alpha - (2\alpha - 1)(1 - t_{app})} \equiv P_s \tag{31}$$

Here P_s is a measure of permselectivity of the m mbrane–electrolyte system.

RESULTS AND DISCUSSION

The membrane potential data obtained with each of the two parchment-supported membranes using various 1:1 electrolytes, are plotted as a function of log $[(C_1 + C_2)/2]$ while the ratio $\nu = C_2/C_1$ fixed at 10. These plots are shown in Figure 1.

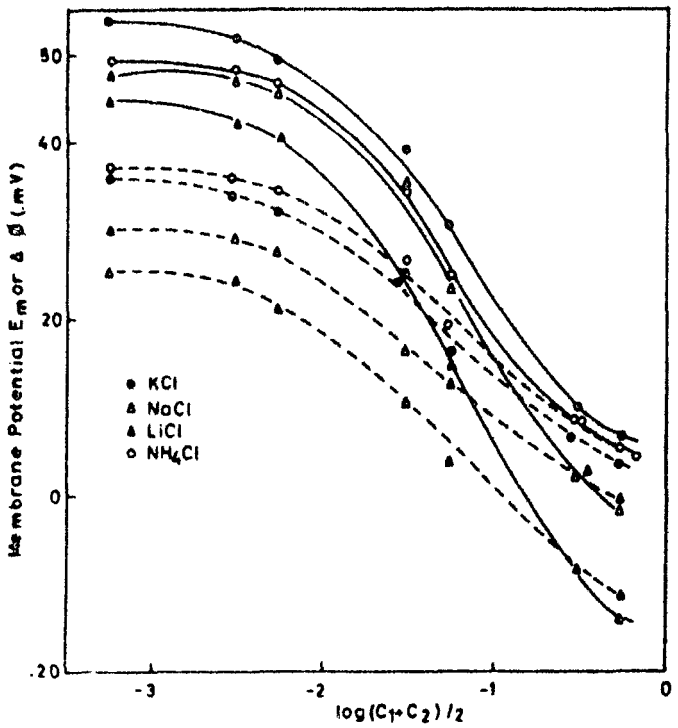

Fig. 1. Plots of observed potential (E_m or $\Delta\phi$) against log $[(C_1 + C_2)/2]$ for various electrolytes with (A) mercuric iodide ( ) and (B) cupric iodide (- -) membranes.

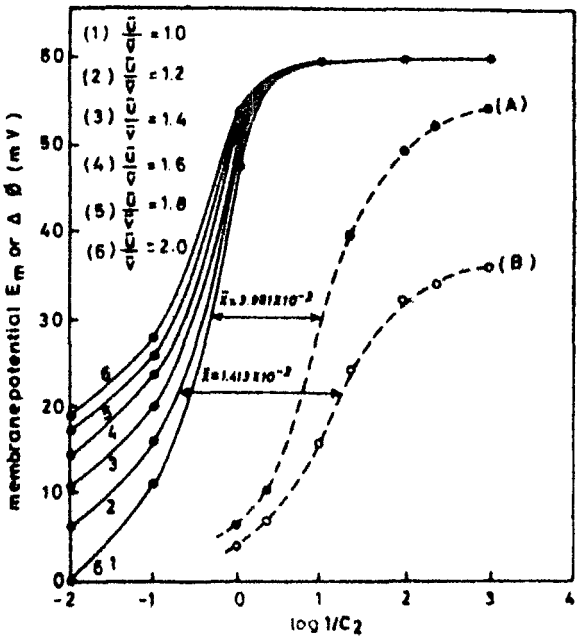

Fig. 2. Evaluation of membrane charge density $\bar{X}$ and mobility ratio $\bar{u}/\bar{v}$ in the membrane phase: (●) different curve for different mobility ratios; observed value of E_m or $\Delta\phi$ for (A) mercuric iodide and (B) cupric iodide membrane for KCl electrolyte plotted against log $1/C_2$.

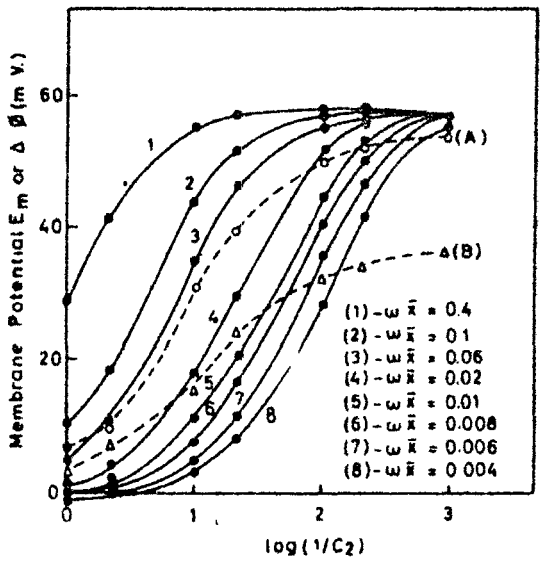

Fig. 3. Plots of membrane potential across (*A*) mercuric iodide (- -O- -) and (*B*) cupric iodide (- Δ -) for KCl electrolyte of varying concentration for fixed charged density against log $1/C_2$ (observed value with broken line).

In the method of Teorell, Meyer, and Siever, the fixed charge $\overline{X}$ is expressed in equivalents/liter and the cation-to-anion mobility ratio in the membrane phase by $\overline{u}/\overline{v}$. For the evaluation of these parameters for the simple case of 1:1 electrolyte and a membrane carrying a net negative charge of unity ($\overline{X} = 1$), the theoretical concentration potentials E_m existing across the membrane were calculated as a function of C_2, the ratio ν being kept at a constant value of 10, for different mobility ratios by using eq. (1). The set of curves on the left in Figure 2 are the theoretical membrane potential curves drawn as a function of $-\log C_2$,

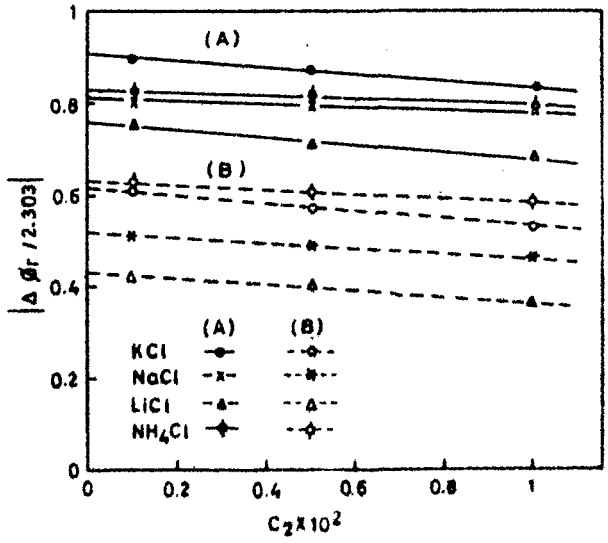

Fig. 4. Plots of $|\Delta\phi_r/2.303|$ vs. $C_2 \times 10^2$ for various electrolytes with (*A*) mercuric iodide (—) and (*B*) cupric iodide (- -) membranes.

TABLE I
Values Derived for the Membrane Parameters $\overline{X}$ and $(\bar{u}/\bar{v})$

Electrolyte	Mercuric iodide		Cupric iodide	
	$\overline{X} \times 10^3$, equiv/l.	$(\bar{u}/\bar{v})$	$\overline{X} \times 10^3$, equiv/l.	$(\bar{u}/\bar{v})$
KCl	3.981	1.0	1.413	1.2
NaCl	3.162	1.0	1.208	1.4
LiCl	3.242	1.2	1.112	1.2
NH_4Cl	3.821	1.0	1.328	1.2

while the observed membrane potential values for both mercuric iodide and cupric iodide membranes with KCl electrolyte are shown by the right-hand curves (*A* and *B*) in the same graph. The experimental curve for any given membrane was shifted horizontally and ran parallel to one of the theoretical curves. The extent of this shift gave log $\overline{X}$ and the parallel theoretical curve gave the value for $(\bar{u}/\bar{v})$. The experiment curves (*A*) and (*B*) were found to coincide approximately with the theoretical curves having mobility ratios 1 and 1.2, respectively. Table I gives the values of $\overline{X}$ and $(\bar{u}/\bar{v})$ derived in this way for both membranes with different electrolytes.

This method gave satisfactory result for the fixed charge-density evaluation, the values of which are found to be low and hence very difficult to determine by the usual exchange reaction. This technique has been used by Kumins and London to estimate the capacity of thin polymer membranes of poly(vinyl chloride) and poly(vinyl acetate). It has also been used by Baxter[36] to determine the charge on keratin and by Lakshminarayaniah[37] and Siddiqi[1-11] to evaluate the fixed charge on thin parlodion- and parchment-supported membranes.

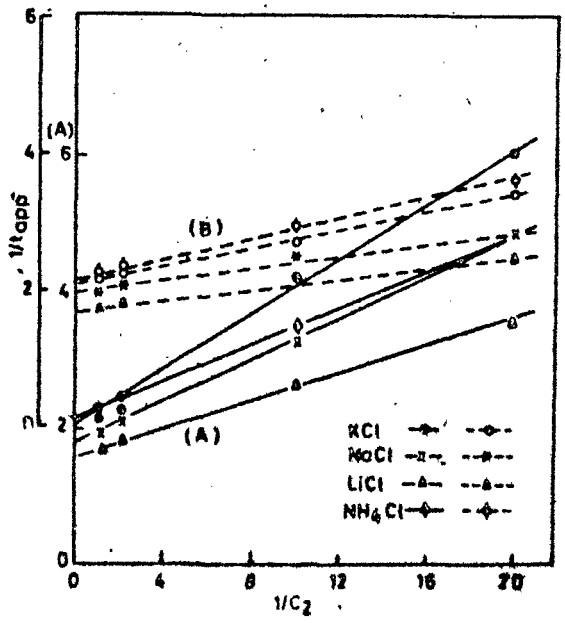

Fig. 5. Plots of $1/t_{app}$ against $1/C_2$ for various electrolytes with (*A*) mercuric iodide (——) and (*B*) cupric iodide (- -) membranes.

TABLE II
Comparison of Charge Density by Different Methods for KCl

Membrane	TMS $\bar{X}$	Altug and Hair $\bar{X}$	Kobatake[a] θ	Kobatake[a] ϕX
Mercuric iodide	3.981×10^{-2}	2.0×10^{-2}	3.8×10^{-2}	7.943×10^{-2}
Cupric iodide	1.413×10^{-2}	1.0×10^{-2}	1.7×10^{-2}	2.113×10^{-2}

[a] θ = Slope $[2(1-\alpha)^2 \ln \nu]/[(1+\beta-2\alpha\beta)(\nu-1)\alpha]$; ϕX from graph of P_s vs. log $[(C_1+C_2)/2]$.

In a modification of this type of plot, Altug and Hair[19] evaluated $\bar{X}$ for glass membranes, choosing the solution values for $\bar{u}$ and $\bar{v}$. In this method, a value of $\bar{X}$ was assumed and the distribution ratios r_1 and r_2 were calculated with the help of equations (3)–(8) for the given electrolyte concentrations C_1 and C_2. The theoretical membrane potentials are then calculated from equations (3)–(8) for the concentration range 1.0 to 1.0×10^{-4}. By following algebraic procedure, a series of theoretical curves were obtained for different $\bar{X}$ values for KCl and are shown by solid lines in Figure 3. At the same time observed potential values for KCl in the same concentration range for both the membranes are also plotted in Figure 3. The theoretical curve which coincided with the experimental curve gave the value for $\bar{X}$ which is given in Table II. The fixed charge density of mercuric iodide and cupric iodide membranes are found to be 2.0×10^{-2} and 1.0×10^{-2} equiv/l., respectively.

For the evaluation of the thermodynamically effective fixed charge density by the method of Kobatake et al., the following procedure was adopted.

Equation (20) indicates that a value of β and a relation between α and θ can be obtained by evaluating the intercept and the initial slope of a plot of $|\Delta\phi_r|$ against C_2. Figure 4 illustrates plots of $|\Delta\phi_r|$ versus C_2 in the region of low concentration that were determined for various electrolytes with both membranes. The value of intercept is equal to $(1/\beta) \ln \nu$, from which β is evaluated. The values are given in Table III.

Equation (23) indicates that the intercept of a plot of $1/t_{app}$ against $1/C_2$ at fixed ν allows the values of α to be determined, which are shown in Figure 5 for both membranes with various electrolytes. The value of the intercept is equal to $1/(1-\alpha)$, from which α is evaluated. The values are given in Table III.

For the evaluation of θ, there are two limiting cases.

In the dilute range ($C = 1.0 \times 10^{-3}$ to $1.0 \times 10^{-2} N$) the slope of eq. (20) is given by

$$\frac{\nu-1}{\alpha\beta\nu}\left(1+\frac{1}{\beta}-2\alpha\right)\frac{1}{\theta}$$

TABLE III
Values of Parameters α, β, and θ for Various Membrane–Electrolyte Systems at $\nu = 10$

Electrolyte	Mercuric iodide membrane α	β	θ	Cupric iodide membrane α	β	θ
KCl	0.55	1.09	3.8×10^{-2}	0.52	1.61	1.7×10^{-2}
NaCl	0.50	1.20	3.5×10^{-2}	0.50	1.92	1.1×10^{-2}
LiCl	0.38	1.30	2.5×10^{-2}	0.41	2.27	1.2×10^{-2}
NH_4Cl	0.54	1.19	2.8×10^{-2}	0.56	1.56	1.2×10^{-2}

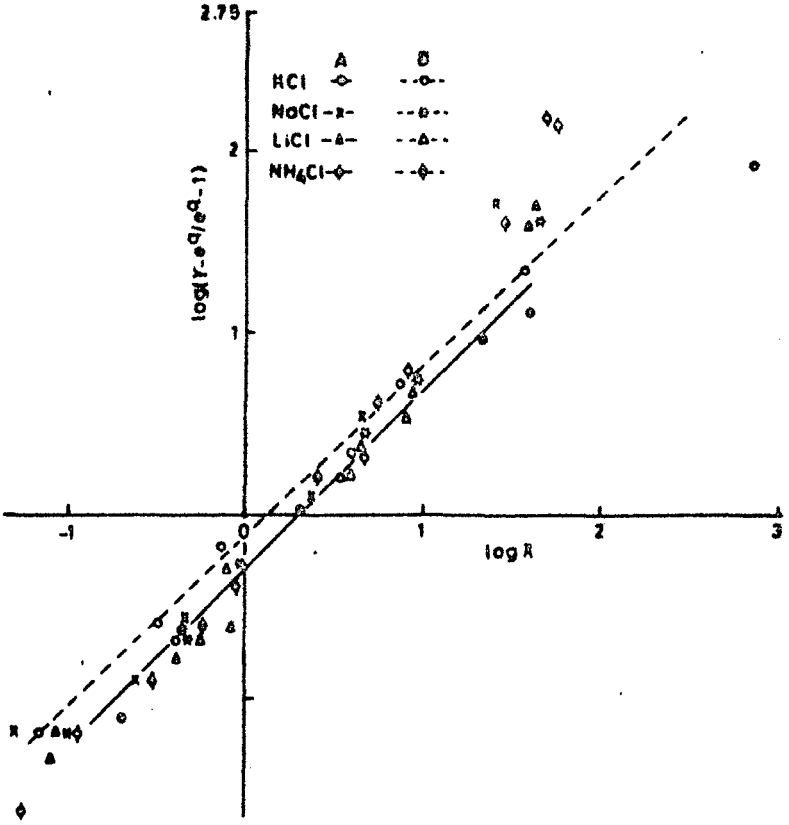

Fig. 6. Plots of log $(r - e^q/e^q - 1)$ against log X for the various electrolytes with (A) mercuric iodide (——) and (B) cupric iodide (· ·) membranes.

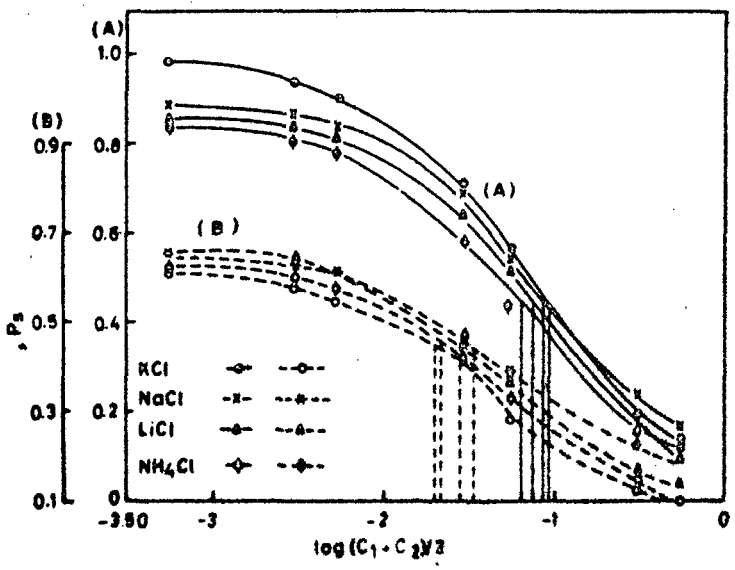

Fig. 7. Plots of P_s defined by eq. (31) against log $[(C_1 + C_2)/2]$ for various electrolytes with (A) mercuric iodide (——) and (B) cupric iodide (· ·) membranes.

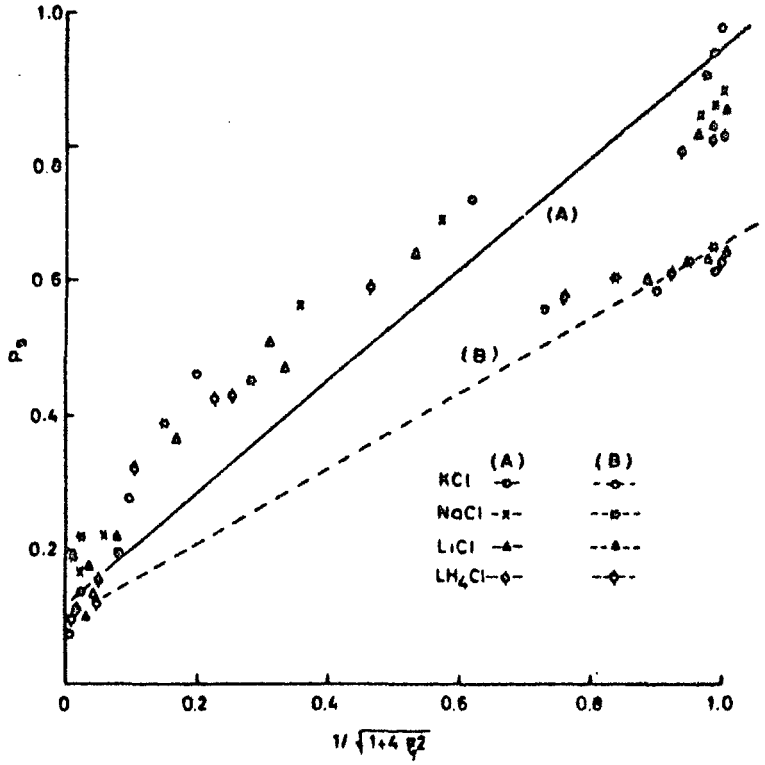

Fig. 8. Plots of P_s against $1/\sqrt{1+4\xi^2}$ for various electrolytes with (*A*) mercuric iodide (——) and (*B*) cupric iodide (- -) membranes.

The graphical value of the slope determined from Figure 4 is equated with the above expression after substituting the values of α and β, and thus the value of θ is obtained.

In the concentration range ($C = 1.0$ to $5.0 \times 10^{-2}N$) using eq. (23) the slope is given by

$$\left[\frac{(1+\beta-2\alpha\beta)(\nu-1)\alpha}{2(1-\alpha)^2 \ln \nu}\right]\theta$$

The graphical value of the slope determined from Figure 5 is equated with the above expression. The values of α and β are substituted, and thus the value of θ is evaluated. Kobatake has suggested that, provided this equation for the membrane potential is correct, then the two values of θ (in the two limiting cases) thus determined from the opposite limits should agree with one another. In the present investigation with parchment-supported membranes, the two values obtained from the opposite limits agree with one another, thereby confirming the applicability of Kobatake et al. equation to these systems also.

Comparison between theoretical and experimental data can be made and the applicability of the equation of Kobatake et al. to both the membranes can be tested by the following analytical technique suggested by Kobatake. Equation (17) may be rewritten as

$$(\nu - e^q)/(e^q - 1) = X \qquad (32)$$

with q and X defined by eqs. (33) and (34), where the X is not the same as the one used by TMS or Altug and Hair.

$$q = \frac{[|\Delta\phi_r| + (1 - 2\alpha) \ln \nu]}{[(1/\beta) + (1 - 2\alpha)]}$$

$$X = C_2/\alpha\beta\theta$$

If this equation is valid the values of $(\nu - e^q)/(e^q - 1)$, together with the predetermined α, β and θ (from Table III) must fall on a straight line which has a unit slope and passes the origin when plotted against X. This behavior should be observed irrespective of the value of ν and the kind of membrane electrolyte (1:1 system) used. Figure 6 demonstrates that the theoretical predictions, based on Kobatake's membrane potential expression is borne out quite satisfactorily by our experimental results on parchment-supported membranes.

For the evaluation of the thermodynamically effective fixed charge density ϕX, the various values of premselectivity P_s were also calculated by substituting the values of α (bulk) and $t_{\bar{a}pp}$ in eq. (31), and then plotted against log $[C_1 + C_2)/2]$. The results are shown in Figure 7. The term ξ has already been defined as the ratio between the average concentration C and the effective fixed charge density ϕX, i.e. $\xi = C/\phi X$. The units of both C and ϕX are expressed in terms of equivalents/liter. When the average concentration C is equal to the effective fixed charge density ϕX, i.e., $C/\phi X = \xi = 1$, the value of P_s must give $1/\sqrt{5} = 0.448$ from the left-hand side of eq. (31). The corresponding concentration is obtained from the plots of P_s versus log C as given in Figure 7. This value of concentration is equal to the fixed charge density ϕX. The ϕX values are given for various electrolytes in Table II. The plots of P_s versus $(1 + 4\xi^2)^{-1/2}$ are drawn for both membrane with KCl and shown in Figure 8. It is evident that the line nearly passes through the origin with unit slope, confirming the applicability of Kobatake's equation to these membranes.

The authors are grateful to Prof. Wasiur Rahman, Head of Department of Chemistry, for providing research facilities and to C.S.I.R. (India) for the award of a fellowship to one of them (S. P. S.).

References

1. F. A. Siddiqi and S. Pratap, *J. Electroanal. Chem.*, **23**, 137 (1969).
2. F. A. Siddiqi and S. Pratap, *J. Electronal. Chem.*, **23**, 147 (1969).
3. F. A. Siddiqi, N. Lakshminarayanaiah, and S. K. Saksena, *Z. Phys. Chem.* (Frankfurt), **72**, 298 (1970).
4. F. A. Siddiqi, N. Lakshminarayanaiah, and S. K. Saksena, *Z. Phys. Chem.* (Frankfurt), **72**, 307 (1970).
5. F. A. Siddiqi, N. Lakshminarayanaiah, and M. N. Beg, *J. Polym. Sci.*, **9**, 2853 (1971).
6. F. A. Siddiqi, N. Lakshminarayanaiah, and M. N. Beg, *J. Polym. Sci.*, **9**, 2868 (1971).
7. W. U. Malik and F. A. Siddiqi *J. Colloid Sci.*, **18**, 161 (1963).
8. W. U. Malik, H. Arif, and F. A. Siddiqi *Bull. Chem. Soc. Japan*, **40**, 1746 (1967).
9. W. U. Malik and F. A. Siddiqi, *Proc. Indian Acad. Sci.*, **A56**, 206 (1962).
10. F. A. Siddiqi, M. N. Beg, S. P. Singh, and A. Haq, *Bull. Chem. Soc. Japan*, in press.
11. F. A. Siddiqi, M. N. Beg, A. Haq, and S. P. Singh, *Bull. Chem. Soc. Japan*, in press.
12. T. Teorell, *Discuss. Faraday Soc.*, **21**, 9 (1956).
13. N. Lakshminarayanaiah and F. A. Siddiqi, *Biophys. J.*, **11**, 603 (1971).
14. N. Lakshminarayanaiah and F. A. Siddiqi, *Biophys. J.*, **11**, 617 (1971).
15. N. Lakshminarayanaiah and F. A. Siddiqi, *Biophys. J.*, **12**, 540 (1972).

16. N. Lakshminarayanaiah and F. A. Siddiqi, in *Membrane Process in Industry and Biomedicine* M. Bier, Ed., Plenum Press, New York, 1971
17. A. M. Liquori and C. Botré, *Ric Sci.*, **34**, 6 (1964).
18. A. M. Liquori and C. Botré, *J. Phys. Chem.*, **71**, 3765 (1967).
19. T. Teorell, *Proc. Soc. Exptl. Biol.*, **33**, 282 (1935); *Proc. Natl. Acad. Sci.* (U.S.), **21**, 152 (1935); *Z. Elektrochem.*, **55**, 460 (1951); *Progr. Biophys. Chem.*, **3**, 386 (1953).
20. K. H. Meyer and J. F. Sievers, *Helv. Chim. Acta.*, **19**, 649, 665, 987 (1936).
21. I. Altug and M. L. Hair, *J. Phys. Chem.*, **72**, 599 (1968).
22. Y. Kobatake, T. Noriaki, Y. Toyoshima, and H. Fujita, *J. Phys. Chem.*, **69**, 3981 (1965).
23. Y. Toyoshima, M. Yuassa, Y. Kobatake, and H. Fujita, *Trans. Faraday Soc.*, **63**, 2803, 2814 (1967).
24. M. Yuassa, Y. Kobatake, and H. Fujita, *J. Phys. Chem.*, **72**, 2871 (1968).
25. N. Kamo, Y. Toyoshima, H. Nazaki, and Y. Kobatake, *Kolloid-Z. Z. Polym.*, **248**, 914 (1971).
26. N. Kamo, Y. Toyoshima, and Y. Kobatake, *Kolloid-Z. Z. Polym.*, **249**, 1061 (1971).
27. N. Kamo, M. Ookawa, and Y. Kobatake, *J. Phys. Chem.*, **77**, 92, 2995 (1973).
28. H. B. Weiser, *J. Phys. Chem.*, **34**, 355, 1826 (1930).
29. L. Michaelis, *Bull. Nat. Res. Council* (U.S.), **69**, 119 (1929).
30. K. Sollner and H. P. Gregor, *J. Phys. Chem.*, **51**, 299 (1947).
31. C. E. Marshall and A. D. Ayers, *J. Amer. Chem. Soc.*, **70**, 1297 (1948).
32. L. Michaelis and H. Fujita, *Biochem. Z.*, **158**, 28 (1925).
33. D. E. Goldman, *J. Gen. Physiol.*, **27**, 37 (1943).
34. G. J. Hills, P. W. M. Jacobs, and N. Lakshminarayanaiah, *Proc. Roy. Soc.* (*London*), **A262**, 246 (1961).
35. E. A. Guggenheim, *Phil. Mag.*, **19**, 588 (1935).
36. S. Baxter, *J. Colloid Sci.*, **2**, 495 (1947).
37. N. Lakshminarayanaiah, *J. Appl. Polym. Sci.*, **10**, 1687 (1966).

Received March 5, 1976
Revised June 22, 1976

Acta Chimica Academiae Scientiarum Hungaricae. Tomus 93 (2), pp. 123 133 (1977)

STUDIES WITH PARCHMENT SUPPORTED MEMBRANES, XIII

DETERMINATION OF THE THERMODYNAMICALLY EFFECTIVE FIXED CHARGE DENSITY AND PERMSELECTIVITY

FASIH A. SIDDIQI, M. NASEEM BEG, SURENDRA P. SINGH and ABDUL HAQ

(Physical Chemistry Division, Department of Chemistry Aligarh Muslim University, Aligarh 202001 INDIA)

AKADÉMIAI KIADÓ, BUDAPEST
PUBLISHING HOUSE OF THE HUNGARIAN ACADEMY OF SCIENCES
VERLAG DER UNGARISCHEN AKADEMIE DER WISSENSCHAFTEN
MAISON D'EDITIONS DE L'ACADEMIE DES SCIENCES DE HONGRIE
ИЗДАТЕЛЬСТВО АКАДЕМИИ НАУК БЕНГРИИ

Acta Chimica Academiae Scientiarum Hungaricae, Tomus 93 (2), pp. 123—133 (1977)

STUDIES WITH PARCHMENT SUPPORTED MEMBRANES, XIII

DETERMINATION OF THE THERMODYNAMICALLY EFFECTIVE FIXED CHARGE DENSITY AND PERMSELECTIVITY

FASIH A. SIDDIQI, M. NASEEM BEG, SURENDRA P. SINGH and ABDUL HAQ

(Physical Chemistry Division, Department of Chemistry Aligarh Muslim University, Aligarh 202001 INDIA)

Received July 26, 1976

The membrane potentials arising across two parchment supported hexacyanoferrate(II) membranes of silver and cadmium are used to evaluate the thermodynamically effective fixed charge densities of KOBATAKE. KOBATAKE's theory is based on the thermodynamics of irreversible processes. KOBATAKE's equation was used under two limiting conditions, namely in the concentration range and in the dilute range. The two limiting forms of KOBATAKE's equation gave identical values of Θ for both membranes. The theoretical predictions for membrane potentials by KOBATAKE's equation are borne out quite satisfactorily by the experimental results obtained with the silver and cadmium hexacyanoferrate(II) membranes investigated.

The theories of transport of charged or uncharged particles through membranes have been treated under the following headings; (a) the idealized theory of TMS [1—2] and its refinement [3], (b) pseudo thermodynamic approach due to SCATCHARD [4] and the treatment based on the thermodynamics of irreversible processes [5—8] and (c) a kinetic approach based on the theory of absolute reaction rates [9—10]. NAGASAWA and KOBATAKE [10] have taken the structure of the membrane into account and by the application of the Poisson—Boltzmann equation computed ionic concentrations in the membrane phase. In order to substantiate our earlier findings [11—19] extensive investigations have been made for the determination of membrane charge density and are reported in this paper on the basis of the thermodynamics of irreversible processes given by KOBATAKE *et al.* [20—25].

Experimental

Preparation of membranes

The membranes of silver and cadmium hexacyanoferrate(II) were prepared by the method of interaction suggested by WEISER [26]. First parchment paper was soaked in distilled water for two hours and then tied carefully to the flat mouth of a beaker which contains 0.2 *M* silver nitrate. This was suspended for about 72 hours in a 0.2 *M* solution of potassium hexacyanoferrate(II). The two solutions were interchanged and kept for another 72 hours. The silver hexacyanoferrate(II) membrane thus prepared was washed with deionized water

for the removal of free electrolyte. A similar procedure was adopted for the preparation of cadmium hexacyanoferrate(II) membrane by taking a 0.2 *M* solution of cadmium chloride and potassium hexacyanoferrate.

Measurement of membrane potential

The potential developed by setting up a concentration cell of the following type described by MICHAELIS [27], SOLLNER and GREGOR [28] and MARSHALL and AYERS [29]

S.C.E.	Solution C_1	Membrane	Solution C_2	S.C.E.

was taken as a measure of membrane potential. The measurements were carried out at 25 °C using a Pye *precision potentiometer* (No. 7568).

Result and discussion

The membrane potential data obtained with the silver and cadmium hexacyanoferrate(II) in various 1 : 1 electrolytes were plotted as a function of $\log \frac{C_1 + C_2}{2}$ with the ratio $r = C_2/C_1$ fixed at 10. These plots are shown in Fig. 1.

KOBATAKE *et al.* [21] derived the following equation for the electric current density $(I)_c$, relative to the frame of reference fixed to the membrane, using the basic flow equation provided by the thermodynamics of irreversible processes,

$$(I)_c = -F(l_+C_+ + l_-C_-)\frac{d\Phi}{dx} - RT\left(l_+C_+\frac{d\ln a_+}{dx} - l_-C_-\frac{d\ln a_-}{dx}\right) + F(C_+ - C_-)U_m. \quad (1)$$

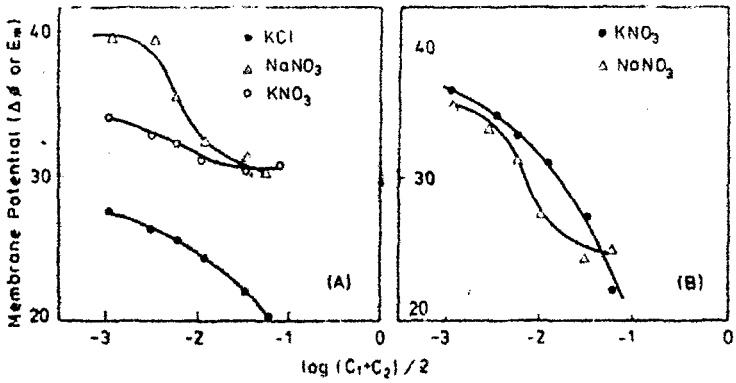

Fig. 1. Plots of observed potential $\Delta\Phi$ against $\log (C_1 + C_2)/2$ for various electrolytes with (A) Cadmium Hexacyanoferrate(II) and (B) Silver Hexacyanoferrate(II) membranes

Here l_+ and l_- are molar mobilities of $+ve$ and $-ve$ ions defined in terms of the mass fixed frame of reference, U_m is the velocity of the local centre of mass, Φ is the electric potential, C_+ and C_- are concentrations of $+ve$ and $-ve$ ions in moles per cubic centimeter of solution, a_+ and a_- are activities of positive and negative ions in moles per cubic centimeter of solution, R is the gas constant, T the absolute temperature of the system and F the Faraday constant.

For the evaluation of U_m, the viscous force acting on 1c.c. of solution in the membrane is represented by $\left(\frac{1}{K}\right) U_m$, where K is a constant which is considered to depend on the viscosity of the solution and the structural details of the polymer network of which the membrane is composed. The same volume of solution undergoes an electric force which is represented by

$$F(C_+ \quad C_-)\left(\frac{d\Phi}{dx}\right). \tag{2}$$

In the steady state, the sum of these two forces is zero, so that

$$U_m = KF(C_+ \quad C_-)\left(\frac{d\Phi}{dx}\right). \tag{3}$$

For convenience, KOBATAKE *et al.* have considered a membrane which is ionized negatively with a charge density Θ (in moles/c.c.). Then the requirement that the electric neutrality must be realized in any element of the membrane gives the relation

$$C_+ \quad C_- = 0. \tag{4}$$

Since in the system considered here no electric field is applied externally across the membrane, no net charge is transported from one side of the membrane to the other. This means that $(I)_c$ must be zero at a cross-section of the membrane. Substituting Eqs 3 and 4 into Eq. 1, putting $(I)_c$ equal to zero, and solving for $\frac{d\Phi}{dx}$, the following expression is obtained

$$\frac{d\Phi}{dx} = \frac{\left(\frac{RT}{F}\right)\left[l_+(C_- + \Theta)\left(\frac{d\ln a_+}{dx}\right) - l_-C_-\left(\frac{d\ln a_-}{dx}\right)\right]}{(l_+ + l_-)C_- + l_+\Theta + KF\Theta^2}. \tag{5}$$

To proceed further, the activities a_+ and a_- must be known as function of C_-.

Assumption for a_+ and a_-:

KOBATAKE *et al.* have assumed the following relations

$$a_+ = C_-; \text{ and } a_- = C_- \tag{6}$$

$$\nu_+ = C_-/(C_- + \Theta); \quad \nu_- = 1 . \tag{7}$$

Here ν_+ and ν_- are the activity coefficients of $+ve$ and $-ve$ ions in the membrane.

Equation for membrane potential

With Eqs 6, 7 assumed for a_+ and a_- Eq. 5 becomes

$$\frac{d\Phi}{dx} = \frac{RT}{F}\left[\frac{(l_+ - l)C_- + l_+\Theta}{[(l_+ + l)C_- + l_+\Theta + KF\Theta^2]C_-}\right]\frac{dC}{dx} \tag{8}$$

when the bulk solution on both sides of the membrane are vigorously stirred. no potential gradient is set up in them, so that the desired membrane potential $\Delta\Phi$ is obtained by integrating $\frac{d\Phi}{dx}$ over the thickness of the membrane. The final expression for the membrane potential is given by

$$\Delta\Phi = \left(\frac{RT}{F}\right)\left[\frac{1}{\beta}\ln\frac{C_2}{C_1} - \left(1 + \frac{1}{\beta} - 2\alpha\right)\ln\left(\frac{C_2 + \alpha\beta\Theta}{C_1 + \alpha\beta\Theta}\right)\right] \tag{9}$$

$$\text{where } \alpha = \frac{l_+}{l_+ + l} \quad \text{and} \quad \beta = 1 + \left(\frac{KF\Theta}{l_+}\right) \tag{10, 11}$$

and the parameters have been assumed to be independent of salt concentration.

KOBATAKE *et al.* [21] have derived two useful limiting forms of Eq. 9. These are (a) when C_2 becomes sufficiently small with ν fixed; Eq. 9 may be expanded to give

$$|\Delta\Phi_\gamma| = \frac{1}{\beta}\ln\nu - \frac{\nu - 1}{\alpha\beta\nu}\left(1 + \frac{1}{\beta} - 2\alpha\right)\left(\frac{C_2}{\Theta}\right) + \cdots \tag{12}$$

where $|\Delta\Phi_\gamma|$ is the absolute value of a reduced membrane potential defined by

$$\Delta\Phi_\gamma = F\Delta\Phi/RT \tag{13}$$

(b) It has also been shown by KOBATAKE *et al.* that at a fixed ν the inverse of an apparent transference number t^-_{app} for the Co-ion species in a negatively

charged membrane is proportional to the inverse of the concentration C_2 in the region of high salt concentration. Here t_{app}^- is defined by the relation

$$|\Delta\Phi_\gamma| = (1 - 2\,t_{app}^-)\ln\nu \tag{14}$$

substituting for $\Delta\Phi$ from Eq. 9 and expanding the resulting expression for t_{app}^- in powers of $1/C_2$ gives

$$\frac{1}{t_{app}^-} = \frac{1}{(1-\alpha)} + \frac{(1+\beta-2\alpha\beta)(\nu-1)\alpha}{2(1-\alpha)^2\ln\nu}\left(\frac{\Theta}{C_2}\right) + \ldots \tag{15}$$

For the evaluation of the thermodynamic effective fixed charge density by the method of KOBATAKE *et al.* the following procedure was adopted.

Equation 12 indicates that a value of β and a relation between α and Θ can be obtained by evaluating the intercept and the initial slope of a plot of $|\Delta\Phi_\gamma|$ against C_2. Figure 2 illustrates plots of $|\Delta\Phi_\gamma|$ *versus* C_2 in the region of low concentration that were determined for electrolyte with both membranes. The value of intercept is equal to $1/\beta\ln\nu$, by which β may be evaluated. Values are given in Table I.

Table I

Values of parameters α, β, Θ and ΦX for various electrolyte system at $\nu = 10$

Membrane	Silver hexacyanoferrate(II)				Cadmium hexacyanoferrate(II)			
Electrolyte	α	β	Θ	ΦX	α	β	Θ	ΦX
KNO_3	0.68	1.69	0.0061	0.00215	0.75	1.81	0.0011	0.0083
KCl	—	—	—	—	0.68	2.27	0.0008	0.0063
$NaNO_3$	0.68	1.64	0.0035	0.00418	0.75	1.48	0.0011	0.0054

Θ are evaluated from the slope $= \dfrac{(1+\beta-2\alpha\beta)(\nu-1)\alpha\Theta}{2(1-\alpha)^2\ln\nu}$

ΦX from graph 5.

Eq. 15 indicates that the intercept of a plot of $\dfrac{1}{t_{app}^-}$ against $1/C_2$ at fixed ν allows the values of α to be determined, which are shown in Fig. 3 for both membranes with the electrolyte. The value of the intercept is equal to $\dfrac{1}{(1-\alpha)}$, from which α may be evaluated. Values are given in Table I.

For the evaluation of Θ, there are two limiting cases

(i) in the dilute range the slope, of Eq. 12 is given by

$$\frac{\nu-1}{\alpha\beta\nu}\left(1+\frac{1}{\beta}-2\alpha\right)\frac{1}{\Theta}.$$

The graphical value of the slope determined from Fig. 2 is equated with the above expression after substituting the value of α and β, Θ may thus be determined.

(ii) in the concentration range using Eq. 15. The slope is given by

$$\frac{(1+\beta-2\alpha\beta)(\nu-1)\alpha}{2(1-\alpha)^2 \ln \nu}\,\Theta$$

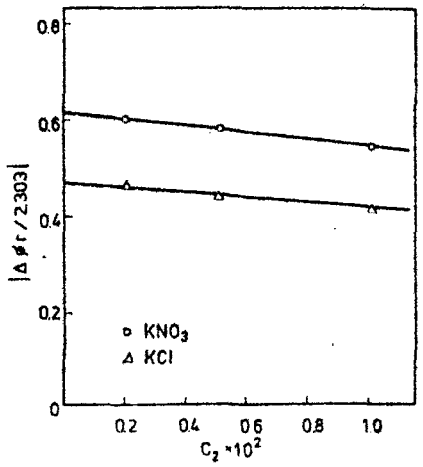

Fig. 2. $|\Delta\Phi_\gamma|/2.303$ *vs.* $C_2 \times 10^2$ plots for electrolyte with (Δ) Cadmium Hexacyanoferrate(II) and (o) Silver Hexacyanoferrate(II) membranes

The graphical value of the slope determined from Fig. 3 is equated with the above expression. The values of α and β are substituted and thus the value of Θ is evaluated. KOBATAKE has suggested that, provided his equation for the membrane potential is correct, then the two values of Θ (in the two limiting cases) thus determined from the opposite limits should agree. In the present

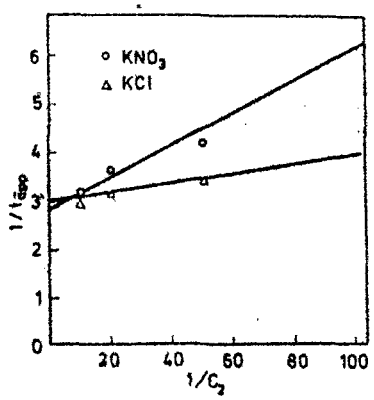

Fig. 3. $1/\bar{t}_{app}$ *vs.* $1/C_2$ plots for electrolyte with (Δ) Cadmium Hexacyanoferrate(II) and (o) Silver Hexacyanoferrate(II) membranes

investigation with parchment supported membranes, the two values obtained from opposite limits agree with one another thereby confirming the applicability of KOBATAKE *et al.* equation to these systems also.

Once the values of the parameters α, β and Θ for a given membrane electrolyte system have been determined, one can calculate the theoretical $\Delta\Phi$ *versus* C_2 curve for the value of ν and then compare it with the corresponding experimental data. For this comparison Eq. 9 may be rewritten in the following form as suggested by KOBATAKE

$$\frac{(\nu - e^q)}{(e^q - 1)} = X$$

with q and X defined by

$$q = \frac{\left[|\Delta\Phi_\gamma| + (1 - 2\alpha)\ln\nu\right]}{\left[\frac{1}{\beta} + (1 - 2\alpha)\right]}$$

and

$$X = \frac{C_2}{\alpha\beta\Theta}.$$

If this equation is valid the values of $\frac{\nu - e^q}{e^q - 1}$ together with the predetermined α, β and Θ (from Table I) must fall on a straight line which has a unit slope and passes through the coordinate origin, when plotted against X. This behaviour should be observed irrespective of the value of ν and the kind of membrane electrolyte (1 : 1 system) used. Figure 4 demonstrates that the theoretical predictions, based on KOBATAKE's membrane potential expression is borne out quite satisfactorily by our experimental results on parchment supported membranes.

KOBATAKE *et al.* developed another theory for the evaluation of charge density of membranes [25]. This theory is based on the expression of permselectivity, which they derived by taking some assumption. Both the activity coefficients and mobilities of small ions in charged membranes can be expressed by the following expression [3]

$$\nu_+ = \nu_+^0(C_- + \Phi X)/(C_- + X), \quad \nu_- = \nu_-^0 \tag{16}$$

$$u_+ = u_+^0(C_- + \Phi X)/(C_- + X), \quad u_- = u_-^0. \tag{17}$$

Here ν_i, u_i, ν_i^0 and u_i^0 $(i = +, -)$ stand for the activity coefficient and mobility of ionic species i in the membrane and in the bulk solution, respectively C_- and X are the concentration of anion adsorbed on the membrane

(in moles per litre of water in the membrane), and the stoichiometric concentration of charges fixed in the membrane. According to the convention suggested by GUGGENHEIM [30] ν_+^0 can be equated with ν_-^0 for 1 : 1 electrolyte, and they are replaced by the mean activity coefficient $\nu_\pm^0$ of the electrolyte component. In Eq. 16, Φ represents the fraction of counter ions in the unbounded form, *i.e.* excluding those tightly bound to the polymer skeleton constituting the membrane. ΦX may be referred to as the thermodynamically effective fixed charge density of the membrane.

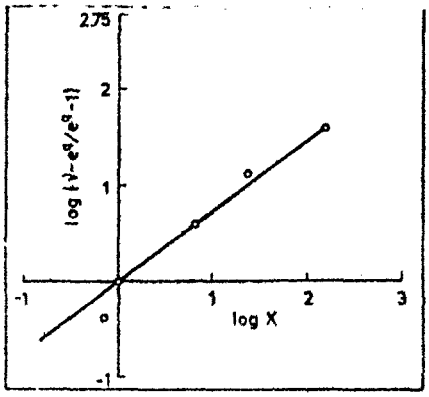

Fig. 4. Plots of log $(\nu - e^q/e^q - 1)$ *vs.* log X for KNO_3 with Silver Hexacyanoferrate(II) membrane

Consider a system in which a negatively charged membrane is immersed in an electrolyte solution of concentration C. Under this condition the Donnan equilibrium for small ions holds between the membrane phase and the solution then we have

$$(\nu_\pm^0)^2 C^2 = \nu_+ C_+ \nu_- C_- . \tag{18}$$

The mass fixed transference number of the anion in the membrane, is defined by

$$\tau_- = u_- C_- / (u_+ C_+ + u_- C_-) . \tag{19}$$

Introducing Eqs 16, 17 and 18 into Eq. 19 together with the electrical neutrality condition, *i.e.* $C_+ = C_- + X$
we obtain

$$\tau_- = 1 - \alpha \frac{(4\zeta^2 + 1)^{1/2} + 1}{(4\zeta^2 + 1)^{1/2} + (2\alpha - 1)} \tag{20}$$

where

$$\zeta = C/\Phi X \tag{21a}$$

and

$$\alpha = \frac{u_+^0}{(u_+^0 + u_-^0)} . \tag{21b}$$

On the other hand, the apparent transference number of the anion in the membrane, t^-_{app} is defined from the observed membrane potential $\Delta\Phi$ by the following Nernst equation

$$\Delta\Phi = -\left(\frac{RT}{F}\right)(1 - 2t_{-app}) \ln \frac{C_2}{C_1}. \tag{22}$$

Here C_1 and C_2 are the concentration of the external solutions on the two sides of the membrane, and R, T, and F have their usual thermodynamics

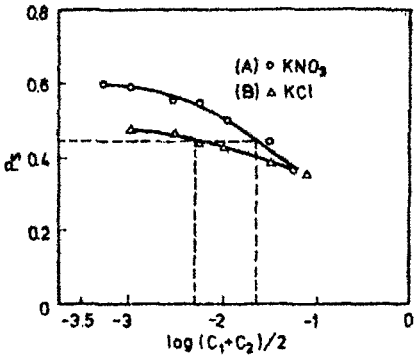

Fig. 5. Plots of P_s defined by equation 23 against $\log (C_1 + C_2)/2$ for electrolyte with (Δ) Cadmium Hexacyanoferrate(II) and (o) Silver Hexacyanoferrate(II) membranes

meaning. It has been found by KOBATAKE *et al.* [18] that the difference between τ_- and t^-_{app} was less than 2% in the wide range of salt concentration, when the averaged concentration $\frac{C_1 + C_2}{2}$ was replaced by C. Therefore, if we replace τ_- by t^-_{app}, and C by $\frac{C_1 + C_2}{2}$ Eq. 20 is applicable even when the concentrations on the two sides of the membrane are different. Rearrangement of Eq. 20 leads to

$$\frac{1}{(4\zeta^2 + 1)^{1/2}} = \frac{1 - t^-_{app} - \alpha}{\alpha - (2\alpha - 1)(1 - t^-_{app})} \equiv P_s. \tag{23}$$

Here P_s is a measure of permselectivity of the membrane–electrolyte system.

For the evaluation of the thermodynamically effective fixed charge density ΦX, the various values of permselectivity P_s were calculated by substituting the values of α (bulk) and t^-_{app} in Eq. 23, and then plotted against $\log \frac{C_1 + C_2}{2}$. The results are shown in Fig. 5 (*vide* Table II). The term ζ has been defined as the ratio between the average concentration C and the

Table II

Values of permselectivity P_s for various electrolytes at different concentrations

Membrane	← Silver hexacyanoferrate(II) →						← Cadmium hexacyanoferrate(II) →					
Electrolyte	Concentrations 'M'						Concentrations 'M'					
	0.1	0.05	0.02	0.01	0.005	0.002	0.1	0.05	0.02	0.01	0.005	0.002
KNO_3	0.35	0.44	0.50	0.54	0.56	0.59	0.49	0.50	0.52	0.52	0.54	0.56
KCl							0.36	0.39	0.43	0.44	0.46	0.48
$NaNO_3$	0.55	0.55	0.59	0.64	0.68	0.69	0.62	0.64	0.65	0.70	0.75	0.76

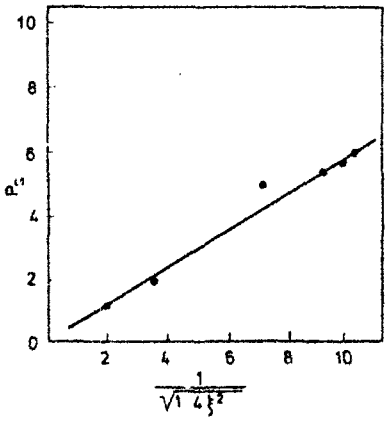

Fig. 6. Plots of P_s vs. $\frac{1}{\sqrt{1+4\zeta^2}}$ for KNO_3 with Silver Hexacyanoferrate(II) membrane

effective fixed charge density ΦX *i.e.* $\zeta = \frac{C}{\Phi X}$ the units of both C and ΦX are expressed in terms of moles or equivalents/litre when the average concentration C is equal to the effective fixed charge density ΦX *i.e.* $C/\Phi X = \zeta = 1$, the value of P_s must give $\frac{1}{\sqrt{5}} = 0.447$ from left hand side of Eq. 23. The corresponding concentration is obtained from the plots of P_s *versus* long C as given in Fig. 5. The value of the concentration is equal to the fixed charge density, the ΦX values are given for electrolytes with both membranes in Table I. Further, the plots of P_s *versus* $(1 + 4\zeta^2)^{-\frac{1}{2}}$ were drawn for one membrane with KCl and shown in Fig. 6. It is evident that the line nearly passes through the origin with unit slope, thereby confirming the applicability of KOBATAKE's equation to these membranes.

*

The authors are grateful to Professor WASIUR RAHMAN, Head of the Department of Chemistry, for providing research facilities. The financial assistance from CSIR (New Delhi, India) to two of us S.P.S. and A.H. is gratefully acknowledged.

REFERENCES

[1] TEORELL, T.: Proc. Soc. Expt. Biol., **33**, 282 (1935); Proc. Natl. Acad. Sci., (U.S.A.), **21**, 152 (1935); Z. Elektrochem. **55**, 460 (1951)
[2] MEYER, K. H., SIEVERS, K. F.: Helv. Chim. Acta., **19**, 649, 665, 987 (1963)
[3] SCHLOGL, R.: Z. Elektrochem., **57**, 195 (1953); Z. Physik. Chem. (Frankfurt), **1**, 305 (1954)
[4] SCATCHARD, G.: J. Am. Chem. Soc., **75**, 2883 (1956)
[5] HILLS, G. J., JACOBES, P. W. N., LAKSHMINARAYANAIAH, N.: Proc. Roy. Soc. (London) A262, 246 (1961)
[6] KOBATAKE, Y.: J. Chem. Phys. **28**, 146 (1958)
[7] LORIMER, J. W., BOTERENBROOD, E. I., HERMANS, J. J.: Disc. Faraday Soc. **21**, 141 (1956)
[8] STAVERMAN, A. J.: Trans. Faraday Soc. **48**, 176 (1952)
[9] NAGASAWA, M., KAGAWA, I.: Disc. Faraday Soc., **21**, 52 (1956)
[10] NAGASAWA, M., KOBATAKE, Y.: J. Phys. Chem., **56**, 1017 (1952)
[11] SIDDIQI, F., A., PRATAP, S.: J. Electroanal. Chem. **23**, 137, 147 (1969)
[12] SIDIQI, F. A., LAKSHMINARAYANAIAH, SAKSENA, K.: Z. Physik Chem. (Frankfurt) **72**, 298, 307 (1970)
[13] SIDDIQI, F. A., LAKSHMINARAYANAIAH, NASIM, Beg, M.: J. Polym. Sci., **9**, 2853, 2869 (1971)
[14] LAKSHMINARAYANAIAH, SIDDIQI, A.: Biophys. J. **11**, 603, 617 (1971)
[15] LAKSHMINARAYANAIAH, SIDDIQI: Biophys. J. **12**, 540 (1972)
[16] LAKSHMINARAYANAIAH, N., SIDDIQI, F. A.: in "Membrane Processes in Industry and Biomedicine" Edited by M. Bier, Plenum Press, New York (1971)
[17] SIDDIQI, F. A., NASIM, Beg, M., SINGH, P., HAQ, A.: Bull. Chem. Soc. Japan. **49**, 2864 (1976)
[18] SIDDIQI, F. A., BEG, M. N., HAQ, A., SINGH, P.: Bull. Chem. Soc., Japan **49**, 2858 (1976)
[19] SIDDIQI, F. A., BEG, M. N., SINGH, S. P.: J. Polym. Sci. **15**, 959 (1977)
[20] KOBATAKE, Y., TAKEGUCHI, N., TOYOSHIMA, Y., FUJITA, H.: J. Phys. Chem. **69**, 3981 (1965)
[21] KAMO, N., TOYOSHIMA, Y., KOBATAKE, Y.: Kolloid-Z, Z-Polym. **249**, 1061 (1971)
[22] KAMO, N., TOYOSHIMA, Y., NOZAKI, H., KOBATAKE, Y.: Kolloid Z, Z-Polym. **248**, 914 (1971)
[23] TOYOSHIMA, Y., YUSSA, M., KOBATAKE, Y., FUJITA, H.: Trans. Faraday Soc., **63**, 2803, 2814 (1967)
[24] YUSSA, M., KOBATAKE, Y., FUJITA, H.: J. Phys. Chem. **72**, 2871 (1968)
[25] KAMO, N., OCKAWA, M., KOBATAKE, Y.: J. Phys. Chem., **77**, 92 (1973)
[26] WEISER, H. B.: J. Phys. Chem. **34**, 355, 1826 (1930)
[27] MICHAELIS, L.: Bull. Natl. Res. Council (U.S.A.), **69**, 119 (1929)
[28] SOLLNER, K., GREGORE, H. P.: J. Phys. Chem. **51**, 299 (1947)
[29] MARSHALL, C. E., AYERS, A. D.: J. Am. Chem. Soc. **70**, 1297 (1948)
[30] GUGGENHEIM, E. A.: Phil. Mag.: **19**, 588 (1935)

Fasih A. SIDDIQI
M. Naseem BEG
Surendra P. SINGH
Abdul HAQ

Aligarh 202001 India.

REPRINTED FROM

BULLETIN
OF THE
CHEMICAL SOCIETY OF JAPAN

VOL. 49, NO. 10, OCTOBER, 1976

THE CHEMICAL SOCIETY OF JAPAN

Studies with Parchment Supported Membranes. VIII. Determination of the Thermodynamic Effective Fixed Charge Density of Barium Phosphate Membrane by Various Methods and Evaluation of Permselectivity

Fasih A. Siddiqi, M. Nasim Beg, Surendra P. Singh, and Abdul Haque

Physical Chemistry Division, Department of Chemistry, Aligarh Muslim University, Aligarh, India

(Received December 8, 1975)

The thermodynamic effective fixed charge density, the most important parameter governing transport phenomena in membranes, was estimated by methods of TMS, Altug and Hair and the most recent one of Kobatake based on the thermodynamics of irreversible processes. Kobatake's equation has also been utilized for the evaluation of permselectivity of membranes. The two limiting forms of his equation for dilute and concentrated ranges gave identical values of θ (charge density) for barium phosphate membrane. The theoretical predictions for membrane potential by the equation were borne out quite satisfactorily by experimental results obtained with the investigated membranes.

The theories of transport of charged or uncharged particles through membranes have been treated on the basis of the following: (a) the idealized theory of TMS[1-3] and its refinements,[3] (b) the pseudo thermodynamic approach due to Scatchard[4] and treatment based on the thermodynamics of irreversible processes,[5-8] and (c) a kinetic approach based on the theory of absolute reaction rates.[9-10] In the preceeding paper[11] we showed that the parchment supported membranes can generate potentials when they are used to separate electrolyte solutions of different concentrations. This is attributed to the presence of a net charge (negative in the case of 1:1 electrolyte and positive in the case of 2:1 or 3:1 electrolyte) on the membrane probably due to the adsorption of anions or cations.[12-19] This communication deals with the evaluation of membrane fixed charge density on the basis of various approaches of TMS,[1-3] Altug and Hair[20] and Kobatake *et al.*[21-28] based on the thermodynamics of irreversible processes.

Experimental

The barium phosphate parchment supported membrane was prepared as described in part VII of this series.[11] The potential developed across the cell was measured by using a Pye Precision Vernier Potentiometer (No. 7568) at 25 °C (±0.1 °C).

S.C.E. | Solution (C_1) | Membrane | Solution (C_2) | S.C.E.

Donnan potential — Donnan potential

← Diffusion potential →

Results and Discussion

The membrane potential data obtained with the barium phosphate parchment supported membrane in various 1:1 electrolyte solutions are plotted as a function of log $(C_1+C_2)/2$ with the ratio ν of concentration C_2/C_1 fixed at 10 and are shown in Fig. 1.

The total membrane potential according to the Teorell[1] and Meyer-Sievers theories[2] consists of two Donnan potential at the two solution-membrane interfaces (π_1 and π_2) and a diffusion potential ($\phi_2-\phi_1$)

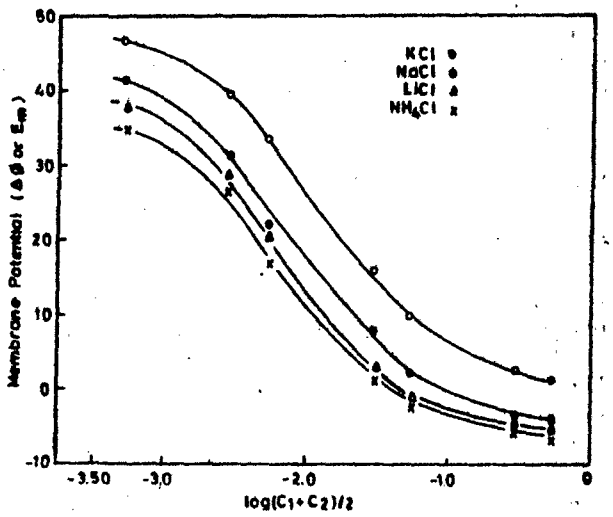

Fig. 1. Plots of observed potentials against log $(C_1+C_2)/2$ for various electrolytes with barium phosphate membrane.

arising from the unequal concentrations of the mobile ions at the two membrane surfaces. The membrane potential E_m or $\Delta\phi$ in millivolts according to TMS theory applicable to a highly idealized system is given by

$$E_m = 59.16\left[\log\frac{C_1(\sqrt{4C_2^2+\bar{X}^2}+\bar{X})}{C_2(\sqrt{4C_1^2+\bar{X}^2}+\bar{X})} + U\log\frac{\sqrt{4C_1^2+\bar{X}^2}+\bar{X}U}{\sqrt{4C_2^2+\bar{X}^2}+\bar{X}U}\right] \quad (1)$$

where $$U = \frac{\bar{u}-\bar{v}}{\bar{u}+\bar{v}}$$

$\bar{u}$ and $\bar{v}$ are the mobilities of cation and anion, respectively, in the membrane phase (the bars refer to the parameters in the membrane phase), $\bar{X}$ is the effective charge on the membrane expressed in equivalents/litre of the imbibed solution. In order to evaluate this parameter for the simple case of 1:1 electrolyte and membrane carrying a net negative charge of unity (*i.e.* $\bar{X}=1$) theoretical values for E_m were calculated as a function of C_2, the ratio ν of C_2/C_1 being kept at 10 for the different values of the mobility ratio $\bar{u}/\bar{v}$ and plotted as shown in Fig. 2.

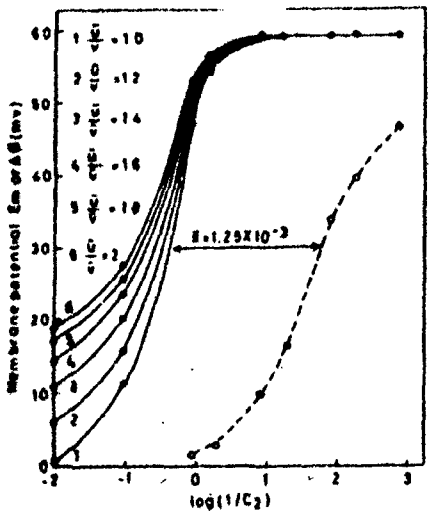

Fig. 2. Evaluation of membrane charge density x and the mobility ratio $\bar{u}/\bar{v}$ in the membrane phase. The different curves for different mobility ratio; O. The observed value E_m for barium phosphate membrane for KCl are plotted against log $(1/C_2)$.

The observed membrane potential values for barium phosphate membrane and KCl electrolyte are plotted in the same graph as a function of log $(1/C_2)$. The experimental curve shifts horizontally and runs parallel to one of the theoretical curves. The extent of this shift gives log $\bar{X}$ and the parallel theoretical curve the value $\bar{u}/\bar{v}$. The values of $\bar{X}$ and $\bar{u}/\bar{v}$ so derived for the barium phosphate membrane and various 1 : 1 electrolytes are given in Table 1.

TABLE 1. VALUES DERIVED FOR THE MEMBRANE PARAMETERS $\bar{X}$ AND $(\bar{u}/\bar{v})$

Membrane	Parameter	KCl	NaCl	LiCl	NH_4Cl
Barium phosphate	$(\bar{X}) \times 10^3$ eq/l	1.259	3.162	1.995	1.995
	$(\bar{u}/\bar{v})$	1.0	1.0	1.0	1.0

In a modification of this type of plotting, Altug and Hair[30] evaluated $\bar{X}$ on the glass membrane chosing the aqueous electrolyte solution values for $\bar{u}$ and $\bar{v}$ and calculating the values for E_m assigning different values for $\bar{X}$. The total membrane potential E_{calcd} is given by

$$E_{calcd} = (\pi_1 + \pi_2) + (\phi_2 - \phi_1) \tag{2}$$

where

$$\pi_1 = -\frac{RT}{F} \ln r_1 \tag{3a}$$

$$\pi_2 = \frac{RT}{F} \ln r_2 \tag{3b}$$

r_1 and r_2 are the Donnan distribution ratios, which are determined by means of the equation

$$r = \left\{1 + \left(\frac{w\bar{X}}{2a}\right)^2\right\}^{1/2} - \left(\frac{w\bar{X}}{2a}\right) \tag{4}$$

where a is the external solution concentration. The diffusion potential $(\phi_2 - \phi_1)$ for 1 : 1 electrolyte is given by

$$(\phi_2 - \phi_1) = \frac{u-v}{u+v} \frac{RT}{F} \ln \left\{\frac{a_1(r_1 u + v/r_1)}{a_2(r_2 u + v/r_2)}\right\} \tag{5}$$

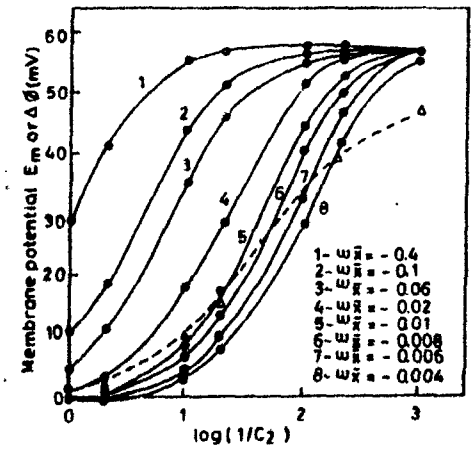

Fig. 3. Plots of membrane potential across barium phosphate membrane for KCl electrolyte of varying concentrations at fixed charge density against log $(1/C_2)$ (observed value are shown by brokenline).

where u and v are the cationic and anionic mobilities respectively, subscripts 1 and 2 referring to the solution on each side of membrane. Substitution in Eq. 2 gives

$$E_m = \frac{u-v}{u+v} \frac{RT}{F} \ln \frac{a_1\left(r_1 u + \frac{v}{r_1}\right)}{a_2\left(r_2 u + \frac{v}{r_2}\right)} + \frac{RT}{F} \ln \frac{r_2}{r_1} \tag{6}$$

Thus the membrane potentials are calculated by Eq. 6 for different values of fixed charge density $\bar{X}$. They are plotted in Fig. 3 as a function of the external solution concentration. The experimental values of membrane potential observed in the case of KCl for barium phosphate membrane are plotted against solution concentration. The theoretical curve which most nearly coincides with the experimental one gives the value of fixed charge density $\bar{X}$. The value of $\bar{X}$ thus calculated for KCl is given in Table 4.

Starting with the basic flow equations provided by the thermodynamics of irreversible processes Kobatake *et al.*[31] derived the following expression for the membrane potential $\Delta\phi$:

$$\Delta\phi = -\left(\frac{RT}{F}\right)\left[\frac{1}{\beta} \ln \frac{C_2}{C_1} - \left(1 + \frac{1}{\beta} - 2\alpha\right) \times \ln \left(\frac{C_2 + \alpha\beta\theta}{C_1 + \alpha\beta\theta}\right)\right] + \cdots \tag{7}$$

where

$$\alpha = \frac{l_+}{l_+ + l_-} \tag{8a}$$

and

$$\beta = 1 + (KF\theta/l_+). \tag{8b}$$

l_+ and l_- are the molar mobilities of $+ve$ and $-ve$ ions, respectively, defined in terms of the mass fixed frame of reference, K is a constant which is considered to depend on the viscosity of the solution and the structural details of the polymer net work of which the membrane is composed, θ is the charge density (in mol/cm³) and F is the Faraday constant. These parameters have been assumed to be independent of salt concentration C_2 and C_1.

For the analysis of data, Eq. 7 can be used under two sets of conditions, two limiting forms thus being

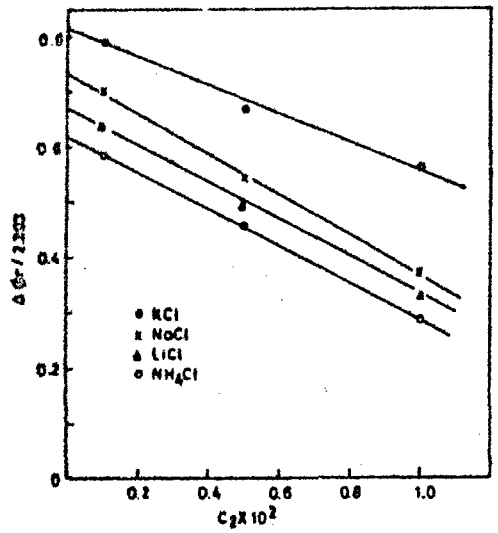

Fig. 4. $|\Delta\phi_r/2.303|$ *vs.* $C_2 \times 10^2$ plots for various electrolytes with barium phosphate membrane.

obtained: (a) when concentration C_2 becomes sufficiently small, (extreme dilute range) Eq. 7 can be expanded to give

$$|\Delta\phi_r| = \frac{1}{\beta}\ln\nu - \frac{\nu-1}{\alpha\beta\nu}\left(1+\frac{1}{\beta}-2\alpha\right)\frac{C_2}{\theta} + \cdots \qquad (9)$$

where $|\Delta\phi_r|$ is the absolute value of reduced potential defined by

$$|\Delta\phi_r| = \frac{F\Delta\phi}{RT}. \qquad (10)$$

Equation 9 indicates that the value of β and a relation between α and θ can be obtained by evaluating the intercept and initial slope of a plot for $|\Delta\phi_r|$ against C_2. Figure 4 shows plots for $|\Delta\phi_r|$ *versus* C_2 in the region of very low concentration determined for four electrolytes with barium phosphate membrane. The values of the intercepts for all electrolytes were equal to $(1/\beta)\ln\nu$ from which the values of β were evaluated (Table 2).

Table 2. Values of parameters α, β, and θ for various electrolyte with barium phosphate membrane at $\nu = 10$

Electrolyte	α	β	θ
KCl	0.51	1.23	0.008
NaCl	0.46	1.33	0.0071
LiCl	0.44	1.53	0.0020
NH_4Cl	0.44	1.69	0.0070

(b) It is well-known experimentally that at fixed ν the inverse of an apparent transference number, *i.e.* $t_{\bar{a}pp}^{-}$, for the co-ion species in a negatively charged membrane is proportional to the inverse of concentration C_2 in the region of high salt concentration. Here $t_{\bar{a}pp}^{-}$ is defined by the relation

$$|\Delta\phi_r| = (1-2t_{\bar{a}pp}^{-})\ln\nu. \qquad (11)$$

Substituting for $\Delta\phi_r$ from Eq. 7 and expanding the resulting expression for $1/t_{\bar{a}pp}^{-}$ in powers of $1/C_2$ gives

$$\frac{1}{t_{\bar{a}pp}^{-}} = \frac{1}{(1-\alpha)} + \frac{(1+\beta-2\alpha\beta)(\nu-1)}{2(1-\alpha)^2\ln\nu}\left(\frac{\theta}{C_2}\right). \qquad (12)$$

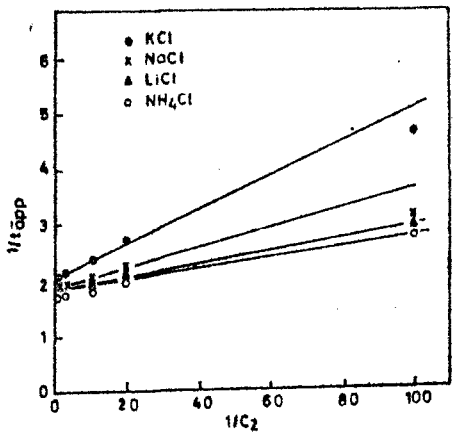

Fig. 5. $1/t_{\bar{a}pp}^{-}$ *vs.* $1/C_2$ plots for various electrolytes with barium phosphate membrane.

This indicates that intercept for a plot of $1/t_{\bar{a}pp}$ against $1/C_2$ at fixed ν allows the value of α to be determined. Plots of $1/t_{\bar{a}pp}^{-}$ against $1/C_2$ for various 1:1 electrolytes are shown in Fig. 5. The values of α are given in Table 2. There are two limiting cases for the evaluation of θ; (i) In the dilute range (1×10^{-3}M) using Eq. 9, the slope is given by

$$\frac{\nu-1}{\alpha\beta\nu}\left(1+\frac{1}{\beta}-2\alpha\right)\times\frac{1}{\theta}.$$

The graphical value of the slope determined from Fig. 4 is equated to the above equation, and the values of α and β are substituted. θ is thus evaluated, the value being designated as θ_d. (ii) In the concentration range (1.0 M) using Eq. 12, the slope is given by

$$\frac{(1+\beta-2\alpha\beta)(\nu-1)}{2(1-\alpha)^2\ln\nu}\times\theta.$$

The graphical value of slope determined from Fig. 5 is equated with the above expression and the values of α and β are substituted. θ is thus evaluated, the value being designated as θ_c.

In the present investigation with barium phosphate membrane, the two values of θ, *viz.* θ_c and θ_d, obtained from the opposite limits agree well with each other (Table 2) confirming the applicability of Kobatake's equation to this system. Also the value of α in Kobatake's treatment is defined by $u_+^0/(u_+^0+u_-^0)$ where u_+^0 and u_-^0 stand for the mobilities of cation and anion respectively in free solution. Thus, the value of α should be 0.5· KCl. The value of α obtained for KCl with barium phosphate membrane (Table 2) is 0.5. This implies that the assumption in the equation of Kobatake holds good for the barium phosphate membrane. It is evident that the constancy of the stoichiometric fixed charge density of the barium phosphate membrane is maintained, which is the basic assumption of the TMS theory[1-2] and its revised form given by Schlögl[3] and Kobatake *et al.*[21-26]

Comparison can be made between theoretical and experimental data and the applicability of Kobatake *et al.* equation to barium phosphate membrane can be tested by the following analytical technique suggested by Kobatake.

Equation 7 can be rewritten as

$$\frac{\nu-e^{q}}{e^{q}-1}=X \tag{13}$$

with q and X defined by

$$q=\frac{[|z|\phi_c|+(1-2\alpha)\ln\nu]}{1/\beta+(1-2\alpha)} \tag{14a}$$

$$X=\frac{C_s}{\alpha\beta\theta}. \tag{14b}$$

(The X is not the same as the one used in TMS or Altug and Hair method for the evaluation of charge density). Thus if Eq. 7 is valid, the values of log $(\nu-e^{q})/(e^{q}-1)$ calculated from measured $\Delta\phi$ and the given value of ν must fall on a straight line, which has a unit slope and passes the coordinate origin when plotted against log X as shown in Fig. 6, the theoretical predictions from the Kobatake *et al.* membrane potential equation are borne out quite satisfactorily by our experimental results with barium phosphate membrane.

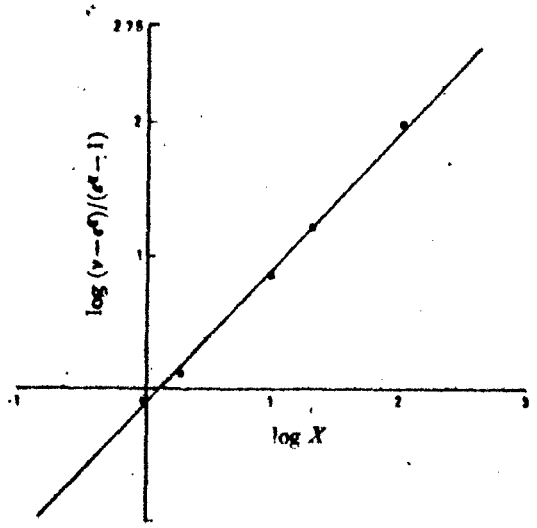

Fig. 6. Plot of log $(\nu-e^{q})/(e^{q}-1)$ *vs.* log X for KCl with barium phosphate membrane.

A method of characterization of the membrane electrolyte system has been developed by Siddiqi and Pratap[19] for parchment supported membranes. Recently a general method of characterization applicable to any system irrespective of ion species has been developed by Kobatake.[20] Consider the present system of negatively charged membrane immersed in an electrolyte solution of average concentration C (*i.e.* $(C_1+C_2)/2$) for which Donnan equilibrium for small ions holds. The mass transference number τ_- of anions in the membrane is given by

$$\tau_-=1-\alpha\frac{(4\xi^2+1)^{1/2}+1}{(4\xi^2+1)^{1/2}+(2\alpha-1)} \tag{15}$$

where ξ and α stand for the relative concentration defined by $C/\phi X$ and $u_+^0/(u_+^0+u_-^0)$ respectively.

On the other hand the apparent transference number of anions in the membrane, *i.e.* $t_{\bar{a}pp}$, is defined from the derived membrane potential by the Nernst equation

$$\Delta\phi=-\frac{RT}{F}(1-2t_{\bar{a}pp})\ln\frac{C_2}{C_1}. \tag{16}$$

The difference between τ_- (in Eq. 15) and $t_{\bar{a}pp}$ (in Eq. 16) was less than 2% within a wide range of salt concentration.[20] If τ_- is replaced by $t_{\bar{a}pp}$, and C by $(C_1+C_2)/2$, Eq. 15 is applicable even when the concentration of the two sides of the membrane differs. Rearrangement of Eq. 15 leads to the following expression

$$\frac{1}{(4\xi^2+1)^{1/2}}=\frac{1-t_{\bar{a}pp}-\alpha}{\alpha-(2\alpha-1)(1-t_{\bar{a}pp})}\equiv P_s \tag{17}$$

where P_s is a measure of permselectivity of the membrane electrolyte system. The value of P_s takes a value between zero and unity depending on the external salt concentration for a given system of a membrane and an electrolyte pair. P_s can be calculated from the data of the membrane potential, while the left hand side of Eq. 17 is a function of the relative concentration $\xi=C/\phi X$ or $(C_1+C_2)/2\phi X$. Thus the values of the right hand side should be independent of the mobilities of ion species involved. Equation 17 implies that the plot of P_s against $(1+4\xi^2)^{-1/2}$ should give a straight line of unit slope.

For the evaluation of the effective fixed charge density, another procedure suggested by Kobatake[20] was also adopted for barium phosphate membrane. The various values of P_s were calculated by substituting the value of α (bulk) and $t_{\bar{a}pp}$ in Eq. 17 (*vide* Table 3) and then plotted against by log $(C_1+C_2)/2$. A curve was obtained as shown in Fig. 7 when the average concentration C, *i.e.* $(C_1+C_2)/2$, becomes equal to the effective fixed charge density ϕX, the value of ξ becomes equal

Table 3. Values of permselectivity P_s for various electrolytes of barium phosphate membrane at different concentrations

Electrolytes	Concentrations (M)						
	1	0.5	0.1	0.05	0.01	0.005	0.001
KCl	0.05	0.06	0.18	0.29	0.58	0.67	0.80
NaCl	0.12	0.14	0.23	0.32	0.53	0.66	0.78
LiCl	0.24	0.26	0.29	0.29	0.58	0.71	0.79
NH_4Cl	−0.08	−0.06	0.0	0.06	0.30	0.47	0.60

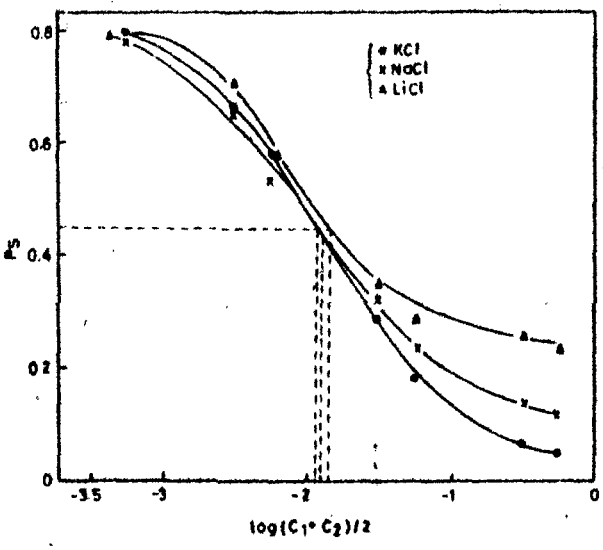

Fig. 7. Plots of P_s defined by Eq. 17 against log $(C_1+C_2)/2$ for various electrolyte with barium phosphate membrane.

Table 4. Comparison of charge density (ϕX or WX or X) by different methods for KCl

Membrane	TMS X	Altug and Hair WX	Kobatake's Eq. 12 θ^*	Kobatake's Eq. 9 θ^*	P_s vs. log $(C_1+C_2)/2$ ϕX
Barium phosphate	0.1259×10^{-3}	0.800×10^{-3}	0.8×10^{-3}	2.0×10^{-3}	1.14×10^{-3}

$$\theta^* = \text{slope}\frac{2(1-\alpha)^2 \ln \nu}{(1+\beta-2\alpha\beta)(\nu-1)\alpha} \qquad \theta^* = \frac{\nu-1(1+1/\beta-2\alpha)}{\text{slope }(\alpha\beta\nu)}$$

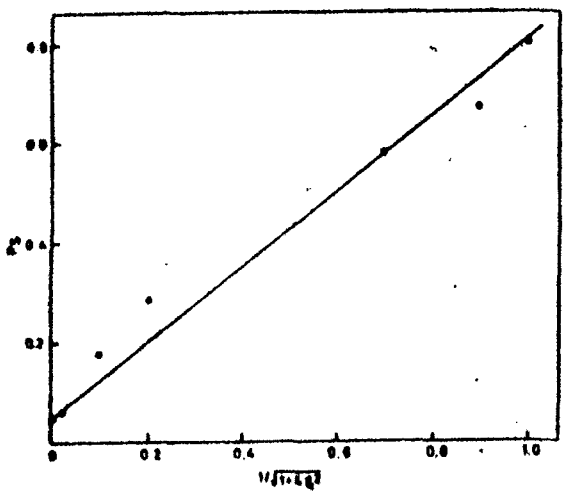

Fig. 8. Plots of P_s against $1/\sqrt{1+4\xi^2}$ for KCl electrolyte with barium phosphate membrane.

to unity, *i.e.* $C/\phi X=1$. Substituting this value of $\xi=1$ into $P_s=1/(4\xi^2+1)^{1/2}$, the value of P_s 0.448 is obtained. At this particular value of 0.448, the corresponding concentration is obtained from the curve P_s *versus* log C (Fig. 7). This value of concentration is equal to the fixed charge density (Table 4). The plot of P_s *versus* $(1+4\xi^2)^{-1/2}$ is drawn for barium phosphate membrane with KCl electrolyte is (Fig. 8). It is evident that the line passes through the origin with unit slope confirming the applicability of Kobatake's equation.

All the theories derived for the fixed charge membrane and used in these investigations give the effective fixed charge density θ or ϕX instead of X itself, when the charge density is evaluated from the data of membrane phenomena such as the membrane potential, ion permeability, electric resistance *etc.* Thus, the values of X do not differ from ϕX ($0<\phi<1$). For the evaluation of true X the titration and isotopic methods were tried. The titration method proved very inconvenient and inaccurate. The isotopic method was discarded in view of strong ionic adsorption phenomenon exhibited by these systems. Consequently the potentiometric method was used.

The authors are grateful to Professor W. Rahman, Head, Department of Chemistry for providing necessary facilities and also to Dr. N. Lakshminarayanaiah of the University of Pennsylvania U.S.A. for valuable discussions. The financial assistance from C.S.I.R. (New Delhi) India to two of us (S.P.S. and A.H.) is gratefully acknowledged.

References

1) T. Teorell, *Proc. Soc. Expt. Biol.*, **33**, 282 (1935); *Proc. Natl. Acad. Sci. U. S. A.*, **21**, 152 (1935); *Z. Elektrochem.*, **55**, 460 (1951); *Progr. Biophys. Chem.*, **3**, 305 (1953).
2) K. H. Meyer and J. F. Sievers, *Helv. Chim. Acta*, **19**, 649, 665, 987 (1936).
3) R. Schlögl, *Z. Elektrochem.*, **57**, 195 (1953); *Z. Physik. Chem. (Frankfurt)*, **1**, 305 (1954).
4) G.Scatchard, *J. Am. Chem. Soc.*, **75**, 2883 (1956).
5) G. J. Hills, P. W. M. Jacobs, and N. Lakshiminarayanaiah, *Proc. R. Soc. London, Ser. A*, **262**, 246 (1961).
6) Y. Kobatake, *J. Chem. Phys.*, **28**, 146 (1958).
7) J. W. Lorimer, E. I. Boterenbrood, and J. J. Hermans, *Discuss., Faraday Soc.*, **21**, 141 (1956).
8) A. J. Staverman, *Trans. Faraday Soc.*, **48**, 176 (1952).
9) M. Nagasawa and I. Kagawa, *Discuss. Faraday Soc.*, **21**, 52 (1956).
10) M. Nagasawa and Y. Kobatake, *J. Phys. Chem.*, **56**, 1017 (1952).
11) Fasih A. Siddiqi, Mohd Nasim Beg, Surendra P. Singh, and Abdul Haque, *Bull. Chem. Soc., Jpn.* **49**, 2858 (1976).
12) Fasih A. Siddiqi and S. Pratap, *J. Electroanal. Chem.*, **23**, 137, 147 (1969).
13) Fasih A. Siddiqi, N. Lakshminarayanaiah, and S. K. Saksena, *Z. Physik Chem. (Frankfurt)*, **72**, 298, 307 (1970).
14) Fasih A. Siddiqi, N. Lakshminarayanaiah, and M. N. Beg, *J. Polym. Sci.*, **9**, 2853, 2868 (1971).
15) Fasih A. Siddiqi, M. Nasim Beg, and Surendra P. Singh, *J. Polym. Sci.*, in press.
16) Fasih A. Siddiqi, M. Nasim Beg, and Poorna Prakash, *J. Electroanal. Chem.*, in press.
17) Wahid U. Malik and Fasih A. Siddiqi, *Proc. Indian Acad. Sci.*, **A56**, 206 (1962).
18) Wahid U. Malik and Fasih A. Siddiqi, *J. Colloid Sci.*, **18**, 161 (1963).
19) Wahid U. Malik, H. Arif, and Fasih A. Siddiqi, *Bull. Chem. Soc. Jpn.*, **40**, 1741 (1967).
20) I. Altug and M. L. Hair, *J. Phys. Chem.*, **72**, 599 (1968).
21) Y. Kobatake, N. Takeguchi, Y. Toyoshima, and H. Fujita, *J. Phys. Chem.*, **69**, 3981 (1965).
22) N. Kamo, Y. Toyoshima, and Y. Kobatake, *Kolloid-Z, Z-Polym.*, **249**, 1061 (1971).
23) N. Kamo, Y. Toyoshima, H. Nazaki, and Y. Kobatake, *Kolloid-Z, Z-Polym.*, **248**, 914 (1971).
24) Y. Toyoshima, M. Yuasa, Y. Kobatake, and H. Fujita, *Trans. Faraday Soc.*, **63**,2803, 2814 (1967).
25) M. Yuasa, Y. Kobatake, and H. Fujita, *J. Phys. Chem.* **72**, 2871 (1968).
26) N. Kamo, M. Oikawa, and Y, Kobatake, *J. Phys. Chem*, **77**, 92 (1973).

Preparation of Cupric Palmitate Membrane, Its Characterization and Evaluation of Thermodynamically Effective Fixed Charge Density

M. NASIM BEG, FASIH A. SIDDIQI[1], AKMAL HUSAIN, and BADRUL ISLAM,
Membrane Research Laboratory, Division of Physical Chemistry, Department of Chemistry, Aligarh Muslim University, Aligarh 202001 (India)

Reprinted from LIPIDS Vol 14 No [illegible] (1979)

Reprinted from LIPIDS, Vol. 14, No. 7, Pages: 682-686 (1979)

Preparation of Cupric Palmitate Membrane, Its Characterization and Evaluation of Thermodynamically Effective Fixed Charge Density

M. NASIM BEG, FASIH A. SIDDIQI[1], AKMAL HUSAIN, and BADRUL ISLAM,
Membrane Research Laboratory, Division of Physical Chemistry, Department of Chemistry, Aligarh Muslim University, Aligarh – 202001 (India)

ABSTRACT

Membrane potentials have been measured across parchment-supported cupric palmitate membrane separating various 1:1 electrolytes at concentrations C_1 and C_2 such that $C_2 = 10\ C_1$. Membrane potential data have been used to calculate transference number of ions, permselectivity and also to derive the thermodynamically effective fixed charge density which is an important characteristic governing the membrane phenomena by utilizing the generally accepted and most widely used theory of Teorell-Meyer and Sievers as well as the recent theories for membrane potential of Kobatake et al. and Nagasawa et al. based on the principles of nonequilibrium thermodynamics. The values of charge densities derived from different theories were almost the same, confirming thereby the validity of the recently developed theories of membrane potential.

INTRODUCTION

Many biologically important substances resemble the membranous structures of the living cells. In recent years considerable attention has been focused on these structures in order to determine their properties, especially their permeability properties. Mueller et al. (1-3) generated the first bimolecular lipid layer membrane which has been used as a model by a number of investigators. Recently other complex membranes have been prepared by Liquori et al. (4-6), Hays (7), De Korosy (8), Lakshminarayanaiah and Siddiqi (9-11), Siddiqi et al. (12), Beg and coworkers (14-18), and utilized as a useful representation of living systems.

One of the most consistent properties of biological systems is the presence of a voltage across the cellular surfaces. The mechanism whereby this potential arises is still in dispute. Some consider it to be a diffusion potential while others suggest it to be an adsorption potential. Teorell (19-20), Meyer and Sievers (21-23) developed fixed charge theory, which is still regarded as the most pertinent starting point for the investigation of the acual mechanisms of the ionic or molecular processes which occur in the membrane phase. Based on the fixed charge concept, a number of mathematically rigorous equations for membrane potentials in recent years have been developed and their validity examined by taking simpler artificial membrane systems.

In this paper we describe the preparation of parchment-supported cupric palmitate membrane to be utilized as a biological model and the evaluation of its thermodynamically effective fixed charge density by the most recently, developed theories for membrane potential including those based on the principles of irreversible thermodynamics.

MATERIALS AND METHODS

Parchment-supported cupric palmitate membrane was prepared by the method of interaction suggested by Beg and coworkers (14-18). To precipitate cupric palmitate in the interstices of parchment paper (supplied by M/S Baird and Tatlock, London Ltd.) an aqueous 0.2 M cupric chloride solution was kept inside a glass tube, to one end of which was tied the parchment paper previously soaked in deionized water. This was suspended in a saturated sodium palmitate solution for 72 hr at room temperature (25 ± 0·1 C). The two solutions were interchanged later and kept for another 72 hr. The membrane thus obtained was thoroughly washed (4-5 times) with deionized water for the removal of free electrolyte. It was then cut into a circular disc form of radius 1.5 cm and clamped between two cylindrical half cells of capacity 50 ml each. The electrochemical cell of the type

$$Hg\,|\,Hg_2Cl_2\,|\,\frac{\text{Satd. KCl}}{\text{agar}}\,|\,\frac{\text{Soln.}}{C_1}\,|\,\frac{\text{Mem-}}{\text{brane}}\,|\,\frac{\text{Soln.}}{C_2}\,|\,\frac{\text{Satd. KCl}}{\text{agar}}\,|\,Hg_2Cl_2\,|\,Hg$$

was set up and was used for measuring electrical potentials arising across the membrane by maintaining a 10-fold difference in electrolyte concentration such that $C_2/C_1 = 10$ in the range 1×10^{-3} to 10^{-1} M using a Pye Precision

[1]Present address: Department of Biophysics, Michigan State University, East Lansing, Michigan 48824 (U.S.A.).

TABLE I

Measured Membrane Potentials[a] E_m (Millivolts) Obtained across Cupric Palmitate Membrane for Various Electrolytes at Different Concentrations

Electrolyte concentrations eq./l	Membrane potentials (millivolts) KCl	NaCl	LiCl
1/0.1	4.05	0.72	15.80
0.5/0.05	1.02	8.29	14.00
0.1/0.01	+7.15	+1.27	−5.83
0.05/0.005	+17.07	+9.55	+1.50
0.01/0.001	+28.10	+17.90	+13.65

[a] Dilute solution side taken as positive.

TABLE II

Transference Number t_+ of Cations Calculated from Membrane Potentials Measured across Cupric Palmitate Membrane for Various Electrolytes at Different Concentrations

Electrolyte concentrations eq./l/l	Transference number KCl	NaCl	LiCl
1/0.1	0.53	0.58	0.63
0.5/0.05	0.51	0.57	0.62
0.1/0.01	0.44	0.49	0.55
0.05/0.005	0.36	0.42	0.49
0.01/0.001	0.26	0.35	0.38

Vernier Potentiometer No. 7568. The solutions in both the half cells were vigorously stirred by a pair of magnetic stirrers. The solutions were replaced by fresh solutions and, when there was no change in potential with the addition of fresh solution, it was taken as true membrane potential. The potentials could be reproduced within a few tenths of a millivolt. The salt solutions were prepared from the analytical grade reagent (BDH India) without further purification and using de-ionized water. Sodium palmitate used in the investigation was obtained by mixing 0.2 M aqueous caustic soda solution with 0.2 M palmitic acid solution previously recrystallized with ethyl alcohol.

RESULT

The measured values of membrane potentials across the cupric palmitate membrane in contact with various uni-univalent electrolytes at different concentrations C_1 and C_2 such that $C_2/C_1 = 10$ are given in Table I.

The values of the transference number calculated from the membrane potential measurements and using the Nernst equation are given in Table II. Thermodynamically effective fixed charge density of the membrane in contact with different electrolytes have been derived following the procedures of Teorell-Meyer and Sievers (19-21), Kobatake and coworkers (24-26) method, and the most recently developed method of Nagasawa et al. (27). The results are given in Table III.

DISCUSSION

When two electrolyte solutions are separated by a membrane, the mobile species penetrate the membrane and vaious transport phenomena are induced into the system. In particular, a potential is generated which depends upon the charge on the membrane and its porosity. When the membrane pores are too wide, any charge does little to generate good potentials, but if the pores are narrow a little charge on it gives a potential E according to the Nernst equation

$$E = \frac{RT}{F} \ln \frac{f_2 C_2}{f_1 C_1}$$

where C_1 and C_2 are the elctrolyte concentrations on either side of the membrane; other symbols have their usual significance.

The values of the membrane potential are smaller when the membrane is used to separate concentrated electrolyte solutions, and when it is separating dilute solutions the values are higher. Such behavior of the membrane is not peculiar to this system (9). The variation of

TABLE III

Derived Values of Mobility Ratio, and Effective Fixed Charge Density of Cupric Palmitate Membrane by Various Methods

Methods / Electrolytes eq./l.	TMS $\bar{u}/\bar{v}$	$\bar{x}$ eq./l	Kobatake et al. $\bar{\rho}x$ eq./l.	Nagasawa et al. $\bar{x}$ eq./l.
KCl	1.0	1.1×10^{-2}	3.2×10^{-2}	1.5×10^{-2}
NaCl	0.3	9.3×10^{-2}	3.7×10^{-2}	1.7×10^{-2}
LiCl	0.6	8.0×10^{-2}	3.0×10^{-2}	1.8×10^{-2}

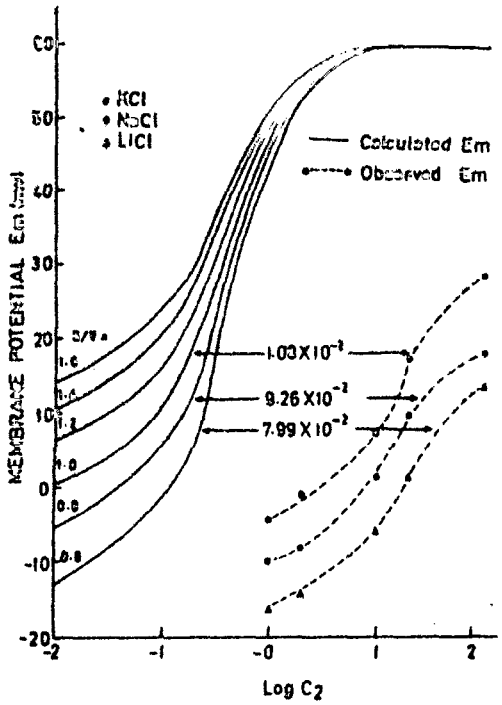

FIG. 1. Evaluation of the membrane charge density $\bar{X}$ and mobility ratio $\bar{u}/\bar{v}$. The smooth curves on the left are the theoretical concentration potentials for a cation selective membrane ($\bar{X}$ = 1) at different mobility ratio $\bar{u}/\bar{v}$. The experimental values of E_m for cupric palmitate membrane are shown by broken lines (see texts.)

membrane potential with electrolyte concentration may be attributed to the change in the selectivity character of the membrane for the ions of the electrolyte at different concentrations. This is in agreement with the values of the transference number given in Table II.

Teorell (19-20), Meyer and Sievers (21-23) considered the membrane as a charged barrier. The total membrane potential was considered to be made up of two Donnan potentials at the two membrane solutions interfaces and a diffusion potential within the membrane. For a highly idealized system, these authors derived the following equation for membrane potential:

$$E_m = 59.16\left[\log\frac{C_2\left(\sqrt{4C_1^2+\bar{X}^2}+\bar{X}\right)}{C_1\left(\sqrt{4C_{22+}^2+\bar{X}^2}+\bar{X}\right)} + \bar{U}\log\frac{\sqrt{4C_2^2+\bar{X}^2}+\bar{X}\bar{U}}{\sqrt{4C_1^2+\bar{X}^2}+\bar{X}\bar{U}}\right] \quad (1)$$

Here

Here $\bar{U} = (\bar{u}-\bar{v})/(\bar{u}+\bar{v})$; and $\bar{u}$ and $\bar{v}$ are the mobilities of the cation and anion, respectively, in the membrane phase, and $\bar{X}$ is the charge on the membrane expressed in equivalents/liter of imbibed solution. In order to evaluate this parameter for the simple case of a 1:1 electrolyte and a membrane carrying net negative charge of unity ($\bar{X}$=1), theoretical concentration potentials E_m existing across the membrane were calculated as a function of C_2, the ratio C_2/C_1 being kept at a constant value of 10 for different mobility ratios $\bar{u}/\bar{v}$ and plotted as shown in Figure 1. The observed membrane potential values with various 1:1 electrolyte solutions were also plotted on the same graph. The experimental curve was shifted horizontally and ran parallel to one of the theoretical curves. The extent of this shift gave log $\bar{X}$, and the parellel theoretical curve gave the value for $\bar{u}/\bar{v}$. The values for $\bar{X}$ and $\bar{u}/\bar{v}$ derived in this way for the membrane electrolyte systems are given in Table III. It may be mentioned here that this method (The TMS method) has been generally used and widely accepted for the evaluation of the effective fixed charge density of a membrane.

Kobatake and Kamo (24-25) derived another equation 2 based on fixed charge concept for membrane potential using a different set of assumptions; viz. (a) the contribution of mass movement is negligible (17), and (b) small ions do not behave ideally in a charged membrane (17).

$$E_m = \frac{RT}{F}\left[\ln\frac{C_2}{C_1} + (2\alpha-1)\times\ln\frac{\sqrt{4C_2^2+\phi^2X^2}+(2\alpha-1)\phi X}{\sqrt{4C_1^2+\phi^2X^2}+(2\alpha-1)\phi X} \ln\frac{\sqrt{4C_2^2+\phi^2X^2}+\phi X}{\sqrt{4C_1^2+\phi^2X^2}+\phi X}\right] \quad (2)$$

where ϕ is a characteristic factor of the membrane-electrolyte pair, and represents a fraction of counterions not tightly bound to the membrane skeleton. The product ϕX is termed the thermodynamically effective fixed charge density of a membrane. Other terms have their usual significance. Equation 2 has the same functional form as that given by the TMS theory for the membrane potential E_m, i.e., Eq. 1 except that the thermodynamically effective fixed charge density ϕX of the membrane is used in place of stoichiometric fixed charge density $\bar{X}$. Equation 2 reduces to the TMS membrane potential for ϕ = 1. Since it is somewhat troublesome to evaluate ϕX at an arbitrary external electrolyte concentration

from the observed membrane potential E_m using eq. 2, Kobatake and Kamo (24) have proposed a simple method using the following approximate equation for the diffusive contribution to the emf of a cell with transport

$$E_m = \frac{RT}{F}(1 - 2T_{-app}) \ln C_2/C_1 \qquad (3)$$

where T_{-app} is the transference number of coions in the membrane phase. Comparison of eqs. 2 and 3 yield

$$T_{app} = \frac{1-2\alpha}{2} \frac{\ln\left(\frac{\sqrt{4\xi_2^2+1}+2\alpha-1}{\sqrt{4\xi_1^2+2}+2\alpha-1}\right)}{\ln\gamma} + \frac{\ln\left(\frac{\sqrt{4\xi_2^2+1}+1}{\sqrt{4\xi_1^2+1}+1}\right)}{2\ln\gamma} \qquad (4)$$

where

$$\xi = C/\phi X \text{ and } \gamma = C_2/C_1$$

On the other hand (17,18), the mass-fixed transference number of coions τ_- in a negatively charged membrane immersed in an electrolyte solution of concentration C was defined by

$$T_- = vc_- / (uc_+ + vc_-) \qquad (5)$$

where C_+ and C_- are the concentrations of cation and anion, respectively, in the membrane phase. This equation was transformed to

$$T_- = 1-\alpha - \frac{\sqrt{4\xi^2+1}+1}{\sqrt{4\xi^2+1}+(2\alpha-1)} \qquad (6)$$

using the equations for the activity coefficients, mobilities of small ions in the membrane phase, and the equilibrium condition for electrical neutrality. The difference between T_{-app} calculated from eq. 4 and T_- from eq. 6 for various reduced concentrations was found to be less than 2%. Therefore, T_{app} and T_- were considered practically the smae. As a result, the apparent transference number T_{app} evaluated from the membrene potential data could be used for the determination of thermodynamically effective fixed charge density ϕX of the membrane at an average salt concentration C

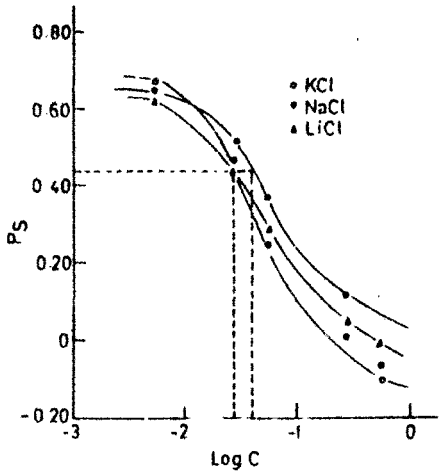

FIG. 2. Plots of P_s vs. log c for cupric palmitate membrane using various 1:1 electrolyte solutions. The dotted horizontal line shows $P_s = 1/\sqrt{5}$, and the vergical lines give the value of ϕX for the membrane-electrolyte system.

(i.e., $(C_1+C_2)/2$) using eq. 6. Rearrangement of equation 6 gave the definition of permselectivity P_s by the expression

$$\frac{1}{(4\xi^2+1)^{1/2}} \quad \frac{1-T_- -\alpha}{\alpha(2\alpha-1)(1-T_-)} = P_s. \qquad (7)$$

This equation was used to find the permselectivity P_s from the membrane potential measurements using eq. 3. If the transport number of coions (T_- or T_{-app}) is zero, the membrane is perfectly selective and $P_s = 1$, while if the transport number of coions has the value in free solution, $P_s = 0$. The values of P_s obtained using the right hand side of eq. 7 were plotted against log C. The concentration at which P_s becomes $1/\sqrt{5}$ (i.e., $\xi = C/\phi X = 1$) gives the value of the thermodynamically effective fixed charge density ϕX as demanded by the left hand side of eq. 7. Figure 2 represents a plot of P_s vs. log C for the parchment-supported cupric palmitate membrane in contact with various 1:1 electrolytes. The values of ϕX thus derived for the membrane-electrolyte systems are given in Table III.

Most recently, Tasaka et al. (27) derived another equation for the membrane potential existing across a charged membrane. The total membrane potential E_m was considered as the sum of a diffusion potential inside the membrane and the electrostatic potential difference between the membrane surfaces and electrolyte solutions on both sides of the membrane. The diffusion potential E_d was obtained by inte-

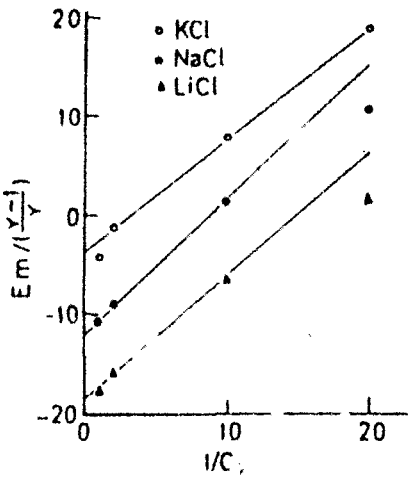

FIG. 3. Plots of membrane potential $E_m/(\gamma-1)/\gamma$ vs $1/c_2$ for cupric palmitate membrane.

grating the basic flow equation for diffusion while the electrostatic potential was calculated from the Donnan's theory. At sufficiently high electrolyte concentrations, these authors derived the following approximate equation for membrane potential E_m

$$E_m = \frac{RT}{F}\left(\frac{\gamma-1}{\gamma}\right)\left(\frac{\phi X}{2}\right)1/c_2 + \ldots \quad (8)$$

Equation 8 predicts a linear relationship between E_m and $1/C_2$ from which ϕX can be calculated. A set of straight lines in Figure 3 are in full agreement with eq. 8. The values of ϕX derived from the slope of the lines are given in Table III.

Table III shows that the values of the charge densities evaluated from the various procedures are not much different from each other and that the values are comparable to those derived by the TMS theory. A slight difference in the values of ϕX may be ascribed to the different graphical procedures adopted for the evaluation. It may therefore be concluded that the recently developed theoretical equations for membrane potential are quite sound and that their use for the evaluation of effective fixed charge density of membrane is justified for at least the systems under investigation.

ACKNOWLEDGMENTS

The authors are grateful to Prof. W. Rahman, Head, Department of Chemistry, Aligarh Muslim University, Aligarh for providing the necessary research facilities and also to C.S.I.R. (India) for the award of fellowship to Akmal Husain and Badrul Islam.

REFERENCES

1. Mueller, P., D.O. Rudin, H.T. Tien, and W.C. Wescott, Circulation 26:1167 (1962).
2. Mueller, P., D.O. Rudin, H.T. Tien, and W.C. Wescott, Nature 194:979 (1962).
3. Mueller, P., D.O. Rudin, H.T. Tien, and W.C. Wescott, J. Phys. Chem. 67:534 (1963).
4. Liquori, A.M., and C. Botre, Rec. Sci. 34(6):71 (1964).
5. Liquori, A.M., and C. Botre, J. Phys. Chem. 71:3765 (1967).
6. Liquori, A.M., L. Constantino, and G. Segre, Ric. Sci. 36:591 (1966).
7. Hays, R.H., J. Gen. Physiol. 51:385 (1968).
8. DeKorosy, F., J. Phys. Chem. 72:2591 (1968).
9. Lakshminarayanaiah, N., and F.A. Siddiqi, Biophys. J. 11:603 (1971).
10. Lakshminarayanaiah, N., and F.A. Siddiqi, Biophys. J. 11:617 (1971).
11. Lakshminarayanaiah, N., and F.A. Siddiqi, Biophys. J. 12:540 (1972).
12. Siddiqi, F.A., N. Lakshminarayanaiah, and M.N. Beg, J. Polym. Sci. A-1, 9:2853 (1971).
13. Siddiqi, F.A., N. Lakshminarayanaiah, and M.N. Beg, J. Polym. Sci. A-1, 9:2869 (1971).
14. Beg, M.N., F.A. Siddiqi, and R. Shyam, Can. J. Chem. 55:1680 (1977).
15. Beg, M.N., F.A. Siddiqi, Radhey Shyam, and M. Arshad, J. Membr. Sci. 2:365 (1977).
16. Beg, M.N., F.A. Siddiqi, R. Shyam, and I. Altaf, J. Electroanal. Chem. Interfacial Electrochem. 89:141 (1978).
17. Siddiqi, F.A., M.N. Beg, M. Ibadur Bahman Khan, A. Haque, S.K. Saksena, and B. Islam, Can. J. Chem. 56:2205 (1978).
18. Siddiqi, F.A., M.N. Beg, M. Ibadur Rahman Khan, and M. Squeel Ahsan, J. Membr. Sci., 4:275 (1978).
19. Teorell, T., Proc. Soc. Exp. Biol. Med. 33:282 (1935).
20. Teorell, T., Proc. Natl. Acad. Sci. USA 21:152 (1935).
21. Meyer, K.H., and J.F. Sievers, Helv. Chem. Acta 19:649 (1936).
22. Meyer, K.H., and J.F. Sievers, Helv. Chim. Acta 19:665 (1936).
23. Meyer, K.H., and J.F. Sievers, Helv. Chim. Acta 19:987 (1936).
24. Kobatake, Y., and N. Kamo, Prog. Polym. Sci. Jpn. 5:257 (1972).
25. Kamo, N., M. Oikawa, and Y. Kobatake, J. Phys. Chem. 77:92 (1973).
26. Kamo, N., M. Oikawa, and Y. Kobatake, J. Phys. Chem. 77:2995 (1973).
27. Tasaka, M., N. Aoki, Y. Konda, and M. Nagasawa, J. Phys. Chem.

[Received September 19, 1978]

J Electroanal. Chem., 80 (1977) 223—238

STUDIES WITH MODEL MEMBRANES

PART IX. EVALUATION OF THE THERMODYNAMIC EFFECTIVE FIXED CHARGE DENSITY AND PERMSELECTIVITY OF PARCHMENT SUPPORTED COBALT TUNGSTATE AND MERCURIC CHROMATE MEMBRANES

FASIH A. SIDDIQI, M. NASIM BEG and POORNA PRAKASH

Physical Chemistry Division, Department of Chemistry, Aligarh Muslim University, Aligarh 202001 (India)

(Received 9th December 1975; in final form 13th August 1976)

ABSTRACT

Thermodynamic effective fixed charge densities of cobalt tungstate and mercuric chromate parchment supported membranes were evaluated by a number of methods particularly those of Teorell-Meyer-Sievers [19]. Altug and Hair [23] and the most recent one of Kobatake et al. [24,27] based on the thermodynamics of irreversible processes. The value of the permselectivity was also obtained for the two membranes based on Kobatake et al.'s procedure. Kobatake et al.' equation was used under two limiting conditions of concentration of electrolyte solution, namely (1) in the concentrated range, and (2) in the dilute range. The charge densities obtained under these conditions namely θ_c and θ_d were found to differ ($\theta_c = \frac{1}{2}\theta_d$), but it was interesting to note that θ_c values were more closer to those of the TMS values. The theoretical predictions for membrane potential using Kobatake et al.'s equation are borne out quite satisfactorily by our experimental results for both membranes.

In order to understand the mechanism of transport through biological systems, a number of studies have been made of model membranes, for example (a) the parchment supported membranes [1—6] which in some formal aspects, behave like gastric mucosal membranes [7] and (b) asymmetric polymeric membranes [8] which mimic some of the properties of nerve cells [9]. In the earlier studies of parchment supported membranes, we have obtained the diffusion rate sequence of biologically important metal cations which, on the basis of Eisenman-Sherry theory [10,11] points towards the weak field strength of fixed charge groups of the membrane matrix [1—3]. Kedem and Katchalsky have discussed the behaviour of complex membranes in a series of theoretical papers [12]. We have approached the problem of understanding the complex behaviour membranes following suggestions by Teorell [7], Sollner [13], Gregor [14], Schmid [15], Helfferich [16], Schlögl [17], Spiegler [18], etc., the most important being the evaluation of the thermodynamic effective fixed charge density.

The various attempts made to calculate membrane potentials fall into three

groups: (a) the idealized theory of Teorell-Meyer-Sievers (TMS) [19] and its refinements [20], (b) the pseudo-thermodynamic approach due to Scatchard and the treatment based on the thermodynamics of irreversible processes [21] and (c) a kinetic approach based on the theory of absolute reaction rates [22]. This paper deals with the evaluation of the thermodynamic effective fixed charge density by different methods, namely those of TMS [19], Altug and Hair [23], and the most recent one of Kobatake et al. [24—27] based on the thermodynamics of irreversible processes.

EXPERIMENTAL

The membranes of (a) cobalt tungstate, and (b) mercuric chromate were prepared by the method of interaction suggested by Weiser [28]. First parchment paper was soaked in distilled water for 2 h and then tied carefully to the flat mouth of a beaker which contains 0.2 mol dm^{-3} cobalt chloride solution. This was suspended for about 72 h in a 0.2 mol dm^{-3} solution of sodium tungstate. The two solutions were then interchanged and kept for another 72 h. The cobalt tungstate membrane thus prepared was washed with deionized water for the removal of free electrolyte. A similar procedure was adopted for the preparation of mercuric chromate membrane by taking a 0.2 mol dm^{-3} solution of mercuric chloride and a 0.2 mol dm^{-3} solution of potassium chromate.

Measurement of membrane potential

The potential developed by setting up a concentration cell of the type described by Michaelis [29], and other authors [30,31] was measured using a Pye potentiometer (No. 7568) at 25° C. Saturated calomel electrodes (SCE) were connected to the solutions via KCl-agar bridges. The cell potential

SCE | Solution | Membrane | Solution | SCE

c_1 ↑ ↑ c_2

Donnan potential — Donnan potential

← diffusion potential →

was taken as a measure of membrane potential. The concentration ratio $\nu = c_1/c_2$ was put equal to 10 throughout the experiment.

Fixed charge theory of Teorell-Meyer-Sievers (TMS)

TMS [19] developed a theory of membranes with charges fixed in the lattice. This theory has been described in detail by Lakshminarayanaiah and others [21] and has also been applied by Siddiqi et al. [1—6] for the determination of thermodynamically effective fixed charge density of parchment supported membranes.

The membrane potential E_m in mV according to TMS theory applicable to a

highly idealized system is given by the equation (at 25°C)

$$E_m = 59.2[\log\{c_1([4c_2^2 + \bar{X}^2]^{1/2} + \bar{X})/c_2([4\,c_1^2 + \bar{X}^2]^{1/2} + \bar{X})\} + \bar{U}\,\log([4\,c_1^2 + \bar{X}^2]^{1/2} + \bar{X}\bar{U})/([4\,c_2^2 + \bar{X}^2]^{1/2} + \bar{X}\bar{U})] \quad (1)$$

where $\bar{U} = (\bar{u} - \bar{v})/(\bar{u} + \bar{v})$; $\bar{u}$ and $\bar{v}$ are the mobilities of the cation and anion respectively, in the membrane phase. c_1 and c_2 are the concentrations of the electrolyte solutions on either side of the membrane and $\bar{X}$ is the charge on the membrane expressed in equivalents dm^{-3}.

Altug and Hair method

Altug and Hair [23] have given an ingenious and indirect method which has been developed on the lines of Teorell's model [19] for the evaluation of membrane charge density $w\bar{x}$, where $\bar{x}$ represents the number of ionised sites per unit volume and $w = \pm 1$ depending on the nature of charged sites.

The essential feature of the original fixed charge theory of Teorell [19] was the assumption that the overall membrane potential was composed of three potential jumps: two Donnan potentials one at each solution-membrane interface (here denoted by π_1 and π_2) and one residing inside the membrane the internal potential or the driving potential being denoted by $(\phi_2 - \phi_1)$. The overall total membrane potential E_{cal} is given by

$$E_{cal} = (\pi_1 + \pi_2) + (\phi_2 - \phi_1) \quad (2)$$

π_1 and π_2 can be calculated according to equations

$$\pi_1 = -(RT/F)\ln r_1 \quad (3a)$$

and

$$\pi_2 = +(RT/F)\ln r_2 \quad (3b)$$

where r_1 and r_2 are the Donnan distribution ratios at the two interfaces and are given by the equation

$$r = \{1 + (w\bar{x}/2\,a)^2\}^{1/2} - (w\bar{x}/2\,a) \quad (4)$$

where a is the external solution activity. The diffusion potential $(\phi_2 - \phi_1)$ for 1 : 1 valent electrolyte is given by

$$(\phi_2 - \phi_1) = (u - v)/(u + v)(RT/F)\,\ln\{a_1(r_1u + v/r_1)/a_2(r_2u + v/r_2)\} \quad (5)$$

where u and v are the cationic and anionic mobilities in the membrane. However in the present calculations, these are assumed to be the same as in the bulk solutions. Subscripts 1 and 2 refer to the solutions on each side of the membrane. The use of concentration, rather than activities, is an assumption based on the practical difficulty of measuring ion activities in a membrane phase as suggested [23]. Substituting these values in eqn. (2) gives

$$E_{cal} = (u - v)/(u + v)(RT/F)\,\ln\{a_1(r_1u + v/r_1)/a_2(r_2u + v/r_2)\} + (RT/F)\ln r_2/r_1 \quad (6)$$

Kobatake et al. theory

Starting with the basic flow equations provided by the thermodynamics of irreversible processes [21], Kobatake et al., describe in detail the derivation of eqn. (7) for the electric potential $\Delta\phi$ arising between two solutions of an uni-univalent electrolyte of different concentrations, c_1 and c_2, separated by an (negatively) ionisable membrane of charge density θ (mol dm^{-3}).

$$\Delta\phi = -(RT/F)\left[\frac{1}{\beta}\ln c_2/c_1 - (1 + 1/\beta - 2\alpha)\ln(c_2 + \alpha\beta\theta/c_1 + \alpha\beta\theta)\right] \quad (7)$$

where $\alpha = (l_+/l_+ + l_-)$; $\beta = 1 + KF\theta/l_+$, l_+ and l_- are molar conductivities of positive and negative ions, and K is a constant dependent on solution viscosity.

Limiting forms of eqn. (7)

Kobatake et al. [24] have derived two useful limiting forms of eqn. (7). These are:

(a) where c_1 becomes sufficiently small with ν fixed; eqn. (7) may be expanded to give

$$|\Delta\phi_r| = \frac{1}{\beta}\ln\nu - \frac{\nu - 1}{\alpha\beta\nu}\left(1 + \frac{1}{\beta} - 2\alpha\right)c_1/\theta \quad (8)$$

where $|\Delta\phi_r|$ is the absolute value of a reduced membrane potential defined by

$$\Delta\phi_r = F\Delta\phi/RT \quad (9)$$

(b) it has also been shown by Kobatake et al. [24] that at a fixed ν the inverse of an apparent transference number t^-_{app} for the co-ion species in a negatively charged membrane is proportional to the inverse of the concentration c_1 in the region of higher salt concentration. Here t^-_{app} is defined by the relation

$$|\Delta\phi_r| = (1 - 2t^-_{app})\ln\nu \quad (10)$$

The derived transport number value has been called the apparent transport number, i.e., t^-_{app}, because in this type of measurement water transport has not been taken into account. This apparent value will be close to the true value, when dilute solutions are used. Substituting for $\Delta\phi$ from eqn. (7) and expanding the resulting expression $1/t^-_{app}$ in powers of $1/c_1$ gives

$$1/t^-_{app} = 1/(1 - \alpha) + \frac{(1 + \beta - 2\alpha\beta)(\nu - 1)\alpha}{2(1 - \alpha)^2\ln\nu}(\theta/c_1) \quad (11)$$

Reduced expression of permselectivity according to Kobatake

Kobatake et al. [27] have derived the following expression for the mass fixed transference number of anion in the membrane phase (negatively charged) immersed in an electrolyte solution of concentration c.

$$r_- = 1 - \alpha[(4\xi^2 + 1)^{1/2} + 1/(4\xi^2 + 1)^{1/2} + (2\alpha - 1)] \quad (12)$$

where $\xi = c/\phi X$, $\alpha = (u^0_+/u^0_+ + u^0_-)$; u^0_i ($i = +, -$) stand for the mobility of ion

species i in the bulk solution, ahd X is a stoichiometric concentration of charges fixed in the membrane. On the other hand, the apparent transference number of anion in the membrane τ_{app}^- is defined by the following Nernst equation:

$$\Delta\phi = -(RT/F)(1 - 2\,\tau_{app}^-)\ln(c_1/c_2) \tag{13}$$

where c_1 and c_2 are the concentration of the external solution in mol dm^{-3} on the two sides of the membrane, and R, T and F have their usual thermodynamic meaning. It has been found by Kobatake et al. [27] that the difference between τ^- and τ_{app}^- was less than 2% in the wide range of salt concentration when the averaged concentration $(c_1 + c_2)/2$ was replaced by c. Therefore, if we replace τ^- by τ_{app}^- and c by $(c_1 + c_2)/2$, eqn. (12) is applicable even when the concentrations on the two sides of the membrane are different. Rearrangement of eqn. (12) leads to

$$1/(4\,\xi^2 + 1)^{1/2} = (1 - \tau_{app}^- - \alpha)/(\alpha - [2\,\alpha - 1][1 - \tau_{app}^-]) \equiv P_s \tag{14}$$

Here P_s is a measure of permselectivity of the membrane electrolyte system.

RESULTS AND DISCUSSION

The membrane potential data obtained with each of the two types of parchment supported membranes using various 1 : 1 electrolytes, are plotted as a function of $\log(c_1 + c_2)/2$ with the ratio ν fixed at 10. These plots are shown in Fig. 1.

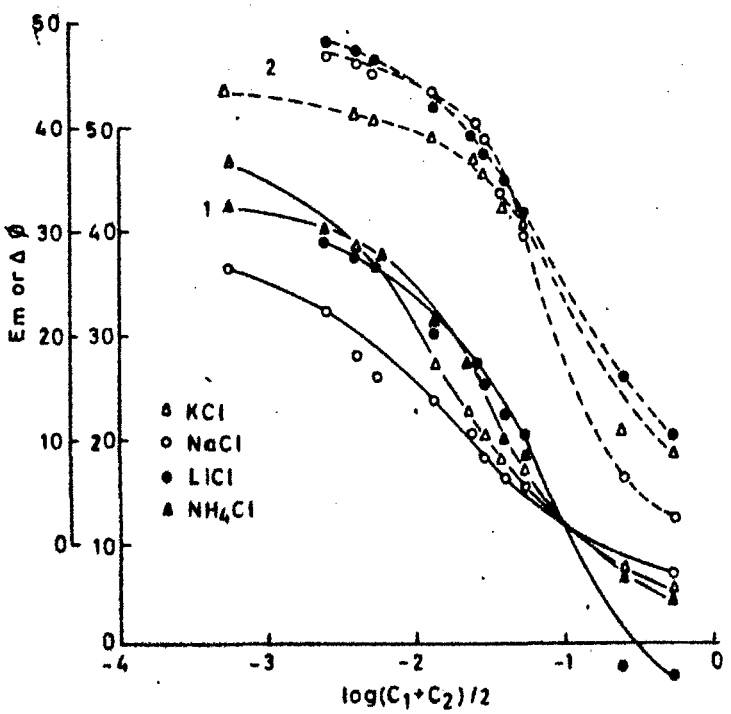

Fig. 1. Plots of observed potentials against $\log(c_1 + c_2)/2$ for various electrolytes. 1, cobalt tungstate((———); 2, mercuric chromate (- - - - - -).

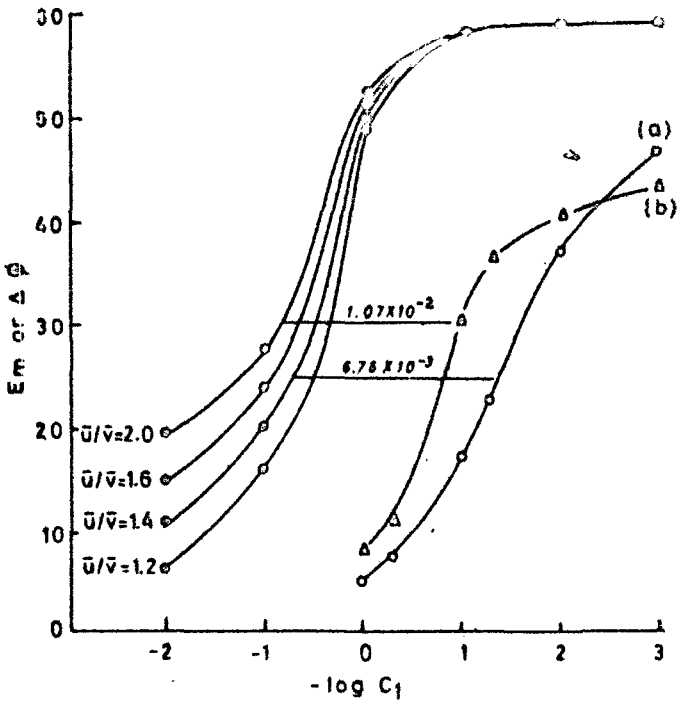

Fig. 2. Evaluation of membrane charge density $\bar{X}$ and the mobility ratio $\bar{u}/\bar{v}$ in the membrane phase. The different curves for different mobility ratio. The observed values of E_m or $\Delta\phi$ for (a), cobalt tungstate; (b), mercuric chromate for KCl electrolyte against $-\log c_1$.

The graphical method of Meyer and Sievers [19] determines the fixed charge $\bar{X}$ in equivalents dm^{-3} and the cation-to-anion mobility ratio in the membrane phase. The sets of curves on the left in Fig. 2 (closed points curves) are the theoretical membrane potentials calculated with the help of eqn. (1) for a cation selective membrane, 1 : 1 electrolyte and constant solution concentration ratio $\nu = 10$, as a function of $-\log c_1$. The different curves are for different mobility ratios $\bar{u}/\bar{v}$, with $\bar{X}$ having constant value of unity expressed in equivalents dm^{-3}. The experimental E_m values for (a) cobalt tungstate and (b) mercuric chromate membranes (open points) with KCl electrolytes are plotted in the same graph against $\log c_1$. These experimental curves were shifted horizontally until they coincided with one of the theoretical curves. This shift gave $\log \bar{X}$ and coinciding theoretical curve gave $\bar{u}/\bar{v}$. But the experimental curves (a) and (b) do not coincide exactly as demanded by the theoretical method of Meyer and Sievers and a very rough approximation has been made particularly with curve (a). The reason for this slight discrepancy is low charge density of both the membranes due to which the maximum value of membrane potential is not obtained. This lies between 44—46 mV with highest dilution ($c = 10^{-3}$ to 10^{-4} mol dm^{-3}) with vigorous stirring. (Theoretical value would be around 59 mV.) In Table 1 are given the values of $\bar{X}$ and $\bar{u}/\bar{v}$ derived in this way for both membranes with different electrolytes.

This analytical method gave satisfactory result for fixed charge density eval-

TABLE 1

Comparison of charge density for different membrane-electrolyte systems

Membrane	Electrolyte	TMS		Altug and Hair	Kobatake et al. values			
		$\bar{u}/\bar{v}$	$\bar{X}$	$\bar{X}$	eqn. (11) θ_c [a]	eqn. (8) θ_d [b]	eqn. (17) ϕX [c]	P_s vs. $\log\frac{c_1+c_2}{2}$ ϕX
Cobalt tungstate	KCl	1.4	0.0067	0.02	0.0054	0.0253	0.0486	0.0209
	NaCl	1.4	0.0054		0.0049	0.0102	0.0438	0.0603
	LiCl	1.0	0.0199		0.0065	0.0367	0.0511	0.0100
	NH_4Cl	1.4	0.0085		0.0046	0.0226	0.0408	0.0380
Mercuric chromate	KCl	2.0	0.0107	0.04	0.0035	0.0449	0.0233	0.0758
	NaCl	1.4	0.0457		0.1189	0.3495	1.2440	0.1148
	LiCl	1.2	0.0336		0.0374	0.1282	0.3582	0.3311

[a] $\theta_c = \frac{2(1-\alpha)^2 \ln \nu}{(1+\beta-2\alpha\beta)(\nu-1)\alpha} \cdot \text{slope}$. [b] $\theta_d = \frac{(\nu-1)\cdot(1+1/\beta-\alpha\alpha)}{\alpha\beta\nu} \cdot \frac{1}{\text{slope}}$. [c] $\phi X = \frac{(1-\alpha)}{\alpha} \cdot \left[\frac{\nu \ln \nu}{\nu-1}\right] \cdot \text{slope}$.

uation, the values of which are quite low and hence very different to determine by the usual exchange reaction. This technique has been used by Kumins and London [32] to estimate the capacity of thin polymer membranes of poly-(vinyl chloride) and poly(vinyl acetate). It has also been used by Baxter [33] to determine the charge on Keratin and by Lakshminarayanaiah [34] and Siddiqi [1—5] to evaluate the fixed charge on thin parlodion and parchment supported membranes.

In a modification of this type of plotting Altug and Hair [23] evaluated $\bar{X}$ for glass membranes, choosing solution values for u and v. In this procedure, a value for $\bar{X}$ was assumed and r_1 and r_2, the distribution ratios, were calculated according to eqns. (3) and (4) for the given electrolyte concentrations c_1 and c_2, the theoretical membrane potential was then determined from eqn. (6) for 1.0 to 1.0 $\times 10^{-4}$ mol dm^{-3} concentration range. By following the algebraic procedure, a series of theoretical curves were obtained for different $\bar{X}$ values with KCl electrolyte and are shown by the solid lines in Fig. 3. At the same time curves were also plotted in same Fig. 3 between the experimentally determined membrane potential values for KCl electrolyte in the same concentration range for both the membranes. The theoretical curves gave the values for $\bar{X}$ which are given in Table 1. Here again, there is a poor fit due to the very low charge density.

The fixed charge density of the mercuric chromate membrane determined by the Altug and Hair [23] method was found to be 0.04 equivalents dm^{-3}. Taking

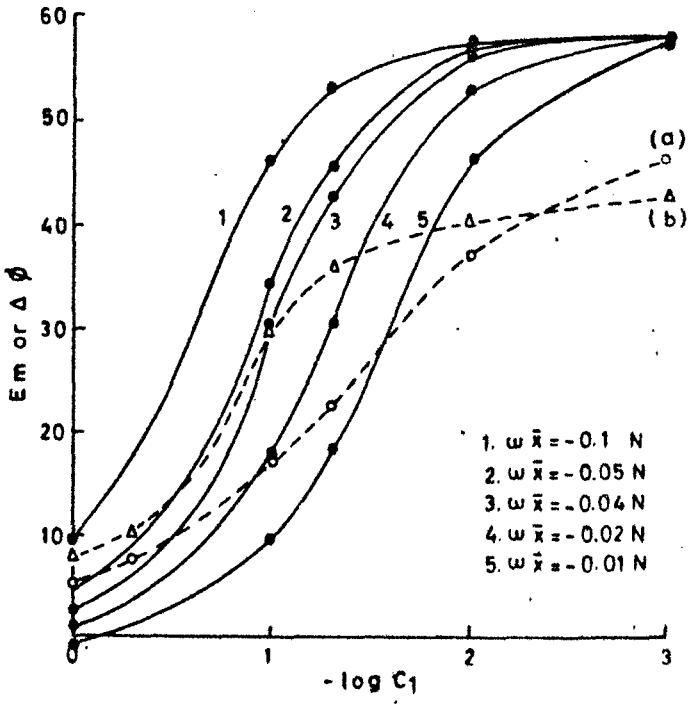

Fig. 3. Plots of membrane potentials across (a), cobalt tungstate; (b), mercuric chromate. For KCl electrolyte of varying concentrations, fixed charge density against $-\log c_1$. Observed values with broken line.

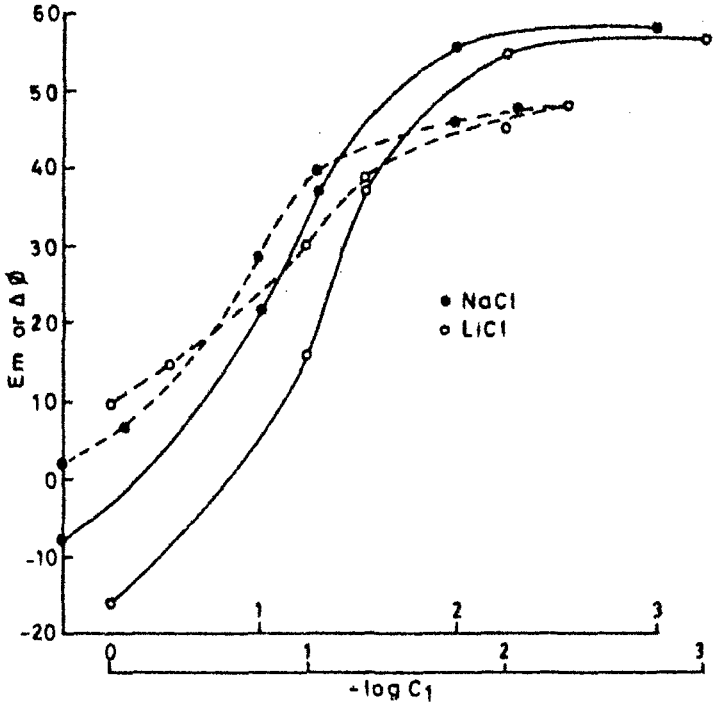

Fig. 4. Membrane potential E_m or $\Delta\phi$ across mercuric chromate of varying concentrations for different electrolytes. (———), calculated values assuming $w\bar{X} = -0.04\ N$; (- - - - - -), observed values.

this value of the charge density, the experimental and calculated value of the membrane potential for NaCl and LiCl is shown in Fig. 4. Fair agreement with theory or theoretical curves is obtained for the NaCl, but not for LiCl. It should be noted that the cation and anion mobilities used in the present calculations are those of the free solution [35]. Diffusion data in literature, however, indicate that the ion mobilities go through a considerable change in a parchment supported membrane. The fair agreement between observed and calculated values in the case of the salt solution, indicates that the membrane is behaving in a manner closely allied to that predicted by TMS [19] and that the cation and anion mobility ratio is little affected by the membrane. In the case of LiCl solution the cation and anion mobility ratio may be altered by the membrane, the mobility of the cation being decreased relative to that of anion.

Method of evaluation of the thermodynamic effective fixed charge density and permselectivity according to Kobatake et al. [24]

Equation (8) indicates that a value of β and a relation between α and θ can be obtained of a plot of $|\Delta\phi_r|$ against c_1 at fixed $\nu = 10$. Figure 5 illustrates plots of $|\Delta\phi_r|$ versus c_1 in the region of very low concentration that were determined for various electrolytes with cobalt tungstate and mercuric chromate membranes. The value of intercept is equal to $(1/\beta)\ln\nu$, from which β may be evaluated. Values are given in Table 2.

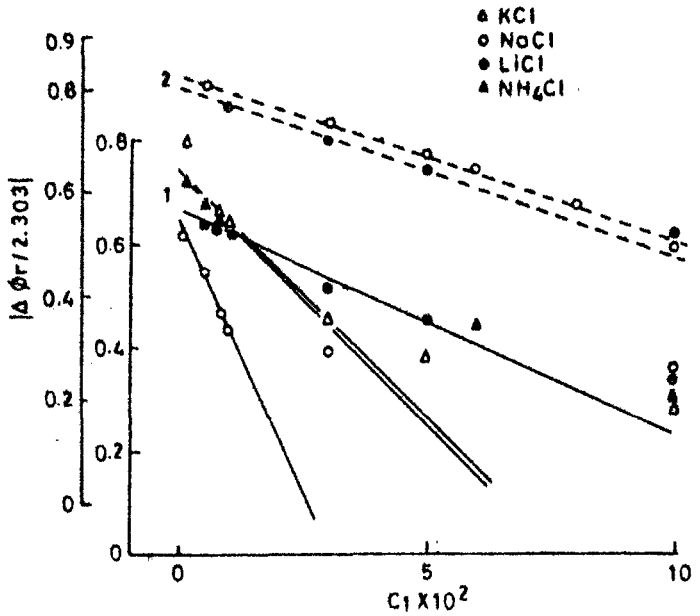

Fig 5. Plots of $|\Delta\phi_r/2.303|$ vs. $c_1 \times 10^2$ for various electrolytes. 1, cobalt tungstate (———); 2, mercuric chromate (- - - - - -).

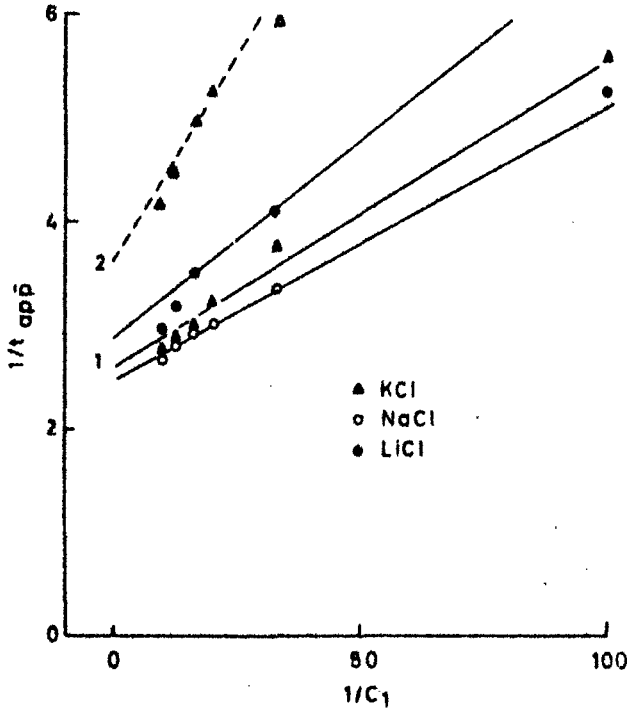

Fig. 6. Plots of $1/\bar{t}_{app}$ vs. $1/c_1$ for various electrolytes. 1, cobalt tungstate (———); 2, mercuric chromate (- - - - - -).

TABLE 2

Values of parameters α, β and θ for various membrane-electrolyte systems at $\nu = 10$

Membrane	Electrolyte	α	β	θ_c [a]
Cobalt tungstate	KCl	0.6123	1.360	0.0054
	NaCl	0.5935	1.538	0.0049
	LiCl	0.6504	1.516	0.0065
	NH_4Cl	0.6213	1.370	0.0046
Mercuric chromate	KCl	0.7312	1.379	0.0035
	NaCl	0.3333	1.227	0.1189
	LiCl	0.5556	1.243	0.0374

[a] $\theta_c = \dfrac{2(1-\alpha)^2 \ln \nu}{(1+\beta-2\alpha\beta)(\nu-1)\alpha} \cdot \text{slope}.$

Equation (11) indicates that the intercept of a plot of $1/t_{app}^-$ against $1/c_1$ at fixed $\nu = 10$ allows the values of α to be determined. Plots of $1/t_{app}^-$ against $1/c_1$ for various 1 : 1 electrolytes are shown in Fig. 6 for both cobalt tungstate and mercuric chromate membranes. The value of intercept is equal to $1/(1-\alpha)$; from which α may be evaluated. Values are given in Table 2.

For the evaluation of θ, there are also two limiting cases: (a) in dilute range ($c = 1 \times 10^{-3}$ to 3×10^{-2} mol dm^{-3}) the slope of eqn. (8) is given by

$$\frac{\nu-1}{\alpha\beta\nu}(1 + 1/\beta - 2\alpha)(1/\theta)$$

The graphical value of the slope determined from Fig. 5 is equated with the above expression, substituting the values α and β, θ may be determined. This value of θ is designated by θ_d (signifying the dilute range); (b) in the concentration range ($c = 1.0$ to 1.0×10^{-2} mol dm^{-3}) using eqn. (11), the slope is given by

$$(1 + \beta - 2\alpha\beta)(\nu - 1)\,\theta/2(1-\alpha)^2 \ln \nu$$

The graphical value of slope determined from Fig. 6 is equated with the above expression. The values of α and β are substituted and thus the value of θ is evaluated. This value of θ is designated θ_c (signifying the concentrated range). Kobatake has suggested [24] that provided his equation for the membrane potential is correct, then the two values of θ i.e. θ_c and θ_d thus determined from the opposite limits should agree. In the present investigation with parchment supported membranes, the θ_d values are found to be higher than θ_c values ($\theta_d = 0.025 > \theta_c = 0.005$). It is also noted that the lower values of θ, i.e. θ_c, are closer to the charge density values determined by TMS method (vide Table 1). Once the value of parameters α, β and θ for a given membrane-electrolyte system have been determined, one can calculate the theoretical $\Delta\phi$ versus c_1 curve for the given value of $\nu = 10$ and then compare it with the corresponding experimental data. For this comparison the equation may be rewritten in the following form as suggested by Kobatake [24]

$$(\nu - e^q)/(e^q - 1) = X \qquad (15)$$

with q and $\bar{X}$ defined by

$$q = [|\Delta\phi_r| + (1 - 2\alpha) \ln \nu]/[(1/\beta) + (1 - 2\alpha)] \quad (16a)$$

$$X = c_1/(\alpha\beta\theta) \quad (16b)$$

(This X has no relation to the $\bar{X}$ used in the TMS and Altug and Hair methods.) Thus if eqn. (7) is valid, the values of $(\nu - e^q)/(e^q - 1)$ calculated from the measured values of $\Delta\phi$, together with the predetermined α, β and θ (from Table 2) and the given value of $\nu = 10$, must fall on a straight line which has a unit slope and passes through the coordinate origin, when plotted against X. This behaviour should be observed irrespective of the value of ν and the kind of membrane/electrolyte (1 : 1 system) used. Figure 7 demonstrates that for NaCl (open circle), the curve nearly passes through the origin with unit slope and the derivation from linearity is very slight, while for NH_4Cl (closed triangles) the deviation is somewhat marked. It may be possible that at the two extreme concentrations ($X = c_1/\alpha\beta\theta$) the curve deviates from ideal behaviour. It may safely be concluded that the theoretical prediction, based on Kobatake's membrane potential equation is borne out quite satisfactorily by our experimental results on parchment supported cobalt tungstate and mercuric chromate membranes for NaCl electrolyte.

For the evaluation of effective fixed charge density ϕX, the various values of permselectivity P_s were calculated by substituting the values of α (bulk) and $\bar{r}_{app}$

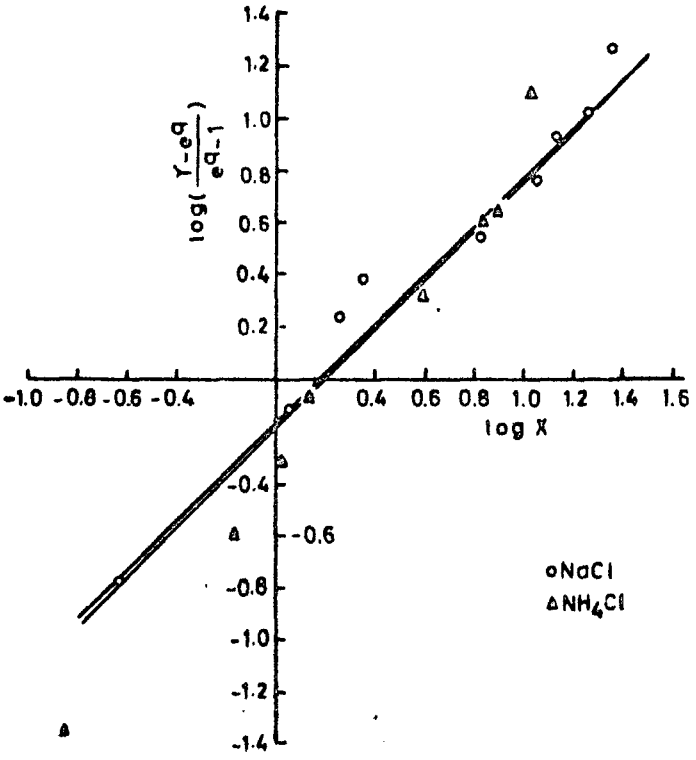

Fig. 7. Plots of $\log(\nu - e^q)/(e^q - 1)$ and $\log X$ for cobalt tungstate with various electrolytes.

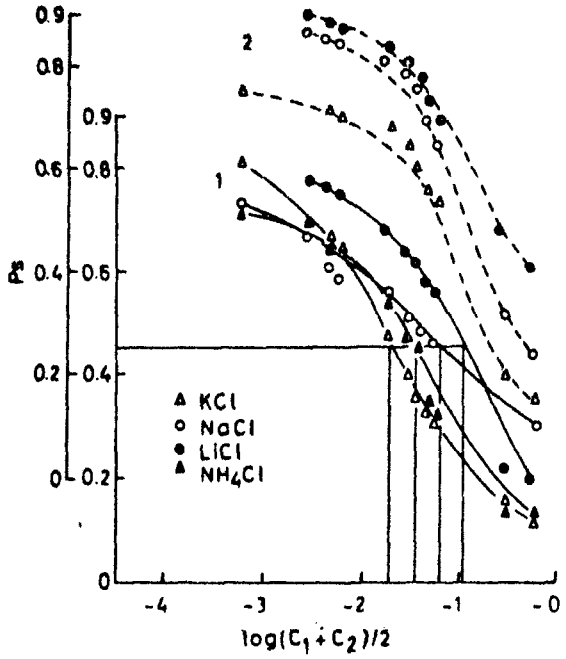

Fig. 8. Plots of P_s vs. $\log(c_1 + c_2)/2$ for various electrolytes. 1, cobalt tungstate (———); 2, mercuric chromate (· · · · · ·).

in eqn. (14), and then plotted against $\log(c_1 + c_2)/2$ ($(c_1 + c_2)/2$ being the average concentration). The results are shown in Fig. 8. The term ξ has already been defined as the ratio between the average concentration c and the effective fixed charge density ϕX i.e. $\xi = c/\phi X$, the units of both c and ϕX are expressed in terms of mol or equivalents dm^{-3}. When the average concentration c is equal to the effective fixed charge density ϕX, i.e. $c/\phi X = \xi = 1$, the values of P_s must give $1/\sqrt{5} = 0.448$ from left hand side eqn. (14). The corresponding concentration is obtained from the plot of P_s versus $\log c$ as given in Fig. 8. This value of concentration is equal to the fixed charge density. The ϕX values are given for various electrolytes in Table 1. Further, the plots of P_s versus $(1 + 4\,\xi^2)^{-1/2}$ were drawn for both membranes with KCl electrolyte and shown in Fig. 9. It is clear from the Figure that the points for both the membranes with KCl electrolyte joined together do not pass through the origin. But if a straight line is drawn with unit slope from the origin, some of the points are above the line (positive deviation) up to the value 0.45 of $1/(1 + 4\,\xi^2)^{1/2}$, while the remaining points are below the straight line after the value of 0.45. It may be concluded that if the mean of the points are joined together, they will fall on a straight line with unit slope passing through the origin, thereby confirming the applicability of Kobatake's equation to these membranes.

Yet another method for the evaluation of effective fixed charge density is given by Kobatake et al. [27] which utilizes the following expression

$$1/\bar{\tau}_{app} = 1/(1-\alpha) + \alpha/(1-\alpha)[(\nu-1)/\nu \ln \nu](\phi X/c_1) \qquad (17)$$

This equation illustrates that the plots of $1/\bar{\tau}_{app}$ against $1/c_1$ with fixed $\nu = 10$

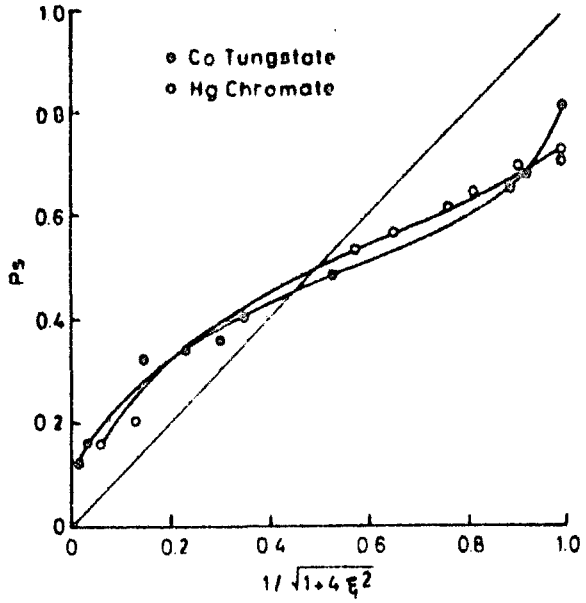

Fig. 9. Plots of P_s vs. $1/\sqrt{1+4\xi^2}$ for KCl electrolytes with various systems.

gives a straight line and the values of α and ϕX of the system can be evaluated from the intercept and the slope of the straight line. The values of ϕX for both membrane electrolytes are given in Table 1.

The conclusions which can be drawn about the relative strengths and weaknesses of each of the theories as applied to parchment supported membranes can be summarized as follows.

The important point emerging from the application of TMS theory is that the mobility ratio goes through a change, considerable in some cases, in the membrane phase. Usually in the case of cation selective membrane (values of $\bar{X}$ high) $(\bar{u}/\bar{v}) \to \infty$ in dilute solutions and only when the membrane is in equilibrium with concentrated solutions does $(\bar{u}/\bar{v}) \to (u/v)_{\text{solution}}$. In view of this, the approach of TMS is unreliable to evaluate $\bar{X}$ for ion-exchange membranes which have a high concentration of fixed groups. This point has been well illustrated by Lakshminarayanaiah [34] for a phenolsulfonate membrane. It is not that unreliable for a membrane which has a low concentration of $\bar{X}$, as found in this study, due to the fact that the change in the values of the factor $(\bar{u}/\bar{v})$ is not as drastic as it is with membranes of high charge density. The limitations of this conceptually useful theory which has stimulated both theoretical and experimental work, are applicable only to an idealized system and this should be borne in mind when it is applied to analyze membrane phenomena.

Altug and Hair's method is principally based on Teorell's model. This alternative method of plotting the membrane potential data may be expected to give $\bar{X}$ values different from those given by TMS method. It is not very realistic to use the solution mobility values for the ratio $\bar{u}/\bar{v}$ in the calculations. It is believed that the approach of Altug and Hair overestimated $\bar{X}$ in comparison to TMS method.

In the Kobatake method, the derivation is based on the thermodynamics of

irreversible processes. They have claimed that their data on an oxidized collodion membrane potential, as well as those of previous workers, are fitted quite accurately by the equation derived by them. They have also stated that no such agreement with experiment was obtained in terms of the earlier theory of TMS. In the present investigation the mean value of charge density obtained by using the different equations of Kobatake is found to be closer to that obtained by the Altug and Hair method. The theoretical predictions from the Kobatake membrane potential equation is borne out quite satisfactorily by our experimental results and hence it may safely be concluded that Kobatake's approach for charge density evaluation is the best among the existing of membrane potential.

ACKNOWLEDGEMENT

Thanks are due to Professor Wasiur Rahman, Head, Department of Chemistry, for providing necessary facilities.

REFERENCES

1 F.A. Siddiqi and S. Pratap, J. Electroanal. Chem., 23 (1969) 137, 147.
2 F.A. Siddiqi, N. Lakshminaraynaiah and S.K. Saksena, Z. Phys. Chem. (Frankfurt), 72 (1970) 298, 307.
3 F.A. Siddiqi, N. Lakshminarayanaiah and M.N. Beg, J. Polymer Sci., 9 (1971) 2853, 2869.
4 F.A. Siddiqi, M.N. Beg and S.P. Singh, J. Polymer Sci., in press.
5 F.A. Siddiqi, M.N. Beg, A. Haq and S.P. Singh, Bull. Chem. Soc. Jap., 49 (1976) 2858, 2864.
6 W.U. Malik and F.A. Siddiqi, Proc. Indian Acad. Sci., A 56 (1962) 206; J. Colloid Sci., 18 (1963) 161; Bull. Chem. Soc. Jap., 40 (1967) 1741.
7 T. Teorell, Discuss. Faraday Soc., 21 (1956) 9.
8 N. Lakshminarayanaiah and F.A. Siddiqi, J. Polymer Sci., 8 (1970) 2949; Biophys. J., 11 (1971) 603, 617; 12 (1972) 150; Z. Phys. Chem., 78 (1972) 150; in M. Bier, (Ed.) Membrane Processes in Industry and Biomedicine, Plenum Press, New York, 1971.
9 A.M. Liquori and C. Botre, Ric. Sci., 34 (1964) 6; J. Phys. Chem., 71 (1967) 3765.
10 G. Eisenman in A. Kleinzer and A. Kotyk, (Eds.) Membrane Transport and Metabolism, Academic Press, New York, 1961, p. 163; Biophys. J. Suppl., 2 (1962) 259.
11 H. Sherry in J.A. Marinsky (Ed.), Ion Exchange Vol. 2, Marcel Dekker, New York, 1968.
12 O. Kedem and A. Katchalsky, Trans. Faraday Soc., 59 (1963) 1918, 1931, 1941.
13 K. Sollner, J. Phys. Chem., 49 (1945) 47, 171; J. Electrochem. Soc., 97 (1950) 139C; Ann. N. Y. Acad. Sci., 57 (1953) 177; J. Macromol. Sci., A3 (1969) 1.
14 H.P. Gregor, J. Amer. Chem. Soc., 70 (1948) 1293; 73 (1950) 642.
15 G. Schmid, Z. Elektrochem., 54 (1950) 424; 55 (1951) 229; 56 (1952) 181; G. Schmid and H. Schwarz, Z. Elektrochem., 55 (1951) 295, 684; 56 (1952) 35.
16 F. Helfferich, Ion Exchange, McGraw Hill, New York, 1962.
17 R. Schlögl, Stofftransport durch Membrane, Dr. Dietrich Steinkopff Verlag, Darmstadt, 1964.
18 K.S. Spiegler, Trans. Faraday Soc., 54 (1958) 1408.
19 K.H. Meyer and J.F. Sievers, Helv. Chim. Acta, 19 (1936) 649, 665, 987; T. Teorell, Proc. Soc. Exptl. Biol. Med., 33 (1935) 282; Proc. Natl. Acad. Sci. (U.S.), 21 (1935) 152; Z. Elektrochem., 55 (1951) 460; Progr. Biophys. Chem., 3 (1953) 305.
20 R. Schlogl, Z. Elektrochem., 57 (1953) 195; Z. Phys. Chem. (Frankfurt), 1 (1954) 305.
21 G. Scatchard, J. Amer. Chem. Soc., 21 (1956) 30; Discuss. Faraday Soc., 21 (1956) 30; G.J. Hills, P.W.M. Jacobs and N. Lakshminarayanaiah, Proc. Roy. Soc. (London), A262 (1961) 257; Y. Kobatake, J. Chem. Phys., 28 (1958) 146; A.J. Staverman, Trans. Faraday Soc., 48 (1952) 176; J.W. Lorimer, E.I. Boterenbrood and J.J. Hermans, Discuss. Faraday Soc., 21 (1956) 141.
22 M. Nagasawa and I. Kogawa, Discuss. Faraday Soc., 21 (1956) 52; M. Nagasawa and Y. Kobatake, J. Phys. Chem., (1952) 1017.
23 I. Altug and M.L. Hair, J. Phys. Chem., 72 (1968) 599.
24 Y. Kobatake, T. Noriaki, Y. Toyoshima and H. Fujita, J. Phys. Chem., 69 (1965) 3981.
25 Y. Toyoshima, M. Yusso, Y. Kobatake and H. Fujita, Trans. Faraday Soc., 63 (1967) 2803, 2874; J. Phys. Chem., 72 (1968) 2871.

26 N. Kamo, Y. Toyoshima, H. Nozaki and Y. Kobatake, Kolloid-Z. Z. Polym., 248 (1971) 914; 249 (1971) 1061.
27 N. Kamo, M. Ockawa and Y. Kobatake, J. Phys. Chem., 77 (1973) 92, 299.
28 H.B. Weiser, J. Phys. Chem., 34 (1930) 335, 1826.
29 L. Michaelis, Bull. Natl. Res. Council (U.S.A.), 69 (1929) 119; Kolloid Z., 62 (1933) 1; Michaelis and Fujita, Biochem. Z., 142 (1923) 398; Z. Phys. Chem., 110 (1924) 286.
30 K. Sollner and H.P. Gregor, J. Phys. Chem., 50 (1946) 58; 51 (1947) 299.
31 C.E. Marshall and A.D. Ayers, J. Amer. Chem. Soc., 70 (1948) 1297.
32 C.A. Kumins and A. London, J. Polymer Sci., 46 (1960) 395.
33 S. Baxter, J. Colloid Sci., 2 (1947) 495.
34 N. Lakshminarayanaiah, J. Appl. Polymer Sci., 10 (1966) 1687.
35 W.J. Moore, Physical Chemistry, Prentice Hall, Englewood Cliffs, N.J., 3rd edn., 1968, p. 337.

Colloid Science · Kolloide

Colloid & Polymer Sci. 256, 552–562 (1978)

ISSN 0303-402X / ASTM-Coden: CPMSB (formerly KZZPAF)

Physical Chemistry Division, Department of Chemistry, Aligarh Muslim University, Aligarh (India)

Studies with model membranes

Evaluation and comparison of the thermodynamic effective fixed charge density by different methods

F. A. Siddiqi, P. Prakash, and *S. P. Singh*

With 8 figures and 3 tables

(Received April 23, 1976)

We have been engaged for quite some time in the studies of membranes which can serve as models for biological membranes, for example (*a*) parchment supported membranes (1–9) which in some formal aspects at least, behaved like gastric mucosal membranes (10) (*b*) asymmetric polymeric membranes (11-14) which mimic some of the properties of nerve cells (15, 16). These studies (2, 4, 6) point towards the weak field strength of fixed charge groups of the membrane matrix. In order to substantiate our earlier findings, extensive investigations of membrane potentials have been made with mercuric phosphate and carbonate parchment supported membranes.

The various attempts made to calculate the membrane potentials and charge density fall into three groups: (*a*) the idealized theory of *Teorell-Meyer-Sievers* (17, 18) and its refinements (19), (*b*) the pseudo-thermodynamic approach due to *Scatchard* (20) and the treatment based on the thermodynamics of irreversible processes (21–24) and (*c*) a kinetic approach based on the theory of absolute reaction rates (25, 26).

This paper deals with the evaluations of (i) transport number using a modified Nernst relation, (ii) the thermodynamic effective fixed charge density by different methods namely those of TMS (17, 18) *Altug* and *Hair* (27) and the recent one of *Kobatake* et al. (28–33). A comparison between various methods have also been made along with the evaluation of permselectivity of investigated membranes. The problem has been approached taking into consideration the views of *Sollner* (34), *Gregor* (35), *Schmid* (36, 37), *Helfferich* (38) etc.

Experimental

The membranes of (1) mercuric phosphate, and (ii) mercuric carbonate were prepared by the method of interaction suggested by *Weiser* (39). First parchment paper was soaked in distilled water for 2 hr. and then tied carefully to the flat mouth of a beaker which contains 0.2 mole L^{-1} mercuric chloride solution. This was suspended for about 72 hr. in 0.2 mole L^{-1} solution of tri sodium orthophosphate. The two solutions were then interchanged and kept for another 72 hr. The mercuric phosphate membrane thus prepared was washed with deionized water for the removal of free electrolyte. A similar procedure was adopted for the preparation of mercuric carbonate membrane by taking a 0.2 mole L^{-1} solution of mercuric-chloride and 0.2 mole L^{-1} solution of sodium carbonate.

Measurement of membrane potential:

The potential developed by setting up a concentration cell of the type described by *Michaelis* (40), *Sollner* and *Gregor* (41) and *Marshal* and *Ayers* (42) was measured using a Pye potentiometer (No. 7568) at 25 °C. Saturated calomel electrodes (S.C.E.) were connected to the solutions via KCl-ager bridges. The cell potential

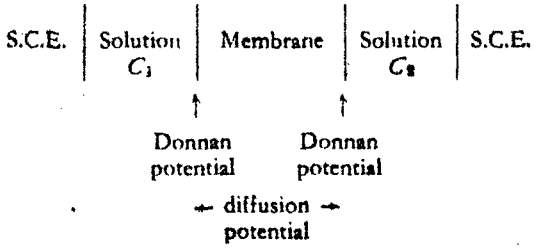

was taken as a measure of membrane potential. The concentration ratio $\gamma = \frac{C_2}{C_1}$ was put equal to 10 throughout the experiment.

Theory:

The electromotive force, E_m, of this cell may be expressed as (43)

$$E_m = -\frac{RT}{F}\int_1^2 (t_c d\ln a_c + t_A d\ln a_A + t_w d\ln a_w) \quad [1]$$

where t is the transference number, a is the activity, and the subscripts C, A and W refer to the cation, anion and water.

Equation [1] expresses the main problem. In order to relate the membrane potential to the physical properties of the membrane, the transference numbers must be determined as function of activities of the various permeating species. Two different approaches can be taken to this problem. The first is the use of a modified Nernstian approach, the second is the use of the TMS fixed charge theory.

(a) Modified Nernstian relation:

There are two main assumptions associated with this approach. The most important one is the use of an average value for the transference number in integration of eq. [1]. The other is to neglect the transference of water. With these assumptions and use of relations

$$a_c = a_A = a_\pm$$

$$T_i = Z_i t_i$$

and

$$T_A + T_c = 1$$

the integration of eq. [1] results in

$$E_m = \frac{RT}{F}(2T_c - 1)\ln\frac{a\pm(2)}{a\pm(1)} \quad [2]$$

where Z_i is the valence, T_c average transport number of the cation in the membrane, and $a\pm(1)$ and $a\pm(2)$ are the mean activities of the salt in solns [1] and [2]. Equation [2] may be rearranged

$$T_c = \frac{E_m + E^\circ}{2E^\circ} = \frac{1}{2}\left(\frac{E_m}{E^\circ} + 1\right) \quad [3]$$

where E_m is the measured membrane potential and E° is the Nernstain potential. Equation [3] permits the calculation of T_c from the measured values of E_m for different solution activities.

Fixed charge theory of Teorell-Meyer-Sievers:

The earliest efforts towards developing a membrane model was by *Michaelis* (44), who considered that the charge on the membrane was due to adsorption of one kind of ion. Later, *Teorell* (17) and *Meyer* and *Sievers* (18) developed a theory of membranes with charges fixed in the lattice. In the TMS theory there is an equilibrium process at each solution-membrane interface which has a formal analogy with the Donnan equilibrium. In addition, there is an internal salt diffusion potential which was first represented by the Henderson equation and later by the more nearly correct Planck expression (45). Further assumptions made are (*a*) the cation and anion mobilities and fixed charge concentration are constant throughout the membrane phase and are independent of the salt concentration and (*b*) the transference of water may be neglected. The implications of these assumptions have been discussed by *Hills*, *Jacobs*, and *Lakshminarayanaih* (21).

In order to use the graphical method of *Meyer* and *Sievers* (18), a further assumption must be made that the activity coefficient of the salt is the same in the membrane and solution phase at each interface. The introduction of activities for concentrations can only be correctly made for the Donnan potential. The expression for the diffusion potential using either the integration of *Planck* or *Henderson* requires concentrations.

According to TMS theory, the membrane potential E_m in millivolts (applicable to a highly idealized system) is given by the equation at 25 °C

$$E_m = 59.2\left[\log\frac{C_1(\sqrt{4C_2^2 + \bar{X}^2} + \bar{X})}{C_2(\sqrt{4C_1^2 + \bar{X}^2} + \bar{X})} + U\log\frac{(\sqrt{4C_1^2 + \bar{X}^2} + \bar{X}0)}{(\sqrt{4C_2^2 + \bar{X}^2} + \bar{X}0)}\right] \quad [4]$$

where $\bar{U} = \left(\frac{\bar{u} - \bar{v}}{\bar{u} + \bar{v}}\right)$, $\bar{u}$ and $\bar{v}$ are the mobilities of the cation and the anion respectively, in the membrane phase (overbar, refer the parameters to the membrane phase). C_1 and C_2 are the concentrations of the electrolyte solution on either side of the membrane and $\bar{X}$ is the charge on the membrane expressed in equivalents/litre.

The graphical potentiometric method of *Meyer* and *Sievers* yield values of $\bar{X}$ and cation-to-anion mobility ratio in the membrane phase $\frac{\bar{u}}{\bar{v}}$. The results of the above analysis have been used by *Hersh* (46) to calculate the membrane transport numbers for glass. Similar procedure is also adopted here for transport number evaluation using the relation

$$\bar{T}_c = \frac{(\bar{u}/\bar{v})\bar{C}_+}{(\bar{u}/\bar{v})\bar{C}_+ + \bar{C}_-} \qquad [5]$$

where $\bar{u}/\bar{v}$ is the mobility ratio in the membrane phase, and $\bar{C}_+$ and $\bar{C}_-$ are the concentrations of the cations and anions respectively in the membrane phase.

The values of $\bar{C}_+$ and $\bar{C}_-$ for a -vely charge membrane have been calculated (46) using the following equations

$$\bar{C}_+ = \frac{1}{2}\left[\sqrt{(\bar{X})^2 + 4C_1^2} + \bar{X}\right] \qquad [6a]$$

$$\bar{C}_- = \frac{1}{2}\left[\sqrt{(\bar{X})^2 + 4C_1^2} - \bar{X}\right] \qquad [6b]$$

Altug and Hair method

Altug and *Hair* (27) have given an ingenious and indirect method which has been developed on the lines of Teorell's model (17) for the evaluation of membrane charge density $W\bar{X}$, where $\bar{X}$ represents the number of ionized sites per unit volume and $W = \pm 1$, depending on the nature of the ionized sites. According to the Teorell's model, the behaviour of a charged membrane in an electrolyte solution can be characterized in terms of ionic mobilities, concentrations and the fixed charge in the membrane.

The essential feature of the original fixed charge theory of *Teorell* (17) was the assumption that the overall membrane potential was composed of three potential jumps: two Donnan potentials at each solution-membrane interface (here denoted by $\bar{\Lambda}_1$ and $\bar{\Lambda}_2$) and one residing inside the membrane- the internal potential or the driving potential being denoted by $(\bar{\varphi}_2 - \bar{\varphi}_1)$. The overall total membrane potential E_{cal} is given by

$$E_{cal} = (\bar{\Lambda}_1 + \bar{\Lambda}_2) + (\bar{\varphi}_2 - \bar{\varphi}_1). \qquad [7]$$

$\bar{\Lambda}_1$ and $\bar{\Lambda}_2$ can be calculated according to equation

$$\bar{\Lambda}_1 = -\frac{RT}{F} \ln r_1 \qquad [8a]$$

and

$$\bar{\Lambda}_2 = \frac{RT}{F} \ln r_2 \qquad [8b]$$

where r_1 and r_2 are the Donnan distribution ratios at the two interfaces and are given by the equation

$$r = \left[1 + \left(\frac{w\bar{x}}{2a}\right)^2\right]^{1/2} - \left(\frac{w\bar{x}}{2a}\right) \qquad [9]$$

where a is the external solution activity. The diffusion potential $(\bar{\varphi}_2 - \bar{\varphi}_1)$ for 1:1 valent electrolyte is given by

$$(\bar{\varphi}_2 - \bar{\varphi}_1) = \left(\frac{u - v}{u + v}\right) \frac{RT}{F} \ln \left(\frac{a_1(r_1 u + v/r_1)}{a_2(r_2 u + v/r_2)}\right) \qquad [10]$$

where u and v are the cationic and anionic mobilities in the membrane. However, in the present calculations these are assumed to be the same as in the bulk solution. Subscripts 1 and 2 refer to the solutions on each side of the membrane. The use of concentration, rather than activities, is an assumption based on the practical difficulty of measuring ion activities in a membrane phase as suggested by *Altug* and *Hair* (27). Substituting values in eq. [7], the final expression is given by

$$E_{cal} = \left(\frac{u - v}{u + v}\right) \frac{RT}{F} \ln \left(\frac{a_1(r_1 u + v/r_1)}{a_2(r_2 u + v/r_2)}\right) + \frac{RT}{F} \ln \frac{r_2}{r_1}. \qquad [11]$$

Kobatake et al. theory

Kobatake et al. (28) derived the following equation for the electric current density $(I)_e$, relative to the frame of reference fixed to the membrane

$$(I)_e = F(l_+C_+ + l_-C_-)\frac{d\emptyset}{dx} - RT\left(l_+C_+\frac{d\ln a_+}{dx} - l_-C_-\frac{d\ln a_-}{dx}\right) + F(C_+ - C_-)U_m . \quad [12]$$

Here $\emptyset$ is the electric potential, C_+ and C_- are concentrations of $+ve$ and $-ve$ ions in moles per cubic centimeter of solution, a_+ and a_- are activities of positive and negative ions in moles per cubic centimeter of solution, l_+ and l_- are molar mobilities of $+ve$ and $-ve$ ions defined in terms of the mass fixed frame of reference, U_m is the velocity of the local centre of mass, R is the molar gas constant, T is the absolute temperature of the system and F is the Faraday constant.

For the evaluation of U_m, the viscous force acting on lcc of solution in the membrane is represented by $\left(\frac{1}{K}\right)U_m$, where K is a constant which is considered to depend on the viscosity of the solution and the structural details of the polymer net work of which the membrane is composed. The same volume of solution undergoes an electric force which is represented by

$$-F(C_+ - C_-)\left(\frac{d\emptyset}{dx}\right) . \quad [13]$$

In the steady state, the sum of these two forces is zero, so that

$$U_m = -KF(C_+ - C_-)\left(\frac{d\emptyset}{dx}\right) . \quad [14]$$

For convenience, *Kobatake* et al. (28) have considered a membrane which is ionized negatively with a charge density θ (in moles/cc). Then the requirement that the electric neutrality must be realized in any element of the membrane gives the relation

$$C_+ - C_- = \theta . \quad [15]$$

Since in the system considered here no electric field is applied externally across the membrane, no net charge is transported from one side of the membrane to other. This means that $(I)_e$ must be zero at a cross section of the membrane. Substituting eq. [14] and [15] into eq. [12], putting $(I)_e$ equal to zero, and solving for $\frac{d\emptyset}{dx}$, the following expression is obtained.

$$\frac{d\emptyset}{dx} = \frac{-\left(\frac{RT}{F}\right)\times 1_+(C_- + \theta)(d\ln a_+/dx) - 1_-C_-(d\ln a_-/dx)}{(1_+ + 1_-)C_- + 1_+\theta + KF\theta^2} . \quad [16]$$

To proceed further, the activities a_+ and a_- must be known as function of C_-.

Assumptions for a_+ and a_-

Kobatake et al. have assumed the following relation

$$a_+ = C_+;\ a_- = C_- \quad [17]$$

or

$$\gamma_+ = \frac{C_-}{(C_- + \theta)};\ \gamma_- = 1 \quad [18]$$

where γ_+ and γ_- are the activity coefficients of $+ve$ and $-ve$ ions in the membrane.

Equation for membrane potential:

With eq. [17], and [18] assumed for a_+ and a_-, eq. [16] becomes

$$\frac{d\emptyset}{dx} = -\left(\frac{RT}{F}\right)\frac{(l_+ - l_-)C_- + l_+\theta}{[(l_+ + l_-)C_- + l_+\theta + KF\theta^2]C_-}\frac{dc_-}{dx} \quad [19]$$

when the bulk solutions on both sides of the membrane are vigorously stirred, no potential gradient is set up in them, so that the desired membrane potential $\Delta\emptyset$ is obtained by the integrating $\frac{d\emptyset}{dx}$ over the thickness of the

membrane. The final expression for the membrane potential is given by

$$\Delta\emptyset = -\left(\frac{RT}{F}\right)\left[\frac{1}{\beta}\ln\frac{C_2}{C_1} - \left(1+\frac{1}{\beta}-2\alpha\right)\times\ln\frac{C_2+\alpha B\theta}{C_1+\alpha B\theta}\right] \quad [20]$$

where

$$\alpha = \frac{1_+}{1_+ + 1_-} \quad [21]$$

$$\beta = 1 + \left(\frac{KF\theta}{1_+}\right) \quad [22]$$

and parameters have been assumed to be independent of salt concentration.

Limiting form of eq. [20]

Kobatake et al. (28) have derived two useful limiting forms of eq. [20]. These are: (*a*) when C_2 becomes sufficiently small with γ fixed; eq. 20 may be expanded to give

$$|\Delta\emptyset_r| = \frac{1}{\beta}\ln\gamma - \frac{\gamma-1}{\alpha\beta\gamma}\left(1+\frac{1}{\beta}-2\alpha\right)\frac{C_2}{\theta} \quad [23]$$

where $|\Delta\emptyset_r|$ is the absolute value of a reduced membrane potential defined by

$$\Delta\emptyset_r = F\Delta\emptyset/RT. \quad [24]$$

(*b*) It has also been shown by *Kobatake* et al. (28) that at a fixed γ the inverse of an apparent transference number t^-_{app} for the co-ion species in a negatively charged membrane is proportional to the inverse of the concentration C_2 in the region of high salt concentration. Here t^-_{app} is defined by the relation

$$|\Delta\emptyset_r| = (1 - t^-_{app})\ln\gamma. \quad [25]$$

The derived transport number value has been called the apparent transport number i.e. t^-_{app} because in this type of measurement water transport has not been taken into account. This apparent value will be close to the true value, when dilute solutions are used. Substituting for $\Delta\emptyset$ from eq. [20] and expanding the resulting expression for $1/t^-_{app}$ in powers of $1/C_2$ gives

$$\frac{1}{t^-_{app}} = \frac{1}{(1-\alpha)} + \frac{(1+\beta-2\alpha\beta)\alpha}{2(1-\alpha)^2\ln\gamma}\left(\frac{\theta}{C_2}\right) + \ldots. \quad [26]$$

Reduced expression of permselectivity according to Kobatake et al.

Both the activity coefficients and mobilities of small ions in charged membranes can be expressed according to *Kobatake* et al. (33) by the following expression.

$$\gamma_+ = \gamma_+^\bullet(C_- + \emptyset X)/(C_- + X),\ \gamma_- = \gamma_-^\bullet \quad [27]$$

$$u_+ = u_+^\circ(C_- + \emptyset X)/(C_- + X),\ u_- = u_-^\circ. \quad [28]$$

Here γ_i, u_i, $\gamma_i^\bullet$ and u_i° ($i = +, -$) stand for the activity coefficient and mobility of ion species i in the membrane and in the bulk solution, respectively, C_- and X are the concentration of anion adsorbed in the membrane (in moles per litre of water in the membrane), and the stoichiometric concentration of charges fixed in the membrane. According to the convention suggested by *Guggenheim* (47), $\gamma_+^\bullet$ can be equated with $\gamma_-^\bullet$ for 1:1 electrolyte, and they are replaced by the mean activity coefficient $\gamma_\pm^\bullet$ of the electrolyte component. In equations [27] and [28], $\emptyset$ represents the fraction of counter-ions in the unbounded form, i.e., excluding those tightly bound to the polymer skeleton constituting the membrane. $\emptyset X$ may be referred to as the thermodynamically effective fixed charge density of the membrane.

Consider a system in which a negatively charged membrane is immersed in an electrolyte of concentration C. Under this condition the Donnan equilibrium for small ions holds between the membrane phase and the solution, then we have

$$(\gamma_\pm^\bullet)^2C^2 = \gamma_+C_+\gamma_-C_- \quad [29]$$

the mass fixed transference number of anion in the membrane, τ_- is defined by

$$\tau_- = \frac{U_-C_-}{(U_+C_+ + U_-C_-)}. \quad [30]$$

Introducing equations [27], [28] and [29] into equation [30] together with the electrical neutrality condition, i.e. $C_+ = C_- + X$ we obtain

$$\tau_- = 1 - \alpha \frac{(4\xi^2 + 1)^{1/2} + 1}{(4\xi^2 + 1)^{1/2} + (2\alpha - 1)} \quad [31]$$

where

$$\xi = \frac{C}{\emptyset X} \quad [32]$$

and

$$\alpha = \frac{U_+^0}{(u_+^0 + u_-^0)} . \quad [33]$$

On the other hand, the apparent transference number of anion in the membrane, $t_{\bar{a}pp}$ is defined by the following Nernst equation

$$\Delta\emptyset = -\left(\frac{RT}{F}\right)(1 - 2t_{\bar{a}pp}) \ln\left(\frac{C_2}{C_1}\right). \quad [34]$$

Here C_1 and C_2 are the concentrations of the external solution in moles litre^{-1} on the two sides of the membrane, and R, T and F have their usual thermodynamic meaning. It has been found by *Kobtake* et al., (33) that the difference between τ_- and $t_{\bar{a}pp}$ was less than 2% in the wide range of salt concentration when the averaged concentration $\frac{C_1 + C_2}{2}$ was replaced by C. Therefore, if we replace τ_- by $t_{\bar{a}pp}$ and C by $\frac{C_1 + C_2}{2}$, equation [31] is applicable even when the concentration on the two sides of the membrane are different. Rearrangement of equation [31] leads to the eqn.

$$\frac{1}{(4\xi^2 + 1)^{1/2}} = \frac{1 - t_{\bar{a}pp} - \alpha}{\alpha - (2\alpha - 1)(1 - t_{\bar{a}pp})} \equiv P_s . \quad [35]$$

Here P_s is a measure of permselectivity of the membrane-electrolyte system.

Results and discussion

The membrane potential data obtained with each of the two types of parchment supported membranes using various 1:1 electrolytes, are

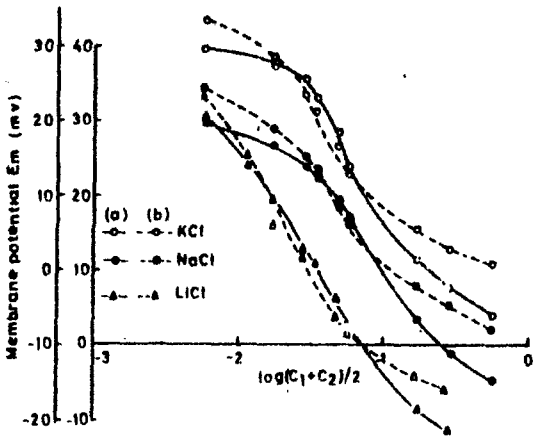

Fig. 1. Plots of observed membrane potential against log $(C_1 + C_2)/2$ for various electrolytes with (a) Mercuric phosphate (—), (b) Mercuric Carbonate (---)

plotted as a function of log $\frac{C_1 + C_2}{2}$, with the ratio γ fixed at 10. These plots are shown in figure 1.

The graphical method of *Meyer* and *Sivers* (18) determines the fixed charge $\bar{X}$ in equivalents/litre, and the cation-to-anion mobility ratio in the membrane phase. The set of curves on the left in figure 2 (closed point curves) are the theoretical membrane potentials for a cation selective membrane, 1:1 electrolyte and constant solution concentration ratio $\gamma = 10$, as a function of $-\log C_2$. The different curves are for different mobility ratios $\bar{u}/\bar{v}$, with a constant value of $\bar{X}$ is unity expressed in equivalents/litre. The experimental E_m values for (*a*) mercuric phosphate and (*b*) mercuric carbonate membranes (open points) with KCl electrolyte were plotted in the same graph as a function of $-\log C_2$. The experimental curve for any membrane was shifted horizontally and ran parallel to one of the theoretical curves. The shift gave $\log \bar{X}$ and coinciding theoretical curve gave $(\bar{u}/\bar{v})$. In table 3 are given values of $\bar{X}$ and $(\bar{u}/\bar{v})$ derived in this way for the above membrane.

This analytical method gave satisfactory result for fixed charge density evaluation, the values of which are quite low and hence very difficult to determine by the usual exchange reaction. This technique has been used by *Kumins* and *London* (48) to estimate the capacity of thin polymer membranes of poly (vinyl chloride) and poly (vinyl acetate). It has also

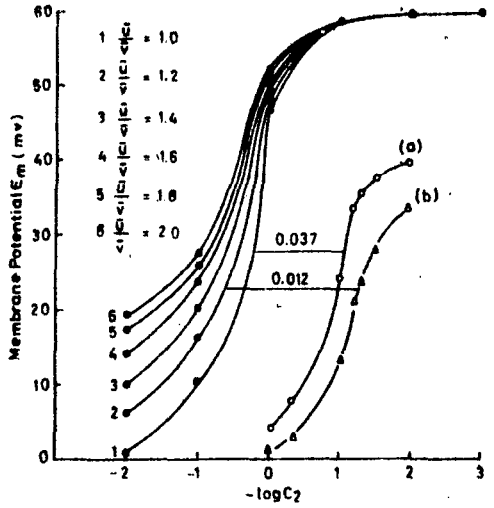

Fig. 2. Evaluation of membrane charge density $\bar{x}$ and the mobility ratio $\bar{u}/\bar{v}$ in the membrane phase. The different curves for different mobility ratio. The observed values of E_m for the (a) Mercuric phosphate, (b) Mercuric Carbonate, for KCl electrolyte against-log C_2

been used by *Bexter* (49) to determine the charge of Keratin and by *Lakshminarayanaiah* (50) and *Siddiqi* (1–6) to evaluate the fixed charge on thin parlodian and parchment supported membranes.

The values of $\bar{X}$ and $(\bar{u}/\bar{v})$ obtained by TMS graphical analysis can be substituted into eq. 5 to calculate values of $\bar{T}_K^+$. The transport number $\bar{T}_K^+$ may also be calculated by the use of eq. [3]. The results of two approaches to the calculation of the potassium ion transport numbers in membrane phase are presented in table 1. The numbers $(\bar{T}_K^+)_N$ and $(\bar{T}_K^+)_T$ were determined by eq. [3] and [5] which are *Nerstian*(N) and TMS(T) values respectively.

Table 1. Transport number of counter ions calculated by modified Nernstian relation (N) and Teorell-Meyer-Sievers method (T) as a function of external KCl electrolyte concentration

S. No.	Concentration	Mercuric Phosphate		Mercuric Carbonate	
		$(\bar{T}_K^+)_N$	$(\bar{T}_K^+)_T$	$(\bar{T}_K^+)_N$	$(\bar{T}_K^+)_T$
1	1.0 M	0.54	0.51	0.51	0.54
2	0.5 M	0.58	0.52	0.53	0.55
3	0.1 M	0.72	0.59	0.62	0.56
4	0.05 M	0.82	0.67	0.72	0.60
5	0.01 M	0.85	0.93	0.79	0.78

In a modification of this type of plotting *Altug* and *Hair* (27) evaluated $\bar{X}$ for glass membranes, choosing the solution values for $\bar{u}$ and $\bar{v}$. In this procedure, a value of $\bar{X}$ was assumed and r_1 and r_2, the distribution ratios were calculated according to eq. [8] and [9] for the given electrolyte concentration C_1 and C_2, the theoretical membrane potential was then determined from eq. [11] for 1.0 to 1.0×10^{-4} moles L^{-1} concentration range. By following the algebraic procedure, a series of theoretical curves were obtained for different $\bar{X}$ values for KCl electrolyte and are shown by the solid lines in figure 3. At the same time curves were also plotted in the same figure 3, between the experimentally determined membrane potential values for KCl electrolyte for both the membranes. The theoretical curve which most nearly coincides with the experimental curves gave the values for $\bar{X}$ which are given in table 3.

Kobatake et al. method of evaluation of the thermodynamic effective fixed charge density and permselectivity:

Equation [23] indicates that a value of β and a relation between α and θ can be obtained by evaluating the intercept and the initial slope of a plot of $\Delta\emptyset_r$ against C_2. Figure 4 illustrates

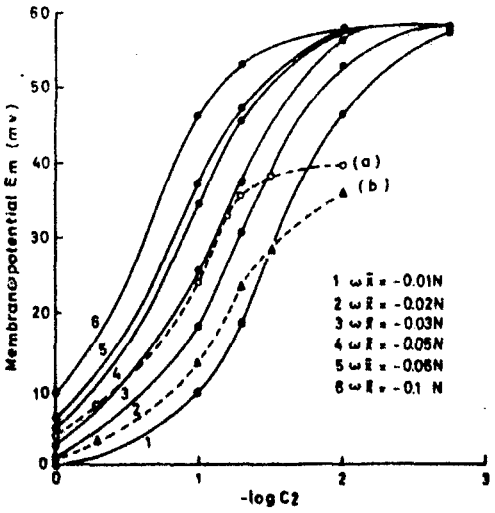

Fig. 3. Plots of membrane potentials across (a) Mercuric phosphate, (b) Mercuric carbonate, for KCl electrolyte in varying concentrations (●) Calculated values assuming $\omega\,\bar{x}$ equal to (1) −0.01, (2) −0.02, (3) −0.03, (4) −0.05, (5) −0.06, (6) −0.1 N; observed values with broken line

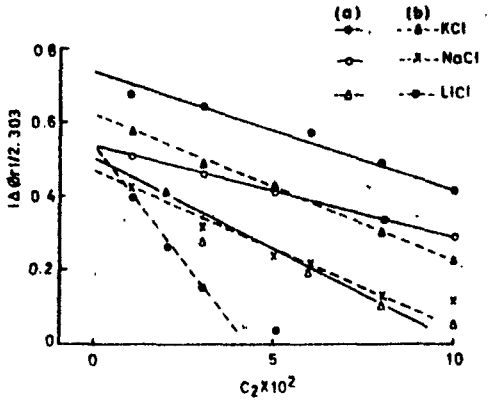

Fig. 4. Plots of $|\Delta\theta r|/2.303$ vs. $C_2 \times 10^2$ for various electrolytes (a) Mercuric phosphate (—), (b) Mercuric Carbonate (---)

plots of $\Delta\theta_r$ versus C_2 in the region of very low concentration that were determined for various electrolyte with mercuric phosphate and carbonate membranes. The value of intercept is equal to $\frac{1}{\beta}\ln\gamma$, from which β may be evaluated. Values are given in table 2.

Equation [26] indicate that the intercept of a plot of $\frac{1}{t_{app}}$ against $1/C_2$ at fixed γ allows the value of α to be determined. Plots of $\frac{1}{t_{app}}$ against $1/C_2$ for various 1:1 electrolytes are shown in figure 5 for both mercuric phosphate and carbonate membranes. The value of the intercept is equal to $\frac{1}{(1-\alpha)}$, from which α may be evaluated. Values are given in table 2. If this value of α is inserted in the relation obtained from the initial slope for $\Delta\theta_r$ vs C_2, the desired value for θ can be determined. Once α and β are known in the manner described above, the values of θ may also be evaluated

Table 2. Values of parameters α, β and θ for various membrane-electrolyte system at $\gamma = 10$

Membrane	Electrolyte	α	β	θ
Mercuric-Phosphate	KCl	0.459	1.351	0.047
	NaCl	0.555	1.851	0.012
	LiCl	0.411	2.000	0.013
Mercuric-Carbonate	KCl	0.524	1.613	0.014
	NaCl	0.444	2.127	0.013
	LiCl	0.333	1.887	0.011

from the initial slope for $\frac{1}{t_{app}}$ vs $1/C_2$. *Kobatake* has suggested (28) that, provided his equation for the membrane potential is correct, the two values of θ obtained in this way from opposite limits should agree with one another. In the present investigation with parchment supported membranes, the two value of θ agree with one another and are shown in table 2.

Once the values of parameters α, β and θ for a given membrane-electrolyte system have been determined, one can calculate the theoretical $\Delta\theta$ versus C_2 curve for the given value of γ and than compare it with the corresponding experimental data. For this comparison equation [20] may be rewritten in the following form as suggested by *Kobatake* (28).

$$\frac{(\gamma - e^q)}{(e^q - 1)} = X \qquad [36]$$

with q and X defined by

$$q = \frac{[|\Delta\theta_r| + (1-2\alpha)\ln\gamma]}{\left[\left(\frac{1}{\beta}\right) + (1-2\alpha)\right]} \qquad [37a]$$

$$X = \frac{C_2}{(\alpha\beta\theta)}. \qquad [37b]$$

(This X has got no relation with X used in TMS and *Altug* and *Hair* methods). Thus if equation [20] is valid, the value of $\frac{(\gamma - e^q)}{(e^q - 1)}$

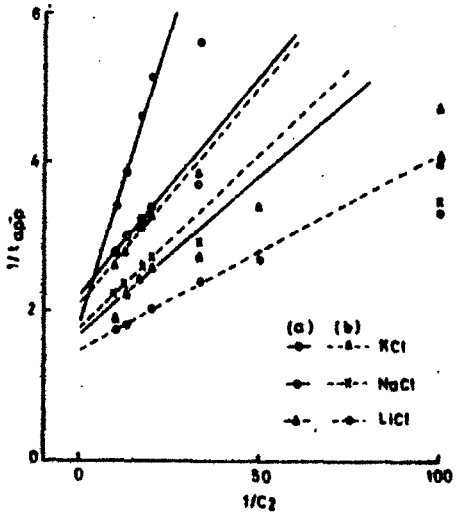

Fig. 5. Plots of $1/t_{app}$ vs. $1/C_2$ for various electrolytes (a) Mercuric phosphate (—), (b) Mercuric Carbonate (—)

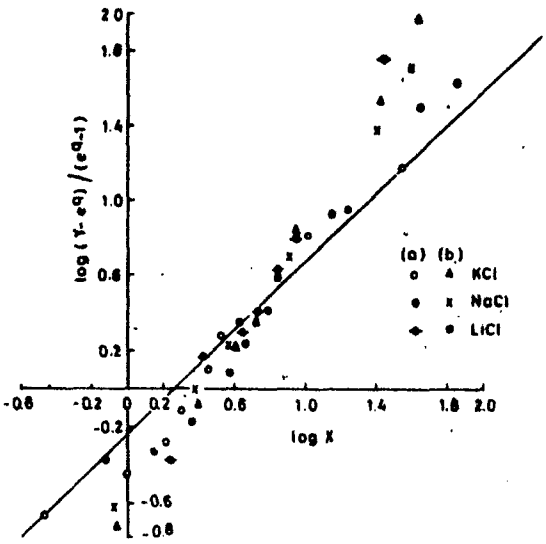

Fig. 6. Plots of log $(\gamma - e^{q})/(e^{q} - 1)$ vs. log X for various electrolytes with (a) Mercuric phosphate, (b) Mercuric Carbonate

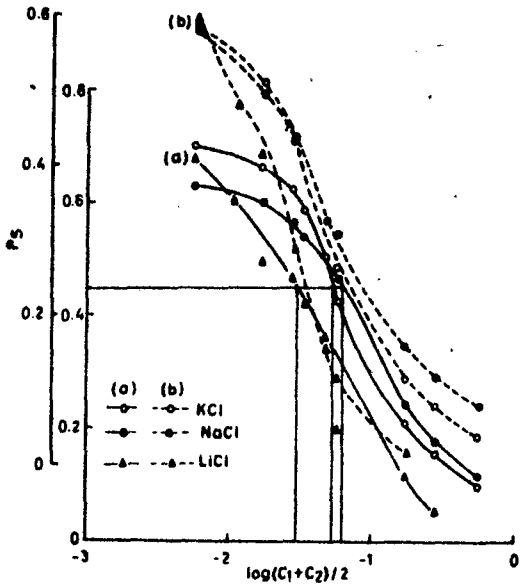

Fig. 7. Plots of P_s vs. log $(C_1 + C_2)/2$ for various electrolytes with (a) Mercuric phosphate (—), (b) Mercuric Carbonate (---)

calculated from the measured values of $\Delta\emptyset$, together with the predetermined α, β and θ and the given value of γ, must fall on a straight line which has a unit slope and passes the coordinate origin, when plotted against X. This behaviour should be observed irrespective of the γ and the kind of membrane/electrolyte (1:1 systems) used. Figure 6 illustrates that, this theoretical predictions, based on Kobatake's membrane potential equation is borne out quite satisfactorily by our experimental results on parchment supported membranes with various electrolytes.

For the evaluation of effective fixed charge density $\emptyset X$, the various values of permselectivity P_s were calculated by substituting the values of α (bulk) and $t_{\bar{a}pp}$ in equation [35], and then plotted against log $\frac{C_1+C_2}{2}$ $\left[\left(\frac{C_1+C_2}{2}\right)\text{being the average concentration}\right]$. The results are shown in figure 7. The term ξ has already been defined as the ratio between the average concentration C and the effective fixed charge density $\emptyset X$ i.e. $\xi = \frac{C}{\emptyset X}$, the units of both C and $\emptyset X$ are expressed in terms of moles or equivalents/litre. When the average concentration C is equal to the effective fixed charge density $\emptyset X$ i.e. $\frac{C}{\emptyset X} = \xi = 1$, the values of P_s must give $\frac{1}{\sqrt{5}} = 0.448$ from left

Table 3. Comparison of charge density for different membrane-electrolyte system

Membrane	Electrolyte	TMS		Altug and Hair	Kobatake et al. Values Equation	P_s vs log $\frac{C_1+C_2}{2}$
		$\bar{a}/\beta$	$\bar{X}$	$\bar{X}$	θ	$\emptyset X$
Mercuric-Phosphate	KCl	1.0	0.037	0.03	0.047	0.053
	NaCl	–	–		0.012	0.063
	LiCl	–	–		0.013	0.029
Mercuric-Carbonate	KCl	1.2	0.012	0.01	0.014	0.026
	NaCl	–	–		0.013	0.025
	LiCl	–	–		0.011	0.016

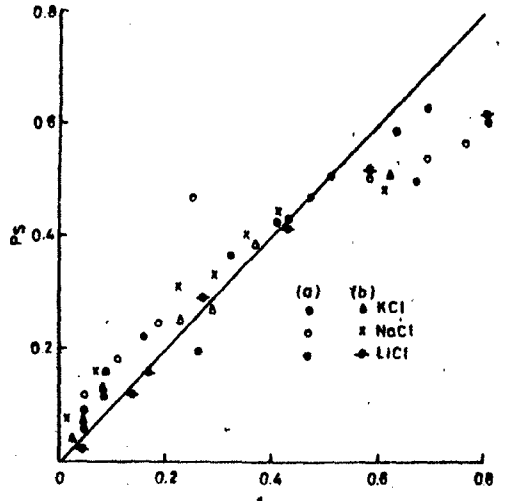

Fig. 8. Plots of P_s vs. $\frac{1}{\sqrt{1+4\xi^2}}$ for various electrolytes with (a) Mercuric phosphate, (b) Mercuric Carbonate

hand side of equation [35]. The corresponding concentration is obtained from the plot of P_s versus log C as given in figure 7. This value of concentration is equal to the fixed charge density. The $\emptyset X$ values are given for various electrolytes in table 3. Further, the plots of P_s versus $(1+4\xi^2)^{-1/2}$ were drawn for both membranes with various electrolytes and are shown in figure 8. It is evident that the line nearly passes through the origin with unit slope, thereby confirming the applicability of Kobatake's equation to these membranes.

In *Kobatake* et al. method, the derivation is based on the thermodynamics of irreversible processes. They have claimed that their data of oxidized collodion membrane potential as well as typical ones of previous workers are fitted quite accurately by the equation derived by them. In the present investigation the mean value of charge density obtained by using different equations of *Kobatake* is found to be closer to that obtained by *Altug* and *Hair* and TMS method. The theoretical predictions from *Kobatake* et al. membrane potential equation is borne out quite satisfactorily by our experimental results and hence it may safely be concluded that *Kobatake* et al. method for charge density evaluation is the best among the existing theories of membrane potential.

Acknowledgement

The authors are grateful to Professor *Wasiur Rahman*, Head of the Department of Chemistry for providing research facilities. The financial assistance from C.S.I.R. (New Delhi, India) to one of us S.P.S. is gratefully acknowledged.

Summary

Thermodynamic effective fixed charge densities of mercuric phosphate and carbonate parchment supported membranes were evaluated by a number of methods particularly those of *Teorell-Meyer-Sievers*, *Altug* and *Hair* and *Kobatake* et al. The value of the permselectivity was obtained for the two membranes based on *Kobatake* et al. procedure. Membrane transport number was calculated using a modified Nernst relation and compared with the values determined by the TMS method. The theoretical predictions for membrane potential using *Kobatake* et al. equation are borne out quite satisfactorily by our experimental results for both membrane.

Zusammenfassung

Es wurden die Dichte der fixierten Ladungen von Quecksilberphosphat und Quecksilberkarbonat-Niederschlagsmembranen nach den Methoden von *Torell-Meyer-Sievers*, *Altug* und *Hair* und *Kobatake* bestimmt. Weiterhin wurden Durchlässigkeit und Transportzahlen ermittelt und mit Werten der TMS-Methode verglichen. Theoretische Voraussagen über das Membranpotential nach den Gleichungen von *Kobatake* stimmen mit den experimentellen Ergebnissen überein.

References

1) *Siddiqi, F. A., S. Pratap*, J. Electroanal. Chem. **23**, 137 (1969).
2) *Siddiqi, F. A., S. Pratap*, J. Electroanal. Chem. **23**, 147 (1969).
3) *Siddiqi, F. A., N. Lakshminarayanaiah, S. K. Saksena*, Z. Physik. Chem. (Frankfurt) **72**, 298 (1970).
4) *Siddiqi, F. A., N. Lakshminarayanaiah, S. K. Saksena*, Z. Physik. Chem. (Frankfurt) **72**, 307 (1970).
5) *Siddiqi, F. A., N. Lakshminarayanaiah, M. Nasim Beg*, J. Polymr. Sci. **9**, 2853 (1971).
6) *Siddiqi, F. A., N. Lakshminarayanaiah, M. Nasim Beg*, J. Polymr. Sci. **9**, 2869 (1971).
7) *Malik, W. U., F. A. Siddiqi*, Proc. Indian Acad. Sci. A **56**, 206 (1962).
8) *Malik, W. U., F. A. Siddiqi*, J. Colloid Sci. **18**, 161 (1963).
9) *Malik, W. U., H. Arif, F. A. Siddiqi*, Bull. Chem. Soc. Japan **40**, 1746 (1969).
10) *Teorell, T.*, Discussion Faraday Soc. No. **21**, 9 (1956).
11) *Lakshminarayanaiah, N., F. A. Siddiqi*, Biophys. J. **11**, 603 (1971).
12) *Lakshminarayanaiah, N., F. A. Siddiqi*, Biophys. J. **11**, 617 (1971).
13) *Lakshminarayanaiah, N., F. A. Siddiqi*, Biophys. J. **12**, 540 (1972).
14) *Lakshminarayanaiah, N., F. A. Siddiqi*, Membrane Processes in Industry and Biomedicine, Editor M. Bier (New York 1971).
15) *Liquori, A. M., C. Botre*, Ric. Sci. **34**, 6 (1964).

16) *Liquori, A. M., C. Botre*, J. Phys. Chem. **71**, 3765 (1967).
17) *Teorell, T.*, Proc. Soc. Expt. Biol. Med. **33**, 282 (1935); Proc. Natl. Acad. Sci. (U.S.A.) **21**, 152 (1935); Z. Elektrochem. **55**, 460 (1951); Prog. Biophys. Biophys. Chem. **3**, 305 (1953).
18) *Meyer, K. H., J. F. Sievers*, Helv. Chim. Acta. **19**, 649, 665, 987 (1936).
19) *Schlögl, R.*, Z. Elektrochem. **57**, 195 (1953); Z. Physik. Chem. (Frankfurt), **1**, 305 (1954).
20) *Scatchard, G.*, J. Am. Chem. Soc. **75**, 2883 (1956).
21) *Hills, G. L., P. W. M. Jacobs, N. Lakshminarayanaih*, Proc. Roy. Soc. (London) **A 262**, 246 (1961).
22) *Kobatake, Y.*, J. Chem. Phys. **28**, 146 (1958).
23) *Lorimer, J. W., E. I. Boterenbrood, J. J. J. Hermans*, Discussion Faraday Soc. **21**, 141 (1956).
24) *Staverman, A. J.*, Trans. Faraday Soc. **48**, 176 (1952).
25) *Nagasawa, M., I. Kagawa*, Discussion Faraday Soc. **21**, 52 (1956).
26) *Nagasawa, M., Y. Kobatake*, J. Phys. Chem. **56**, 1017 (1952).
27) *Altug, I., M. L. Hair*, J. Phys. Chem. **72**, 599 (1968).
28) *Kobatake, Y., T. Noriaki., Y. Toyoshima, H. Fujita*, J. Phys. Chem. **69**, 3981 (1965).
29) *Toyoshima, Y., M. Yusso, Y. Kobatake, H. Fujita*, Trans. Faraday. Soc. **63**, 2803, 2814 (1967).
30) *Yuasa, M., Y. Kobatake, H. Fujita*, J. Phys. Chem. **72**, 2871 (1968).
31) *Kamo, N., Y. Toyoshima, H. Nozaki, Y. Kobatake*, Kolloid-Z. Z. Polym. **248**, 1914 (1971).
32) *Kamo, N., Y. Toyoshima, Y. Kobatake*, Kolloid-Z. Z. Polym. **249**, 1061 (1971).
33) *Kamo, N., M. Ockawa, Y. Kobatake*, J. Phys. Chem. **77**, 92, 2995 (1973).
34) *Sollner, K.*, J. Phys. Chem. **49**, 47, 171 (1945); J. Electrochem. Soc. **97**, 139C (1950); Ann. N.Y. Acad. Sci. **57**, 177 (1953); J. Macromol. Sci. **A3**, 1 (1969).
35) *Gregor, H. P.*, J. Am. Chem. Soc. **70**, 1293 (1948); **73**, 642 (1950).
36) *Schmid, G.*, Z. Elektrochem. **54**, 424 (1950); **55**, 229 (1951), **56**, 181 (1952).
37) *Schmid, G., H. Schwarz*, Z. Elektrochem. **55**, 295, 684 (1951); **56**, 35 (1952).
38) *Helfferich, F.*, Ion Exchange, (New York 1962).
39) *Weiser, H. B.*, J. Phys. Chem. **34**, 335, 1826 (1930).
40) *Michaelis, L.*, Bull. Natl. Res. Council (USA) **69**, 119 (1929).
41) *Sollner, K., H. P. Gregor*, J. Phys. Chem. **51**, 299 (1947); ibid **50**, 58 (1946).
42) *Marshall, C. E., A. D. Ayers*, J. Am. Chem. Soc. **70**, 1297 (1948).
43) *Amphlett, C. B.*, Inorganic Ion Exchangers (New York 1964).
44) *Michaelis, L., A. Fujita*, Biochem. Z. **158**, 28 (1925).
45) *Goldman, D. E.*, J. Gen. Physiol. **27**, 37 (1943).
46) *Hersh, L. S.*, J. Phys. Chem. **72**, 2195 (1968).
47) *Guggenheim, E. A.*, Phil. May **19**, 588 (1935).
48) *Kumins, C. A., A. London*, J. Polymer. Sci. **46**, 395 (1960).
49) *Baxter, S.*, J. Colloid. Sci. **2**, 495 (1947).
50) *Lankshminarayanaiah, N.*, J. Appl. Polymer. Sci. **10**, 1687 (1966).

Authors' address:

Fasih A. Siddiqi, Poorna Prakash, and *Surendra P. Singh*
Physical Chemistry Division,
Department of Chemistry,
Aligarh Muslim University
Aligarh (India)

Reprinted from

Canadian Journal of Chemistry

Réimpression du

Journal canadien de chimie

Studies with inorganic precipitate membranes: Part XIV. Evaluation of effective fixed charge densities

M. Nasim Beg, Fasih A. Siddiqi, and Radhey Shyam

Volume 55 • Number 10 • 1977

Pages 1680–1686

National Research Council Canada

Conseil national de recherches Canada

Studies with inorganic precipitate membranes: Part XIV. Evaluation of effective fixed charge densities

M. NASIM BEG, FASIH A. SIDDIQI, AND RADHEY SHYAM

Division of Physical Chemistry, Department of Chemistry, Aligarh Muslim University, Aligarh-202001, India

Received October 25, 1976

M. NASIM BEG, FASIH A. SIDDIQI, and RADHEY SHYAM, Can. J. Chem. 55, 1680 (1977).

Effective fixed charge densities of cobalt and nickel sulphide (parchment supported) membranes in contact with various 1:1 electrolyte solutions have been evaluated from membrane potential measurements. The methods used for the estimation of charge densities were: (*a*) the Teorell–Meyer Sievers method (TMS) and (*b*) the methods developed recently by Kobatake and co-workers. The two limiting forms of Kobatake's equation for dilute and concentrated solutions gave identical values of charge densities. The theoretical predictions for membrane potential were borne out quite satisfactorily by experimental results obtained with both the membranes. Apparent transference numbers of coions and permselectivities of the membranes for electrolytes have also been calculated. A method based on permselectivity values for the determination of charge density was also used. It was interesting to note that the charge densities evaluated from different methods of Kobatake and co-workers gave identical values and that the results were comparable to those derived from the TMS method.

M. NASIM BEG, FASIH A. SIDDIQI et RADHEY SHYAM, Can. J. Chem. 55, 1680 (1977).

On a évalué, à partir de mesures de potentiel de membranes, les densités effectives de charges fixes pour des membranes de sulfures de cobalt et de nickel (supportés sur du parchemin) en contact avec diverses solutions d'électrolytes 1:1. Les méthodes utilisées pour évaluer les densités de charges sont: (*a*) la méthode de Teorell–Meyer–Sievers et (*b*) les méthodes développées récemment par Kobatake et ses collaborateurs. Les deux formes limites de l'équation de Kobatake pour des solutions diluées et concentrées conduisent à des valeurs identiques pour les densités de charge. Les prédictions théoriques pour les potentiels des membranes concordent bien avec les résultats expérimentaux obtenus avec les deux membranes. On a aussi calculé les nombres apparents de transferts des coions et les permsélectivités des membranes pour les électrolytes. On a aussi utilisé une méthode basée sur des valeurs de permsélectivité pour la détermination de la densité de charge. Il est intéressant de noter que les densités de charges évaluées par diverses méthodes de Kobatake et ses collaborateurs conduisent toutes à des valeurs identiques et que les résultats sont comparables à ceux que l'on peut obtenir à partir de la méthode TMS.

[Traduit par le journal]

In a series of communications (1–10) on parchment supported membranes, Siddiqi, Beg, and co-workers (1–6) have, on the basis of the Eisenman–Sherry model of membrane selectivity (11, 12) and by the application of the theory of rate processes to diffusion (13), demonstrated the small density of fixed charge on the membrane matrix. In order to substantiate these findings, membrane potential measurements have been carried out for the evaluation of effective fixed charge density which is an important characteristic of a membrane by various methods (14–16) including those developed recently by Kobatake and co-workers (17–23).

Experimental

Parchment supported cobalt and nickel sulphide membranes were prepared by the method of interaction suggested by Siddiqi, Beg, and co-workers (1–6). To precipitate these substances in the interstices of the parchment paper, a 0.2 *M* solution of sodium sulphide was placed inside a glass tube, to one end of which was tied parchment paper. The tube was suspended for 72 h in a 0.2 *M* solution of either cobalt(II) or nickel(II) chloride. The two solutions were interchanged later and kept for another 72 h. The membranes were washed with deionized water to remove free electrolyte.

Electrochemical cells of the type

Reference electrode Ag–AgCl	Solution C_2	Membrane	Solution C_1	Reference electrode Ag–AgCl

Donnan potential — Donnan potential

←Diffusion→ potential

TABLE 1. Observed membrane potential E_m (mV) across parchment supported cobalt(II) and nickel(II) sulphide membranes in contact with various 1:1 electrolytes at different concentrations (at 25 ± 1°C)

Electrolyte concentration (mol/ℓ)	E_m (mV)							
	Cobalt sulphide				Nickel sulphide			
	KCl	NaCl	LiCl	NH_4Cl	KCl	NaCl	LiCl	NH_4Cl
$1/1 \times 10^{-1}$	5.1	0.6	−12.8	0.8	2.3	−5.3	−11.1	3.8
$5 \times 10^{-1}/5 \times 10^{-2}$	7.6	2.7	−11.5	1.2	3.3	−3.9	−10.8	5.5
$1 \times 10^{-1}/1 \times 10^{-2}$	19.3	15.2	−9.2	8.7	20.8	5.5	0.00	14.1
5×10^{-2} 5×10^{-3}	24.8	18.9	0.1	14.0	22.4	10.7	5.4	18.0
$1 \times 10^{-2}/1 \times 10^{-3}$	36.2	24.2	18.9	30.8	31.0	24.9	20.3	30.0
5×10^{-3} 5×10^{-4}	36.8	24.7	22.5	33.1	37.0	26.4	25.2	34.0
1×10^{-3} 1×10^{-4}	37.0	25.0	23.8	35.1	37.2	26.5	26.0	34.3

were used for measuring membrane potentials. The reference electrodes used were reversible Ag–AgCl standing in chloride solutions. The total potential difference between Ag–AgCl electrodes placed on either side of the membrane is the algebraic sum of the electrode potential, *i.e.* concentration potential and the membrane potential E_m (2, 24). A tenfold difference in concentration of chloride solutions (*i.e.* $C_2/C_1 = 10$) was maintained and measurements were made using a Pye precision potentiometer (No. 7568). The solutions were replaced by fresh solutions and when there was no change in potential with the addition of fresh solutions, with constant vigorous stirring by a pair of magnetic stirrers, it was taken as the true total potential difference across the Ag–AgCl electrodes. In both the membranes it could be reproduced within a few tenths of a mV. The whole cell was immersed in a water thermostat maintained at 25 ± 0.1°C. The various salt solutions (chlorides of Li^+, Na^+, K^+, and NH_4^+) were prepared from B.D.H. A.R. grade chemicals and deionized water. The parchment paper was supplied by M/S Baird and Tatlock (London) Ltd.

Results and Discussion

The values of membrane potential measured across two sulphide membranes in contact with various 1:1 electrolytes are given in Table 1.

When two electrolytic solutions having different concentrations are separated by a membrane, the mobile species penetrate the membrane and various transport phenomena are induced into the system (23). The fixed charge concept of Teorell (14) and Meyer and Sievers (15) (the TMS theory) for charged membranes is a pertinent starting point for the investigation of the actual mechanisms of the ionic or molecular processes which occur in the membrane phase. These authors obtained the following mathematical expression eq. 1 for the emf across a charged membrane by integrating the equation for the emf due to diffusion of ions within a membrane and subsequently adding the two phase-boundary (Donnan) potentials to the intramembrane diffusion potential

$$[1]\quad E_m = 59.2\left[\log \frac{C_2\,(\sqrt{4C_1^2 + \bar{X}^2} + \bar{X})}{C_1\,(\sqrt{4C_2^2 + \bar{X}^2} + \bar{X})} + \bar{U}\log \frac{\sqrt{4C_2^2 + \bar{X}^2} + \bar{X}\bar{U}}{\sqrt{4C_1^2 + \bar{X}^2} + \bar{X}\bar{U}}\right]$$

Here, $\bar{U} = (\bar{u} - \bar{v})/(\bar{u} + \bar{v})$, $\bar{u}$ and $\bar{v}$ are the mobilities of cation and anion, respectively, in the membrane phase, and $\bar{X}$ is the charge on the membrane expressed in equiv./ℓ of imbibed solution. In order to evaluate this parameter for the simple case of a 1:1 electrolyte and a membrane carrying a net negative charge of unity ($\bar{X} = 1$), theoretical concentration potentials E_m existing across the membrane were calculated as a function of C_2, the ratio (C_2/C_1) being kept at a constant value of 10 for different mobility ratios $(\bar{u}/\bar{v})$ and plotted as shown in Fig. 1. The observed membrane potential values for different membranes and KCl electrolyte were plotted in the same graph. The experimental curve for any given membrane was shifted horizontally and ran parallel to one of the theoretical curves. The extent of this shift gave $\log \bar{X}$ and the parallel theoretical curve gave the value for $(\bar{u}/\bar{v})$. The values of $\bar{X}$ and $(\bar{u}/\bar{v})$ derived in this way for the different membranes and electrolytes are given in Table 2.

Recently Kobatake *et al.* (17) derived the following equation for the electrical potential E_m which arises when a negatively-charged membrane separates two solutions of a 1:1 electrolyte of concentrations C_1 and C_2 $(C_1 < C_2)$:

$$[2]\quad E_m = -\frac{RT}{F}\left[\frac{1}{\beta}\ln\frac{C_2}{C_1} - \left(1 + \frac{1}{\beta} - 2\alpha\right)\ln\left(\frac{C_2 + \alpha\beta\bar{X}}{C_1 + \alpha\beta\bar{X}}\right)\right]\ldots$$

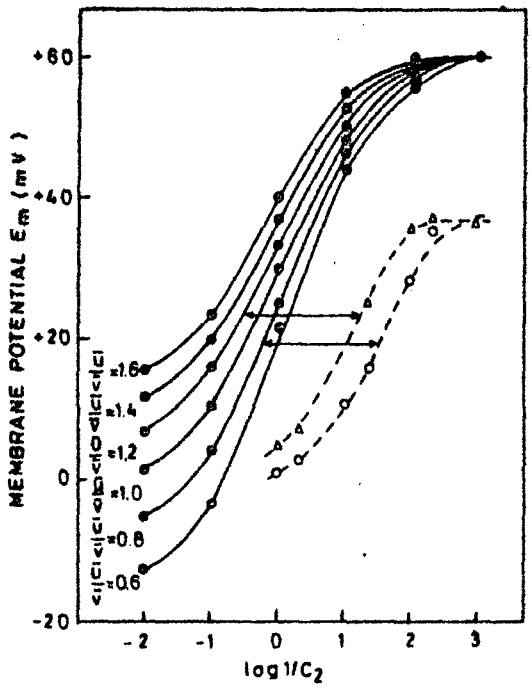

FIG. 1. Evaluation of membrane charge density $\bar{X}$ and the mobility ratio $\bar{u}/\bar{v}$ in the membrane phase. Smooth curves on the left are the theoretical concentration potentials for a cation - selective membrane ($\bar{X} = 1$) using 1:1 electrolytes at different mobility ratios $\bar{u}/\bar{v}$. The experimental values of E_m for (Δ) cobalt and (○) nickel sulphide membranes and KCl electrolyte solution are shown by the broken lines, see text.

TABLE 2. Derived values for membrane parameters ($\bar{X}$) and ($\bar{u}/\bar{v}$) using Teorell–Meyer–Sievers theory

	Cobalt sulphide		Nickel sulphide	
Electrolyte	$(\bar{X}) \times 10^2$, equiv./ℓ	$\bar{u}/\bar{v}$	$(\bar{X}) \times 10^2$, equiv./ℓ	$\bar{u}/\bar{v}$
KCl	3.8	1.2	2.3	0.8
NaCl	3.0	0.8	1.6	0.6
LiCl	2.5	1.0	2.2	0.8
NH_4Cl	2.2	0.8	1.5	1.0

where

$$\alpha = u/(u + v)$$

$$\beta = 1 + KFX/u$$

F and K represent, respectively, the Faraday constant and a constant dependent upon the viscosity of the solution and structural details of the polymer network of which the membrane is composed. To evaluate the membrane parameters, β and X, two limiting forms of the above equation were derived. When the external salt concentration C is sufficiently small,

$$[3] \quad |E_m^\circ| = \frac{1}{\beta} \ln \gamma - \left(\frac{\gamma - 1}{\alpha\beta\gamma}\right) \times \left(1 + \frac{1}{\beta} - 2\alpha\right)\left(\frac{C_2}{X}\right) + \ldots$$

where

$$|E_m^\circ| = FE_m/RT$$

and

$$\gamma = C_2/C_1$$

When the salt concentration C is high,

$$[4] \quad \frac{1}{t_-} = \frac{1}{1-\alpha} + \frac{(1 + \beta - 2\alpha\beta)(\gamma - 1)}{2(1-\alpha)^2 \ln \gamma}\left(\frac{X}{C_2}\right) + \ldots$$

where t_- is the apparent transference number of coions (anions) in a negatively-charged membrane defined by

$$[5] \quad |E_m^\circ| = (1 - 2t_-) \ln \gamma$$

The values of t_- calculated from observed membrane potentials using [5] are given in Table 3. Equation 3 was used to give the value of β and a relation between α and X by evaluating the intercept and the initial slope of the plot of $|E_m^\circ|$ against C_2 (Fig. 2), while [4] was used to evaluate α from the intercept of a plot of $1/t_-$ against $1/C_2$ (Fig. 3). The value of X (or X_d) was determined by inserting this value of α in the relation between α and X obtained earlier. Once α and β are known in the manner described above, X (or X_c) was also evaluated from the initial slope of $1/t_-$ against $1/C_2$. Kobatake and co-workers (17) have suggested that provided their equation for the membrane potential is correct then the two values of charge densities namely X_c and X_d obtained under opposite limiting conditions (concentrated and dilute) should be the same. In the present case, the two values thus obtained agree well with each other (Table 4), thereby confirming the applicability of the Kobatake and co-workers equation to parchment supported membranes.

Once the values of the parameters α, β, and X for a given membrane electrolyte system have been determined, one can get the theoretical E_m *vs.* C_2 curve using [2] for any given γ ($= C_2/C_1$) and compare it with the corresponding experimental data. For this comparison eq. 2 can be rewritten in the following form as suggested by Kobatake and co-workers (17)

TABLE 3. Transference number t_- of coions derived from observed membrane potential at various electrolyte concentrations

Electrolyte concentrations (mol/ℓ)	t_-							
	Cobalt sulphide*				Nickel sulphide*			
	KCl	NaCl	LiCl	NH_4Cl	KCl	NaCl	LiCl	NH_4Cl
$1/1 \times 10^{-1}$	0.46	0.44	0.65	0.49	0.48	0.55	0.59	0.47
$5 \times 10^{-1}/5 \times 10^{-2}$	0.44	0.48	0.59	0.48	0.47	0.53	0.59	0.45
$1 \times 10^{-1}/1 \times 10^{-2}$	0.34	0.37	0.57	0.42	0.33	0.45	0.50	0.38
$5 \times 10^{-2}/5 \times 10^{-3}$	0.30	0.34	0.50	0.38	0.31	0.41	0.45	0.35
$1 \times 10^{-2}/1 \times 10^{-3}$	0.20	0.30	0.34	0.24	0.24	0.30	0.39	0.25
$5 \times 10^{-3}/5 \times 10^{-4}$	0.19	0.29	0.31	0.22	0.19	0.29	0.29	0.21
$1 \times 10^{-3}/1 \times 10^{-4}$	0.19	0.29	0.30	0.20	0.18	0.28	0.28	0.19

*Membrane.

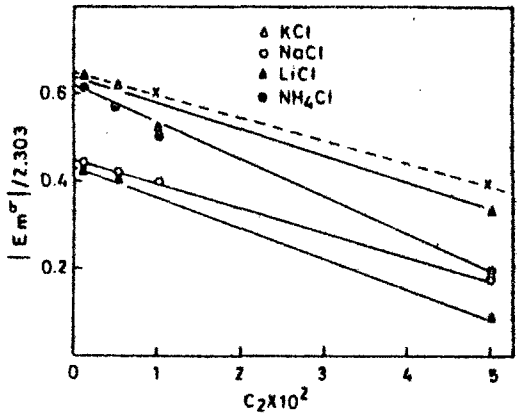

FIG. 2. Plots of $|E_m^\circ|/2.303$ *vs.* $C_2 \times 10^2$ for nickel sulphide membrane (-) in contact with various 1:1 electrolyte solutions and (---) for cobalt sulphide membrane with KCl solutions.

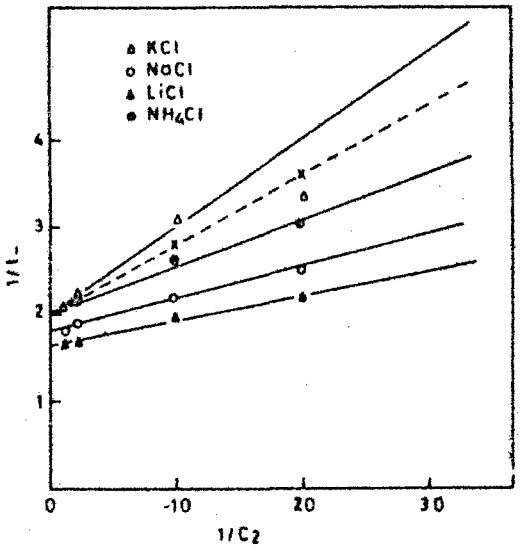

FIG. 3. Plots of $1/t_-$ *vs.* $1/C_2$ for nickel sulphide membrane (—) in contact with various 1:1 electrolyte solutions and cobalt sulphide membrane (---) with KCl solution.

$$[6] \qquad \frac{(\gamma - e^q)}{(e^q - 1)} = Z$$

with q and Z defined by

$$q = \frac{[|E_m^\circ| + (1 - 2\alpha) \ln \gamma]}{1/\beta + (1 - 2\alpha)}$$

and $Z = C_2/\alpha\beta X$. Thus if [6] is valid, the value of $(\gamma - e^q)/(e^q - 1)$ calculated from the measured E_m with predetermined α, β, and X and the given value of γ must fall on a straight line which has a unit slope and passes the co-ordinate origin when plotted against Z. This behaviour should be observed irrespective of the value of γ and the kind of membrane electrolyte system used. Figure 4 demonstrates that the theoretical prediction of [6] (or eq. 2) is borne out quite satisfactorily by our experimental results on parchment supported membranes.

Kobatake and Kamo (23) derived another equation (eq. 7) for membrane potential using a different set of assumptions, namely: (*a*) the contribution of mass movement is negligible (23), and (*b*) small ions do not behave ideally in a charged membrane (23).

$$[7] \quad E_m = \frac{RT}{F}\left[\ln \frac{C_2}{C_1} + (2\alpha - 1) \times \ln \frac{\sqrt{4C_2^2 + \phi^2 X^2} + (2\alpha - 1)\phi X}{\sqrt{4C_1^2 + \phi^2 X^2} + (2\alpha - 1)\phi X} - \ln \frac{\sqrt{4C_2^2 + \phi^2 X^2} + \phi X}{\sqrt{4C_1^2 + \phi^2 X^2} + \phi X}\right]$$

TABLE 4. Values of the effective fixed charge densities (X_c, X_d, ϕX^* or ϕX) for various membrane electrolyte systems derived from different methods of Kobatake *et al.*

	Value							
	Cobalt sulphide*				Nickel sulphide*			
Parameter‡	KCl†	NaCl†	LiCl†	NH_4Cl†	KCl†	NaCl†	LiCl†	NH_4Cl†
$X_c \times 10^2$ equiv./ℓ (eq. 4)	3.0	2.5	1.7	2.0	2.1	1.5	2.1	1.4
$X_d \times 10^2$ equiv./ℓ (eq. 3)	3.2	2.0	2.2	2.8	2.3	1.8	2.5	3.7
$\phi X^* \times 10^2$ equiv./ℓ (eq. 13)	2.5	1.0	2.9	3.8	2.7	1.9	2.5	3.0
$\phi X \times 10^2$ equiv./ℓ (eq. 10)	2.3	2.7	2.6	4.0	2.8	1.4	1.5	4.0

*Membrane.
†Electrolyte.
‡$X_c = \frac{2(1-\alpha)^2 \ln \gamma}{(1+\beta-2\alpha\beta)(\gamma-1)} \times$ slope; $X_d = \frac{(\gamma-1)(1+1/\beta)}{\alpha\beta\gamma} \times$ slope, ϕX^* is derived from the plot P_s *vs.* log $(C_1 + C_2)/2$;
$\phi X = \frac{1-\alpha}{\alpha} \times \left[\frac{\gamma \ln \gamma}{\gamma - 1}\right] \times$ slope

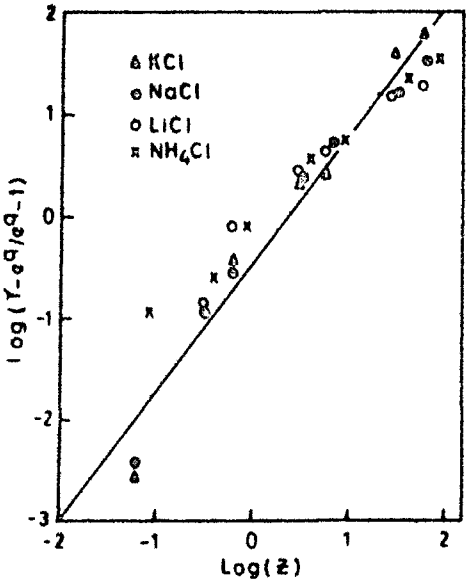

FIG. 4. Plot of $\log(\gamma - e^q)/(e^q - 1)$ *vs.* $\log Z$ for nickel sulphide membrane in contact with various 1:1 electrolyte solutions.

where ϕ is a characteristic factor of the membrane–electrolyte pair, and represents a fraction of counterions not tightly bound to the membrane skeleton. The product ϕX is termed the thermodynamically effective fixed charge density of a membrane. Other terms have their usual significance. Equation 7 has the same functional form as that given by the TMS theory for the membrane potential E_m (*i.e.* eq. 1) except that the thermodynamically effective fixed charge density ϕX of the membrane is used in place of stoichiometric fixed charge density $\bar{X}$. Equation 7 reduced to the TMS membrane potential for $\phi \simeq 1$. Since it is somewhat troublesome to evaluate ϕX at an arbitrary external electrolyte concentration from the observed membrane potential E_m using [7], Kobatake and Kamo (23) have proposed a simple method using the following approximate equation for the diffusive contribution to the emf of a cell with transport.

$$[8] \qquad E_m = -\frac{RT}{F}(1 - 2\tau_{app}) \ln C_2/C_1$$

where τ_{app} is the transference number of coions in the membrane phase. Comparison of [7] and [8] gives

$$[9] \qquad \tau_{app} = \frac{1-2\alpha}{2} \frac{\ln\left(\frac{\sqrt{4\xi_2^2 + 1} + 1 + 2\alpha - 1}{\sqrt{4\xi_1^2 + 1} + 1 + 2\alpha - 1}\right)}{\ln \gamma} + \frac{\ln\left(\frac{\sqrt{4\xi_2^2 + 1} + 1}{\sqrt{4\xi_1^2 + 1} + 1}\right)}{2 \ln \gamma}$$

where $\xi \simeq C/\phi X$, when the concentration of the external salt solution is large as compared to the effective charge density ϕX, *i.e.* when $C_1/\phi X = \xi_1 \gg 1$, [9] is expanded to

$$[10] \qquad 1/\tau_{app} = \frac{1}{1-\alpha} + \frac{\gamma - 1}{\gamma \ln \gamma} \frac{\alpha}{1-\alpha}\left(\frac{\phi X}{C_1}\right) + O\left(\frac{1}{C_1}\right)^2$$

This equation indicates that the plot of $1/\tau_{app}$ *vs.* $1/C_1$ with a fixed γ (or C_2/C_1) should give a straight line, and the values of α and ϕX in the concentrated solution for a given combination of membrane and electrolyte can be determined

from the intercept and the slope of the line. The values of thermodynamically effective fixed charge densities thus derived using Fig. 5 for two sulphide membranes in contact with various 1:1 electrolytes are given in Table 4.

On the other hand (22, 23), the mass-fixed transference number of coions in a negatively-charged membrane immersed in an electrolyte solution of concentration C is defined by

$$[11] \qquad \tau_- = vC_-/(uC_+ + vC_-)$$

where C_+ and C_- are the concentrations of cation and anion respectively in the membrane phase. This equation is transformed to

$$[12] \quad \tau_- = 1 - \alpha\frac{\sqrt{4\xi^2 + 1} + 1}{\sqrt{4\xi^2 + 1} + (2\alpha - 1)}$$

using equations given by Kobatake and co-workers (22, 23) for the activity coefficients, mobilities of small ions in the membrane phase, and the equilibrium condition for electrical neutrality. The difference between τ_{app} calculated from [9] and τ_- from [12] for various reduced concentrations ξ is found to be less than 2%. Therefore τ_{app} and τ_- are considered practically the same. As a result, the apparent transference number τ_{app} evaluated from the membrane potential data permits the determination of the thermodynamically effective fixed charge density ϕX of the membrane at a given average salt concentration C (*i.e.* $(C_1 + C_2)/2$) using [12]. At the same time rearrangement of [12] leads to the definition of permselectivity P_s by the

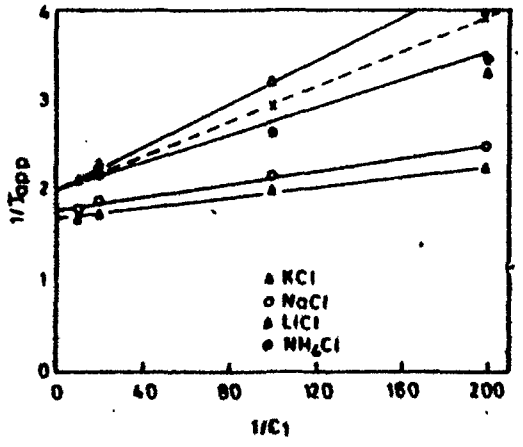

FIG. 5. Plots of $1/\tau_{app}$ *vs.* $1/C_1$ for nickel sulphide membrane (—) in contact with various 1:1 electrolyte solutions and cobalt sulphide membrane (---) with KCl solutions.

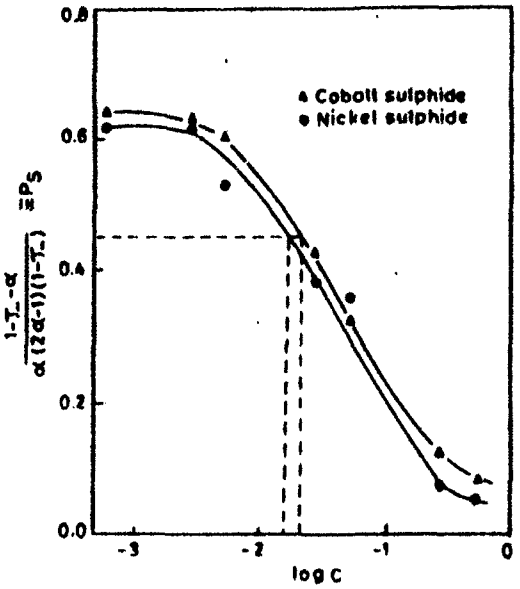

FIG. 6. Plots of P_s *vs.* $\log (C_1 + C_2)/2$ for membranes using different concentrations of KCl solutions.

expression

$$[13] \quad \frac{1}{(4\xi^2 + 1)^{1/2}} = \frac{1 - \tau_- - \alpha}{\alpha - (2\alpha - 1)(1 - \tau_-)} \equiv P_s$$

This equation can be used to find the permselectivity P_s from the membrane potential measurements using [8]. If the transport number of coions (τ or τ_{app}) is zero, the membrane is perfectly selective and $P_s = 1$, while if the transport number of coions has the value in free solution, $P_s = 0$. The values of P_s obtained using the right-hand side of [13] were plotted against log C. The concentration at which P_s becomes $1/\sqrt{5}$ (*i.e.* $\xi = C/\phi X = 1$) gives the value of the thermodynamically effective fixed charge density ϕX as demanded by the left-hand side of [13]. Figure 6 represents a typical plot of P_s *vs.* log C for two parchment supported sulphide membranes in contact with the KCl electrolyte. The values of ϕX thus derived from both the membranes and 1:1 electrolyte combinations are given in Table 4. Further, it is noted from Tables 2 and 4 that the charge densities found by the three theories are of the same magnitude.

Acknowledgement

Thanks are due to Professor Wasiur Rahman, Head, Department of Chemistry, for providing necessary facilities.

1. F. A. Siddiqi, N. Lakshminarayanaiah, and M. N. Beg. J. Polym. Sci. 9, 2853 (1971).
2. F. A. Siddiqi, N. Lakshminarayanaiah, and M. N. Beg. J. Polym. Sci. 9, 2869 (1971).
3. F. A. Siddiqi, M. N. Beg, S. P. Singh, and A. Haque. Bull. Chem. Soc. Jpn. 49(10), 2869 (1976).
4. F. A. Siddiqi, M. N. Beg, S. P. Singh, and A. Haque. Bull. Chem. Soc. Jpn. 49(10), 2858 (1976).
5. F. A. Siddiqi, M. N. Beg, and S. P. Singh. J. Polym. Sci. In press.
6. F. A. Siddiqi, M. N. Beg, and P. Prakash. J. Electroanal. Chem. In press.
7. F. A. Siddiqi and S. Pratap. J. Electroanal. Chem. 23, 137 (1969).
8. F. A. Siddiqi and S. Pratap. J. Electroanal. Chem. 23, 147 (1969).
9. F. A. Siddiqi, N. Lakshminarayanaiah, and S. K. Saksena. Z. Phys. Chem. (Frankfurt), 72, 298 (1970).
10. F. A. Siddiqi, N. Lakshminarayanaiah, and S. K. Saksena. Z. Phys. Chem. (Frankfurt), 72, 307 (1970).
11. G. Eisenman. Membrane transport and metabolism. *Edited by* A. Kleinzer and A. Kotyk. Academic Press, New York, NY. 1961. p. 163; Biophys. J. Suppl. 2, 259 (1962).
12. H. Sherry. Ion exchange. Vol. 2. *Edited by* J. A. Marinsky. Dekker, New York, NY. 1968.
13. S. Glasstone, K. S. Laidler, and H. Eyring. The theory of rate processes. McGraw Hill, New York, NY. 1941. (*a*) p. 525; (*b*) p. 544.
14. T. Teorell. Proc. Soc. Exp. Biol. 33, 282 (1935); Proc. Natl. Acad. Sci. (USA), 21, 152 (1935); Z. Electrochem. 55, 460 (1951); Prog. Biophys. Chem. 3, 385 (1953).
15. K. H. Meyer and J. F. Sievers. Helv. Chim. Acta, 19, 649 (1936); 19, 665 (1936); 19, 987 (1936).
16. T. Teorell. Discuss. Faraday Soc. No. 21, 9 (1956).
17. Y. Kobatake, T. Noriaki, Y. Toyoshima, and H. Fujita. J. Phys. Chem. 69, 3981 (1965).
18. Y. Toyoshima, M. Yussa, Y. Kobatake, and H. Fujita. Trans. Faraday Soc. 63, 2803 (1967); 63, 2814 (1967).
19. M. Yussa, Y. Kobatake, and H. Fujita. J. Phys. Chem. 72, 2871 (1968).
20. N. Kamo, Y. Toyoshima, H. Nozaki, and Y. Kobatake. Kolloid-Z.,Z. Polym. 248, 214 (1971).
21. N. Kamo, Y. Toyoshima, and Y. Kobatake. Kolloid-Z. Z. Polym. 249, 1061 (1971).
22. N. Kamo, M. Ockawa, and Y. Kobatake. J. Phys. Chem. 77, 92 (1973); 77, 2995 (1973).
23. Y. Kobatake and N. Kamo. Prog. Polym. Sci. Jpn. 5, 257 (1972).
24. N. Lakshminarayanaiah. Transport phenomena in membranes. Academic Press, New York, NY. 1969. p. 196.

Journal of Membrane Science, 2 (1977) 245—261

STUDIES WITH MODEL MEMBRANES.

XI. EVALUATION OF THERMODYNAMIC PARAMETERS FOR DIFFUSION AND FIXED CHARGE DENSITY BY METHODS BASED ON THERMODYNAMICS OF IRREVERSIBLE PROCESSES

FASIH A. SIDDIQI, IBADUR RAHMAN KHAN, S.K. SAKSENA and M. AQUEEL AHSAN

Division of Physical Chemistry, Department of Chemistry, Aligarh Muslim University, Aligarh (India)

(Received May 2, 1977)

Summary

The various ionic processes occurring in membrane systems notably (i) ionic transport, (ii) membrane potential, (iii) electrical conductivity, and (iv) ionic distribution and the potentials within the membrane have been thoroughly studied with a parchment-supported silver phosphate membrane. By applying the theory of absolute reaction rates, various thermodynamic parameters, namely $\Delta H^{\neq}$, $\Delta F^{\neq}$, and $\Delta S^{\neq}$, were evaluated. The $\Delta S^{\neq}$ values were found to be negative, indicating that diffusion takes place with partial immobilization in the membrane phase. The effective fixed charge density was also evaluated by methods based on the thermodynamics of irreversible processes.

We have been engaged for some time in studies of model systems which mimic some of the properties of biological membranes. For example, parchment-supported membranes [1—4] and certain polymeric membranes [5—7], in some formal aspects at least, behaved like gastric mucosal membrane [8]. This series of communications deals with the application of the Nernst-Planck formulas for electrical potential to the study of diffusion rates as well as the evaluation of the thermodynamically effective fixed charge density by recent methods based on the thermodynamics of irreversible processes [9—15].

Experimental

Preparation of membrane

The parchment-supported silver phosphate membrane was prepared by the method of interaction suggested by Siddiqi et al. [2], to which the reader is referred. In the present case, the membranes were prepared from 0.2 *M* solutions of $AgNO_3$ and sodium di-*ortho*-hydrogen phosphate.

Apparatus and procedure

The apparatus and procedures used to determine diffusion rates are those

described by Siddiqi et al. [2—4]. The half cells contained 125 ml of the electrolyte solutions while the capacity of each of the half cells holding the membrane was about 130 ml. Initially these concentrations, C_1 and C_2, were 0.001 *M* and 0.1 *M*. Each half cell had two platinized-platinum electrodes firmly fixed in order to follow concentration changes on a conductivity bridge (Cambridge Instrument Co., England, No. 350140), and two anion-reversible Ag/AgCl electrodes, one a disc type to pass a small d.c. current and the other a J-shaped wire electrode used to measure membrane potential (by Pye-Precision Vernier Potentiometer No. 7568). The whole cell was immersed in a water thermostat maintained at 10, 20, 25, or 35°C (±0.1°C) for measuring the diffusion rates of various electrolytes through the parchment-supported silver phosphate membrane. The various salt solutions (chlorides of K^+, Na^+, Li^+, Ca^{2+}, Ba^{2+}, Sr^{2+}, Mg^{2+}, and Al^{3+}) were prepared from BDH (AR) grade chemicals using deionized water.

Once the cell was set up, the experimental procedure used was to follow the conductance change on the dilute side of the membrane with time. The exact concentration of the solution at any given time was estimated from a calibration curve of conductance against concentration. The J-type electrodes monitored the membrane potential with time. The membrane resistance, R_m, was determined by applying an external emf to the disc-type Ag/AgCl electrodes and measuring the change in potential across the membrane using the J-type electrodes.

For the evaluation of membrane charge density, another cell of the following type

Ag/AgCl	Solution 1	Membrane	Solution 2	Ag/AgCl
	C_1		C_2	

was set up to measure membrane potential. The membrane potential was measured by keeping a fixed concentration ratio, i.e. $C_1/C_2 = \gamma = 10$, throughout the experiment. The observed membrane potential is the sum of the cell potential and the concentration potential. The pressure and temperature were also kept constant throughout the experiment. The potentials were measured at 25°C.

Results and discussion

Diffusion of electrolytes

When an ionic gradient is maintained using two solutions of different concentrations of the same electrolyte on either side of the membrane, diffusion of electrolyte from the region of high concentration takes place. In addition, an electric field due to differences in the ionic mobilities is established across the membrane. If the membrane contains a large number of fixed charged groups, the potential generated will be many times larger than the liquid junction potential normally observed when the same two solutions are brought together with or without an "uncharged" membrane in between.

The data obtained in the present study indicate that electrolyte permeation gives rise to negative values of $\Delta S^{\neq}$ whose magnitude depends on the value chosen for λ (λ has been assumed to be between 3 Å and 5 Å for different electrolytes). Since the membrane used in this study is fairly thick, it is believed that the membrane itself and not the membrane-solution interfaces controlled the electrolyte diffusion process. As suggested by Schuler et al. [22], the negative values of $\Delta S^{\neq}$ indicate that electrolyte diffusion occurs with partial immobilization in the membrane, the immobilization increasing with the valence of the ions. In Fig. 4 the individual ionic contribution to the properties of aqueous ions, namely $\Delta H_{\text{hydration}}$, $\Delta F_{\text{hydration}}$ and $\Delta S_{\text{hydration}}$ of various cations, are plotted against the corresponding $\Delta H^{\neq}$, $\Delta F^{\neq}$, and $\Delta S^{\neq}$ values for diffusion through the parchment membrane. It was found that at least some formal relationship exists between these thermodynamic parameters.

Evaluation of membrane charge density

The membrane potential across the silver phosphate membrane observed when it was used to separate two solutions of different concentrations of the same 1:1 electrolyte are plotted against log $((C_1 + C_2)/2)$ and are shown in Fig. 5 for various electrolytes at 25°C. Recently, Kobatake et al. [9–13] have obtained various expressions for the membrane potential derived from the thermodynamics of irreversible processes for the electrical potential, $\Delta\phi$, across a (negatively) ionizable membrane. The final expression for the

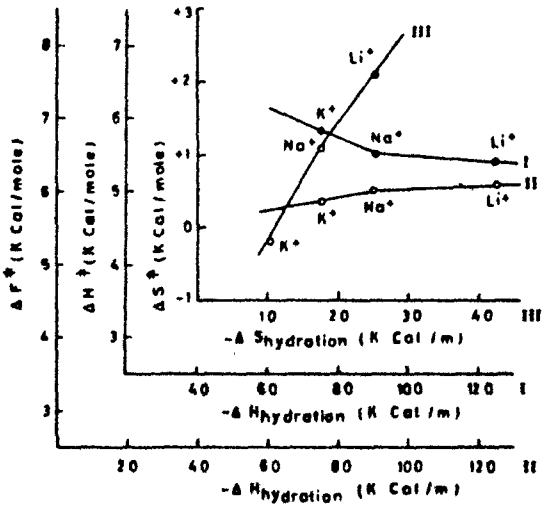

Fig. 4. Plots of (I) $\Delta H^{\neq}$, (II) $\Delta F^{\neq}$, and (III) $\Delta S^{\neq}$ vs. $\Delta H_{\text{hydration}}$, $\Delta F_{\text{hydration}}$, and $\Delta S_{\text{hydration}}$ for the diffusion of cations across a silver phosphate membrane. The solution data were taken from Noyes [25].

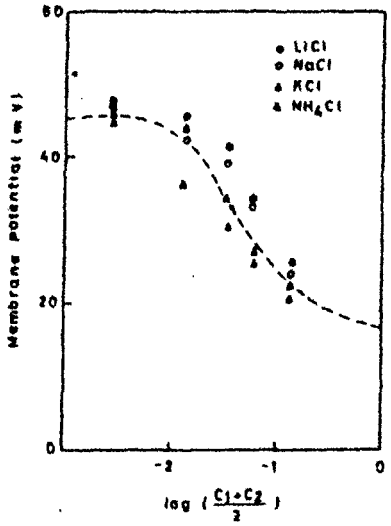

Fig. 5. Observed membrane potential vs. $\log(C_1 + C_2)/2$ across a silver phosphate membrane for various electrolytes at 25°C.

membrane potential is

$$\Delta\phi = -\frac{RT}{F}\ \frac{1}{\beta}\ \ln\frac{C_2}{C_1} - \left(1 + \frac{1}{\beta} - 2\alpha\right)\ln\left(\frac{C_2 + \alpha\beta\theta}{C_1 + \alpha\beta\theta}\right) \tag{11}$$

where $\alpha = \dfrac{u_+}{u_+ + u_-}$ 12(a)

and $\beta = 1 + \dfrac{KF\theta}{u_+}$, 12(b)

where u_+ and u_- are the molar mobilities of positive and negative ions, K is a constant which depends on the viscosity of the solution and the structural details of the polymer network of which the membrane is composed, and θ is the charge density. These parameters are assumed to depend on salt concentration.

Kobatake [9—13] has derived two limiting forms of eqn. 11 useful for the analysis of experimental data on membrane potential:

(*i*) when C_2 becomes sufficiently small with γ fixed, eqn. 11 reduces to

$$|\Delta\phi_r| = \frac{1}{\beta}\ln\gamma - \frac{(\gamma - 1)}{\alpha\beta\gamma}\left(1 + \frac{1}{\beta} - 2\alpha\right)\frac{C_2}{\theta} + \ldots \tag{13}$$

where $|\Delta\phi_r| = \dfrac{F\Delta\phi}{RT}$, (14)

which is the absolute value of the reduced membrane potential.

(*ii*) It is well known experimentally that at fixed γ the inverse of an apparent transference number (t_{app}) for the co-ion species in a negatively charged membrane is proportional to the inverse of the concentration C_2 in the region of high salt concentration. Here t_{app} is defined by

$$|\Delta\phi_r| = (1 - 2t_{app}) \ln \gamma . \tag{15}$$

Now eqn. 11 may be expanded to give

$$\frac{1}{t_{app}} = \frac{1}{(1-\alpha)} + \frac{(1+\beta-2\alpha\beta)(\gamma-1)\alpha}{2(1-\alpha)^2 \ln \gamma}\left(\frac{\theta}{C_2}\right) \tag{16}$$

Eqns. 13 and 16 indicate that the values of β and α may be obtained by evaluating the intercept of plots of $|\Delta\phi_r|$ against C_2 and $1/t_{app}$ against $1/C_2$ at fixed γ. These plots are shown for various uni-univalent electrolytes through the parchment-supported silver phosphate membrane at 25°C in Figs. 6 and 7, respectively. The intercepts are equal to $(1/\beta) \ln \gamma$ and $1/(1-\alpha)$ from which β and α may be evaluated. From these α and β values, θ values may be obtained for various 1:1 electrolytes.

To compare theory and experiment, Kobatake made the following suggestion. Because

$$\frac{\gamma - e^q}{e^q - 1} = Z , \tag{17}$$

where

$$q = \frac{|\Delta\phi_r| + (1-2\alpha)\ln\gamma}{\frac{1}{\beta} + (1-2\alpha)} \tag{18}$$

and

$$Z = \frac{C_2}{\alpha\beta\theta} , \tag{19}$$

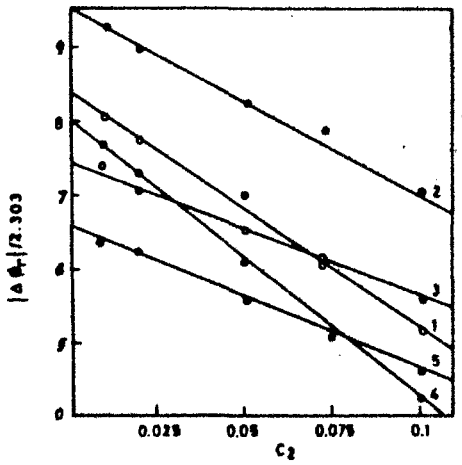

Fig. 6. Plots of $|\Delta\phi_r|/2.303$ vs. C_2 for (1) LiCl, (2) CH_3COOK, (3) NaCl, (4) NH_4Cl, and (5) KCl across a silver phosphate membrane at 25°C.

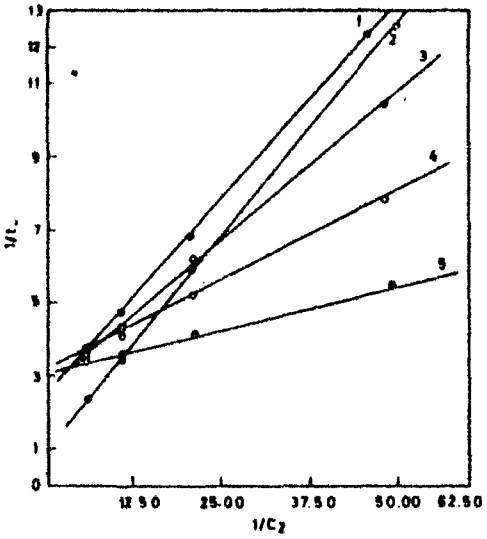

Fig. 7. Plots of $1/t_-$ vs. $1/C_2$ for (1) LiCl, (2) CH_3COOK, (3) NaCl, (4) NH_4Cl, and (5) KCl across a silver phosphate membrane at 25°C.

then, if eqn. 11 is valid, a plot of $(\gamma - e^q)/(e^q - 1)$ (calculated from measured $\Delta\phi$ values with the α, β, and θ values determined above and the known value of γ) against t must be a straight line with unit slope and passing through the origin. This behavior must be valid irrespective of the value of γ and the kind of membrane-electrolyte system. This prediction is borne out quite satisfactorily by our experimental results.

The mass transference number of anions in the membrane is given by Kobatake [9—13]:

$$\tau_- = 1 - \alpha \frac{(4\epsilon^2 + 1)^{1/2} + 1}{(4\epsilon^2 + 1)^{1/2} + (2\alpha - 1)}, \qquad (20)$$

where ϵ stands for the relative concentration defined by $C/\phi X$, where ϕX is the charge density of the membrane.

On the other hand the apparent transference number $T_{\bar{a}pp}$ is defined by the Nernst equation

$$\Delta\phi = -\frac{RT}{F}(1 - 2\,T_{\bar{a}pp}) \ln\left(\frac{C_2}{C_1}\right) \qquad (21)$$

The difference between τ_- and $T_{\bar{a}pp}$ was less than 2% in Kobatake's experiments within a wide range of salt concentration [9—13].

If we replace τ_- by $T_{\bar{a}pp}$ and C by $(C_1 + C_2)/2$, eqn. 20 may be rearranged to give

$$\frac{1}{(4\epsilon^2 + 1)^{1/2}} = \frac{1 - \tau_{\bar{a}pp} - \alpha}{\alpha - (2\alpha - 1)(1 - T_{\bar{a}pp})} \equiv P_s, \qquad (22)$$

where P_s is a measure of the permselectivity of the membrane-electrolyte system.

Kobatake suggested a procedure for evaluating the membrane charge density which was adopted for the present investigation. The various values of P_s were calculated by substituting the values of α (bulk) and τ_{app} into eqn. 22 and then P_s was plotted against log C. Thus a curve was obtained as shown in Fig. 8. When $C = \phi X$, the value of ϵ automatically becomes equal to unity and P_s becomes 0.448 from $P_s = 1/(4\epsilon^2 + 1)^{1/2}$. At this value of P_s the corresponding concentration is obtained from the plot of P_s versus log C. This value of concentration is equal to the fixed charge density of the membrane and such values are given in Table 2 for various electrolytes.

The emf $\Delta\phi$ may be expressed by the modified Nernst equation

$$\Delta\phi = \Delta\phi_N \ (2\,\overline{T}_C - 1) \tag{23}$$

where $\Delta\phi$ is the measured membrane potential in mv and $\Delta\phi_N$ is the Nernst potential. $\overline{T}_C$ is the cation transference number which was calculated from measured potentials for different solution activities.

Another method was also developed to evaluate the transference number by using Hersh's equation [26]:

$$T_C = \frac{(\bar{u}/\bar{v})\ \overline{C}_+}{(\bar{u}/\bar{v})\ \overline{C}_+ + \overline{C}_-} \tag{24}$$

$$\text{where } \overline{C}_+ = \frac{1}{2}\left[\sqrt{(\phi X)^2 + 4C_1^2} + \phi X\right] \tag{25a}$$

$$\text{and } \overline{C}_- = \frac{1}{2}\left[\sqrt{(\phi X)^2 + 4C_1^2} - \phi X\right], \tag{25b}$$

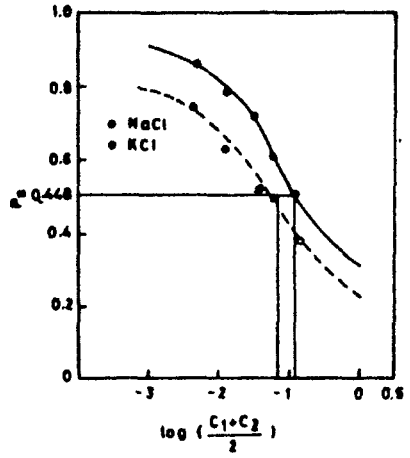

Fig. 8. Permselectivity P_s vs. $\log(C_1 + C_2)/2$ for various electrolytes across a silver phosphate membrane at 25°C.

TABLE 2

Charge-density (ϕX) of a parchment-supported silver phosphate membrane obtained by two methods, at $\gamma = 1.0$

Electrolyte	ϕX from Kobatake's method (eq. I')	ϕX from Nagasawa's method (eq. I')
KCl	0.035	0.025
NaCl	0.026	0.025
LiCl	0.032	0.036
NH_4Cl	0.020	0.050

where $(\bar{u}/\bar{v})$ is the mobility ratio in the membrane phase and $\overline{C}_+$ and $\overline{C}_-$ are the cation and anion concentrations in the membrane phase. Thus, values of T_C were evaluated from eqn. 23 as well as from eqn. 24. These values were found to be in close agreement.

Recently, Nagasawa et al. [14] developed a new method for the evaluation of the charge density of membranes. The system considered was analogous to the Kobatake method [9—13]. The solutions on both sides of the membrane were maintained at the same pressure and temperature throughout the experiment. The fluxes of water and ions relative to the cell were expressed by the following linear equations:

$$-J_0 = L_{00} \operatorname{grad} \bar{\mu}_0 + L_{0+} \operatorname{grad} \bar{\mu}_+ + L_{0-} \operatorname{grad} \bar{\mu}_- \quad (26a)$$

$$-J_+ = L_{+0} \operatorname{grad} \bar{\mu}_0 + L_{++} \operatorname{grad} \bar{\mu}_+ + L_{+-} \operatorname{grad} \bar{\mu}_- \quad (26b)$$

$$-J_- = L_{-0} \operatorname{grad} \bar{\mu}_0 + L_{-+} \operatorname{grad} \bar{\mu}_+ + L_{--} \operatorname{grad} \bar{\mu}_- \quad (26c)$$

Here subscripts +, —, and zero represent the cation, anion, and water molecule, respectively, and the J's are the mass fluxes, L's the phenomenological coefficients, and μ's the chemical potentials including the contribution due to external forces.

The concentration of the electrolyte in the solution was so low that the flow rate of solutions (J_v) was approximated by $J_0/\overline{C}_0$, where J_0 and C_0 are defined as mole/cm^2-min and mole/cm^3, respectively. Thus we have:

$$-(L_{i0}/L_{00})\, J_0 \approx -(\overline{C}_i/\overline{C}_0)\, J_0 \quad . \quad (27)$$

The distribution of ions in the membrane is not uniform. Most counterions are accumulated around the fixed charges in the membrane matrix due to their strong electrostatic forces. The effective concentration of coions is approximately equal to $\overline{C}_-$, whereas the effective concentration of counterions may be expressed by $\overline{C}_- + \phi X$, where ϕX is the charge density of the membrane. Thus, the following equations were obtained

$$-J_+ = -\left(\frac{\overline{C}_- + \phi X}{\overline{C}_0}\right) J_0 + (\overline{C}_- + \phi X)\, u_+ \operatorname{grad} \bar{\mu}_+ \quad (28a)$$

$$-J_- = -\left(\frac{\bar{C}_-}{\bar{C}_0}\right) J_0 + \bar{C}_- u_- \operatorname{grad} \bar{\mu}_- \qquad (28b)$$

where u_+ and u_- are the cation and anion mobilities in the membrane phase.

From the condition of no current at steady state, i.e. $J_+ = J_- = J_s$ for a 1:1 electrolyte system, eqns. 28 were rearranged to give

$$-J_s = -\left(\frac{J_0}{C_0}\right) \frac{\bar{C}_-(\bar{C}_- + \phi X)(u_+ + u_-)}{(\bar{C}_- + \phi X) u_+ + \bar{C}_- u_-} + \frac{(2\bar{C}_- + \phi X) u_+ u_- RT}{(\bar{C}_- + \phi X) u_+ + \bar{C}_- u_-} \operatorname{grad} \bar{C}_- . \qquad (29)$$

On integrating across the membrane, this equation gave:

$$-J_s = \left(\frac{RT}{\delta}\right) \frac{2u_+ u_- A_1 (A_1 - \phi X)\ A_1 - \phi X/2}{(u_+ + u_-)(A_1 - A_2)\left(A_1 - \frac{\phi X u_+}{u_+ + u_-}\right)} \ln\left(\frac{\bar{C}_{2-} + A_1}{\bar{C}_{1-} + A_1}\right) +$$

$$\frac{RT}{\delta} \frac{2u_+ u_- A_2 (A_2 - \phi X)\left(A_2 - \frac{\phi X}{2}\right)}{(u_+ + u_-)(A_2 - A_1)\left(A_2 - \frac{\phi X u_+}{u_+ + u_-}\right)} \ln\left(\frac{\bar{C}_{2-} + A_2}{\bar{C}_{1-} + A_2}\right), \qquad (30)$$

where $A_i = \frac{1}{2(u_+ + u_-)} \left[\phi X u_+ + \frac{2RT \bar{C}_0 u_+ u_- k}{J_0} + (-1)^i \left\{\left(\phi X u_+ - \frac{2RT \bar{C}_0 u_+ u_- k}{J_0}\right)^2 + 4(\phi X)^2 u_+ u_-\right\}^{1/2}\right] . \qquad (31)$

The parameter δ is the thickness of the membrane, and k is a constant which was evaluated by integrating the equation

$$\frac{d\bar{C}_-}{dX} = \bar{C}_- + \frac{\phi X}{2} - 1 \left[\bar{C}_-^2 \frac{J_0 (u_+ + u_-)}{2RT \bar{C}_0 u_+ u_-} + \bar{C}_- \left(\frac{\phi X J_0}{2RT \bar{C}_0 u_-} + k\right) - \frac{(\phi X)^2 J_0}{2RT \bar{C}_0 (u_+ + u_-)} + \frac{\phi X u_+ k}{u_+ + u_-}\right] . \qquad (32)$$

The membrane potential arising on both sides of the membrane ($\Delta\phi = \Delta\phi_1 - \Delta\phi_2$) was taken as the sum of the diffusion potential ($\Delta\phi_d$) inside the membrane and the electrostatic potential differences ($\Delta\phi_e$) between the membrane and electrolyte solution phases on both sides of the membrane, i.e.

$$\Delta\phi = \Delta\phi_d + \Delta\phi_e , \qquad (33)$$

where $-\Delta\phi_d = -\int_1^2 \left(\frac{J_0}{F\bar{C}_0}\right) \frac{\phi X}{(\bar{C}_- + \phi X)\,u_+ + \bar{C}_- u_-}\,dx +$

$$\frac{RT}{F}\int_1^2 \frac{(\bar{C}_- + \phi X)\,u_+}{(\bar{C}_- + \phi X)\,u_+ + \bar{C}_- u_-}\,d\ln \bar{a}_+ -$$

$$\frac{RT}{F}\int_1^2 \frac{\bar{C}_- u_-}{(\bar{C}_- + \phi X)\,u_+ + \bar{C}_- u_-}\,d\ln \bar{a}_- \qquad 33(a)$$

and $-\Delta\phi_e = -\frac{RT}{F}\ln\left(\frac{\bar{a}_{1-}\,\bar{a}_{2-}}{a_{1-} - \bar{a}_{2-}}\right)$. 33(b)

For $J_0 = 0$, eqn. 33 on integration gives

$$-\Delta\phi = \left(\frac{RT}{2F}\right)\ln\left(\frac{\bar{C}_{2-}(\bar{C}_{1-} + \phi X)}{\bar{C}_{1-}(\bar{C}_{2-} + \phi X)}\right) +$$

$$\left(\frac{RT}{F}\right)\frac{2\phi X u_+ u_- \left(A_1 - \frac{\phi X}{2}\right)}{(u_+ + u_-)^2\,(A_1 - A_2)\left(A_1 - \frac{\phi X u_+}{u_+ - u_-}\right)}\ln\left(\frac{\bar{C}_{2-} + A_1}{\bar{C}_{1-} + A_1}\right) +$$

$$\left(\frac{RT}{F}\right)\frac{2\phi X u_+ u_- \left(A_2 - \frac{\phi X}{2}\right)}{(u_+ + u_-)^2\,(A_2 - A_1)\left(A_2 - \frac{\phi X u_+}{u_+ + u_-}\right)}\ln\left(\frac{\bar{C}_{2-} + A_2}{\bar{C}_{1-} + A_2}\right) \qquad (34)$$

while if J_0 was small and $\phi X J_0 << 2RT\bar{C}_0 u_- k$, then eqn. 34 changes to

$$-\Delta\phi = \frac{RT}{2F}\ln\left(\frac{(C_{1-} + \phi X)}{\bar{C}_{1-}(\bar{C}_{2-} + \phi X)}\right) + \left(\frac{RT}{F}\right)\left(\frac{u_+ - u_-}{u_+ + u_-}\right)\left[\frac{1 - \frac{\phi X J_0}{RT\bar{C}_0(u_+ - u_-)k}}{1 - \frac{\phi X J_0}{2RT\bar{C}_0 u_- k}}\right] X$$

$$\ln\left[\frac{\bar{C}_{2-} + \frac{\phi X u_+}{u_+ + u_-} - \frac{(\phi X)^2 J_0}{2RT\bar{C}_0(u_+ + u_-)k}}{\bar{C}_{1-} + \frac{\phi X u_+}{u_+ + u_-} - \frac{(\phi X)^2 J_0}{2RT\bar{C}_0(u_+ + u_-)k}}\right] +$$

$$\frac{RT\phi X}{2Fu_+u_-}\left(\frac{J_0}{RT\bar{C}_0k}\right)^2\left[\frac{\left(1-\frac{\phi XJ_0(u_++u_-)}{4RT\bar{C}_0u_+u_-k}\right)}{\left(1-\frac{\phi XJ_0}{2RT\bar{C}_0u_-k}\right)^2}\right]\left(\bar{C}_{2-}-\bar{C}_{1-}\right) \tag{35}$$

In the limit of high concentration, eqn. 34 becomes

$$-\Delta\phi=\frac{RT}{F}\left(\frac{\phi X}{2}\right)\left(\frac{\gamma-1}{\gamma}\right)\frac{1}{C_1}+\frac{RT}{F}\left(\frac{u_+-u_-}{u_++u_-}\right)\left[\frac{1-\frac{\phi XJ_0}{RT\bar{C}_0(u_+-u_-)k}}{1-\frac{\phi XJ_0}{2RT\bar{C}_0u_-k}}\right]\ln\gamma+$$

$$\frac{RT\phi X}{2Fu_+u_-}\left(\frac{J_0}{RT\bar{C}_0k}\right)^2\left[\frac{\left(1-\frac{\phi XJ_0(u_++u_-)}{4RT\bar{C}_0u_+u_-k}\right)}{\left(1-\frac{\phi XJ_0}{2RT\bar{C}_0u_-k}\right)^2}\right](\gamma-1)C_1 \tag{36}$$

At significant electrolyte concentration, eqn. 36 reduces to

$$-\Delta\phi=\frac{RT}{F}\left(\frac{\gamma-1}{\gamma}\right)\left(\frac{\phi X}{2}\right)\frac{1}{C_1} \tag{37}$$

which predicts a linear relationship between $\Delta\phi$ and $1/C_1$ from which ϕX can be calculated. Fig. 9 demonstrates that such a relationship exists in the

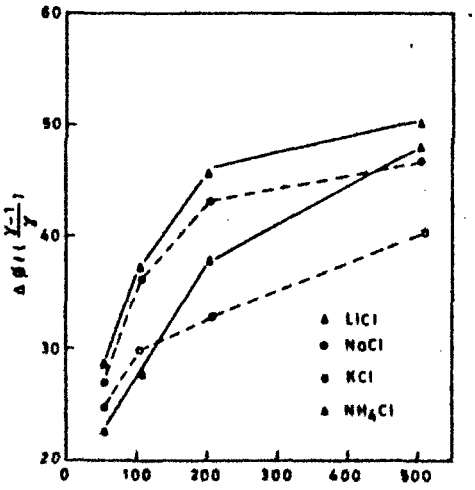

Fig. 9. Plots of $\Delta\phi/(\frac{\gamma-1}{\gamma})$ vs. $1/C_1$ for various electrolytes across a silver phosphate membrane at 25°C.

membrane-electrolyte system under investigation. The values of ϕX derived from the initial slope in this way are given in Table 2, for a parchment-supported silver phosphate membrane.

Acknowledgements

The authors are grateful to Prof. W. Ranman, Head of the Department of Chemistry, Aligarh Muslim University, Aligarh, for providing the necessary research facilities, and also to C.S.I.R. (India) for the award of fellowships to I.R.K., S.K.S., and M.A.A.

References

1 Fasih A. Siddiqi and S. Pratap, J. Electroanal. Chem. 23 (1969) 137; ibid, 23 (1969) 147.
2 Fasih A. Siddiqi, N. Lakshminarayanaiah, and S.K. Saksena, Z-phys. Chem. (Frankfurt), 72 (1970) 298; ibid., 72 (1970) 307.
3 Fasih A. Siddiqi, N. Lakshminarayanaiah, and M.N. Beg, J. Polym. Sci., 9 (1971) 2853; ibid., 9 (1971) 2868.
4 N. Lakshminarayanaiah and Fasih A. Siddiqi, Biophy. J., II (1971) 617; ibid., II (1971) 603.
5 N. Lakshminarayanaiah and Fasih A. Siddiqi, in M. Bier (Ed.), Membrane Processes in Industry and Biomedicine, Plenum Publishing Co., N.Y., 1971, p. 301.
6 N. Lakshminarayanaiah and Fasih A. Siddiqi, J. Polym. Sci., 8 (1970) 2949.
7 N. Lakshminarayanaiah and Fasih A. Siddiqi, Z-phys. Chem. (Frankfurt), 78 (1972) 150.
8 T. Teorell, "Membrane phenomena", Discussion Faraday Soc. No. 21, 1956, p. 9.
9 Y. Kobatake, T. Nariabi, and F. Hiroski, J. Phys. Chem., 69 (1965) 3981.
10 Y. Toyoshima, M. Yussa, Y. Kobatake, and H. Fujita, Trans. Faraday Soc., 63 (1967) 2803, 2814.
11 M. Yussa, Y. Kobatake, and H. Fujita, J. Phys. Chem., 72 (1968) 2871.
12 N. Kamo, Y. Toyoshima, and Y. Kobatake, Kolloid Z.Z.Poly., 249 (1971) 1061; 248 (1971) 914.
13 N. Kamo, M. Oikawa, and Y. Kobatake, J. Phys. Chem., 77 (1973) 92.
14 M. Tasaka and N. Aoki, J. Phys. Chem., 79 (1975) 1307.
15 N. Kamo, Y. Toyoshima, H. Nozaki, and Y. Kobatake, Kolloid Z.Z. Poly., 248 (1971) 914.
16 G. Schmid and H. Schwarz, Z.Electrochem., 55 (1951) 295; ibid., 55 (1951) 684.
17 W.W. Kittleberger, J. Phys. and Colloid Chem., 53 (1949) 392.
18 G. Eisenman, in A. Kleinzeller and A. Kotyk (Eds.), Membrane Transport and Metabolism, Academic Press, New York, 1961.
19 G. Eisenman, Biophys. J., 2 (1962) 259.
20 G. Eisenman, The Glass Electrode, Interscience, New York, 1965.
21 H. Sherry in J.A. Marinsky (Ed.), Ion Exchange, Vol. 72, Dekker, New York, 1968.
22 K.E. Schuler, C.A. Dames, and K.J. Laidler, J. Chem. Phys., 17 (1949) 860.
23 B.Z. Zwolinski, H. Eyring, and C.E. Reese, J. Phys. Chem., 53 (1949) 1426.
24 S. Glasstone, K.J. Laidler, and Eyring, The Theory of Rate Processes, McGraw Hill, N.Y., 1941, pp. 525—544.
25 R.M. Noyes, J. Amer. Chem. Soc., 84 (1962) 513.
26 L.S. Hersh, J. Phys. Chem., 72 (1968) 2195.

Journal of Membrane Science, 2 (1977) 365–374
© Elsevier Scientific Publishing Company, Amsterdam — Printed in The Netherlands

STUDIES WITH INORGANIC PRECIPITATE MEMBRANES

XXV. EVALUATION OF MEMBRANE PARAMETERS AND TEST OF RECENTLY DEVELOPED FIXED CHARGE THEORIES FOR MEMBRANE POTENTIAL

M. NASIM'BEG, FASIH A. SIDDIQI, RADHEY SHYAM and M. ARSHAD

Division of Physical Chemistry, Department of Chemistry, Aligarh Muslim University, Aligarh-202001 (India)

(Received April 18, 1977; in revised form August 18, 1977)

Summary

Effective fixed charge densities of parchment-supported cobalt and nickel phosphate membranes in contact with various 1 : 1 electrolyte solutions have been evaluated from membrane potential measurements. The methods used for the estimation of charge densities were: (a) Teorell—Meyer—Sievers; (b) two different methods of Kobatake et al.; and (c) a more recently developed method of Nagasawa et al. The charge densities evaluated from different methods were of the same magnitude. The apparent transference number of coions and permselectivities of the membranes for electrolytes have also been calculated.

In a series of communications on parchment-supported membranes, Siddiqi and Beg et al. [1—9] have, on the basis of the Eisenman—Sherry model of membrane selectivity [10,11] and by the application of the theory of rate processes to diffusion [12], demonstrated the low density of fixed charge groups on the membrane matrix and the partial immobilization of ions within the membrane. In order to substantiate these findings, the apparent transference number, the permselectivity for ions, and the effective fixed charge density of cobalt and nickel phosphate membranes have been evaluated in this paper through membrane potential measurements. Various fixed charge theories [13—20] for membrane potential, including those developed by Kobatake et al. [17—19] and more recently by Nagasawa et al. [20] based on the principles of irreversible thermodynamics, have been utilized for the charge density determinations in order to examine their validity in the system under investigation.

Experimental

Various inorganic precipitate membranes embedded in different polymeric materials have been prepared by a number of investigators [21—23] including Alberti et al. [22] who first used $ZrO(H_2PO_4)$ and Teflon under high pressure to prepare a membrane. Parchment-supported membranes of cobalt and nickel

phosphate were prepared by the method of interaction suggested by Siddiqi and Beg et al. [1—9]. To precipitate these substances in the interstices of the parchment paper, a 0.2 *M* solution of tri-sodium orthophosphate was placed inside a glass tube, to one end of which parchment paper was tied. The tube was suspended for 72 h in a 0.2 *M* solution of either Co(II) or Ni(II) chloride. The two solutions were interchanged later and kept for another 72 h. The membranes thus obtained were washed with deionized water to remove free electrolyte. Electrochemical cells of the type

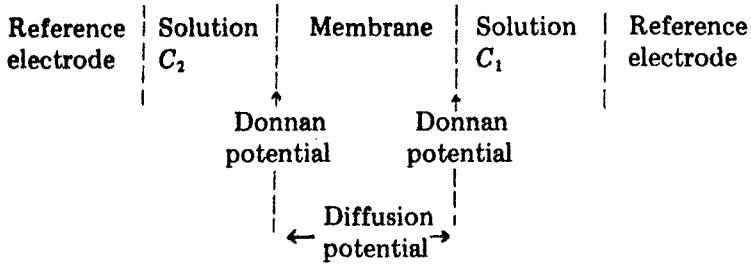

were used for measuring membrane potentials. The reference electrodes used were reversible saturated calomel electrodes connected to the solutions via KCl—agar bridges. A tenfold difference in concentration of the chloride solution (i.e. $C_2/C_1 = 10$) in the range 1×10^{-5} *N* to 0.1 *N* was maintained, and measurements were made using a Pye precision vernier potentiometer (No. 7568). The solutions were replaced by fresh solutions and when there was no change in potential with the addition of fresh solution it was taken as the true membrane potential. In the membranes under investigation, the potential could be reproduced within a few tenths of a mV. The whole cell was immersed in a water thermostat maintained at 25 ± 0.1°C. The solutions in both chambers were stirred by magnetic stirrers. The salt solutions (chlorides of Li^+, Na^+, and K^+) were prepared from B.D.H. AR grade chemicals and deionized water. The parchment paper was supplied by M/S Baird and Tatlock (London) Ltd.

TABLE 1

The values of the membrane potential E_m (mV) across cobalt and nickel phosphate membranes

Electrolyte concentration (*N*)	Cobalt phosphate membrane			Nickel phosphate membrane		
	KCl	NaCl	LiCl	KCl	NaCl	LiCl
0.1/0.01	−34.30	−38.65	−35.65	−42.40	−40.30	−40.50
0.05/0.005	−31.36	−36.80	−32.60	−40.25	−40.28	−38.00
0.01/0.001	−28.50	−21.70	−16.40	−32.00	−24.50	−21.50
0.005/0.0005	−10.50	−14.50	−10.40	−15.00	−13.00	−6.90
0.001/0.0001	+1.50	−5.00	+5.00	+1.50	+9.00	+4.50
0.0005/0.00005	+9.00	+10.00	+15.50	+10.25	+10.25	+8.00
0.0001/0.00001	+10.00	+15.00	+20.00	+12.50	+12.50	+15.25

Results and discussion

The values of membrane potential across both cobalt and nickel phosphate membranes in contact with various 1 : 1 electrolytes are given in Table 1.

When two electrolytic solutions having different concentrations are separated by a membrane, the mobile species penetrate the membrane and various transport phenomena are induced in the system [19]. The fixed charge concept of Teorell [14] and Meyer and Sievers [15] for charged membranes is a pertinent starting point for the investigation of the actual mechanisms of the ionic or molecular processes which occur in the membrane phase. These authors obtained eqn. (1) for the emf across a charged membrane by integrating the equation for the emf due to diffusion of ions within a membrane and subsequently adding the two phase-boundary (Donnan) potentials to the intramembrane diffusion potential:

$$E_m = 59.2\left[\log\frac{C_2}{C_1}\frac{(\sqrt{4C_1^2+\bar{X}^2}+\bar{X})}{(\sqrt{4C_2^2+\bar{X}^2}+\bar{X})} + \bar{U}\log\frac{\sqrt{4C_2^2+\bar{X}^2}+\bar{X}\bar{U}}{\sqrt{4C_1^2+\bar{X}^2}+\bar{X}\bar{U}}\right] \quad (1)$$

Here, $\bar{U} = (\bar{u} - \bar{v})/(\bar{u} + \bar{v})$, where $\bar{u}$ and $\bar{v}$ are the mobilities of the cation and anion, respectively, in the membrane phase, and $\bar{X}$ is the charge on the membrane expressed in equivalents/liter of imbibed solution. In order to evaluate this parameter for the simple case of a 1 : 1 electrolyte and a membrane carrying a net negative charge of unity ($\bar{X} = 1$), theoretical concentration potentials E_m existing across the membrane were calculated as a function of C_2, the ratio (C_2/C_1) being kept at a constant value of 10 for different mobility ratios $(\bar{u}/\bar{v})$ and plotted as shown in Fig. 1. The observed membrane potential values for the membranes obtained with an NaCl solution are plotted on the same graph. The experimental curve for any given membrane was shifted horizontally and run parallel to one of the theoretical curves. The extent of this shift gave $\log \bar{X}$ and the parallel theoretical curve gave the value for $(\bar{u}/\bar{v})$. The values of $\bar{X}$ and $(\bar{u}/\bar{v})$ derived in this way for both membranes and various 1 : 1 electrolytes are given in Table 2.

Kobatake et al. [17], on the basis of the thermodynamics of irreversible processes, derived the following equation for the electrical potential E_m which arises when a negatively-charged membrane separates two solutions of a 1 : 1 electrolyte of concentration C_1 and C_2 ($C_1 < C_2$):

$$E_m = -\left(\frac{RT}{F}\right)\left[\frac{1}{\beta}\ln\frac{C_2}{C_1} - \left(1+\frac{1}{\beta}-2\alpha\right)\ln\left(\frac{C_2+\alpha\beta X}{C_1+\alpha\beta X}\right)\right] \quad (2a)$$

where $\alpha = u/u + v$ (2b)

$$\beta = 1 + (KFX/u) \quad (2c)$$

and where K is a constant dependent upon the viscosity of the solution and

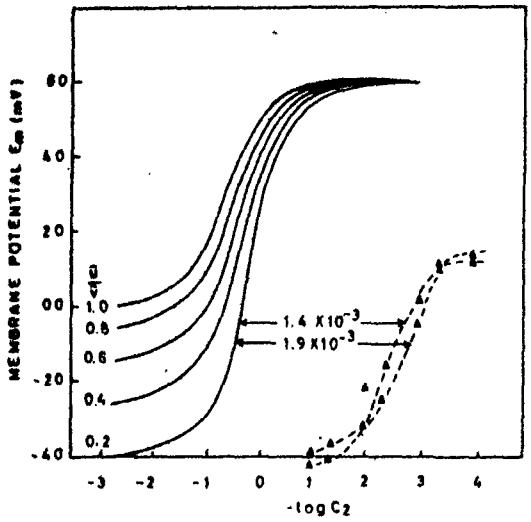

Fig. 1. Evaluation of membrane charge density $\bar{X}$ and the mobility ratio ($\bar{u}/\bar{v}$) in the membrane phase. The smooth curves on the left are the theoretical concentration potentials for a cation-selective membrane ($\bar{X} = 1$) using electrolytes at different mobility ratios $\bar{u}/\bar{v}$. The experimental values of E_m for cobalt (△) and nickel (▲) phosphate membranes and an NaCl solution are shown by the broken lines. See text for details.

TABLE 2

Values of the effective fixed charge densities of cobalt and nickel phosphate membranes in contact with various 1 : 1 electrolytes derived from different theories

Electrolyte	Cobalt phosphate			Nickel phosphate		
	KCl	NaCl	LiCl	KCl	NaCl	LiCl
$(\bar{X}) \times 10^3$, eq/l (TMS Method)	1.64	1.90	2.90	1.80	1.40	2.50
$\left(\frac{\bar{u}}{\bar{v}}\right)$	0.2	0.2	0.2	0.2	0.2	0.2
$(\bar{X}) \times 10^3$, eq/l (eqn. (4))	5.30	2.50	3.70	1.90	4.70	4.20
$(\phi X) \times 10^3$, eq/l (eqn. (11))	4.50	3.20	3.20	3.20	3.20	3.20
$(\phi X) \times 10^3$, eq/l (eqn. (14))	1.10	1.70	2.00	1.10	2.00	2.20

structural details of the polymer network of which the membrane is composed. To evaluate the membrane parameters α, β, and X, two limiting forms of eqn. (2) were derived. When the external salt concentration C is sufficiently small,

$$|E_m^o| = \frac{1}{\beta}\ln\gamma - \left(\frac{\gamma-1}{\alpha\beta\gamma}\right)\left(1+\frac{1}{\beta}-2\alpha\right)\left(\frac{C_2}{X}\right)+\ldots \quad (3)$$

where $|E_m^o| = FE_m/RT$ and $\gamma = C_2/C_1$.

When the salt concentration C is high,

$$1/t_- = \frac{1}{1-\alpha}+\frac{(1+\beta-2\alpha\beta)(\gamma-1)}{2(1-\alpha)^2\ln\gamma}\left(\frac{X}{C_2}\right)+\ldots \quad (4)$$

where t_- is the apparent transference number of the coion (anion) in a negatively charged membrane, defined by

$$|E_m^o| = (1-2t_-)\ln C_2/C_1 \quad (5)$$

The values of t_- calculated from observed membrane potentials using eqn. (5) are given in Table 3. Eqn. (3) was used to obtain the value of β and a relation between α and X by evaluating the intercept and the initial slope of a plot of $|E_m^o|$ against C_2 (Fig. 2), while eqn. (4) was used to evaluate α from the intercept of a plot of $1/t_-$ against $1/C_2$ (Fig. 3). The values of X were determined by inserting this value of α in the relation between α and X obtained earlier. The values of X derived in this way for both membranes and 1 : 1 electrolytes are given in Table 2.

Recently Kobatake et al. [19] derived another equation (eqn. (6)) for the membrane potential starting with the basic flow equation provided by the thermodynamics of irreversible processes and using a different set of assumptions, namely: (a) the contribution of mass movement is negligible [19], and (b) small ions do not behave ideally in a charged membrane [19]. Their result is:

$$E_m = -\frac{RT}{F}\left[\ln\frac{C_2}{C_1}+(2\alpha-1)\ln\frac{\sqrt{4C_2^2+\phi^2X^2}+(2\alpha-1)\phi X}{\sqrt{4C_1^2+\phi^2X^2}+(2\alpha-1)\phi X}-\ln\frac{\sqrt{4C_2^2+\phi^2X^2}+\phi X}{\sqrt{4C_1^2+\phi^2X^2}+\phi X}\right] \quad (6)$$

where ϕ is a characteristic factor of the membrane-electrolyte pair and represents the fraction of counterions not tightly bound to the membrane skeleton. The product ϕX is termed the thermodynamically effective fixed charge density of a membrane; the other terms have their usual significance. Eqn. (6) reduces to the TMS membrane potential for $\phi = 1$. Since it is somewhat troublesome to evaluate ϕX at an aribitrary external electrolyte concentration from the observed membrane potential using eqn. (6), Kobatake et al.

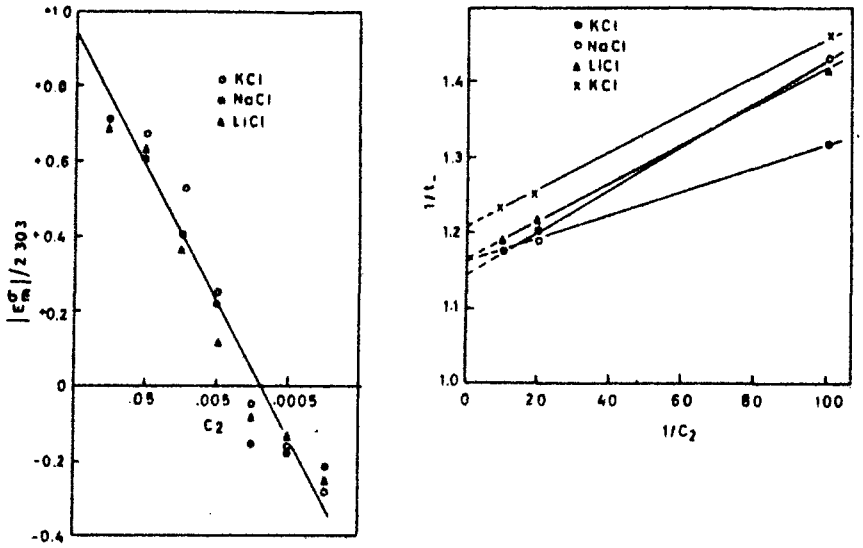

Fig. 2. Plots of $|E_m|/2.303$ vs. C_2 for a nickel phosphate membrane in contact with various 1 : 1 electrolyte solutions.

Fig. 3. Plots of $1/t_-$ against $1/C_2$ for various 1 : 1 electrolyte solutions at constant γ (γ = 10) with a nickel phosphate membrane. A set of data for KCl and a cobalt phosphate membrane (X) is also shown.

TABLE 3

Transference number t_- of coions derived from observed membrane potentials at various electrolyte concentrations

Electrolyte concentration (N)	Cobalt phosphate			Nickel phosphate		
	KCl	NaCl	LiCl	KCl	NaCl	LiCl
0.1/0.01	0.78	0.82	0.81	0.85	0.85	0.84
0.05/0.005	0.75	0.80	0.77	0.83	0.84	0.82
0.01/0.001	0.74	0.68	0.63	0.76	0.70	0.76
0.0005/0.0005	0.60	0.62	0.58	0.62	0.60	0.56
0.001/0.0001	0.49	0.54	0.45	0.46	0.42	0.46
0.0005/0.00005	0.42	0.41	0.37	0.41	0.41	0.43
0.0001/0.00001	0.41	0.37	-.33	0.39	0.34	0.37

[19] have proposed a simple method using the following approximate equation for the diffusive contribution to the emf of a cell with transport:

$$E_m = -\frac{RT}{F}(1 - 2\tau_{app}) \ln (C_2/C_1) \tag{7}$$

where τ_{app} is the apparent transference number of coions in the membrane phase. Comparison of eqns. (6) and (7) gives

$$\tau_{app} = \frac{1 - 2\alpha}{2} \frac{\ln\left(\frac{\sqrt{4\epsilon_2^2 + 1} + 2\alpha - 1}{\sqrt{4\epsilon_1^2 + 1} + 2\alpha - 1}\right)}{\ln \gamma} + \frac{\ln\left(\frac{\sqrt{4\epsilon_2^2 + 1} + 1}{\sqrt{4\epsilon_1^2 + 1} + 1}\right)}{2 \ln \gamma} \tag{8}$$

where $\epsilon = C/\phi X$.

On the other hand [18,19], the mass-fixed transference number of coions τ_- in a negatively charged membrane immersed in an electrolyte solution of concentration C was defined by

$$\tau_- = \nu \bar{c}_- / (u\bar{c}_+ + \nu \bar{c}_-) \tag{9}$$

where c_+ and c_- are the concentrations of cation and anion, respectively, in the membrane phase. This equation was transformed to

$$\tau_- = 1 - \alpha \frac{\sqrt{4\epsilon^2 + 1} + 1}{\sqrt{4\epsilon^2 + 1} + (2\alpha - 1)}, \tag{10}$$

using certain equations for the activity coefficients, mobilities of small ions in the membrane phase, and the equilibrium condition for electrical neutrality [18,19]. The difference between the apparent transference number τ_{app} calculated from eqn. (8) and τ_- from eqn. (10) for various reduced concentrations ϵ ($\epsilon = C/\phi X$) was found to be always less than 2% over a wide range of external electrolyte concentrations. Therefore τ_{app} and τ_- were considered practically the same. As a result, the apparent transference number evaluated from the membrane potential data was used for the determination of the thermodynamically effective fixed charge density ϕX of the membrane at a given average salt concentration C ($C = (C_1 + C_2)/2$) using eqn. (10). At the same time rearrangement of eqn. (10) provides a definition of permselectivity P_s, given by the expression

$$\frac{1}{(4\epsilon^2 + 1)^{1/2}} = \frac{1 - \tau_- - \alpha}{\alpha - (2\alpha - 1)(1 - \tau_-)} \equiv P_s \tag{11}$$

This equation can be used to find the permselectivity from membrane potential measurements using eqn. (7). If the transport number of coions (τ_- or τ_{app}) is zero, the membrane is perfectly selective and $P_s = 1$, while if the transport number of coions has the free solution value, $P_s = 0$. The values of P_s obtained using the right hand side of eqn. (11) were plotted against log C. The concentration at which P_s (where $\epsilon = C/\phi X = 1$) becomes $1/5^{1/2}$ gives the

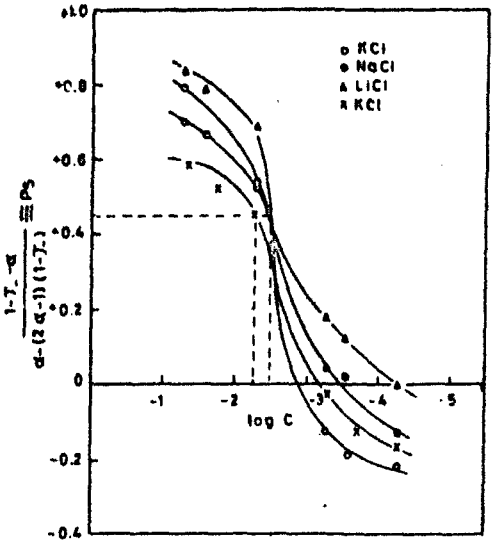

Fig. 4. Plots of P_s vs. log C for a nickel phosphate membrane using various 1 : 1 electrolyte solutions and for a cobalt phosphate membrane (X) using KCl solution. The dotted horizontal line shows $P_s = 1/\sqrt{5}$ and the vertical lines give the value of ϕX for the membrane electrolyte system.

value of the thermodynamically effective fixed charge density ϕX as required by the left hand side of eqn. (11). Fig. 4 presents plots of P_s versus log C for the parchment-supported cobalt and nickel phosphate membranes in contact with various 1 : 1 electrolytes. The values of ϕX thus derived for the membranes and 1 : 1 electrolyte combinations are given in Table 2.

More recently, Nagasawa et al. [20] derived an equation for the membrane potential existing across a charged membrane. The total membrane potential E_m was considered as the sum of a diffusion potential E_d inside the membrane and the electrostatic potential differences E_e between the membrane surfaces and the electrolyte solutions on both sides of the membrane. The diffusion potential E_d was obtained by integrating the basic flow equation for diffusion [20], while the electrostatic potential difference was calculated from the Donnan theory. Stated mathematically,

$$E_m = E_d + E_e \tag{12a}$$

where

$$-E_d = -\int_1^2 \frac{J_0}{F\bar{C}_0}\frac{\phi X}{(\bar{C}_- + \phi X)u + \bar{C}_- v}\,dx + \frac{RT}{F}\int_1^2 \frac{(\bar{C}_- + \phi X)u}{(\bar{C}_- + \phi X)u + \bar{C}_- v}\,d\ln \bar{a}_+ -$$

$$\frac{RT}{F}\int_1^2 \frac{\bar{C}_- v}{(\bar{C}_- + \phi X)u + \bar{C}_- v}\,d\ln \bar{a}_- \tag{12b}$$

and

$$-E_0 = -\frac{RT}{F}\ln\left(\frac{\bar{a}_{1-}\,a_{2-}}{a_{1-}\,\bar{a}_{2-}}\right) \tag{12c}$$

where a_1 and a_2 are the activities of the electrolytes on the two sides of the membrane, and the overbar refers to phenomena in the membrane phase. J_0 is the flow of electrolyte in the absence of an external electric field; the other symbols have their usual significance. On integrating eqn. (12) in the limit of high electrolyte concentrations across the membrane, one obtains the following equation for the membrane potential:

$$-E_m = \frac{RT}{F}\left(\frac{\phi X}{2}\right)\left(\frac{\gamma-1}{\gamma}\right)\frac{1}{C_1} + \frac{RT}{F}\left(\frac{u-v}{u+v}\right)\left[\frac{1-\dfrac{\phi X J_0}{RT\bar{C}_0(u-v)K}}{1-\dfrac{\phi X J_0}{2RT\bar{C}_0 vK}}\right]\ln\gamma +$$

$$+\frac{RT\phi X}{2Fuv}\left(\frac{J_0}{RT\bar{C}_0 K}\right)^2\frac{\left[1-\dfrac{\phi X J_0(u+v)}{4RT\bar{C}_0 uvK}\right]}{\left(1-\dfrac{\phi X J_0}{2RT\bar{C}_0 vK}\right)^2}(\gamma-1)C_1 \tag{13}$$

At high electrolyte concentrations, eqn. (13) can be approximated by

$$-E_m = \frac{RT}{F}\left(\frac{\gamma-1}{\gamma}\right)\left(\frac{\phi X}{2}\right)1/C_1 + \ldots \tag{14}$$

Eqn. (14) predicts a linear relationship between E_m and $1/C_1$ from which ϕX can be calculated. Plots of E_m vs. $1/C_1$ are presented in Fig. 5; they are

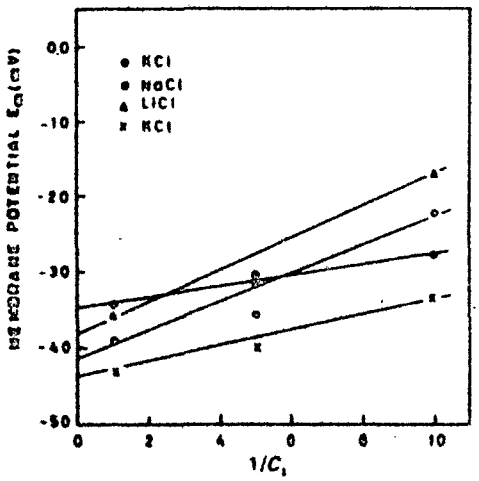

Fig. 5. Plots of membrane potential E_m(mV) vs. $1/C_1 \times 10^{-2}$ for cobalt phosphate and nickel phosphate (X) membranes.

straight lines, in agreement with eqn. (14). The values of ϕX derived from the slope of the lines are given in Table 2. It may be noted in Table 2 that the charge densities evaluated from the different theories are of the same magnitude.

Acknowledgement

Thanks are due to Professor Wasiur Rahman, Head, Department of Chemistry, for providing the necessary facilities.

References

1 Fasih A. Siddiqi, N. Lakshminarayanaiah and M. Nasim Beg, J. Polymer Sci., 9 (1971) 2853.
2 Fasih A. Siddiqi, N. Lakshminarayanaiah and M. Nasim Beg, J. Polymer Sci., 9 (1971) 2869.
3 Fasih A. Siddiqi, M. Nasim Beg, Surendra P. Singh and Abdul Haque, Bull. Chem. Soc. Jpn., 49 (1976) 2864.
4 Fasih A. Siddiqi, M. Nasim Beg, Surendra P. Singh, and Abdul Haque, Bull. Chem. Soc. Jpn., 49 (1976) 2868.
5 Fasih A. Siddiqi, M. Nasim Beg and Surendra P. Singh, J. Polymer Sci., 15 (1977) 959.
6 Fasih A. Siddiqi, M. Nasim Beg and Poorna Prakash, J. Electroanal. Chem., 80 (1977) 223.
7 Fasih A. Siddiqi, M. Nasim Beg, Surendra P. Singh and Abdul Haque, Electrochimica Acta., 22 (1977) 361.
8 Fasih A. Siddiqi, M. Nasim Beg, Surendra P. Singh and Abdul Haque, Electrochimica Acta., 22 (1977) 368.
9 M. Nasim Beg, Fasih A. Siddiqi and Radhey Shyam, Can. J. Chem., 55 (1977) 10.
10 G. Eisenman, in A. Kleinzer and A. Kotyle (Eds.), Membrane Transport and Metabolism, Academic Press, New York, 1961, p. 163; Biophys. J. Suppl., 2 (1962) 259.
11 H. Sherry, in J.A. Marinsky (Ed.), Ion Exchange, Vol. 2, Dekker, New York, 1968.
12 S. Glasstone, K.S. Laidler and H. Eyring, The theory of Rate Processes, McGraw Hill, New York, 1941, (a) p. 525, (b) p. 544.
13 T. Teorell, Disc. Faraday Soc., 21 (1956) 9.
14 T. Teorell, Proc. Soc. Expt. Biol., 33 (1935) 282; Proc. Natl. Acad. Sci. (USA), 21 (1935) 152; Z. Electrochem., 55 (1951) 460; Prog. Biophys. Chem., 3 (1953) 385.
15 K.H. Meyer and J.F. Sievers, Helv. Chim. Acta., 19 (1936) 649, 665, 987.
16 I. Altug and M.L. Hair, J. Phys. Chem., 72 (1968) 599.
17 Y. Kobatake, T. Noriaki, Y. Toyoshima and H. Fujita, J. Phys. Chem., 69 (1965) 3981.
18 N. Kamo, M. Oikawa, and Y. Kobatake, J. Phys. Chem., 77 (1973) 92, 2995.
19 Y. Kobatake and N. Kamo, Prog. Poly. Sci. Jpn., 5 (1972) 257.
20 M. Tasaka, N. Aoki, Y. Konda and M. Nagasawa, J. Phys. Chem., 79 (1975) 1307.
21 N. Lakshminarayanaiah, Transport Phenomena in Membranes, Academic Press, New York, 1969, p. 32.
22 G. Alberti, Atti Accad. Nazl. Lincei Rend. Classe Sci. Fis. Mat. Nat., 31 (1961) 427.
23 G. Alberti, A. Conte and E. Torroca, Atti Accad. Nazl. Lincei Rend. Classe Sci. Fis. Mat. Nat., 35 (1963) 548.

CHAPTER 8

THEORIES OF BI-IONIC POTENTIALS AND ITS APPLICATIONS

J. Electroanal. Chem., 98 (1979) 231—240

STUDIES WITH INORGANIC PRECIPITATE MEMBRANES

PART XXVI. EVALUATION OF MEMBRANE SELECTIVITY FROM ELECTRIC POTENTIAL AND CONDUCTIVITY MEASUREMENTS

M. NASIM BEG, FASIH A. SIDDIQI, R. SHYAM and I. ALTAF

Physical Chemistry Division, Department of Chemistry, Aligarh Muslim University, Aligarh 202001 (India)

(Received 9th July 1976; in final form 10th July 1978)

ABSTRACT

Biionic and multiionic potentials arising across parchment supported nickel and cobalt phosphate membranes using various combinations of 1 : 1 electrolytes at different concentrations have been measured. The intramembrane permeability ratio of cations has been derived using the plotting method. Conductivity of membranes in contact with simple 1 : 1 electrolytes has been experimentally determined in order to evaluate selectivity of membranes using the predetermined values of the intramembrane permeability ratio. The selectivity sequence of both the membranes has been found as $K^+ > Na^+ > Li^+$, which on the basis of the Eisenman-Sherry model of membrane selectivity, points towards the weak field strength of the charge groups on the membrane matrix. Perfect Donnan exclusion of coions was realized in the dilute limit of the external solution. Potentiometric selectivity constants K_{ij}^{pot} have also been evaluated by the improved method of Buck et al. based on the integrated form of the Nernst-Planck flux equation.

INTRODUCTION

When two electrolytic solutions having different concentrations are separated by a membrane, the mobile species penetrate the membrane and various transport phenomena are induced in the system [1]. The total electric potential difference observed under zero current flow between two aqueous solutions separated by a membrane has been one of the most widely characterized electrochemical and bioelectric phenomena [2—10]. The fixed charge concept of Teorell [11] and Meyer and Sievers [12] for the charged membranes is a pertinent starting point for the investigation of the actual mechanisms of ionic or molecular processes which occur in the membrane phase. For biological membranes the electrical potential difference is usually described in terms of the Goldman-Hodgkin-Katz [13,14] equation whereas for certain ion exchange membranes permeable solely to species of one sign, it is described by a generalized Nernst equation. Both the Goldman-Hodgkin-Katz and the Nernst equations contain ionic permeability ratio terms. Depending on the transport mechanism, or the assumptions made in the derivation, the permeability ratio has been given various physical meanings as: mobility ratio [15], ion exchange equilibrium constant [16], the product of the mobility ratio and the Donnan ratio [11,12], the product of the mobility ratio and the distribution coefficient ratio [14], the product of the

mobility ratio and ion exchange equilibrium constant [17,18] or the product of the equivalent conductance ratio and the ratio of partition coefficients [2]. Sandblom et al. [2,3,19] have discussed the significance and implications of the observed permeability ratio. Recently a number of reviews have appeared dealing with the ion selectivity of membranes [20–22].

In Part XXI of this series [6] we described (a) the behavior of cobalt and nickel phosphate membranes in contact with various 1 : 1 electrolytes and (b) the evaluation of thermodynamically effective fixed charge density from membrane potential measurements. In this paper a series of biionic potential, multiionic potential and conductivity measurements have been carried out for the evaluation of the intramembrane permeability ratio and the selectivity coefficient of the membranes for ions of the electrolytes.

EXPERIMENTAL

The membranes were prepared by the method of interaction described in Part XXI of this series [6]. The biionic and multiionic potentials were measured by constructing an electrochemical cell of the following type, and using a Pye precision vernier potentiometer.

SCE	Electrolyte solution iX (')	Membrane	Electrolyte solution jX ('')	SCE

For the measurement of electrical conductivity, membranes were first dipped and equilibrated in an appropriate electrolyte solution. They were then clamped between two half cells and measurements were made as shown in Fig. 1 using a conductivity bridge (Cambridge Instrument Co. Ltd., England). All measurements were carried out at 25 ± 0.1°C. The error in measurement of membrane potential was within ± 1% whereas electrical conductivity could be measured to better than 0.05%.

RESULTS AND DISCUSSION

When an ion exchange membrane is interposed between two solutions of the same electrolyte, but of different concentrations, the potential difference developed is called the concentration potential or the membrane potential. The sign and magnitude of this e.m.f. gives the selectivity of the membrane towards the

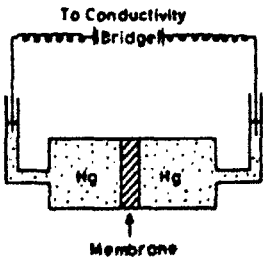

Fig. 1. Cell for measuring the electrical conductivity of membranes.

ions of the electrolyte. But if the membrane is used to separate solution of two electrolytes of the type iX and jX (or iX and iY), the steady potential developed is called biionic potential (BIP) [23] which is a measure of the selectivity of the membrane for ions of the same sign. The BIP has been considered by Helfferich [17] in accordance with the concepts of the TMS theory [11,12], as being the algebraic sum of two interfacial potentials and an internal diffusion potential. A complete mathematical discussion under conditions: (a) membrane diffusion control, (b) film diffusion control, and (c) coupled membrane film diffusion control has been presented [17]. For a general case involving complete membrane diffusion control, the total BIP for counterions is given by

$$E = (RT/zF) \ln \bar{D}_i a_i' \bar{v}_j K_i / \bar{D}_j a_j'' \bar{v}_i K_j = (RT/zF) \ln [K_{ji} (\bar{D}_i a_i' \bar{v}_j / \bar{D}_j a_j'' \bar{v}_i)] \quad (1)$$

where a_i'/a_j'', $\bar{D}_i/\bar{D}_j$, $\bar{v}_i/\bar{v}_j$ are the ratio of the activities, diffusion coefficients, and the activity coefficients of the counterions i and j, respectively. Overbars refer the phenomena in the membrane phase; R, T, z and F have their usual meanings. Using the Einstein relation $D_i = U_i RT$ and the generalized Nernst equation in which the permeability ratios are independent of the external electrolyte solution [16,24], equation (1) reduces to the form

$$E = \frac{RT}{zF} \ln \left[\frac{a_i' \bar{U}_i}{a_j'' \bar{U}_j} K_{ji} \right] = \frac{RT}{zF} \ln \left[\frac{a_i' \bar{P}_i}{a_j'' \bar{P}_j} \right] \quad (2)$$

Equation (2) gives

$$\bar{P}_i / \bar{P}_j = K_{ji} \, \bar{U}_i / \bar{U}_j \quad (3)$$

This equation has also been derived most recently by Sandblom and Eisenman [19] from thermodynamic treatment for fixed site membranes which implies that the permeability ratio is, quite generally, related to the ion exchange equilibrium constant K_{ij} and the ratio of mobilities of the critical ions. Further, using the well known relation $\bar{U}_i/\bar{U}_j = \bar{\lambda}_i/\bar{\lambda}_j$ eqn. (3) gives

$$\bar{P}_i / \bar{P}_j = K_{ji} \, \bar{U}_i / \bar{U}_j = K_{ji} \, \bar{\lambda}_i / \bar{\lambda}_j \quad (4)$$

where $\bar{\lambda}_i$ is the conductivity of the membrane when it is wholly in i form and $\bar{\lambda}_j$ is the conductivity of the membrane when it is wholly in the j form.

The quantity $\bar{P}_i/\bar{P}_j$ is considered truly a membrane property [19]. It is independent of the changes made in the activities a_i and a_j of the external solution. Thus it is apparent from eqn. (2) that a plot of log a_i against potential for a constant a_j should give a straight line. Similarly a straight line should be obtained if a_j is varied and a_i is kept constant. Both these lines should show potential changes of RT/F or 59.2 mV at 25°C for each tenfold change in activity when membranes are separating 1 : 1 electrolytes. Accordingly BIP values across cobalt and nickel phosphate parchment supported membranes were determined for various electrolyte pairs, viz. NaCl-LiCl, KCl-NaCl and KCl-LiCl, taking the concentration of one of the electrolyte constant (0.05 M) and varying the concentration of the other electrolyte between 0.001 M to 0.05 M. In the second set of experiment the concentration of the other electrolyte was kept constant (0.05 M) and the concentration of the first electrolyte was varied. The biionic potentials thus observed were plotted against logarithm of the mean molal activ-

ity. Two sets of straight lines in accordance with the expectation of eqn. (2) are obtained (Fig. 2). The straight lines confirm the views of Nicolsky [16] and Eisenman [24] that the permeability ratios are independent of external solution conditions. In order to derive the values of the permeability ratio, these straight lines were extended to cut the activity axis at zero potential. Thus two sets of a_i and a_j values for which potential E was zero were obtained. At zero potential the ratio a_i/a_j was equal to $\overline{P}_j/\overline{P}_i$. The values of $\overline{P}_i/\overline{P}_j$ derived in this way for the membranes and different electrolyte pairs are as follows: $\overline{P}_{K^+}/\overline{P}_{Na^+} = 1.99$, $\overline{P}_{K^+}/\overline{P}_{Li^+} = 1.71$, $\overline{P}_{Na^+}/\overline{P}_{Li^+} = 1.18$ for cobalt phosphate membrane; and $\overline{P}_{K^+}/\overline{P}_{Na^+} = 1.72$, $\overline{P}_{K^+}/\overline{P}_{Li^+} = 1.50$, $\overline{P}_{Na^+}/\overline{P}_{Li^+} = 1.36$ for nickel phosphate membrane. The values of $\overline{P}_i/\overline{P}_j$ are generally low which point towards the fact that the membranes are relatively more imbibed in an equilibrium water content [27]. The values of the intramembrane permeability ratio also refer to the selectivity sequence of the membranes for the cations as follows:

$$K^+ > Na^+ > Li^+$$

This order of selectivity on the basis of the Eisenman-Sherry model of membrane selectivity [24–26] points towards the weak field strength of the charge groups attached to the membrane matrix. This is in accordance with our earlier findings of charge density (charge density $\approx 10^{-3}$ mol l^{-1}) determinations of cobalt and nickel phosphate membranes [6].

Biionic potential measurements were also carried out by interposing the membrane between two different electrolyte solutions at the same concentration. The BIP values were low when the membrane was used to separate concentrated electrolyte solutions whereas it increased with decreasing salt concentrations (Table 1). The permeability ratio $\overline{P}_i/\overline{P}_j$ calculated from these BIP values using

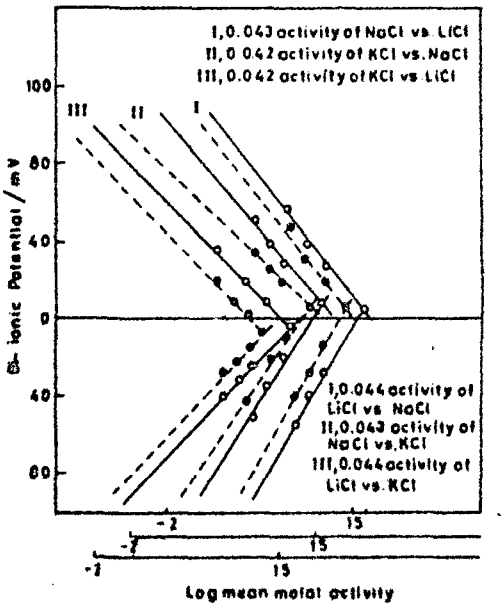

Fig. 2. Plots of biionic potentials (KCl side taken as positive) vs. logarithm of mean molal activity for cobalt (- - - - - -) and nickel (———) phosphate membranes.

TABLE 1

Values of experimentally observed biionic potentials BIP (mV) across parchment supported cobalt and nickel phosphate membranes

Membrane	Cobalt phosphate			Nickel phosphate		
pair	KCl[a]-NaCl	KCl[a]-LiCl	NaCl[b]-LiCl	KCl[a]-NaCl	KCl[a]-NaCl	NaCl[b]-LiCl
Concentration/ mol l^{-1}						
0.1/0.1	2.41	−4.52	−4.21	2.26	−3.94	−3.26
0.05/0.05	2.55	−2.46	−2.46	4.54	−2.74	−2.03
0.02/0.02	6.69	−0.90	0.63	6.28	−0.30	2.13
0.01/0.01	6.80	2.62	0.99	8.57	2.60	2.24
0.005/0.005	13.30	5.11	3.45	11.65	3.45	4.15
0.002/0.002	18.85	12.36	8.29	19.06	9.55	10.14
0.001/0.001	19.80	18.50	9.76	19.84	16.00	13.46

[a] KCl side taken as positive.
[b] NaCl side taken as positive.

eqn. (2) were seen to be concentration dependent. This behavior was seen with both the membranes and different electrolyte pairs. The variation in BIP caused by the changes produced in the permeability ratio may be ascribed due to structural changes produced at the membrane—solution interfaces. Parchment supported inorganic precipitate membranes contain exchangeable groups as part of its structure which may account for its negative charge. The exchangeable cations will be free to move in the pores. Within the pores there will be a diffuse ionic atmosphere from the charged wall. Since the membrane under investigation carries low site densities (charge density 1×10^{-3} mol l^{-1}), anion encroachment

TABLE 2

Values of the intramembrane permeability ratios of various 1 : 1 electrolyte ion pairs for cobalt and nickel phosphate membranes

Membrane	Cobalt phosphate			Nickel phosphate		
Electrolyte ion pair	$\bar{P}_{K^+}/\bar{P}_{Na^+}$ KCl/NaCl	$\bar{P}_{K^+}/\bar{P}_{Li^+}$ KCl/LiCl	$\bar{P}_{Na^+}/\bar{P}_{Li^+}$ NaCl/LiCl	$\bar{P}_{K^+}/\bar{P}_{Na^+}$ KCl/NaCl	$\bar{P}_{K^+}/\bar{P}_{Li^+}$ KCl/LiCl	$\bar{P}_{Na^+}/\bar{P}_{Li^+}$ NaCl/LiCl
Concentration/mol l^{-1}						
0.1/0.1	1.10	0.83	0.84	1.09	0.85	0.88
0.05/0.05	1.24	0.90	0.90	1.19	0.90	0.92
0.02/0.02	1.29	1.00	1.02	1.27	1.00	1.08
0.01/0.01	1.30	1.10	1.04	1.44	1.09	1.09
0.005/0.005	1.68	1.22	1.14	1.57	1.14	1.19
0.002/0.002	2.08	1.61	1.38	2.09	1.45	1.46
0.001/0.001	2.16	1.95	1.46	2.17	1.86	1.68

into the membrane seems to be the most probable phenomenon. The thickness of the atmosphere depends upon the electrolyte concentration. In very dilute solutions of electrolyte, the thickness becomes so great that only cations are present in the pores and the membrane becomes impermeable to anions, a condition necessary for the derivation of eqn. (2) with constant permeability ratio. Thus the best data on $\overline{P}_i/\overline{P}_j$ are that from the most dilute solutions. It may therefore be concluded that the existence of an expression for E with constant permeability ratios can not be characteristic of all the membranes but is restricted to certain physical situations, most notably those in which a membrane is permeable only to species of one sign. This is in agreement with the mathematical treatment advanced by Sandblom and Eisenman [19].

In order to have a knowledge of selectivity K_{ij} from the predetermined values of $\overline{P}_i/\overline{P}_j$, the ratio of electrical conductivities $\overline{\lambda}_i/\overline{\lambda}_j$ as demanded by eqn. (4) must be known. Membrane conductance measurements were carried out when it was wholly in the form i or wholly in the form j. The values of membrane conductance at various electrolyte concentration are given in Table 3. The values are relatively more dependent upon the concentration of the electrolyte within the membrane as shown in Fig. 3. This implies that the membranes have a relatively high Donnan uptake of anion and a low selectivity constant value. This is in agreement with the findings of Heymann and Rabinov [28], Spiegler et al. [29] and our own findings with ion exchange membranes [4—8]. The values of selectivity K_{ij} evaluated from the ratio of electrical conductivities $\overline{\lambda}_i/\overline{\lambda}_j$ and the intramembrane permeability ratio $\overline{P}_i/\overline{P}_j$ using eqn. (4) are given in Table 4.

In order to substantiate our findings, potentiometric selectivity constants K_{ij}^{pot} have also been evaluated using the most recently developed method of Dole [30], and modified and improved by Buck et al. [31—37], although a number of methods [34] have been suggested for the determination of it by taking mixtures of electrolytes across the membrane and measuring the electric potentials developed. The general equation (eqn. 5) for membrane potential E in an electrochemical cell of the type

Electrolyte solution (′) (i + j)	Membrane	Electrolyte solution (″) i or j or (i + j)

has often been used to derive the value of K_{ij}^{pot} of membrane electrolyte systems

$$E = \frac{nRT}{F} \ln[(a_i')^{1/n} + (K_{ij}^{pot} a_j')^{1/n}] / [(a_i'')^{1/n} + (K_{ij}^{pot} a_j'')^{1/n}] \qquad (5)$$

where

$$K_{ij}^{pot} = K_{ij}(\overline{U}_j/\overline{U}_i)^{1/n}$$

If $n = 1$ and the concentrations on side (″) are held constant eqn. (5) gives

$$E = \text{const} + (RT/F) \ln[a_i' + (K_{ij}^{pot} a_j')] \qquad (6)$$

Equation (6) is considered a normal form for ideal behavior of ion selective electrode responsive to species i and j. If the response for cation is more positive for solutions of species i than for j at equal activities then K_{ij}^{pot} is a number less than unity and the electrode is more sensitive to i than to j [32]. Equation (6) has been used in various ways for the evaluation of potentiometric selectivity con-

TABLE 3

Observed values of membrane conductances (S m^{-1}) for monovalent electrolytes at 25 ± 0.1°C

Membrane	Cobalt phosphate			Nickel phosphate		
Electrolyte	KCl	NaCl	LiCl	KCl	NaCl	LiCl
Concentration/mol l^{-1}						
0.1/0.1	0.64	0.62	0.41	0.91	0.52	0.35
0.05/0.05	1.04	1.02	0.70	1.6	1.0	0.82
0.02/0.02	2.3	2.2	1.4	3.1	2.0	1.8
0.01/0.01	3.6	3.5	2.4	3.4	2.6	2.2
0.005/0.005	4.6	4.6	3.2	4.0	3.2	2.8
0.002/0.002	7.0	6.0	4.5	6.0	5.0	3.0
0.001/0.001	8.0	7.8	5.0	8.0	7.0	6.8

stants K_{ij}^{pot}. Various aspects of eqn. (6) for the evaluation of K_{ij}^{pot} have been reviewed by Lakshminarayanaiah [34]. Mixture methods based on eqn. (6) were first developed and used extensively by Lengyel and Blum [35] and later by Eisenman [36]. Srinivasan and Rechnitz [37] examined several methods for the determination of K_{ij}^{pot} while Pungor and Toth [38,39] strongly recommended another form of the mixture method. A convenient form of the mixture methods is the titration procedure of Dole [30] which has recently been modified and improved by Buck et al. [31–33]. This method provides extensive sets of data for the determination of K_{ij}^{pot} (apparent). In this method a set of mixture response potentials ΔE_{ij} and pure response potentials ΔE_i are measured and the

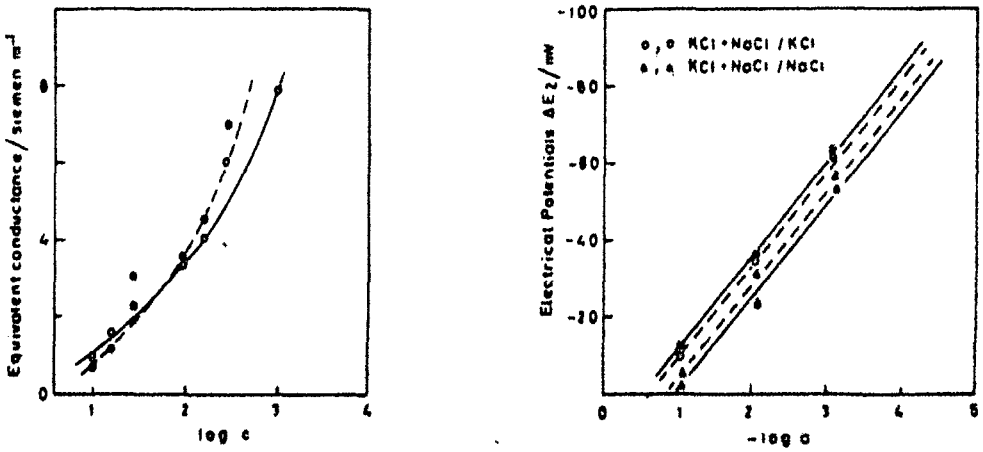

Fig. 3. Typical plots of equivalent conductance vs. log c for cobalt (· · · · · ·) and nickel (———) phosphate membranes using potassium chloride.

Fig. 4. Plots of electrical potentials ΔE_i vs. −log a for cobalt (· · · · · ·) and nickel (———) phosphate membranes.

TABLE 4

Values of the selectivity K_{ij} derived from intramembrane permeability ratio and the ratio of electrical conductivities at various electrolyte concentrations

Membrane	Cobalt phosphate			Nickel phosphate		
Selectivity	K_{NaK}	K_{LiK}	K_{LiNa}	K_{NaK}	K_{LiK}	K_{LiNa}
Concentration/ mol l^{-1}						
0.1/0.1	1.06	0.53	0.56	0.62	0.33	0.6
0.05/0.05	1.20	0.63	0.67	0.74	0.46	0.76
0.02/0.02	1.23	0.62	0.68	0.90	0.62	0.94
0.01/0.01	1.25	0.73	0.72	1.10	0.72	0.93
0.005/0.005	1.60	0.87	1.03	1.25	0.76	0.99
0.002/0.002	1.84	1.04	1.01	1.68	1.03	1.28
0.001/0.001	2.07	1.33	1.04	1.80	1.43	1.52

selectivity coefficient calculated from the equation

$$\ln K_{ij}^{pot}\,(\text{apparent}) = \ln\{\exp[(\Delta E_{ij} - E_i)/S] - 1\} - \ln(a_j/a_i) \qquad (7)$$

where S is the slope of the pure a_i response curve (Fig. 4).

Electrical potentials ΔE_{ij} across the electrochemical cell of the type shown above were measured by taking fixed concentrations of both the primary ions (i.e. i and j) on the side (') and varying the concentration of the ion species i and j on the side ("), whereas in another experiment only one ion either i or j on the side (") at different concentration was taken and electrical potentials ΔE_i or ΔE_j were plotted against log a_i or log a_j. Parallel straight lines, as shown in Fig. 4 were obtained which refers to the ideal behavior of the membrane systems. The slope S of the line was used to derive the value of K_{ij}^{pot} (apparent) using eqn. (7). The values of K_{ij}^{pot} derived in this way for both cobalt and nickel phosphate membranes using various 1 : 1 electrolytes are given in Table 5.

Parchment supported cobalt and nickel phosphate membranes in contact with various 1 : 1 electrolytes are thus considered as homogeneous membrane ele-

TABLE 5

Values of the potentiometric selectivity constant (K_{ij}^{pot}) for the membranes at various electrolyte concentrations

Membrane	Cobalt phosphate			Nickel phosphate		
Selectivity constant	$K_{K\text{-}Na}$	$K_{K\text{-}Li}$	$K_{Na\text{-}Li}$	$K_{K\text{-}Na}$	$K_{K\text{-}Li}$	$K_{Na\text{-}Li}$
Concentration/ mol l^{-1}						
0.1	0.82	0.49	0.60	0.64	0.35	0.49
0.01	1.2	1.2	1.4	1.1	1.2	1.34
0.001	3.5	4.01	3.2	4.01	5.2	2.18

ments with charged rigid capillary structure or gels having a diameter large as compared to the thickness of the electrical double layer at the walls [11,12,16]. Flow of electrolyte by diffusion, because of the presence of a net charge on the membrane gives rise to membrane potential which regulates the flow of electrolyte by increasing the speed of the slow moving ion and also by decreasing the speed of the fast moving ion. The electrical double layer at the membrane solution interface seems to control the ion permeation as suggested by Tien and Ting [40] for bilayer membranes and our own findings with inorganic precipitate membranes. Perfect Donnan exclusion of coions was realized in the dilute limit of the external solution and that the selectivity sequence of the membranes for alkali metal cations was $K^+ > Na^+ > Li^+$.

ACKNOWLEDGEMENTS

The authors are grateful to Prof. Wasiur Rahman, Head, Department of Chemistry, for providing research facilities and to C.S.I.R. and U.G.C. (India) for the award of fellowships to R.S. and I.A.

REFERENCES

1 Y. Kobatake and N. Kamo, Progr. Polymer Sci. Jap., 5 (1973) 257.
2 J. Sandblom, G. Eisenman and J.L. Walker, Jr., J. Phys. Chem., 71 (1967) 3862, 3871.
3 J. Sandblom and F. Orme in G. Eisenman (Ed.), Membranes, Vol. 1, Marcel Dekker, New York, 1972, p. 125.
4 Fasih A. Siddqi, N. Lakshminarayanaiah and M. Nasim Beg, J. Polymer Sci., 9 (9171) 2853, 2869.
5 M. Nasim Beg, Fasih A. Siddiqi and R. Shyam, Can. J. Chem., 55 (1977) 1660.
6 M. Nasim Beg, Fazih A. Siddiqi, R. Shyam and I. Altaf, J. Electroanal. Chem., 89 (1978) 141.
7 Fasih A. Siddiqi, M. Nasim Beg and P. Prakash, J. Electroanal. Chem., 80 (1977) 223.
8 Fasih A. Siddiqi, M. Nasim Beg, Surendra P. Singh and Abdul Haq, Bull. Chem. Soc. Jap., 49 (1976)c 2858, 2864.
9 Fasih A. Siddiqi, M. Nasim Beg, Surendra P. Singh and Abdul Haq, Electrochim. Acta, 22 (1977) 361, 368.
10 Fasih A. Siddiqi, M. Nasim Beg and Surendra P. Singh, J. Polymer Sci., 15 (1977) 959.
11 T. Teorell, Proc. Soc. Expt. Biol. Med., 33 (1935) 282; Proc. Natl. Acad. Sci. (USA), 21 (1935) 152; Z. Elektrochem., 55 (1951) 460; Progr. Biophys. Chem., 3 (1953) 305.
12 K.H. Meyer and J.F. Sievers, Helv. Chim. Acta, 19 (1936) 649, 665, 987.
13 D. Goldman, J. Gen. Physiol., 27 (1943) 37.
14 A.L. Hodgkin and B. Katz, J. Physiol., 108 (1949) 37.
15 M. Planck, Ann. Phys. Chem., 40 (1890) 561.
16 B.P. Nicolsky, Acta Physicochim. USSR, 7 (1937) 592.
17 F. Helfferich, Ion Exchange, McGraw-Hill, New York, 1962.
18 G. Karreman and G. Eisenman, Bull. Math. Biophys., 24 (1962) 413.
19 J.P. Sandblom and G. Eisenman, Biophys. J., 7 (1967) 217.
20 R.P. Buck, J. Anal. Chem., 48 (1976) 23R.
21 J. Koryta, Anal. Chim. Acta, 91 (1977) 1.
22 R.P. Buch, Electroanalytical Chemistry of Membranes, March 1976, p. 323.
23 J.R. Wilson, Demineralization by Electrodialysis, Butterworths, London-Washington, 1960, p. 84.
24 G. Eisenman, Proc. XXIIIrd Intern. Congr. Physiol. Sci., 97 (1965) 489.
25 G. Eisenman in A. Kleinzer and A. Kotyk (Eds.), Membrane Transport and Metabolism, Academic Press, New York, 1961, p. 163; Biophys. J. Suppl., 2 (1962) 259.
26 H. Sherry in J.A. Marinsky (Ed.), Ion Exchange, vol. 2, Marcel Dekker, New York, 1968.
27 M.R.J. Wyllie and S.L. Kanaan, J. Phys. Chem., 58 (1959) 73.
28 E. Heymann and G. Rabinov, J. Phys. Chem., 47 (1943) 655.
29 K.S. Spiegler, R.L. Yoest and M.R.J. Wyllie, Discuss. Faraday Soc., 21 (1956) 174.
30 M. Dole, J. Amer. Chem. Soc., 53 (1931) 4260.
31 R.P. Buck, Anal. Chim. Acta, 75 (1974) 321.
32 R.P. Buck, Electroanalytical Chemistry of Membranes, 1976, p. 323 (Carolina).

33 R.P. Buck, J.H. Boles, R.D. Porter and J.A. Margolis, Anal. Chem., 46 (1974) 255.
34 N. Lakshminarayanaiah, Membrane Electrode, Academic Press, New York, 1976, p. 124.
35 B. Lengyel and E. Blum, Trans. Faraday Soc., 30 (1934) 461.
36 G. Eisenman in C.N. Reilley (Ed.), Advances in Analytical Chemistry and Instrumentation, Vol. 4, Interscience, New York, 1965.
37 K. Srinivasan and G.A. Rechnitz, Anal. Chem., 41 (1969) 1203.
38 E. Pungor and K. Toth, Anal. Chim. Acta, 47 (1969) 291.
39 E. Pungor and K. Toth, Analyst (London), 95 (1970) 625.
40 H.T. Tien and H.P. Ting, J. Colloid Interface Sci., 27 (1968) 702.

Studies with Model Membranes. XXII. Evaluation of Thermodynamic Parameters and Testing of Theories of Membrane and Bi-ionic Potential Based on Nonequilibrium Thermodynamics

FASIH A. SIDDIQI, M. NASIM BEG, and POORNA PRAKASH,
Membrane Research Laboratory, Department of Chemistry, Aligarh Muslim University, Aligarh, India

Synopsis

Thermodynamically effective fixed-charge density of mercuric phosphate and carbonate parchment-supported membranes have been evaluated by the most recent method of Nagasawa et al., based on the thermodynamics of irreversible processes and compared with the values obtained by the Kobatake et al. and Teorell–Meyer-Sievers (TMS) methods. Bi-ionic potential (BIP) has also been measured for these membranes with three pairs of electrolyte solutions: KCl-NaCl, KCl-LiCl, and NaCl-LiCl. Theoretical values of BIP have been calculated by using the membrane potential and BIP theories recently developed by Toyoshima et al., based on nonequilibrium thermodynamics. Various parameters have also been evaluated and it was found that the theoretical equation of BIP is applicable to these parchment-supported membranes.

INTRODUCTION

In a series of articles[1-23] we have applied the theories of Teorell–Meyer–Sievers,[24,25] Sollner,[26] Gregor,[27] Schmid,[28,29] Helfferich,[30] and Eisenman and Sherry[31-34] to explain various ionic processes that occur across parchment-supported[1-15,21-23] and that polymeric[16-20] membranes can serve as models for a biological system.[35,36] More recently theories based on the thermodynamics of irreversible processes, in particular the work of Spiegler,[37] Spiegler, Yoest, and Wyllie,[38] Scatchard,[39,40] Lorimer et al.,[41] and Scattergood and Lightfoot,[42] have been applied to the evaluation of different parameters such as the Maxwell diffusivity constant and hydraulic permeabilities of some of these membranes. The membrane potential theory of Kobatake et al.[43-48] has been applied to an evaluation of thermodynamically effective fixed-charge density and permselectivity of membranes. This article deals with the testing and application of the most recent theories of membrane and bi-ionic potential developed by Nagasawa et al.[49-51] and Toyoshima and Nozaki,[52] based on the thermodynamics of an irreversible process on parchment-supported membranes.

EXPERIMENTAL

Preparation of Membranes

The membranes of mercuric phosphate and mercuric carbonate were prepared by the interaction method suggested by Siddiqi et al.[1-15] First parchment paper

Journal of Polymer Science: Polymer Chemistry Edition, Vol. 17, 539–550 (1979)

0360-6376/79/0017-0539$01.00

was soaked in distilled water for 2 hr and then tied carefully to the flat mouth of a beaker that contained 0.2 mole liter^{-1} of mercuric chloride solution. This was suspended for about 72 hr in a 0.2 mole liter^{-1} solution of trisodium orthophosphate. The two solutions were then interchanged and kept for another 72 hr. The mercuric phosphate membrane thus prepared was washed with deionized water for the removal of free electrolyte. A similar procedure was adopted for the preparation of mercuric carbonate membrane by taking a 0.2 mole liter^{-1} solution of mercuric chloride and a 0.2 mole liter^{-1} solution of sodium carbonate.

Measurement of Membrane Potential and Bi-ionic Potential

The electrochemical cell of the type

$$\text{Ag–AgCl} \left| \begin{matrix}\text{solution} \\ C_1\end{matrix} \right| \text{membrane} \left| \begin{matrix}\text{solution} \\ C_2\end{matrix} \right| \text{AgCl–Ag}$$

was used to measure electrical potentials arising across the membrane by maintaining a tenfold difference in concentration ($C_2/C_1 = 10$) and using a Pye Precision Vernier potentiometer (No. 7568) at 25°C. The bi-ionic potentials were determined by setting up an electrochemical cell of the type

$$\text{Ag–AgCl} \left| \begin{matrix}\text{solution} \\ \text{AP}\end{matrix} \right| \text{membrane} \left| \begin{matrix}\text{solution} \\ \text{BP}\end{matrix} \right| \text{AgCl–Ag}$$

by keeping the concentration of both AP and BP electrolytes the same. The various salt solutions (chloride of Li^+, Na^+, and K^+) were prepared from analytical-grade reagents (BDH) with deionized water. The parchment paper was supplied by M/S Baird and Tatlock Ltd. (London).

RESULTS AND DISCUSSION

The membrane potential data obtained with mercuric phosphate and mercuric carbonate parchment-supported membranes with various 1 : 1 electrolytes were plotted as a function of log $(C_1 + C_2)/2$ with a ratio γ $(=C_2/C_1)$ fixed at 10. These plots are shown in Figure 1.

Nagasawa et al.[51] derived eqs. (1) for a membrane potential existing across a negatively charged membrane. Consider a cell in which a membrane separates two aqueous solutions of different concentrations (C_1 and C_2 in moles liter^{-1}) of an electrolyte. The solutions on both sides of the membrane are maintained at the same pressure and temperature. The fluxes of water and ions relating to the cell may be expressed by the linear equations

$$-J_0 = L_{00} \operatorname{grad} \bar{\mu}_0 + L_{0+} \operatorname{grad} \bar{\mu}_+ + L_{0-} \operatorname{grad} \bar{\mu}_- \quad (1a)$$

$$-J_+ = L_{+0} \operatorname{grad} \bar{\mu}_0 + L_{++} \operatorname{grad} \bar{\mu}_+ + L_{0+} \operatorname{grad} \bar{\mu}_- \quad (1b)$$

$$-J_- = L_{-0} \operatorname{grad} \bar{\mu}_0 + L_{-+} \operatorname{grad} \bar{\mu}_+ + L_{--} \operatorname{grad} \bar{\mu}_- \quad (1c)$$

Here, subscripts +, −, and 0 refer to cation, anion, and water molecule, respectively, Js, to the mass fluxes (mole cm^{-2} min^{-1}), Ls, to the phenomenological coefficients, and μs, to the chemical potentials. By substituting eq. (1a) into eq. (1b) and eq. (1c) we have

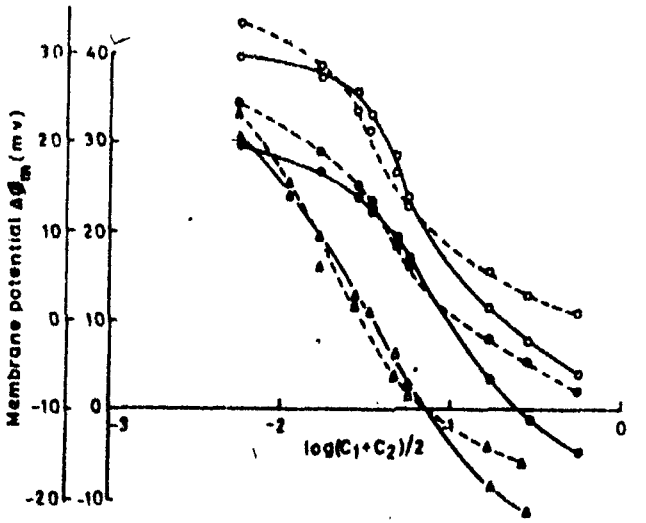

Fig. 1. Plots of membrane potentials ΔO_m vs. log $(C_1 + C_2)/2$ for (a) (-O-, KCl. ●, NaCl; -Δ-, LiCl) mercuric phosphate and (b) (- -O- -, KCl; - -●- -, NaCl; - -Δ- -, LiCl) mercuric carbonate membranes in contact with various 1 : 1 electrolyte solutions at 25°C.

$$-J_+ = -\left(\frac{L_{+0}}{L_{00}}\right)J_0 + \left(L_{++} - \frac{L_{+0}L_{0+}}{L_{00}}\right) \times \text{grad}\,\bar{\mu}_+ + \left(L_{+-} - \frac{L_{+0}L_{0-}}{L_{00}}\right)\text{grad}\,\bar{\mu}_- \quad (2a)$$

$$-J_- = -\left(\frac{L_{-0}}{L_{00}}\right)J_0 + \left(L_{-+} - \frac{L_{-+}L_{0+}}{L_{00}}\right) \times \text{grad}\,\bar{\mu}_+ + \left(L_{--} - \frac{L_{-0}L_{0-}}{L_{00}}\right)\text{grad}\,\bar{\mu}_- \quad (2b)$$

Equations (2a) and (2b) may be approximated as

$$-J_+ = -\left(\frac{\bar{C}_- + X}{\bar{C}_0}\right)J_0 + (\bar{C}_- + X)\bar{U}\,\text{grad}\,\bar{\mu}_+ \quad (3a)$$

$$-J_- = -\left(\frac{\bar{C}_-}{\bar{C}_0}\right)J_0 + \bar{C}_-\bar{V}\,\text{grad}\,\bar{\mu}_- \quad (3b)$$

where $\bar{C}_-$ is the effective concentration of counterions, X is the concentration of fixed charge, and $\bar{U}$ and $\bar{V}$ are the mobilities in the membrane phase.

From the condition of no current at the steady state, that is, $J_+ = J_- = J_0$ for 1:1 eleotrolytes, we have

$$-F\,\text{grad}\,\psi = -\left(\frac{J_0}{\bar{C}_0}\right)\frac{X}{(\bar{C}_- + X)\bar{U} + \bar{C}_-\bar{V}} + \frac{(\bar{C}_- + X)\bar{U}}{(\bar{C}_- + X)\bar{U} + \bar{C}_-\bar{V}}\,\text{grad}\,\mu_+ - \frac{\bar{C}_-\bar{V}}{(\bar{C}_- + X)\bar{U} + \bar{C}_-\bar{V}}\,\text{grad}\,\mu_- \quad (4)$$

The values of $\bar{C}_+$ and $\bar{C}_-$ for a negatively charged membrane have been calculated by using the expression given by Hersh[53]:

$$\bar{C}_+ = \tfrac{1}{2}(\sqrt{(X)^2 + 4C_i^2} + X) \quad (5a)$$

$$\bar{C}_- = \tfrac{1}{2}(\sqrt{(X)^2 + 4C_i^2} - X) \quad (5b)$$

The total membrane potential ΔO_m was considered the sum of diffusion potential ΔO_d inside the membrane and the electrostatic potential difference ΔO_e between the membrane surfaces and electrolyte solutions on both sides of the membrane. The diffusion potential ΔO_d was obtained by integrating eq. (4) for diffusion from one side of membrane to the other, whereas the electrostatic potential difference was calculated from Donnan's theory[54]:

$$\Delta O_m = \Delta O_d + \Delta O_e \tag{6a}$$

where

$$-\Delta O_d = -\int_1^2 \frac{J_0 X}{F\bar{C}_0(\bar{C}_- + X)U + \bar{C}_- V}\,dx + \frac{RT}{F}\int_1^2 \frac{(\bar{C}_- + X)U}{(\bar{C}_- + X)U + \bar{C}_- V}\,d\ln \bar{a}_+ - \frac{RT}{F}\int_1^2 \frac{\bar{C}_- V}{(\bar{C}_- + X)U + \bar{C}_- V}\,d\ln \bar{a}_- \tag{6b}$$

and

$$-\Delta O_e = -\frac{RT}{F}\ln\left(\frac{\bar{a}_1 a_2}{a_1 \bar{a}_2}\right) \tag{6c}$$

where a_1 and a_2 are the activities of the electrolytes on two sides of the membrane, the overbar refers to the phenomena in membrane phase, and J_0 is the flow of electrolyte in the absence of electric field; other symbols have their usual significance. By integrating eq. (6) and putting the limit of high electrolyte concentrations across the membrane the following equation for membrane potential is obtained:

$$-\Delta O_m = \frac{RT}{F}\left(\frac{X}{2}\right)\left(\frac{\gamma - 1}{\gamma}\right)\frac{1}{C_1} + \frac{RT}{F}\left(\frac{U - V}{U + V}\right)\left(\frac{1 - XJ_0/RT\bar{C}_0(U - V)K}{1 - XJ_0/2RT\bar{C}_0 VK}\right) \times \ln\gamma + \frac{RT}{2F}\left(\frac{X}{UV}\right)\left(\frac{J_0}{RT\bar{C}_0 K}\right)^2\left(\frac{1 - XJ_0(U + V)/4RT\bar{C}_0 UVK}{1 - XJ_0/2RT\bar{C}_0 VK}\right)^2 \times [(\gamma - 1)C_1]^{-1} \tag{7}$$

At high electrolyte concentrations eq. (7) was put in the following approximate form:

$$-\Delta O_m = \frac{RT}{F}\left(\frac{\gamma}{\gamma - 1}\right)\left(\frac{X}{2}\right)\frac{1}{C_1} \tag{8}$$

Equation (8) predicts a relationship between ΔO_m and $1/C_1$ from which X can be calculated. Figures 2 and 3 show plots between $\Delta O_m/(\gamma - 1/\gamma)$ and $1/C_1$ from which X is derived from the slope and is given in Table I.

The electromotive force ΔO_m may also be expressed by the modified Nernstian equation:

$$\Delta O_m = \Delta O_N(2\bar{T}_e - 1) \tag{9}$$

where ΔO_m is the observed membrane potential in mV, ΔO_N is the Nernstian

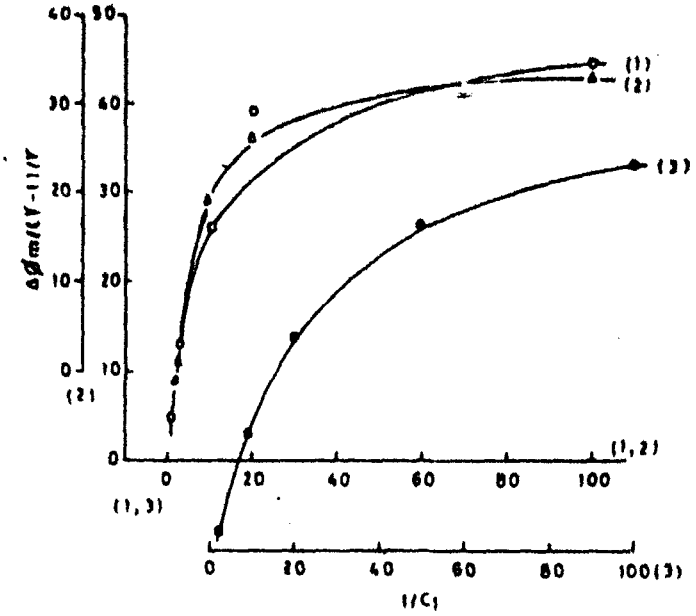

Fig. 2. Plots of $\Delta O_m/(\gamma - 1/\gamma)$ vs. $1/C_1$ for various electrolytes with mercuric phosphate membranes. ○, KCl; △, NaCl; ●, LiCl.

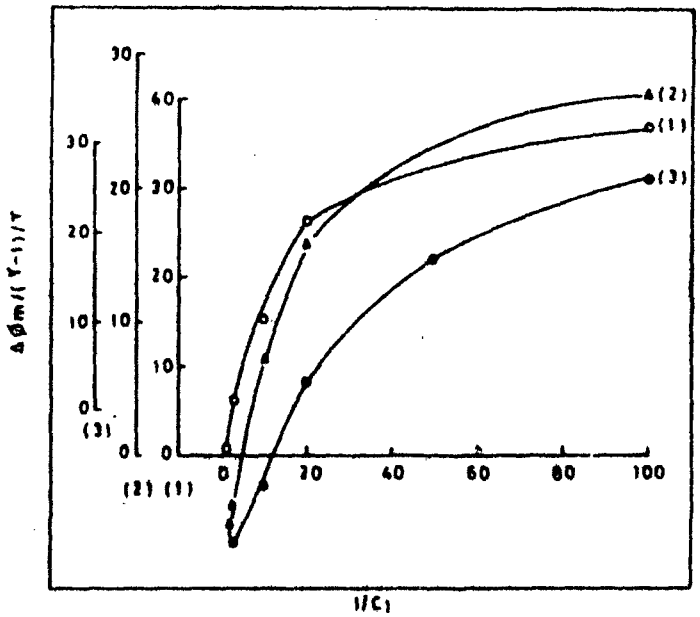

Fig. 3. Plots of $\Delta O_m/(\gamma - 1/\gamma)$ vs. $1/C_1$ for various electrolytes with mercuric carbonate membranes. ○, KCl; △, NaCl; ●, LiCl.

potential, and $\bar{T}_c$, is the cationic transference number in the membrane phase which is calculated from measured potential for different solution activities and is given in Table II.

The transference number was calculated by using Hersh's equation[53]:

$$\bar{T}_c = \frac{(\bar{U}/\bar{V})\bar{C}_+}{(\bar{U}/\bar{V})\bar{C}_+ + \bar{C}_-} \tag{10}$$

TABLE I
Comparison of Charge Density for Different Membrane Electrolyte Systems

Membrane	Electrolyte	TMS[28] $\bar{U}/\bar{V}$	TMS[28] X	Kobatake et al.[43] X	Nagasawa et al.[51] X
Mercuric phosphate	KCl	1.0	0.037	0.047	0.019
	NaCl	—	—	0.012	0.028
	LiCl	—	—	0.013	0.022
Mercuric carbonate	KCl	1.2	0.012	0.014	0.018
	NaCl	—	—	0.013	0.019
	LiCl	—	—	0.011	0.022

where $(\bar{U}/\bar{V})$ is the mobility ratio in the membrane phase and $\bar{C}_+$ and $\bar{C}_-$ have been calculated from eq. (5); $\bar{T}_c$ was calculated by using eq. (10) and substituting the value of X and $(\bar{U}/\bar{V})$ from Table I, as given in Table II. The values of $\bar{T}_c$ derived by both methods are closer to each other.

Bi-ionic Potential (BIP)

A steady electromotive force for a bi-ionic cell containing two electrolytes, AP and BP, separated by a membrane is called bi-ionic potential (BIP). This potential is a measure of selectivity of a membrane for the ions of the same sign. Various mathematically rigorous equations have been derived on the basis of thermodynamics of irreversible processes by Scatchard[40] and Helfferich.[30] Bi-ionic potential has also been reported by Michaelis,[55] Marshall and Krenbill,[56] Meyer and Bernfield,[57] Sollner et al.,[58,59] Manecke,[60] and Wyllie[61]. Toyoshima and Nozaki[52] derived the equation for BIP and membrane potential on the basis of nonequilibrium thermodynamics by using the appropriate assumptions for the mobilities and activity, coefficients of small ions in the membrane phase which are applied here to our system of parchment-supported membranes.

Consider a system in which two large compartments contain the aqueous solution composed of two simple 1 : 1 electrolytes, AP and BP. Here A and B represent the cationic species and P is the common anion. The electric charges carried by the membrane matrix are negative and are distributed uniformly with a charge density X. By neglecting interacting flows between ions of different species and the effect of mass flow we find that the fluxes of the ions A, B, and P are given by

$$J_N = -u_N C_N (RTD \ln a_N/dx + Fd/dx) \qquad (N = A,B) \qquad (11a)$$

TABLE II
Transport Number of Counterions as a Function of External KCl Electrolyte Concentration

Sample No.	Concentration (mole liter^{-1})	Mercuric phosphate $\bar{T}_{K^+}$ eq. (9)	Mercuric phosphate $\bar{T}_{K^+}$ eq. (10)	Mercuric carbonate $\bar{T}_{K^+}$ eq. (9)	Mercuric carbonate $\bar{T}_{K^+}$ eq. (10)
1	$1/1 \times 10^{-1}$	0.54	0.51	0.51	0.54
2	$5 \times 10^{-1}/5 \times 10^{-2}$	0.58	0.52	0.53	0.55
3	$1 \times 10^{-1}/1 \times 10^{-2}$	0.72	0.59	0.62	0.56
4	$5 \times 10^{-2}/5 \times 10^{-3}$	0.82	0.67	0.72	0.60
5	$1 \times 10^{-2}/1 \times 10^{-3}$	0.85	0.93	0.79	0.76

$$J_P = -u_P C_P(RTd \ln a_P/dx - Fd/dx) \quad (11b)$$

where $J_i (i = A,B,P)$ is the flux of ionic species i according to the frame of reference fixed to the membrane, and u_i, C_i, and a_i are the mobility (relative to local center of mass), molar concentration, and activity of ion i. The gradient of the electrochemical potential of the anion is represented in terms of J_P, a_P, and $U_P C_P$. If I and II indicate the value in the external solution 1 and 2 ΔO is the difference in the electric potential between two bulk solutions, then $O^{II} - O^{I}$, is the BIP:

$$\Delta O = (J_P/F) \int_0^L (1/u_P/C_P)dx + (RT/F) \text{ in } (a_P^{II}/a_P^{I}) \quad (12)$$

In the system of a negatively ionizable membrane and a 1 : 1 electrolyte the following assumptions are made for the concentration depencence of u_i and a_i of ion $i (i = +,-)$ in the membrane phase[52]:

$$u_+C_+ = u_+^0(\bar{C}_- + OX)$$
$$u_-C_- = u_-^0\bar{C}_- \quad (13a)$$
$$a_+ = \gamma_+^0(C_- + OX)$$
$$a_- = \gamma_-^0 C_- \quad (13b)$$

Here u_i^0 and γ_i^0 are the mobility and activity coefficients of ion i in free solution. The quantity OX is called the thermodynamically effective concentration of counterion dissociated from the ionizable groups fixed on membrane matrix.

The system is now composed of four kinds of electrolyte, AP, BP, AM, and BM; M represents the negatively ionizable groups fixed on the membrane skeleton. Applying eqs. (13a) and (13b) for this system and assuming[52] that the ratio of C_{AM} to C_{BM} is equal to that of C_{AP} to C_{BP}

$$\frac{C_{AM}}{C_{BM}} = \frac{C_{AP}}{C_{BP}} \quad (14a)$$

and the requirement that the electric neutrality must be realized in any element of the membrane gives the relation

$$C_{AM} + C_{BM} = X \quad (14b)$$

The expressions for the activities and mobilities of small ions in the membrane are given by

$$a_A = C_{AP}[1 + OX/(C_{AP} + C_{BP})]$$
$$a_B = C_{BP}[1 + OX/(C_{AP} + C_{BP})] \quad (15a)$$
$$a_P = C_{AP} + C_{BP}$$
$$u_A C_A = u_A^0 a_A$$
$$u_B C_B = u_B^0 a_B \quad (15b)$$
$$u_P C_P = u_P^0 a_P$$

Here C_{AP}, C_{BP}, C_{AM}, and C_{BM} are the concentration of the electrolytes AP, BP, AM, and BM, respectively, and O is a characteristic constant of the given membrane.

Equation (12) for the bi-ionic potential may be rewritten in the following form:

$$O = -\left(\frac{RT}{F}\right)\left[\ln\left(\frac{\gamma_L + \eta_L - 1}{\xi_0 + \eta_0 - 1}\right) - (2J - 1)\ln\left(\frac{\xi_L + \eta_L - J}{\xi_0 + \eta_0 - J}\right)\right] \tag{16}$$

where ξ_0 and ξ_L are the values of ξ in the membrane phase at $x = 0$ and $x = L$ and η_0 and η_L are the corresponding values of η; ξ and η are the reduced concentrations, defined by $\xi = (C_{AP}OX) + C_{AP}/(C_{AP} + C_{BP})$ and $\eta = (C_{BP}/OX) + C_{BP}/(C_{AP} + C_{BP})$.

By assuming that at both membrane surfaces the equilibrium distribution for every ion species is maintained between the membrane phase and external bulk solutions[52] and also neglecting the effect of osmotic pressure produced between the two phases, the following expressions are obtained:

$$\begin{aligned} K_N^2(a_{NP})_I^2 &= (a_N)_0(a_P)_0 \\ K_N^2(a_{NP})_{II}^2 &= (a_N)_L(a_P)_L \end{aligned} \tag{17}$$

where $(a_{NP})_I$ and $(a_{NP})_{II}$ are the mean activities of the electrolyte NP(N = A,B) in solutions I and II, respectively, defined by

$$\begin{aligned} (a_{NP})_I^2 &= a_N^I a_P^I \\ (a_{NP})_{II}^2 &= a_N^{II} a_P^{II} \end{aligned} \tag{18}$$

$(a_i)_0$ and $(a_i)_L (i = A,B,P)$ are the single ion activities of species i in the membrane phase at $x = 0$ and $x = L$ and K_N (N = A,B) is defined by

$$1/K_N = \exp\,(u_N^{0m} - u_N^{0b} + u_P^{0m} - u_P^{0b})/2RT \tag{19}$$

In eq. (19) u_N^{0m} is the standard chemical potential of cation N in the membrane phase, u_N^{0b} is the external bulk solution, and u_P^{0m} and u_P^{0b} are the corresponding values of anion P.

By solving these equations Toyoshima et al.[52] derived an equation for BIP in this form:

$$\Delta O = \left[2\ln\left(\frac{K_A}{K_B}\right) + \ln\left(\frac{JV_A + 1}{JV_B + 1}\right)\right]\left(\frac{F}{RT}\right) \tag{20}$$

J can be obtained from the relation

$$(2J + 1)\ln\left(\frac{g_A + 2J}{g_B + 2J}\right) - \ln\left(\frac{JV_A + 1}{JV_B + 1}\right) - \ln\left(\frac{g_A}{g_B}\right) = 0 \tag{21}$$

where

$$v_N = 1 + (\mu_N^0/\mu_P^0) \tag{22a}$$

$$g_N = 1 + \left[1 + \left(\frac{2K_N C}{X}\right)^2\right]^{1/2} \tag{22b}$$

Knowing the value of parameters K_A, K_B, X, v_A, and v_B, we can calculate the value of ΔO by eq. (20). For the evaluation of these parameters separate experiments for membrane potential were carried out.

The value of membrane potential ΔO_m[52] arising between two solutions of a 1 : 1 electrolyte of different concentrations and separated by an (negatively) ionizable membrane is given by

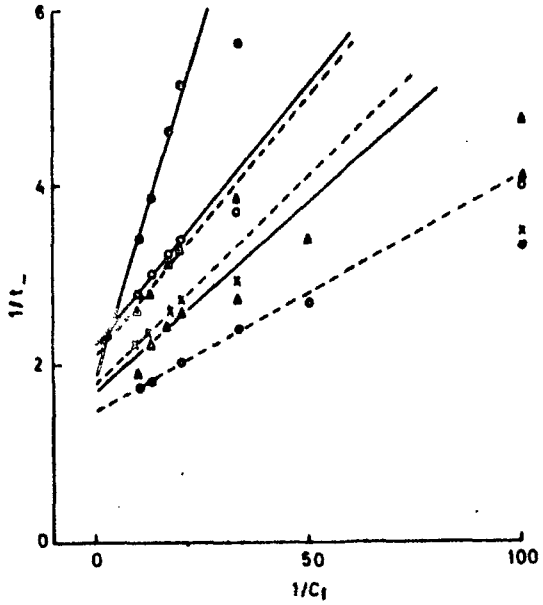

Fig. 4. Plots of $1/t_-$ vs. $1/C_1$ for (a) mercuric phosphate and (b) mercuric carbonate membranes with various 1 : 1 electrolytes. (a) -●-, KCl; -○-, NaCl; -Δ-, LiCl. (b) - -Δ- -, KCl; - -X- -, NaCl; - -⊙- -, LiCl.

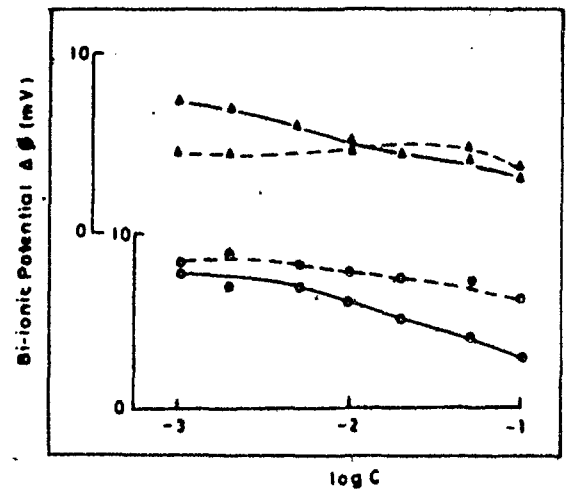

Fig. 5. Plots of observed (—) and calculated (- - -) bi-ionic potentials ΔO vs. log C for different pairs of electrolytes with mercuric phosphate membranes. ●, KCl-LiCl (I); Δ, NaCl-LiCl (II).

$$\left(\frac{F}{RT}\right)\Delta O_m = -\ln\gamma - \left(1-\frac{2}{\upsilon_N}\right)\ln\left(\frac{[1+(2C_N^{\prime}K_N/X)^2]^{1/2}+(1-2/\upsilon_N)}{[1+(2C_N^{\prime}K_N/X)^2]^{1/2}+(1-2/\upsilon_N)}\right)$$

$$+\ln\left(\frac{[1+(2C_N^{\prime}K_N/X)^2]^{1/2}+1}{[1+(2C_N^{\prime}K_N/X)^2]^{1/2}+1}\right) \quad (23)$$

where $\gamma = C_N^{\prime}/C_N^{\prime}$. Expansion of eq. (23) in powers of $(1/C_N^{\prime})$, in which the concentration ratio is kept constant yields

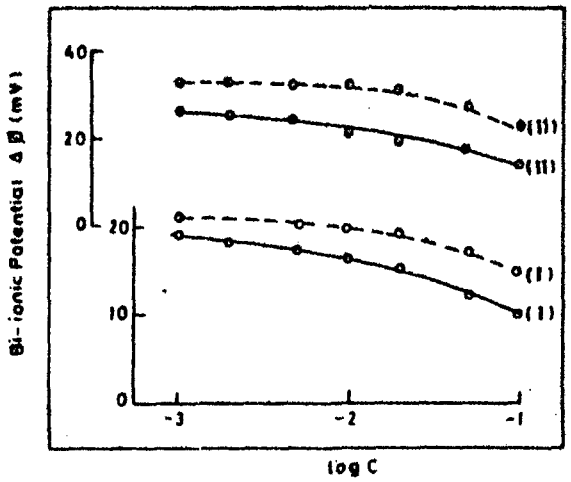

Fig. 6. Plots of observed (—) and calculated (- - -) bi-ionic potentials ΔO vs. log C for different pairs of electrolytes with mercuric carbonate membranes. O, KCl-NaCl (I); ●, KCl-LiCl (II).

$$-\left(\frac{F}{RT}\right)\Delta O_m = -\left(1-\frac{2}{\upsilon_N}\right)\ln\gamma - 2\left(1-\frac{1}{\upsilon_N}\right)\left(\frac{1}{\upsilon_N}\right)\left(1-\frac{1}{\gamma}\right)X\left(\frac{X}{K_N}\right)\left(\frac{1}{C_N^I}\right) \quad (24)$$

The apparent transference number t_- for co-ion species is defined by the Nernst equation:

$$-\left(\frac{F}{RT}\right)\Delta O_m = (1-2t_-)\ln\gamma \quad (25)$$

By introducing eq. (24) into eq. (25) and expanding $1/t_-$ as a power series in $1/C_N^I$, we obtain the following expression:

$$\frac{1}{t_-} = \upsilon_N + (\upsilon_N - 1)\left(\frac{\gamma-1}{\gamma\ln\gamma}\right)\left(\frac{X}{K_N}\right)\left(\frac{1}{C_N^I}\right) \quad (26)$$

Using eq. (26), we determine the values of υ_N and (X/K_N) from the ordinate intercept and initial slope of a plot for $1/t_-$ against $1/C_N^I$ at a given γ.

Equation (26) indicates that the intercept of a plot of $1/t_-$ against $1/C_N^I$ at fixed $\gamma = 10$ allows the values of υ_N to be determined. Plots of $1/t_-$ against $1/C_N^I$ for various 1 : 1 electrolytes are shown in Figure 4 for both mercuric carbonate and phosphate membranes. For the evaluation of (X/K_N) the slope of eq. (26), which is given by the following, is first determined:

$$(\upsilon_N - 1)[(\gamma-1)/\gamma\ln\gamma](X/K_N)$$

The graphical value of the slope determined from Figure 4 is equated with this expression and by substituting υ_N the value of (X/K_N) is determined.

The value of g_N is calculated from eq. (22) at different concentrations. By substitution of the value of g_N and υ_N in eq. (21) J is evaluated. By substitution of the values of υ_N, (X/K_N), g_N, and J in eq. (20) the theoretical BIP is calculated. These theoretical values of BIP are plotted against log C and are shown by broken lines in Figures 5 and 6. For comparison the observed values of BIP are also plotted and are shown by solid lines in the same graph. It is quite evident from these diagrams that the agreement between the observed and theoretical values are quite fair and it may be concluded that the theory of BIP developed by

Toyoshima et al.[52] is applicable to our system of parchment-supported membranes.

The authors are grateful to Professor Wasiur Rahman, Head of the Department of Chemistry, for providing research facilities and to C.S.I.R. (India) for the fellowship award to one of them (P.P.).

References

1. F. A. Siddiqi, M. N. Beg, and S. P. Singh, *J. Polym. Sci.*, **15**, 959 (1977).
2. F. A. Siddiqi, S. K. Saksena, and I. R. Khan, *J. Polym. Sci.*, **15**, 1935 (1977).
3. F. A. Siddiqi, M. N. Beg, S. P. Singh, and A. Haque, *Electrochim. Acta*, **22**, 631, 638 (1977).
4. F. A. Siddiqi, M. N. Beg, A. Haque, and S. P. Singh, *Bull. Chem. Soc. Jpn.*, **49**, 2854, 2864 (1976).
5. F. A. Siddiqi, M. N. Beg, and P. Prakash, *J. Electroanal. Chem.*, **80**, 223 (1977).
6. F. A. Siddiqi, P. Prakash, and S. P. Singh, *Kolloid Z.Z. Polym.*, **256**, 652 (1978).
7. F. A. Siddiqi, M. N. Beg, P. Prakash, and S. P. Singh, *Indian J. Chem.*, **16A**, 7 (1978).
8. F. A. Siddiqi, M. N. Beg, S. P. Singh, and A. Haque, *Acta Chim.*, **93**(2), 123 (1977).
9. F. A. Siddiqi, M. N. Beg, A. Haque, M. A. Ahsan, and M. I. R. Khan, *J. Chim. Phys.*, **74**, 932 (1977).
10. F. A. Siddiqi, S. K. Saksena, M. I. R. Khan, and M. A. Ahsan, *J. Mem. Sci.*, **2**, 245 (1977).
11. M. N. Beg, F. A. Siddiqi, and R. Shyam, *Can. J. Chem.*, **55**, 1680 (1977).
12. M. N. Beg, F. A. Siddiqi, R. Shyam, and I. Altaf, *J. Electroanal. Chem.*, **89**, 141 (1978).
13. F. A. Siddiqi and S. Pratap, *J. Electroanal. Chem.*, **23**, 137, 147 (1969).
14. F. A. Siddiqi, N. Lakshminarayanaiah, and S. K. Saksena, *Z. Phys. Chem. (Frankfurt am Main)*, **72**, 298, 307 (1970).
15. F. A. Siddiqi, N. Lakshminarayanaiah and M. N. Beg, *J. Polym. Sci.*, **9**, 2853, 2869 (1971).
16. N. Lakshminarayanaiah and F. A. Siddiqi, *J. Polym. Sci.*, **8**, 2949 (1970).
17. N. Lakshminarayanaiah and F. A. Siddiqi, *Biophys. J.*, **11**, 603, 1617 (1971).
18. N. Lakshminarayanaiah and F. A. Siddiqi, *Biophys. J.*, **12**, 540 (1972).
19. N. Lakshminarayanaiah and F. A. Siddiqi, *Z. Phys. Chem. (Frankfurt am Main)*, **78**, 150 (1972).
20. N. Lakshminarayanaiah and F. A. Siddiqi, in *Membrane Process in Industry and Biomedicine*, M. Bier, Ed., Plenum, New York, 1971, p. 301.
21. W. U. Malik and F. A. Siddiqi, *J. Colloid Sci.*, **18**, 161 (1963).
22. W. U. Malik and F. A. Siddiqi, *Proc. Indian Acad. Sci.*, **A56**, 206 (1962).
23. W. U. Malik, F. A. Siddiqi, and H. Arif, *Bull. Chem. Soc. Jpn.*, **40**, 1741 (1967).
24. T. Teorell, *Discuss. Faraday Soc.*, 21, 9 (1956); *Proc. Soc. Exp. Biol. Med.*, **33**, 282 (1935); *Proc. Nat. Acad. Sci. USA*, **21**, 152 (1935); *Prog. Biophys. Biophys. Chem.*, **3**, 305 (1953).
25. K. H. Meyer and J. F. Sievers, *Helv. Chim. Acta*, **19**, 649, 665, 987 (1936).
26. K. Sollner, *J. Phys. Chem.*, **49**, 47, 171 (1945); *J. Electrochem.*, **97**, 139 (1950); *Ann. NY Acad. Sci.*, **57**, 177 (1953); *J. Macromol. Sci.*, **A3**, 1 (1969).
27. H. P. Gregor, *J. Am. Chem. Soc.*, **70**, 1293 (1948); *ibid.*, **73**, 642 (1950).
28. G. Schmid, *Z. Elektrochem.*, **54**, 424 (1950); *ibid.*, **55**, 229 (1951); *ibid.*, **56**, 35 (1952).
29. G. Schmid and H. Schwarz, *Z. Elektrochem.*, **55**, 295 (1951); *ibid.*, **56**, 35 (1952).
30. F. Hefferich, *Ion Exchange*, McGraw-Hill, New York, 1962.
31. G. Eisenman, *The Glass Electrode*, Interscience, New York, 1965, p. 163.
32. G. Eisenman, *Biophys. J.*, **2**, 259 (1962).
33. G. Eisenman, *Membrane Transport and Metabolism*, A. Kleinzellers and A. Kotgk, Eds., Academic, New York, 1961.
34. H. Sherry, *Ion Exchange, Vol. 2*, J. A. Marinsky, Ed., Marcel Dekker, New York, 1968.
35. A. M. Liquori and C. Botre, *Ric. Sci.*, **34**, 6 (1964).
36. A. M. Liquori and C. Botre, *J. Phys. Chem.*, 71, 3765 (1967).
37. K. S. Spiegler, *Trans. Faraday Soc.*, **54**, 1408 (1958).
38. K. S. Spiegler, R. L. Yoest, and M. R. J. Wyllie, *Discuss. Faraday Soc.*, **21**, 174 (1956).
39. G. Scatchard, *J. Am. Chem. Soc.*, **21**, 30 (1956).
40. G. Scatchard, *Discuss. Faraday Soc.*, **21**, 30 (1956).

41. J. W. Lorimer, E. I. Boterenbrood, and J. J. Hermans, *Discuss. Faraday Soc.*, **21**, 141 (1956).
42. F. M. Scattergood and E. N. Lightfoot, *Trans. Faraday Soc.*, **64**, 1135 (1968).
43. Y. Kobatake, T. Noriaki, Y. Toyoshima, and H. Fujita, *J. Phys. Chem.*, **69**, 3981 (1965).
44. Y. Toyoshima, M. Yuasa, Y. Kobatake, and H. Fujita, *Trans. Faraday Soc.*, **63**, 2803, 2814 (1967).
45. M. Yuasa, Y. Kobatake, and H. Fujita, *J. Phys. Chem.*, **72**, 2871 (1968).
46. N. Kamo, Y. Toyoshima, H. Nozaki, and Y. Kobatake, *Kolloid Z.Z. Polym.*, **248**, 914 (1971).
47. N. Kamo, Y. Toyoshima, and Y. Kobatake, *Kolloid Z.Z. Polym.*, **249**, 1061 (1971).
48. N. Kamo, M. Ockawa, and Y. Kobatake, *J. Phys. Chem.*, **77**, **92**, 2995 (1973).
49. M. Nagasawa and I. Kagawa, *Discuss. Faraday Soc.*, **21**, 52 (1956).
50. M. Nagasawa and Y. Kobatake, *J. Phys. Chem.*, **56**, 1017 (1952).
51. M. Tasaka, N. Aoki, Y. Konda, and M. Nagasawa, *J. Phys. Chem.*, **79**, 1307 (1975).
52. Y. Toyoshima and H. Nozaki, *J. Phys. Chem.*, **74**, 2704 (1970).
53. L. S. Hersh, *J. Phys. Chem.*, **72**, 2145 (1968).
54. F. G. Donnan and E. A. Guggenheim, *Z. Phys. Chem., Abt A*, **162**, 346 (1932).
55. L. Michaelis, *Kolloid Z.*, **62**, 2 (1933).
56. C. E. Marshall and C. A. Krinbill, *J. Am. Chem. Soc.*, **64**, 1814 (1942).
57. K. H. Meyer and P. Bernfield, *Helv. Chim. Acta*, **28**, 962 (1945).
58. K. Sollner, *J. Phys. Chem.*, **53**, 1211, 1226 (1949).
59. K. Sollner, S. Dray, E. Grim, and R. Neihof, *Ion Transport Across Membrane*, Academic, New York, 1954, p. 144.
60. G. Manecke, *Z. Elektrochem.*, **55**, 672 (1951).
61. M. R. J. Wyllie, *J. Phys. Chem.*, **58**, 167 (1959).

Received November 3, 1977
Revised December 23, 1977

2696 BULLETIN OF THE CHEMICAL SOCIETY OF JAPAN, VOL. 52 (9), 2696—2698 (1979) [Vol. 52, No. 9

Studies on Inorganic Precipitate Membranes: Membrane Potential and Bi-ionic Potential

M. Nasim Beg,* Fasih A. Siddiqi,† Surendra P. Singh,
(Miss) Veena Gupta, and Poorna Prakash
Physical Chemistry Division, Department of Chemistry, Aligarh Muslim University, Aligarh, U.P., India

(Received August 19, 1978)

Electrical potentials arising across barium(II) phosphate, mercury(II) iodide and cobalt(II) chromate membranes using various 1:1 electrolytes are reported. Thermodynamically effective fixed charge density, which is an important parameter governing the membrane phenomena, has been evaluated by the theory of Toyoshima and Nozaki. Using the values of effective fixed charge density determined, the theory of bi-ionic potentials developed by Toyoshima and Nozaki based on the principles of the irreversible thermodynamics has been examined. Theoretical predictions were borne out quite satisfactorily by our experimental results.

In recent years we have studied a large number of parchment supported inorganic precipitate and polymeric composite membranes.[1-6] Various transport parameters such as ion migration, self diffusion coefficient, hydrodynamic permeability *etc.* occuring across the membranes have been evaluated in the light of the theory described by Speigler[7] and by the use of the generalized Stefan-Maxwell equations. The theory of absolute reaction rates,[8] Eisenman-Sherry theory of membrane selectivity[9] and the theory of irreversible thermodynamics developed by Kedem and Katchalsky,[10] Smit and Staverman,[11] Bearman and Krikwood,[12] and Kobatake and coworkers[13-16] have been applied to evaluate apparent fixed charge density as well as to examine the various aspects of membranes.

In this communication a series of membrane potentials and bi-ionic potentials observed across parchment supported barium(II) phosphate, mercury(II) iodide and cobalt(II) chromate membranes using various 1:1 electrolytes are presented. Thermodynamically effective fixed charge density, which is an important parameter governing the membrane phenomena has been evaluated by the recently developed theory of Toyoshima and Nozaki based on the principles of irreversible thermodynamics.[17] An effort has been made to examine the validity of the theory of Toyoshima and Nozaki[17] for bi-ionic potential.

Experimental

Preparation of Membranes. Parchment supported barium(II) phosphate, mercury(II) iodide and cobalt(II) chromate membranes were prepared by the method of interaction suggested by Siddiqi, Beg, and coworkers.[1-6] To precipitate barium(II) phosphate in the interstices of parchment paper, a 0.2 M solution of barium(II) chloride was placed inside a glass tube, to one end of which was tied the parchment paper (supplied by M/s- Baird and Tatlock London Ltd.). The tube was suspended for 72 h in a 0.2 M solution of potassium dihydrogenphosphate. The two solutions were interchanged later and kept for another 72 h. The membrane was taken out and washed with deionized water to remove free electrolyte. Similar procedure was adopted for the preparation of mercury(II) iodide and cobalt(II) chromate membranes by taking 0.2 M solutions of mercury(II) chloride and potassium iodide, cobalt(II) chloride and potassium chromate, respectively.

Measurements of Membrane Potential and Bi-ionic Potential. Membrane potential E_m were obtained by constructing a cell of the following type taking different concentrations C'_x and C''_x of an electrolyte such that $C''_x/C'_x=10$

SCE	Solution C'_x	Membrane	Solution C''_x	SCE

and the bi-ionic potentials (BIP) were determined by setting up another cell of the type

SCE	Solution AP	Membrane	Solution BP	SCE

and keeping the same concentration of both the electrolytes AP and BP. The various salt solution (chlorides of Li^+, Na^+, K^+) were prepared from analytical grade reagents and deionized water. All measurements were carried out using a water thermostate maintained at 25±0.1 °C. The solutions on either sides of the membrane were vigorously stirred by a pair of magnetic stirrer.

Results and Discussion

When two electrolyte solutions of different concentrations are separated by a membrane, the mobile species penetrate the membrane and various transport phenomena are induced in the system. The fixed charge theory of Teorell-Meyer-Seivers (TMS) for charged membranes is a pertinent starting point for the investigation of the actual mechanisms of the ionic or molecular processes which occur in the membrane phase. Based on the fixed charge concept various mathematically rigorous equations for membrane potential and bi-ionic potential have in recent years been derived.[17-22] Most recently Toyoshima and Nozaki[17] have derived equations for membrane potential and bi-ionic potential using the principles of non-equilibrium thermodynamics and by utilizing appropriate assumptions for the mobilities and activity coefficients of small ions in the membrane phase.[17] The effect of ionic interaction, mass flow and osmotic effect were neglected. For a negatively charged membrane separating two 1:1 electrolytes (common co-ions) of the same concentration, these authors derived following expression for bi-ionic potential, E_{BIP},

$$E_{BIP} = (F/RT)[2\ln K_A/K_B + \ln(JV_A + 1/JV_B + 1)]. \quad (1)$$

Knowing the values of parameters K_A, K_B, V_A, V_B and the flux J, the values of theoretical E_{BIP} can be

† Present address: Department of Biophysics, Michigan State University, East Lansing, Michigan 48824, (U.S.A.).

Table 1. The values of membrane potentials, E_m (mV) observed across parchment supported barium(II) phosphate, mercury(II) iodide and cobalt(II) chromate membranes at 25±0.1 °C

Membrane concentration* (M)	Barium(II) phosphate			Mercury(II) iodide			Cobalt(II) chromate		
	KCl	NaCl	LiCl	KCl	NaCl	LiCl	KCl	NaCl	LiCl
1/0.1	1.51	−4.39	−4.98	6.68	−1.35	−13.40	−5.30	−7.90	−14.32
0.5/0.05	2.90	−3.89	−4.01	10.03	2.24	−8.27	−3.20	−5.50	−11.50
0.1/0.01	9.82	2.10	1.96	31.11	25.59	14.77	4.50	−1.23	−5.50
0.05/0.005	16.34	7.95	2.50	39.58	34.35	25.22	8.80	2.63	−1.00
0.01/0.001	33.78	22.05	20.15	49.86	46.32	40.63	21.20	16.83	13.80

* Dilute solution side taken as positive.

Table 2. The values of the membrane parameters V_N and $(\bar{X}/K_N)$ derived from the Toyoshima and Nozaki theory for parchment supported membrane

Membrane parameters	Mercury(II) iodide		Barium(II) phosphate		Cobalt(II) chromate	
	V_N	$\bar{X}/K_N$	V_N	$\bar{X}/K_N$	V_N	$\bar{X}/K_N$
KCl	2.05	0.438	2.00	0.092	1.75	0.012
NaCl	1.73	0.474	1.88	0.066	1.75	0.013
LiCl	1.53	0.490	1.86	0.026	1.55	0.010

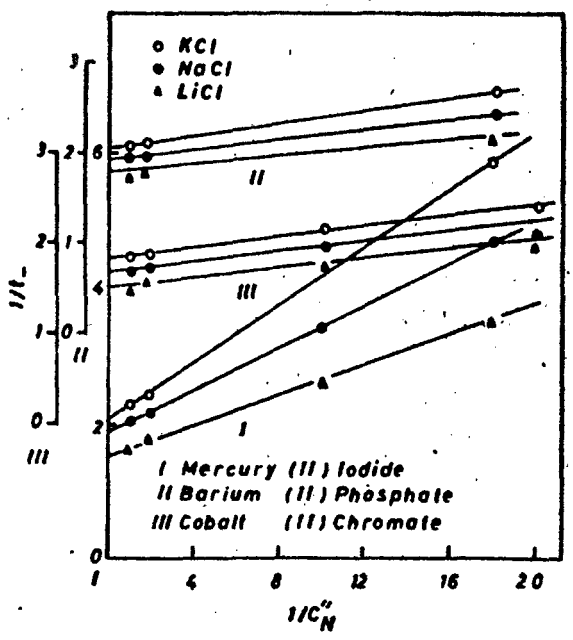

Fig. 1. Plots of $1/t$ against $1/C$ for various electrolytes across (i) mercury(II) iodide, (ii) barium(II) phosphate and (iii) cobalt(II) chromate membranes.

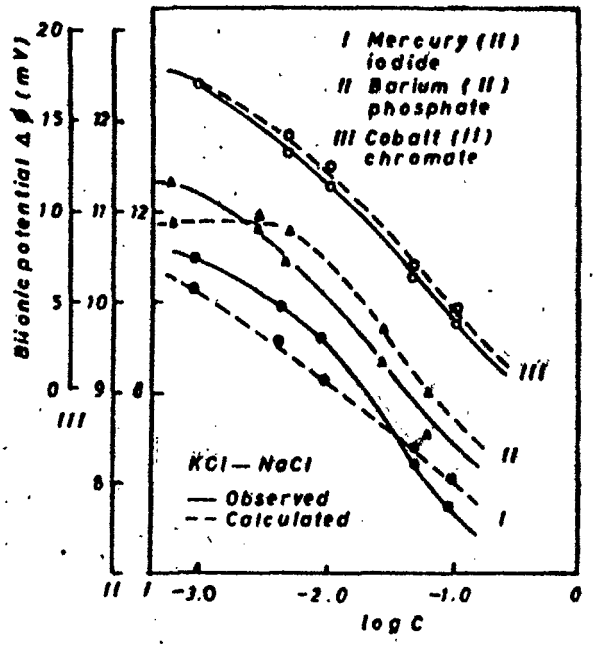

Fig. 2. Plots of bi-ionic potentials against log C for KCl–NaCl pair of electrolytes across (i) mercury(II) iodide, (ii) barium(II) phosphate and (iii) cobalt(II) chromate membranes.

calculated using Eq. 1. For the evaluation of these parameters, following equations have been forwarded[17]

$$(2J+1)\ln(g_A+2J/g_B+2J) - \ln(JV_A+1/JV_B+1) - \ln(g_A/g_B) = 0 \quad (2)$$

where

$$V_N = 1 + V_N^*/V_P^* \quad (N=A, B) \quad (3a)$$

and

$$g_N = 1 + [1+(2K_NC/\bar{X})^2]^{1/2} \quad (N=A, B) \quad (3b)$$

In Eq. 3a, V_N^* and V_P^* are the mobilities of cation N and anion P, respectively in bulk solution. In Eq. 3b, $\bar{X}$ is the effective charge density of the membrane and K_N is defined by

$$1/K_N = \exp[(\mu_N^{0m} - \mu_N^{0b} + \mu_P^{0m} - \mu_P^{0b})/2RT] \quad (3c)$$

where μ_N^{0m} is the standard chemical potential of cation N ion in the membrane phase and μ_N^{0b} is that in bulk solution and μ_P^{0m} and μ_P^{0b} are the corresponding values of anion P. In order to derive the values of the parameters V_N and $\bar{X}$ occuring in Eq. 3a and 3b Toyoshima and Nozaki[17] derived another equation for membrane potential E_m arising across a membrane when it is used to separate two solutions of an electrolyte at

different concentrations C'_N and C''_N

$$(F/RT)E_m = -\ln\gamma - (1-2/V_N)X \ln\frac{\sqrt{1+(2C''_NK_N/\bar{X})^2}+(1-2/V_N)}{\sqrt{1+(2C'_NK_N/\bar{X})^2}+(1-2/V_N)} + \ln\frac{\sqrt{1+(2C''_NK_N/\bar{X})^2}+1}{\sqrt{1+(2C'_NK_N/\bar{X})^2}+1} \quad (4)$$

where $\gamma=C''_N/C'_N$.

Equation 4 on expansion in powers of concentration ratio=10 being kept constant yield

$$(F/RT)E_m = -(1-2/V_N)\ln\gamma - 2(1-1/V_N)X (1/V_N)(1-1/\gamma)(\bar{X}/K_N)(1/C''_N) + \cdots \quad (5)$$

The apparent transference number t_- for co-ion was defined by the Nernst equation

$$-(F/RT)E_m = (1-2t_-)\ln\gamma. \quad (6)$$

Combining Eqs. 5 and 6 and expanding $1/t_-$ as a power of series of $1/C''_N$, following expression was obtained

$$1/t_- = V_N + (V_N-1)\left[\frac{\gamma-1}{\gamma\ln\gamma}\right]\left(\frac{\bar{X}}{K_N}\right)\left(\frac{1}{C''_N}\right) + \cdots \quad (7)$$

Equation 7 predicts a linear relationship between $1/t_-$ and $1/C''_N$. The values of V_N and $(\bar{X}/K_N)$ can be determined from the ordinate intercept and initial slope of a plot for $1/t_-$ against $1/C''_N$. The apparent transference number t_- was calculated from membrane potential data (Table 1) using Eq. 6. The values of V_N and $\bar{X}/K_N$ thus derived for the membrane and various 1:1 electrolyte systems using Fig. 1 are given in Table 2. The values of V_N and $(\bar{X}/K_N)$ were then used to calculate J and g_N using Eqs. 2 and 3. Once the membrane parameters V_N, g_N, J and $(\bar{X}/K_N)$ are known for the membrane electrolyte systems, one can calculate theoretical bi-ionic potential using Eq. 1. The bi-ionic potential thus obtained were plotted as a function of log C in Fig. 2 (shown by dotted lines). In order to compare theoretical bi-ionic potential values, the observed bi-ionic potentials were also plotted in the same graph (shown by solid lines). Figure 2 demonstrates that the theoretical predictions are borne out quite satisfactorily by our experimental results on parchment supported membranes. However, a slight deviation in the values may be accounted due to various reasons, most notably due to the various degree of interaction of ions with the membranes of low fixed charge site.

The authors are grateful to Professor Wasiur Rahman, Head, Department of Chemistry for providing research facilities and to C.S.I.R. (India) for the award of fellowship to SPS, VG, and PP.

References

1) F. A. Siddiqi, M. N. Beg, S. P. Singh, and A. Haque, *Bull. Chem. Soc. Jpn.*, **49**, 2854, 2864 (1976); *Electrochim. Acta*, **22**, 631, 638 (1977).
2) F. A. Siddiqi, M. N. Beg, P. Prakash, and S. P. Singh, *Indian J. Chem.*, **16A**, 7 (1978).
3) F. A. Siddiqi, M. N. Beg, and P. Prakash, *J. Electroanal. Chem.*, **80**, 223 (1977); *J. Polym. Sci.*, in press; *J. Electroanal. Chem.*, in press.
4) N. Lakshminarayanaiah and F. A. Siddiqi, *J. Polym. Sci.*, **8**, 2849 (1970); *Biophys. J.*, **11**, 603, 617 (1971); **12**, 150 (1972); *Z. Phys. Chem. (Fr.)*, **78**, 150 (1972).
5) M. N. Beg, F. A. Siddiqi, and R. Shyam, *Can. J. Chem.*, **55**, 1680 (1977).
6) M. N. Beg, F. A. Siddiqi, R. Shyam, and M. Arshad, *J. Membrane Sci.*, **2**, 365 (1977).
7) K. S. Speigler, *Trans. Faraday Soc.*, **54**, 1408 (1958); K. S. Speigler, R. L. Yoest, and M. R. J. Wyllie, *Discuss. Faraday Soc.*, **21**, 174 (1956).
8) B. J. Zwolinsky, H. Eyring, and C. E. Reese, *J. Phys. Chem.*, **53**, 1426 (1949).
9) G. Eisenman, *Biophys. J.*, **2**, 259 (1962); "In Membrane Transport and Metabolism," ed by A. Kleinzellers and A. Kotyk, Acad. Press, New York (1961); H. Sherry, "Ion Exchange, Vol. 72," ed by J. A. Marinsky, Dekker, New York (1968).
10) O. Kedem and A. Katchalsky, *Trans. Faraday Soc.*, **59**, 1918, 1931, 1941 (1963); *Biochem. Biophys. Acta*, **27**, 229 (1958).
11) J. A. M. Smit and A. J. Staverman, *J. Phys. Chem.*, **74**, 966 (1970).
12) R. J. Bearman and J. W. Kirkwood, *J. Chem. Phys.*, **28**, 136 (1958).
13) Y. Kobatake, N. Takeguchi, Y. Toyoshima, and H. Fujita, *J. Phys. Chem.*, **69**, 3981 (1965).
14) Y. Toyoshima, M. Yuasa, Y. Kobatake, and H. Fujita, *J. Phys. Chem.*, **72**, 2871 (1968); *Trans. Faraday Soc.*, **63**, 2803, 2814 (1967).
15) N. Kamo, Y. Toyoshima, H. Nozaki, and Y. Kobatake, *Kolloid-Z. Z. Polym.*, **248**, 914 (1971); **249**, 1061 (1971).
16) N. Kamo, M. Ookawa, and Y. Kobatake, *J. Phys. Chem.*, **77**, 92, 299 (1973).
17) Y. Toyoshima and H. Nozaki, *J. Phys. Chem.*, **74**, 2704 (1970).
18) C. E. Mrarshall, *J. Phys. Chem.*, **52**, 1284 (1948).
19) K. Sollner, *J. Phys. Chem.*, **53**, 1211 (1952); *ibid.* **53**, 1226 (1949).
20) M. R. J. Wyllie, *J. Phys. Chem.*, **58**, 67 (1954).
21) R. P. Buck, "CRC Critical Reviews in Analytical Chemistry," (1976), p. 323.
22) F. Helfferich, "Ion Exchange," McGraw Hill, New York (1962).

Electrochimica Acta, Vol 24, pp 85-88
© Pergamon Press Ltd 1979 Printed in Great Britain

0019-4686/79/0101-0085 $02.00/0

STUDIES WITH INORGANIC PRECIPITATE MEMBRANE: EVOLUTION OF THERMODYNAMICALLY EFFECTIVE FIXED CHARGE DENSITY AND TEST OF THE MOST RECENTLY DEVELOPED THEORY OF MEMBRANE POTENTIAL BASED ON THE PRINCIPLES OF NON-EQUILIBRIUM THERMODYNAMICS

M. NASIM BEG, FASIH A. SIDDIQI,* SURENDRA P. SINGH, POORNA PRAKASH and VEENA GUPTA

Physical Chemistry Division, Department of Chemistry, Aligarh Muslim University, Aligarh, (U.P.) India

(*Received* 28 *February* 1978; *in revised form* 4 *July* 1978)

Abstract Electrical potentials developed across nickel, manganese chromate and cupric iodide membranes using various 1:1 electrolytes are reported. Thermodynamically effective fixed charge density, which is an important parameter governing the membrane phenomena, has been evaluated by the recently developed theory of Nagasawa *et al.* Most recently developed theories of Toyoshima and Nozaki based on the principles of the irreversible thermodynamics has been examined to predict the bi-ionic potentials developed across the membranes. Theoretical predictions were borne out quite satisfactorily by our experimental results.

INTRODUCTION

We have been engaged for quite some time in the studies of parchment supported[1-6] and polymeric composite membranes[7]. Their importance lies in the fact that they happen to bear a close resemblance to cell membrane of living systems. In a series of theoretical papers Kedem and Katchalsky[8] have discussed the behavior of complex membranes. Such complex membranes have been prepared by us and by a large number of investigators[9-11]. Theoretical expressions based on irreversible thermodynamics by Kedem and Katchalsky[8] and Kobatake *et al*[12, 13] and other transport equations developed by Smit and Staverman[14], Speigler[15], Bearman and Kirkwood[16], Richardson[17], and Scatchard[18] including Nernst–Planck flux equation have been applied for the elucidation of various aspects of membrane behavior.

In this paper a series of membrane potentials and bi-ionic potentials developed across nickel, manganese chromate and cupric iodide membranes using various 1:1 electrolytes are reported. The thermodynamically effective fixed charge density, which is an important parameter governing membrane phenomena has been evaluated by the recently developed fixed charge theory of Nagasawa *et al*[19]. An effort has been made to examine the validity of the most recently developed theory of Toyoshima and Nozaki[20] for membrane potential and bi-ionic potential based on the principles of the irreversible thermodynamics.

* Department of Biophysics, Michigan State University, East Lansing, Michigan 48824, U.S.A.

EXPERIMENTAL

Preparation of membranes

Parchment supported nickel, manganese chromate and cupric iodide membranes were prepared by the method of interaction suggested by Siddiqi, Beg *et al*[1-7]. To precipitate nickel chromate in the interstices of parchment paper a 0.2 M solution of nickel chloride was placed inside a glass tube, to one end of which was tied the parchment paper (supplied by M/S Baired and Tatlock London Ltd.). The tube was suspended for 72 h in a 0.2 M solution of potassium-chromate. The two solutions were interchanged later and kept for another 72 h. The membrane was taken out and washed with deionized water to remove free electrolyte. Similar procedure was adopted for the preparation of manganese chromate and cupric iodide membranes by taking 0.2 M solutions of manganese chloride, potassium chromate, cupric chloride and potassium iodide.

Measurement of membrane potential and bi-ionic potential

Membrane potential E_m were obtained by constructing a cell of the following type taking different concentrations C'_N and C''_N of an electrolyte such that $C''_N/C'_N = 10$

sce	Solution C'_N	Membrane	Solution C''_N	*sce*

and the bi-ionic potentials (BIP) were determined by

Table 1. The Values of Membrane potentials E_m(mV) observed across parchment supported cupric iodide, manganese chromate and nickel chromate membranes at 25±0.1 C

Membrane / Concentration (N)	Cupric iodide KCl	Cupric iodide NaCl	Cupric iodide LiCl	Manganese chromate KCl	Manganese chromate NaCl	Manganese chromate LiCl	Nickel chromate KCl	Nickel chromate NaCl	Nickel chromate LiCl
1.0/0.1	3.98	−0.63	−11.10	11.28	5.69	1.02	−1.90	−8.00	−12.00
0.5/0.05	7.13	2.27	−8.42	12.02	5.80	1.94	−0.90	−7.30	−10.53
0.1/0.01	15.70	12.48	4.09	14.93	7.95	3.92	0.20	2.30	−1.10
0.05/0.005	24.76	16.51	10.83	18.13	12.48	7.34	10.53	7.50	4.30
0.01/0.001	32.12	27.70	21.08	32.98	27.91	23.48	29.90	25.23	20.23

setting up another cell of the type

sce	Solution AP	Membrane	Solution BP	*sce*

and keeping the same concentration of both the electrolytes AP and BP. The various salt solutions (chlorides of Li^+, Na^+, K^+) were prepared from analytical grade reagents and deionized water. All measurements were carried out using a water thermostat maintained at 25±0.1°C. The solutions on either sides of the membrane were vigorously stirred by a pair of magnetic stirrers.

RESULTS AND DISCUSSION

The values of membrane potential observed across parchment supported nickel chromate, manganese chromate and cupric iodide membranes in contact with various 1:1 electrolyte solutions are given in Table 1.

When two electrolyte solutions of different concentrations are separated by a membrane, the mobile species penetrate the membrane and various transport phenomena are induced in the system. The fixed charge concept of Teorell–Meyer–Sievers (TMS) for charged membranes is a pertinent starting point for the investigation of the actual mechanisms of the ionic or molecular processes which occur in the membrane phase. Recently Nagasawa *et al*[19] based on the fixed charge concept developed a theory for membrane potential and used it for the evaluation of effective fixed charge density of membranes. The total membrane potential E_m was considered as algebraic sum of diffusion potential E_d inside the membrane and electrostatic potential difference E_e between the membrane-solution interfaces on either side of the membrane, stated mathematically

$$E_m = E_d + E_e \tag{1a}$$

The diffusion potential E_d was obtained by integrating the basic flow equation for diffusion while the electrostatic potential difference E_e was calculated from Donnan's theory as follows

$$-E_d = -\left(\frac{J_0}{F\bar{C}_0}\right)\int_{'}^{''}\frac{\bar{X}}{(\bar{C}_- + \bar{X})u + \bar{C}_- v}\,dx + \left(\frac{RT}{F}\right)\int_{'}^{''}\frac{\bar{C}_- v}{(\bar{C}_- + \bar{X})u + \bar{C}_- v}\,d\ln \bar{a}_- \tag{1b}$$

$$-E_e = -\left(\frac{RT}{F}\right)\ln\left(\frac{\bar{a}'_- a''_-}{a'_- \bar{a}''_-}\right) \tag{1c}$$

where a' and a'' are the activities of the electrolytes on two sides of membrane, overbar refers the phenomena in the membrane phase. J_0 is the flow of water in absence of the external electric field, other symbols have their usual significance. On integration and putting the limit of high electrolyte concentrations, (1) gave the following approximate expression for membrane potential

$$E_m = \frac{RT}{F}\left(\frac{\nu-1}{\nu}\right)\left(\frac{\bar{X}}{2}\right)1/C''_N + \cdots \tag{2}$$

Equation 2 predicts a linear relationship between membrane potential E_m and $1/C''_N$. The straight line plots in Fig. 1 are in accordance (2). The values of $\bar{X}$ derived from the slope of the lines are given in Table 2.

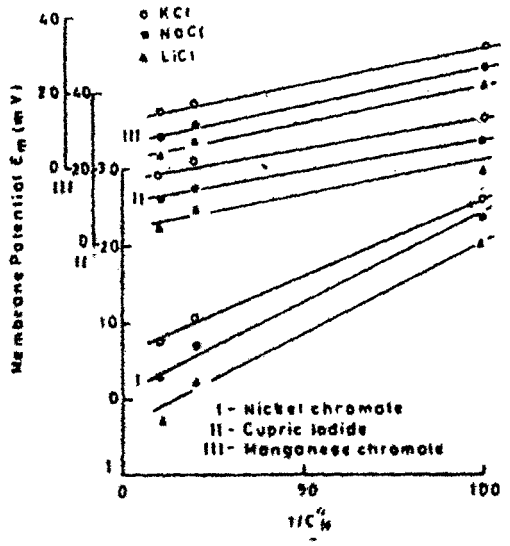

Fig. 1. Plots of membrane potentials E_m against $1/C''_N$ for various 1:1 electrolytes across (i) nickel chromate, (ii) manganese chromate, and (iii) cupric iodide membranes.

Table 2. The values of the thermodynamically effective fixed charge density (eq/l) of the parchment supported membranes

Membrane / Electrolyte	Nickel chromate	Cupric iodide	Manganese chromate
KCl	0.007	0.021	0.016
NaCl	0.009	0.030	0.017
LiCl	0.007	0.062	0.014

Low values of charge densities are in full agreement with our earlier findings[1, 2] of diffusion rate studies.

Bi-ionic potential

A steady state electromotive force of a cell containing two electrolytes AP and BP (*ie*, of the type NaCl and KCl) separated by a membrane is called the bi-ionic potential. This potential is a measure of selectivity of the membrane for the ions of the same sign. Various mathematically rigorous equations have been derived[21–23] and reviewed recently[24, 25]. More recently, Toyoshima and Nozaki[20] have derived an equation for membrane potential and bi-ionic potential using the principles of non-equilibrium thermodynamics and appropriate assumptions for the mobilities and activity coefficients of small ions in the membrane phase[20]. The effect of ionic interaction, mass flow and osmotic effect were neglected. For a negatively charge membrane separating two 1:1 electrolytes (common co-ions) of the same concentration, these authors derived the following expression for bi-ionic potential

$$E_{BP} = [2\ln K_A/K_B + \ln(JV_A + 1/JV_B + 1)](F/RT) \quad (3)$$

Knowing the values of parameters K_A, K_B, V_A, V_B and the flux J, the values of theoretical E_{BP} can be calculated using (3). For the evaluation of these parameters, following equations have been forwarded[20]

$$(2J + 1)\ln(g_A + 2J/g_B + 2J) - \ln(JV_A + 1/JV_B + 1) - \ln(g_A/g_B) = 0 \quad (4)$$

$$(N = A, B)$$

where

$$V_N = 1 + V_N^0/V_P^0 \quad (5a)$$

and

$$g_N = 1 + [1 + (2K_N C/\bar{X})^2]^{1/2} \quad (5b)$$

In order to derive the value of the parameters V_N and $\bar{X}$ occurring in (5a, 5b), Toyoshima and Nozaki[20] derived another equation (6) for membrane potential E_m arising across a membrane when it is used to

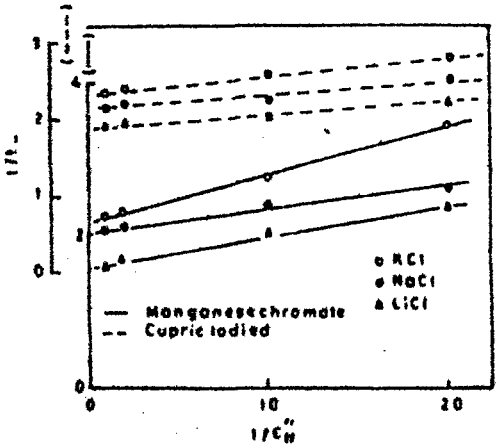

Fig. 2. Plots of $1/t_-$ against $1/C''_N$ across manganese chromate (——) and cupric iodide (- - -) membranes.

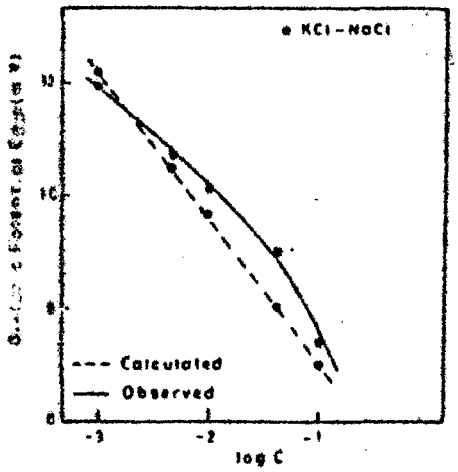

Fig. 3. Plots of bi-ionic potentials against log C for KCl–NaCl pair of electrolyte across manganese chromate membrane.

separate two solutions of an electrolyte at different concentrations C'_N and C''_N

$$(F/RT)E_m = -\ln v - (1 - 2/v_N) \times \ln \frac{\sqrt{1 + (2C''_N K_N/\bar{X})^2} + (1 - 2/v_N)}{\sqrt{1 + (2C'_N K_N/\bar{X})^2} + (1 - 2/v_N)} + \ln \frac{\sqrt{1 + (2C''_N K_N/\bar{X})^2} + 1}{\sqrt{1 + (2C'_N K_N/\bar{X})^2} + 1} \quad (6)$$

where

$$v = C''_N/C'_N$$

Equation (6) on expansion in powers of concentration, ratio $v = 10$ being kept constant, yield

$$(F/RT)E_m = -(1 - 2/v_N)\ln v - 2(1 - 1/v_N) \times (1/v_N)(1 - 1/v)(\bar{X}/K_N)(1/C''_N) + \cdots \quad (7)$$

The apparent transference number t_- for co-ion was defined by the Nernst equation

$$-(F/RT)E_m = (1 - 2t_-)\ln v \quad (8)$$

Combining equations (7) and (8) and expanding $1/t_-$ as a power of series of $1/C''_N$, following expression was obtained

$$1/t_- = v_N + (v_N - 1)\left[\frac{v - 1}{v \ln v}\right]\left(\frac{\bar{X}}{K_N}\right)(1/C''_N) + \cdots \quad (9)$$

Table 3. The values of the membrane parameters V_N and $(\bar{X}/K_N)$ derived from the Toyoshima and Nozaki theory for parchment supported membranes

Membrane	Cupric iodide		Manganese chromate	
Parameters	V_N	$\bar{X}/K_N$	V_N	$\bar{X}/K_N$
KCl	2.10	0.155	2.45	0.035
NaCl	1.95	0.123	2.25	0.032
LiCl	1.08	0.150	2.05	0.031

Equation 9 predicts a linear relationship between $1/t_-$ and $1/C_N^n$. The values of v_N and $(\bar{X}/K_N)$ can be determined from the ordinate intercept and initial slope of a plot for $1/t_-$ against $1/C_N^n$. The values of v_N and $(\bar{X}/K_N)$ thus derived for the membrane and various 1:1 electrolyte systems using Fig. 2, are given in Table 3. These values of v_N and $(\bar{X}/K_N)$ were then used to calculate J and g_N using (4) and (5). Once the membrane parameters v_N, g_N, J and $(\bar{X}/K_N)$ are known for the membrane-electrolyte systems, one can calculate theoretical bi-ionic potential using (3). The bi-ionic potential thus obtained were plotted as a function of log C in Fig. 3 (shown by broken line). In order to compare the theoretical bi-ionic potential values, the observed bi-ionic potentials were also plotted in the same graph (shown by solid lines). Fig 3 demonstrates that the theoretical predictions are borne out quite satisfactorily by our experimental results on parchment supported membranes. However, a slight deviation in the values may be accounted due to various reasons, most notably due to the low fixed charge density of the membranes.

Acknowledgements - The authors are grateful to Professor Wasiur Rahman, Head, Department of Chemistry for providing research facilities and to C.S.I.R. (India) for the award of fellowship to SPS, PP and VG.

REFERENCES

1. F. A. Siddiqi, M. N. Beg, S. P. Singh and A. Haque, *Electrochim. Acta* **22**, 631, 638 (1977); *Bull. Chem. Soc. Japan* **49**, 2854, 2864 (1976).
2. F. A. Siddiqi, M. N. Beg and P. Prakash, *J. electroanal. Chem.* **80**, 223 (1977); *J. Polymer Sci.* (in press); *J. electroanal. Chem.* (in press).
3. F. A. Siddiqi, M. N. Beg, P. Prakash and S. P. Singh, *Indian J. Chem.* **16A**, 7 (1978).
4. F. A. Siddiqi, M. N. Beg and S. P. Singh, *J. Polymer Sci.* **15**, 959 (1977).
5. M. N. Beg, F. A. Siddiqi and R. Shyam, *Can. J. Chem.* **55**, 1650 (1977).
6. M. N. Beg, F. A. Siddiqi, R. Shyam and M. Arshad, *J. Membrane Sci.* **2**, 365 (1977).
7. N. Lakshminarayanaiah and F. A. Siddiqi, *J. Polymer Sci.* **8**, 2949 (1970); *Biophys. J.* **11**, 603, 1617 (1971); *ibid.* **12**, 540 (1972); *Z. phys. Chem.* (Frankfurt) **78**, 150 (1972); in *Membrane Process in Industry and Biomedicine*, (Edited by M. Bier). Plenum Press New York (1971).
8. O. Kedem and A. Katchalsky, *Trans. Faraday Soc.* **59**, 1918, 1931, 1941 (1963).
9. A. M. Liquori and C. Botre, *Ric. Sci.* **34**(6), 71 (1964); *J. phys. Chem.* **71**, 3765 (1967).
10. R. M. Hays, *J. Gen. Physiol.* **51**, 385 (1968).
11. F. De Korosy, *J. phys. Chem.* **72**, 2591 (1968).
12. Y. Kobatake, T. Noviaki, Y. Toyoshima and H. Fujita, *J. phys. Chem.* **60**, 3981 (1965).
13. Y. Toyoshima, M. Yuassa, Y. Kobatake and H. Fujita, *Trans. Faraday Soc.* **63**, 2803, 2814 (1967); *J. phys. Chem.* **72**, 2871 (1968).
14. J. A. M. Smit and A. J. Staverman, *J. phys. Chem.* **74**, 966 (1970).
15. K. S. Speigler, *Trans. Faraday Soc.* **54**, 1408 (1958).
16. R. J. Bearman and J. W. Kirkwood, *J. chem. Phys.* **28**, 136 (1958).
17. I. W. Richardson, *Bull. Math. Biophysics.* **32**, 237 (1970).
18. G. Scatchard, *Discuss. Faraday Soc.* **21**, 30 (1956); *J. Am. Chem. Soc.* **21**, 30 (1956).
19. M. Tasaka, N. Aoki, Y. Konda and M. Nagasawa, *J. phys. Chem.* **79**, 1307 (1975).
20. Y. Toyoshima and H. Nozaki, *J. phys. Chem.* **74**, 2704 (1970).
21. C. E. Marshall, *J. phys. Chem.* **52**, 1284 (1948).
22. K. Sollner, *J. phys. Chem.* **53**, 1211 (1952); *ibid.* **53**, 1226 (1949).
23. M. R. J. Wyllie, *J. phys. Chem.* **58**, 67 (1954).
24. R. P. Buck, *CRC Critical Reviews in Analytical Chemistry* (1976).
25. F. Helfferich, *Ion Exchange*. McGraw-Hill, New York (1962).

Journal of Membrane Science, 4 (1978) 275–281
Elsevier Scientific Publishing Company, Amsterdam – Printed in The Netherlands

Short Communication

STUDIES WITH MODEL MEMBRANES

XXV. EVALUATION OF MEMBRANE PARAMETERS AND TEST OF THE THEORY OF BI-IONIC POTENTIAL BASED ON THE THERMODYNAMICS OF IRREVERSIBLE PROCESSES

M. NASIM BEG, FASIH A. SIDDIQI*, M. IBADUR RAHMAN KHAN, M. AQUEEL AHSAN and BADRUL ISLAM

Membrane Research Laboratory, Department of Chemistry, Aligarh Muslim University, Aligarh, U.P. (India)

(Received November 7, 1977, in revised form June 27, 1978)

Summary

Membrane potentials and bi-ionic potentials observed across polystyrene-based cupric phosphate and aluminum vanadate membranes using various 1 : 1 electrolytes are reported. Theoretical equations derived recently by Toyoshima and Nozaki for the membrane potential and bi-ionic potential based on non-equilibrium thermodynamics have been used for the evaluation of various membrane parameters. The derived membrane parameters have been used to examine the validity of the theory utilized. Theoretical predictions were borne out quite satisfactorily by our experimental results.

Introduction

In order to elucidate the mechanism of transport through biological systems, we have developed a large number of parchment supported [1–4] and polymeric composite membranes [5, 6] which can serve as models for biological cells [7–14]. The Kedem Katchalsky theory of composite membranes [15] has been used for the evaluation of various membrane parameters. Spiegler's model [16] and equations developed by Scattergood and Lightfoot [17] have also been used successfully to obtain Maxwell diffusivity coefficients. Recently developed theories of Kobatake et al. [18–20] and Nagasawa et al. [21–24] for membrane potentials based on the thermodynamics of irreversible processes have been applied to determine the thermodynamically effective fixed charge density and permselectivity of the membranes [25, 26].

In this communication, membrane potentials and bi-ionic potentials observed across polystyrene-based cupric phosphate and aluminum vanadate

*Present address: Department of Biophysics, Michigan State University, East Lansing, Michigan, 48824, U.S.A.

membranes using various 1 : 1 electrolytes are described. An attempt has been made to examine the validity of the recently developed theory of Toyoshima and Nozaki [27] for membrane potential.

Experimental

Cupric phosphate and aluminum vanadate precipitates were obtained by mixing an aqueous solution of 0.2 *M* cupric nitrate with 0.2 *M* sodium orthophosphate, and 0.2 *M* aluminum chloride with 0.2 *M* sodium orthovanadate solutions, respectively. Cupric phosphate and aluminum vanadate ion exchange precipitates thus obtained were washed well with deionized water, dried, and powdered. The membranes were then prepared by the method based on U.S. Patent No. 2,614,976 [28]. The ion exchanger was mixed with 200 mesh polystyrene granules and pressed under suitable conditions of temperature and pressure. The optimum temperature and pressure for cupric phosphate and aluminum vanadate membranes were 97 and 80° C, and 11,000 and 10,800 psi, respectively. Mechanically strong membranes giving reproducible results were obtained when the cupric phosphate was embedded in 32% by weight polystyrene. Somewhat less binder (25%) was required for the aluminium vanadate membranes. Bi-ionic potentials (BIP) arising across the membrane were measured by constructing a cell of the type

Ag AgCl	Solution C′	Membrane	Solution C″	Ag AgCl

by taking the same concentration of the two electrolyte solutions on the two sides of the membrane. The membrane potential E_m was obtained by taking the same electrolyte at different concentrations on the two sides of the membrane, such that the concentration ratio $a = C'/C'' = 10$. The potentials were monitored by means of a Pye precision Potentiometer No. 7568. The membrane potential E_m observed across Ag AgCl electrodes is equal to the sum of the membrane potential E_m and the concentration potential E_c. The concentration potential E_c was calculated from the Nernst equation $E_c = (RT/F) \ln (f'C'/f''C'')$, and the membrane potential E_m was obtained by subtraction. All measurements were carried out using a water thermostat maintained at 25 ± 0.1° C. The solutions in both compartments were stirred with a magnetic stirrer. Various salt solutions were prepared from analytical grade reagents and deionized water.

Results and discussion

The values of observed membrane potentials generated across polystyrene-based cupric phosphate and aluminum vanadate membranes using various 1 : 1 electrolytes are given in Tables 1 and 2. Bi-ionic potential values are depicted in Fig.1.

When an ion exchange membrane is interposed between two solutions of the

TABLE 1

Observed membrane potentials E_m (mV) for various electrolytes at different concentrations across a cupric phosphate membrane at 25 ± 0.1° C

Electrolyte	E_m at concentration value given in eq./l							
	1	0.5	0.2	0.1	0.05	0.02	0.01	0.005
	0.1	0.05	0.02	0.01	0.005	0.001	0.001	0.0005
KCl	0.42	6.03	15.63	26.75	34.57	47.50	51.56	52.54
NaCl	4.14	1.18	11.56	24.06	30.88	51.09	52.43	52.50
NH_4Cl	3.39	0.25	3.98	14.80	18.50	31.82	37.30	41.90

TABLE 2

Observed membrane potentials E_m (mV) for various electrolytes at different concentrations across an aluminum vanadate membrane at 25 ± 0.1° C

Electrolyte	E_m at concentration value given in eq./l					
	1.0	0.1	0.05	0.01	0.005	0.001
	0.1	0.01	0.005	0.001	0.0005	0.0001
KCl	6.58	5.15	9.25	26.56	34.00	47.50
NaCl	2.16	2.00	6.50	13.00	15.55	36.58
NH_4Cl	5.30	3.15	7.50	28.00	32.23	43.90
LiCl	−12.19	−7.05	0.85	5.66	10.06	20.18

same electrolyte at different concentrations, the potential difference developed is called the concentration potential or the membrane potential. The sign and magnitude of this emf gives the selectivity of the membrane toward the ions of the electrolyte. If the membrane separates two different electrolates of the same concentration, the potential developed is called the bi-ionic potential which is a measure of the selectivity to ions of the same sign. Various theories for the potential generated across a membrane have been put forward and reviewed recently by a number of investigators [15—24]. Most recently Toyoshima and Nozaki developed theoretical equations for the bi-ionic potential considering a negatively charged membrane interposed between two simple 1 : 1 electrolytes (with common coion) at the same concentration. The system considered was isothermal and no electric field was applied externally. The following assumptions for the concentration dependence of mobilities and activities of the ions were also used in the derivation:

$$u_+c_+ = u_+^\circ (c_- + \theta) \quad (1)$$

$$u_-c_- = u_-^\circ c_- \quad (2)$$

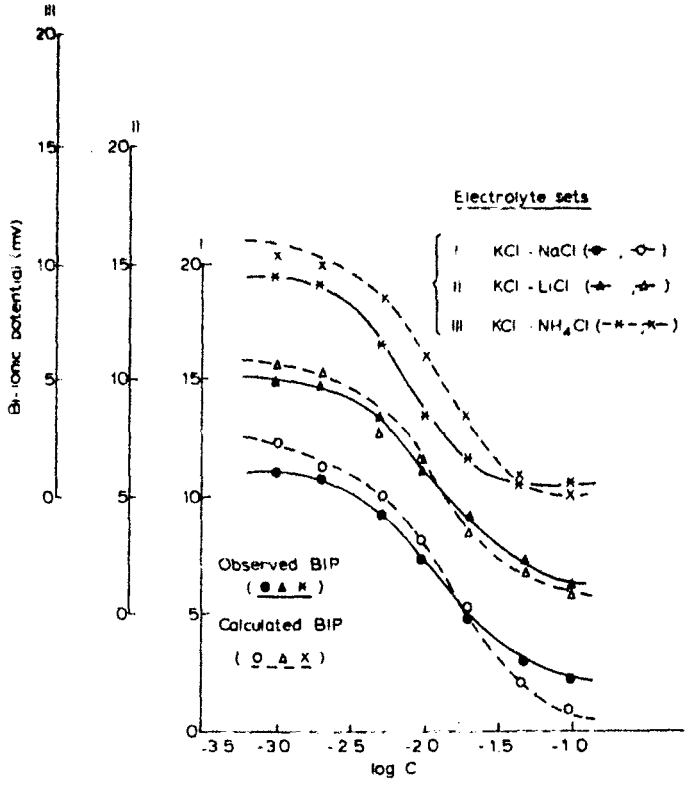

Fig. 1. Plots of observed and theoretically calculated bi-ionic potentials (mV) against log C using a polystyrene-based aluminum vanadate membrane at 25 ± 0.1° C.

$$a_+ = \gamma_+^0 (c_- + \theta) \quad (3)$$

$$a_- = \gamma_-^0 \quad (4)$$

where u_i, c_i, and a_i are the mobility, molar concentration, and activity of ion i (i = + or −); and u_i^0 and γ_i^0 are the mobility and activity coefficient of ion i in free solution. The quantity θ is the thermodynamically effective fixed charge density of the membrane. Thus, the following equation for the bi-ionic potential was derived [27]

$$E_{BIP} = (RT/F)\ [2\ln(K_A/K_B) + \ln(JV_A + 1)/(JV_B + 1)] \quad (5)$$

where J and g were defined as

$$(2J+1)\ln(g_A+2J)/(g_B+2J) - \ln(JV_A + 1)/(JV_B + 1) - \ln(g_n/g_B) = 0$$

and

$$g_N = [1 + \{1 + (2CK_N/\theta)^2\}^{1/2}] \quad (7)$$

V_N is the cationic mobility (N ≡ A or B) and J is the electrolyte flux. The other symbols have their usual significance.

Using the same basic flow equations and assumptions for mobilities and activities of movable ions within the membrane, Toyoshima and Nozaki [27] derived the following equation for the membrane potential E_m

$$E_m = \left(\frac{RT}{F}\right)\left[-\ln\sigma - (1 - 2/V_N)\ln\frac{\sqrt{1 + (2K_N C''_N/\theta)^2} + (1 - 2/V_N)}{\sqrt{1 + (2K_N C'_N/\theta)^2} + (1 - 2/V_N)}\right.$$

$$\left. + \ln\frac{\sqrt{1 + (2K_N C''_N/\theta)^2} + 1}{\sqrt{1 + (2K_N C'_N/\theta)^2} + 1}\right] \qquad (8)$$

On expanding in powers of $1/C'_N$, with the concentration ratio being kept constant, eqn. (8) yields

$$-E_m = \left(\frac{RT}{F}\right)[(1 - 2/V_N)\ln\sigma - 2(1 - 1/V_N)(1/V_N)(1 - 1/\sigma)(\theta/K_N)(1/C'_N) + \ldots] \qquad (9)$$

The apparent transference number $t_{-\,app}$ of the coion was defined by the Nernst equation

$$E_m = -\left(\frac{RT}{F}\right)(1 - 2\,t_{-app})\ln C'/C'' \qquad (10)$$

Introducing eqn. (9) into (10) and expanding the resulting equation as a power series in $1/C'_N$, the following expression was obtained:

$$1/t_{-app} = V_N + (V_N - 1)\{(\sigma - 1)/\sigma\ln\sigma\}(\theta/K_N)(1/C'_N) + \ldots \qquad (11)$$

Eqn. (11) predicts a linear relationship between $1/t_{-app}$ and $1/C'_N$. The values of V_N and θ/K_N for a membrane-electrolyte system can be evaluated from the

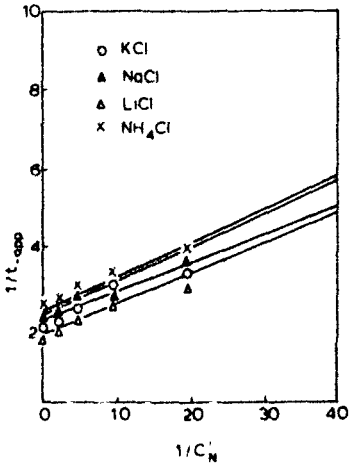

Fig. 2. Plots of $1/t_{-app}$ against $1/C'_N$ using various 1:1 electrolytes through polystyrene based aluminium vanadate membrane at 25 ± 0.1° C.

TABLE 3

Derived values of V_N and θ/K_N for polystyrene-based inorganic precipitate membranes in contact with various 1 : 1 electrolyte solutions at 25 ± 0.1° C

Electrolyte	Cupric phosphate		Aluminum vanadate	
	V_N (cm sec^{-1})	θ/K_N	V_N (cm sec^{-1})	θ/K_N
KCl	2.00	0.160	1.88	0.021
NaCl	1.80	0.120	1.90	0.023
LiCl			1.70	0.022

TABLE 4

Values of the parameter g_N for polystyrene-based membranes in contact with various 1 : 1 electrolyte solutions at different concentrations at 25 ± 0.1° C

Membrane	Electrolyte	g_N at concentration value given in eq./l						
		0.1	0.05	0.02	0.01	0.005	0.002	0.001
Cupric phosphate	KCl	2.25	2.17	2.03	2.01	2.00	2.00	2.00
	NaCl	2.90	2.30	2.05	2.01	2.00	2.00	2.00
	LiCl	3.00	2.80	2.55	2.40	2.11	2.00	2.00
Aluminum vanadate	KCl	10.50	5.80	3.20	2.30	2.01	2.01	2.00
	NaCl	9.75	5.34	2.73	2.40	2.30	2.05	2.00
	LiCl	10.10	6.35	3.40	2.70	2.20	2.03	2.00

ordinate intercept and initial slope of a plot of $1/t_{-app}$ vs. $1/C'_N$. The values of V_N and θ/K_N so obtained using Fig.2 are given in Table 3. These values of V_N and θ/K_N may now be utilized to give the value for g_N (Table 4) using eqn. (7). Once the membrane parameters V_N, g_N, and θ/K_N for a membrane-electrolyte system are known, one can calculate the theoretical BIP at an electrolyte concentration using eqns. (5) and (6). The values of BIP thus calculated are plotted in Fig.1 as a function of electrolyte concentration C (shown by dashed lines). These calculated values can be compared with the observed bi-ionic potentials (shown by solid lines). Fig.1 demonstrates that the theoretical predictions are quite satisfactorily borne out by our experimental results, thereby confirming the validity of Toyoshima and Nozaki's theory to the system under investigation. The slight deviation observed may be due to the interaction of ions with the membranes of low fixed charge density [29].

Acknowledgements

The authors are grateful to Prof. Wasiur Rahman, Head of Department of

Chemistry, Aligarh Muslim University, Aligarh, for providing the necessary research facilities, and to C.S.I.R. (India) for the award of fellowships to M.I.R.K. M.A.A. and B.I.

References

1 F.A. Siddiqi, M. Ibadur Rahman Khan, S.K. Saksena and M. Aqueel Ahsan, J. Membrane Sci., 2 (1977) 245.
2 F.A. Siddiqi, M. Naseem Beg, A. Haq, M. Aqueel Ahsan and M. Ibadur Rahman Khan, J. De Chimie Physique, 74 (1977) 932.
3 F.A. Siddiqi, S.K. Saksena and M. Ibadur Rahman Khan, J. Polym. Sci., 15 (1977) 1935.
4 F.A. Siddiqi, M.N. Beg, A. Haq and S.P. Singh, Bull. Chem. Soc. Jap., 49, No. 10 (1976) 2858.
5 W.U. Malik and F.A. Siddiqi, J. Colloid Sci., 18 (1963) 161; Proc. Indian Acad. Sci., A56 (1962) 206.
6 W.U. Malik, F.A. Siddiqi and H. Arif, Bull. Chem. Soc. Jap., 40 (1967) 1741.
7 F.A. Siddiqi, N. Lakshminarayanaiah and M.N. Beg, J. Polym. Sci., A-1, 9 (1971) 2853, 2868.
8 N. Lakshminarayanaiah and F.A. Siddiqi, Biophys. J., 11 (1971) 603, 617; ibid., 12 (1972) 540.
9 N. Lakshminarayanaiah and F.A. Siddiqi, in M. Bier (Ed.), Membrane Processes in Industry and Biomedicine, Plenum Press, New York, 1971, p. 301; J. Polym. Sci., 8 (1970) 2949; Z. Physik. Chem. (Frankfurt), 78 (1972) 150.
10 T. Teorell, Discuss. Faraday Soc., No. 21 (1956) 9.
11 A.M. Liquori and C. Botre, Ric. Sci., 34 (1964) 6.
12 A.M. Liquori and C. Botre, J. Phys. Chem., 71 (1967) 3765.
13 A.M. Liquori, L. Constantino and G. Segree, Ric. Sci., 36 (1966) 591.
14 C. Botre, S. Borghi and M. Merchetti, Biochim. Biophys. Acta., 135 (1967) 162, 208; ibid.,4 (1966) 1064.
15 O. Kedem and A. Katchalsky, Trans. Faraday Soc., 59 (1963) 1918, 1931, 1941.
16 K.S. Spiegler, Trans. Faraday Soc., 54 (1958) 1408.
17 E.M. Scattergood and E.N. Lightfoot, Trans. Faraday Soc., 64 (1968) 1135.
18 Y. Kobatake, N. Takeguchi, Y. Toyoshima and H. Fujita, J. Phys. Chem., 69 (1965) 3981.
19 Y. Kobatake, Y. Toyoshima and N. Takeguchi, J. Phys. Chem., 70 (1966) 1187.
20 N. Kamo, M. Oikawa and Y. Kobatake, J. Phys. Chem., (1973) 77, 92.
21 M. Nagasawa and Y. Kobatake, J. Phys. Chem., 56 (1952) 1017.
22 M. Nagasawa and I. Kagawa, Discuss. Faraday Soc., 21 (1956) 52.
23 M. Tasaka, N. Aoki, Y. Kondo and M. Nagasawa, J. Phys. Chem., 79 (1975) 1307.
24 M. Nagasawa, in E. Selegny (Ed.), Polyelectrolytes, D. Ridel, Dordrecht, The Netherlands, 1974, p. 57.
25 M.N. Beg, F.A. Siddiqi, R. Shyam and M. Arshad, J. Membrane Sci., 2 (1977) 365.
26 M.N. Beg, F.A. Siddiqi and R. Shyam, Canadian J. Chem., 55 (1977) 1680.
27 Y. Toyoshima and H. Nozaki, J. Phys. Chem., 74 (1970) 2704.
28 W.U. Malik, S.K. Srivastava, V.M. Bhandari and S. Kumar, J. Colloid Interface Sci., 47 (1974) 1.
29 J.P. Sandblom and J. Eisenman, Biophys. J., 7 (1967) 217.

Indian Journal of Technology
Vol. 21, February 1983, pp. 78-82

Evaluation of Membrane Selectivity and Biionic Potential of Polystyrene-Based Ferric Orthovanadate Membrane

M NASIM BEG, FASIH A SIDDIQI & M AQUEEL AHSAN
Membrane Research Laboratory, Department of Chemistry, Aligarh Muslim University, Aligarh 202001

Indian Journal of Technology
Vol. 21, February 1983, pp. 78-81

Evaluation of Membrane Selectivity and Biionic Potential of Polystyrene-Based Ferric Orthovanadate Membrane

M NASIM BEG, FASIH A SIDDIQI & M AQUEEL AHSAN
Membrane Research Laboratory, Department of Chemistry, Aligarh Muslim University, Aligarh 202001

Received 26 *April* 1982; *accepted* 30 *December* 1982

Membrane potential, biionic potential and membrane conductance through polystyrene moulded ferric orthovanadate membrane in contact with alkali metal chlorides were experimentally measured. Equations derived by Toyoshima and Nozaki for the membrane potential and biionic potential based on non-equilibrium thermodynamics were used to calculate the theoretical biionic potentials. The theoretical predictions were borne out satisfactorily by our experimental results. The observed biionic potential and membrane conductance values were also used to evaluate membrane selectivity and permeability ratio using emperical equations of Wyllie and Kanaan and the equations developed by Sandblom and Eisenman. The membrane was found to have low selectivity values and its selectivity was in the order $K^+ > Na^+ > Li^+$.

We have in the past attempted to understand model membranes[1-3] such as parchment supported and polymeric composite membranes[4,5] which bear a close resemblance to the gastric mucosal membrane[6] and the nerve cell[7,8] respectively. In this paper we report a series of membrane potentials, biionic potentials and membrane conductance through polystyrene based ferric orthovanadate membrane and use them for the evaluation of membrane selectivity and permeability ratio obtained using the theoretical equations developed by Sandblom and Eisenman[9,10] based on thermodynamics of irreversible processes. The observed biionic potentials (BIP) have been compared with these calculated using the theory developed by Toyoshima and Nozaki[11].

Experimental Procedure

Preparation of membrane - Polystyrene-based ferric orthovanadate membrane was prepared by mixing 0.2 *M* ferric chloride and 0.2 *M* sodium orthovanadate solutions. The ferric orthovanadate gel thus obtained was well washed with deionized water, dried and finely powdered. The membrane was prepared by the method suggested by Siddiqi *et al.*[12]. Polystyrene granules were grined into fine particles and sieved by 100 mesh. The optimum quantity of binder to be embedded in order to get membrane of adequate mechanical strength was found by using different ratios of binder. The ferric orthovanadate membrane prepared by embedding 25% of binder was found suitable for our purpose. Those containing larger amount of binder did not give reproducible results while those containing lesser amount were unstable. The membrane was moulded at 70 C under a pressure of 10,000 psi. The ferric orthovanadate membrane thus prepared was found to give quite reproducible results.

Measurement of membrane potentials and biionic potentials Biionic potentials arising across the membrane were measured using alkali metal halide solutions in a cell of the type:

$$\text{Hg-Hg}_2\text{Cl}_2 \,|\, \underset{\text{KCl}}{\text{Saturated}} \,|\, \underset{(')}{\text{Solution}} \,|\, \text{Membrane} \,|\, \underset{('')}{\text{Solution}} \,|\, \underset{\text{KCl}}{\text{Saturated}} \,|\, \text{Hg-Hg}_2\text{Cl}_2$$

The concentrations of electrolyte solutions were the same on both sides of the membrane. The membrane potential was obtained by taking different concentrations of the same electrolyte on the two sides of the membrane, such that the concentration ratio $\sigma = C'/C'' = 10$. The solutions were stirred by means of magnetic stirrers. The potentials were monitored with the help of a Pye precision vernier potentiometer (No. 7568).

Measurement of membrane conductance - For the measurement of membrane conductance the membrane was first dipped and equilibrated in an appropriate electrolyte solution and then clamped between two half cells as shown in Fig. 1. The measurements were made using a conductivity bridge (Cambridge Instrument Co. Ltd, England).

All the measurements were carried out in a water thermostat at 25 C. Various salt solutions were prepared from analytical grade reagents and deionized water.

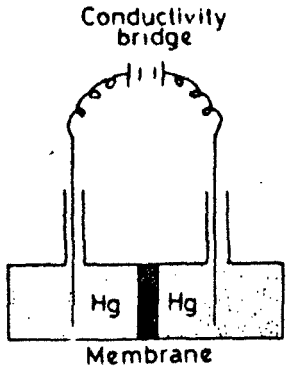

Fig. 1 Schematic diagram of the cell for measurement of membrane conductance

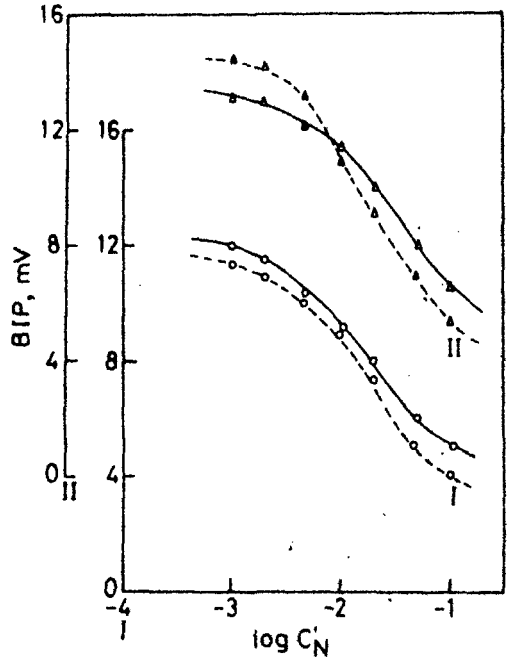

Fig. 2 Comparison of observed (– – –) and calculated (——) BIP for KCl-NaCl (○), and KCl-LiCl (Δ) electrolyte sets through ferric orthovanadate membrane

Result and Discussion

The observed BIP through ferric orthovanadate membrane with the uni-univalent electrolytes at different concentrations are depicted in Fig. 2.

The most important property of a membrane governing the membrane phenomena is its electromotive behaviour in concentration chains. If a membrane is interposed between two solutions, of the same electrolyte at different concentrations an electromotive force arises that is different in most instances from the liquid junction potential. The electromotive force arising in such a membrane—concentration chain is customarily referred to as the membrane potential. The sign and magnitude of the membrane potential depend on the concentration ratio, the nature of the electrolyte used and the nature of the membrane.

The dynamic membrane potential which arises across a membrane separating the solutions of two electrolytes having different "critical" cations which are able to exchange across the membrane, and the same "noncritical" ion species for which the membrane is ideally impermeable is called the biionic potential. The sign and magnitude of the BIP depend on the relative ease with which the two species of critical ions can penetrate across the membrane. The BIP as a measure for the selectivity of a membrane for the ions of the same sign has been the subject of many theoretical and experimental studies but it appears that no satisfactory results have as yet been established. Mathematically rigorous equations were derived on the basis of the thermodynamics of irreversible processes by Scatchard[13] and Helfferich[14]. In their derivations[11], Toyoshima and Nozaki[11] neglected the effect of flow of anion on the BIP. Moreover, these types of treatment did not provide much information about the actual mechanism which produces the observed BIP.

In a system of negatively charged ionizable membrane and a uni-univalent electrolyte, Toyoshima and Nozaki[11] proposed the following assumptions:

$$u_+ C_+ = u_+^0 (C + \theta) \quad \ldots (1)$$

$$u_- C_- = u_-^0 C \quad \ldots (2)$$

$$a_+ = \gamma_+^0 (C + \theta) \quad \ldots (3)$$

$$a_- = \gamma_-^0 C \quad \ldots (4)$$

where u_i^0 and γ_i^0 are the mobility and activity coefficient of ion i (i = +, −) in free solutions. The quantity θ is often called the "thermodynamically effective fixed charge density" of the membrane. a_i and C_i are the activity and concentration of ion i (i = +, −) in membrane phase. Toyoshima and Nozaki[11] derived the following theoretical equations for BIP and membrane potential using the appropriate assumptions for the mobilities and activity coefficients of small movable ions in the membrane phase and the basic flow equations for a system consisting of two uni-univalent electrolytes separating a negatively charged membrane.

$$\mathrm{BIP} = \left[2 \ln\left(\frac{K_A}{K_B}\right) + \ln(JV_A + 1)/(JV_B + 1) \right] \frac{RT}{F} \quad \ldots (5)$$

where K_A/K_B is the selectivity constant of a membrane for positive ions and the terms V_N, g_N and J are defined as

$$V_N = (1 + u_+^0 - u_-^0) \quad \ldots (6)$$

$$(2J+1)\ln(g_A + 2J)(g_B + 2J) - \ln(JV_A + 1)/(JV_B + 1) - \ln(g_A/g_B) = 0 \quad \ldots (7)$$

$$\ldots [1 + \{1 + (2C_N K_N/\theta)^2\}^{1/2}] \quad \ldots (8)$$

λ_N is the cationic mobility, (N = A or B) and J is the electrolyte flux. Other symbols have their usual significance.

In order to evaluate V_N and θ/K_N the following equation for membrane potential, E_m, is used:

$$E_m = \left(\frac{RT}{F}\right)\left[-\ln\sigma - (1-2V_N)\ln\frac{\sqrt{1+(2K_N C'_N/\theta)^2}+(1-2V_N)}{\sqrt{1+(2K_N C''_N/\theta)^2}+(1-2V_N)} + \ln\frac{\sqrt{1+(2C'_N K_N/\theta)^2}+1}{\sqrt{1+(2C''_N K_N/\theta)^2}+1}\right] \quad \ldots (9)$$

where C' and C'' are the concentrations of electrolyte solution on the two sides of the membrane in each case and σ is the concentration ratio. In the derivation of Eq. (9), the effect of the stagnant layers has been neglected and its expansion in powers of $1/C'$ with concentration ratio being kept constant yields:

$$-E_m = \left(\frac{RT}{F}\right)\left[\left(1-\frac{2}{V_N}\right)\ln\sigma - 2\left(1-\frac{1}{V_N}\right)\left(\frac{1}{V_N}\right)\left(1-\frac{1}{\sigma}\right)\left(\frac{\theta}{K_N}\right)\left(\frac{1}{C'_N}\right) + \ldots\right] \quad \ldots (10)$$

The apparent transference number t_{app} for anions is defined by the Nernst equation

$$E_m = -\frac{RT}{F}(1-2t_{app})\ln\frac{C'}{C''} \quad \ldots (11)$$

On introducing Eq. (10) into Eq. (11) and expanding $1/t_{app}$ as a power series in $1/C'_N$ the following equation was obtained.

$$\frac{1}{t_{app}} = V_N + (V_N - 1)\{(\sigma-1)\sigma\ln\sigma\}\left(\frac{\theta}{K_N}\right)\left(\frac{1}{C'_N}\right) + \ldots \quad \ldots (12)$$

Eq. (12) indicates that the slope and intercept of a plot of $1/t_{app}$ against $1/C'_N$ at fixed σ (Fig. 3) allows the calculation of the values of V_N and θ/K_N. These values of V_N and θ/K_N may now be utilized to evaluate the value of g_N from Eq. (7). Once these parameters for a membrane-electrolyte system are known, one can calculate the theoretical BIP at an electrolyte concentration using Eq. (5). The values of BIP thus calculated are plotted as a function of electrolyte concentration C'_N (shown by dotted lines in Fig. 2). The observed BIP values across ferric orthovanadate membrane were also plotted in the same graph (shown by solid lines in Fig. 2). It is apparent from Fig. 2 that the agreement between the observed and theoretical values of BIP are fair for polystyrene moulded ferric orthovanadate membrane and it may be concluded that the theory of BIP developed by Toyoshima and Nozaki[11] based on the thermodynamics of irreversible processes is applicable to the polystyrene based inorganic precipitate membranes.

The BIP for counterions of equal valence is also given by the expression

$$\text{BIP} = \frac{RT}{ZF}\ln\left(\frac{\bar{D}_i\bar{a}_i\gamma'_i}{\bar{D}_j\bar{a}_j\gamma''_j}\right) \quad \ldots (13)$$

The symbols a, D and γ represent respectively the activities, diffusion coefficients and activity coefficients of ions (i and j) on the two sides ($'$) and ($''$). The bar refers to the membrane phase. Other symbols have their usual significance. Eq. (13) reduces to

$$\text{BIP} = \frac{RT}{ZF}\ln\left(\frac{a_i\bar{u}_i}{a_j\bar{u}_j}\right) \quad \ldots (14)$$

provided that $\gamma'_i = \gamma''_j$ and the diffusion coefficient $\bar{D}_i/\bar{D}_j$ is replaced by intramembrane mobility ratio $(\bar{u}_i/\bar{u}_j)$. The intramembrane mobility ratio has been related to the selectivity constant or the ion exchange equilibrium constant K_{ij} by the expression[15,16].

$$\frac{\bar{u}_i}{\bar{u}_j} = k_{ij}\left(\frac{\lambda_i}{\lambda_j}\right) \quad \ldots (15)$$

where λ_i and λ_j are the experimentally measured conductivity of the membrane when it is purely in the form of i or j. Membrane conductance measurements were carried out when it is wholly in the form of i or j.

The conductance of ferric orthovanadate membrane bathed in different concentrations of potassium, sodium and lithium chloride solutions are plotted against concentration in Fig. 4. For all the three electrolytes conductance of the membrane increases with decrease in concentration of the bathing electrolyte solutions and attains a maximum limiting value. The flow of ion and water are generally larger in the more open structure of the membrane and decrease as the membrane shrinks in more concentrated solution in part at least due to the increased

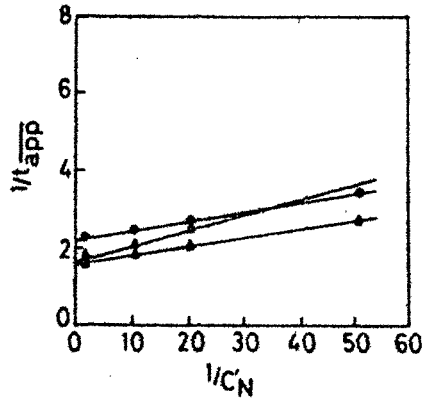

Fig. 3— Plots of $1/t_{app}$ vs $1/C'_N$ for KCl (●), NaCl (▲) and LiCl (Δ) electrolytes through ferric orthovanadate membrane

obstruction of the polymer matrix as diffusional pathways become more tortuous and the fractional pore volume decreases. On the other hand, the membrane conductance should increase with the increased salt uptake. These two opposing effects operate simultaneously and at higher concentration as shown in Fig. 4, the effect of salt uptake by the membrane overcomes the effect of increased tortuousity and thus membrane conductance become almost constant. The sequence of membrane conductance for the alkali metal ions was found to be

$$K^+ > Na^+ > Li^+$$

which follows the order of their ionic radii. A similar behaviour is observed by others[17-24]. Our own findings with inorganic precipitate membranes[4,5,12] also bears this out.

The BIP values were used to calculate intramembrane mobility ratio (u_i/u_j) using Eq. (14). The selectivity constant K_{ij} was thus evaluated from the predetermined values of intramembrane mobility ratio

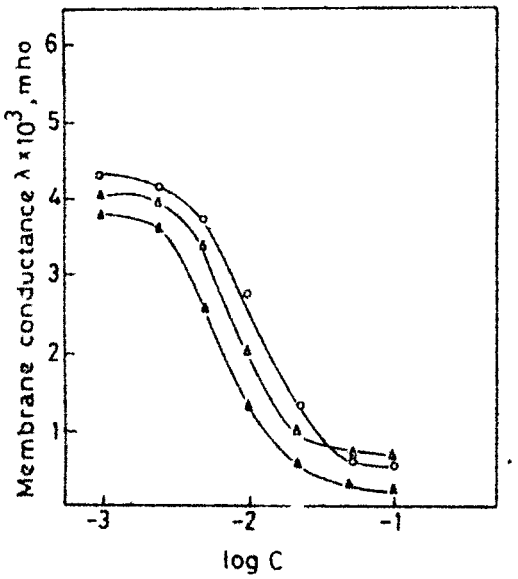

Fig. 4 Plots of membrane conductance $\times 10^3$ (mohs) vs concentration for KCl (○), NaCl (▲) and LiCl (△) electrolytes through ferric orthovanadate membrane

and experimentally observed membrane conductance and are given in Table 1. These values of K_{ij} point towards the fact that the selectivity of the membrane increases with the decrease in the concentration of the external electrolyte solutions. According to Eisenman[25,26] the selectivity depends upon the energy of hydration of ion-site interaction. For ion exchangers with fixed charge groups having weak field strength, the selectivity sequence is governed by difference in the hydration energy of counterions. In such cases the normal sequence, $Li^+ < Na^+ < K^+ < Rb^+ < Cs^+$, is followed. On the other hand, for ion exchangers with fixed charged groups having high field strength, the selectivity sequence is governed by the crystallgraphic radii of counterions. In such cases a reverse selectivity sequence, $Cs^+ < Rb^+ < K^+ < Na^+ < Li^+$, should result. This sequence refers to the fact that the size of the ions would be the major factor in the diffusion process. Their hydration would not only restrict permeations through the pore but would also adversely affect the exchange adsorption. There would, however, be an important opposing factor, viz., smaller ion association due to hydration which facilitates the diffusion of ions. The combined effect of the former two factors would outweight the latter with the result that the hydrated ions would penetrate slower than less hydrated ions[25,26].

A number of theoretical papers[24-30] dealing with different aspects of ion permeation in various membrane-electrolyte systems have appeared. One of the most important parameters of a membrane-electrolyte system is the permeability ratio (P_i/P_j) of the ions transporting through the opposite sides of the membrane. Depending upon the transport mechanism, or the assumptions made in the derivations, the permeability has been given such various physical meanings as mobility ratio, ion exchange equilibrium constant, the product of the mobility ratio and the Donnan ratio, the product of the mobility ratio and ion exchange equilibrium constant or the product of the mobility ratio and the distribution coefficient ratio[9,10,15,16]. Sandblom and Eisenman[9,10] have

Table 1 - Values of Membrane Selectivity K_{ij} and Permeability Ratio P_i/P_j for Ferric Orthovanadate Membrane with Two Sets of Electrolytes at Different Concentrations

Parameters	Electrolyte sets	Concentrations, *M*						
		0.10	0.05	0.02	0.01	0.005	0.002	0.001
K_{ij}	KCl-NaCl	0.454	0.484	0.537	0.986	0.800	1.372	1.460
	KCl-LiCl	0.145	0.217	0.290	0.771	1.144	1.287	1.386
P_i	KCl-NaCl	0.676	0.609	0.692	-	1.140	2.070	2.263
P_j	KCl-LiCl	0.185	0.306	0.438	1.250	1.988	2.188	2.453

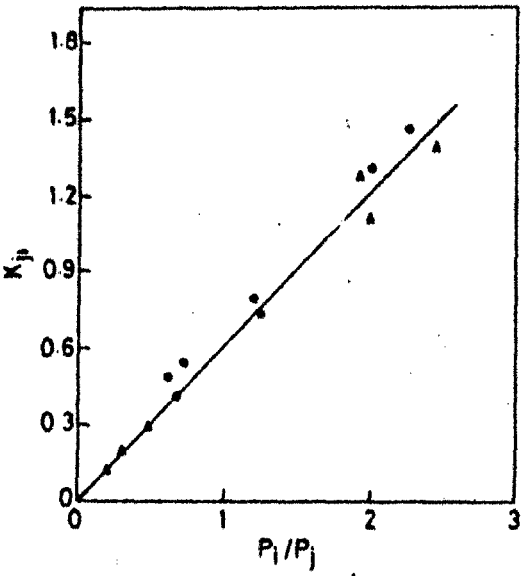

Fig. 5— Plots of membrane selectivity K_{ji} vs permeability ratio P_i/P_j for KCl-NaCl(●) and KCl-LiCl(▲) electrolyte pairs through ferric orthovanadate membrane

discussed the significance and implications of the permeability ratio and represented it by the following mathematical expressions.

$$\frac{P_i}{P_j} = \frac{\exp(\mu_i^0(\text{sol}) - \mu_i^0)/RT}{\exp(\mu_j^0(\text{sol}) - \mu_j^0)/RT} \frac{\bar{u}_i}{\bar{u}_j} = K_{ji}\frac{\bar{u}_i}{\bar{u}_j} \quad \ldots (16)$$

$$\text{where } K_{ji} = \frac{\exp(\mu_i^0(\text{sol}) - \mu_i^0)/RT}{\exp(\mu_j^0(\text{sol}) - \mu_j^0)/RT} \quad \ldots (17)$$

and μ^0 refer to the standard electrochemical potential. The permeability ratio P_i/P_j is a function of standard chemical potential in the membrane phase, μ^0, and in the solution phase, μ^0 (sol). Thus if $\bar{u}_i/\bar{u}_j$ and K_{ji} are known for a membrane-electrolyte system one can calculate the permeability ratio P_i/P_j using Eq. (16). The values of permeability ratio for ferric orthovanadate membrane at different electrolyte concentrations thus evaluated are given in Table 1. These values of permeability ratio show a regular increase with the decrease in the concentration of the electrolyte across the membrane and the order of selectivity for cations is $K^+ > Na^+ > Li^+$. This order of selectivity according to the Eisenman-Sherry model of membrane selectivity refers to the fact that the membrane carried a small density of fixed charge groups. It has been concluded that ionic species retain their hydration shell, at least partially, while diffusing through the membrane pores. To test the validity of Eisenman and Sandblom equation[9,10] with the system of polystyrene based ferric orthovanadate membrane the calculated values of membrane selectivity, K_{ji} are plotted against permeability ratio P_i/P_j in Fig. 5. A good straight line passing through the origin is obtained which thereby testifies the theory of Eisenman and Sandblom[9,10] with the polystyrene based inorganic precipitate ion exchange membranes.

Acknowledgement

Thanks are due to the Council of Scientific and Industrial Research, New Delhi, for financial assistance.

References

1 Siddiqi F A, Beg M N, Khan I R, Saksena S K & Ahsan M A, *J Membrane Sci*, 2 (1977) 245.
2 Siddiqi F A, Beg M N, Haq A, Ahsan M A, Khan M I R & Khan S A, *J Chim Phys Phys-Chim Biol*, 76 (1979) 57.
3 Siddiqi F A, Lakshminarayanaiah N & Beg M N, *J Polym Sci*, 9 (1971) 2853, 2868.
4 Siddiqi F A, Beg M N, Haq A, Ahsan M A & Khan M I R, *J Chim Phys-Chim Biol*, 74 (1978) 932.
5 Beg M N, Siddiqi F A & Ahsan M A, *Indian J Technol*, 19 (1981) 135.
6 Teorell T, *Discuss Faraday Soc*, 21 (1956) 9.
7 Liquori A M & Botre C, *Ric Sci*, 34 (1964) 6; *J Phys Chem*, 71 (1967) 3765.
8 Liquori A M, Constantino L & Segre G, *Ric Sci*, 36 (1966) 591.
9 Sandblom J P & Eisenman G, *Biophys J*, 7 (1967) 217.
10 Sandblom J P & Orme F, *Membrane*, Vol 1, edited by G Eisenman (Marcel Dekker, New York) 1972 125.
11 Toyoshima Y & Nozaki H, *J Phys Chem*, 74 (1970) 2704.
12 Siddiqi F A, Beg M N, Khan M I R, Ahsan M A & Islam B, *J Membrane Sci*, 4 (1978) 275.
13 Schatchard G, *J Am Chem Soc*, 75 (1956) 2883.
14 Helfferich F, *Ion-exchange* (McGraw-Hill, New York) 1962.
15 Wyllie M R J & Kanaan S L, *J Phys Chem*, 58 (1954) 73.
16 Wyllie M R J, *J Phys Chem*, 58 (1954) 67.
17 George J H B & Courant R A, *J Phys Chem*, 71 (1967) 246.
18 Manecke G & Laupenmuhlen E O, *Z Phys Chem*, (Frankfurt), 2 (1954) 336.
19 Gregor H P, Jacobson H, Shail R C & Westone D M, *J Phys Chem*, 61 (1957) 141.
20 Gregor H P, Kawabe K, Jacobson H & Miller I F, *J Colloid Interface Sci*, 21 (1966) 79.
21 Subramanyan V & Lakshminarayanaiah N, *J Phys Chem*, 72 (1968) 4314.
22 Ijima T, Obara T, Isshiki M, Sekj T & Adachi K, *J Colloid Sci*, 63 (1978) 421.
23 Heyman H & Rabinov G, *J Phys Chem*, 47 (1943) 655.
24 Spiegler K S, Yoest R L & Wyllie M R J, *Discuss Faraday Soc*, 21 (1956) 174.
25 Eisenman G, Sandblom J P & Walker (Jr) J L, *Science*, 155 (1967) 965.
26 Eisenman G, *Biophys J Suppl*, 2 (1962) 259.
27 Buck R P, *J Anal Chem*, 48 (1976) 2312.
28 Lakshminarayanaiah N, *Membrane electrode*, (Academic Press New York) 1976, 69.
29 Lakshminarayanaiah N, *Transport phenomena in membrane* (Academic Press, New York) 1969.
30 Rechnitz G A, *Chem Eng News*, 45 (1967) 146.

J. Electroanal. Chem., 92 (1978) 231–238

STUDIES WITH PARCHMENT SUPPORTED MEMBRANES

PART XXIII. TEST OF THE THEORIES OF MEMBRANE POTENTIAL AND BI-IONIC POTENTIAL BASED ON NON-EQUILIBRIUM THERMODYNAMICS

FASIH A. SIDDIQI, M.N. BEG and POORNA PRAKASH

Membrane Research Laboratory, Physical Chemistry Division, Department of Chemistry, Aligarh Muslim University, Aligarh-202001 (India)

(Received 7th November 1977; in revised form 31st January 1978)

ABSTRACT

The thermodynamically effective fixed charge density of cobalt and mercuric tungstate parchment supported membranes has been evaluated by the use of the most recent method of Tasaka et al. [36] based on the thermodynamics of irreversible processes and have been compared with the values obtained by the methods of Kobatake et al. [31] and Teorell-Meyer-Sievers (TMS) [19,20]. Bi-ionic potentials (BIP) have also been measured for the above membranes with different pairs of electrolyte solutions. Theoretical values of BIP have been calculated by utilizing the theories of membrane potential and BIP recently developed by Toyoshima and Nozaki [37] based on non-equilibrium thermodynamics. The various parameters have been evaluated and it was found that the theoretical equations of BIP are applicable to these parchment supported membranes.

We are engaged in the study of membranes [1–17] which can serve as models for biological systems [18], particularly parchment membranes which in some formal aspects at least, according to Teorell [19] behave exactly like gastric mucosal membranes. Membrane theories of Teorell [19], Meyer and Sievers [20], Schmid [21], Sollner [22], Gregor [23], Eisenman [24] and Sherry [25], etc. have been applied for the evaluation of various parameters. Recently the work of Kedem and Katchalsky [26], Spiegler [27], Scatchard [28], Helfferich [29], Schlögl [30], Kobatake et al. [31–34] etc. based on non-equilibrium thermodynamics has been applied to elucidate the mechanism of transport through parchment supported [1–10] and polymeric composite membranes [13–17]. This communication deals with the application and test of the most recent theories of membrane potential developed by Nagasawa et al. [35,36] based on the thermodynamics of irreversible processes as well as those of Toyoshima and Nozaki [37] on bi-ionic potential.

EXPERIMENTAL

The membranes of cobalt tungstate and mercuric tungstate were prepared by the method of interaction suggested by Siddiqi et al. [1–15].

Measurement of membrane potential and bi-ionic potential

The electrochemical cell of the type

SCE	Solution	Membrane	Solution	SCE
	c_1		c_2	

was used for measuring electrical potentials arising across the membrane by maintaining a tenfold difference in concentration (i.e. $c_2/c_1 = 10$) and using a Pye Precision Vernier potentiometer (No. 7568). The bi-ionic potentials were measured by setting up an electrochemical cell of the following type

SCE	Solution	Membrane	Solution	SCE
	AP		BP	

and keeping the concentration of both AP and BP electrolytes the same. The various salt solutions (chloride and nitrate of K^+, Na^+, Li^+ and NH_4^+) were prepared from analytical grade reagents (B.D.H.) by using deionized water. In both the measurements of membrane potential and bi-ionic potential the solutions were vigorously stirred and temperature was maintained at 25°C. The parchment paper was supplied by Baird and Tatlock Ltd. (London).

RESULTS AND DISCUSSION

The membrane potential data obtained with cobalt tungstate and mercuric tungstate parchment supported membranes using various 1 : 1 electrolytes are plotted as a function of $\log[(c_1 + c_2)/2]$ with the ratio v ($= c_2/c_1$) fixed at 10. These plots are shown in Fig. 1.

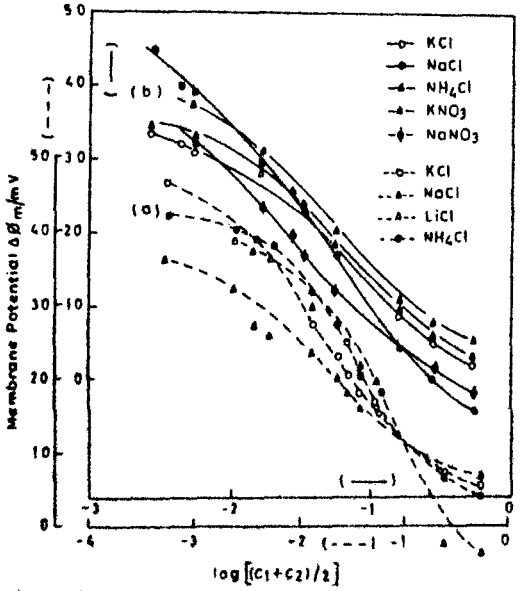

Fig. 1. Plots of membrane potentials $\Delta\phi_m$ vs. $\log(c_1 + c_2)/2$ for (a) cobalt tungstate and (b) mercuric tungstate membranes in contact with various 1 : 1 electrolyte solutions at 25°C.

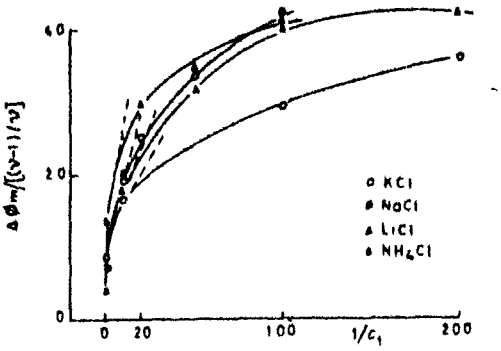

Fig. 2. Plots of $\Delta\phi_m/(\nu - 1)/\nu$ vs. $1/c_1$ for various electrolyte with cobalt tungstate membrane.

Tasaka et al. [36] derived a general equation for membrane potential existing across a negatively charged membrane. In the limit high electrolyte concentrations they found the following approximate form (their equation 31)

$$-\Delta\phi_m = (RT/F)[\nu/(\nu - 1)](X/2)\ 1/c_1 + \cdots \quad (1)$$

where X is the concentration of fixed charge on the membrane. Equation (1) predicts a relationship between $\Delta\phi_m$ vs. $1/c_1$, from which X can be calculated. Figures 2 and 3 show plots between $\Delta\phi_m/[(\nu - 1)/\nu]$ vs. $1/c_1$. The tangents from which the slopes are evaluated are shown by the dotted lines. The values of charge densities X obtained from the various slopes are given in Table 1 with different electrolytes.

The transport number was calculated using Hersh's equation [38]

$$\bar{T}_c = (\bar{U}/\bar{V})\bar{c}_+/(\bar{U}/\bar{V})\bar{c}_+ + \bar{c}_- \quad (2)$$

where $(\bar{U}/\bar{V})$ is the mobility ratio in the membrane phase and $\bar{c}_+$ and $\bar{c}_-$ have

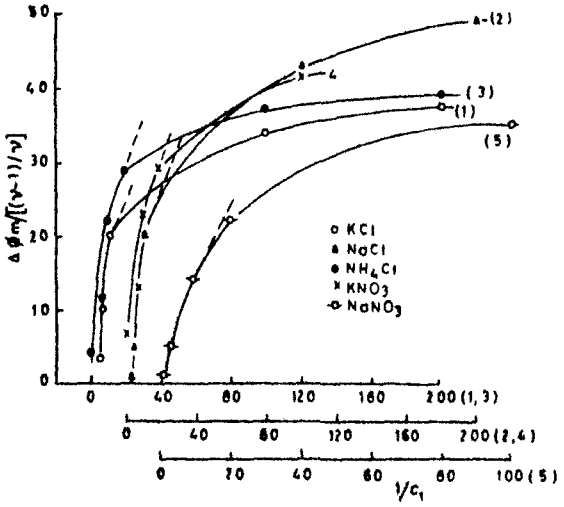

Fig. 3. Plots of $\Delta\phi_m/(\nu - 1)/\nu$ vs. $1/c_1$ for various electrolyte with mercuric tungstate membrane.

TABLE 1

Comparison of charge density for different membrane-electrolyte systems

S_1 = cobalt tungstate and S_2 = mercuric tungstate

Membrane	Electrolyte	TMS [19,20]		Kobatake et al. [31]	Tasaka et al. [36]
		$\bar{U}/\bar{V}$	10^2X/mol dm^{-3}	10^2X/mol dm^{-3}	10^2X/mol dm
S_1	KCl	1.4	0.67	0.54	0.97
	NaCl	1.4	0.54	0.49	0.87
	LiCl	1.0	1.99	0.65	0.85
	NH_4Cl	1.4	0.85	0.46	0.93
S_2	KCl	1.0	2.8	1.4	1.4
	NaCl	1.2	1.2	1.9	1.5
	NH_4Cl	1.0	3.5	1.2	1.4
	KNO_3	1.0	4.4	1.0	1.5
	$NaNO_3$	1.0	2.1	0.8	1.5

been calculated using the expression given by Hersh [38]

$$\bar{c}_+ = \tfrac{1}{2}\left(\sqrt{(X)^2 + 4\,\bar{c}_1^2} + X\right) \tag{3a}$$

$$\bar{c}_- = \tfrac{1}{2}\left(\sqrt{(X)^2 + 4\,\bar{c}_1^2} - X\right) \tag{3b}$$

The transport number of the counter ions in the membrane phase was calculated using eqn. (2) by substituting the value of X and $(\bar{U}/\bar{V})$ from Table 1, and are given in Table 2 for two membranes with different electrolytes.

Bi-ionic potential (BIP)

A steady electromotive force of a bi-ionic cell containing two electrolytes AP and BP separated by a membrane, is called bi-ionic potential (BIP). This potential

TABLE 2

Transport number of counter ions as a function of external electrolyte concentration

S_1 = cobalt tungstate and S_2 = mercuric tungstate

Membrane	Electrolyte	Concentrations/mol dm^{-3}					
		1.0	0.5	0.1	0.05	0.01	0.001
S_1	KCl	0.58	0.59	0.60	0.61	0.73	—
	NaCl	0.58	0.58	0.68	—	0.70	0.98
	LiCl	0.50	0.51	0.55	0.59	0.85	—
	NH_4Cl	0.58	0.59	0.60	0.62	0.76	0.99
S_2	KCl	0.50	0.51	0.57	0.63	0.91	—
	NaCl	0.55	0.55	0.56	0.60	0.70	—
	NH_4Cl	0.51	0.52	0.58	0.66	0.92	—
	KNO_3	0.51	0.52	0.54	0.71	0.94	—
	$NaNO_3$	0.50	0.51	0.55	0.61	0.86	—

is a measure of selectivity of a membrane for ions of the same sign. Various mathematically rigorous equations have been derived on the basis of thermodynamics of irreversible processes by Scatchard [28] and Helfferich [29]. Bi-ionic potentials have also been reported by Michaelis [39], Marshall and Krinbill [40], Meyer and Bernfeld [41], Sollner et al. [42], Manecke [43] and Wyllie [44], etc. Recently Toyoshima and Nozaki [37] have derived the equation for BIP and membrane potential on the basis of non-equilibrium thermodynamics, using the appropriate assumptions for the mobilities and activity coefficients of small ions in the membrane phase which is applied here to our system of parchment supported membranes.

They considered a system in which two large compartments contain the aqueous solutions composed of two simple 1 : 1 electrolytes AP and BP. Here A and B represent the cationic species and P is the common anion. The electric charges carried by the membrane matrix are negative charges and are distributed uniformly with a charge density X. They showed that the apparent transport number of the anion is approximately given by (their eqn. 36)

$$1/t_- = V_N + (V_N - 1)[(\nu - 1)/\nu \ln \nu]X(X/K_N)1/c_N^I \tag{4}$$

where

$$V_N = 1 + u_N^0/u_P^0, \tag{5}$$

u^0 are the limiting mobilities and K_N is defined by

$$\begin{aligned} K_N^2(a_{NP})_I^2 &= (a_N)_0(a_P)_0 \\ K_N^2(a_{NP})_{II}^2 &= (a_N)_L(a_P)_L \end{aligned} \tag{6}$$

where $(a_{NP})_I$ and $(a_{NP})_{II}$ are the mean activities of the electrolyte NP (N = A, B) in both solution I and II, respectively, defined by

$$\begin{aligned} (a_{NP})_I^2 &= a_N^I a_P^I \\ (a_{NP})_{II}^2 &= a_N^{II} a_P^{II} \end{aligned} \tag{7}$$

$(a_i)_0$ and $(a_i)_L$ (i = A, B, P) are the single ion activities of species i in the membrane phase at $X = 0$ and $X = L$ and K_N(N = A, B) is defined by

$$1/K_N = \exp(\mu_N^{o^m} - \mu_N^{o^b} + \mu_P^{o^m} - \mu_P^{o^b})/2\,RT \tag{8}$$

In eqn. (8), $\mu_N^{o^m}$ and $\mu_N^{o^b}$ are the standard chemical potentials of cation N in the membrane phase and the external bulk solution, respectively, and $\mu_P^{o^m}$ and $\mu_P^{o^b}$ are the corresponding values of anion P. Using eqn. (4), the values of V_N and (X/K_N) can be determined from the ordinate intercept and initial slope of a plot for $1/t_-$ against $1/c_N^I$ at a given ν.

Equation (4) indicates, that the intercept of a plot of $1/t_-$ against $1/c_N^I$ at fixed $\nu = 10$, allows the value of V_N to be determined. Plots of $1/t_-$ against $1/c_N^I$ for various 1 : 1 electrolytes are shown in Fig. 4 for both cobalt and mercuric tungstate membranes. For the evaluation of (X/K_N), the slope of eqn. (4), which is given by the following, is first determined

$$(V_N - 1)[(\nu - 1)/\nu \ln \nu](X/K_N)$$

The graphical value of the slope determined from Fig. 4 is equated with the

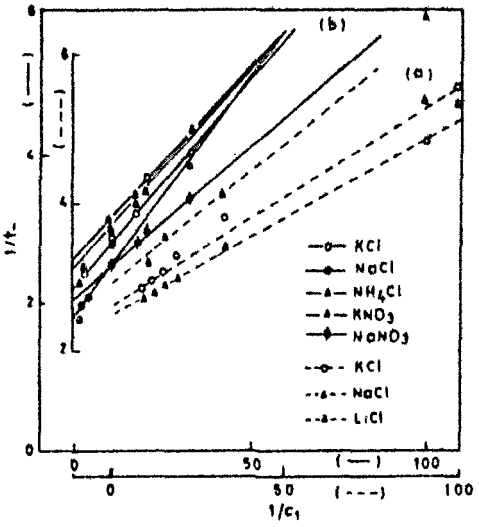

Fig. 4. Plots of $1/t_-$ vs. $1/c_1$ for (a) cobalt tungstate and (b) mercuric tungstate membranes with various 1 : 1 electrolyte.

above expression and then by substituting V_N, the value of (X/K_N) is determined.

The value of g_N is calculated from eqn. (9) at different concentrations (equation 39 of Toyoshima et al. [32]) and

$$g_N = 1 + \{1 + (2\,K_N c/X)^2\}^{1/2} \tag{9}$$

By substituting the values of V_N and g_N in eqn. (10) J, the reduced flux, is evaluated.

$$(2\,J + 1)\ln(g_A + 2\,J/g_B + 2\,J) - \ln(JV_A + 1/JV_B + 1) - \ln(g_A/g_B) = 0 \tag{10}$$

With the help of these parameters namely V_N, (X/K_N), g_N and J the theoretical

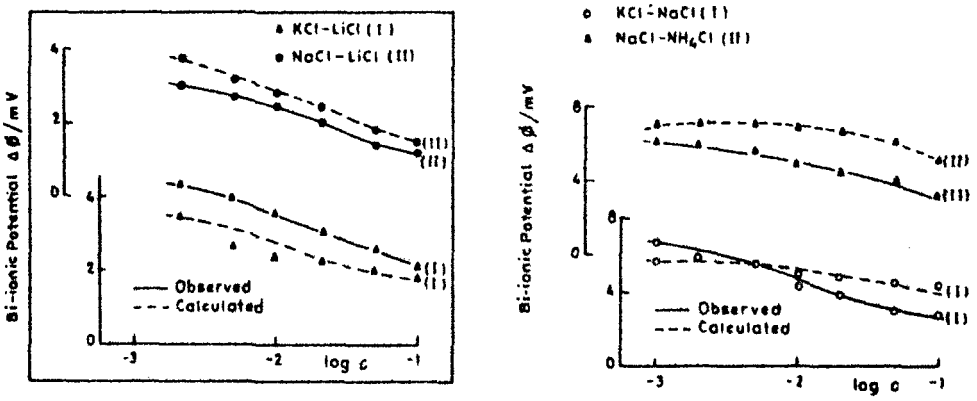

Fig. 5. Plots of observed (——) and calculated (- - -) bi-ionic potentials $\Delta\phi$ vs. log c for different pairs of electrolyte with cobalt tungstate membrane.

Fig. 6. Plots of observed (——) and calculated (- - -) bi-ionic potentials $\Delta\phi$ vs. log c for different pairs of electrolyte with mercuric tungstate membrane.

BIP is calculated from the equation (Toyoshima et al., eqn. 38)

$$\Delta\phi = [2 \ln K_A/K_B + \ln(JV_A + 1/JV_B + 1)](F/RT)$$

These theoretical values of BIP thus obtained are plotted against log c and are shown by broken lines in Figs. 5 and 6. For comparison the observed values of BIP are also plotted and are shown by solid lines in the same graph. It is quite evident from the Figures that the agreement between the observed and theoretical values is quite fair and it may be concluded that the theory of BIP developed by Toyoshima and Nozaki [37] is applicable to our system of parchment supported cobalt and mercuric tungstate membranes.

ACKNOWLEDGEMENTS

The authors are grateful to Prof. Wasiur Rahman, Head of the Department of Chemistry for providing research faciiities and to C.S.I.R. (India) for the award of a fellowship to one of them (P.P.).

REFERENCES

1 F.A Siddiqi, M.N. Beg and P. Prakash, J. Electroanal. Chem., 80 (1977) 223.
2 F.A. Siddiqi and S. Pratap, J. Electroanal. Chem., 23 (1969) 137, 142.
3 F.A. Siddiqi, M.N. Beg, S.P. Singh and A. Haque, Electrochim. Acta, 22 (1977) 631, 638.
4 F.A. Siddiqi, M.N. Beg, A. Haque and S.P. Singh, Bull. Chem. Soc. Jap., 49 (1976) 2854, 2864.
5 F.A. Siddiqi, P. Prakash and S.P. Singh, Kolloid-Z.Z. Polym., (1977) in press.
6 F.A. Siddiqi, M.N. Beg and S.P. Singh, J Polymer Sci., 15 (1977) 959.
7 F.A. Siddiqi, S.K. Saksena and I.R. Khan, J. Polymer Sci., 15 (1977) 1936.
8 F.A. Siddiqi, M.N. Beg, P. Prakash and S.P. Singh, Indian J. Chem., 16A (1978) 7.
9 F.A. Siddiqi, S.K. Saksena, M.I.R. Khan and M.A. Ahsan, J. Mem. Sci., 2 (1977) 245.
10 F.A. Siddiqi, M.N. Beg, A. Haque, M.A. Ahsan and M.I.R. Khan, J. Chim. Phys., 74 (1977) 932.
11 F.A. Siddiqi, N. Lakshminarayanaiah and S.K. Saksena, Z. Phys. Chem. (Frankfurt), 72 (1970) 298, 307.
12 F.A. Siddiqi, N. Lakshminarayanaiah and M.N. Beg, J. Polymer Sci., 9 (1971) 2853, 2869.
13 F.A. Siddiqi, M.N. Beg, S.P. Singh and A. Haque, Acta Chim., 93 (1977) 123.
14 M.N. Beg, F.A. Siddiqi and R. Shyam, Can. J. Chem., 55 (1977) 1680.
15 M.N. Beg, F.A Siddiqi, R. Shyam and I. Altaf, J. Electroanal. Chem., 89 (1978) 141.
16 W.U. Malik and F.A. Siddiqi, Proc. Indian Acad. Sci., A56 (1962) 206; J. Colloid Sci., 18 (1963) 161; Bull. Chem. Soc. Jap., 40 (1967) 1741.
17 N. Lakshminarayanaiah and F.A. Siddiqi, J. Polymer Sci., 8 (1970) 2949; Biophys. J., 11 (1971) 603; 12 (1972) 150; Z. Phys. Chem. (Frankfurt), 78 (1972) 150; in M. Bier (Ed.), Membrane Process in Industry and Biomedicine, Plenum Press, New York, 1971, p. 301.
18 A.M. Liquori and C. Botre, Ric. Sci., 34 (1964) 6; J. Phys. Chem., 71 (1967) 3765.
19 T. Teorell, Proc. Soc. Exptl. Biol. Med., 33 (1935) 282; Proc. Natl. Acad. Sci. (U.S.), 21 (1935) 152; Z. Elektrochem., 55 (1951) 460; Progr. Biophys. Chem., 3 (1953) 305; Discuss. Faraday Soc., 21 (1956) 9.
20 K.H. Meyer and J.F. Sievers, Helv. Chim. Acta, 19 (1936) 649, 665, 987.
21 G. Schmid, Z. Elektrochem., 54 (1950) 424; 55 (1951) 229; 56 (1952) 35; G. Schmid and H. Schwartz, Z. Elektrochem., 55 (1951) 295; 56 (1952) 35.
22 K. Sollner, J. Phys. Chem., 49 (1945) 47, 171; J. Electrochem. Soc., 97 (1950) 139; Ann. N.Y. Acad. Sci., 57 (1953) 177; J. Macromol. Sci., A3 (1969) 1.
23 H.P. Gregor, J. Amer. Chem. Soc., 70 (1948) 1293; 73 (1950) 642.
24 G. Eisenman in A. Kleinzellrs and A. Kotvk (Eds.), Membrane Transport and Metabolism, Academic Press, New York, 1961, p. 163; Biophys. J., 2 (1962) 259.
25 H. Sherry in J.A. Marinsky (Ed.), Ion Exchange, Vol. 2, Marcel Dekker, New York, 1968.
26 O. Kedem and A. Katchalsky, Trans. Faraday Soc., 59 (1963) 1918, 1931, 1941.
27 K.S. Spiegler, Trans. Faraday Soc., 54 (1958) 1408.
28 G. Scatchard, J. Amer. Chem. Soc., 21 (1956) 30; Discuss. Faraday Soc., 21 (1956) 80.
29 F. Helfferich, Ion Exchange, McGraw Hill, New York, 1962.

30 R. Schlögl, Stofftransport durch Membrane, Dr. Dietrich Steinkopff Verlag, Darmstadt, 1964.
31 Y. Kobatake, T. Noriaki, Y. Toyoshima and H. Fujita, J. Phys. Chem., 60 (1965) 3981.
32 Y. Toyoshima, M. Yuasa, Y. Kobatake and H. Fujita, Trans. Faraday Soc., 63 (1967) 2803, 2814; J. J. Phys. Chem., 72 (1968) 2871.
33 N. Kamo, Y. Toyoshima, H. Nozaki and Y. Kobatake, Kolloid-Z.Z. Polym., 249 (1971) 1061; 248 (1971) 914.
34 N. Kamo, M. Ockawa and Y. Kobatake, J. Phys. Chem., 77 (1973) 92, 2995.
35 M. Nagasawa and I. Kagawa, Discuss. Faraday Soc., 21 (1956) 52.
36 M. Tasaka, N. Aoki, Y. Konda and M. Nagasawa, J. Phys. Chem., 79 (1975) 1307.
37 Y. Toyoshima and H. Nozaki, J. Phys. Chem., 74 (1970) 2704.
38 L.S. Hersh, J. Phys. Chem., 72 (1968) 2195.
39 L. Michaelis, Kolloid-Z., 62 (1933) 2.
40 C E. Marshall and C.A. Krinbill, J. Amer. Chem. Soc., 64 (1942) 1814.
41 K.H. Meyer and P. Bernfeld, Helv. Chim. Acta, 28 (1945) 962.
42 K. Sollner, S. Dray, E. Grim and R. Neihof, Ion Transport Across Membranes, Academic Press, New York, 1954, p. 144.
43 G. Manecke, Z. Elektrochem., 55 (1951) 672.
44 M.R.J. Wyllie, J. Phys. Chem., 58 (1954) 167.

Reprinted from

Canadian Journal of Chemistry

Réimpression du

Journal canadien de chimie

Studies with model membranes. Part XXIV. Evaluation of thermodynamic activation parameters, effective fixed charge density, and test of the theory of bi-ionic potential based on the thermodynamics of irreversible processes

FASIH A. SIDDIQI, M. NASIM BEG, M. IBADUR RAHMAN KHAN, ABDUL HAQ, S. K. SAKSENA, AND BADRUL ISLAM

Membrane Research Laboratory, Department of Chemistry, Aligarh Muslim University, Aligarh, 202001 India

Can. J. Chem. 56, 2205 (1978).

National Research Council Canada

Conseil national de recherches Canada

Studies with model membranes. Part XXIV. Evaluation of thermodynamic activation parameters, effective fixed charge density, and test of the theory of bi-ionic potential based on the thermodynamics of irreversible processes

FASIH A. SIDDIQI, M. NASIM BEG, M. IBADUR RAHMAN KHAN, ABDUL HAQ, S. K. SAKSENA, AND BADRUL ISLAM

Membrane Research Laboratory, Department of Chemistry, Aligarh Muslim University, Aligarh 202001, India

Received November 3, 1976[1]

FASIH A. SIDDIQI, M. NASIM BEG, M. IBADUR RAHMAN KHAN, ABDUL HAQ, S. K. SAKSENA, and BADRUL ISLAM. Can. J. Chem. 56, 2205 (1978)

The various ionic processes in the membrane system, notably (*a*) ionic transport, (*b*) membrane potential, (*c*) electrical conductivity, (*d*) ionic distribution equilibria, and (*e*) spatial distribution of ions and the potential within the membrane have been thoroughly studied with parchment-supported membranes. By applying the theory of absolute reaction rate, various thermodynamic parameters, namely, enthalpy of activation ΔH^*, energy of activation ΔF^*, and entropy of activation ΔS^* were evaluated. The ΔS^* values were found to be negative, indicating that diffusion takes place with partial immobilization in the membrane phase. A formal relation between $\Delta H_{\text{hydration}}$, $\Delta F_{\text{hydration}}$, and $\Delta S_{\text{hydration}}$ of cations with corresponding values of ΔH^*, ΔF^*, and ΔS^* for diffusion was also worked out. Thermodynamically fixed charge density was evaluated using methods based on thermodynamics of irreversible processes. Potentiometric selectivity and recent theory of bi-ionic potential based on nonequilibrium thermodynamics was tested and found applicable to parchment membranes

FASIH A. SIDDIQI, M. NASIM BEG, M. IBADUR RAHMAN KHAN, ABDUL HAQ, S. K. SAKSENA et BADRUL ISLAM. Can. J. Chem. 56, 2205 (1978).

On a étudié d'une façon extensive, à l'aide de membranes supportées par des parchemins, les divers processus ioniques des systèmes de membranes, à savoir: (*a*) le transport ionique, (*b*) le potentiel de la membrane, (*c*) la conductivité électrique, (*d*) les équilibres de distributions ioniques, (*e*) la distribution spatiale. Une application de la théorie des vitesses absolues a permis d'évaluer divers paramètres thermodynamiques, à savoir l'enthalpie d'activation ΔH^*, l'énergie libre d'activation ΔF^* et l'entropie d'activation ΔS^*. On a trouvé que les valeurs de ΔS^* sont négatives; ceci indique que la diffusion a lieu par une immobilisation partielle dans la phase de la membrane. On a aussi pu établir une relation formelle entre les $\Delta H_{\text{hydratation}}$, $\Delta F_{\text{hydratation}}$ et $\Delta S_{\text{hydratation}}$ des cations avec les valeurs correspondantes de ΔH^*, ΔF^* et ΔS^* pour la diffusion. On a évalué la densité de charge fixe thermodynamique en faisant appel à des méthodes basées sur la thermodynamique de processus irréversibles. On a évalué la sélectivité potentiométrique et la théorie récente du potentiel bi-ionique, basée sur la thermodynamique des phénomènes irreversibles, et on a trouvé qu'on peut l'appliquer aux membranes de parchemin.

[Traduit par le journal]

Introduction

We have been engaged in the studies of (*a*) parchment-supported, (*b*) polymeric-composite, and (*c*) polystyrene-based ion exchange membranes (1–8) which can serve as models for biological systems. Membrane theories of Kedem and Katchalsky (9), Spiegler (10), Scathchard (11), Scattergood and Lightfoot (12), etc., have been used to evaluate various membrane parameters.

This article deals with the following aspects of parchment-supported membranes: (*A*) application of Nernst-Planck flux equations and Fick's diffusion law (13) and evaluation of various thermodynamic activation parameters, (*B*) evaluation of thermodynamically effective fixed charge density by the most recent methods of Nagasawa and co-workers (14, 15) and others (16–21) based on thermodynamics of irreversible processes, and (*C*) evaluation of potentiometric selectivity coefficient and test of the most recent theories of membrane potential and bi-ionic potential developed by Toyoshima and Nozaki (22) based on non-equilibrium thermodynamics.

Experimental

Preparation of Parchment-supported Membranes

The membranes of silver tungstate and chromic ferricyanide were prepared by the method of interaction suggested by Weiser (23) and Siddiqi *et al.* (2). First parchment was soaked in distilled water for about 2 h and then tied carefully to the flat mouth of a beaker in which 0.2 *M* solution of $AgNO_3$ was taken. This was suspended for about 72 h in a 0.2 *M* sodium tungstate solution. The temperature was kept at 25 C. The two solutions were interchanged and kept for another 72 h.

[1]Revision received April 20, 1978.

In this way fine deposition of silver tungstate was obtained on the surface of parchment paper. Similar procedure was adopted for chromic ferricyanide membrane by taking 0.2 *M* solutions of chromic chloride and potassium ferricyanide. The temperature maintained in this case was kept at 72 *C* and the time for deposition was 3 h. Both the membranes thus prepared were well washed with deionized water for the removal of free electrolytes. The vegetable parchment paper was supplied by M/S Baird and Tatlock (London) Ltd

Part A. Studies of Diffusion of Electrolytes Through Parchment-supported Silver Tungstate Membrane

The apparatus and procedures used to measure membrane potential $\Delta\phi_m$, membrane resistance R_m, and electrolyte concentrations are those described by Siddiqi *et al.* (2-4). The half cells contained 125 ml of the electrolyte solutions while the capacity of each of the cells holding the membrane was about 130 ml. Initially the concentrations C_1 and C_2 across parchment-supported silver tungstate membrane were 0.001 *M* and 0.1 *M* of the same electrolyte, respectively. Each of the half cell was fitted with two platinized platinum electrodes firmly fixed to follow concentration changes and two anion reversible Ag AgCl electrodes: one a disc type to pass a small d.c. current and the other a J-shaped wire electrode placed very near the membrane surface to measure membrane potential (by Pye Precision Potentiometer No. 7568) and changes in membrane potential following current flow. The solutions in both the half cells were kept well stirred by magnetic stirrers. The whole cell assembly was immersed in a water thermostat maintained at 10, 15, 20, 25, and 30 C (±0.1 C).

The changes in conductance on the dilute solution side was followed by means of the conductivity bridge (Cambridge Instrument Co., England, No. E-350140). The exact concentration of the solution at any given time was estimated from a calibration curve. The membrane resistance was determined by applying an external emf to the disc-type Ag AgCl electrodes and measuring the change in potential across the membrane using J-type wire electrodes. The current passed through the membrane system was determined by measuring *IR* drop across a precision Kilo-Ohm resistor. The current was kept very low in order to minimize the ion transfer during the period (2-3 min) required for each resistance measurement. The direction of current flow was reversed in each successive measurement. The surface of the membrane was controlled during membrane resistance measurements but on account of the changes in salt concentration due to diffusion on the dilute solution side, the control was not 100% perfect. However, reproducible results were obtained during resistance measurements. The d.c. current densities at the electrode and membrane surfaces were also determined in mA cm^{-2}. The resistance measurements gave a value of the entire system, namely,

Electrolyte film - Membrane - Electrolyte film

In order to measure R_m directly the wire electrodes should be placed strictly on the membrane surfaces. When this was done, membrane resistance values were not 100% reproducible. The value of membrane resistance determined in this way includes additional film (very thin) resistance which is outside of the membrane itself. Although the membrane potential could be measured to a better accuracy than ±1%, the estimation of membrane resistance was accurate to ±4%.

Part B. Membrane Potential Measurements

Separate measurements of membrane potentials were carried out by setting another electrochemical cell of the following type

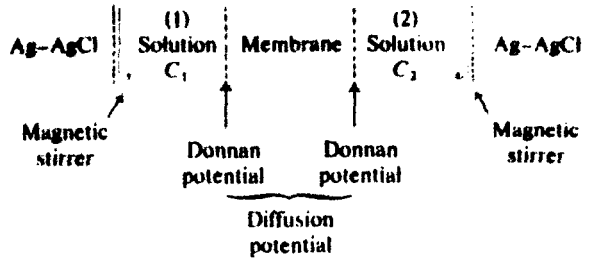

with fixed concentration ratio $C_1/C_2 = \sigma \approx 10$ throughout the experiment (concentration varied from 1.0 *M* to 1.0×10^{-3} *M*). The temperature was kept constant at 25 ± 0.1 C and the solutions were vigorously stirred. The membrane potentials were measured for parchment-supported silver tungstate and chromic ferricyanide membranes.

Part C. Bi-ionic Potential Measurements

The measurements were recorded by constructing another new electrochemical cell of the following type

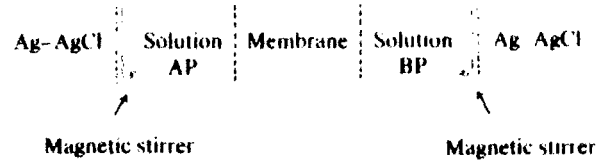

In this cell concentrations of both AP and BP types of electrolyte solutions (KCl NaCl, KCl LiCl, and KCl NH_4Cl) were kept the same on both sides of the membrane (parchment supported silver tungstate membrane only). The bi-ionic potentials were measured at 25 C (±0.1 C) across the parchment-supported silver tungstate membrane using KCl NaCl, KCl-LiCl, and KCl NH_4Cl electrolyte sets in each successive measurement. The solutions were vigorously stirred by means of the magnetic stirrers on both sides of the membrane. The measurements were recorded when three changes in the test solutions did not lead to potential variation ±0.2 mV. At least two membranes were utilized in each experiment. The membrane potential measurements with silver tungstate membrane were further carried out to obtain two membrane parameters V_N and θ/K_N (N = A, B) which are required for the evaluation of theoretical values of bi-ionic potentials. The membrane potentials were measured by constructing a cell of the type described in Part B. The concentration ratio σ was kept constant at 10 for each electrolyte solution (e.g. KCl, NaCl, LiCl, NH_4Cl etc.) used in the present investigation.

Results and Discussion

Part A. Evaluation of Activation Parameters, Namely, ΔH^*, ΔF^*, and ΔS^* for Diffusion of Various Electrolytes through Parchment-supported Silver Tungstate Membrane

When an ionic gradient is maintained using two solutions of different concentrations of the same electrolyte on either side of the membrane, diffusion of electrolytes from the region of higher concentration takes place. These transport phenomena are often described by some extended form of Nernst Planck flux equation (24). Evaluation of flows require integration of these flux equations under suitable boundary conditions governing the behavior

of the membrane-electrolyte system Kittelberger (25) from the simple laws of electrolysis developed the following equation [1] for the evaluation of diffusion rates through membranes. This equation is found to be applicable as is evident from Fig. 1 to the system of parchment-supported silver tungstate membrane.

$$[1]\quad \frac{dQ_1}{dt} = \frac{1}{\bar{Z}_1 F R_m}\left[\frac{RT}{\bar{Z}_1 F}\ln\frac{a_2}{a_1} - \Delta\phi_m\right] \times \left[\frac{Z_1 Z_-}{\bar{Z}_1 + \bar{Z}_-} \frac{\Delta\phi_m}{(RT/F)\ln a_2/a_1} + \frac{Z_+}{\bar{Z}_1 + \bar{Z}_-}\right]$$

where Q_1 is the milliequivalents of cation diffusing in time t s, Z_+ and Z_- are the valencies of the cation and anion, respectively. R_m is the resistance in ohms of the membrane, $\Delta\phi_m$ is the membrane potential in mV, a_1 and a_2 are the activities of the two electrolyte solutions on either side of the membrane, R, T, and F have their usual meanings.

The rates at which various electrolytes diffuse through the membrane were calculated at different temperatures from eq. [1]. The calculated values of diffusion rate (dQ/dt) or D_r in mol/s at 25 ± 0.1°C are given in Table 1. The changes in R_m and $\Delta\phi_m$ and electrolyte flux (dQ/dt) or D_r through silver tungstate membrane are shown in Fig. 2. The diffusion rate derived electrometrically or conductometrically determined changes in the salt concentration of the test solution C_1 is called 'observed' diffusion rate while the values computed from the measured concentration potential and electrolytic resistance of the membrane is designated the 'computed' diffusion rate. The observed and computed diffusion rates are plotted against time (Fig. 1) for various electrolytes diffusing through silver tungstate membrane at 25 ± 0.1 C. It is found that the two methods show somewhat systematic deviations. The reason for these deviations probably has its origin in additional film resistances to mass transfer which are outside of the membrane itself. It was also noted that very small error in the measured salt concentration can produce a large error in the 'observed' diffusion rate. The physical imperfections in the membranes can also contribute towards the deviation.

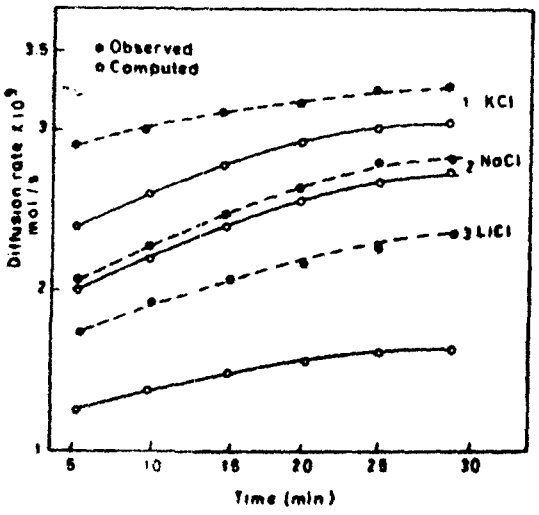

FIG. 1. Plots of observed and computed diffusion rates against time for diffusion of electrolytes through silver tungstate membrane.

The emf measured across the membrane using J-type Ag AgCl electrodes is made up of two components. The first is the electrode potential difference $\Delta\phi_e$ due to the Ag AgCl electrodes existing in two chloride solutions of different activities a_1 and a_2 of the same electrolyte and second is due to the membrane potentials $\Delta\phi_m$ arising across the membrane due to flow of electrolyte through it.

$\Delta\phi_e$ is given by the following equation:

$$[2]\quad \Delta\phi_e = (RT/Z\ F)\ln(C_2\gamma_2)/C_1\gamma_1)$$

where γ_1 and γ_2 are the activity coefficients of the electrolyte solutions on either side of the membrane (taken from the literature). Since Z_+ is always unity and $C_1\gamma_1(a_1)$ and $C_2\gamma_2(a_2)$ are known, $\Delta\phi_e$ can be computed. As $(\Delta\phi_e + \Delta\phi_m)$ is measured directly, the value of $\Delta\phi_m$ can be evaluated by subtraction.

$\Delta\phi_m$ values for various electrolytes display a very interesting phenomena. In the case of 1:1 electrolytes, the values are all positive indicating that the membrane is cation selective. On the other hand, for 2:1 and 3:1 systems of electrolytes $\Delta\phi_m$ changes sign. It means that the membrane is now anion selective. This change in the selectivity character of the membrane is evidently due to adsorption of multivalent ions leading to a state where a net positive charge is

TABLE 1. Experimental activation energies and the activation parameters derived from transition state theory of rate process for diffusion of various electrolytes by the end of 2 h periods at 25 ± 0.1°C through parchment-supported silver tungstate membrane

Electrolytes	Parameters			
	$D_r \times 10^9$ (mol/s)	$D \times 10^7$ (cm²/s)	E_a (kcal/mol)	d.c. density (mA/cm²)
KCl	2.96	3.90	6.21	4.08×10^{-3}
NaCl	2.09	2.49	5.98	3.46×10^{-3}
LiCl	1.77	2.02	5.75	3.40×10^{-3}
$BaCl_2$	1.56	1.16	4.83	4.42×10^{-3}
$CaCl_2$	2.14	1.97	5.53	4.40×10^{-3}
$MgCl_2$	2.01	1.64	5.18	3.72×10^{-3}
$AlCl_3$	0.94	0.45	6.44	2.67×10^{-3}

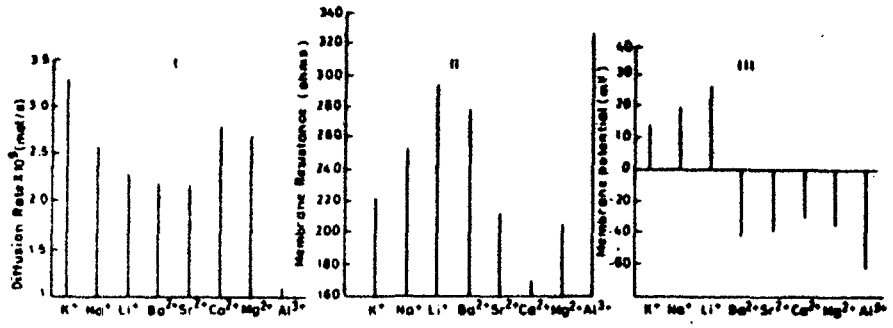

FIG. 2. Plots of diffusion rates, membrane resistance, and membrane potential through silver tungstate membrane against various cations.

left on the membrane surface making it anion selective. Adsorption of Al^{3+} makes the membrane more anion selective than it is with the adsorption of divalent cations. At any given time the membrane resistance R_m increases in the following order

$$LiCl > NaCl > KCl$$

and

$$BaCl_2 > SrCl_2 > MgCl_2 > CaCl_2$$

for 1:1 and 2:1 electrolytes and 3:1 system of electrolyte produces the highest value for membrane resistance.

The rate of flow measured for different electrolytes through silver tungstate membrane follows the sequence

$$KCl > NaCl > LiCl$$

and

$$CaCl_2 > MgCl_2 > SrCl_2 > BaCl_2$$

for 1:1 and 2:1 systems of electrolytes. The diffusion rates are calculated at different temperatures through the investigated membrane and are plotted against $1/T$ (K) (Fig. 3).

The theory of absolute reaction rates has been applied to diffusion by several investigators (26-28). According to Laidler and co-workers (27, 28) the integral diffusion coefficient D is given by

$$[3] \qquad D = Ae^{-E_a/RT}$$

where E_a is the observed activation energy for diffusion and A is the frequency factor. Thus if $\log D_t$ is plotted against $1/T$ (K), the slope gives the value of E_a. The values derived in this way for E_a are given in Table 1 at 25 ± 0.1 C. The derived values of D from eq. [3] are also given in Table 1. Various thermodynamic activation parameters, namely, enthalpy of activation, ΔH^*, entropy of activation, ΔS^*, and free energy of activation, ΔF^*, are also calculated with the help of Gibbs Helmholtz equations. The derived values of ΔH^*, ΔS^*, and ΔF^* are given in Table 2. The values of ΔS^* are found to be negative.

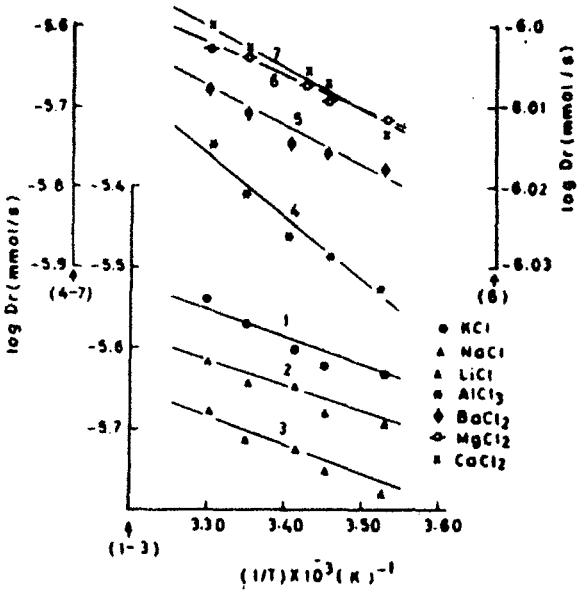

FIG. 3. Plots of diffusion rates of various electrolytes against different temperatures through silver tungstate membrane.

TABLE 2. The thermodynamic activation parameters calculated from the transition state theory of rate processes for electrolyte diffusion at 25 ± 0.1°C through silver tungstate membrane

Electrolytes	ΔH^* (kcal/mol)	ΔS^* (eu)	ΔF^* (kcal/mol)
KCl	5.62	−0.12	5.66
NaCl	5.39	−1.79	5.93
LiCl	5.16	−2.98	6.06
$BaCl_2$	4.24	−7.13	6.37
$CaCl_2$	4.97	−3.83	6.09
$MgCl_2$	4.59	−5.46	6.22
$AlCl_3$	5.85	−3.82	6.99

The negative ΔS^* indicates that the electrolyte diffusion is taking place with the partial immobilization in the membrane phase (28). This partial immobility increases in a relative manner with increase in the

valence of ions constituting the electrolyte with parchment-supported silver tungstate membrane.

Part B. Evaluation of Thermodynamically Effective Fixed Charge Density by the Use of Membrane Potential Values

Both the most recent method by Nagasawa and co-workers (14, 15) as well as the method developed by Kobatake and co-workers (16–21) are based on thermodynamics of irreversible processes applied here for the evaluation of fixed charge density of membranes.

The Method by Kobatake and Co-workers

The following expression used for charge density evaluation is given by Kobatake and co-workers (16–21):

$$[4] \quad \Delta\phi = -\frac{RT}{F}\left[\frac{1}{\beta}\ln\frac{C_2}{C_1} - \left(1+\frac{1}{\beta}-2\alpha\right) \times \ln\frac{C_2+\alpha\beta\theta}{C_1+\alpha\beta\theta}\right]$$

where

$$[5] \quad \alpha = [u_+/(u_+ + u_-)]$$

and

$$[6] \quad \beta = [1 + (KF\theta/u_+)]$$

The symbols u_+ and u_- represent the molar mobilities of positive and negative ions; K is a constant which is considered to depend upon the viscosity of the solution and the structural details of the polymer network of which the membrane is composed; θ is the fixed charge density (in equivalent/ℓ) of the membrane; C_1 and C_2 are the concentrations of electrolyte solutions across the membrane; R, T, and F have their usual meanings.

Kobatake and co-workers (16–21) have derived two limiting forms of eq. [4] useful for the analysis of experimental data on membrane potential. These are

(*a*) When C_2 becomes sufficiently small with σ fixed, eq. [4] may be expanded to give

$$[7] \quad |\Delta\phi_r| = \frac{1}{\beta}\ln\sigma - \left(\frac{\sigma-1}{\alpha\beta\sigma}\right)\left(1+\frac{1}{\beta}-2\alpha\right)\frac{C_2}{\theta}$$

where $|\Delta\phi_r|$ is the absolute value of reduced membrane potential defined by

$$[8] \quad |\Delta\phi_r| = F\Delta\phi/RT$$

Equation [7] indicates that the value of β and a relation between α and θ may be obtained by determining the intercept and the initial slope of a plot for $|\Delta\phi_r|$ against C_2. The value of intercept is given by $(1/\beta) \times \ln\sigma$ from which β may be evaluated.

(*b*) In the region of high concentration the apparent transference number t_{-app} is defined by

$$[9] \quad |\Delta\phi_r| = (1 - 2t_{-app})\ln\sigma$$

Substituting for $|\Delta\phi_r|$ in eq. [4] and expanding the resulting expression for $1/t_{-app}$ in powers of $1/C_2$ gives

$$[10] \quad \frac{1}{t_{-app}} = \frac{1}{1-\alpha} + \frac{(1+\beta+2\alpha\beta)(\sigma-1)\alpha\theta}{2(1-\alpha)^2(\ln\sigma)C_2}$$

Equation [10] indicates that the intercept for a plot of $1/t_{-app}$ against $1/C_2$ at fixed σ allows the value of α to be determined. For the evaluation of α from eq. [10], plots of $1/t_{-app}$ against $1/C_2$ for various electrolytes through parchment-supported silver tungstate and chromic ferricyanide membranes are drawn (Fig. 4). The value of intercept is given by $1/(1-\alpha)$ from which α is evaluated. Therefore from the predetermined β and α values, θ is evaluated and its values are given in Table 3 for various electrolytes with investigated membranes.

Test of the Kobatake Theory

Kobatake and co-workers (16–21) also suggested the following procedure for comparison of the theory

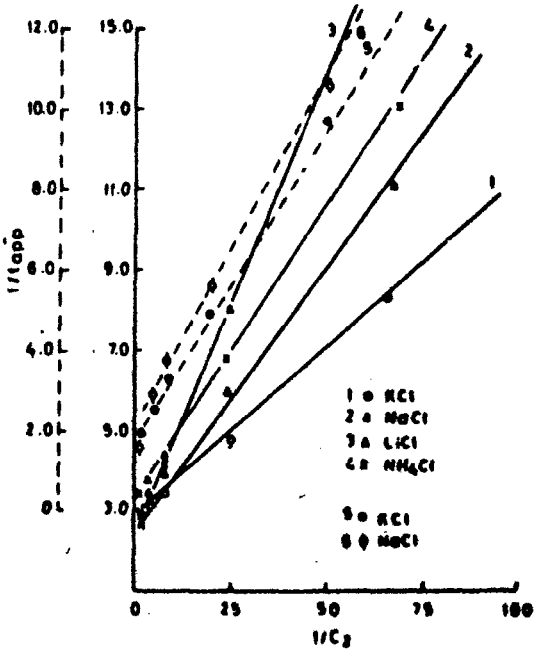

FIG. 4. Plots of $1/t_{-app}$ against $1/C_2$ for various electrolytes through (*i*) — silver tungstate and (*ii*) — chromic ferricyanide membranes. (*i*) KCl (○), NaCl (△), LiCl (▲), and NH_4Cl (×); (*ii*) KCl (●), NaCl (◇).

TABLE 3. Values derived for thermodynamically effective fixed charge density θ (in equiv./ℓ) of parchment-supported membranes at σ = 10

	Membranes			
	Silver tungstate		Chromic ferricyanide	
Electrolytes	Kobatake method	Nagasawa method	Kobatake method	Nagasawa method
KCl	0.0557	0.032	0.045	0.020
NaCl	0.0813	0.032	0.031	0.080
LiCl	0.0610	0.024	—	—
NH_4Cl	0.0730	0.048	—	—

and experiment by taking the following expressions

$$[11] \qquad (\sigma - e^q)/(e^q - 1) = Z$$

where

$$[12] \qquad q = \frac{|\Delta\phi_r| + (1 - 2\alpha)\ln\sigma}{1/\beta + 1 - 2\alpha}$$

and

$$[13] \qquad Z = C_2/\alpha\beta\theta$$

Thus if eq. [4] is valid, the values of $(\sigma - e^q)/(e^q - 1)$ calculated from measured $\Delta\phi$ and predetermined α, β, and θ values at a known value of σ (= 10) must fall on a straight line which has a unit slope and passes through the origin when plotted against log Z. Figure 5 demonstrates that the theoretical prediction from membrane potential equation is borne out quite satisfactorily by our experimental results with these investigated membranes.

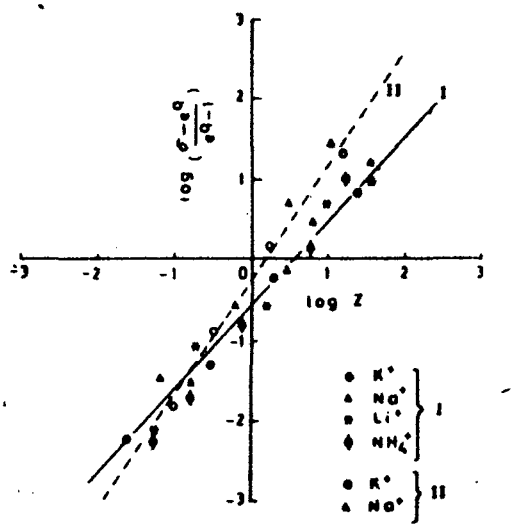

FIG. 5. Plots of log $(\sigma - e^q)/(e^q - 1)$ against log Z for various electrolytes through (*i*) — silver tungstate and (*ii*) --- chromic ferricyanide membranes. (*i*) KCl (●), NaCl (▲), LiCl (•), and NH_4Cl (◆); (*ii*) KCl (○), NaCl (△).

The Method of Nagasawa and Co-workers

Nagasawa and co-workers (14, 15) used the following equations by making various assumptions for activity and mobility of small ions, which are applied here. The membrane potential equation is given by

$$[14] \quad -\Delta\phi = \frac{RT\theta}{F}\frac{\sigma - 1}{2}\frac{1}{\sigma}\frac{1}{C_2} + \frac{RT}{F}\frac{u_+ - u_-}{u_+ + u_-}\frac{\left[1 - \dfrac{\theta J_0}{RT\bar{C}_0(u_+ - u_-)K}\right]}{\left[1 - \dfrac{\theta J_0}{2RT\bar{C}_0 u_- K}\right]}\ln\sigma + \frac{RT\theta}{2Fu_+u_-}\left(\frac{J_0}{RT\bar{C}_0 K}\right)^2\frac{\left[1 - \dfrac{\theta J_0(u_+ + u_-)}{4RT\bar{C}_0 u_+ u_- K}\right]}{\left[1 - \dfrac{\theta J_0}{2RT\bar{C}_0 u_- K}\right]}(\sigma - 1)C_2$$

where J_0 is the flux of water, θ is the thermodynamically effective fixed charge density, $\bar{C}_0$ is the concentration of water in the membrane phase, u_+ and u_- are the cation and anion mobilities in the membrane phase, σ is the concentration ratio equal to C_1/C_2, K is a constant defined by

$$[15] \qquad K = \frac{1}{\delta}\left\{\bar{C}_{-(2)} - \bar{C}_{-(1)} - \frac{\bar{C}_{-(2)} + \bar{C}_{-(1)}}{2RT\bar{C}_0 u_-} + \frac{\theta^2 J_0}{4RT\bar{C}_0(\bar{C}_{-(2)} - \bar{C}_{-(1)})}\ln\frac{\bar{C}_{-(2)} + \frac{\theta}{2}}{\bar{C}_{-(1)} + \frac{\theta}{2}}\right\}$$

where $\bar{C}_{-(1)}$ and $\bar{C}_{-(2)}$ are the anionic concentrations in the membrane phase for ions 1 and 2 on two sides 1 and 2 of the membrane; δ is the thickness of the membrane (in cm). At significant electrolyte concentration eq. [14] reduces to

$$[16] \qquad -\Delta\phi = \frac{RT}{F}\frac{\theta}{2}\frac{\sigma - 1}{\sigma}\frac{1}{C_2}$$

except at extremely high concentrations where the potential is significantly affected by J_0. The plots of $[\Delta\phi/\{(\sigma - 1)/\sigma\}]$ against $1/C_2$ are drawn (Fig. 6) for the evaluation of θ, the thermodynamically effective fixed charge density of membrane. The slope of eq. [16] is given by

$$[17] \qquad \frac{RT}{F}\cdot\frac{\theta}{2}$$

This was equated to the graphical value of the slope obtained from Fig. 6. The values of θ thus determined are given in Table 3 for various electrolytes through the investigated membranes.

Part C. Determination of Potentiometric Selectivity Coefficient K_A^{Pot} and Test of Nozaki's Theory of Bi-ionic Potential (BIP)

The mechanism of bi-ionic potential has been considered in detail by a number of workers (29-35). Sollner (35) found that not only the mobility of counter ions is important but the selectivity of the membrane material plays a significant role in the development of BIP. The relations of selectivity of membranes to the various physicochemical parameters have also been given by a number of investigators. The selectivity of membrane is governed by both the mobility of ions in the membrane phase and the equilibrium that exists at the membrane solution interfaces (e.g., partition coefficients, ion-exchange equilibrium constants). The various factors responsible for the selectivity of the parchment membrane arising from differences in the mobilities of the ions in the membrane are described here. The factors controlling or responsible for the membrane selectivity due to physicochemical equilibrium conditions have been analysed by Reichenberg (36) and intensively pursued by Eisenman and co-workers (37-43). The important facts emerging from the studies of investigators are that (*i*) the pattern of selectivity is predominantly governed by field strength, (*ii*) the number of water molecules in the neighbourhood of the cationic and anionic sites influences only the magnitude and not the sequence of selectivity, and (*iii*) the spatial distribution of anionic site influences the selectivity through the overlap of electrostatic forces.

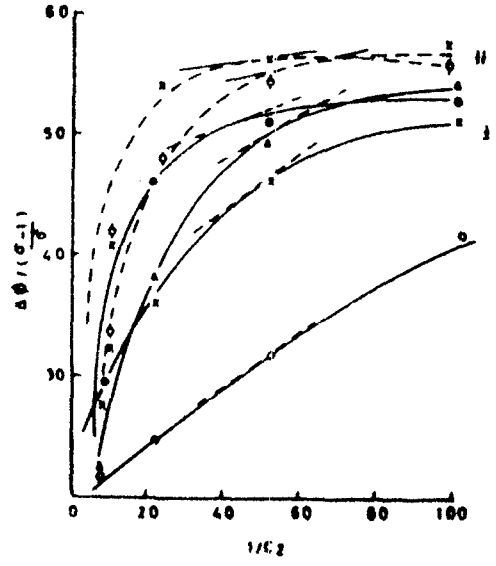

FIG. 6. Plots of $\Delta\phi\sigma/(\sigma - 1)$ against $1/C_2$ for various electrolytes through (*i*) silver tungstate (—) and (*ii*) chromic ferricyanide (---) membranes. (*i*) KCl (●), NaCl (×), LiCl (○), and NH_4Cl (▲); (*ii*) KCl (◇), NaCl (×).

Marshall and Krinbill (44) developed the following equation [18] for the bi-ionic potential

$$[18] \qquad \Delta\phi_{BIP} = (RT/F)\ln(a_A\bar{u}_A/a_B\bar{u}_B)$$

where $(\bar{u}_A/\bar{u}_B)$ is the mobility ratio in the membrane phase of the two ions. The values derived for mobility ratios across silver tungstate membrane for 1:1 set of electrolytes are given in Table 4. The BIP values are related to the potentiometric selectivity coefficient K_{BA}^{Pot} by the following relation:

$$[19] \quad \Delta\phi_{BIP} = \text{constant} + (nRT/F) \times \ln\{a_A^{1/n} + (K_{BA}^{Pot}a_B)^{1/n}\}$$

which is the extended form of Nicolsky's equation (45-51), with n, R, T, and F having their usual meanings. Super Pot signifies potentiometric selectivity coefficient. According to an IUPAC report # 43, January 1975 on nomenclature for ion selective electrodes, the potentiometric selectivity coefficient is designated K_{BA}. However, the present existing litera-

TABLE 4. Values derived for mobility ratios (u_A/u_B) across silver tungstate membrane

	u_A/u_B		
Concentration	KCl-NaCl	KCl LiCl	KCl-NH_4Cl
0.1/0.1	1.27	1.22	1.14
0.05/0.05	1.30	1.25	1.19
0.02/0.02	1.35	1.29	1.24
0.01/0.01	1.38	1.30	1.26
0.005/0.005	1.41	1.36	1.35
0.002/0.002	1.43	1.41	1.40
0.001/0.001	1.47	1.54	1.50

TABLE 5. Values derived for $K_{B_A}^{Pot}$ for different sets of electrolytes across silver tungstate membrane at 25 ± 0.1°C

KCl-NaCl	KCl-LiCl	KCl-NH_4Cl
1.131	1.096	1.131

ture uses the nomenclature above almost exclusively (52). Conti and Eisenman (53-55) and others (56, 57) have given most complete derivation and analysis of various equations involving the term potentiometric selectivity for permeable ions of the same sign through membranes containing a distribution of *fixed sites, including the usual uniform distribution.* The various values of BIP obtained with silver tungstate membrane are plotted against mean ion activities and straight lines as shown in Fig. 7 are obtained. From the slopes of the lines the values of $K_{B_A}^{Pot}$ are thus obtained and are given in Table 5 for various 1:1 sets of electrolytes (KCl-NaCl, KCl-LiCl, and KCl-NH_4Cl) through silver tungstate membrane.

More recently Toyoshima and Nozaki (22) derived various theoretical equations for membrane potential and bi-ionic potential based on thermodynamics of irreversible processes which are applied and tested here with parchment-supported silver tungstate membrane. The various assumptions for the concentration dependence of u_i and a_i of ion i ($i = +, -$) in the membrane phase are as follows:

$$[20] \qquad u_+C_+ = u_+^0C_+(C_- + \theta)$$

$$[21] \qquad u_-C_- = u_-^0C_-$$

$$[22] \qquad a_+ = \gamma_+^0(C_- + \theta)$$

$$[23] \qquad a_- = \gamma_-^0C_-$$

Here u_i^0 and γ_i^0 are the mobility and activity coefficients of ion i in the free solution. The quantity θ is the thermodynamically effective fixed charge density of the membrane.

According to Toyoshima and Nozaki (22) the system studied consists of two kinds of 1:1 electrolytes (KCl and NaCl) separating a negatively charged membrane. No electric field is applied externally across the membrane, and no electric charge is transported from one side of the membrane to the other. The theoretical equation eq. [24] for bi-ionic potential using variables which contains four parameters (V_{K^+}, V_{Na^+}), (θ/K_{K^+}, θ/K_{Na^+}), (g_{K^+}/g_{Na^+}) and (K_{K^+}/K_{Na^+}) is given by

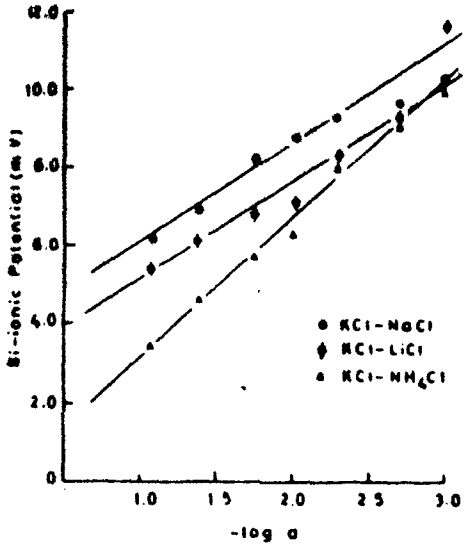

FIG. 7. Plots of observed bi-ionic potential (mV) against $-\log a$ through silver tungstate membrane for various sets of electrolytes at 25 ± 0.1°C.

$$[24] \qquad \Delta\phi_{BIP} = \left(2 \ln \frac{K_{K^+}}{K_{Na^+}} + \ln \frac{JV_{K^+} + 1}{JV_{Na^+} + 1}\right) \frac{F}{RT}$$

where (K_{K^+}/K_{Na^+}) is the selectivity constant of a membrane for positive ion species K^+ to Na^+.

$$[25] \qquad V_{K^+} = 1 + (u_{K^+}^0/u_{Cl^-}^0)$$

and

$$[26] \qquad V_{Na^+} = 1 + (U_{Na^+}^0/U_{Cl^-}^0)$$

For the evaluation of flux J of ion species, Toyoshima and Nozaki (22) gave the following equation [27] which is also used in the present investigation

$$[27] \qquad (2J + 1) \ln \frac{g_{K^+} + 2J}{g_{Na^+} + 2J} - \ln \frac{JV_{K^+} + 1}{JV_{Na^+} + 1} - \ln \frac{g_{K^+}}{g_{Na^+}} = 0$$

where

$$[28] \qquad g_{K^+} = 1 + [1 + (2K_{K^+}C/\theta)^2]^{1/2}$$

and

$$[29] \qquad g_{Na^+} = 1 + [1 + (2K_{Na^+}C/\theta)^2]^{1/2}$$

In order to evaluate (V_{K^+}, V_{Na^+}), (θ/K_{K^+}, θ/K_{Na^+}) for KCl-NaCl set of uni-univalent electrolytes, the following equation [30] given by Toyoshima and Nozaki (22) for membrane potential, $\Delta\phi$, is utilized here.

For KCl electrolyte

$$[30]\quad \Delta\phi_{KCl} = -\ln\sigma - \frac{1.2}{V_{K^+}}\ln\frac{[1+(2C_2K_{K^+}/\theta)^2]^{1/2}+(1-2/V_{K^+})}{[1+(2C_1K_{K^+}/\theta)^2]^{1/2}+(1-2/V_{K^+})} + \ln\frac{[1+(2C_2K_{K^+}/\theta)^2]^{1/2}+1}{[1+(2C_1K_{K^+}/\theta)^2]^{1/2}+1}\frac{RT}{F}$$

For NaCl electrolyte

$$[31]\quad \Delta\phi_{NaCl} = -\ln\sigma - \left(1-\frac{2}{V_{Na^+}}\right)\ln\frac{[1+(2C_2K_{Na^+}/\theta)^2]^{1/2}+(1-2/V_{Na^+})}{[1+(2C_1K_{Na^+}/\theta)^2]^{1/2}} + \left(1-\frac{2}{V_{Na^+}}\right)\ln\frac{[1+(2C_2K_{Na^+}/\theta)^2]^{1/2}+1}{[1+(2C_1K_{Na^+}/\theta)^2]^{1/2}+1}\left(\frac{RT}{F}\right)$$

where C_1 and C_2 are the concentrations of electrolyte solution on two sides of the membrane in each case

$$[32]\quad \sigma = C_1/C_2$$

Expanding eqs. [30] and [31] in powers of $1/C_2$ with fixed σ yields:

For KCl electrolyte

$$[33]\quad \Delta\phi_{KCl} = -\left(1-\frac{2}{V_{K^+}}\right)\ln\sigma - 2\left(1-\frac{1}{V_{K^+}}\right)\left(\frac{1}{V_{K^+}}\right)\left(1-\frac{1}{\sigma}\right)\left(\frac{\theta}{K_{K^+}}\right)\left(\frac{1}{C_2}\right)$$

For NaCl electrolyte

$$[34]\quad \Delta\phi_{NaCl} = -\left(1-\frac{2}{V_{Na^+}}\right)\ln\sigma - 2\left(1-\frac{1}{V_{Na^+}}\right)\left(\frac{1}{V_{Na^+}}\right)\left(1-\frac{1}{\sigma}\right)\left(\frac{\theta}{K_{Na^+}}\right)\left(\frac{1}{C_2}\right)$$

The transference number $t_{-_{app}}$ for anion is defined by eq. [9]. Introducing eq. [33] into eq. [9] and eq. [34] into eq. [9] and expanding separately $1/t_{-_{app}}$ as a power series in $1/C_2$, the following expressions are obtained.

For KCl electrolyte

$$[35]\quad \frac{1}{t_{-_{app}}} = V_{K^+} + (V_{K^+}-1)\left(\frac{\sigma-1}{\sigma\ln\sigma}\right)\times\left(\frac{\theta}{K_{K^+}}\right)\left(\frac{1}{C_2}\right)$$

For NaCl electrolyte

$$[36]\quad \frac{1}{t_{-_{app}}} = V_{Na^+} + (V_{Na^+}-1)\left(\frac{\sigma-1}{\sigma\ln\sigma}\right)\times\left(\frac{\theta}{K_{Na^+}}\right)\left(\frac{1}{C_2}\right)$$

The above equations, [35] and [36], were used for the evaluation of V_{K^+}, V_{Na^+}, θ/K_{K^+}, and θ/K_{Na^+} in the following way:

The different values of $1/t_{-_{app}}$ were plotted against $1/C_2$ (Fig. 4) for KCl and NaCl electrolytes through silver tungstate membrane at fixed $\sigma = 10$. Equations [35] and [36] indicate that the intercept of a plot of $1/t_{-_{app}}$ against $1/C_2$ at fixed σ allows the values of V_{K^+} and V_{Na^+} to be determined. For the evaluation of θ/K_{K^+} and θ/K_{Na^+}, the slopes of eq. [35] and eq. [36] are given by the following factors.

For KCl electrolyte

$$[37]\quad \left[\frac{(V_{K^+}-1)(\sigma-1)}{\sigma\ln\sigma}\right]\left(\frac{\theta}{K_{K^+}}\right) = \text{Slope}_{K^+}$$

For NaCl electrolyte

$$[38]\quad \left[\frac{(V_{Na^+}-1)(\sigma-1)}{\sigma\ln\sigma}\right]\left(\frac{\theta}{K_{Na^+}}\right) = \text{Slope}_{Na^+}$$

are first determined. The graphical values of slopes evaluated from Fig. 4 are equated with the above factors, [37] and [38], and then by substituting V_{K^+} and V_{Na^+}, the values of θ/K_{K^+} and θ/K_{Na^+} are evaluated. The same procedures were employed for the other sets of electrolytes (KCl LiCl and KCl NH_4Cl); V and θ/K thus determined for various electrolytes, namely KCl, NaCl, LiCl, and NH_4Cl and the values are given in Table 6. The values of g (for K^+, Na^+, Li^+, and NH_4^+) were calculated by substituting θ/K in eq. [28] and eq. [29] for KCl and NaCl electrolytes and the values of g are given in Table 7. The same method was adopted for NH_4Cl and LiCl and the values of g are given in Table 7. The theoretically determined values of BIP from eq. [24] are plotted against log C (Fig. 8) (for KCl NaCl set). For comparison the observed values of BIP are plotted in the same figure with silver tungstate membrane. For other sets (KCl LiCl, and KCl NH_4Cl) the calculated and observed BIP were also plotted in Fig. 8. It is quite evident from Fig. 8 that

TABLE 6. Values derived for V and (θ/K) for different electrolytes across silver tungstate membrane

Electrolytes	V	(θ/K)
KCl	2.56	0.0984
NaCl	2.82	0.1120
LiCl	2.40	0.0625
NH_4Cl	2.80	0.0682

TABLE 7. Values derived for g with different electrolytes across silver tungstate membrane

Concentration (equiv./ℓ)	g			
	KCl	NaCl	LiCl	NH_4Cl
0.01	2.01	2.01	2.03	2.00
0.02	2.07	2.05	2.24	2.01
0.05	2.40	2.28	2.55	2.08
0.10	3.23	2.97	4.01	2.29
0.20	5.10	4.70	6.78	2.94

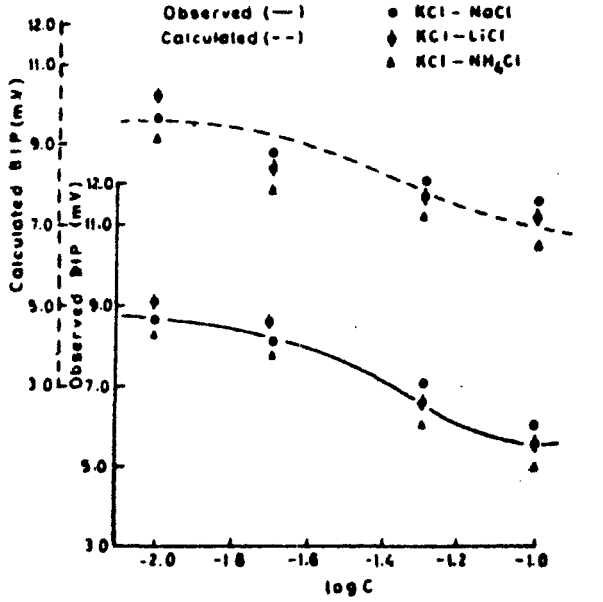

FIG. 8. Plots of observed and theoretically calculated BIP values against log C for various sets of electrolytes through silver tungstate membrane at 25 ± 0.1°C.

the agreement between the observed and theoretical values of BIP are quite fair and it may be concluded that the theory of BIP developed by Toyoshima and Nozaki (22) based on thermodynamics of irreversible processes is applicable to the system of parchment-supported membrane.

Acknowledgements

The authors are grateful to Professor Wasi-ur-Rahman, Head, Department of Chemistry, Aligarh Muslim University, India, for providing research facilities and also to C.S.I.R. (India) for the award of fellowships to M.I.R.K., A.H., and B.I.

1. F. A. SIDDIQI and S. PRATAP. J. Electroanal. Chem. **23**, 137 (1969).
2. F. A. SIDDIQI, N. LAKSHMINARAYANAIAH, and S. K. SAKSENA. Z. Phys. Chem. Frankfurt, **72**, 298 (1970).
3. F. A. SIDDIQI, N. LAKSHMINARAYANIAH, and M. N. BEG. J. Polym. Sci. **9**, 2853 (1971); **9**, 2868 (1971).
4. N. LAKSHMINARAYANAIAH and F. A. SIDDIQI. Biophys. J. **11**, 603 (1971).
5. N. LAKSHMINARAYANAIAH and F. A. SIDDIQI. Biophys. J. **11**, 617 (1971); **12**, 540 (1972).
6. N. LAKSHMINARAYANAIAH and F. A. SIDDIQI. *In* Membrane processes in industry and biomedicine. *Edited by* M. Bier. Plenum Publishing Corporation, New York. 1971. p. 301.
7. W. U. MALIK and F. A. SIDDIQI. Proc. Indian Acad. Sci. **A56**, 206 (1962).
8. N. LAKSHMINARAYANAIAH and F. A. SIDDIQI. J. Polym. Sci. **8**, 2949 (1970); Z. Phys. Chem. Frankfurt, **78**, 150 (1972).
9. O. KEDEM and A. KATCHALSKY. Trans. Faraday Soc. **59**, 1918 (1963); **59**, 1931 (1963); **59**, 1941 (1963).
10. K. S. SPEIGLOR. Trans. Faraday Soc. **54**, 1408 (1958).
11. G. SCATCHARD. Discuss. Faraday Soc. **21**, 30 (1956).
12. E. M. SCATTERGOOD and E. N. LIGHTFOOT. Trans. Faraday Soc. **64**, 1135 (1968).
13. M. PLANCK. Ann. Phys. **39**, 161 (1890); **40**, 561 (1890).
14. M. NAGASAWA and Y. KOBATAKE. J. Phys. Chem. **56**, 1017 (1952).
15. M. TASAKA, N. AOKI, Y. KONDO, and M. NAGASAWA. J. Phys. Chem. **79**, 1307 (1975).
16. Y. KOBATAKE and H. FUJITA. J. Phys. Chem. **72**, 2871 (1968).
17. N. KAMO, M. OIKAWA, and Y. KOBATAKE. J. Phys. Chem. **77**, 92 (1973).
18. Y. KOBATAKE, N. TAKEGUCHI, Y. TOYOSHIMA, and H. FUJITA. J. Phys. Chem. **69**, 3981 (1965).
19. N. KAMO, Y. TOYOSHIMA, and Y. KOBATAKE. Kolloid Z. Z. Polym. **249**, 1061 (1971).
20. N. KAMO, Y. TOYOSHIMA, H. NOZAKI, and Y. KOBATAKE. Kolloid Z. Z. Polym. **248**, 914 (1971).
21. Y. TOYOSHIMA, M. YUASA, Y. KOBATAKE, and H. FUJITA. Trans. Faraday Soc. **63**, 2803 (1967); **63**, 2814 (1967).
22. Y. TOYOSHIMA and H. NOZAKI. J. Phys. Chem. **74**, 2704 (1970).
23. H. B. WEISER. J. Phys. Chem. **34**, 335 (1930); **34**, 1826 (1930).
24. R. SCHLÖGL. Stofftransport durch Membrane Steinkopff. Darmstadt, 1964; Ber. Bunsenges. Phys. Chem. **70**, 400 (1966).
25. W. W. KITTELBERGER. J. Phys. Chem. **53**, 392 (1949).
26. B. J. ZWOLINSKI, H. EYRING, and C. E. REESE. J. Phys. Chem. **53**, 1426 (1949).
27. S. GLASSTONE, K. J. LAIDLER, and H. EYRING. The theory of rate processes. McGraw-Hill, New York. 1941. p. 525.
28. K. E. SHULER, C. A. DAMES, and K. J. LAIDLER. J. Chem. Phys. **17**, 860 (1949).
29. T. TEORELL. Proc. Soc. Exptl. Biol. Med. **33**, 282 (1935); Proc. Natl. Acad. Sci. U.S. **21**, 152 (1935).
30. T. TEORELL. Z. Elektrochem. **55**, 460 (1951).
31. T. TEORELL. Prog. Biophys. Chem. **3**, 305 (1953).
32. K. H. MEYER and J. F. SIEVERS. Helv. Chim. Acta, **19**, 649 (1936); **19**, 665 (1936); **19**, 987 (1936).

33. A. ILANI. Biochim. Biophys. Acta, 94, 415 (1965).
34. K. SOLLNER, S. DRAY, E. GRIM, and R. NEIHOF. *In* Ion transport across membranes. *Edited by* H. T. Clarke and D. Nachmanshon. Academic Press, New York. 1954. p. 144; *In* Electrochemistry in biology and medicine. *Edited by* T. Shedlovsky. Wiley, New York. 1955. p. 65.
35. K. SOLLNER. J. Phys. Chem. 53, 1211 (1949); 53, 1226 (1949); *In* Encyclopedia of electrochemistry. *Edited by* C. A. Hampel. Reinhold, New York. 1964. p. 806.
36. D. REICHENBERG. *In* Ion-exchange. Vol. 1. *Edited by* J. A. Marinsky. Dekker, New York. 1968. p. 227.
37. G. EISENMAN. Bol. Inst. Estud. Med. Biol. (Univ. Nac. Auton Mex.) 21, 155 (1963); Proc. Int. Congr. Physiol Sci. 23rd, Tokyo. 1965 p. 489.
38. G. EISENMAN, D. O. RUDIN, and J. U. CASBY. Science, 126, 831 (1957).
39. G. EISENMAN. Biophys. J. Suppl. 2, 314 (1962).
40. G. EISENMAN (*Editor*). Glass electrodes for hydrogen and other cations, principles and practice. New York. 1967.
41. G. EISENMAN. Adv. Anal. Chem. Instrum. 4, 213 (1965); also reprinted in G. Eisenman, R. Bates, G. Mattock, and S. M. Friedman. The glass electrode. Wiley, Interscience, New York. 1966.
42. G. EISENMAN. *In* Ion selective electrodes. *Edited by* R. A. Durst. Natl. Bur. of Std. Spec. Publ. 314, Washington, DC. 1969. p. 1.
43. G. EISENMAN. *In* Symp. membrane transport metabolism. *Edited by* A. Kleinzeller and A. Kotyk. Academic Press, New York. 1961. p. 163.
44. C. E. MARSHALL and C. A. KRINBILL. J. Am. Chem. Soc. 64, 1814 (1942).
45. B. P. NICOLSKY. Acta Physicochim. URSS, 7, 597 (1937).
46. R. M. GARRELS, M. SATO, M. E. THOMPSON, and A. H. TUESDELL. Science, 135, 1045 (1962).
47. E. PUNGOR. Anal. Chem. 39, 28A (1967).
48. E. PUNGOR and K. TOTH. Anal. Chim. Acta, 47, 291 (1969).
49. E. PUNGOR and K. TOTH. Analyst, 95, 625 (1970).
50. H. R. WUHRMAN, W. E. MORF, and W. SIMON. Helv. Chim. Acta, 56, 1011 (1973).
51. W. E. MORF, D. AMMAN, E. PRETSCH, and W. SIMON. Pure Appl. Chem. 36, 421 (1973).
52. R. P. BUCK. Critical reviews in analytical chemistry. 1976. pp. 342–382.
53. F. CONTI and G. EISENMAN. Biophys. J. 5, 247 (1965); 5, 511 (1965).
54. G. EISENMAN (*Editor*). Membranes. Vol. 1. Dekker, New York. 1972. Vol. 2, New York. 1973.
55. F. CONTI and G. EISENMAN. Biophys. J. 6, 227 (1966).
56. F. HELFFERICH and H. D. OCKER. Z. Phys. Chem. Frankfurt, 10, 213 (1957); Discuss. Faraday Soc. 21, 83 (1956); 21, 133 (1956).
57. W. R. J. WYLLIE and S. L. KANAAN. J. Phys. Chem. 58, 73 (1954).

MISCELLANEOUS STUDIES

[Reprinted from the Journal of Physical Chemistry, 66, 356 (1962)]

Studies on the Sol–Gel Transformation of the Ferro- and Ferricyanides of Some Metals. Part III. Gelation in Chromic Ferrocyanide

By Wahid U. Malik and Fasih A. Siddiqi

[Reprinted from the Journal of Physical Chemistry, 66, 356 (1962).]

STUDIES ON THE SOL–GEL TRANSFORMATION OF THE FERRO- AND FERRICYANIDES OF SOME METALS. PART III. GELATION IN CHROMIC FERROCYANIDE

By Wahid U. Malik and Fasih A. Siddiqi

Chemical Laboratories, Muslim University, Aligarh, India

Received August 23, 1961

During the course of the work on heavy metal ferrocyanides we came across an unusual reaction, *viz.*, that between chromic chloride and potassium ferrocyanide, where unlike other metal ferrocyanides a soluble complex (reddish brown in color) of the composition[1,2] $KCr^{III}Fe^{II}Cy_6$ is formed. On carrying out the reaction at 80° an insoluble complex, highly viscous in nature and showing a tendency to gelatinize, is obtained. A study of some colloidal aspects of this compound was undertaken.

Experimental

The chromic ferrocyanide sol did not reveal vulnerability toward electrolytes as is generally the case with typical hydrophobic sols. However, interesting results were obtained on keeping it in the electrophoresis tube. Thus with a mixture of $CrCl_3$ and K_4FeCy_6 (concn. 0.075 and 0.025 *M*, respectively) of molar ratio $Cr^{3+}/FeCy_6^{4-}$ of 3:1, well-defined rings in the cathodic limb were formed; the liquid in the anodic limb depressed to about 1 cm. in about one hr. 15 min. (potential applied: 150 v.; current 2 to 5 mamp.). Mixtures of the molar ratio 1:3 (concn. $CrCl_3$ = 0.016 *M* and K_4FeCy_6 0.05 *M*) underwent movement toward the anode; with the equilibrium mixture (concn. 0.05 *M* of each reactant) there was no perceptible movement toward either of the electrodes.

The time of setting of chromic ferrocyanide gel as influenced by the $Cr^{3+}/FeCy_6^{4-}$ ratio was studied by Fleming's method[3] with the following four sets of mixtures. (i) 3.5 cc. of 0.78 *M* K_4FeCy_6 mixed with 1.0, 1.5, 2.0. . . . . .6.0, 6.5 cc. of 1.25 *M* $CrCl_3$. Total volume made up to 10 cc. (Molar ratio varied from 0.45:1 to 2.97:1.0); (ii) 5.0 cc. of 0.78 *M* K_4FeCy_6 mixed with 1.0, 1.2, ...4.2, 4.5 cc. of 1.25 *M* $CrCl_3$. Total volume made up to 15.0 cc. (Molar ratio varied from 0.32:1 to 1.8:1.0). (iii) 2.8 cc. of 0.78 *M* K_4FeCy_6 mixed with 0.96, 1.2,1.28,. . . . . 3.06, 3.2 cc. of 1.25 *M* $CrCl_3$. Total volume made up to 10 cc. (Molar ratio varied from 0.53:1.0 to 1.83:1.0); (iv) 1.8 cc. of 0.78 *M* K_4FeCy_6 mixed with 0.6, 0.8,. . . . . .2.0, 2.2 cc. of 1.25 *M* $CrCl_3$. Total volume made up to 10 cc. (Molar ratio varied from 0.534:1 to 2.0:1.0). The results are depicted in Figs. 1 and 2 (curves 1, 2, 3 and 4, respectively).

The time of gelation, besides being influenced by the $Cr^{3+}/FeCy_6^{4-}$ also was found to be dependent upon the concentration of the reactants. Thus the time of gelation of the mixture containing 3.5 cc. of 0.78 *M* K_4FeCy_6 and 2.5 cc. of 1.25 *M* $CrCl_3$ (molar ratio 1.1:1.0) increased from 12 min. to 15, 17, 28, 60, 155 min., respectively, on diluting the reactants to 4/5th, 3/5th, 2/5th, 1.5/5th and 1/5th of the original concentration.

Discussion

The results on the sol–gel transformation of chromic ferrocyanide reveal many points of dissimilarity with other metal ferrocyanides.[4] These are (i) lesser solubility of the complex with increasing temperature, optimum condition for gelation being reached in the vicinity of 80°; (ii) non-destructibility of the colloidal state by the addition of foreign ions; (iii) slow movement in the electrophoresis tube and indistinct separation of the phases at the interface; (iv) the tendency of the particles to assume a positive as well as negative charge (depending upon the excess of chromic or ferrocyanide ions). That the two types of gel-forming mixtures exist can be seen from the results on the time of gelation. Thus with the increasing concentration of the chromic ions a continuous decrease in the time of gelation is not realized. On the other hand, after reaching a minimum value for the equimolar mixture gradual increase in the time of gelation takes place (Figs. 1 and 2). However, in both cases the time of gelation is highly dependent upon the $Cr^{3+}/FeCy_6^{4-}$ ratio.

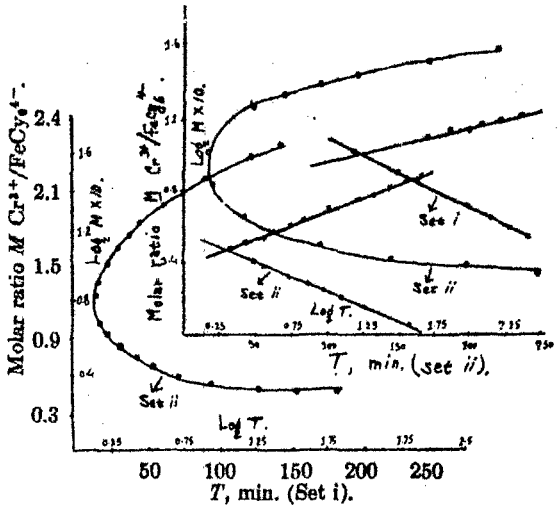

Fig. 1.—Set i and ii.

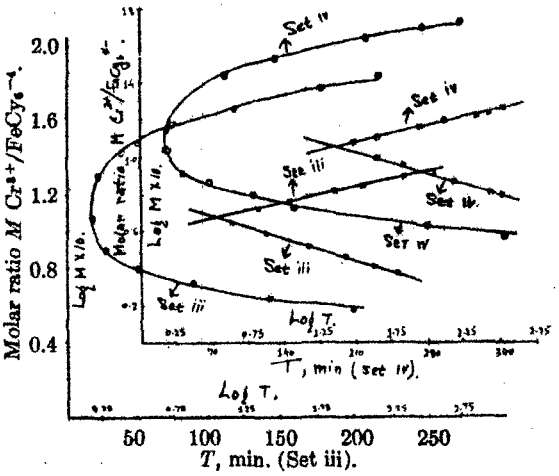

Fig. 2.—Set iii and iv.

The behavior, *viz.*, decrease in the time of gelation for mixtures of minimum gelation time (molar ratio 1.1:1.0) with increase in the concentration of the reactions is not unexpected since with concentrated solutions the degree of supersaturation increases and chances of gelation are enhanced.

A plot of log *M* against log *T* gives a pair of straight lines. The exponential nature of the curves can be represented by the empirical relationship

$$(T - \alpha M^{n})(T - \beta M^{-m}) = 0$$

(1) W. U. Malik, *J. Sci. Ind. Research* (India), **18**, 463 (1959).
(2) W. U. Malik, *ibid.*, **20B.8**, 213 (1961).
(3) Fleming, *Z. Physik*, **41**, 427 (1902).
(4) K. Nasiruddin, W. U. Malik and A. K. Bhattacharya, *J. Phys. Chem.*, **59**, 488 (1955); W. U. Malik and A. K. Bhattacharya, *ibid.*, **59**, 490 (1955).

M being molar ratio and T the time of gelation, where α, β, n and m are constants. Their values for the four sets are α = 5.8, 19.9, 18.6, 10.0; β = 19.05, 14.2, 17.78, 36.14; n = 3.4, 5.0, 6.9, 6.25 and m = 2.91, 2.68, 4.16 and 4.68. The fact that the values of the constants are not the same may be due to the varying influence of factors like solubility, degree of supersaturation, extent of hydration and dilution during gelation.

Acknowledgment.—Thanks are due to Dr. A. R. Kidwai for providing facilities and to C.S.I.R. (India) for the award of a fellowship to F.A.S.

[Reprinted from the Journal of Physical Chemistry, 66, 357 (1962).]

Studies on the Sol–Gel Transformation of the Ferro- and Ferricyanides of Some Metals. Part IV. Variations in Viscosity and Hydrogen Ion Concentration During the Gelation of Chromic Ferrocyanide

By Wahid U. Malik and Fasih A. Siddiqi

[Reprinted from the Journal of Physical Chemistry, 66, 357 (1962).]

STUDIES ON THE SOL–GEL TRANSFORMATION OF THE FERRO- AND FERRICYANIDES OF SOME METALS. PART IV. VARIATIONS IN VISCOSITY AND HYDROGEN ION CONCENTRATION DURING THE GELATION OF CHROMIC FERROCYANIDE

By Wahid U. Malik and Fasih A. Siddiqi

Chemical Laboratories, Muslim University, Aligarh, India

Received August 23, 1961

The conductivity method, which was successfully employed[1] earlier in studying gelation of Prussian and Turnbull's blues, did not give any useful information here, and hence the methods based on the variations in viscosity and *p*H were adopted. The latter method was particularly chosen with a view to ascertain the hydrolytic effects operative during gel formation.

Experimental

Viscosity measurements were carried out at 80 ± 0.1° (Fisher Unitized constant temperature oil-bath) with the help of an Ostwald viscometer after applying a vacuum of 1 cm. (manometer tube supplied with koppeos viscometer unit was used for this purpose) at the head of the viscometer tube. Beckman *p*H meter (model H2) was used for *p*H measurements. Seven sets were studied, containing 0.25 *M* K_4FeCy_6 and varying concn. of $CrCl_3$ (0.083, 0.125, 0.18, 0.25, 0.375, 0.50 and 0.625 *M*) in the reaction mixture. The results are summarized in Table I.

Table I

Set	$Cr^{3+}/FeCy_6^{4-}$	Time interval for abrupt change in viscosity η (min.)	Change in η during this interval (centipoise)	Value of $(\eta_t - \eta_0)/\eta_0$ at abrupt change	*p*H change during gelation
I	0.33:1.0	218–250	0.70–2.4	0.75	4.0–7.25
II	0.5:1.0	120–140	0.95–2.7	0.90	3.8–6.8
III	0.75:1.0	72–80	1.15–4.8	1.10	3.6–4.0
IV	1:1	28–33	1.28–2.75	1.30	3.5–3.25
V	1.5:1.0	48–55	1.35–5.0	1.70	3.3–2.75
VI	2.0:1.0	120–150	1.45–3.6	2.10	3.12–2.02
VII	2.5:1.0	225–250	1.90–3.75	2.63	2.7–1.7

Discussion

The results on viscosity variations provide the following useful information regarding the gelation of chromic ferrocyanide: (1) the abrupt change in viscosity may be taken as a measure of the time of gelation since the values obtained by this and Fleming's method compare favorably (times of setting for the gelation mixtures of molar ratios 0.50:1.0, 1.0:1.0 and 2.0:1.0 being 25, 17, 85 minutes, respectively, by Fleming's method and 120, 28 and 120 minutes, respectively, by the viscosity method), provided due allowance is given to the disturbances experienced by the gel-forming mixture during its movement through the capillary; (2) similar types of curves are obtained by the two methods on plotting the time of setting against the molar ratio (Fig. 1), confirming thereby the existence of two types of gels in chromic ferrocyanide

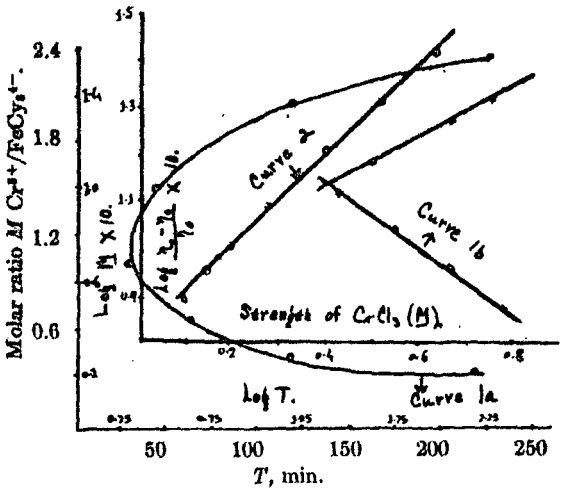

Fig. 1.—Curve 1a, *T vs. M*; curve 1b, log *T vs.* log *M*; curve 2, strength of $CrCl_3$ *vs.* log $(\eta_t - \eta_0)/\eta_0$.

(Part III); (3) a straight line is obtained on plotting log $(\eta_t - \eta_0)/\eta_0$ (for abrupt change) against the concentration of chromic chloride (Fig. 1, curve 2) (Cr^{3+} concn. for sets I to VII), which indicates a thixotropic behavior of chromic ferrocyanide gel (a linear relationship $\log \theta = A - Bc$, where θ is the time of setting and c is the concentration of the electrolyte and A and B are constants, was found by Freundlich,[2] Schalek and Szegvari[3] for the gelation of ferric oxide sol).

The results on *p*H measurements, besides confirming the results on viscometry (the time when constancy in *p*H value is reached being taken as the time of setting), throw some light on the nature of the chromic ferrocyanide gel. As expected the mixtures containing excess of chromic ions have lower *p*H values and those containing excess of potassium ferrocyanide have higher *p*H values. But with lapse of time the *p*H of the mixtures having $Cr^{3+}/FeCy_6^{4-} > 1$ continuously decreases, while for those having $Cr^{3+}/FeCy_6^{4-} < 1$ the variations are of the reverse order. The behavior can be explained by assuming (a) the hydrolysis of chromic chloride, and (b) the hydrolytic decomposition of potassium ferrocyanide in the presence of chromic ions.[4,5] In the latter case the reaction takes the course

$$K_4FeCy_6 + H_2O \rightleftharpoons K_3(FeCy_6 \cdot H_2O) + KCN$$

$$KCN + H_2O \rightleftharpoons KOH + HCN$$

thereby making the mixture less acidic. However, another significant point worth considering is that with mixtures having a molar ratio 1:1, the variations in *p*H with time are negligible (Table I).

Acknowledgment.—Thanks are due to Dr. A. R. Kidwai for providing facilities and C.S.I.R. (India) for the award of fellowship to F.A.S.

(1) W. U. Malik and A. K. Bhattacharya, *J. Phys. Chem.*, **59**, 490 (1955).

(2) H. Freundlich, "Thixotropy," Paris, 1935, pp. 7, 29.

(3) E. Schalek and A. Szegvari, *Kolloid-Z.*, **33**, 326 (1923).

(4) W. U. Malik, *J. Sci. Ind. Research* (India), **18**, 463 (1959).

(5) W. U. Malik, *ibid.*, **20B**, 5, 213 (1961).